COALBED METHANE

PRINCIPLES & PRACTICES

Second Edition

Courtesy of

HALLIBURTON

Rudy Rogers
Muthukumarappan Ramurthy
Gary Rodvelt
Mike Mullen

Coalbed Methane: Principles and Practices

Coalbed Methane: Principles and Practices

Rudy Rogers
Mississippi State University

Kumar Ramurthy
Halliburton

Gary Rodvelt
Halliburton

Mike Mullen
Halliburton

Oktibbeha Publishing, LLC, Starkville, MS 39759

Coalbed Methane: Principles and Practices
Rogers, R., Ramurthy, K., Rodvelt, G., and Mullen, M.

ISBN 978-0-9794084-1-0

Oktibbeha Publishing Co., LLC
Starkville, MS.
Registered, *Books in Print*

Cover Design: Halliburton

For more information on ordering this book, contact:

R.E. Rogers
2017 South Montgomery
Starkville, MS 39759

Phone 662-323-0252
rudyrogers@hotmail.com

Printed in the United States of America
10 9 8 7 6 5 4 3 2 1

ISBN 978-0-9794084-1-0

Note: This book was previously published by
Prentice-Hall, Inc. now known as Pearson Education, Inc.
(previously ISBN 0-13-016353-8)
Rogers, Rudy E.
Coalbed methane: principles and practice / Rudy E. Rogers.
p. cm.
Includes bibliographical references and index.
1. Coalbed methane. 1. Title.
TN844.5.R64 1994 93-39681
622'.3385---dc20 CIP

Contents

Chapter 1—Introduction

Chapter 2—Geological Influences on Coal

Chapter 3—Sorption

Contents

Chapter 6—Formation Evaluations, Logging

Chapter 7—Completions

Contents

Preface

It is not often that a new industry unexpectedly appears and flourishes in only a few years—especially in the field of energy. Such is the case, however, with the coalbed methane industry. It began as an altruistic effort to make coal mines safe from the explosions that have been the nemesis of miners for two centuries. The effort was more than successful; the coalbed methane process is now a self-supporting, profitable enterprise.

The value of the coalbed methane process is not just as a profitable business. The process reduces loss of lives in coal mine explosions, reduces greenhouse gas emissions from mines, reduces air pollution as a clean-burning fuel, reduces a country's reliance on imported fossil fuels, and helps utilize vast coal resources around the world. The process has abruptly introduced an energy source not previously considered in estimating world energy reserves. At a time when needs for abundant energy supply and clean environment often conflict, coalbed methane is a welcome remedy. Such was the case in the United States, where the advent of the coalbed methane process introduced an abundant and cheap supply of the cleanest-burning fossil fuel at a time of heightened environmental awareness, at a time of rapidly decreasing domestic oil production and increasing oil importation, and at a time of increasing consumer demand for energy. Many countries now seek information on the process in the United States where the technology originated and continues to be developed. *Coalbed Methane: Principles and Practices* is written to make available an explanation of the technology comprehensive enough to assist these countries.

The timing of the introduction of the coalbed methane process was right; however, industries and governments must continue to fully utilize the potential. So far, both institutions are doing so. Industry is steadily making technical improvements to increase the methane recovery factor and to produce methane more economically. This current edition of *Coalbed Methane: Principles and Practices* includes an update by Halliburton of process technical improvements now practiced in the field, which they and others have introduced in recent years. During the process infancy stage of research, the federal government established a tax credit for produced methane that helped establish the process.

Coalbed Methane: Principles and Practices is intended for a wide audience. Prior to publication of the book, hundreds of individual articles appeared throughout the technical literature that described most aspects of the process, but the principles and their applications had not been organized into a single reference text. This is the first cohesive book on the subject. The original manuscript described technologies and innovations from two industries that were melded to make coalbed methane technology an entity itself. Coal mining technology and oilfield technology were combined to produce coalbed methane, but field practices from each parent had to be modified. In making these modifications, a viable process resulted to produce coal gas. The book details the modifications, but more importantly, states the principles that made the changes necessary.

Engineers coming from the oil and gas industry to work on producing methane from coalbeds may lack working knowledge of gas adsorption and diffusion in micropores, and they may be unfamiliar with coal mechanical properties or chemistry. This textbook begins with the rudiments of coal formation, chemical structure, and physical/mechanical properties (including the pervading influence of rank) that should endow the newcomer with essential background information.

A chapter is devoted to reservoir engineering principles. These principles are discussed from the standpoint of coal being a reservoir rock as well as a source rock for methane. Subsequent chapters deal with water production and disposal, well completion practices, fracturing, and economics. Thus, the book is an

overview of the important principles of methane genesis through production. In each of the topics, case histories or field data are taken primarily from the Black Warrior and the San Juan basins and secondarily from the Appalachian, Piceance, or Powder River basins. A new section is added in this edition on well logging and stimulation. Additionally, technology updates are included on all of the topics from the original edition.

Creation of *Coalbed Methane: Principles and Practices* is exciting because it reports the pioneering work of a new energy technology. One perceives the excitement as an undercurrent of feeling among the geologists, engineers, and managers developing the process. It is reflected in their enthusiasm. Secondarily, the book gives well-deserved recognition to the people who began the process a few years ago and who are still making basic contributions to process improvement. As a new addition to the book, valuable insight into the coalbed methane process is incorporated by Halliburton from their many years of field experience. Finally, it is satisfying to present a text that could help further the development of a natural resource with potential benefits to so many people in multiple ways.

Chapter 1

Introduction

1.0 Introduction

Methane burns more cleanly than any other fossil fuel. Methane is cheap, and it comes from domestic sources; a U.S. source of about 800 trillion cubic feet (Tcf) of methane has been discovered in coalbeds. This significant energy source has been converted from a centuries-old mining hazard into an environmentally friendly fuel.

Production of coalbed methane (CBM) in a short time has become an important industry, providing an abundant, clean-burning fuel in an age when concerns about pollution and fuel shortages preoccupy the thoughts of many Americans. Other than in the U.S.A., CBM is being produced in Queensland, Australia and the United Kingdom. Pilot projects are underway in China and India. Test or pilot programs are underway in approximately 15 other countries.

Use of CBM could improve the environments of Eastern Europe and China. In the United States, it could be an alternative fuel for automotive vehicles or the clean fuel of the future in power plants.

Consider that the use of CBM could fulfill national goals, such as the following:

- Provide a clean-burning fuel.
- Increase substantially the natural gas reserve base.
- Improve safety of coal mining.
- Decrease methane vented to the atmosphere from coal mines that might affect global warming.
- Provide a means to use an abundant coal resource that is often too deep to mine.

The process may be applicable wherever coal is found. Much potential exists internationally. Spain, France, Poland, Australia, Canada, the Peoples Republic of China, Great Britain, Germany, Zimbabwe, and Russia are a few of the countries that have undertaken projects after the initial success in the United States. Over 60 countries have substantial coal reserves, and most of them are interested in recovering the methane. In Eastern Europe, for example, coal may be the only natural energy resource of a country. In this region, CBM holds the intriguing potential to help supply energy needs for revitalizing industries—and in a manner that improves air quality. The same intriguing potential exists in other developing countries where industry and environment suffer parallel fates.

CBM, an emerging industry, developed over a span of 5 years after 5 years of research and pilot projects. Initial process improvements came rapidly to bolster its success where these innovations improved production, economics, reservoir management, and drilling. The primary catalyst for CBM development was possibly a federal tax credit that overcame the inertia of starting a new industry.

Employed in the coalfields have been oilfield techniques, sometimes modified and improved. In many ways the CBM process has merged technologies from the oil industry and the coal industry. For example, during the preceding generation, methane was produced for local use from wells drilled into coals, but it took the fracturing of those coals and their dewatering, along with other oilfield technology, to increase production rates to commercial levels. Research generated by the activity delved into coal properties and associated phenomena on a scale not undertaken before for coal.

Future technical advancements may turn properties that are now marginal into successful commercial ventures. Breakthroughs may make production of the methane of deep coals profitable because a vast resource lies at depths heretofore not considered for mining or methane recovery—exciting challenges for industry.

Material in this book is a compilation of current knowledge of CBM and its processes and the work is meant to serve as a single reference for the many parties who now seek information needed to develop a coal property. The book

draws from a large body of information generated during the several years of the CBM process.

An engineer from the oil and gas industry entering into a CBM project for the first time may be faced with problems not previously encountered, such as adsorption, diffusion, coal mechanical properties, and stress-dependent permeabilities; he may find that geology impacts his reservoir in an unexpected manner. From another viewpoint, if one first sees CBM from the perspective of a long-time association with coal mining, then familiarity with fracturing or completion techniques of the oil and gas industry may be of particular benefit. The new process is an amalgam of oilfield and coal-mining practices that has merged as one and has often beneficially caused the engineer to investigate limits of parameters previously ignored.

Since the process was developed in the United States, other countries with substantial coal reserves look there for the knowledge to produce the methane. Independent operators and major companies seeking an investment need a ready source of information on all aspects of CBM to encourage participation. The college student anticipating a competitive job market should seek information on this new technology. Government agencies concerned with a cheap, abundant, clean energy source should understand the principles of CBM. Thus, the text is prepared to assist many individuals, corporations, and countries interested in developing a valuable natural resource.

1.1 U.S. Clean Energy Needs

Growth of U.S. industry and upward population growth will continue to require more energy. More importantly, a high-quality energy source will be demanded to protect the environment. The United States and other industrialized countries are now exploring for energy sources to (1) replace gasoline and diesel vehicular fuels and (2) provide clean fuels for power plants.

In addition to environmental quality, other requirements are placed on the fuel. It must be abundant, cheap, and a domestic resource with reserves sufficient to carry the nation well into the 21st Century. These are extremely stringent demands.

Energy consumption in the U.S. has followed the trend given in Fig. 1.1. As the country has grown in population, industry, and transportation sophistication since 1950, total energy needs have more than doubled. The energy trend is toward inexorable growth, following society's quest for a higher standard of living, and slowed only by recessionary periods. It is noteworthy that the total energy requirement has increased more than efficiency improvements, such as better automobile mileage to better insulated housing.

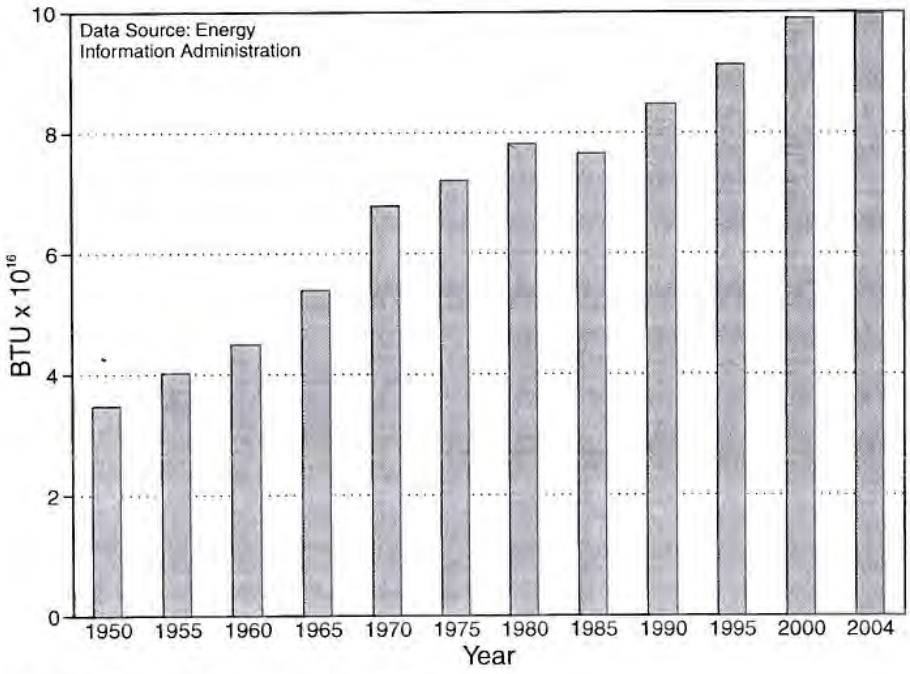

Fig. 1.1—U.S. energy consumption.

The energy mix has changed in recent decades. For example, nuclear energy was introduced for electric power generation. Changing supply and cost factors altered the mix. Safety and convenience of use continue to influence choice. Environmental factors are in the forefront of changing future patterns of use. Not only will the country experience the need for an increasing energy supply to fuel its progress, but stringent controls on public safety and on environmental effects will alter the present energy mix. The task to fulfill the need is made monumental by the extraordinary magnitude of energy volume needed by an industrialized country.

In 2002, U.S. energy consumption of 9.75×10^{16} BTU came from a mix of coal, natural gas, nuclear fuel, and crude oil. The energy supplied by each source is presented in Fig. 1.2. Oil is the leading energy supplier by a large margin. Note, however, that more than one-half of the oil is imported.

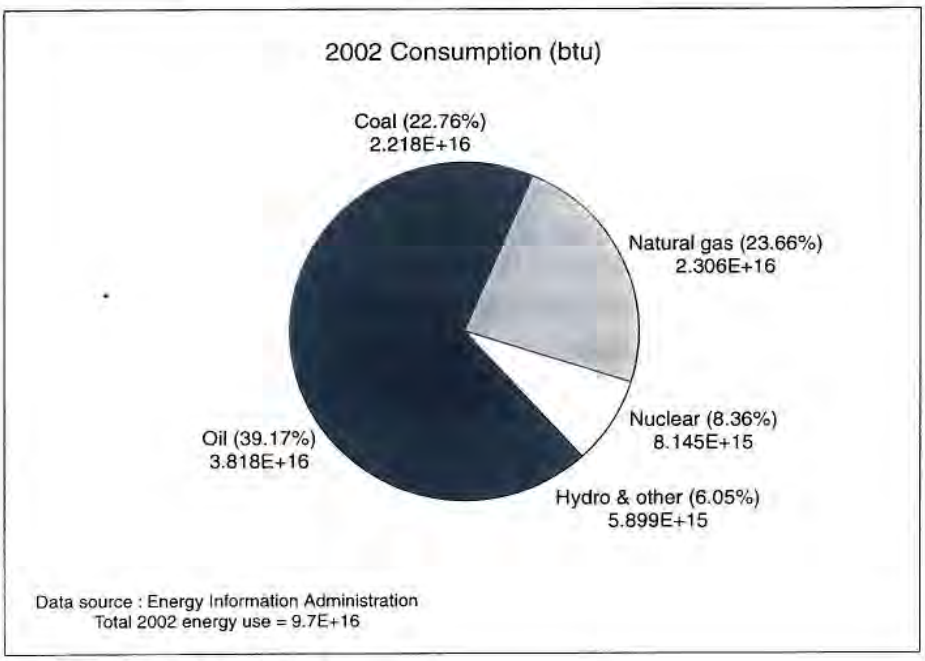

Fig. 1.2—Mix of energy use.

Among the most important consumers of energy were power plants for generating the nation's electricity in the year 2002 (Fig. 1.3).[1] In that year, oil and gas supplied 21% of power plant fuel needs. Over 50% of the electricity was generated directly from coal and over 15% from nuclear energy.

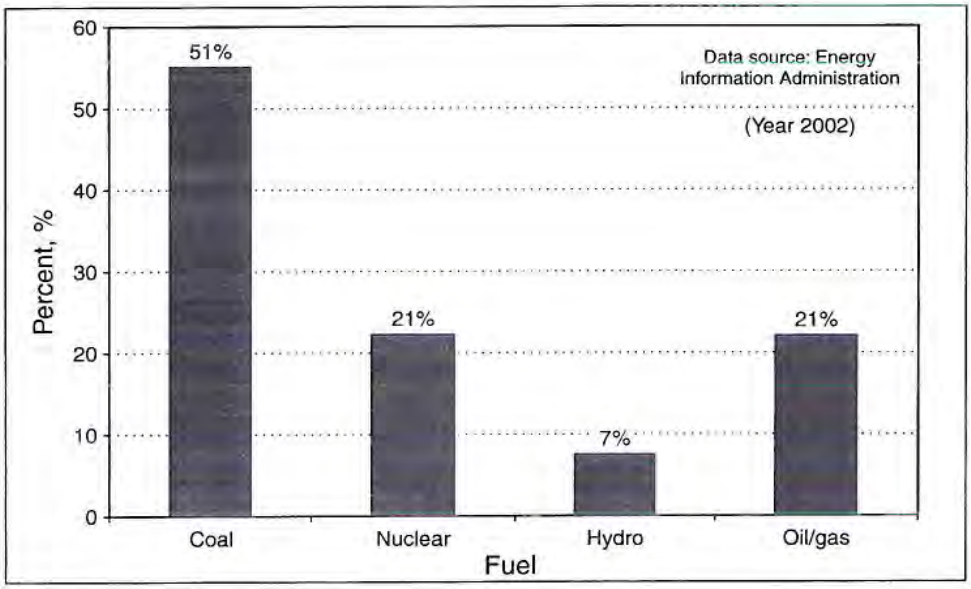

Fig. 1.3—Power-plant fuels.

Consequently, the facts emphasize that any abundant new energy source that meets or exceeds the strict rules of usage and economics must be studied and, if possible, developed.

1.2 Future Role of Natural Gas

The primary energy source of the United States throughout the country's history follows the order: wood, coal, and oil. If the next primary source is natural gas, a progressive order is noted from the dirtiest to the cleanest fuels. It is in this scenario that CBM enters the market.

Several circumstances should encourage a larger share for natural gas of the nation's energy consumption in the future than the 23.66% of Fig. 1.2. Supply and environmental problems with oil, environmental problems with coal, safety problems with nuclear power, and a scarcity of alternative sources may influence a shift in usage toward natural gas.

Overall, the generation of greenhouse gases could probably be reduced with the expanded use of natural gas. Gas may have the best combination of abundance, supply, price, cleanliness, and safety. Carson[2] relates improvements of a natural gas power plant over a coal-fired plant in areas of less SO_2 emissions, no solid waste disposal, 60% lower CO_2 emissions, and 87% lower NO_x emissions with an estimate of a capital cost 65% less than its nuclear counterpart.

As shown in Fig 1.4, the Energy Information Administration (EIA) anticipates increased natural-gas usage in power plants until 2025. From 2002 to 2025, electricity consumption is projected to increase 2.2% per year in the commercial sector, 1.6% per year in the industrial sector and 1.4% per year in the residential sector. According to EIA, most new electricity generation is expected to be from natural-gas-fired power plants because natural-gas-fired generators have the following advantages over coal-fired generators: lower capital costs, higher fuel efficiency, shorter construction lead times, and lower emissions. Natural gas consumption by power plants is projected to increase from 5.6 Tcf in 2002 to 6.7 Tcf in 2010 and 8.4 Tcf in 2025.[1]

A traditional problem of power plants has been the need to have a long-term supply contract for fuel purchase. Because CBM production exhibits a steady, moderate decline rate with long well lives on the order of 20 years, the CBM

source may be attractive for power plant use. Conventional natural gas reservoirs do not usually exhibit such longevity.

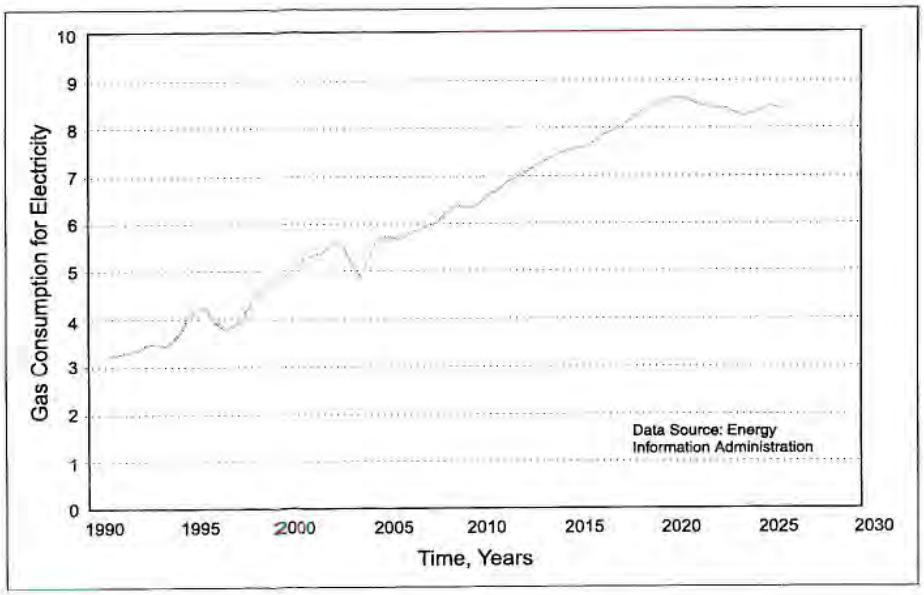

Fig. 1.4—Natural gas to power plants.

Another application outside the utility industry that may accelerate the upward trend of natural gas consumption is to power automotive vehicles, especially fleet vehicles. Gasoline and diesel fuels have come under increasing criticism for air pollution, and natural gas is a viable alternative.[3]

At the time of the 1990 Clean Air Act, 30,000 fleet vehicles in the United States were powered by compressed natural gas. At that point 500,000 vehicles were powered by natural gas worldwide.[4] The American Gas Association reports that more than 130,000 natural-gas vehicles (NGV) are in operation today in the United States and there are more than 1 million worldwide.

Natural gas has an octane number of 130. Burning natural gas reduces emissions of particulate matter from diesel fuels to negligible amounts. Compressed natural gas (CNG) engines reduce the carbon monoxide emission to less than 50% of that of gasoline engines.[5] CNG to fuel automotive vehicles is a proven concept that would substantially reduce air pollution in the United States.

With research and development progress, another large potential market for natural gas exists in residential and commercial refrigeration units.

1.3 The Conventional Natural Gas Resource

Against the backdrop of increasing demand for natural gas, expanding markets, and the accelerating demand for environmental quality, consider natural gas production during recent decades. Fig. 1.5 gives the production of natural gas in Tcf in the United States from 1949 to 2002. Production peaked in 1973, and an increasing trend was seen again from 1986. Forecasts are for 29.1 Tcf of gas demand in the United States by 2025 in the low economic growth case and 34.2 Tcf demand under a rapid technology case, as compared with 22.6 Tcf in 2002.[1]

Natural gas reserves, the gas that has been discovered and is economical to produce, indicate the replacement efficiency for produced gas. The proven conventional natural gas reserves, not including CBM, of the contiguous 48 states show the trend since 1966 depicted in Fig. 1.6. It should be remembered that the reserve estimates are dependent upon price and the profitability to develop gas discoveries. From a peak reserve of about 280 Tcf in 1966, a decrease of over 100 Tcf has steadily reduced that high point until the year 2000. For the years after the mid-1980s, gas surpluses and low prices discouraged drilling for new reserves, especially in deep wells. This trend started to reverse in the year 2000 and can be seen with addition of new reserves.

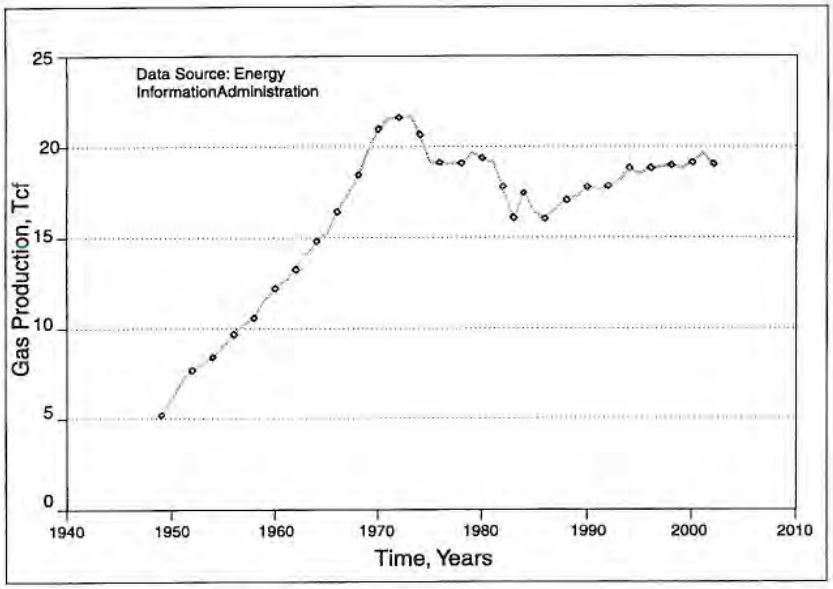

Fig. 1.5—U.S. natural gas production.

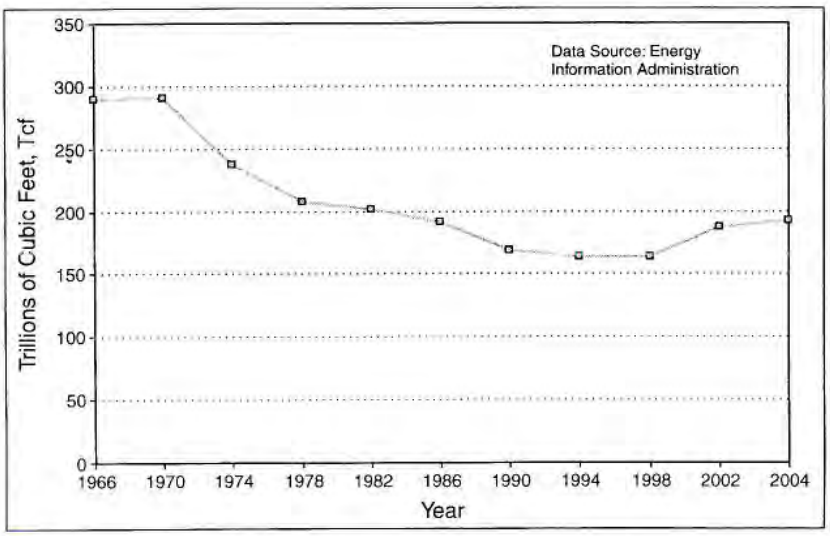

Fig. 1.6—U.S. natural gas reserves.

The 2000 U.S. conventional gas reserve was 177 Tcf. The 2000 CBM recoverable reserve was estimated to be 90 Tcf, out of a possible 750 Tcf of CBM in place, a relative magnitude that emphasizes the significance of the new source of domestic natural gas.[6]

Natural gas prices have responded to disruptions of crude oil supply, changing tax laws, governmental regulation of the industry, and supply/demand in a manner illustrated in Fig. 1.7. The low cost of gas after World War II reflects the general abundance of energy relative to the country's needs. The Arab embargo of crude oil initiated a steep, 8-year rise in prices that lost some markets. Subsequent price decreases in the late 1980s regained market but created a cautious response because of an impression of less predictable future prices. However, within the price range (given as dollars per 1,000 cubic feet [Mcf] of gas) shown in Fig. 1.7, natural gas will remain economically competitive with other energy sources.

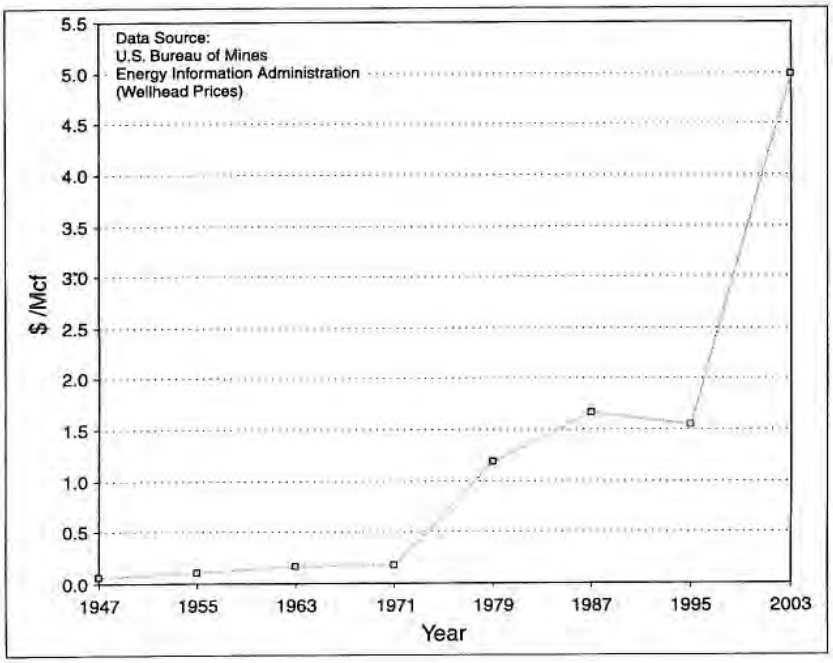

Fig. 1.7—Natural gas prices.

1.4 The Coal Resource

Coal, the largest energy natural resource in the country, has been widely mined in the United States since the 18th Century. Coal is an extensive resource in the United States; 300 billion tons that are recoverable (less than 4,000 ft deep) underlie 380,000 sq miles in 36 states.[1,7] This represents one-fourth of the world's total reserves. Americans have long relied on coal as a primary energy source, and still over 50% of the electricity generated in the United States comes from coal. Deeper coals beyond the range of mining have mostly been ignored; possibly, with further development of technology, the methane in their seams may be within reach and a partial benefit from the coal realized.

The coal in the contiguous 48 states is located in 14 major basins and coal regions, as listed in Table 1.1. Activity in methane recovery is necessarily centered in the 22 states touched by these basins. Where the basins had been most heavily mined, adequate data were available to launch the CBM industry. Lesser-mined areas with large coal reserves are now being considered for the process.

Outside the United States, at least 60 countries have appreciable coal reserves, and there are an estimated 13 trillion metric tons of coal in place in the world.[8] The figure is expanded to 25 trillion tons with the inclusion of low-rank coals.[9] Most of the coal is located in the 10 countries as given in Table 1.2. The finding costs of CBM are usually lower than for conventional natural gas, providing some incentive for development in these countries.[10]

Main constraints to producing the methane are usually lack of geologic characterization of the coals, lack of engineering and operating experience in producing the CBM, and lack of investment capital. Markets may not exist, or the coal may be far removed from markets in that country. Therefore, a tandem requirement may be to develop both the market and the resource. On-site use of the gas for electrical power generation or heating is common.[10] Governmental assistance, such as the U.S. tax credit, may be necessary to self-start the industry in many countries.

Table 1.1—Major U.S. Coal Basins[11]

Basin	Location
San Juan	Colorado, New Mexico
Black Warrior	Alabama, Mississippi
Raton Mesa	New Mexico, Colorado
Piceance	Colorado
Greater Green River	Wyoming, Colorado
Powder River	Montana, Wyoming
Northern Appalachian	West Virginia, Pennsylvania, Ohio, Kentucky, Maryland
Central Appalachian	West Virginia, Virginia, Kentucky, Tennessee
Western Washington (Pacific Coal Region)	Washington, Oregon
Wind River	Wyoming
Illinois	Illinois, Indiana, Kentucky
Arkoma	Oklahoma, Arkansas
Uinta	Utah, Colorado
Cherokee	Kansas, Oklahoma, Missouri

The environmental aspect of CBM emissions into the atmosphere from mines is an international problem, as can be surmised from the diversity of coal locations in the world. Emissions from coal mines are estimated to account for as much as 10% of methane emissions from all sources worldwide. Further, 70% of the mine emissions may come from the first three countries of Table 1.2: Russia, China, and the United States, plus Poland.[10]

It is estimated that 90% of all coals in the United States cannot be mined under the standards set for their extraction.[11] Since it is in the national interest to use the large coal resource for the benefit of society, CBM is a partial solution

because it has the following attributes: (1) production of the methane reduces further mining hazards; (2) coalbeds too deep to mine economically may eventually be used to extract the methane as technology advances; (3) methane is the cleanest-burning fossil fuel; (4) drilling for the methane is a benign operation with extremely low risk of blowout or spill because air is often used instead of drilling muds; and (5) methane emissions to the atmosphere from mines are reduced.

Table 1.2—Worldwide Coal In Place[8-10]

Country	Billion Tons
Russia	4,860
China	4,000
U.S.	2,570
Australia	600
Canada	323
Germany	247
United Kingdom	190
Poland	139
India	81
South Africa	72
Others	229

1.5 The CBM Resource

Methane has been traditionally extracted from coals to reduce mining hazards, but the gas was vented to the atmosphere with large fans in the mines. Some methane was tapped from coal by vertical wells earlier in the last century and the gas was used locally. For example, CBM was produced commercially from the Mulky coalseam in southeastern Kansas from 1920 into the Great Depression.

The output from vertical wells drilled to approximately 1,000 ft was termed shaly gas without producers realizing it came from the Mulky coalseam.[12] Records suggest use of methane from artesian wells of clean formation waters flowing from coalbeds in the Powder River basin of Montana to heat ranch buildings[13] and the pressure of the coal gas contributing to artesian flow of waters in northern Wyoming.[14]

Low explosive limits of methane in the air have made it necessary to vent great volumes of the gas from gassy coals of mines before working in the mines. It is estimated that a volume of 250 million cubic feet per day (MMcf/D) of methane was vented from U.S. coal mines directly into the atmosphere in the early 1980s. This increased to 300 MMcf/D in 1990.[15] Venting has occurred in U.S. coal mines since the 19th Century.[16] The necessity of sweeping out the methane with large amounts of air is apparent upon considering that explosive limits of methane in air are 5–15%, by volume. In Alabama, multiple fans requiring as much as 14,000 hp have the capacity to sweep from mines up to 20 MMcf/D of methane with 3,4 MMcf/min of air, venting directly to the atmosphere.[17] As mining extends deeper, more methane must be removed further, and the costs compound. According to the EPA's Coalbed Methane Outreach Program (CMOP), emissions decreased by 30% from 1990 to 2001 because of (1) the increased consumption of CH_4 collected by mine degasification systems and (2) a shift toward surface mining.

The venting procedure as a contributor to the greenhouse effect has received mounting environmental concerns. It is estimated that methane from all sources, not just coal, contributed 9% of the detrimental effects of global warming during the year 2001, although the methane has a much shorter longevity than carbon dioxide.[18,19] About 10% of the methane going into the atmosphere can be attributed to coal mines.[15]

Development of the commercial CBM process is a positive step for the environment worldwide. However, environmental effects of vented methane were not the driving force for developing the CBM process. Rather, the initial

incentive was to improve mine safety. As the process was improved, it became apparent that a substantial commercial value existed either in pipeline sales or in supplying on-site energy needs. This realization provided the final incentive for widespread development in mines as well as in vertical boreholes not associated with mines. Table 1.3 summarizes significant events in the commercial development of CBM.

Rightmire *et al.* estimated that 400–850 Tcf of CBM in-place gas exists in major coal basins of the continental United States.[7] The estimate does not include coals deeper than 4,000 ft. It has been reported[6] that 750 Tcf of CBM in-place gas exist in the major coal basins of the continental United States, which agrees with the range provided by Rightmire *et al.*[7] It is estimated that the five foremost basins in the United States have 259 Tcf of CBM in place.[6,16] The CBM recoverable reserves have increased the current U.S. natural gas reserves by almost 50%.

An indication of the early vitality of the industry is the growth evident from data of the Alabama Oil and Gas Board for the number of CBM well permits to drill in the Black Warrior basin after the first commercial project at Pleasant Grove, Alabama in 1980 (Fig. 1.8).

Table 1.3—Highlights of Coalbed Methane Development	
1920–1933	Wells drilled into S.E. Kansas coalbeds inadvertently and methane produced.
1928	Rice suggested vertical wells to drain CH_4 from coalseams before mining.[20]
1931	Coalbed CH_4 found upon abandoning conventional gas well in West Virginia. Produced 212 MMcf until 1968.
1954	First coalbed methane well fractured by Halliburton experimental project with USBM.
1973	USBM funded project to improve degasification preceding mining. Studied fracturing in PA, VA, WV, OH, and IL mines.
1978	DOE, Gas Research Institute (GRI) undertook joint project in Warrior basin of Alabama; studied response of coalseams to fracturing. Evaluated CH_4 commercial possibilities.
1980	Federal tax credit established for coalbed methane.
1983	Gas Research Institute and U.S. Steel began Rock Creek Research Project.
1985	Regional coalbed methane information centers established by GRI near Warrior and San Juan basins.
1992	1.5 Bcf/D production of coalbed methane from 5,500 wells.
1994	U.S. EPA's Coalbed Methane Outreach Program (CMOP) initiated.
1995	The first GRI Regional Coalbed Methane Center to open in Tuscaloosa, AL was closed.
2000	3.7 Bcf/D production of coalbed methane from 13,986 wells.
2003	The Regional Information Center in Denver (the final one in operation) established by GRI closed.

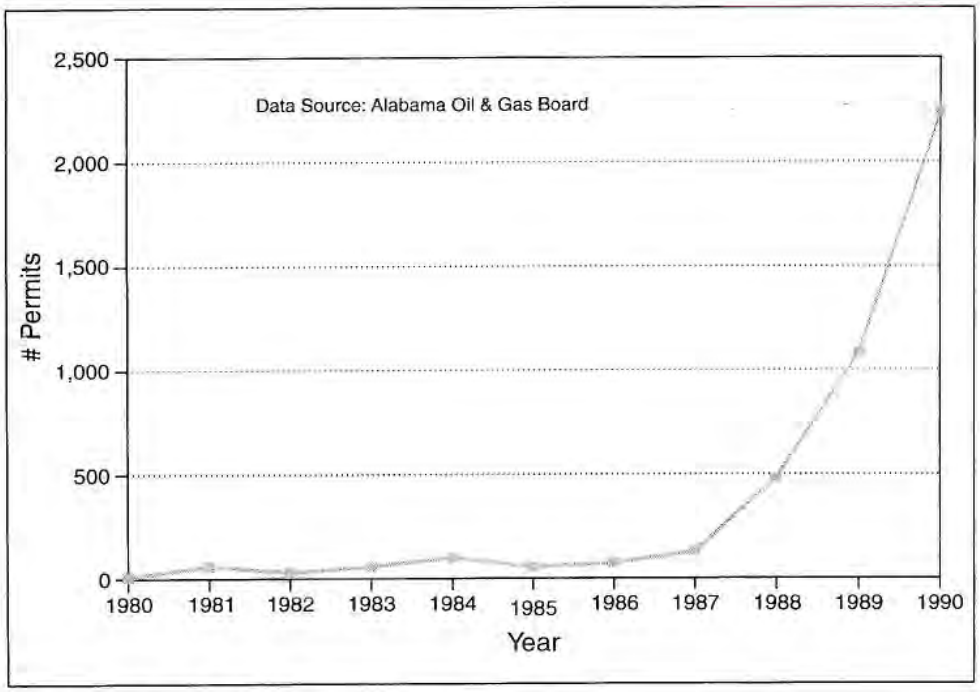

Fig. 1.8—Growth of CBM well permits.

Improvements in the process helped the growth, but the federal tax credit provided the main incentive. Before the tax credit was scheduled to expire, drilling accelerated. After the period indicated on the graph in 1991 and 1992, permits dropped back to 183 and 152, respectively. The data reflect the incentives provided by the Section 29 tax credit.

1.6 Overview: CBM vs. Conventional Reservoir

An overview of CBM principles is presented to put the process in perspective, and a comparison is made with the production of natural gas from conventional reservoirs as a means to understand readily its operating requirements.

Drilling and production techniques of the oil and gas industry were employed initially to extract methane from coal. However, significant differences in the coalbed reservoir properties, gas storage mechanisms, the gas-transport phenomenon, resource decline, and water disposal have required innovations and changes to the conventional procedures.

Emerging is a process unique to CBM production. Research behind these innovations has added knowledge often applicable to conventional oil and gas operations, as illustrated by two examples. First, for the first time, minethroughs provide visual study of fractures from hydraulic fracturing. Second, the effects of in-situ stresses and extreme rock properties on the coal reservoir performance are so important that their study has added significantly to the pool of oilfield knowledge.

1.6.1 Gas Composition

Gas produced from coalbeds may be initially higher in methane than the gas produced from conventional reservoirs. Ethane and heavier, saturated hydrocarbons are more strongly adsorbed than methane; consequently, they may not be as readily desorbed at first. Analyses of gases produced from the Oak Grove coalfield of the Warrior basin and from the D seam of the Piceance basin are given in Table 1.4.[21,22] Note that the Warrior gas is high in methane and low in ethane but that the nitrogen content is 3.40%. Nitrogen is less strongly adsorbed than methane.

Table 1.4 shows that the coals of the Piceance basin have a relatively high 6.38% carbon dioxide, as do the sister Uinta basin[23] and other western coals. Relatively

high CO_2 contents in the Fruitland coals[24] of the northwestern part of the San Juan basin have been postulated to come from biogenic sources of fairly young age as a result of bacteria entering with meteoric waters.

Table 1.4—Composition of Coalbed Gas[21,22]

Component	Composition Mary Lee Seam Warrior Basin (Mole %)	Composition D Coalseam Piceance Basin (Mole %)
Methane	96.2	90.25
Ethane	0.01	2.66
Carbon Dioxide	0.1	6.38
Nitrogen	3.4	—
Hydrogen	0.01	—
Helium	0.26	—
C_{3+}	0.71	0.71
BTU/scf	978	—

The gas produced in the two Appalachian basins have compositions similar to that of the Warrior.[22] Therefore, surface facilities to remove contaminants are an exception rather than the rule. Coalbed gas is usually of high quality, suitable for direct input into natural gas pipelines.

1.6.2 Adsorption

The mechanism by which hydrocarbon gases are stored in the coal reservoir contrasts with the mechanism of gas storage in the conventional reservoir. Instead of occupying void spaces as a free gas between sand grains, the methane is held to the solid surface of the coal by adsorption in numerous micropores. The inordinately large surface area within the micropores and the close proximity of

methane molecules on the internal solid surfaces allow the surprisingly large volumes of gas to be stored in the coal. Some free gas exists in the natural fractures of the coal and some methane dissolves in the waters in the coal, but the bulk of the methane comes from the micropores. The adsorption mechanism creates the paradox of high gas storage in a reservoir rock of porosity less than 2.5%.

A clear illustration of the enormous surface area in the micropores of the coal is that 1 lb of coal has a surface area of 55 football fields, or 1 billion sq ft per ton of coal.[26] A good coalbed well in the San Juan or Warrior basin would hold two to three times more gas in a given reservoir volume than a sandstone reservoir of like depth having 25% porosity and 30% water saturation.[26]

Facilitated by the removal of water, the adsorbed gases are released upon reduction of pressure in the matrix of the coal.

1.6.3 Water Production

Another contrasting feature of CBM production is normally the prolific generation of formation waters from natural fractures in the coal. These waters must be removed before methane can be desorbed in the early production life of a well. The large volumes of water in the first year or two of production decrease thereafter to relatively small volumes for the remaining life of the well, which might be 20 years. In contrast, conventional gas reservoirs would have the connate water of the pore spaces held immobile, and water would not be expected to be produced in volume with the gas until encroachment of aquifer waters signaled an impending demise of gas production.

Initial costs can be high to dispose of large volumes of water early in the life of the CBM well, but the costs decline rapidly thereafter. For example, the water production rate in the Warrior basin has a dramatic drop-off of 70–90% after the first 1–2 months. The water production rate will thereafter decline slowly to

some low steady-state value.[27] The early cost of processing and disposing of large amounts of water, as well as the environmental concerns of the disposal, are important factors that must be dealt with in the CBM process.

Exceptions to the pattern of coalbed water production occur when wells are located near active coal mines that have already dewatered through years of mining. For example, water production is relatively low in some wells of the Central Appalachian basin, and wells in the Big Run field of the Northern Appalachian basin are reported to have no water production.[25] Another exception is the underpressured coalbeds in some western Cretaceous coals.

1.6.4 Gas Flow

Contrasting with conventional reservoirs is the mechanism of gas flow through the formation to the wellbore. For coals, an additional mechanism of gas diffusion through the micropores of the coal matrix is involved, where the mass transport depends upon a methane concentration gradient across the micropores as the driving force. Upon encountering a fracture or a cleat, the gas will flow according to Darcy's law as in a conventional reservoir where the mass transport depends upon a pressure gradient.

1.6.5 Rock Physical Properties

Conventional oil and gas formations are inorganic. Organic formations contain CBM; these formations may contain about 10–30% inorganic ash. For example, the coals of Jefferson County, Alabama, in the Warrior basin, range in ash content from 3.3% to 13.8%.[21,28] Coals of optimum rank for methane are brittle and friable with low values of Young's modulus and high Poisson's ratio. The coal usually has low permeability and depends on natural fractures to act as gas and liquid conduits. Without hydraulic fracturing, these low-permeability coals are usually commercially nonproductive. The permeability is stress-dependent, so

low values of permeability develop rapidly with depth in the absence of unusual tectonic forces. Deep coals, or highly stressed coals, may exhibit a permeability of less than 0.1 md, such as in some areas of the Piceance basin.[29] Coals of permeability this low will not accommodate economical methane flow rates, even with hydraulic fracturing.

Whether the coals exhibit a low permeability or exhibit an extensive, unstressed network of fractures with high permeability is a critical parameter in any decision to invest in a CBM process.

1.6.6 Gas Content

Current state-of-the-art logging techniques cannot determine whether coals contain methane gas. The coal can be located by logs with the assurance that at some geologic time, gas saturated it, for it is a source rock as well as a reservoir rock. However, the gas may have been desorbed and lost either to the atmosphere or to an adjacent porous sandstone. Unfortunately, gas adsorbed on the coal cannot be detected on geophysical logs as in a conventional reservoir, and the gas amount must be determined by volumetric calculations based on coring data.

Gas content of coals may increase with depth as do conventional gas reservoirs, but in contrast, the content increases because of the positive influence of pressure on adsorptive capacity rather than the compressibility of the gas. However, gas content is dependent on more variables than depth. The amount of adsorbed gas also depends on ash content, rank of coal, burial history, chemical makeup of the coal, temperature, and gas lost over geologic time.

Some ranges for the gas content of the major basins include:

- Less than 74 scf/ton in the shallow coals of the Powder River basin.
- Approximately 600 scf/ton in the San Juan basin at 3,500 ft.[29]
- 680 Scf/ton in the Central Appalachian basin at 1,700 ft.
- From 115 to 492 scf/ton in the Vermejo coals of the Raton basin (>2,000 ft).
- From 23 to 193 scf/ton in the Raton coals of the Raton basin (<2,000 ft).[30]

1.6.7 Coal Rank

As mentioned in the previous section, gas content depends on the coal's rank, a measure of the quality and thermal maturity of the organic matter. Mechanical properties of the coal also depend on rank. Table 1.5 presents the ranks given to coals as specified in Standard D388-88 in the annual book of standards for the American Society for Testing and Materials (ASTM). Coal passes through four classes in its maturation: lignite, subbituminous, bituminous, and anthracite. Further subgrouping expands the listing to 13 groups. The ranks and abbreviations of ranks given in Table 1.5 are used throughout the text.

Table 1.5—ASTM Coal Rank[31]

Class	Group	Abbreviation
Anthracitic	Meta-Anthracite	ma
	Anthracite	an
	Semianthracite	sa
Bituminous	Low Volatile	lvb
	Medium Volatile	mvb
	High Volatile A	hvAb
	High Volatile B	hvBb
	High Volatile C	hvCb
Subbituminous	Subbituminous A	subA
	Subbituminous B	subB
	Subbituminous C	subC
Lignitic	Lignite A	ligA
	Lignite B	ligB

1.6.8 Gas Production

Comparison of the decline curves of gas production from conventional reservoirs to methane production from coalbeds reveals differences in their production patterns. Gas-decline coefficient and drainage areas were determined from coal well-decline behavior, and the results have been compared with reported and simulated declines in the Warrior, Powder River, and San Juan basins.[32] Computer simulations indicate that CBM may be produced for 20–30 years from reservoirs. Actually, wells in the Big Run coal field of West Virginia produced over 2 Bcf of CH_4 from 1932 until 1975. A single well in the field produced 200 MMcf in 30 years without the benefit of hydraulic fracturing.[25]

The extended producing life of a coalbed well, in contrast to a conventional gas well, may be conducive to long-term contracts desired by the electric utilities.

Coalbeds feature production rates of methane that initially increase and then slowly decline as gas production continues over a long period. This behavior is dictated by the pressure-lowering process of dewatering.

In summary, the CBM process has many similarities to the development of gas from conventional reservoirs. However, outstanding differences in the two reservoirs have a great impact on profitability and operations. As the process to produce CBM has grown in just a few years, it has taken on a character of its own. The innovations in drilling, completing, and producing methane are responsible in large part for the economic viability of the process. The comparisons will be dealt with in detail in the chapters that follow.

1.7 CH_4 Potential of Major U.S. Coal Basins

The potential of producing methane from coals in the United States has been evaluated for about the last 20 years. Although the estimate of recoverable and in-place gas in shallow coals is an approximation, it is anticipated that about 145 Tcf of methane are recoverable from the major coal basins of the contiguous 48

states, according to the 1990 Potential Gas Committee.[33] This estimate represented a rise of 60% over the previous 2 years. However, the recoverable CBM reserve was estimated to be 90 Tcf in the year 2000 out of a possible 750 Tcf of CBM gas in place. This recoverable reserve number could change with the recent success in the Piceance basin of Colorado and the Atlantic rim of the Washakie basin in Wyoming. It seems apparent that the reserve estimates will be low if technology improves to allow production of CH_4 from the deeper coals and to allow production from marginally economical wells. Although commercial CBM production has been confined to the United States and a few other countries, at least 4,000 Tcf of methane exists in coals of the 10 major coal-bearing countries listed in Table 1.2.[9] Here, the estimate has even more error.

Fig. 1.9 depicts the locations, relative sizes, and CBM potentials of the major U.S. coal basins.[34] The eastern coals in Appalachia and the coals along the Rocky Mountains contain most of the in-place gas. In general, the older coals of the east have attained a higher rank with less ash, and the coals of the west are contained in thicker seams. An extensive infrastructure of pipelines and oilfield services exists for the eastern coal region but not for the western coalfields.

Each of the basins has unique conditions determining the economics of methane production: depth of the coal, gas content, thickness of seams, permeability, access to pipelines, coal mining history in region, presence of logs from conventional gas wells, volume and quality of waters in the seams, and water-disposal limitations. Therefore, important characteristics of each of the 14 basins will be summarized in the following sections of this chapter. Discontinuous seams, different nomenclature of investigators, and changes in seam designations across state boundaries often cause confusion in tabulations of a basin's contents. It is probable that any coal basin around the world having prospective commercial CBM would be similar to one of these examples.

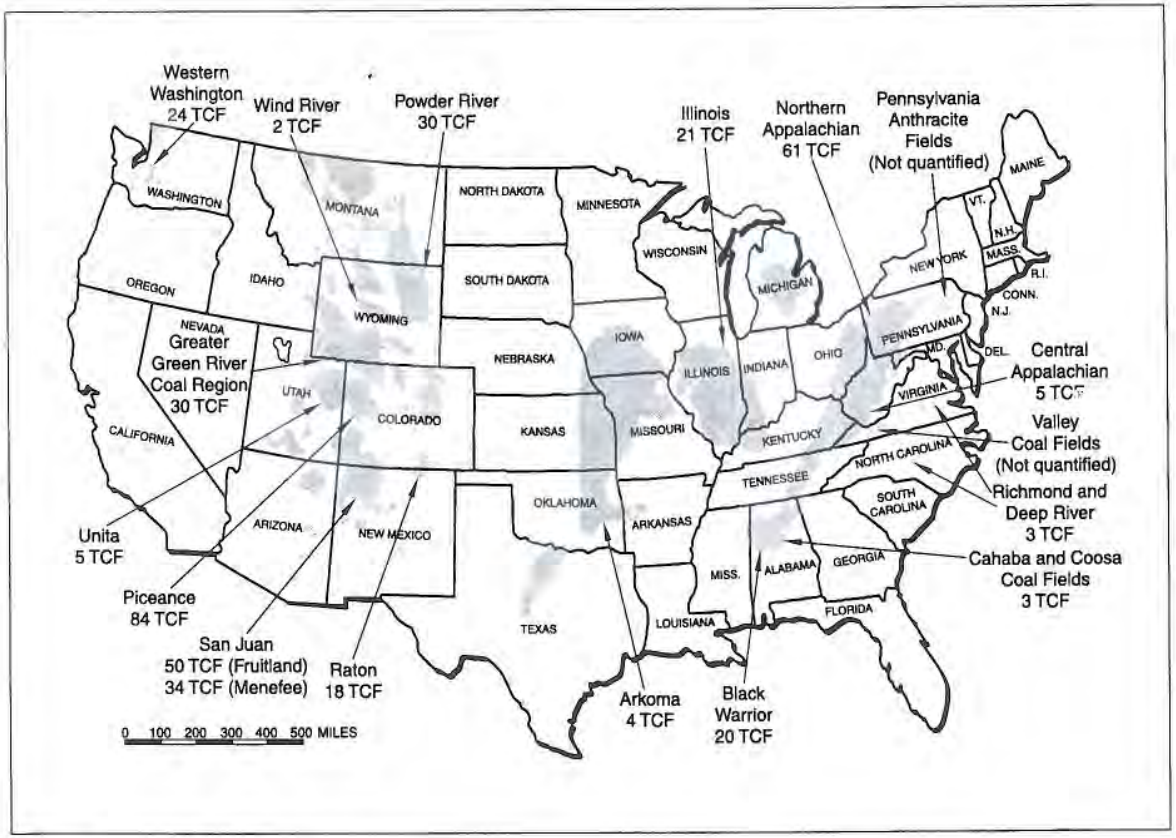

Fig. 1.9—Major U.S. coal basins.

1.7.1 San Juan Basin

The San Juan basin extends 100 miles wide and 140 miles long over southwestern Colorado and northwestern New Mexico, covering mountainous terrain of public property and tribal reservations. One of its most noteworthy features, however, is that it has the most profitable and prolific CBM production of any basin in the world along the border of the two states.[28,35]

Historical highlights of CBM development in the basin are as follows:[28,36-38]

- 1896—Conventional natural gas first produced commercially.
- 1953—Natural gas pipeline constructed to West Coast market.
- 1953—First CBM well completed in the New Mexico portion of the basin by Phillips Petroleum Co.
- 1977—First CBM well drilled by Amoco.
- 1991—2,032 wells producing; 270 Bcf CBM produced during 1991.
- 1992—359.2 Bcf methane produced from Fruitland in first 10 months.
- 2000—CBM well spacing reduced to 160 acres from 320 acres.
- 2003—810 Bcf methane produced from Fruitland coals during 2003.

The basin has experienced highly successful CBM production because of favorable coalseam thickness, permeability, gas content, depth, and coal rank in a large area. Development of the coals for methane was assisted by extensive drilling in previous decades into the gas-containing Pictured Cliffs sandstone below the coals, which resulted in an in-place infrastructure to handle the gas. Additional data came from mining in the basin near outcrops. The high flow rate of some of its wells makes it the leading producer in the United States and a model for exploration in the other countries.

Individual seams occur up to 40 ft thick, and net thicknesses of coal in a single well may reach 100 ft, although average net thicknesses of 30–50 ft are common.[35,39-41]

The basin is conveniently divided into three areas that have substantially different coal reservoir properties[42] (see Fig. 1.10). Area 1 of Fig. 1.10 represents

the heavily drilled area of high permeability, high rank, and overpressuring, so most of that area represents a fairway of prolific production. Production from the Cretaceous coals in the basin is assisted by a permeability of 1.5–50 md with an average of 5 md realized over the Fruitland formation and with 50 md occurring in highly fractured areas.[40,43,44]

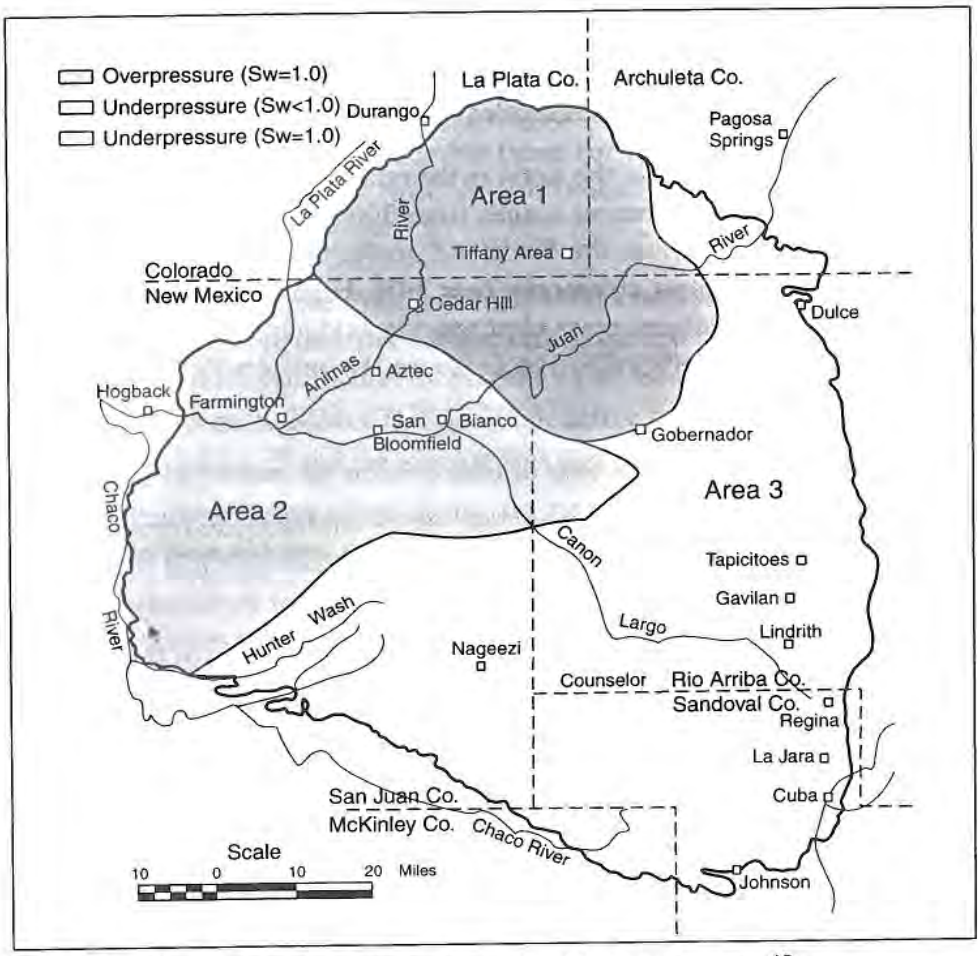

Fig. 1.10—San Juan basin's three zones for CBM producibility.[42]

The coals are ranked as high as low-volatile bituminous in the north to as low as subbituminous B in the south, their rank not necessarily dependent on present burial depth. The critical level of rank in the basin for the most successful wells, which are cavity completed, is hvAb. Even the next lower rank of hvBb encounters much less success. Large amounts of in-place gas, about 50 Tcf in the Fruitland formation, exist because of thick seams, high gas content, and large areal extent. The favorable permeability means extensive reserves of methane estimated for the basin.[39] The estimated gas in place for the Menefee coals in the San Juan basin is approximately equivalent to 34 Tcf.[6]

Favoring CBM production in the basin is the relatively high gas content of the coals in Area 1. The gas content ranges from 300–600 scf/ton. The inorganic matter is a high 10–30% in the Fruitland coals, and the ash content from proximate analysis is most commonly near 20%. High mineral matter content reduces methane content, increases cleat spacing, and may create an anomaly in gamma ray readings of well logs (affects the mineral's variability in radioactivity).

It is estimated that 350 billion tons of coal exist in the basin.[6] In the Fruitland coals, 50 Tcf of in-place methane are present at depths between 400–4,200 ft, and 11 Tcf of the methane has been recovered so far, with possibly another 20 Tcf that could be recovered.[29,35,38,45]

Although coal is found throughout the Cretaceous sediments of the basin, the Fruitland formation (100–600 ft thick) is the primary coal-bearing stratum and the main target. The Fruitland is extensive, containing 16 seams spread over 7,500 square miles of the basin.[45] It has 2–14 seams in the depth interval of 2,500 to 3,800 ft.[43] Logan[40] gives a typical example of the Fruitland: at a depth of 3,100 ft in a 170-ft interval, shale and sand lenses reduce the net coal thickness to a typical 54 ft in the interval. Individual seams are discontinuous, but the coal persists over most of the basin. Fassett found that single seams do not continue beyond 2–25 miles.[46] The thickest seams occur in the overpressured northern part of the basin (Area 1 of Fig. 1.10) and contain about 35 Bcf/sq mile of methane.[45]

Located below the Fruitland, the Pictured Cliffs sandstone, target for conventional gas reservoirs, formed the base of the Fruitland peat swamps as the Cretaceous Seaway regressed.[47] Historically, while drilling the 17,000 oil and gas wells in the basin, companies considered it a nuisance to drill through the coal. In these sandstone formations below the coal are located gas reserves second in size in the United States to the Hugoton field of Kansas.[46] Gas in the Pictured Cliffs originated in the coals of the Fruitland formation. In areas where the Pictured Cliffs sandstone intertongues with the Fruitland, the coal and sandstone sources of the produced gas may be indistinguishable. Here, decline curves of the sandstone may resemble those for coal, further indicating their inseparability. The coal has thin, discontinuous laminations of shale and sandstone mingled with it.[48]

In 1992, active wells in the Fruitland coals produced 359.2 Bcf of gas.[49] Wells have an average reserve of 3 Bcf and are drilled on 320-acre spacings. The most prolific well in the basin is that of Meridian Oil, which reached a production plateau in excess of 20 MMcf/D.[36] In 2003, active wells in the Fruitland coals produced 810 Bcf gas,[38] and the spacing was downsized to 160 acres.

Some problems encountered in the San Juan basin included: (1) altitudes of 5,000–7,000 ft, (2) water salinity necessitating disposal wells, (3) in a few reservoirs, desorbed methane contaminated with 4–6% carbon dioxide, (4) environmental concerns in a national forest, and (5) difficult access to remote locations. Initially, there was limited distribution infrastructure for distributing the gas produced. Yet despite these problems, profitability was high enough in Area 1 of Fig. 1.10 to sustain operations without the tax credit, and 60 companies were drilling and producing CBM in the basin at the beginning of 1991.

The coalseams of the Fruitland formation in the northwest are about 30% overpressured because of the outcrop of the permeable formation at a high elevation near Durango, Colorado, where meteoric waters overpressure the steeply dipping coals southward beneath terrain of lower elevation.[50] Moreover, the overpressuring is indicative of good permeability in the seams. In the

Northeast Blanco unit of the northwestern part of the basin, pressure gradient is 0.55 psi/ft,[40] as compared to the normal 0.43 psi/ft of the Pictured Cliffs sandstone beneath the Fruitland. The pressure gradient in the Tiffany area of the San Juan basin varies between 0.50 and 0.53 psi/ft.[44] This contrasts with an underpressured southern region.

A deeper formation, the Menefee, has an estimated[41] 38 Tcf of additional gas over an areal extent of 12,000 sq miles, but the Menefee has not yet been developed. It consists of thinner, less continuous beds intermingled with shale.[29]

Tables 1.6 and 1.7 summarize some significant facts of the San Juan basin. The low sulfur content of the coals of less than 1% indicates fresh water in the peat-forming swamps that developed inland from the Cretaceous Seaway.

Table 1.6—San Juan Basin Description[29,43-45]

Depth of Coal (ft)	Fruitland: Outcrop to 4,200 ft
	Menefee: Outcrop to 6,500 ft
Net Coal Thickness, Max. (ft)	110
Individual Coalseam Thickness (ft)	50 (Max.), 8 to 15 (Avg.), Fruitland 15 (Max.), 4 (Avg.), Menefee
Gas Content (scf/ton)	300 to 609
Gas In Place (Tcf)	88
Coal Rank	hvBb to lvb
Ash Content (%)	8 to 30
Sulfur Content (%)	<1.0
Moisture Content (%)	2 to 10
Permeability (md)	1.5 to 50

Table 1.7—San Juan Basin Producing Horizons[45,51]

Age Sediments	Formations	Depth (ft)	Rank	Bed/Net Thickness (ft)
Upper Cretaceous	Fruitland (16 Seams)	Surface to 4,200	subB to hvAb (South and West) to lvb (North)	50 to 80/ 110 to 140
	Menefee		hvCb to lvb	10/ 35 to 60
Lower Cretaceous	Dakota		hvCb to hvAb	9 to 13/ 27

1.7.2 Black Warrior Basin

The CBM industry began in the Black Warrior basin of Alabama, and from the basin has come much of the data for development of the process. Research from the Gas Research Institute's Rock Creek facility and field data from the many companies in the basin made the process viable there, especially for multiple, thin seams that are often marginally profitable. Coal mining in the Warrior for the previous 100 years provided a source of geologic and engineering data that gave impetus to early development. The propitious depths and existing mines allowed field studies and development at reduced economic risk.

Coal mines in the area have experienced safety problems throughout the history of mining there because coals of the Black Warrior are gassy. Deep mines may have 500–600 scf/ton of methane, and 51 mine explosions of methane have killed 974 people over the years. The first explosion occurred in 1911 and killed 128 miners.[52] To make the shafts safer to work, the methane is mixed with air and vented to the atmosphere via multiple fans of 2,000–3,500 hp each.[17]

Another method to rid coals in the Warrior basin of methane began in 1977 with a joint project between the DOE and U.S. Steel to drill a vertical wellbore ahead of a mining operation to demethanize the coal and use the gas on-site for electricity generation. Because the technique proved so successful, it was developed into a stand-alone commercial enterprise. Significant events related to development of the CBM industry in Alabama are

- 1886—First coal mining in Alabama's Warrior basin.
- 1911—First coal mine explosion, 128 killed.
- 1976—23 Well programs of USBM and U.S. Steel began at Oak Grove.
- 1977—Production began at Oak Grove.
- 1977—Test of vertical wellbore to vent.
- 1981—First permit to drill CBM well.
- 1983—Rock Creek research site established by GRI.
- 1985—Eastern Region Coalbed Methane Resource Center established by GRI at University of Alabama.
- 1990—Cumulatively, 4,308 wells permitted; 3,587 wells drilled.
- 1992—3,089 wells producing; 92 Bcf produced for the year; 290 Bcf cumulative production.
- 1992—End-of-year demise of the federal tax credit on new wells reduces drilling in basin.
- 1995—Eastern Region Coalbed Methane Resource Center closed.
- 2002—3,474 Wells producing; 116 Bcf produced for the year; 1.4 Tcf cumulative production.[53]

The industry grew rapidly in the Black Warrior basin as the decade of the 1980s progressed, creating a boom atmosphere locally in the midst of an oil and gas industry depression nationwide. The self-start of the industry, centered along a Tuscaloosa-to-Birmingham axis, was assisted by an infrastructure of service companies and accessible pipelines already in place to serve the conventional natural gas produced from the Black Warrior basin since 1953. About 4,308 wells had been permitted by the beginning of 1991, and drilling expenditures had exceeded $1.138 billion. Production reached 36.5 Bcf for 1990, a 56% increase over the previous year; 1,770 wells were producing in 1990, a 94% increase over the previous year.[54] Production reached 116 Bcf for the year 2002, a 21% increase from 1992 when the tax credit ended.[53] Because producing multiple thin

seams is often marginally economical, the termination of the federal tax credit on new wells at the end of 1992 seriously affected drilling in the Warrior basin.

The Black Warrior basin is not considered as profitable as the San Juan basin for the production of methane from coal, primarily because the multiple, thin seams are more difficult and costly to complete and are of limited production rate.

However, economic feasibility of CBM production in the Black Warrior basin depends on numerous factors. Although economics of producing methane from the coals of the Warrior are hurt by the cost of producing from multiple, thin zones, advancements in completion techniques and fracturing have made the process more profitable. Also, favorable state regulations for surface-water disposal have contributed to economic feasibility; water-disposal costs are generally less than in western basins. The Section 29 federal tax credit, as mentioned previously, was important in establishing marginal economic properties in the basin. Other positive factors include good permeability of the formations, high gas content of the coals, and data from previous coal and natural gas operations. Finally, proximity to gas pipelines and infrastructure in the basin helped make the coal gas commercially attractive.

Coalseams in the 18,000-sq mile Black Warrior basin, from which methane is commercially produced, range in depth from 500 ft in the Cobb seams to 4,500 ft in the Black Creek seams.[55] However, the most productive depths are at about 1,500 to 3,000 ft. Individual seam thicknesses run from 1 ft or less to 8 ft with multiple seams occurring over a 1,000-ft interval. Net thickness of coalseams in any well may reach a maximum of 20–30 ft.[29,56]

Normal faults occur in this foreland basin and trend northwestward, having displacements of perhaps several hundred feet.[29,57] The basin covers much of northern Alabama and northern Mississippi, bounded by the Appalachian tectonic belt on the east, the Oauchita front on the south, and the Nashville and Ozark domes on the north.[58]

Roughly one-half of the basin extends into Mississippi, but no mining or CBM production has occurred in Mississippi. Reports[59,60] confirm the presence of coalseams in the Mississippi portion of the basin, but the lack of data has discouraged development. In both the Mississippi and Alabama Warrior basins, much conventional natural gas production has been realized since about 1953.[61] The location of gas-bearing sands below the coal suggests the coal as a source rock throughout the basin.

The coal in Alabama occurs in the Pottsville formation of lower Pennsylvanian Age rock. Four main coal groups occur in the Pottsville formation: Cobb, Pratt, Mary Lee, and Black Creek. The coal groups outcrop in the northern part of the basin. Additionally, a later interest has been shown in the Gwin group above the Cobb and the J-Interval below Black Creek. Rank of the coals is medium- to high-volatile bituminous, the Black Creek group being of higher rank. The coals generally have low ash content, low sulfur content, and high methane content. Typically, profitable wells in the Warrior basin may produce an average peak rate of 150–400 Mcf/D. Methane content of the gas is a high 96%, and there are negligible amounts of carbon dioxide or nitrogen present. Therefore, heat content is near 978 BTU/Mcf.

A significant factor in establishing the process in the Warrior has been the ground-level treatment and disposal of produced waters. The lack of suitable formations to dispose of produced waters made the procedure necessary and cooperation with government, along with close environmental monitoring, made it successful. By the third quarter of 1990, 52.3 million barrels of water had been produced and disposed of at the surface since the inception of the process.[62] By the end of 1993, water production had reached a peak of 107 million bbl; this could be a result of the large number of wells drilled to meet the expiration of the tax credit deadline in 1992. A total of 59 million bbl of water was produced during 2002.[53] Part of the decline in water production could be attributed to declining water production from mature wells.

An estimated 20 Tcf of CBM exist in the Alabama portion of the Warrior basin. The figure includes neither the expectations of the Warrior basin in Mississippi nor the gas that might exist deeper than 4,200 ft.

Tables 1.8 and 1.9 summarize characteristics of the Black Warrior basin coalseams. These are similar to other Pennsylvanian Age coals in the eastern United States and are regarded as a benchmark for the coals of the other basins.

Typically, production is from net coalseam thickness ranges of 15–25 ft of Pratt, Mary Lee, and Black Creek groups.[63] The Mary Lee seams are the primary targets because of favorable depth-permeability relationships, gas content, and seam thickness. Although the Mary Lee seams produce the most methane, the deeper Black Creek seams contain the most in-place gas but at lower coal permeability.[64]

Table 1.8—Black Warrior Basin Description[29,56,65]

Depth of Coal, Max. (ft)	4,200
Net Coal Thickness, Max. (ft)	25
Individual Coalseam Thickness, Max. (ft)	8
Gas Content (scf/ton)	Mary Lee/Blue Creek Coal – 420 (excluding residual gas) Black Creek Coal – 430 to 520
Gas In Place (Tcf)	20
Coal Rank	hvAb to mvb

Table 1.9—Black Warrior Basin Producing Horizons[69]

Formation and Age Sediments	Coal Groups	Important Seams	CH_4 In Place Tcf	Depth	Rank
Pottsville	Cobb	Upper Cobb	1.3	448 to 1,656	hvAb
		Lower Cobb			
		Thomas			
Lower Pennsylvania	Pratt	Pratt	4.2	710 to 1,480	hvAb
		Nickel Plate		1,606 to 2,038	
		American		729 to 2,071	
		Curry		—	
		Gillespie		1,663 to 2,275	
	Mary Lee	New Castle	6.7	1,148 to 2,729	hvAb
		Mary Lee		520 to 2,810	
		Blue Creek		2,362 to 2,819	
		Jagger		—	
		Ream		1,264 to 3,044	
	Black Creek	Lick Creek	7.6	1,414 to 3,156	hvAb
		Jefferson		481 to 3,272	
		Black Creek		537 to 3,339	

1.7.3 Raton Basin

The smallest of the major coal basins is Raton Mesa, covering 2,200 sq miles astride the northeastern New Mexico border and the southeastern Colorado border. Bounded on the north by the Wet Mountains and bounded on the west by the Sangre de Cristo Mountains, heights of 9,000 ft are reached in the basin.

Late Cretaceous and Paleocene coals in the Raton basin are found in the Vermejo and Raton formations; the upper Raton formation intertongues with the Vermejo. Below the Vermejo is the Trinidad sandstone. The low-volatile bituminous coal exists in seams of 14-ft maximum thickness, averaging 3 to 8 ft in the Vermejo formation and 12-ft maximum thickness in the Raton formation; generally the seams are thin, but they may be numerous for a given well.[66] Although a few miles is the limit of their trace, as many as 40 seams exist in these formations, with a cumulative thickness of 90 ft from outcrop to a depth of 4,000 ft. Most seams are lenticular and discontinuous. Despite the small areal extent of the basin, CBM is estimated by DOE to be as high as 8–18 Tcf of in-place gas. Stevens[67] estimated 10.2 Tcf of methane in place in the basin. A brief description of the basin is given in Table 1.10.

Table 1.10—Raton Basin Description[29,56,68]

Depth of Coal, Max. (ft)	4,000
Net Coal Thickness, Max. (ft)	90
Individual Coalseam Thickness, Max. (ft)	Vermejo, 14 ft Raton, 12 ft
Gas Content (scf/ton)	250 to 569 (Max.)[a]
Gas In Place (Tcf)	8 to 18
Coal Rank	hvCb to lvb
Maximum Production Rates	300 Mcfd to 1 MMcfd
Permeability (md)	10 (Central)

[a] *510 scf/ton at 1,192 ft reported.*

The coals of the basin are found to be the source rock for conventional gas produced from the Trinidad sandstone below the Vermejo formation.[11] In regard to their proximity to the coal, charging of their sands from the coal, conventional

gas production and depositional history, the Trinidad sandstone is similar to the Pictured Cliffs sand below the Fruitland coals of the San Juan basin, although an overpressured region like the fairway of the San Juan basin is not present.[66] Note that coalbeds are discontinuous in the Raton basin, and the naming of them is inconsistent[68] (see Table 1.11).

Table 1.11—Raton Producing Horizons[51,68]

Age Sediments	Formations	Coal Groups	Depth (ft)	Rank
Cretaceous/ Paleocene	Raton	Discontinuous	390 to 2,600	hvCb to lvb
Late Cretaceous	Vermejo	Discontinuous	625 to 3,300	hvAb to an

Coal has been mined in the basin since the 1870s from 371 coal mines. Gassy coals are indicated. Tremain[68] reports that the coal of the Allen mine had a gas content of 514 scf/ton and that methane at the rate of 410 Mscf/D was vented from the mine during 1974–76, when nearly 2 million tons of coal was produced. Coal reserves of 17 billion tons are estimated for the basin.[56] The gas content of the coal can be characterized as a relatively high 250–569 scf/ton across the basin.

Moderate GBM activity began in the basin in the mid-1980s, and the spotty drilling program was not sufficient to define the production potential of the Raton basin. In 1989, Pennzoil began a test program with the drilling of 19 wells in the Vermejo formation shallower than 2,000 ft.[26] Amoco has drilled in the basin. Fifty wells drilled to depths of 1,200–2,000 ft have been shut in. One well was reported to produce 239 Mcf/D upon testing. Six Vermejo wells exhibited initial production of 0–160 Mcf/D and water rates from 41–574 barrels of water per day (BWPD). Water production ranges from 0–1,200 BWPD from the wells.[45] Sixteen wells were abandoned because of excessive water or low gas content. There are several operators currently active in the basin, and they produced 88 Bcf gas from 1,800 wells in 2003.[38]

Certain drawbacks to commercial CBM production in the Raton basin are still present, including:

- Inadequate pipeline infrastructure for markets outside the basin curtails development.
- Thin and discontinuous coalseams.
- Excessive produced waters. CBM water is replenished in certain parts of the basin.

1.7.4 Piceance Basin

The Piceance basin in western Colorado is an elliptically shaped basin divided by the Colorado River into one-third of the area south of the river. It contains coal of Late Cretaceous Age that underlies 6,570 sq miles.[70] It is one of three basins touching Colorado to give the state an estimated 100 Tcf of CBM in place. Seventeen companies were active in CBM development in the Piceance by 1991.

As a result of high gas content and thick seams in the Piceance basin, in-place gas has been estimated at 84 Tcf, but the actual value could range from 30–110 Tcf.[11] The coal is gassy with methane contents reported in the range of 438 to 569 scf/ton. Individual seams are 50 ft thick near Rifle, Colorado. Net thicknesses of seams in single wells are 120 ft in the south and 250 ft in the northeast part of the basin.[71] Important characteristics of the basin are given in Table 1.12.

Table 1.12—Piceance Basin Description[29,70,71]

Depth of Coal, Max. (ft)	Outcrop to 12,200
Net Coal Thickness, Max. (ft)	60 to 200
Individual Coalseam Thickness, Max. (ft)	50 (usually 20 to 30)
Gas Content (scf/ton)	438 to 569 (Max.)
Gas In Place (Tcf)	84
Coal Rank	hvCb (Northeast) sa (Southeast, Interior)

Three primary coal groups exist in the Mesaverde group: Black Diamond, Cameo, and Coal Ridge. The Black Diamond coal group is restricted mostly to the northern one-half of the basin, the Cameo group across the entire basin, and the Coal Ridge group about one-fourth of the basin.[70] The latter two groups of the Williams Fork formation in the southeast, where interbedded sandstone is also a target,[72] are the main target seams. The sequence of seams and their characteristics are presented in Table 1.13.

- **Black Diamond Coal group**—The coals in this group are mostly low-volatile bituminous, which exist as an outcrop to depths of 12,200 ft; maximum cumulative seam thickness is 30 ft. Estimated gas in place in the Black Diamond is 8.8 Tcf.
- **Cameo Coal group**—The Cameo coals of the Williams Fork formation extend across the 6,600 sq mi Piceance basin even reaching depths of 10,000 ft in the northeast part of the basin. The rank of semi-anthracite, denoting a localized thermal maturity, in the deeper part of the basin is a higher rank than observed in other areas of the basin. A total seam thickness of up to 60 ft exists in the basin and the estimated gas-in-place for the Cameo coals of the Williams Fork formation is 65.2 Tcf. The Cameo coal group contains the most extensive individual coalseams of the Mesaverde group. The coal group can locally be divided into eight seams, which in ascending order are A, B, C, D, E, F, K, and L coalseams. The lowermost "A" and middle "D" seams are the thickest and most extensive coalseams in the basin.[73] Separating the "A" coalseam from the additional Cameo group coalseams are interbeds of sandstone, siltstone, and shale. In the Parachute field of Garfield County, wells in the Cameo coals at 5,000–6,000 ft depth average 430 Mcf/D and produce less than 10 BWPD; some of the gas-producing wells produce no water.[54]
- **Coal Ridge group**—This group exists south of the Colorado River and has an areal extent of 1,600 sq miles. Rank is hvBb to lvb. The Coal Ridge group is the uppermost of the three major target coal groups and usually occurs about 200 ft above the Cameo coal group.[75] The Coal Ridge group reaches a maximum depth of 8,000 ft and attains net seam thickness of 40–50 ft. Estimated gas in place is 9.9 Tcf.

Table 1.13—Piceance Basin Producing Horizons[24,70,71,75]

Age Sediments	Formations	Coal Groups	Important Seams	Depth (ft)	Rank
Cretaceous	Mesaverde-Williams Fork	Coal Ridge	2 to 5 Seams	5,335 to 8,000	lvb to hvBb
		Cameo	A to D	2,000 to 11,000	sa to hvBb
			E,F,K,L	Discontinuous	sa to hvBb
Late Cretaceous	Mesaverde-Iles	Black Diamond		0 to 12,200	sa to lvb to hvCb

The Gas Research Institute, recognizing the abundance of the resource deeper than 3,000 ft, but with a lack of data to characterize coal at those depths,[74] established a project near Rifle, Colorado to develop technology for producing deep CBM.[54]

Initial production rates of methane from wells in the basin are reported to range from 14 Mcf/D to 1.5 MMcf/D accompanying 0–2,500 BWPD.[71] The following three examples are from the Piceance basin: (1) Wells into Cameo coals at 6,500–7,500 ft averaged 656 Mcf/D and 26 BWPD; (2) a well drilled to 6,502–6,725 ft in the Cameo coal had initial production of 776 Mcf/D and no water;[56] (3) Barrett Resources drilled 12 wells of 5,000–7,000 ft into Cameo coals or Mesaverde sandstone. They reported 370–900 Mcf/D and 20 BWPD. Many Cameo coals are dual-sandstone producers.[75] In the first quarter of 2002, Tom Brown, Inc. (currently Encana) reported production of 33 MMcf/D out of their White River Dome field (including production from the Mesaverde sands). In 2003, the cumulative production from all the coals in the Piceance basin was 1.98 Bcf from 163 wells.[38] This number will only move up with the increased activity by Encana and other operators.

Although thick seams and good gas content are characteristics of the basin, the coal is deep. Permeabilities that fall below 1 md in the northeastern part of the basin do not provide the natural fracture network for commercial flow rates of gas.[76] In the southeast part of the basin, the permeabilities improve because of structural deformations that have left the rock fractured. In the southeast, the overpressured nature of the coal improves gas content.[29] Overall, however, the depth of the basin gives a low permeability, which is its greatest impediment to development.

1.7.5 Greater Green River Coal Region

The Greater Green River Coal region has an areal extent of 21,000 sq miles, which makes it one of the larger coal regions with methane potential.[29] The basin extends from southwestern Wyoming into northwestern Colorado and is bounded on the north, west, south, and east by the Wind River Mountains, Overthrust belt, Uinta Mountains uplift, and Rock Springs uplift, respectively.

Five component basins within the region offer individual potential for CBM production: (1) Sand Wash basin of northwestern Colorado and southern Wyoming; (2) Great Divide basin of Wyoming; (3) Hanna basin of Wyoming; (4) Green River basin proper; and (5) Washakie basin in Wyoming.

Of these five component basins, the Sand Wash basin has had more coal mined than any other basin in Colorado—7 million tons in 1989. Surface and underground mining of the subbituminous to high-volatile bituminous coal occurs in the Yampa field of the southern part of the Sand Wash basin. Major coalbeds of the Sand Wash basin are in the Fort Union formation (Paleocene) and the Williams Fork and Iles formations of the Mesaverde group (Upper Cretaceous). The older and deeper Mesaverde has coals of higher rank, where individual seam thicknesses of 30 ft and net thicknesses of 18–136 ft occur. The Williams Fork has more continuous and thicker coals than the Iles of the

Mesaverde group.[77] In comparison, the Fort Union formation in the north has seams that reach 114-ft net thickness with 50-ft single seams.[71]

Depths of the seams in the Sand Wash basin are 2,000–7,000 ft. Meteoric waters enter on the eastern boundary where the Mesaverde outcrops in the mountains. Consequently, high water production rates are encountered from wells drilled into the coals on the eastern margin.[77] A few pilot projects were initiated by operators active in the Sand Wash basin toward the end of the last decade and into the early part of the present decade. It was found that several factors stood in the way of commercial CBM development in the basin:

- Mostly unsaturated coals.
- High water production with aquifer sands lying between the coals.
- Thin coalseams.
- Low to very low permeability.
- Normal to underpressured coalseams.

A summary of some important characteristics of the Greater Green River Coal region is given in Table 1.14. A synopsis of the coal-bearing formations of the basins is presented in Table 1.15.

Table 1.14—Greater Green River Coal Region Description[29,35,62,78]

Depth of Coal, Max. (ft)	7,837
Net Coal Thickness, Max. (ft)	95
Individual Coalseam Thickness, Max. (ft)	20 to 50
Gas Content (scf/ton)	544 at 3,500 ft, 500 (Mesaverde)
Gas In Place (Tcf)	9 to 31
Coal Rank	subC, hvCb to hvAb

Table 1.15—Greater Green River Producing Horizons[68,79]

Basin	Age Sediments	Formation	Depth (ft)	Rank
Hanna	Paleocene/Eocene	Ferris/Hanna	1,574 to 4,500	subB to hvCb
Sand Wash	Paleocene	Almond	725 to 3,000	
		Wasatch		
		Fort Union	1,831 to 5,800	subC to subB
		Lance	2,887 to 3,106	subC to subB
	Upper Cretaceous	Williams Fork	1,500 to 5,000	subB to hvAb
		Iles	1,453 to 6,833	an to sa to hvCb
Great Divide	Cretaceous	Rock Springs	2,000 to 4,540	hvCb to subC
		Almond	3,806 to 3,822	
		Lance	2,587 to 3,106	
		Blair	3,460 to 6,000	
Washakie		Wasatch	3,000 to 3,300	
		Almond	5,800 to 7,000	
Green River		Mesaverde	3,393 to 4,500	
		Rock Springs	5,500	
Overthrust		Bear River		
		Frontier		hvBb
		Adaville	5,300	sub
		Evanston		

Coal has been mined from the Frontier formation of the Overthrust belt in Wyoming since about 1900.[79]

CBM drilling began in 1989 in the region. Wells drilled near Rock Springs, Wyoming show that coals above about 2,700 ft have been naturally desorbed. However, as the coal depths approach 4,000 ft, gas content exceeds 500 scf/ton, and water salinity increases. Mud logs from conventional wells show the presence of gas.[35]

Activity in the Greater Green River Coal region in 1990[79] included coalbed wells drilled as deep as 7,837 ft in the Mesaverde group and as shallow as 1,453–1,473 ft in the Williams Fork formation. A 904-mile pipeline of 36-in. diameter and 1.2-Bcf/D capacity has been completed from the Green River basin to Bakersfield, California. A pilot study was completed by Barrett Resources (currently Williams) toward the end of the 1990s and early 2000 in the Hanna basin.

There has been no commercial CBM production in the Hanna basin. However, there is one successful CBM play in the Greater Green River basin. It is the Atlantic Rim CBM play, located on the shallow eastern margin of the Washakie basin, in Carbon County, Wyoming. The target coalseams are the Almond and Allen Ridge formations, belonging to the Upper Cretaceous Mesaverde group. The coals are of subbituminous A to high-volatile C bituminous rank. Merit Energy, Anadarko Petroleum, Double Eagle Petroleum, and Yates Petroleum Corporation are active in this area. Based on adsorption isotherms and measured gas content at initial reservoir pressure, both the Almond and the Allen Ridge coals are fully saturated or slightly undersaturated. The gas contents varied anywhere from 21–266 scf/ton for the Almond coals and 53–295 scf/ton for the Allen Ridge coals. These values are on as-received basis. Pore pressure gradients varied from 0.48–0.67 psi/ft, indicating that these coals are overpressured. Based on some measured data and also based on the high water production (up to 3,000 BWPD) the coals have high permeability in this play.[80]

At depths of 1,100 to 2,750 ft, the coal thickness ranges from 40 to 100 ft based on a bulk-density cutoff of 2.0 gm/cc. Water produced is disposed into the Deep Creek sandstone (3,000–4,000 ft deep) or the Nugget sandstone (9,600 ft deep) at

rates of 5,000 to 10,000 BWPD and the water quality within the coals ranges from 1,000–1,450 ppm total dissolved solids.

Approximately 10.8 MMcf/D of gas and 48,000 BWPD were being produced as of July 2004 out of the 34 wells in the three pods (Cow Creek, Sun Dog, and Blue Sky Pod) of the Atlantic Rim play area.[80]

1.7.6 Powder River Basin

Thick coals of subbituminous rank occur in the Powder River basin of northeastern Wyoming and southeastern Montana. It is an elongated basin of 25,800 sq miles, trending from the northwest to the southeast. The Black Hills and Big Horn Mountains bound it on the east and west.[14]

The profound characteristic of the basin is the extraordinary thicknesses of individual seams; most of this resource is at a depth of 2,500 ft or less. The record reported in the United States is a 220-ft thick seam near Buffalo, Wyoming in the Wasatch formation (Eocene). Net coalseam thicknesses in the basin reach 300 ft. Near Recluse, net thicknesses of seams average 150 ft.[83] Since the shallow coals are not thermally mature, gas content is only approximately 71 scf/ton at a depth of 1,200 ft.[29] Average gas content of the entire basin has been estimated at 25 scf/ton.[14] Despite the low gas contents, the thick subbituminous seams that comprise 1.3 trillion tons of coal[82] hold an estimated 30 Tcf of gas. Of this in-place gas, 16 Tcf may be recoverable[83] from shallow wells that can be drilled at low cost.

A summary of important properties of the Powder River basin is given in Table 1.16.

Table 1.16—Powder River Basin Description[29,83–85]

Depth of Coal, Max. (ft)	Outcrop to 2,500
Net Coal Thickness, Max. (ft)	170 to 300
Individual Coalseam Thickness, Max. (ft)	50 to 220
Gas Content, scf/ton	74 (Max.)
Gas in Place, Tcf	30 to 39
Coal Rank	lig to subB
Ash (%)	5.1
Sulfur (%)	0.34
Permeability	up to 1.5 Darcy

The coal-bearing formations are outlined in Table 1.17.[62] The Canyon coalbed of the Tongue River member of the Fort Union formation (Paleocene) is the thickest and most prevalent,[83] and the Tongue River may contain 8 to 10 seams, reaching 200 ft in net thickness.[82] The Wyodak-Anderson bed is locally up to 150-ft thick, averaging 50 to 100 ft. Note: Besides the Tongue River, the Fort Union formation has two other members with thin coalseams, the Tullock and Lebo.

Table 1.17—Powder River Basin Producing Horizons[14,51,82,84]

Age Sediments	Formations	Coal Groups	Important Seams	Depth (ft)	Rank
Eocene	Wasatch	Lake de Smet	Big George	500 to 2,500	sub
Paleocene	Fort Union	Tongue River	Wyodak	334 to 1,200	sub
			Anderson (Big George)	104 to 681	sub
			Canyon	302 to 681	lig to sub
			Cook	375 to 520	sub
			Wall	1,000	sub
			Cache		sub

Sandstone formations, charged with gas from the coal, are dispersed within the coalbeds. It is no surprise then that 20 conventional, shallow gas fields in the area have been discovered in sandstone-interlocked coals since 1916. Moreover, surface seepage of the gas has been reported in the area for many years, including artesian wells charged with methane.[35,84] The Ft. Union coals are freshwater aquifers. In 1988, 50 wells were drilled into the dry sands between coalbeds, but such production does not qualify for the tax credit. Fracturing was not performed to avoid tapping the aquifers of the coalbeds.[83]

Coal in the Powder River basin has been mined for many years because it has low ash and low sulfur content. Excessive water production in the central part of the basin at 1,000–2,000 ft has made the economics less attractive than the eastern part of the basin where relatively little water must be pumped from the coals at 250–1,500 ft.[62]

Much of the early CBM work in the basin has been in northeastern Wyoming in Campbell County.[54] The target coalseam is the Wyodak. Since the coal permeability was very high, these coals were not stimulated; instead, they were completed openhole by underreaming. Such openhole completions in the Fort Union formation (211–600 ft) of northeastern Wyoming[54,61,72] have had flows that ranged from 10 Mcf/D to 298 Mcf/D with negligible water production. Generally, the wells in the basin produce 25–500 Mcf/D. The increased activity in this basin over the last 10 years has made it the second-largest CBM producer in the United States after the San Juan basin. Cumulative gas production in 2003 for Powder River basin was about 344 Bcf from approximately 12,145 wells.[81]

In summary, factors favoring CBM production in the Powder River basin are:[83]

- Thick coalseams.
- Low drilling and completion costs.
- High permeability.
- Sands charged with CBM at less than 2,500 ft.

Unfavorable characteristics are low-rank coals, low methane content of coals, water disposal and problems with water rights.

1.7.7 Northern Appalachian Basin

The Northern Appalachian basin occupies 43,000–44,000 sq miles in West Virginia, Pennsylvania, Ohio, Kentucky, and Maryland[11] and contains an estimated 61 Tcf of CBM in place. Residing from outcrop to 2,000-ft deep, the Pennsylvanian Age coals in the basin are shallower than its counterparts to the south, the Central Appalachian and Black Warrior basins. The important seams in the Northern Appalachian basin lie above the Pottsville formation, which contains the seams of the Central Appalachian and Warrior basins.

Because the Black Warrior basin has been characterized and developed so extensively for CBM, the similarities of the Northern and Central Appalachian basins are often emphasized.

Compared to the Black Warrior basin, the Northern Appalachian basin has similar thin seams and cumulative coalseam thicknesses; individual seams of 1–3 ft are normal. Sediment age and structures are similarly of the Carboniferous stratigraphic period with a mean age of about 300 million years ago (m.y.a.). The rank increases to the east because of heat and pressure generated from tectonic activity near the Appalachian front. Because of the extensive mining in the area, the coals are underpressured and produce less water than the Black Warrior basin, although the chloride content and total solids content are higher in the Northern Appalachian basin. Because the coals are shallower, more underpressured, and generally lower rank than the Warrior coals, their gas content is lower at 150–200 scf/ton.[86] Some important characteristics of the basin are summarized in Table 1.18.

Table 1.18—Northern Appalachian Basin Description[11,25,29,86]

Depth of Coal, Max. (ft)	2,000 ft
Net Coal Thickness, Max. (ft)	28 ft
Individual Coalseam Thickness, Max. (ft)	12 ft
Gas Content (scf/ton)	106 to 201 440 (East)
Gas In Place (Tcf)	61
Coal Rank	hvAb, hvBb (West) hvAb (Interior) mvb to lvb to an (East)

The major seams and formations are summarized in Table 1.19. The Allegheny, Conemaugh, Monongahela, and Dunkard groups contain the most important coalseams of Clarion, Kittanning, Freeport, Pittsburgh, Sewickley, and Waynesburg.[72]

Table 1.19—Northern Appalachian Producing Horizons[25,51,54,72,86]

Age Sediments	Formations	Coal Groups	Depth (ft)	Rank
Pennsylvanian	Monongahela/ Dunkard	Waynesburg	152 to 1,600	hvAb
		Sewickey	377 to 960	hvAb
	Monongahela	Redstone	480	
		Pittsburgh	386 to 1,222	hvAb
	Conemaugh	Bakerstown	892 to 1,417	
		Mahoning	1,052 to 1,540	
		Freeport	1,689 to 1,693	hvAb
	Allegheny	Kittanning	1,191 to 1,800	
		Clarion	1,320 to 1,883	hvAb
	Pottsville	Mercer	1,538	
		Quakerston		

Important dissimilarities with the Warrior are the lower permeability and longer sorption times of the Northern Appalachian coals. The sorption time is longer than most basins; Hunt[25] estimates 100 to 900 days. Thus, longer time required to produce the gas leaves a higher residual gas content of the coals at the economic limit.

Because comparisons are so often made between the Northern Appalachian, Central Appalachian, and Warrior basins, their generalized stratigraphic columns are presented in Fig. 1.11.[87]

Historically, numerous CBM wells were drilled and produced in the Northern Appalachian basin from 1932 until 1980. These wells were unstimulated or inadequately stimulated, producing 12–150 Mcf/D of methane. With proper fracture stimulation and multiple-seam completions, suitable wells have the potential of 200 Mcf/D.[25]

The cumulative methane production from the Northern Appalachian basin in 2003 was 8.5 Bcf.[88] Legal questions on gas ownership and water disposal hampered the early development of the CBM production in the basin.

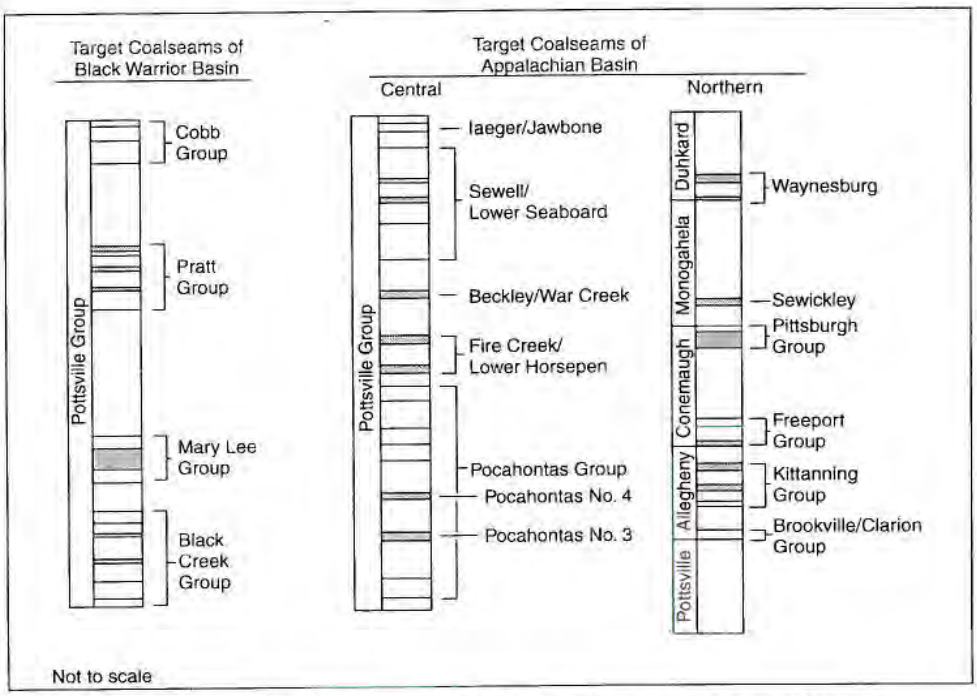

Fig. 1.11—Comparison of Northern and Central Appalachian and Warrior basins.[87]

1.7.8 Central Appalachian Basin

The narrow 23,000-sq mile Central Appalachian basin extends over portions of West Virginia, Virginia, Kentucky, and Tennessee in a northeast to southwest direction with the area of most promise and highest gas content near its center. The Central Appalachian Basin has an estimated 5 Tcf of methane in place.[25]

Again, the Central Appalachian basin has many similarities with the Northern Appalachian and Warrior basins. These similarities are commonly used to describe the basin. Coal is mined as deep as 2,500 ft in the Central basin, deeper than in the Northern Appalachian basin. Methane emissions from mines in the Central Appalachian basin have reached 7 MMscf/D.[56]

Mining in the basin has reduced the amount of water to be removed to achieve gas production (average of 5 to 10 BWPD).[89] Gas content and permeabilities are similar to the Warrior basin, but both properties are higher than the Northern Appalachian. The Pennsylvanian Age coal generally ranges from high-A to low-volatile bituminous, a higher rank than accorded its northern counterpart. Table 1.20 summarizes important characteristics of the central Appalachian basin.

Table 1.20—Central Appalachian Basin Description[25,29,72,86,87]

Maximum Depth of Coal (ft)	2,500
Individual Coalseam Thickness (ft)	5 to 10
Gas Content (scf/ton)	660 (Max.) Pocahontas #3, (Basin Center)
Gas In Place (Tcf)	5
Coal Rank	hvAb to lvb
Sorption Times (Days)	1 to 3
Methane Concentration (%)	95
Permeabilities (md)	5 to 27

Because of coal mining, the coal properties are well characterized. Hunt[25] states that coals near the center of the basin at 1,500–2,500 ft depth have a reported gas content as high as 660 scf/ton; 1,500- to 2,500-ft depths have 500–660 scf/ton coals. Permeabilities range from 2 md to 25 md. Target seams for the Central Appalachian basin are the Pocahontas No. 3, Pocahontas No. 4, Beckley, and Jawbone. Seams average 2–3 ft in thickness, although the range is from inches to 7 ft.[56] Table 1.21 presents the formations and major coal groups of the basin.

Table 1.21—Central Appalachian Producing Horizons[25,86]

Age Sediments	Formations	Coal Groups	Depth (ft)	Rank
Pennsylvanian	Pottsville	Iaeger/Jawbone	400 to 673	mvb
		Sewell	900	
		Beckley	558 to 1221	lvb
		Fire Creek	1,100	lvb
		Pocahontas 4	1,450	lvb
		Pocahontas 3	671 to 2,500	lvb

Note: Rank of most of the seams is high-volatile bituminous, but the Pocahontas No. 3 seam tested as high as 660 scf/ton.[25] Central Appalachian coals are generally only 80–90% saturated with water.

Faulting is not oriented in any particular direction. Although early wells were unstimulated or were inadequately stimulated, productions of 20 to 140 Mcf/D have been reported.[25] Average production of 85 wells brought onstream in 1992 was 100 Mcf/D with 4 BWPD; nitrogen foam and limited-entry completions were frequently used.[72] By the beginning of 1992, there were 101 wells operating in the Central Appalachian basin on 80-acre spacing and averaging 100 Mcf/D.[72] The cumulative CBM production from the Central Appalachian basin in 2003 was about 62.5 Bcf.[90]

In summary, production prospects are boosted by relatively high permeabilities, low water production, and high gas contents in the Central Appalachian basin.

1.7.9 Western Washington

Western Washington contains a series of small coal-bearing areas, trending north-south, stretching along the western foothills of the Cascade Mountains from the Canadian border on the north to the Oregon border on the south.[51] It has the potential of containing between 3.6 and 24 Tcf of methane in place.[11] The coal deposits are interbedded with shale, siltstones, arkoses, and conglomerates. They belong to the Eocene Age.[51]

The coals within the Carbonado formation range from 1 to 5 ft in thickness with a maximum thickness of 15 ft.[91] Only a small amount of data exists for the region. Development of the CBM process in the region is hampered by complex geology and lack of oilfield services infrastructure.[92]

A lucrative market for the gas and possibly good gas contents of the coals generate the interest. El Paso Energy and Duncan Energy were recently active in the basin. However, commercial production of CBM has not been realized in the region, despite these recent efforts and earlier drilling of approximately 25 exploratory wells. In Table 1.22 some characteristics of the region are listed.

Table 1.22—Western Washington Description[11,29,92]

Depth of Coal (ft)	Outcrop to 4,000
Net Coal Thickness, Max. (ft)	45
Individual Coalseam Thickness, Max. (ft)	1 to 15 (Max.); 2 to 5 (Avg.)
Gas Content (scf/ton)	50 to 425
Gas In Place (Tcf)	3.6 to 24
Coal Rank	subC to hvBb

1.7.10 Wind River Basin

The Wind River basin includes 8,100 sq miles in west-central Wyoming. Coal underlies much of it to the extent of a 125×45-mile swath. The deepest coals occur near the northern boundary of the basin. Coals at depths of less than 3,000 ft exhibit a rank of subbituminous A. Coalseams are known to exist to a depth of 14,000 ft, but the rank and potential of those below 3,000 ft are not well known.[11,29] Seam thickness is generally 1–10 ft, but thicker beds are found in a limited area of western Wyoming.

Where the Cretaceous strata outcrop, seven coalfields have been mined. They are Muddy Creek, Pilot Butte, Hudson, Beaver Creek, Big Sand Draw, Alkali Butte, and the Arminto field. Much of the data on the coals of the basin comes from these outcrops. Commercial coal mining began in the basin in 1870. Although 58 mines have operated in the basin, the coal production peaked in the 1920s. Because of the basin's remoteness and the existence of larger mines elsewhere in the state, coal is no longer produced in the basin.[93]

Extreme topographic features give elevations ranging from 4,400 to 13,000 ft. Only 6.5% of the basin is owned privately. Considerable reserves of oil and gas are present in the area. Coalseam discontinuity presents difficulty in correlating the seams throughout the basin. Tables 1.23 and 1.24 present some characteristics of the basin.

Table 1.23—Wind River Basin Description[11,29]

Depth of Coal (ft)	Outcrop to 14,000
Net Coal Thickness, Max. (ft)	100
Individual Coalseam Thickness (ft)	28 (Max.) 1 to 10 (Avg.)
Gas In Place (Tcf)	2
Coal Rank	lig to hvAb (Range) subC to subA (Common)

Table 1.24—Wind River Producing Horizons[51,93]

Age Sediments	Formations	Depth (ft)	Rank
Paleocene	Fort Union	6,500 to 10,600	subB
Upper Cretaceous	Lance	6,100 to 7,488	subA to C
	Meeteetse		subA to C
	Mesaverde	3,270 to 3,869	subA to C
	Frontier		subA to C

1.7.11 Illinois Basin

The Illinois basin is the largest of the coal basins, with an areal extent of 53,000 sq miles. It is strategically located near major cities, covering much of the state of Illinois, western Kentucky, and southwestern Indiana. Its coals are found in the Pennsylvanian Age rocks shallower than 3,000 ft, and its major seams occur shallower than 1,000 ft.[94] The U.S. Geological Survey estimates that 365 billion tons of coal are in the basin. Of the 75 different seams that have been identified, 20 have been mined. The surface and underground mines were operated around the shallow perimeter of the basin, and the coals in the vicinity of these abandoned mines have become a target for CBM.

Carbondale and Spoon formation coals have been found to have the potential for gas production in the Illinois basin. They vary in thickness from a few inches to over 15 ft. The gas content for the basin varies from a low of 5–6 scf/ton along the shallow areas of the basin, 80–150 scf/ton in the center part of the basin, to 230 scf/ton in the southern part of the basin where the higher-rank coals are present.[95] A general range of 150–225 scf/ton[95] is obtained from the adsorption data. The gas is mostly of biogenic nature and the coals are undersaturated. In the Illinois basin, the permeability of coals varies from less than 10 md in southern Illinois and western Kentucky and single digits to over 50 md in the central part of the basin.

An increasing number of CBM wells are being drilled in the Illinois basin, mostly into closed and abandoned mines.[94] Some characteristics of the coals of the basin are presented in Table 1.25. Based on GRI (now known as GTI) information, the current gas in place in the Illinois basin has been estimated at 21 Tcf, but based on new data available, the current in-place gas is considerably less but still significant.[95] In the Carbondale and Spoon formations, the expected gas-in-place reserves are estimated to be 1.5–5.0 Bcf of gas per section, assuming 15–30 ft of coal. This is dependent on the recovery factor, location, and depth of coals in the basin; further, the calculation does not account for the presence of 15–20% nitrogen. The factors favoring CBM production in the Illinois basin are:

- Multiple coalseams from 100–1,700 ft.
- Net coal thickness: 15–35 ft.
- Low water production.
- Strong local and regional gas markets.
- Minimum environmental opposition.

The negatives impacting the development of CBM in the Illinois basin are:

- Low gas contents.
- Poor permeability in many areas.
- High nitrogen content.
- Undersaturated coals.

Table 1.25—Illinois Basin Description[11,29,94,95,96]

Depth of Coal (ft)	Outcrop to 3,000
Target Formations	Carbondale and Spoon
Net Coal Thickness, Max. (ft)	16
Individual Coalseam Thickness (ft)	15 (Max.); 4 to 6 (Avg.)
Gas Content (scf/ton)	30 to 150
Gas In Place (Tcf)	5 to 21
Coal Rank	hvCb to hvAb (Range); hvBb (Common)
Moisture (%)	5 to 19
Ash (%)	1 to 25
Sulphur (%)	2 to 11
Volatile Matter (%)	28 to 41

1.7.12 Arkoma Basin

The Arkoma basin covers 13,488 sq miles along the border of central Arkansas and Oklahoma. The east-to-west trending basin is about 250 miles long and 20–50 miles wide. Important characteristics of the basin are given in Table 1.26. As with other coalfields west of the Mississippi River, initial mining began with the extension of the railroad into the territory between 1870 and 1888. The first commercial coal mining began in Oklahoma in 1872. Gas emissions from the mines indicate their gassy characteristics,[34] especially mines in the Hartshorne coals that have high gas content.[89]

The coal groups and formations in the Arkoma basin are presented in Table 1.27. Note the similarities with the Black Warrior basin.

Table 1.26—Arkoma Basin Description[11,29,89,97]

Depth of Coal, Max. (ft)	6,000
Net Coal Thickness, Max. (ft)	10
Individual Coalseam Thickness (ft)	9 (Max.) 2 to 5 (Avg.)
Gas Content (scf/ton)	73 to 211 (NW) 200 to 700 (Central)
Gas In Place (Tcf)	1.5 to 5.0
Coal Rank	hvBb to sa
Moisture (%)	1.0 to 7.0
Ash (%)	4 to 11
Sulphur (%)	0.5 to 5.0
Permeability (md)	4.5[a]

[a] *Permeability from Hartshorne coal.*

Table 1.27—Arkoma Basin Producing Horizons[11,97]

Age Sediments	Formations	Coal Groups	Depth (ft)	Rank
Pennsylvanian	Senora	Croweburg		hvBb to sa
	Boggy	Secor[b]		hvBb to sa
	Savanna[a]	Cavanal		hvBb to sa
	McAlester	McAlester[b] (Stigler)	1,905 to 3,218	hvBb
	Hartshorne	Upper Hartshorne[b] Lower Hartshorne[b]	192 to 6,000	hvBb to sa

[a] *Coals in Savanna formation in Arkansas known as Paris seam and Charleston seam.*

[b] *These three groups contain 93% of basin coal. Most extensive groups.*

The three most important coals in the Oklahoma part of the basin are the Hartshorne, Stigler, and Secor. It has been estimated that 10 individual seams that are 1–7 ft thick exist in the Oklahoma part of the basin. The best gas content is reported to be as high as 700 scf/ton at a 3,000-ft depth in Le Flore County.[11] The Hartshorne coalseam is the main target at 600–1,400 ft depth, 3–9 ft thick, and with good permeability of 3–30 md.[89] Coals in the basin are of Pennsylvanian Age.

Even before CBM wells had been drilled, extensive conventional gas production occurred from sands interbedded with coal. Historically, conventional natural gas has been produced since 1910–1915 from three fields in the Hartshorne sandstone, which may have been commingled with gas from the coals. Consequently, a widespread infrastructure for gas production exists in the Arkoma basin.

The prospects appear good for the growth of the CBM process in the basin. The first 18 commercial methane wells before 1993 produced 50–300 Mcf/D with typical water production rates of only 0.5 BWPD. As an indication of mounting interest, about 80 wells were drilled in 1993.[98] Thus, the coals are shallow, gassy, of optimum rank, 3–30 md permeability, and have low water rates. Further, a pipeline infrastructure already exists.[89] These factors provide a positive economic indicator. According to the Oklahoma Geological Survey, 749 vertical CBM wells drilled in the Oklahoma part of the Arkoma basin produced 44 Bcf of gas from 1989–2003. There were 249 horizontal wells drilled in the Oklahoma part of the Arkoma basin; they produced 28 Bcf from 1998–2003.[99]

1.7.13 Uinta Basin

The Uinta Basin of northeastern Utah and northwestern Colorado is a westward extension of the Piceance basin. The best-tested coalfield in the basin has been the Book Cliffs, where cores from test wells were analyzed to have a gas content of 443 scf/ton; 25 mines exist in eight coalbeds.[23] Because of available data on the coals near the mines, early CBM developments clustered in the vicinity of the

mines. One stimulated CBM well in the Book Cliffs field reportedly flowed 120 Mcf/D initially.[56] Average gas production of 121 Mcf/D with 318 BWPD is reported.[23] Adjacent sandstones charged with gas from the coals are also targets. Table 1.28 gives a summary of the basin's characteristics.

Table 1.28—Uinta Basin Description[11,23,29]

Depth of Coal (ft)	Outcrop to 7,000 Targets 2,000 to 4,500
Individual Coalseam Thickness, Max. (ft)	20 to 25
Gas Content (scf/ton)	352 to 443
Gas In Place (Tcf)	8 to 10
Coal Rank	hvBb to hvAb
Gas Composition	89% CH_4 1% C_2H_6 10% CO_2

As more data accumulated, estimates of gas in place were increased by the Utah Geological Survey[23] from early estimates of 1–5 Tcf to 8–10 Tcf. Upper Cretaceous, Mesaverde group coals are the main targets. The coals of the Blackhawk formation of the Mesaverde group are sketched and named in Fig. 1.12.[23] Production from five wells in coals of the Blackhawk formation of the Mesaverde group averaged 92 Mcf/D and 356 BWPD on 320-acre spacing. Initially, it was necessary to construct pipelines to remedy a marketing problem.[100]

The Ferron coals within the Ferron sandstone are the main targets in the Drunkard's Wash field. The Ferron coals range from 1,200–3,400 ft in depth with an average depth of 2,400 ft. These are high-volatile, B bituminous coals with a vitrinite reflectance value of 0.69%. The average ash and fixed carbon content of the Ferron coals are 14.6% and 48.6% respectively.[101] The CBM activity in the

basin picked up in the 1990s and the cumulative production for 2003 was approximately 83 Bcf out of 600 wells.[38]

1.7.14 Cherokee Basin

The Cherokee basin begins near the Oklahoma-Kansas-Missouri border and extends northward along the Kansas-Missouri border. To its south is the Arkoma basin and to the north is the Forest City basin, all part of the Western Interior Coal region.

The Weir-Pittsburgh (3–5 ft thick) is the most important coal at 220 scf/ton[89] gas content; the Mulky seam in the Cabaniss formation and the Rowe and Riverton seams in the Krebs formation are also important.[98]

Wells tend to produce an average 50 Mcf/D. Small amounts of oil of low gravity (degrees American Petroleum Institute) have been reported from the coals.[89] Generally, gas rates have reached as high as 250 Mcf/D, and based on the current activity levels in the basin, it appears that long-term commercial production of CBM has been established. In a manner similar to the Arkoma basin, low water production rates and high permeability encourage commercial development of the shallow seams (600–1,200 ft deep). Wells were first drilled to develop the coal resource in 1990, although conventional gas-containing-coal gas was produced commercially many years before targeting the coals.[12] CBM production from the northeastern Oklahoma part of the Cherokee basin reached approximately 11 Bcf per year and from the southeastern Kansas part of the basin reached approximately 10 Bcf per year in 2003.[102]

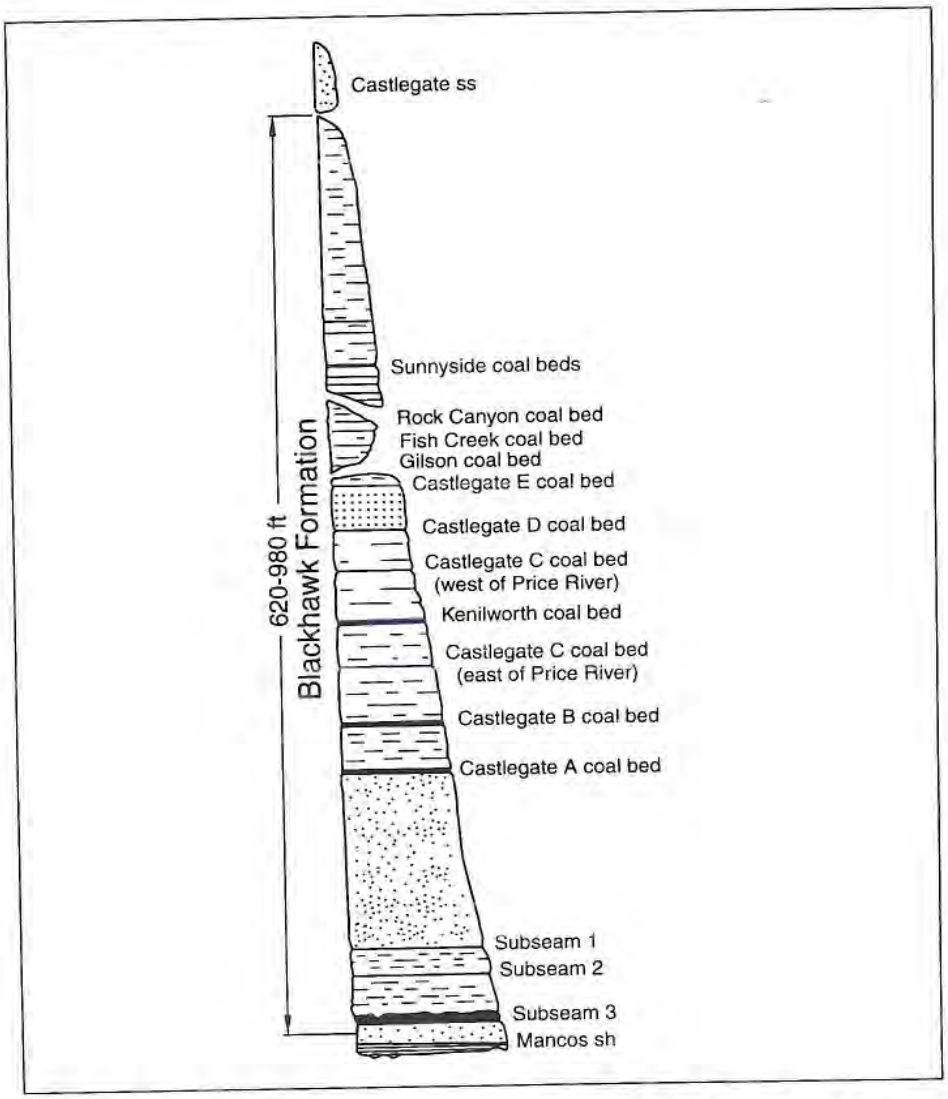

Fig. 1.12—Composite section of coals in Book Cliffs coalfield, Uinta basin, Utah.[23]

References

[1]"Annual Energy Outlook 2004 with Projections to 2025," *Market Trends–Oil and Natural Gas*, Energy Information Administration.

[2]Carson, M., Stram, B.N., and Roberts, M.A.: "Enron's 1993 Outlook for U.S. Gas Reflects New Technologies, Markets," *Oil & Gas J.* (May 1993) 91, No. 18, 97-100.

[3]"U.S. Industry Pushes Natural Gas Motor Fuel," *Oil & Gas J.* (March 18, 1991) 89, No. 11, 133.

[4]"Natural Gas Vehicles Issue Summary," American Gas Association.

[5]"IGU Details Environmental Quantities of Gas," *Oil & Gas J.* (July 1991) 89, No. 29, 31.

[6]US CBM recoverable reserve estimate was obtained from *Harts E&P*.

[7]Coalbed Methane Resources of the United States, Rightmire, C.T., Eddy, G.E., and Kirr, J.N. (eds.), *AAPG Studies in Geology*, Series #17 (1984).

[8]Boyer, C.M.: "Coalbed Methane: A New International Natural Gas Play?" paper presented at the 1992 Eastern Coalbed Methane Forum, Tuscaloosa, Alabama, 14 January.

[9]Kuuskraa, V.A., Boyer, C.M. II, and Kelafant, J.A.: "Hunt for Quality Basins Goes Abroad," *Oil & Gas J.* (October 1992) 90, No. 40, 49-54.

[10]Boyer, C.M. II, Kelafant, J.R., and Kruger, D.: "Diverse Projects Worldwide Include Mined, Unmined Coals," *Oil & Gas J.* (December 1992) 90, No. 50, 366-41.

[11]Byrer, C.W., Mroz, T.H., and Covatch, G.L.: "Coalbed Methane Production Potential in U.S. Basins," *JPT* (July 1987) 39, No. 7, 821-834.

[12]Stoeckinger, W.T.: "Kansas Coalbed Methane Comes on Stream," *Oil & Gas J.* (June 1990) 88, No. 23, 88-90.

[13]Campen, B.: "Exploring the Coalbeds of Montana," *Western Oil World* (July 1990) 24-27.

[14]Larsen, V.E.: "Preliminary Evaluation of Coalbed Methane Geology and Activity in the Recluse Area, Powder River Basin, Wyoming," *Quarterly Review of Methane from Coalseams Technology* (June 1989) 6, Nos. 3 and 4, 2-10.

[15]Carter, R.A.: "Underground Developments in Methane Recovery," *Coal* (December 1990) 55-59.

[16]McMurray, T.A.: "Tax Credit is Giving Life to Coal Gas," *American Oil & Gas Reporter* (January 1989) 21-27.

[17]Mills, R.A. and Stevenson, J.W.: "History of Methane Drainage at Jim Walter Resources, Inc.," *Proc., Coalbed Methane Symposium*, Tuscaloosa, Alabama (May 1991) 143.

[18]Kruger, D.W.: "Coalbed Methane, Environmental Protection at a Profit," *Proc., Coalbed Methane Symposium*, Tuscaloosa, Alabama (May 1991) 193.

[19]Inventory of U.S. Greenhouse Gas Emissions and Sinks: 1990-2001 - EPA 430-R-03-004, Final Version.

[20]Rice, G.S.: "Safety in Coal Mining," RI 277, USBM (1928).

[21]Hewitt, J.L.: "Geologic Overview, Coal, and Coalbed Methane Resources of the Warrior Basin-Alabama and Mississippi," in C.T. Rightmire, G.E. Eddy, and J.N. Kirr (eds.), *Coalbed Methane Resources of the United States: American Association of Petroleum Geologists Studies in Geology,* (1984) 17, 73-104.

[22]Unconventional Natural Gas, M. Satriana (ed.), Noyes Data Corp., Park Ridge, New Jersey (1980) 150.

[23]Gloyn, R.W. and Sommer, S.N.: "Exploration for Coalbed Methane Gains Momentum in Uinta Basin," *Oil & Gas J.* (May 1993) 91, No. 22, 73-76.

[24]Law, B.E., Nuccio, V.F., and Stanton, R.W.: "Evaluation of Source-Rock Characteristics, Thermal Maturation and Pressure History, of the Upper Cretaceous Cameo Coal Zone, Deep Seam Well, Piceance Basin, Colorado," *Proc., Coalbed Methane Symposium*, Tuscaloosa, Alabama (April 1989) 343.

[25]Hunt, A.M. and Steele, D.J.: "Coalbed Methane Development in the Northern and Central Appalachian Basins--Past, Present and Future," *Proc., Coalbed Methane Symposium*, Tuscaloosa, Alabama (May 1991) 127.

[26]Kuuskraa, V.A. and Brandenburg, C.F.: "Coalbed Methane Sparks a New Energy Industry," *Oil & Gas J.* (October 1989) 87, No. 41, 49.

[27]Burkett, W.C., McDaniel, R., and Hall, W.L.: "The Evaluation and Implementation of a Comprehensive Production Water Management Plan," *Proc., Coalbed Methane Symposium*, Tuscaloosa, Alabama (May 1991) 43.

[28]*GRID, Gas Research Institute Digest* (Summer 1989) 12. No.2.

[29]Ayers, W.B. and Kelso, B.S.: "Knowledge of Methane Potential for Coalbed Resources Grows, But Needs More Study," *Oil & Gas J.* (October 1989) 87, No. 43, 64.

[30]Tyler, R., Kaiser, W.R., Scott, A.R., Hamilton, D.S., and Ambrose, W.A.: "Geological and Hydrologic Assessment of Natural Gas from Coal: Greater Green River, Piceance, Powder River, and Raton Basins, Western United States:" Bureau of Economic Geology, Texas, Report of Investigations, 1995.

[31]ASTM D388-88, "Standard Classification of Coals by Rank," *Annual Book of ASTM Standards* (April, 1979), Part 26.

[32]Seidle, J.P.: "Coal Well Decline Behavior and Drainage Areas: Theory and Practice," paper SPE 75519 presented at the 2002 SPE Gas Technology Symposium, Calgary, Alberta, Canada, 30 April-2 May.

[33]"U.S. Natural Gas Resource Base Increases," *Oil & Gas J.* (August 5, 1991) 89, No. 31, 23.

[34]"The United States Coalbed Methane Resource," ICF Resources, Inc., *Quarterly Review of Methane from Coalseams Technology* (March 1990) 7, No. 3, 10-11.

[35]Wheatstrom, C.: Lecture to Coalbed Methane Forum, Tuscaloosa, Alabama (July 1991).

[36]"Telemetry and Process Instruments Control Coal Gas Production," *Oil & Gas J.* (November 1990) 88, No. 46, 98-103.

[37]McMurray, T.A.: "Tax Credit is Giving Life to Coal Gas," *The American Oil & Gas Reporter* (January 1989) 21-27.

[38]Production data from PetroData source.

[39]"Devon Pressing Fruitland Coalseam Program," *Oil & Gas J.* (November 5, 1990) 88, No. 45, 28-30.

[40]Logan, T.L., Clark, W.F., and McBane, R.A.: "Comparing Different Coalbed Methane Completion Techniques, Hydraulic Fracture and Openhole Cavity, at the Northeast Blanco Unit, San Juan Basin," *Proc., Coalbed Methane Symposium*, Tuscaloosa, Alabama (April 1989) 265.

[41]Wellborn, J. and Van Meter, J.R.: "Geological Overview: Evaluation of the Fruitland Coal and the Menefee and Point Lookout Tight Gas Sandstone Reservoirs," an Internal Report submitted to Halliburton Integrated Solutions and Markwest Resources by SCA Consultants, Denver.

[42]Paul, G.W. and Boyer, C.M. II: "Methane from Coal Deposits. Technical Evaluation and Data Base," *Quarterly Review of Methane from Coalseams Technology* (November 1991) 9, No. 1, 28-31.

[43]Ayers, W.B. and Zellers, S.D.: "Geologic Controls on Occurrence and Producibility of Coalbed Methane, Fruitland Formation, North-Central San Juan Basin, New Mexico," *Proc., Coalbed Methane Symposium*, Tuscaloosa, Alabama (April 1989) 75.

[44]Ramurthy, M., Young, G.B.C., Daves, S.B. and Witsell, F.: "Case History: Reservoir Analysis of the Fruitland Coals Results in Optimizing Coalbed Methane Completions in the Tiffany Area of the San Juan Basin," paper SPE 84426 presented at the 2003 SPE Annual Technical Conference and Exhibition, Denver, Colorado, 5-8 October.

[45]Ayers, W.B. Jr. et al.: "Geologic Evaluation of Critical Production Parameters for Coalbed Methane Resources," annual report, GRI-90/0014.1, Part 1, San Juan Basin (January 1990).

[46]Fassett, J.E.: "Geometry and Depositional Environments of Fruitland Formation Coalbeds, San Juan Basin, New Mexico and Colorado: Anatomy of a Giant Coal-Bed Methane Deposit," *Proc., Coalbed Methane Symposium*, Tuscaloosa, Alabama (November 1987) 19.

[47]Kelso, B.S. et al.: "GRI Geologic and Economic Appraisal of Coalbed Methane in the San Juan Basin," *Proc., Coalbed Methane Symposium*, Tuscaloosa, Alabama (November 1987) 119.

[48]"Fracturing Key Element in Fruitland Methane Activity," *Oil & Gas J.* (October 1989) 87, No. 41, 57.

[49]Schwochow, S.D. and Stevens, S.H., (eds.): "San Juan Basin Colorado and New Mexico," *Quarterly Review of Methane from Coalseams Technology* (April 1993) 10, No. 4, 3-4.

[50]Kaiser, W.R. and Swartz, T.E.: "Fruitland Formation and Producibility of Coalbed Methane in the San Juan Basin, New Mexico and Colorado," *Proc., Coalbed Methane Symposium*, Tuscaloosa, Alabama (April 1989) 87.

[51]Coalbed Methane Technology, Halliburton Logging Services, Inc., Charles Jackson, Technical Marketing (June 6, 1991).

[52]Masingill, J.: "Development of Warrior Basin Coals," paper presented at the 1989 Mississippi Energy Futures Symposium, Jackson, Mississippi, May.

[53]Alabama State Oil & Gas Board.

[54]"Black Warrior Basin, Alabama," *Quarterly Review of Methane from Coalseams Technology* (July 1991) 8, No. 4, 6-9.

[55]"Coalbed Stimulations are Optimized in Alabama Basins," *Oil & Gas J.* (October 1989) 87, No. 41, 61.

[56]"Raton Basin, Colorado and New Mexico," *Quarterly Review of Methane from Coalseams Technology* (March 1990) 7, No. 3, 6-7.

[57]Telle, W.R. and Thompson, D.A.: "Coalbed Methane Development Prospects in Southern Tuscaloosa County, Alabama," *Proc., Coalbed Methane Symposium*, Tuscaloosa, Alabama (April 1989) 225.

[58]Sexton, T.A. and Mancini, E.A.: "Coalbed Methane Gas Development in Northwestern Alabama-A New Frontier," *Oil & Gas J.* (April 1988) 86, No. 17, 55-58.

[59]Grazzier, C.A. and Henderson, K.S.: "Interest Aroused Over Coal, Coalbed Gas Resource Potential of Mississippi Region," *Oil & Gas J.* (August 1989) 87, No. 35, 61-63.

[60]Rogers, R.E.: "Development of Coalbed Methane in Mississippi Warrior Basin," Final Report, M.M.R.I. Grant #91-7F (August 1991).

[61]Zorbalas, K. and Rogers, R.E.: "Much More Gas Remains to be Discovered in Mississippi's Black Warrior Basin," *Oil & Gas J.* (November 1992) 90, No. 48, 69-72.

[62]Schwochow, S.D. (ed.): "Powder River Basin Wyoming and Montana," *Quarterly Review of Methane from Coalseams Technology*, Gas Research Institute (April 1991) 8, No. 3, 3.

[63]Telle, W.R., Thompson, D.A., and Malone, P.G.: "Preliminary Burial-Thermal History Investigations of the Black Warrior Basin: Implications for Coalbed Methane and Conventional Hydrocarbon Development," *Proc., Coalbed Methane Symposium*, Tuscaloosa, Alabama (November 1987) 37.

[64]Diamond, W.P. *et al.*: "Measuring the Extent of Coalbed Gas Drainage After 10 Years of Production at the Oak Grove Pattern, Alabama," *Proc., Coalbed Methane Symposium*, Tuscaloosa, Alabama (April 1989) 185.

[65]Malone, P.G., Briscoe, F.H., and Camp, B.S.: "Discovery and Explanation of Low Gas Contents Encountered in Coalbeds at the GRI/USSC Big Indian Creek Site, Warrior Basin, Alabama," *Proc., of the Coalbed Methane Symposium*, Tuscaloosa, Alabama, (November 1987), 63-72.

[66]Stevens, S.H.: "Raton Basin-Colorado and New Mexico," *Quarterly Review of Methane from Coalseams Technology* (August 1993) 11, No. 1, 33-36.

[67]Stevens, S.H. et al.: "A Geologic Assessment of Natural Gas from Coalseams in the Raton and Vermejo Formation, Raton Basin," topical report, GRI-92/0345 (June 1992) 84.

[68]Tremain, C.M.: "The Coal Bed Methane Potential of the Raton Mesa Coal Region, Raton Basin, Colorado," open file report 80-4, Colorado Geological Survey (1980).

[69]McFall, K.S., Wicks, D.E., and Kuuskraa, V.A.: "A Geologic Assessment of Natural Gas from Coalseams in the Warrior Basin, Alabama," topical report, GRI (November 1986).

[70]McFall, K.S. *et al.*: "An Analysis of the Coalseam Gas Resource of the Piceance Basin, Colorado," *JPT* (June 1988) 40, No. 6, 740.

[71]Tremain, C.M.: "Coalbed Methane Development in Colorado," Information Series 32, Colorado Geological Survey, U.S. Dept. of Natural Resources (September 1990).

[72]Schwochow, S.D. (ed.): "Northern and Central Appalachian Basins," *Quarterly Review of Methane from Coalseams Technology* (July 1992) 10, No. 1, 5.

[73]Decker, A.D. and Seccombe J.C.: "Geologic Parameters Controlling Natural Gas Production from a Single Deeply Buried Coal Reservoir in the Piceance, Mesa County Colorado," paper SPE 15221, presented at the 1986 SPE Unconventional Gas Symposium, Louisville, Kentucky, 18-21 May.

[74]Schwoebel, J.J., Logan, T.L., and Horner, D.M.: "Deep Coalseam Project-Advances Made in Coalbed Gas Recovery from Deep Cretaceous Coal Reservoirs, Piceance Basin," *Proc., Coalbed Methane Symposium*, Tuscaloosa, Alabama (November 1987) 217.

[75]"Piceance Basin, Colorado," *Quarterly Review of Methane from Coalseams Technology* (February 1991) 8, No. 2, 6-7.

[76]Decker, A.B. and Horner, D.M.: "Origins and Production Implications of Abnormal Coal Reservoir Pressure," *Proc., Coalbed Methane Symposium*, Tuscaloosa, Alabama (November 1987) 51.

[77]Kaiser, W.R., Scott, A.R., and Tyler, R.: "Geologic and Hydrologic Controls on Coalbed Methane Production-Western Basin," *Quarterly Review of Methane from Coalseams Technology* (July 1992) 10, No. 1, 18-22.

[78]Tyler, R., Kaiser, W.R., and McMurray, R.G.: "Geologic and Hydrologic Controls on Coalbed Methane Production," *Quarterly Review of Methane from Coalseams Technology* (April 1993) 10, No. 4, 19-24.

[79]Schwochow, S.D. (ed.): "Greater Green River Coal Region, Wyoming and Colorado," *Quarterly Review of Methane from Coalseams Technology* (April 1991) 8, No. 3, 3.

[80]Lamarre, R.A. and Ruhl, S.K.: "Atlantic Rim Coalbed Methane Play the Newest Successful CBM Play in the Rockies," presented at the 2004 Rocky Mountain Section AAPG Meeting, Denver, Colorado. 9-11 August.

[81]Wyoming Oil & Gas Conservation Commission.

[82]Law, B.E., Rice, D.D., and Flores, R.M.: "Coalbed Gas Accumulations in the Paleocene Fort Union Formation, Powder River Basin, Wyoming," *Coalbed Methane of Western North America*, Rocky Mountain Association of Geologists, S.D. Schwochow (ed.), Denver, Colorado (1991) 179-190.

[83]Larsen, V.E.: "Preliminary Evaluation of Coalbed Methane Geology and Activity in the Recluse Area, Powder River Basin, Wyoming," *Quarterly Review of Methane from Coalseams Technology* (June 1989) 6, Nos. 3 and 4, 2-10.

[84]Randall, A.G.: "Shallow Tertiary Gas Production, Powder River Basin, Wyoming," *Proc., Coalbed Methane Symposium*, Tuscaloosa, Alabama (May 1991) 509.

[85]"Montana," *Western Oil World* (July 1990) 24-27.

[86]Zebrowitz, M.J., Kelafant, J.R., and Boyer, C.M.: "Reservoir Characterization and Production Potential of the Coalseams in Northern and Central Appalachian Basins," *Proc., Coalbed Methane Symposium*, Tuscaloosa, Alabama (May 1991) 391.

[87]Hunt, A.M. and Steele, D.J.: "Coalbed Methane Technology Development in the Appalachian Basin," topical report, GRI-90/0288 (January 1991) 53.

[88]Production data obtained from West Virginia Geological and Economical Survey and Bureau of Oil & Gas Management, Pennsylvania

[89]Schwochow, S.D. (ed.): "Cherokee Basin, Kansas and Oklahoma," *Quarterly Review of Methane from Coalseams Technology* (April 1992) 9, Nos. 3 and 4, 5.

[90]Production data obtained from Department of Mines, Minerals and Energy, Virginia.

[91]Gard, L.M.: "Bedrock Geology of the Lake Tapps Quadrangle, Pierce County, Washington," U.S. Geological Survey Professional Paper 388-b (1968).

[92]Stevens, S.H.: "Pacific Coal Region," *Quarterly Review of Methane from Coalseams Technology* (August 1993) 11, No. 1, 21-23.

[93]Rieke, H.H.: "Geologic Overview, Coal, and Coalbed Methane Resources of the Wind River Basin, Wyoming," Wind River Basin report, TRW, Inc., U.S. DOE (March 1981).

[94]Stevens, S.H.: "Illinois Basin, Illinois Indiana, and Kentucky," *Quarterly Review of Methane from Coalseams Technology* (August 1993) 11, No. 1, 18-20.

[95]Tedsco, S., Atoka Coal Labs LLC: "Coalbed Methane in the Illinois Basin: An Update," presented at the 2004 International Coalbed Methane Symposium, Tuscaloosa, Alabama, 3-7 May.

[96]Archer, P.L.: "Pennsylvania Geology and Coal and Coalbed Methane Resource of the Illinois Basin, Illinois, Indiana, and Kentucky," Illinois Basin report, TRW, Inc., U.S. DOE.

[97]Rieke, H.H.: "Geologic Overview Coal and Coalbed Methane Resources of the Arkoma Basin, Arkansas and Oklahoma," TRW, Inc., U.S. DOE, Morgantown, WV.

[98]Stevens, S.H. and Sheehy, L.D.: "Western Interior Coal Region (Arkoma, Cherokee, and Forest City Basins)," *Quarterly Review of Methane from Coalseams Technology* (August 1993) 11, No. 1, 43-48.

[99]Cardott, B.J., Oklahoma Geological Survey: "Coalbed Methane Activity in Oklahoma," 2004 Update, presented at the OGS Conference on Unconventional Energy Resources in the Southern Mid-continent, Oklahoma City, Oklahoma, 10 March.

[100]Schwochow, S.D. (ed.): "Uinta Basin, Utah," *Quarterly Review of Methane from Coalseams Technology* (July 1992) 10, No. 1, 3-4.

[101]Burns, T.D. and Lamarre, R.A.: "Drunkards Wash Project: Coalbed Methane Production from Ferron Coals in East-Central Utah," paper 9709 presented at the 1997 International Coalbed Methane Symposium, Tuscaloosa, Alabama, 12-16 May.

[102]*PTTC Newsletter*, Vol. 10, No. 1, 1st Quarter 2004. pp 8.

Chapter 2

Geological Influences on Coal

2.1 Formation of Coals

Coal begins when plants are deposited in swamps, then submerged rapidly enough to limit oxidation but to allow microbial decomposition. Shallow waters of a constant depth, such as created between fluvial systems in plains along the coast of seaways or behind coastal barriers, allow enough plant mass and its covering of sediment to accumulate as undisturbed peat.

The peatification process continues as the decomposing plants are progressively covered with sediments, physical processes act to compress, and biochemical processes alter the remains in an environment of warm temperatures and abundant rainfall. When the organic mass becomes deeply buried, coalification transforms it as a function of pressure, temperature, and time. Of these parameters, temperature is the most important in the geochemical reactions that occur.

As temperature and time progressively change the molecular structure of coals, a point is reached where thermogenic methane is evolved in large volumes, micropores develop to store extraordinary amounts of methane per unit of coal, and fractures permeate the coal to transport the excess methane. Thus, methane is generated to be stored and dissipated over geologic time.

2.1.1 Stratigraphic Periods

The U.S. coals originated in the Tertiary, Cretaceous, or Carboniferous periods.[1] The stratigraphic periods for coal formation are given in Fig. 2.1. It should be noted that the Carboniferous period generated most of the coals. Younger coals in the Cretaceous, Paleocene, and Eocene periods are of lower rank or maturity unless a localized heat source occurred to accelerate the normal metamorphism or burial history was altered by tectonic action.

Lignite exists in various parts of the world from younger Miocene and Pliocene deposits; current peat deposits began during the Quaternary era.[2,3]

2.1.2 Tertiary Coals of Western United States

Shallow coals in the Powder River basin of northern Wyoming and southeastern Montana were formed during Paleocene and Eocene periods. The lignite to subbituminous A coals have the thickest individual seams in the country, exceeding 100 ft.

In the Paleocene period, the Cretaceous Seaway regressed, leaving an extensive coastal plain cut by stream channels all along its western coast (Fig. 2.2). The sea ran from what is now eastern Alaska to the Gulf of Mexico. During this time, fluvial-channel and fluvial-lake sediments accumulated to form the Fort Union formation in the Powder River basin, where large peat swamps developed between the meandering stream channels.

Into the Eocene period, the deposition was similar so that the interface of the sediments may be hard to distinguish. The Wasatch formation contains the Eocene coals of the Powder River basin. Especially noteworthy is the 200-ft-thick Lake de Smet coalbed.[4]

2.1.3 Cretaceous Coals of Western United States

The western U.S. coals of current interest were deposited primarily in the Cretaceous Age about 90–120 million years ago (m.y.a.) at the western coast of the Cretaceous Seaway.[5] This sea ran approximately parallel to the present Continental Divide. As Fasset points out, the Fruitland formation of the San Juan basin, the most productive of all U.S. coal basins, resulted from the last regression of that coast[6] (see Fig. 2.2).

The coals of the Fruitland formation of the San Juan basin have the most prolific coalbed methane (CBM) production in the world. The sediments of the Fruitland accumulated during the Cretaceous Age in a manner similar to the other coal basins along the Cretaceous Seaway.

The fluvial system in the delta flowed northeastward into the sea, leaving fluvial-channel sediments that now constitute the sandstone formations pointing like fingers northeastward in the Fruitland. Peat swamps formed within the fluvial system and rested upon a base of Pictured Cliffs sandstone deposited from the regressed seaway. Therefore, the coals intertongue with the Pictured Cliffs sands at the present northeastern boundary of the basin.

Age	Millions of Years: Mean Age of Coals	Millions of Years: Duration of Period	Stratigraphic Period			Principal Species of Animals
	----	----		Quarternary	Holocene	Mammalia, Man Insects
	<1	1			Pleistocene	
-1-						
	2	11			Pliocene	Domination of Mammalia Fishes, Birds.
-12-						
	15	11			*Miocene*	
-23-			Cenozoic	*Tertiary*		
	28	12			Oligocene	
-35-						
-55-	60	20			*Eocene*	
		15			*Paleocene*	
-70-						
					Upper	Dwindling of Ammonites, Belemnites and Sauria; origin of
	120	65		*Cretaceous*	Lower (Weald)	Mammamlia and Birds.
-135-						
					Upper	Domination of Reptilia and Amphibia, (Dinosauria and Ichthyosauria).
	160	45	Mesozoic	Jurrassic	Middle	Mollusca (Ammonites and
					Lower	Belemnites)
-180-						
					Upper	
	200	40		Triassic	Middle	Crustacea,
					Lower	First Reptilia and Mammalia
-220-						
				Permian		Protozoa, Fishes, Mollusca, Arthropoda (Insects). First Amphibia.
-270-						
		50			*Upper carbonifer.*	
	300			*Carboniferous*		
-320			Palaeozoic		*Lower carbonifer.*	
		30				
-350-	380	50		Devonian		Domination of Coelentrata, Mollusca.
-400-						Protozoa,
		90		Silurian		First Fishes.
-490-		110		Cambian		Protozoa, Coelentrata, First Mollusca.
-600-						
		>1,000	Proterozoic	Algonkian		
				Archaean		

Fig. 2.1—Periods of coal formation.[7]

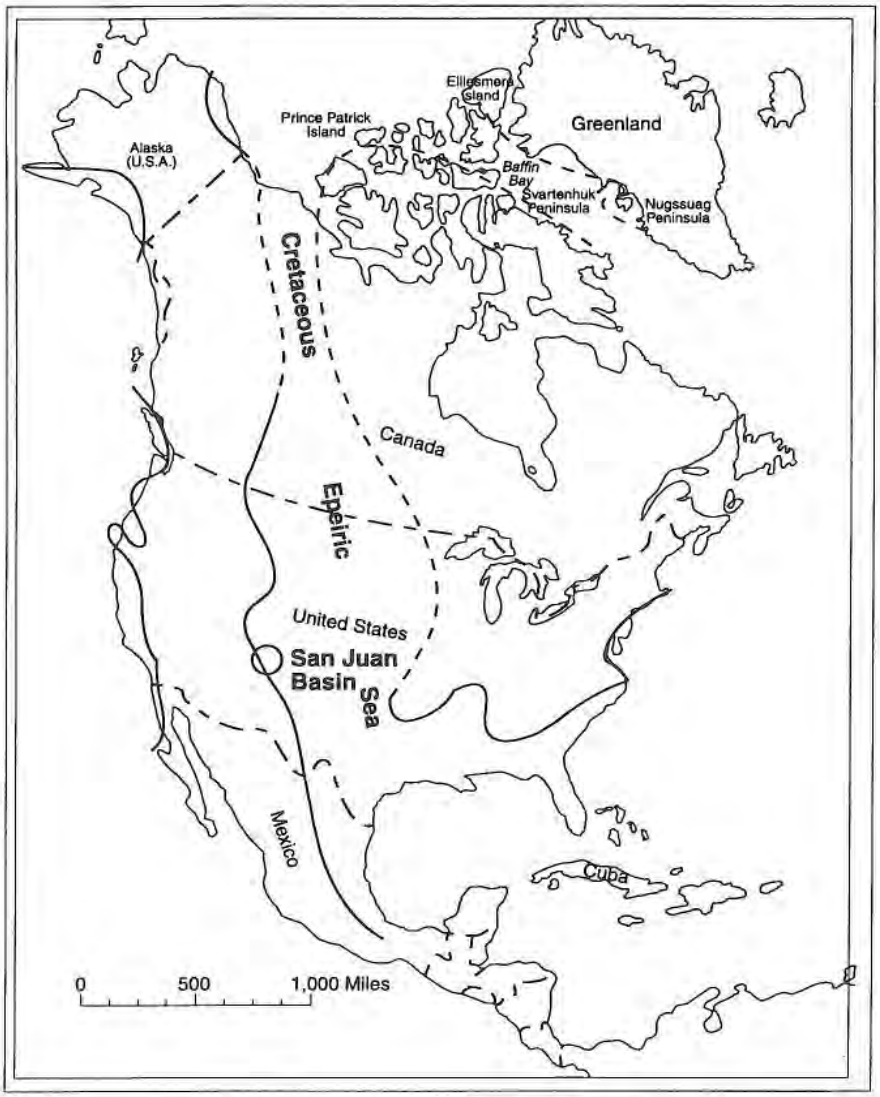

Fig. 2.2—Cretaceous Seaway and western coals.[6]

Donaldson[8] has presented a concept of coalseam discontinuities that is applicable to a depositional environment, such as the Fruitland formation (Fig. 2.3).[9]

In Sketch A of Fig. 2.3, the fluvial sand deposits occurred at the same time as the peat formation to give an intertonguing of the two. In Sketch B, an intruding channel removed the peat and replaced it with sand sediments. In Sketch C, the fluvial sediments occurred after peat formation, not replacing but depositing upon the organic matter where later compaction stressed the coal. A similar stressing of the coal would occur in Sketch D where the peat formed upon the previously deposited channel sand.

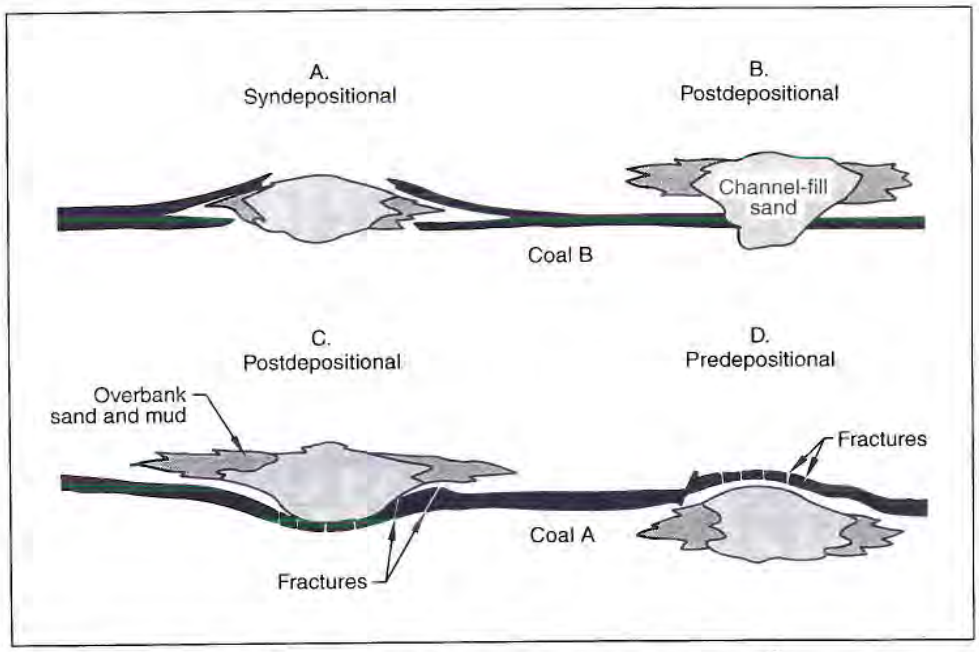

Fig. 2.3—Influence of fluvial deposition on coalseam geometry.[9]

Other large coalbeds in multiple basins stretching into Canada developed along the western coast of that Cretaceous Seaway, creating a large potential CBM resource that now exists as thick coals extending along the Rocky Mountains in Montana, Wyoming, Colorado, and New Mexico. For example, the coals in Montana developed near the shoreline of the Cretaceous Seaway intertongued with the clastic sediments coming from the mountains uplifted to the west of the shoreline.[10]

The low sulfur content (<0.8%) of these coals indicates formation along the flood plains of the rivers coursing into the seaway from the mountains to the west, as well as formation in fresh water behind coastal barriers,[5] and indicates the absence of relatively high concentrations of the sulfate ion that would be in brines.

2.1.4 Carboniferous Coals of Eastern United States

Eastern U.S. coals, older by about 150 million years, exhibit many properties different from the coals of the western states. The coals along the Appalachian Mountains were formed in the Pennsylvanian Age of the Paleozoic era, and they usually have properties characteristic of a higher rank than the Cretaceous and younger coals.

In the Warrior basin of Alabama, the coals are located in the Pottsville formation, a 2,500–4,500-ft sandstone interbedded with siltstone, shale, and coalbeds. These coals are generally far enough along in the maturation process to exhibit a rank of high-volatile A bituminous to low-volatile bituminous, an optimum rank for CBM production. The high sulfur content, 2–3% typically, indicates formation in saline waters of a shallow embayment.[5]

2.1.5 Influence of Coal Properties

Dissimilar plant life, deposition environments, tectonic actions, residence times, and temperatures initiated coals in the two major stratigraphic periods with understandably different properties today. These differences translate into completion and production practice variations for the CBM process in the Carboniferous coals of the eastern United States and the Cretaceous or younger coals of the western part of the country. Some characteristics of the Black Warrior basin coals are compared with those of the San Juan basin in Table 2.1. Seam thickness and rank are the most notable differences; however, the conditions in the two regions are representative of those to be encountered worldwide in developing the CBM. As a consequence, study of the commercial processes of the Black Warrior basin of Alabama and the San Juan basin of Colorado/New Mexico will cover most of the variations to be expected worldwide.

Table 2.1—Comparing Coals

	Black Warrior	San Juan
Age (m.y.a.)	300	120
Rank	lvb	hvAb
Sulfur (%)	2 to 3	<0.8
Single Seam Thickness (ft)	1 to 4	30 to 50
Gas Content (scf/ton)	500 to 600	400 to 500

2.1.6 A Genesis Model of Coal

For a period in the Carboniferous Age, lasting about 10–25 million years, lateral compressive forces on the crustal plates caused inward buckling to create concavities of large areas of the earth's surface. According to a geosyncline theory,[7] these depressions accumulated sediments as they subsided.

Subsequently, as the rate of subsidence slowed in relation to the sediment buildup, the depressions eventually filled (current rate of accumulation of peat has been measured at 1 mm per year[11]). A point was reached where the stagnant waters of the basins were of the depth and conditions for vegetation to form and begin peat swamps.

Distinct and layered seams of coal in a group now observed are explained by another increase in subsidence that submerged the peat and renewed the cycle. The organic sediment was submerged beneath stagnant water and other sediments to forego oxidation. When the driving lateral forces were finally removed, mountains arose. The resultant folding caused the steep inclines of many coalseams encountered in current CBM exploration. It also helps explain the presence of higher rank and maturation in some coals that would have required greater temperatures than their current burial depths justify. Subsequent erosion removed many of the sedimentary levels. Thus, an equilibrium was established between the sedimentation rate and the subsidence rate, and that equilibrium was maintained for long periods.[11]

Generally, the peat swamps formed behind coastal barriers or in river deltas where the peatification process slowly evolved. Flooding of swamps by the melting of the polar ice caps, changing courses of rivers, subsidence, tectonic action, and climate changes have been suggested as reasons for termination of the peat-forming process.

Consider that many types of plants form the coals, and the vegetation changes with time. These facts alone suggest a likely wide variation in physical and chemical properties of coals from different basins as well as lateral and depth variations within a given coal group, which has significance for the CBM process. Plant forms of sufficient foliage to provide the massive biomass required to form peat initially developed during the Devonian Age of about 380 m.y.a.[11]

Besides the organic matter, mineral matter indigenous to the plants enters the coal. Additional mineral matter is airborne or comes from erosion of rocks as rock fragments. Inorganic matter to be eventually precipitated also enters with

the water.[12] Clays, pyrite, calcite, and quartz are thus incorporated in the coals along with other minerals. These inorganic substances are an integral part of all coals and affect overall chemical and physical properties of the coals.

2.1.7 Geochemical Transformation

Peatification, the first stage in the development of coal, is the biochemical and physical process of converting organic matter to peat with only secondary assistance from the geochemical process. The biogenic methane generated by bacteria in the peatification stage is lost unless burial of the peat is rapid enough and sealing shale lenses are interbedded to form a trap.[13] Later, however, biogenic methane from other locales may migrate to the developing coal and be adsorbed.

Although the largest amounts of CBM are from thermogenic sources, biogenic methane may be retained in quantities of commercial value, as in the thick coalseams of the Fort Union formation of Paleocene Age and the overlying Wasatch formation of Eocene Age of the Powder River basin of Montana/ Wyoming.[14] These lignite-to-subbituminous coals may have a gas content of only 15 scf/ton, but seams on the order of 100 ft thick may contain 16 Tcf of recoverable methane.[4] Therefore, even though production of biogenic methane occurs from the subbituminous coals of the Fort Union formation,[15] it is the combination of thick seams and shallow depths that make the production practical.

After the peatification stage comes coalification, the geochemical process of converting organic material in peat to coal over geologic time with secondary assistance from physical processes. The geochemical reactions are influenced by temperature, time, pressure, and composition of the organic matter. Temperature is the important parameter most affecting the dynamic chemical structure of the coal. Higher temperatures promote the geochemical reactions; higher pressures retard the reactions.[16] Progressively higher temperatures are necessary to reach

successively higher levels of maturation.[2] Compaction forces and stresses from tectonic action continually change the physical characteristics of the coal, but pressure is considered to have a minor role in the chemical process[7] and a primary role in altering some physical properties. Pressure increases from subsidence reduce porosity and expel moisture in the low-rank coals.[16] Time alone has been shown to be insufficient to complete the maturation process.

Radiation will create chemical changes in coal in a manner similar to the coalification process,[16] but the influence of the radiation is limited to a short radial distance from the source. Therefore, the presence of localized radioactive sources could result in an elevated coal maturity nearby.

Igneous intrusion influences coal maturity and chemical status in a localized manner, as volcanic action raises temperature of the coal near an intrusion. Localized heating from extreme stresses also accelerates the maturation to achieve high ranks of the impacted coal. Temperatures as high as 572°F may be needed to achieve anthracite—higher than the normal temperature increase with subsidence.[16]

Carbon dioxide and water are the first volatiles generated. They evolve before subsidence takes burial to depths where temperatures attain 212–300°F, the temperatures when bituminous coals form. Relatively little CH_4 is thermally generated at cooler temperatures than these. The methane generation becomes appreciable from hvAb coals, where breakdown of the carbon-carbon bond in the linear-chain components requires the high temperature (see Fig. 2.4). The rapid generation of methane thereafter until reaching the anthracite rank supplies much more gas than can be retained by the coal, possibly generating 7,000 scf/ton, yet retaining only 500–600 scf/ton.[11]

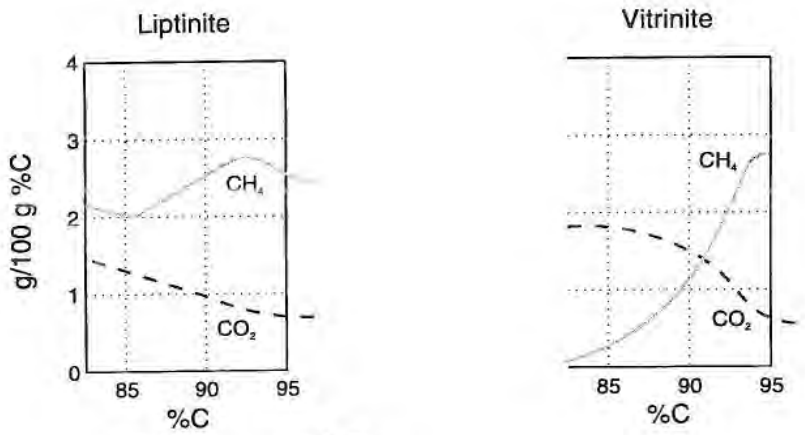

Fig. 2.4—CH_4 generated.[11,17]

Volatiles of CH_4, CO_2, H_2O, and N_2 are liberated during the coalification stage. In the stage going from peat to lignite, mainly CO_2 is liberated.[16] The thermogenic carbon dioxide, albeit more strongly adsorbed to the coal matrix than the other volatiles, is more easily dissipated because of its solubility in water. Gas produced from the San Juan coals ranges from 1–13% CO_2, where the lowest CO_2 concentration occurs in the south of the basin. However, all CO_2 adsorbed currently may not have come from geochemical reactions in the coal's maturation. Biogenic action from microbes in meteoric waters moving toward the basin through the permeable coals from outcrops in the northwest have generated 6% or more CO_2 in the overpressured, higher bottomhole pressure, dry gas, hvAb coals of the prolific fairway of the San Juan basin.[18]

It is concluded[18] that the meteoric waters entering at the coal outcrop in the northwest of the basin introduce microbes that generate methane as well as carbon dioxide. This biogenic source of methane, which has lower amounts of heavier alkanes than does thermogenic methane, exists in the overpressured coals that also adsorb the carbon dioxide.

Being the smallest molecule and more weakly adsorbed than methane or carbon dioxide, nitrogen is more easily dissipated by diffusion during coalification.

It is hypothesized that loss of volatiles, especially water and methane, contributes to the formation of coal cleat systems induced by the shrinkage of the coal matrix upon losing the volatiles.

Thermogenic methane is primarily produced after the maturation reaches about the high-volatile A bituminous rank,[15] coming predominantly from the liptinite maceral. The evolution of large amounts of methane by the liptinite maceral in ascending ranks beginning at a volatile content of 29% (about 85% carbon, dry mineral matter free on a total carbon basis, or about 1.0% reflectance) has led Stach[16] to refer to a coalification break at this point, where a distinct change occurs in the chemical structure of coal. The coalification break signifies the point at which physical properties are altered so that microscopic cracks appear in the coal because of shrinkage from accelerated methane loss and previous moisture or volatile losses at lower ranks.

The coalification break on a large scale is evident in the large production increases from cavitation completions in the San Juan basin in those coals of hvAb or above, and the lack of a coalification break is evident in the poor cavitation results in ranks of coal lower than hvAb. Multiple properties of the coal conducive to cavitation success develop at the coalification break. Good permeability, extensive fracturing, close cleat spacing, low-strength coal, and high gas content are properties conducive to cavitation success that can develop above the coalification break.

Chemical changes continue to occur throughout the coalification process, and general trends may be followed. Condensation, polymerization, and crosslinking reactions increase. Aromatization increases. Functional groups of oxygen decrease; carbonyl, carboxyl, phenol, ester, and ether linkages are lost in volatiles of carbon dioxide and water. Other functional groups containing nitrogen and sulfur decrease.[11]

Coal's diverse chemical and physical nature accentuates the need for orderliness in its study. This has prompted investigators to categorize microscopic organic particles in the coal, called macerals, according to the part of the plant from which they came. Each maceral has been found to contribute different amounts of methane during metamorphism, and each maceral represents a family of characteristic chemical behavior that tends to identify itself with increasing maturation. The maceral approach helps in the categorization and orderliness of studies. Although numerous macerals have been identified, three are primary—vitrinite, liptinite, and inertinite.

Another major step, introduced by van Krevelen,[7] in establishing orderliness to the complex structural nature of coal involves following its maturation path from peat to anthracite and tracking the relative amounts of atomic hydrogen, carbon, and oxygen present along the path. Along the path, volatiles are lost and the percentage of carbon thus increases, while the atomic hydrogen-to-carbon ratio (H/C) and the oxygen-to-carbon ratio (O/C) contents of the coal decrease until the ratios converge for all macerals when a high rank of coal is reached.[19]

A plot of the H/C ratio versus O/C ratio has been developed.[11] Fig. 2.5, a modified van Krevelen diagram,[7] plots the path of the maturation of vitrinites, liptinites, and inertinites; the different branches of the diagram denote the organic source.[13] Although the H/C and O/C atomic ratios differ by large amounts in the beginning, they converge to a similar value by the time anthracite coal is reached.[19] Therefore, chemical compositions of the macerals, which began as highly dissimilar in peat, converge at anthracite.[12] Graphite would be the ultimate state of the coalification process.

The scenario of coal origin, the somewhat precarious requirements of its development, and its burial history help to visualize the variances that must occur in seam continuity, thickness, composition, impurities, depth, and maturation-factors that impact the viability of a commercial CBM process.

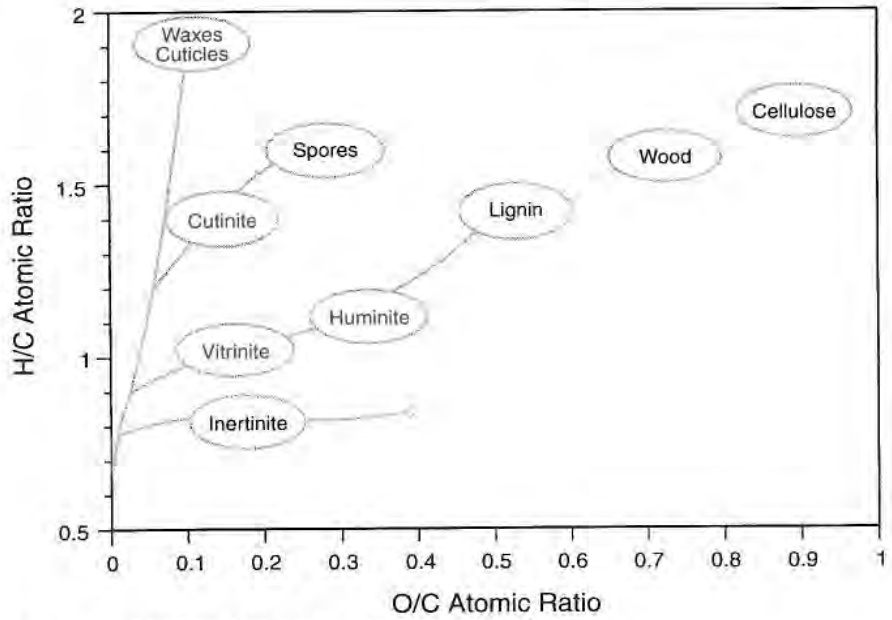

Fig. 2.5—Modified van Krevelen diagram.[13]

2.2 Coal Chemistry

2.2.1 Molecular Structure

Initially and through most of the maturation until the macerals become similar at anthracite, the chemical structure of coal is dependent on depositional environment. The type vegetation and the chemical constituents of that vegetation provide the starting material in the coalification process that later determines parameters ranging from the amount of gas liberated to the degree of cleating.

Type of vegetation varies with geologic age; that is, more advanced plants are expected in the Cretaceous than the Carboniferous period. Even within a given age, the vegetation varies according to locale. Further, environments of fresh water or seawater in the swamp determine the types of plants growing there as well as the eventual sulfur and iron contents of the coal.

After the establishment of composition initially in the peat, chemical structure of the organic matter is time-dependent; structural changes become a function of burial history. In the beginning, the extent of oxidation of the plant material depends on the initial rate of water submergence, sedimentary coverage, and subsidence. Later, burial depth establishes pressure and temperature, but the time at a maximum temperature and the magnitude of the maximum temperature are the primary determinants of the dynamic chemical structure.

There is no single molecular structure that represents a coal molecule; the variation of its structure is too great. Berkowitz,[2] however, refers to a statistical average molecule in terms of units that are most often repeated but with no intent to imply that the common structure represents all coals of all ranks.

The Berkowitz model is summarized as:

- The coal structure is envisioned as similar to synthetic compounds of copolymers, forming with varying molecular weights.
- The basic, repeating coal molecule is composed of a core of two or three condensed, aromatic rings (20–80% organic carbon).
- The clusters of aromatic rings are joined by aliphatic -CH_2- and -0- linkages (10–15% of organic carbon).

Wiser[20] provides another model of an envisioned coal molecule in Fig. 2.6, where the primary functional groups, cyclic and aliphatic components, are represented. In the sketch, arrows indicate reactive sites of probable cleavage of the molecule. Note that the model represents clusters of three to four aromatic rings. As those weaker links between clusters break thermally during coalification, the molecule realigns, releasing volatiles and even hydrocarbon liquids in some instances. Also, condensation reactions occur, such as two

aromatic molecules combining to form a single higher molecular-weight compound with the release of volatile matter.

Researchers agree that regardless of the choice of model, the coal molecule is comprised of cores or clusters of aromatic rings bridged by cyclic or aliphatic crosslinks surrounded by functional groups on the periphery.[11] Over geologic time, under the primary influence of temperature, volatiles of CO_2, CH_4, and H_2O are released, mainly from the non-aromatic component[21] in a continual altering of the molecular structure toward an aromatic bias.

Coal has a net negative surface charge.[22]

Attempts to study the structure of coal have been by various methods, each method providing some insight, but each being incomplete. X-ray diffraction studies, solvent extraction, and oxidation reactions have given the most information about the molecular structure of coals. The studies agree that aromatics represent 20–80% of carbon in the makeup of coal, probably closer to 32–35% as an average.[2] The aromatic rings occur in repetitive units of two to three condensed benzene rings tied together by -O- or -CH_2- groups.

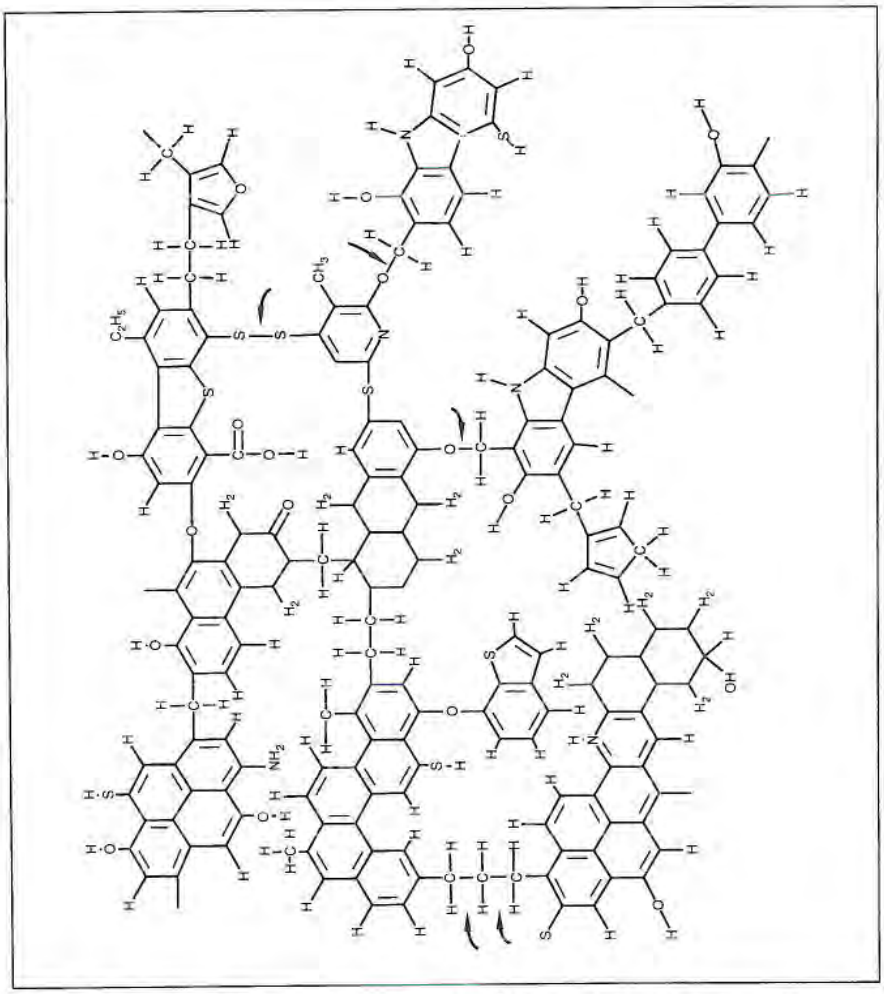

Fig. 2.6—Representative coal molecule.[20] Reprinted with permission from ACS Publications Division. Copyright 1991 American Chemical Society.

Two investigators have presented results on the aromaticity of coal based on X-ray scattering and solvent extractions. Hirsch[23] reported 50–80% of the carbon contained in aromatic structures. From solvent extracts, Given[24] reported

aromatic carbon exceeding 20% for low-rank coals and exceeding 50% for high-rank coals.

Aliphatics comprise 10–15% of the total carbon content of the coal. In the subbituminous coals, polycyclic aliphatic rings are more common and the aliphatic rings along with the straight-chain aliphatics eventually convert to aromatics in the coalification process.[1]

Lee[25] studied eight coals of Paleocene, Cretaceous, and Pennsylvanian vintage, which ranged in rank from lignite to low-volatile bituminous and found that the straight-chain, n-alkane component increased by a factor of about 5 from lignite to high-volatile A bituminous. After the coalification break, the amount of normal alkanes dropped by a factor of 50 at low-volatile bituminous. Lee found that the ratio of odd-to-even number of carbons in these normal alkanes showed approximately an exponential decline from lignite to low-volatile bituminous.

Aromaticity increases with coal rank. Whitehurst[1] gives a correlation in Fig. 2.7. Percentage of carbon in aromatic structures increases from about 40% for subbituminous to 60% for bituminous to over 90% for anthracite. The trend of coals to a more aromatic chemical makeup as rank progresses impacts physical as well as chemical properties important to the CBM. The aromatic clusters and their realignment are instrumental in establishing the micropore network and in releasing volatiles.

Noncarbon components of the coal's molecular structure are hydrogen, oxygen, nitrogen, and sulfur. Nitrogen represents about 1.0% of the structure.[7]

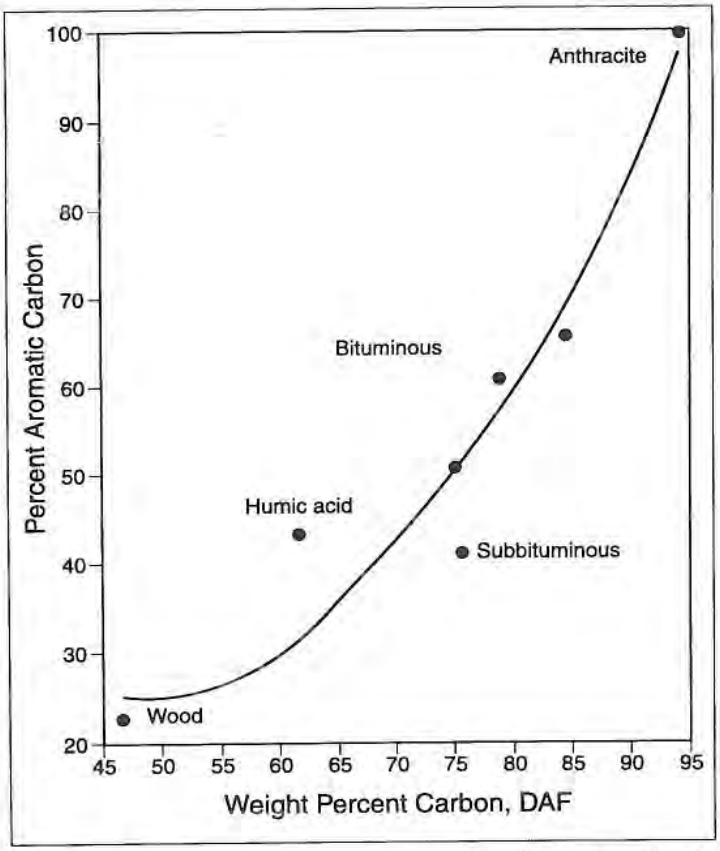

Fig. 2.7—Progression of aromatic content.[1] *Reprinted with permission from ACS Publications Division. Copyright 1978 American Chemical Society.*

2.2.2 Macerals

Macerals are the smallest distinguishable organic particles of coal that can be seen under a microscope. They differ in optical properties and chemical composition because of their origin in different parts of the plant.

There are three maceral groups: vitrinite, liptinite, and inertinite—their names indicating source, appearance, or reactivity. Each of the three groups contains subgroups of macerals with similarities of origin, optical properties, and composition.

Generally, vitrinite is the most abundant maceral of coal and is the most homogeneous maceral. U.S. coals typically contain as much as 80% vitrinite,[1] and it is the main contributor to the shiny black strands so familiar in coals. Vitrinite is formed partly from lignin, an amorphous, polymeric substance that provides the structure of the plant cell wall in conjunction with cellulose. Additionally, vitrinite is formed from cellulose and woody parts of the plant that create a chemical structure high in oxygen and aromatics. Its oxygen content is higher than the liptinite maceral. The vitrinite maceral is capable of producing hydrocarbon gas but only small amounts of oil;[26] vitrinite contains more straight-chain carbon groups.[3] Vitrinite is the maceral most conducive to forming a cleat system in coals.[12]

Liptinite, also called exinite, originates from spores, pollen, resins, oily secretions, algae, fats, bacterial proteins, and waxes. Thus, it has subgroups of macerals designated as resinite, alginite, and cutinite. The cuticle refers to a thin film found on the outside walls of higher plants that is a continuous, protective, fatty deposit; the cuticle forms the cutinite maceral in the liptinite group.[16] The macerals of liptinite have chemical structures high in hydrogen and in aliphatics. Many of the volatiles, including methane, emitted by the coal during coalification come from the liptinite. These macerals have the potential of producing hydrocarbon gases and oil.[26]

Inertinite is the oxidized or charcoaled cell walls or trunks of plants, resulting in high carbon and aromatic content but less hydrogen. Inertinite has relatively more carbon than the other macerals, and its name is derived from its lack of chemical reactivity. Inertinites originated from forest fires, bacterial action, and oxidation from the air before the coalification stage was reached.[11] Only small amounts of volatiles are generated by the inertinites. Further, there is practically

no potential of these macerals to produce hydrocarbons.[26] Inertinite is the hardest of the macerals, and it is seen on a polished surface as a bright protrusion.[16] High inertinite content of coal makes the coal less conducive to forming cleats.[12]

All of the macerals trend toward the same chemical composition as the rank of the coal increases, and they become almost indistinguishable after 94% carbon is reached.[2] As time proceeds after deposition and geochemical reactions occur, volatile matter containing more hydrogen and oxygen than carbon is lost. Van Krevelen's graph[13] of H/C versus O/C atomic ratios explain in Fig. 2.5 the convergence of the macerals in the coal. It is observed that the three macerals ultimately converge to a common composition.

Another way of viewing Fig. 2.5 is that maturity is a function of the hydrogen-to-carbon ratio of the coal's molecular structure. To a large extent, the ratio reflects the coal's capability to evolve methane during coalification. Therefore, from an interpretation of Fig. 2.5, liptinite is most responsible for methane generation. Inertinite contributes little to methane generation.

In Fig. 2.8, where liptinite and vitrinite attain the same composition, carbon represents about 89% of the elemental analysis. At 94% carbon, the three macerals become almost indistinguishable; their reflectance is similar at 95% carbon. At this latter point, the weaker bonds of functional groups have been broken, volatiles have been evolved, and the structure has reduced to the stronger bonds of the aromatic clusters arranged in a more orderly manner. Physical and chemical properties of the coal have therefore changed accordingly.

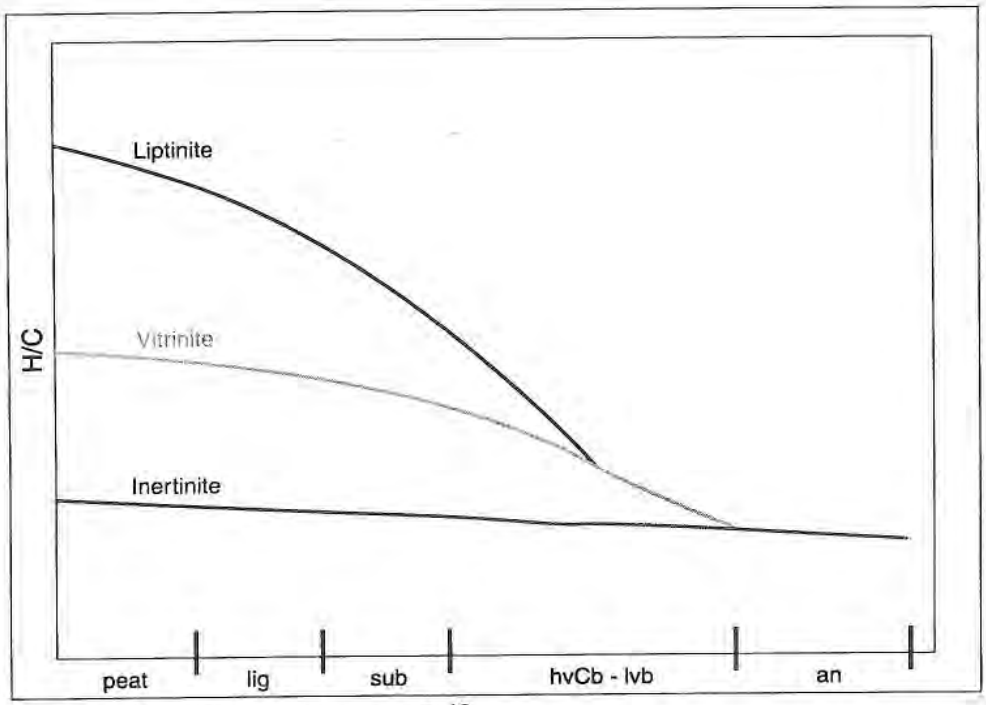

Fig. 2.8—Convergence of macerals.[12]

2.2.3 Lithotypes

On a microscopic basis, macerals classify the makeup of coal according to the plant source.

On a macroscopic basis, lithotypes classify bands of coal that are visibly discernible according to their dominant and minor maceral contents. It is a classification intended to describe coal composition by means of the brightness or dullness of the bands to the unaided eye.

The four lithotypes are:

- Vitrain.
- Clarain.
- Durain.
- Fusain.

Vitrain is composed primarily of vitrinite. Minor amounts of the inertinite and liptinite macerals are present. They are the familiar bright black bands seen in coal. Vitrain is friable and brittle and thus plays an important role in cleat formation. Fissures are common in it,[16] and because of this, the fines generated in a producing CBM well should be weighted toward the vitrain. Vitrain is the most important lithotype in establishing a successful CBM.

Although a bright component of coal, clarain is not as bright as vitrain.[3] It contains less vitrinite and more inertinite and liptinite. The presence of inertinite hinders the formation of fractures; inertinite is hard and difficult to crush.[27]

Durain is a dull lithotype. It contains more mineral matter and inertinite than vitrain or clarain. It is tough and difficult to fracture. Therefore, blocks of it, rather than the fines, would separate from the seam. Durain is not conducive to building good permeability in a coalseam.

Fusain resembles charcoal.[2,3,16,27] It is fibrous and soft and is easily broken. Fusain is the least important of the lithotypes in the CBM process.

Obviously, the greatest usefulness of the lithotypes to the CBM process lies in easily distinguishing the bright bands where vitrinite is concentrated. These components of such bright bands impart to the coal fracturing characteristics that are precursors of good permeability.

2.2.4 Functional Groups

In this section, some attributes of coal structure that affect the CBM process are presented. Functional groups and organic families of coal impact the following:

- Retained gas content of the coal.
- Volatiles generated during coalification.
- Micropores and their size, spacing, and distribution.
- Trends of structure change with maturation.
- Oxidation or swelling of matrix upon adsorption.
- Cleating and fracturing.

Some trends of molecular structure during maturation are significant:

- Aromaticity increases.
- Functional groups containing O, N, S decrease.
- Aliphatic compounds decrease.
- Clustering of aromatic rings increases.

Functional groups containing oxygen in coal are primarily those given in Table 2.2.[2]

Table 2.2—Functional Groups of Oxygen in Coal

Functional Group	Structure
Phenolic	–OH
Methoxyl	$-OCH_3$
Carboxyl	$^{-}COOH$
Carbonyl	$^{-}C{=}O$
Oxygen Residual	Ether, ring structures

As seen earlier in the van Krevelen diagram of Fig. 2.5, the relative amount of oxygen in relation to carbon decreases as the coal becomes more thermally mature. These oxygen functional groups in coal dissipate during the coalification process as the volatiles CO_2, CO, and H_2O, with less CO being generated than

the other two compounds.[1] The vitrinite maceral contains the most groups with oxygen. As maturation proceeds and the rank of the coal increases, the percentage of oxygen found in each of the primary functional groups is decreased in a manner described by Fig. 2.9.[2,28] The total oxygen decreases to less than 5% near anthracite.

Whitehurst[1] ranks the number of oxygen functional groups in the order of phenolic and etheric as most plentiful, then carboxyls, and finally carbonyls.

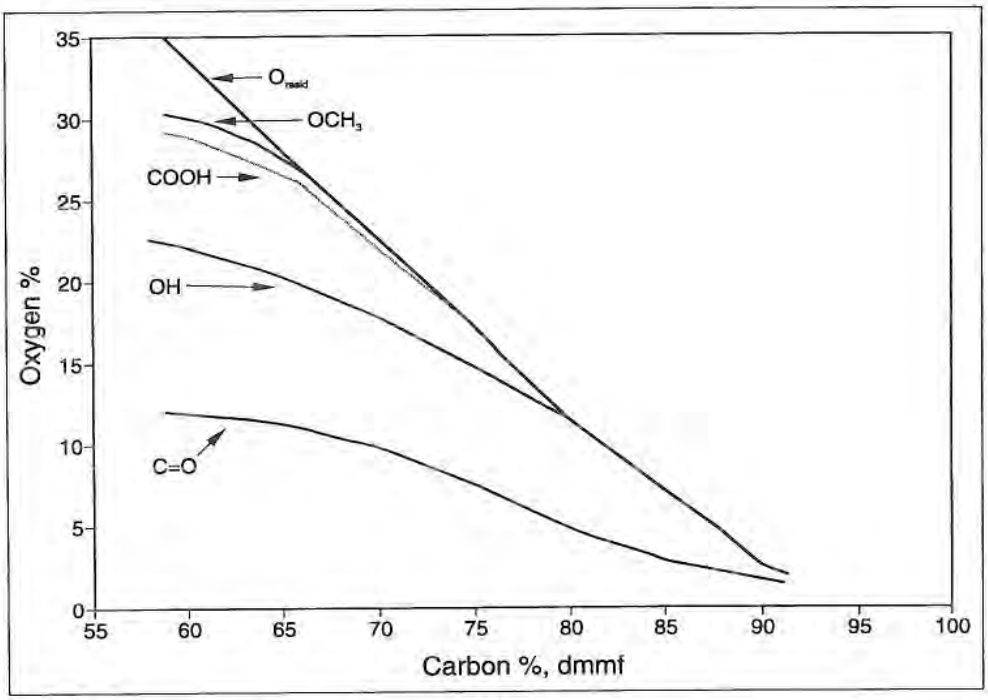

Fig. 2.9—Oxygen in functional groups.[2,28]

Below temperatures of 158°F, oxidation occurs slowly in coals. The oxygen is first chemisorbed from the air whereupon peroxides or acidic functional groups

of -COOH, -OH phenolic, and C=O are produced. With adequate time, the molecular structural units may be oxidized to smaller units.[2]

The oxygen functional groups are responsible for the retention of water by hydrogen bonding in the lower ranks of coal. Porosities of the lignite or subbituminous coals are high and the water adsorbed in the micropores may be 30–50%, or higher. As the oxygen-containing groups dissipate with coal maturation, water content decreases as part of the volatiles emitted.

2.2.5 Proximate Analysis

By definition, coal must contain at least 50% of its weight, or 70% of its volume as organic, carbonaceous matter. A proximate analysis is a common laboratory procedure to provide fundamental composition of the coal.

Proximate analyses of coal provide the percentage composition in coal of the following:

- Ash.
- Fixed carbon.
- Volatile matter.
- Moisture.

The tests are specified by procedure D-3172, ASTM Standards. Each of the four measured parameters has significance to the CBM process.

The ash measured in the proximate analysis represents that part of the mineral matter left after thermal degradation of the sample by combustion (ASTM D-3174). A small (1–2 gram) sample of the coal is completely burned in air at 725 ±25°C. The residue is the ash content. It has a value near that of the percentage of mineral matter. An increasing ash content, from a proximate analysis indicating mineral matter, proportionately lowers the amount of methane that can be adsorbed. Mineral matter also has a deleterious effect on fracturing in the coal. Being a determinant in limiting cleat formation and gas content, mineral

matter thus impacts two of the most important parameters in the commercial CBM—permeability and adsorbed methane capacity. The inorganic particles that comprise the ash of the analysis are distributed throughout the coal as clay minerals, carbonate minerals, sulfide minerals (pyrite), and silica minerals (quartz).

Moisture content affects methane adsorption capacity. Moisture contents are determined (ASTM D-3173) by heating a small coal sample for 1 hour in a vacuum or in a nitrogen atmosphere to 107 ±4°C. The weight loss as a percentage of the original sample is reported as moisture content. Before beginning the analysis, the sample is crushed to <60 mesh.[2]

Volatile matter is determined from the thermal decomposition, without oxidation, of a 1-gm crushed sample (<60 mesh) at 950 ±20°C for 7 minutes in a muffle furnace (ASTM D-3175). Volatile matter and fixed carbon of the proximate analysis are used to specify higher coal ranks above hvAb in the United States.

Carbon content increases with maturation until graphite of 100% carbon would be reached ultimately. Fixed carbon from the preceding three tests is calculated using Eq. 2.1.

$$\%FC = 100 - (\%Ash + \%H_2O + \%VM) \qquad (2.1)$$

where:

FC = calculated fixed carbon of the coal
$\%Ash$ = measured by ASTM D-3174
$\%H_2O$ = measured by ASTM D-3173
$\%VM$ = measured by ASTM D-3175

The percentages of ash, fixed carbon, volatile matter, and moisture of the proximate analysis may be presented on the following bases:

- As received—Percentages based on all four measured components, which represent the coal as received in the laboratory, approximating the conditions in the seam.
- Ash-free (AF)—Percentages based on three measured components without inclusion of ash.
- Dry—Percentages based on the three components of volatile matter, fixed carbon, and ash.
- Dry, ash-free (DAF)—Percentages based on the two components of volatile matter and fixed carbon.

Table 2.3 gives a proximate analysis for an hvAb coal presented on an as-received, dry, and dry ash-free basis for comparison. Note that volatile matter and fixed carbon percentages appear regardless of the basis on which the analysis is made.

Table 2.3—Example Proximate Analysis

	As Received (%)	Dry (%)	DAF (%)
Moisture	1.4	—	—
Volatile Matter	36.3	36.8	41.3
Fixed Carbon	51.6	52.3	58.7
Ash	10.7	10.9	—
Total	100.0	100.0	100.0

Ash content of coals can vary significantly from seam to seam in the same CBM or over several vertical feet of a single seam. The inhomogeneity affects gas content estimates and physical properties, although the inhomogeneities are seldom compensated for in gas content estimates because such extensive coring and analysis would be impractical. In an effort to circumvent the difficulty and estimate fixed carbon and volatile matter from well logs, Hawkins, Schraufnagel,

and Olszewski noted that the volatile matter and fixed carbon content of proximate analyses are linearly related to the ash content.[29] If the proximate analysis parameters of a formation could be evaluated from well logs, a more continuous analysis would result to account for inhomogeneities. For example, if density from geophysical logs could be correlated with ash content, the proximate analysis could be estimated from calculated ash content to give a practical solution without numerous cores and proximate analyses. Their correlations from core data of moisture, volatiles, and fixed carbon content with percentage of ash are given in Fig. 2.10 for the San Juan basin, where the linear relationship holds even though data were taken from three wells over a 40-sq mi area.

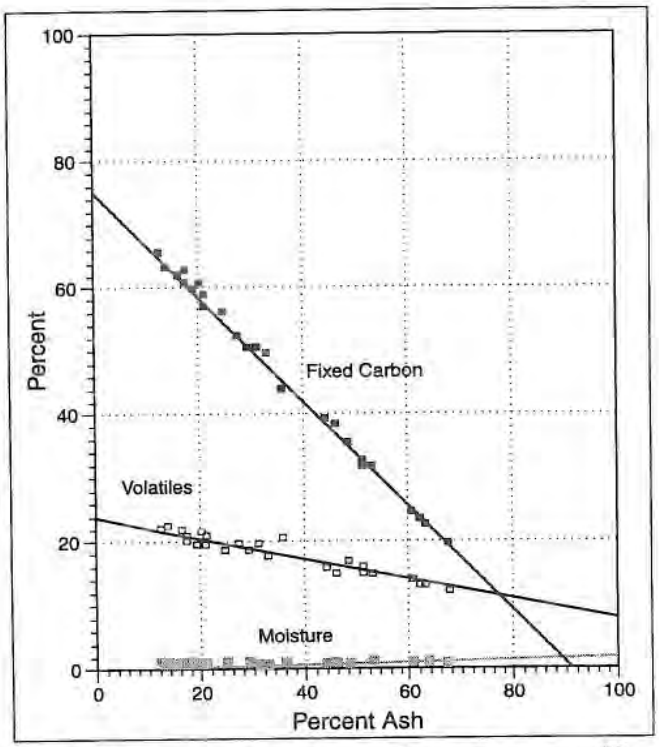

Fig. 2.10—Proximate analyses of Fruitland coals.[29]

Fig. 2.11 shows the wide variation of ash content from 10 seams over 1,235 vertical ft of a single well in the Appalachian basin.[29] Again, the linear relationships hold for moisture, ash, and volatiles with ash content.

A problem to be resolved with the technique is the correlation of the density with ash content. Core analysis provides the standardization of the logs, but the standardization remains site-specific.

Technical advancements, such as the use of well logs to characterize a coal reservoir, are needed to make the CBM process more economical in the future, especially prospective properties that might be marginally profitable.

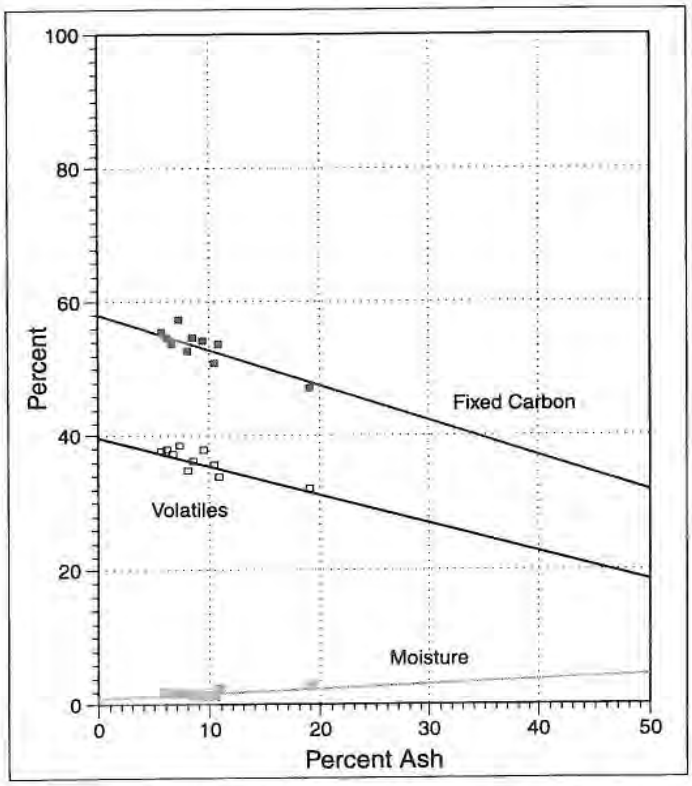

Fig. 2.11—Proximate analyses of Appalachian basin coal.[29]
Copyright 1992 Society of Petroleum Engineers.

2.2.6 Ultimate Analysis

Ultimate analysis provides the elemental composition of oxygen, carbon, hydrogen, sulfur, and nitrogen.

The annual book of ASTM standards presents the standard method for ultimate analysis as procedure D-3176. It specifies that carbon and hydrogen of the coal will be determined from the gaseous products of the material's complete combustion (D-3178). The total sulfur (D-3177), nitrogen (D-3179), and ash (D-3174) are to be determined from the entire material in separate calculations. For lack of a suitable test for oxygen, its percentage content in the coal is determined by subtracting from 100 the sum of the percentages of the other components. A small error is taken for granted but cannot be compensated for in the procedure because some hydrogen and oxygen will be derived from the bound water of clay, shale, or carbonate impurities in the coal.

The elemental analysis of coal obtained by this procedure, when converted from a weight basis to a mole basis, provides the ratios of O/C and H/C used in the van Krevelen diagram[7] to define the maturation state of coal.

The following ultimate analysis[30] applies to a mvb coal of the Blue Creek seam of the Warrior basin that contains 4.82% ash: (1) carbon, 83.46%; (2) hydrogen, 4.39%; (3) nitrogen, 1.81%; (4) sulfur, 0.47%; and (5) oxygen, 5.05%.

2.3 Significance of Rank

Coal progresses through a maturation process driven primarily by temperature and secondarily by time and pressure that goes from the freshly deposited organic matter in swamps to a graphite-like material at the end of the progression. Physical as well as chemical properties of the coal change along the route, and properties that are stereotyped for discrete points in the maturation are developed. Rank is used to define these discrete points in the maturation process. Rank is a harbinger of success of any prospective CBM venture because it

implies the potential for gas content, permeability, and mechanical and physical properties of the coal.

Rank may vary laterally and vertically within a seam, and it varies from seam to seam within a given coal group.[31]

2.3.1 Definition and Measurement

Designation of rank as a measure of the coal maturity is given in Table 2.4. Coals are divided into lignitic, subbituminous, bituminous, and anthracitic classes, and further subdivided into 13 groups. Coals of the bituminous class are most sought after in the CBM process because most properties are optimum at this rank. Specifically, coals of hvAb through lvb are best. More gas has been generated by this point in the maturation process and retention capabilities have been improved. Also, physical properties and mechanical properties of the coal as a reservoir rock are optimum.

Table 2.4—ASTM Coal Rank

Class	Group	Abbreviation
Anthracitic	Meta-Anthracite	ma
	Anthracite	an
	Semianthractie	sa
Bituminous	Low Volatile	lvb
	Medium Volatile	mvb
	High Volatile A	hvAb
	High Volatile B	hvBb
	High Volatile C	hvCb
Subbituminous	Subbituminous A	subA
	Subbituminous B	subB
	Subbituminous C	subC
Lignitic	Lignite A	ligA
	Lignite B	ligB

Physical properties often reach a maximum or minimum at the upper bituminous level with a better cleat system and propensity to fracture. Beyond the bituminous ranks, alterations in the chemical structure of anthracite lead to permeability regression.

As seen in the modified van Krevelen diagram of Fig. 2.5, the carbon content of coals increases, hydrogen content decreases, and oxygen content decreases with rank and maturity. That is, volatiles are being lost as maturation advances. The relationship suggests multiple properties that could be used to designate rank—notably carbon content, hydrogen content, or volatile matter. In fact, these three properties are used to designate rank.

Not only are the preceding three properties used, but other valid measures of rank also exist. For example, a common means to characterize rank of the bituminous and anthracite coals is by vitrinite reflectance, which uses the optical properties of the coal as those optical properties change with maturation. The vitrinite reflectance increases with maturation because of the aromatization of the molecular structure of coal as aliphatic groups are dissipated as volatiles, or converted to aromatics, especially in the bituminous range.[3,21] Therefore, vitrinite reflectance measurements in the laboratory make use of the steady progression of optical properties of the vitrinite maceral with geochemical reactions during steadily increasing temperatures. It should be noted that near 95% carbon content, the optical properties of vitrinite, inertinite, and liptinite converge.

Vitrinite reflectance to establish rank of bituminous coals has the following advantages: (1) steady increase of vitrinite reflectance with rank; (2) independence from composition or homogeneity of the reflectance measurement; (3) independence of sample size; and (4) minimal effects of oxidation.[19]

Berkowitz[2] used data from published sources of North American and European coals to prepare the correlation of vitrinite reflectance with coal rank in Fig. 2.12. Note the lack of scatter in the data (reproducibility within 0.08%) despite coming from independent sources.[3] The steady increase of the reflectivity through the

bituminous coals (as a function of increasing aromaticity) and the reproducibility of its measurements make it an important means to accurately identify rank, especially at the high ranks where reflectivity is highly sensitive to changes in carbon content.

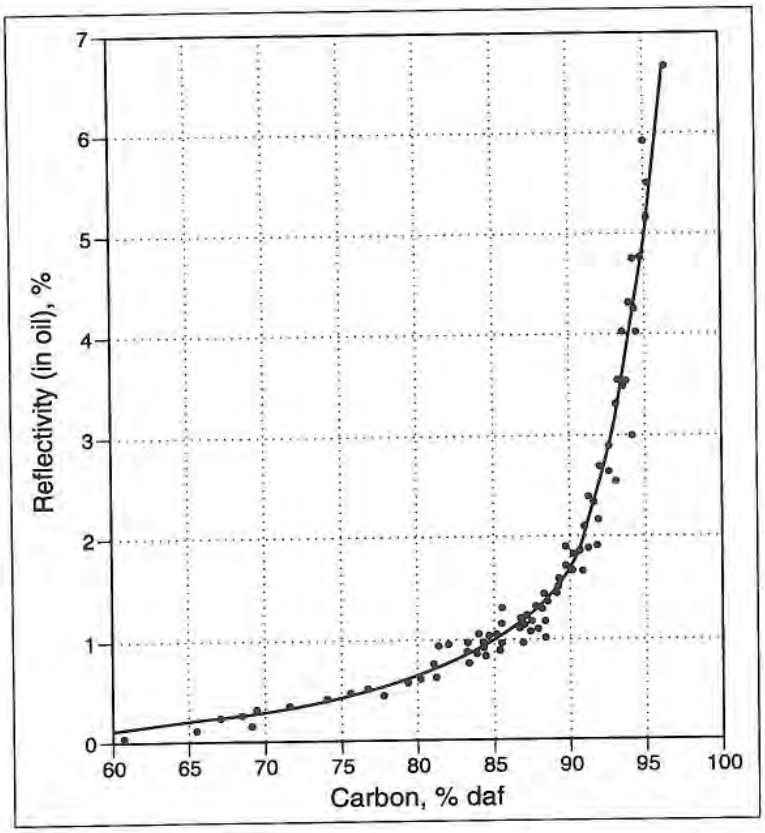

Fig. 2.12—Vitrinite reflectance by rank.[2]

Vitrinite reflectance, fixed carbon content, and percent volatile matter are convenient measures of coal maturity at higher ranks. However, caloric heating

values may be used to distinguish lower rank coals.[13] Also, moisture content in the lower ranks changes steadily in the early stages of maturation and is a reliable indicator of lignite and subbituminous coals. Since the CBM process is more concerned with the higher-rank coals, moisture and heating value are not often used as rank indicators in the CBM industry.

There are various means to establish rank. The ASTM establishes percentage of fixed carbon content and percentage of volatile matter on a dry, ash-free basis as the standard for designating ranks of coals at hvAb or higher in America. In Europe,[21] the designation of rank may be based on percentage of carbon in the elemental analysis on a dry, ash-free basis, rather than on a percentage of fixed carbon. Universally, an important criterion that is highly accurate for the high-ranking coals most encountered in CBM projects, and which is also independent of maceral content variations, is the maximum vitrinite reflectance. As seen in Fig. 2.12, reflectivity is sensitive to minor carbon content changes above approximately 85% carbon, daf. Below hvAb, calorific content or percentage of moisture best indicates the rank. Comparisons of the methods for designating rank are presented in Table 2.5.

Table 2.5—Parameters Determining Coal Rank

Rank	Maximum Reflectance (%)[a]	Volatile Matter (%)	Fixed Carbon (% daf)[b]	Carbon Content (% daf)[c]
an	>3	2 to 8[b]	>92	>92
sa	2.05 to 3.00	8 to 14[b]	86 to 92	91 to 92
lvb	1.50 to 2.05	14 to 22[b]	78 to 86	89 to 91
mvb	1.10 to 1.50	22 to 31[b]	69 to 78	86 to 89
hvAb	0.71 to 1.10	>31[b] 31 to 39[c]	<69	81 to 86
hvBb	0.57 to 0.71	39 to 42[c]		76 to 81
hvCb	0.47 to 0.57	42 to 47[c]		66 to 76
sub	<0.47	>47[c]		<66

[a] *Davis.*[32]

[b] *ASTM D–388–88 (Proximate Analysis)*

[c] *Stach.*[21]

The interrelationship of vitrinite reflectance, carbon, hydrogen, H/C, and volatile matter used to establish rank is given[21] in Fig. 2.13. Note the change of carbon content at the coalification break that occurs at about 85% carbon content.

Values of vitrinite reflectance[32] and Fig. 2.13 and ASTM standards are combined in Table 2.5 to give reference values of reflectance, volatile matter, fixed carbon content, and elemental carbon content for the coal ranks. Reflectance values range from 0.47 to greater than 3 for high-volatile bituminous C to anthracite coals, while elemental carbon content on a dry, ash-free basis goes from 66% to greater than 92% over those ranks.

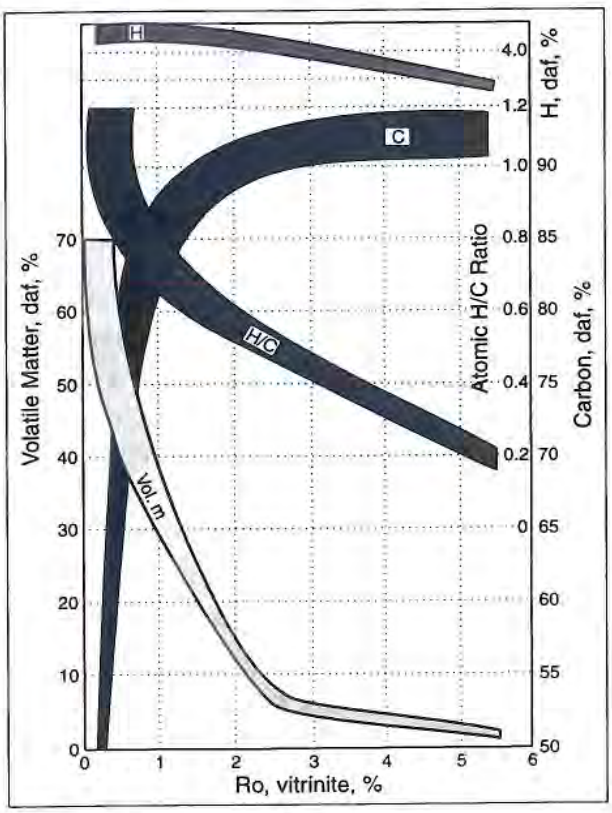

Fig. 2.13—Measures of rank.[21]

2.3.2 Vitrinite Reflectance Measurement

The macerals of the coal may be distinguished under the microscope by means of their different light-reflecting properties. Vitrinite can even be viewed without microscopic assistance.[7] Further, the stage of maturation can be defined by a quantitative measurement of the light reflected by the vitrinite maceral from a vertical beam of incident light of a specified wavelength,[19] typically 546 nm.[3] Submerged beneath an oil under incident light, the macerals give the following appearance: (1) vitrinite, dark-light gray; (2) liptinite, dark; and (3) inertinite, highly reflective.[16] The reflected light is measured from the surface of a highly polished coal sample submerged under the standard oil of specified refractive index, typically 1.518 at 23°C,[3] to improve image contrast.[16]

The reflectance may be calculated from Eq. 2.2.

$$R_o = \frac{[(n - n_o)^2 + n^2 k^2]}{[(n + n_o)^2 + n^2 k^2]} \qquad (2.2)$$

where

Ro = reflectance of vitrinite under oil
n_o = refractive index of the oil
n = refractive index of the maceral
k = absorptive index of the maceral

Measurement of vitrinite reflectance is a straightforward laboratory procedure governed by ASTM standards.[33] The surface of the coal sample is polished[34] and reflected light, filtered to a monochromatic green, is determined with a microscope of magnification between 500X and 750X; calibration is made against reflectance of standard optical glass prisms. The sample is analyzed under oil of specified refractive index.

The reflectance under oil, R_o, varies by about 8% in its value, depending upon the orientation of the sample. Therefore, maximum reflectance values are recorded and a mean maximum reflectance reported from at least 100 measurements from the polarized light. These measurements must be reproducible within ±0 02 of actual percent reflectance.

Polarized light is preferred for the reflectance measurement. If, however, non-polarized light is used, a random reflectance is measured. The relationship between the maximum reflectance, $R_{o,max}$, and the random measurement, $R_{o,random}$, is approximated by Eq. 2.3.

The standard procedure for making the mean maximum reflectance measurement is specified by ASTM D 2798, "Microscopical Determination of the Reflectance of the Organic Components in a Polished Specimen of Coal," and D 2797 for the preparation of the coal sample.

$$R_{o,\max} = 1.066 \times R_{o,random} \qquad (2.3)$$

Law and coworkers used vitrinite reflectance to estimate the thermal and burial history of coals in the Piceance basin. The correlation of vitrinite reflectance with burial depth of organic matter shows a discontinuity as presented in Fig. 2.14.[26] The Cameo coals between 5,550 and 5,750 ft were analyzed from core samples and found to contain mainly the vitrinite maceral and to have matured at 260–265°F to mvb rank of reflectance 1.20–1.29%.

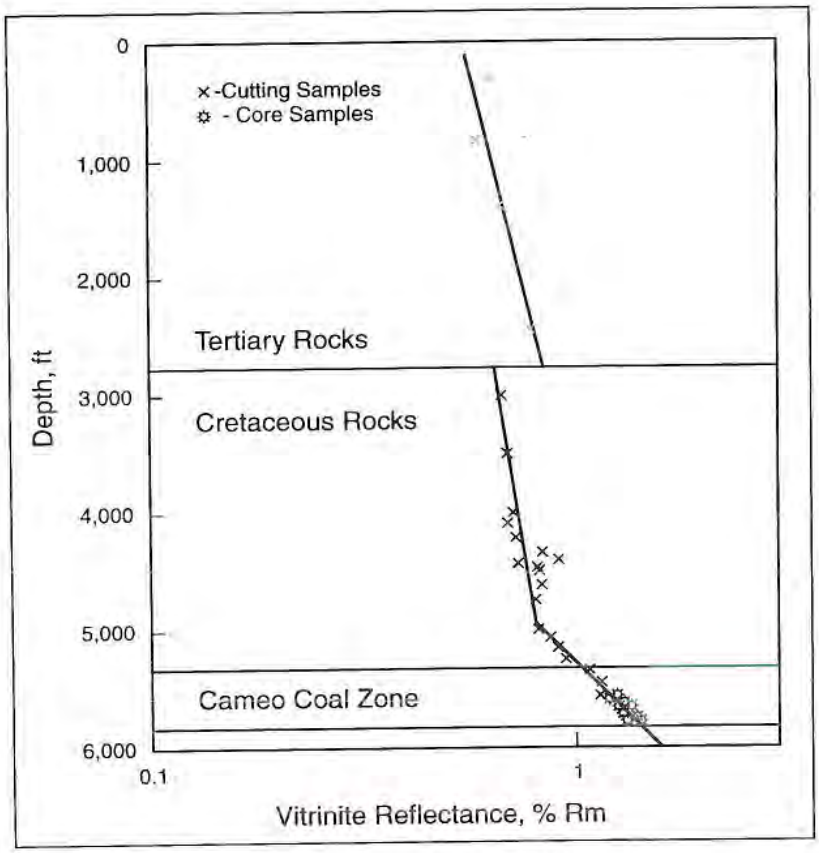

Fig. 2.14—Depth influence on coal maturity.[26]

2.3.3 Physical Properties

The designation of rank implies physical properties of the coal since the properties attain characteristic values for each rank. Most of these properties peak as minimum or maximum values in the mid-bituminous classes.

Compressive strength of coal varies with rank. Compressive strength reaches a minimum at a fixed carbon content near the beginning of the rank of high-volatile A bituminous and persists through the medium volatile bituminous rank (see Fig. 2.15). Implications of low compressive strength in the mid-bituminous range are the generation of natural fractures and cleats in the coal if subjected at that particular stage to undue stresses from tectonic action or from matrix contraction as a result of volatiles or moisture loss.

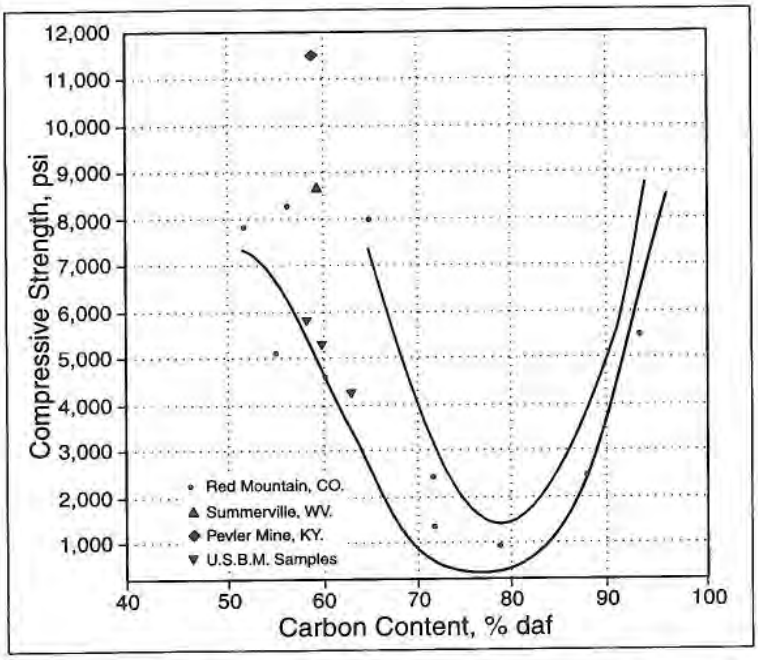

Fig. 2.15—Coal's unconfined compressive strength by rank.[35]

The coals at that stage would be conducive to hydraulic fracturing or cavity completions. The lack of compressive strength also has implications for withstanding induced stresses during drilling or completion of a CBM well.

The cleat system of the coal varies with rank partly because brittleness increases with rank. Fractures do not develop in lignite because it is ductile at that low rank. As seen in Fig. 2.15, subbituminous and lignite have relatively high compressive strengths. The cleat system reaches its maximum development with hvAb to lvb. In that range, the coal becomes friable and easily disintegrates. As the coals mature further to anthracite, the cleats close, possibly from molecular crosslinking reactions that bridge across the fractures and leave the healed fractures that may be visible.[19] Also, it is evident from Fig. 2.15 that the higher compressive strength of anthracite would make it more difficult to fracture.

Thermogenic methane evolves at an accelerated pace in the mid-bituminous ranks. If the gas is not lost from the coals, a progression of rank should be evident in an increase of gas content of the coal. However, the additional gas may have been lost over geologic time at lower pressures by erosion or uplifting, by faulting, or by other mechanisms. An idealized concept of the increase of gas content with rank is shown by Kim in Fig. 2.16.[36]

Pore size of coal is the largest in lignite. Porosity, the fraction of the bulk volume that is void space, decreases to a minimum with low-volatile bituminous coals before increasing again with the anthracites (see Fig. 2.17).

In the low-rank coals, two or three molecular layers of aromatic clusters of 5 to 10 aromatic rings exist in a stack of about 10–15 A° diameter.[21] In these low-rank coals, aliphatic groups containing oxygen link the multilayered stacks. The aliphatics and oxygen functional groups at that point have not yet been dissipated as volatiles in the coalification process. The nonaromatic linkages in low-rank coals act as a standoff between stacks of aromatic clusters to create relatively large micropores between the stacks. The oxygen of the linkages helps bind moisture in the micropores. The consequence on porosity is seen in Fig. 2.17. As the coal matures, it is compressed with increasing burial depth. Oxygen-containing compounds and other volatiles are lost, water is lost, and the multilayered stacks rearrange to make their micropores smaller.

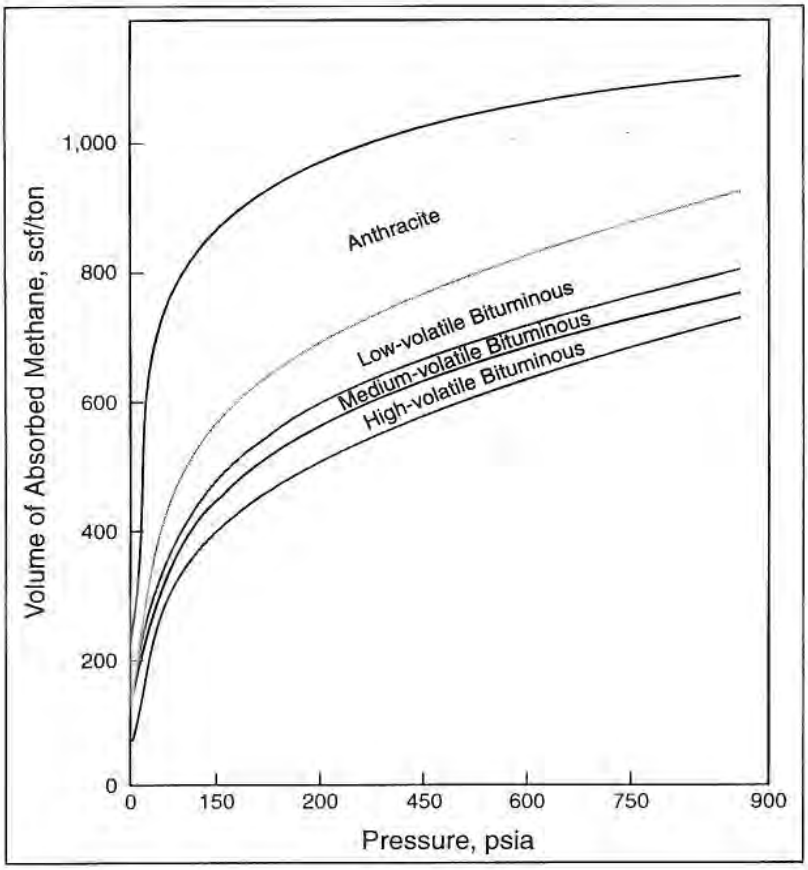

Fig. 2.16—Gas content of maturing coals.[36]

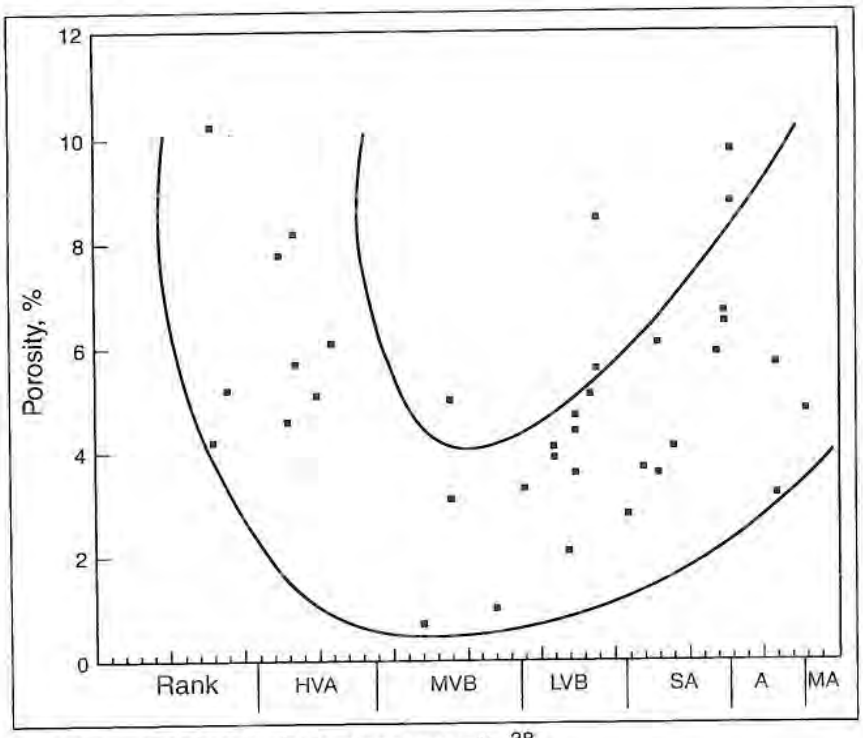

Fig. 2.17—Coal rank determines porosity.[38]

Moisture content also varies over the wide range from lignite to anthracite as the coals assume characteristic chemical and physical properties. Bed moisture, also called inherent or capacity moisture, is contained in the micropores and capillaries of the coal matrix and is characterized by a lower vapor pressure than normal. Because of more and larger micropores, shallower depths, and retention forces of oxygen in functional groups of the molecular structure, the lower-rank coals have large bed-moisture contents. This water trapped within the matrix is highest for the lowest-rank coals and decreases (as illustrated in Fig. 2.18) as carbon content increases to the bituminous coals. The bed moisture reduces the

adsorptive capacity of the coal for methane because it occupies so much of the available space in the micropores for adsorption sites.

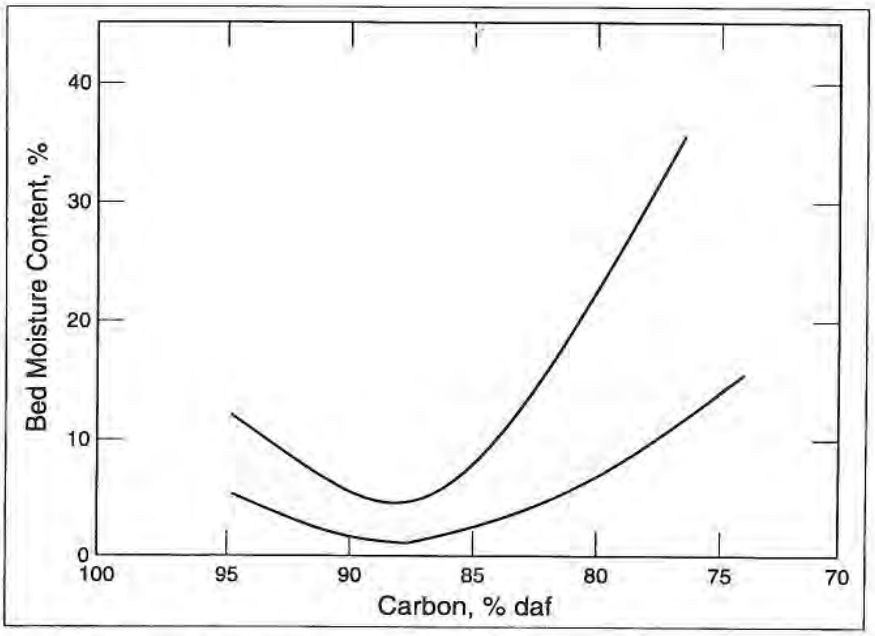

Fig. 2.18—Influence of rank on capacity moisture.[2]

Besides bed moisture, another type of moisture is held in the cleats and natural fissures of the coalseam. It is free moisture, also referred to as adherent, bulk, or superficial moisture. Free moisture is not included in Fig. 2.18 but is instead dependent upon the extent of natural fracturing and saturation of the coals. Free moisture depends on a large secondary porosity of the natural fracture system of the coal. There, free moisture reduces relative permeability to methane flow and is part of the hydrostatic head that controls desorption.

Not included in Fig. 2.18 is the hydration moisture of inorganic minerals entrapped in the coal. Also, the graph does not refer to any water that might be chemically formed during high-temperature pyrolysis or coalification.

Apparent densities of coal are measured by the displacement of a liquid by the coal. The apparent density varies with rank of the coal as determined with water by Franklin[37] and presented in Fig. 2.19. Note again the minimum value of a physical property of coal in the upper bituminous ranks. In this case, the trend of density reflects relative values of cleats, pore volumes, and compositions. When anthracite is reached in rank, cleat and pore volumes are being reduced; the orderly arrangements of the aromatic clusters create a more compact matrix and thus increase bulk density.

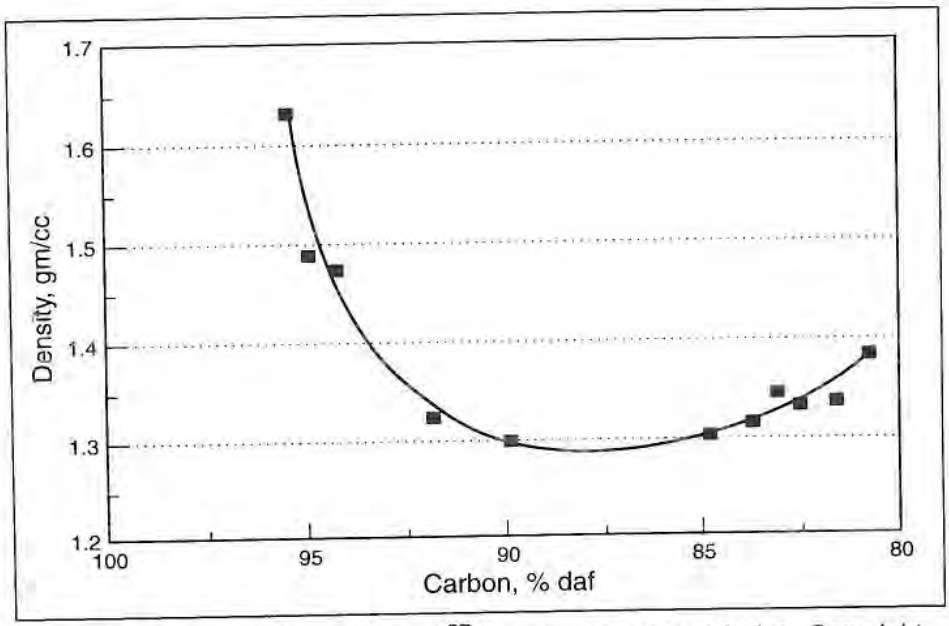

Fig. 2.19—Apparent density of coal.[37] Reprinted with permission. Copyright 1948 Butterworth-Heinemann Ltd.

Although the Hardgrove grindability index (H.G.I.) is commonly used to select coal to be powdered for coal-fired furnaces, the index has significance to the CBM.[3] H.G.I. is related to the attrition of a coalseam from the flow of sand-laden fracturing fluid, to the penetration of the seam by a drill bit, or to the bursting of

the coal upon fracture initiation. The index is a measure of the pulverizing tendency of the coal. The H.G.I. is obtained by grinding a 50-gram sample of sieved coal of -16 to +30 mesh in a ball mill under specified conditions (ASTM D 409-72) and afterward determining the weight of the sample contained as particles of size -200 mesh.[39] The index is then given by Eq. 2.4.

$$H.G.I. = 13 + 6.93\ w_p \qquad (2.4)$$

where

$H.G.I.$ = Hardgrove grindability index
w_p = weight of -200 mesh product

As with most of the physical properties of coal, the Hardgrove index varies with rank. In the case of Fig. 2.20, rank is represented by percentage volatile matter. The index reaches a peak value with medium-volatile and low-volatile bituminous coals[2] in those ranks of primary interest to the CBM process.

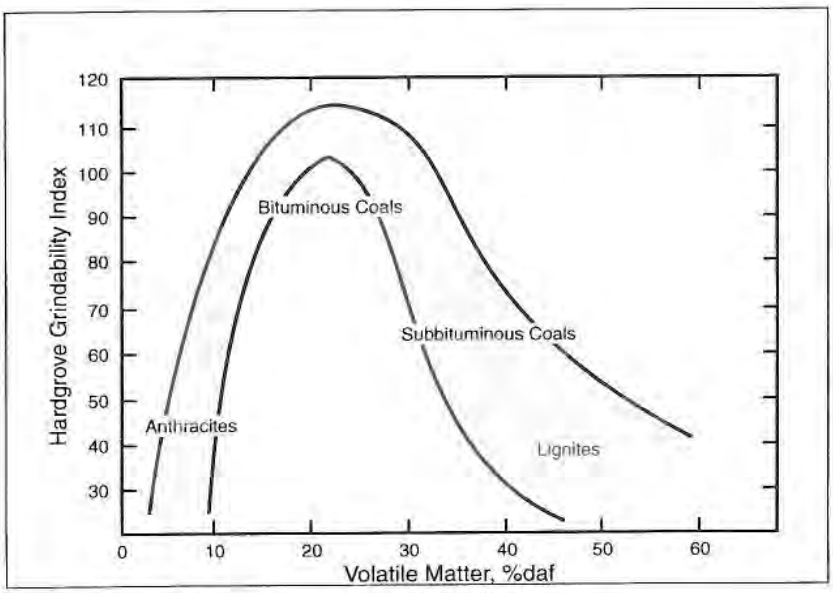

Fig. 2.20—Pulverizing tendency of coal.[2]

Low-rank coals are ductile. Mechanical energy input to them deforms the coals but does not easily break them. (Explosives may be necessary to displace lignite in mining.) In contrast to these lignites and subbituminous coals, the bituminous coals of higher rank are brittle, and the mechanical energy input readily breaks the hvAb, mvb, and lvb coals. The phenomenon is apparent by the correlation of brittleness with rank in Fig. 2.21 and helps explain the likelihood of a developed cleat system in the high-rank bituminous coals and not in ranks below hvAb. The property has obvious importance to CBM production since the viability of the process depends on good permeability being attained by fractures.

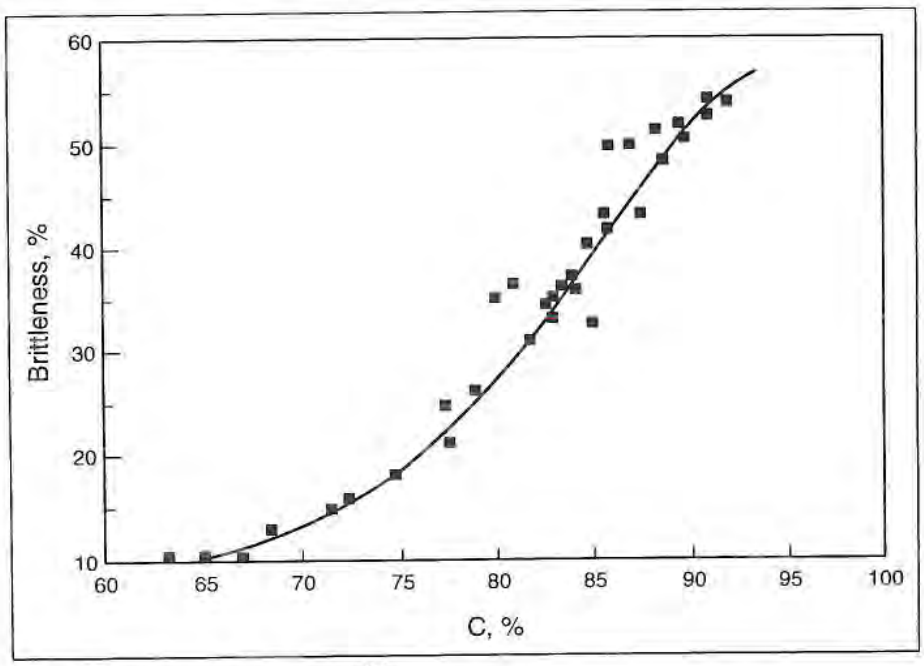

Fig. 2.21—Brittleness of coal.[15]

2.3.4 Volatiles Generated

Fig. 2.22 illustrates the relatively small amounts of thermogenic methane produced in the lower ranks of coal. Rapid generation of methane begins at a carbon content of about 85%, daf basis.[15] Thus, the implication for methane production from a prospective, low-rank coal is that much of the methane must come from biogenic sources.

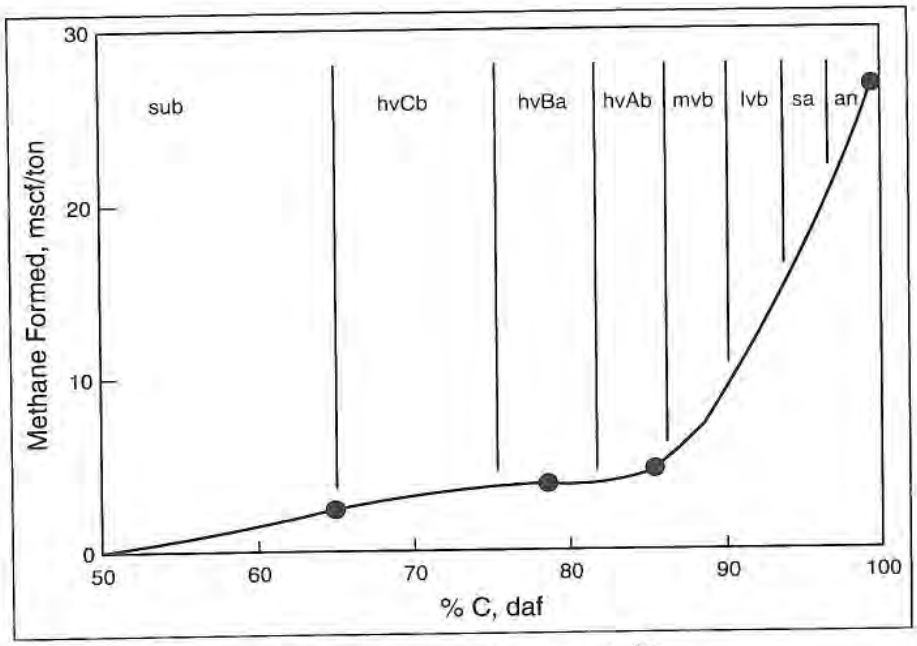

Fig. 2.22—Thermogenic CH_4 generated from coals.[15]

In completing the maturation process, more methane is generated than can be retained—10 times as much in some instances. Gas content is further dependent on the efficiency of retention, as determined by rank, pressure, ash, and bed water content. Of the volatiles generated, the quantity retained also depends on

permeability and faults of the surrounding rock as well as depth, which control the methane's capability to dissipate to adjacent sands or to the surface.

It is evident from Fig. 2.22 that bituminous coal is a prolific source rock for methane. Further, one can surmise that methane not retained by its coal source could charge adjacent sands under proper permeability and trapping conditions.

Methane originates from the liptinite, vitrinite, and inertinite in decreasing order. Temperatures in the coals of 200–300°F over geologic time are required to generate the methane.

2.3.5 Micropores

Coal has a dual pore system of macropores and micropores. In laboratory tests, mercury is accessible only to the macropores or cleats and other natural fissures, but helium is accessible to micropores as well as to macropores. Mercury is excluded by the size of the small openings of the micropores.

The micropore cavities are estimated to have a maximum 40-Angstrom diameter and have connecting passageways of 5–8 Angstroms diameter in coals of interest in the CBM process.[2] Van Krevelen estimates an average micropore cavity diameter of 20 Angstroms based on surface area data.[7] These pore sizes are not uniform. They are not unimodal in distribution, and they change with the molecular reorientation of rank change.[16]

Since the total heat of adsorption released depends on the internal surface area accessible to the molecules, Bond[40] was able to show that a bimodal distribution of 5- and 8-Angstrom diameter passageways blocked the entrance to the cavities as he measured heats of adsorption involving adsorbate molecules of these critical diameters.

A postulated micropore system is envisioned in Fig. 2.23 from the report of Zwietering and van Krevelen.[41]

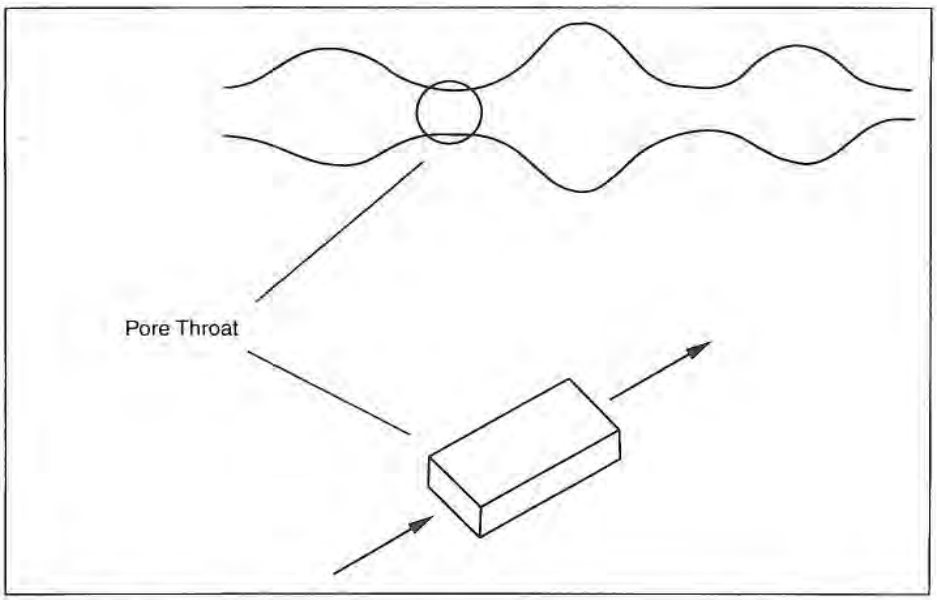

Fig. 2.23—Coal micropore geometry.

The passageways controlling entrance to the cavities may exist as flat, parallel plates of 5 or 8 Angstroms distance between. The cavities that the constricted passageways lead to may also exist as space between flat, parallel plates of the aromatic clusters with distances up to 40 Angstroms apart but averaging 20 Angstroms.[7] The plate configuration is suggested by the plate-like clusters of aromatic molecules in the structure of coal.[16] Nonaromatic linkages of aliphatics and oxygen functional groups between the plates are dissipated as coalification moves into the bituminous ranks.

The model of the micropores in Fig. 2.23 suggests that temperature fluctuation could change the aperture diameter. In fact, lowering the temperature to 77°K in the laboratory causes contraction of the matrix and restricts entry to the micropores of coal to only helium, constricting the openings to the extent of excluding nitrogen and methane.

The model also suggests a pore-opening access that could be blocked or restricted by hydrocarbons heavier than methane liberated in the micropores, such as the paraffins experienced in some CBM wells of the San Juan basin.

It is also understandable from this concept of micropore geometry that reported clearing of the paraffin obstructions can be accomplished with induced microbial action. In these cases, injecting microbes has resulted in increased methane production.

Another implication of the pore model is the constriction of the pore openings as a consequence of swelling of the coal matrix caused by adsorption of CO_2 or other substances having strong adsorptive affinities.

2.4 Cleat System and Natural Fracturing

The network of natural fractures and cleats in a coal determines to a large extent the mechanical properties of the coal and the permeability of the coal.[42] Therefore, to complete a well and produce CBM, it is necessary to understand the genesis and function of the variety of natural fractures.

A fully fractured coal may have the following natural fractures:

- Face cleats (primary).
- Butt cleats (secondary).
- Tertiary cleats.
- Fourth-order cleats.
- Joints.

Face cleats are the continuous fissures of the common orthogonal set found in coals. These primary cleats are longer and generally have wider aperture openings than the butt cleats found approximately perpendicular to them. Face cleats form before butt cleats as evidenced by their continuous nature. Well interference observed during production of water and gas in the Warrior and San Juan basins attests to sometimes long distances of open, interconnected cleats.

Methane moves through the face and the butt cleats to the wellbore, and the permeability of the coal is dependent on them. Permeability anisotropy results because the face cleats usually give a directional permeability toward their orientation, for example, 25 md of face cleats vs. 9 md of accompanying butt cleats.[43] In the San Juan basin, the permeability in the face cleats is expected to be at least 2.8 times greater than in the butt cleats. In other basins, directional permeability ratios of 4 to 1 are reported, and even greater values exist.

The third and fourth order cleats (if present) develop later than face and butt cleats, so they terminate at the face and butt cleats.[44] The higher-order cleats may be characterized as being 45° to their primary and secondary counterparts.[45] In the fairway of the San Juan basin, these higher-order fissures boost the permeability of the coal and assist in the success of cavity completions.

Joints are natural fractures that often run parallel to the face cleats.[27] They form at a later time than the face cleats and occur in the formation much further apart than cleats. The faces of joints show no slippage relative to each other. Joints may traverse the coals vertically, crossing interbedded inorganic layers and crossing the interface of the bounding rock. Thus, the joints can improve vertical permeability and be important for high-producing wells.[44] They are farther apart than any of the four orders of cleats.

Four mechanisms are proposed for creation of the cleating system of coals:

- Dehydration during coalification.
- Devolatilization during coalification.
- Tectonic forces.
- Compaction.

Loss of water and loss of volatiles have related effects upon cleating. Large volumes of water are held in the pores of lignite and subbituminous coals (30–40%), trapped and compressed by the organic sediments during peatification. The many oxygen functional groups in the immature coals have an affinity for the water to help hold the water in place. As pressures and temperatures progress, volatiles containing oxygen are dissipated because of the

geochemical reactions. The maturing coals, therefore, progressively lose water. The loss of oxygen-containing volatiles and water results in a shrinkage of the coal matrix, initiating cracks. As the coalification continues past hvAb, methane release is accelerated. Elevation of the pore pressures of the coal results in further cleavage of the coal matrix.

As an example of the extent of dewatering and compaction, coalbeds in the Powder River basin that are now 100–200 ft thick were once over 700 ft thick.[30]

Tectonic force as a mechanism causing cleating is readily accepted. Tectonic forces fracture the coals, especially if the action occurs after the high-volatile bituminous stage is reached and physical properties have reached a state prone to fracturing.

Compaction as a mechanism in cleating is not thought to be a major factor. The regular spacing of cleats or the uniform directional trends of cleats would not have occurred from an irregular differential compaction of organic sediments.

The mechanisms that cause cleating may create highly variable cleat frequencies in different coals. Less space between cleats or higher cleat frequency is important in elevating permeability of the coal. Cleats may be 0.1 in. apart for lvb coals to 3 or 4 ft apart for lignite.[27] The frequency is highly variable. Why? Four factors establish cleat frequency when tectonic forces and matrix shrinkage from water and volatiles losses occur:

- Lithotypes and maceral types.
- Thickness of coal/inorganic interbedding.
- Rank.
- Current depth and historical burial depth.

Lithotypes are the macroscopic population of specific macerals in the coal. They are discernible by the naked eye as bands. Lithotypes of main importance to the CBM process are vitrain and clarain. Vitrain contains primarily the vitrinite maceral and only small amounts of liptinite and inertinite. It appears as the bright band so familiar in coal. Clarain is the lithotype containing only small amounts of

vitrinite but more inertinite and liptinite interspersed with mineral matter. Clarain appears as a bright coal but duller than vitrain. Vitrain is friable; clarain is tough.

Fracturing occurs more readily in vitrain and thus the cleats are closer together in vitrain. Fracturing is suppressed by the inertinite maceral. High percentages of the inertinite maceral reduce the capability of the coal to cleat.[12] Therefore, a direct indication of fracture extent and potential coalbed process success is the presence of bright coals. Bright coals may have 30 times the number of cleats per unit length than do dull coals from the same mine.[27]

Mavor[44,46] found that the most extensive fracturing occurs in the San Juan basin in the coals of high rank with vitrain layers interbedded with discrete layers of shale. Differences of rock mechanical properties of the two layers contributed to fractures that have developed readily in the coal, terminating at the inorganic layer. Frequency of the cleats is inversely proportional to the thickness of the vitrain layers.

The presence of ash-forming minerals in the coal diminishes cleat formation regardless of the coal's rank. The presence of ash impacts the frequency and occurrence of cleats in the Fruitland coals as seen in Fig. 2.24.[45] Note that fracture frequency increases with lower ash content, and that the coal tends to disintegrate into rubble in those zones of low ash content. Clay and quartz tend to bind the coal particles together and decrease the natural fractures.

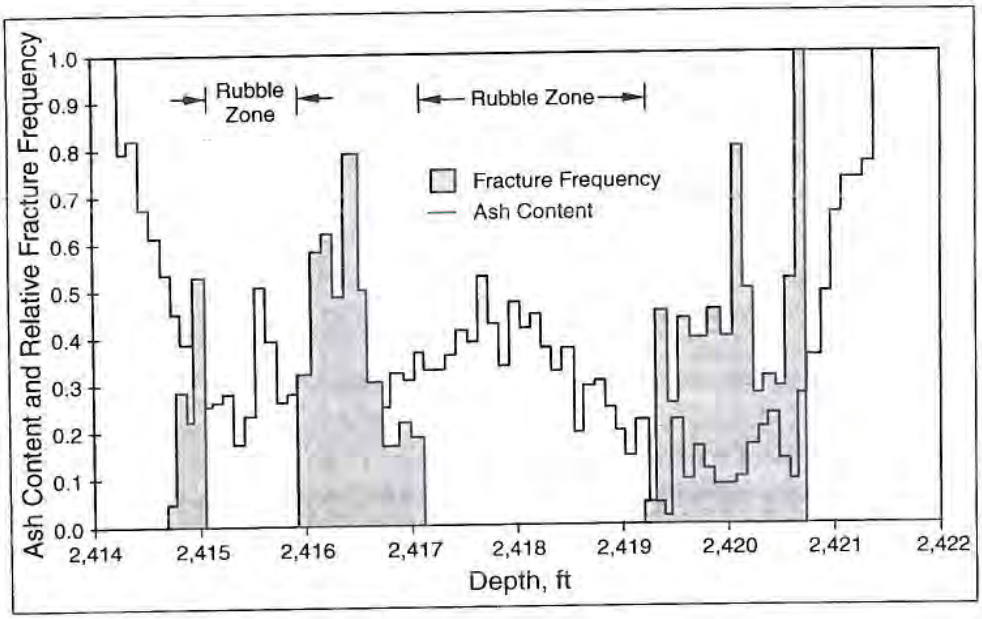

Fig. 2.24—Role of ash content in cleat formation.[45]

Thin bands of vitrain interbedded with thin layers of shale increase cleat frequency, but interspersion of the clay particles in the vitrain lithotype reduces cleat frequency.

Ranks of hvAb to lvb optimize cleat frequency.[47] At these ranks, compressive strength is a minimum and brittleness and Hardgrove grindability index are a maximum. Further along the maturation process, anthracite coals do not have the cleat system of the bituminous coals. Whether this is due to a different path during coalification, such as localized hotspots from igneous intrusion,[15] whether it is due to extremely high tectonic forces, whether it is due to a healing process of polymeric reaction across the crack interfaces, or whether the cleats become filled with minerals is not known. Possibly, crosslinking occurs across contact points of the cleat in which the fusion is influenced by the higher temperatures and pressures.

In a study by Law,[48] cleat spacing was measured in outcrops and cores of coals. The data were taken from bright-banded coals of beds at least 1 ft thick, so that these two facets in cleat frequency were essentially constant. The face-cleat spacing decreases with increasing rank, as determined by mean random vitrinite reflectance, in the exponential manner given in Fig. 2.25.

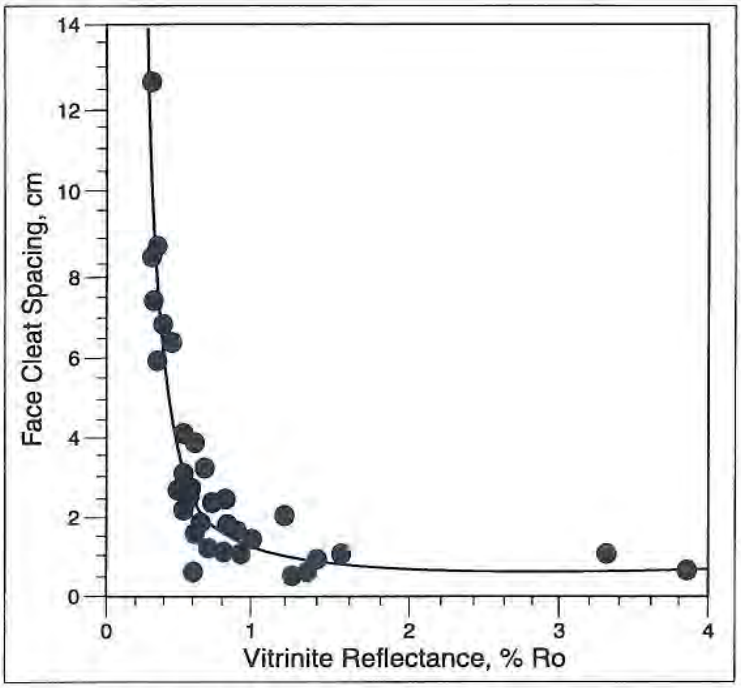

Fig. 2.25—Face cleat frequency.[48]

Law describes the relationship by Eq. 2.5.

$$C_f = 0.473\, e^{0.917/R_o} \qquad (2.5)$$

where

C_f = mean face cleat spacing, cm

R_o = % mean random vitrinite reflectance

For butt cleats, a similar relationship is given in Fig. 2.26. In this case, the mean butt-cleat spacing, Cb, is given by Eq. 2.6.

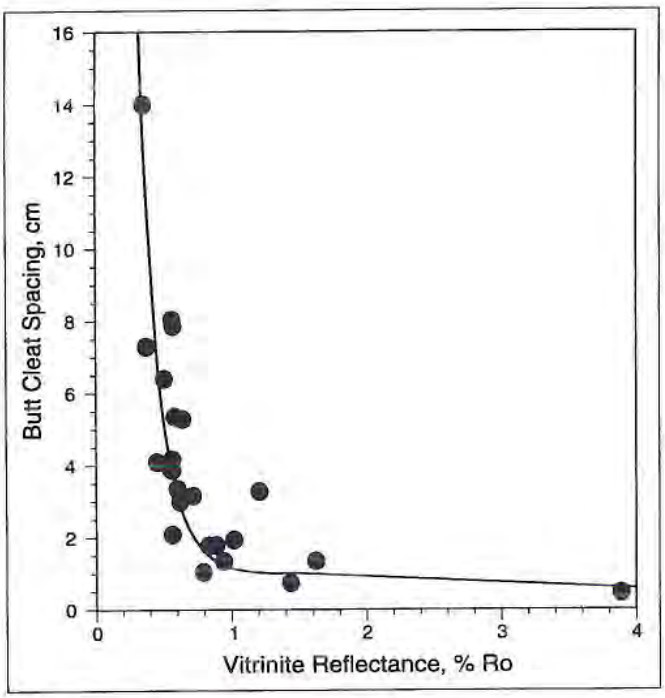

Fig. 2.26—Butt cleat frequency.[48]

$$C_b = 0.568\, e^{1.065/R_o} \qquad (2.6)$$

The impact of rank on cleat frequency is illustrated by two different cleat systems in the Fruitland of the San Juan basin. Coals of hvAb and mvb in the northwest part of the basin in Colorado exhibit extensive cleating and high permeability; coals of hvCb and hvBb in the south-central part of the basin in New Mexico exhibit very low permeability and poorly developed cleats. The difference is

attributed primarily to rank, because the cleats developed in mvb and hvAb but did not in hvCb or even in hvBb (see Table 2.6). Table 2.7 lists some characteristics of cleat frequency/cleat aperture width in the San Juan basin.[45]

Table 2.6—Rank Affects Cleat Development (*After* Mavor and McBane[46])

Location	San Juan Basin NW Location Colorado	San Juan Basin South–Central Location New Mexico
Formation	Fruitland	Fruitland
Rank	mvb	hvCb
Depth (ft)	2,408 to 2,452	2,226 to 2,246
Permeability (md)	36	0.004
Cleat Aperture Width (in.)	0.002	≈0
Cleat Frequency	25 per in.	≈0

Table 2.7—Cleat Characteristics San Juan Basin[45]

Well	Average Cleat Aperture Width (cm)	Average Cleat Frequency (cm^{-1})
Hamilton 3	0.06	3
Northeast Blanco Unit	0.02	6
Southern Ute Mobil 36–1	0.06	10
Colorado 32–7 No. 9	0.05	7
Southern Ute Tribal H	0.02	6
Southern Ute Tribal J	0.02	5

The fourth factor influencing greater cleat frequency is the deep burial of the coal followed by uplifting or erosion that drastically reduces overburden pressure.[27]

Calcite and pyrite present in the coal cleats indicate the minerals to have been deposited from the movement of water through a well-developed cleat system.[12] The mineral fillings may reduce the permeability of high-rank coals significantly.[48]

An extensive natural fracture network is essential for the development of a CBM property. With good permeability of a comprehensive natural fracture system in place, the role of the engineer becomes one of connecting the network to the wellbore by hydraulic fracturing or cavity completing. Difficulties may still arise from high in-situ stresses or man-made formation damage that reduce permeability of the fractures, but the presence of the cleats and joints presages a potential for commercial flow rates.

References

[1]Whitehurst, D.D.: "A Primer on the Chemistry and Constitution of Coal," Organic Chemistry of Coal, J.W. Larsen (ed.), ACS Symposium Series 71, American Chemical Society, Washington, DC (1978).

[2]Berkowitz, N.: An Introduction to Coal Technology, Academic Press, New York (1979) 345.

[3]Coal Geology and Coal Technology, C.R. Ward (ed.), Blackwell Scientific Publications, Australia (1984) 345.

[4]Larsen, V.E.: "Preliminary Evaluation of Coalbed Methane Geology and Activity in the Recluse Area, Powder River Basin, Wyoming," Quarterly Review of Methane from Coalseams Technology (June 1989) 6, No. 3 and 4, 2-9.

[5]Given, P.H.: "An Essay on the Organic Geochemistry of Coal," Coal Science, M.L. Gorbaty, J.W. Larsen, and I. Wender (eds.), Academic Press, New York (1984) 3, 70.

[6]Fassett, J.E.: "Geometry and Depositional Environments of Fruitland Formation Coalbeds, San Juan Basin, New Mexico and Colorado: Anatomy of a Giant Coal-Bed Methane Deposit," Proc., Coalbed Methane Symposium, Tuscaloosa, Alabama (November 1987) 19-35.

[7]van Krevelen, D.W.: Coal, Elsevier Publishing Company, Amsterdam (1961).

[8]Donaldson, A.C.: "Origin of Coalseam Discontinuities," Carboniferous Coal Guidebook, West Virginia Geol. and Econ. Survey Bull. B-37-1, 102-132.

[9]Ayers, W.B. Jr., Epsman, M.L., and Mink, R.M.: "Geologic Evaluation of Critical Production Parameters for Coalbed Methane Resources," Quarterly Review of Methane from Coalseams Technology (June 1989) 6, No. 3 and 4, 52-58.

[10]Campen, B.: "Exploring the Coalbeds of Montana," *Western Oil World* (July 1990) 24.

[11]Tissot, B.P. and Welte, D.H.: Petroleum Formation and Occurrence, second edition, Springer & Verlag, New York (1984) 699.

[12]Johnston, D.J. and Scholes, P.L.: "Predicting Cleats in Coalseams from Mineral and Maceral Composition with Wireline Logs," Guidebook for the Rocky Mountain Association of Geologists Fall Conference and Field Trip, Glenwood Springs, Colorado (September 1991) 123-136.

[13]Rightmire, C.T.: "Coalbed Methane Resource," Coalbed Methane Resources of the United States, American Association of Petroleum Geologists Studies (1984) No. 17, 3.

[14]Law, B.E., Rice, D.D., and Flores, R.M.: "Coalbed Gas Accumulations in the Paleocene Fort Union Formation, Powder River Basin, Wyoming," Coalbed Methane of Western North America, S.D. Schwochow, D.K. Murray, and M.F. Fahy (eds.), Rocky Mountain Association of Geologists, Glenwood Springs, Colorado (September 1991) 179-190.

[15]Das, B.M., Nikols, D.J., Das, A.U., and Hucka, V.J.: "Factors Affecting Rate and Total Volume of Methane Desorption from Coalbeds," Guidebook for the Rocky Mountain Association of Geologists Fall Conference and Field Trip, Glenwood Springs, Colorado (September 1991) 69-76.

[16]Stach, E.: "Basic Principles of Coal Petrology: Macerals, Microlithotypes and Some Effects of Coalification," Coal and Coal-Bearing Strata, D. Murchison and T.S. Westoll (eds.), American Elsevier Publishing Company, Inc., New York (1968).

[17]Jüntgen, H. and Karweil, J.: "Gas Formation and Gas Storage in Anthracite Coal Layers, Part I and Part II," Petroleum and Coal Gas Petrochemicals (1966) 19, 251-258 and 339-344.

[18]Ayers, W.B. Jr.: "Geologic Evaluation of Critical Production Parameters for Coalbed Methane Resources," Quarterly Review of Methane from Coalseams Technology (February 1991) 8, No. 2, 27-32.

[19]Levine, J.R.: Coal Petrology with Application to Coalbed Methane R & D, Short Course, Tuscaloosa, Alabama (September 1990).

[20]Wiser, N.: Fuel Division of ACS Meeting (1975) 20, No. 2, 122.

[21]Stach, E. et al.: Textbook of Coal Petrology, third edition, Borntraeger, Stuttgart and Berlin, Germany (1982) 42.

[22]Conway, M.W.: Coalbed Methane Shortcourse, Gas Research Institute, Birmingham, Alabama (October 1992).

[23]Hirsch, P.B.: "Science in the Use of Coal," Proc. Inst. Fuel Conf., Sheffield, England (1958) A-29.

[24]Given, P.H. and Peover, M.E.: Fuel (1960) 39, 463.

[25]Lee, M.L.: "Appraisal of the Heavy Hydrocarbons in Coal," Quarterly Review of Methane from Coalseams Technology (July 1991) 8, No. 4, 45-47.

[26]Law, B.E., Nuccio, V.F., and Stanton, R.W.: "Evaluation of Source-Rock Characteristics, Thermal Maturation and Pressure History, of the Upper Cretaceous Cameo Coal Zone, Deep Seam Well, Piceance Basin, Colorado," Proc., 1989 Coalbed Methane Symposium, Tuscaloosa, Alabama (April 17-20, 1989) 341-353.

[27]Ting, F.T.C.: "Origin and Spacing of Cleats in Coal Beds," *J. of Pressure Vessel Tech.* (November 1977) 99, 624-626.

[28]Blom, L.: PhD dissertation, Delft University of Technology, Delft, The Netherlands (1960).

[29]Hawkins, J.M., Schraufnagel, R.A., and Olszewski, A.J.: "Estimating Coalbed Gas Content and Sorption Isotherm Using Well Log Data," paper SPE 24905 presented at the 1992 SPE Annual Technical Conference and Exhibition, Washington, DC, 2-7 October.

[30]Conway, M.W.: "Coal-Fluid Interactions," GRI Coalbed Methane Shortcourse, Birmingham, Alabama, 21 October 1992.

[31]Olszewski, A.J. and Schraufnagel, R.A.: "Development of Formation Evaluation Technology for Coalbed Methane Development," Quarterly Review of Methane from Coalseams Technology (October 1992) 10, No. 1, 27-35.

[32]Davis, A.: "The Measurement of Reflectance-Its Automation and Significance," Technical Report 10, Pennsylvania State University, State College, Pennsylvania (1978) 88.

[33]"Standard Method for Microscopical Determination of the Reflectance of the Organic Components in a Polished Specimen of Coal," Annual Book of ASTM Standards (April 1979).

[34]"Standard Method for Preparing Coal Samples for Microscopical Analysis by Reflected Light," Annual Book of ASTM Standards, Part 26 (April 1979).

[35]Jones, A.H., Bell, G.J., and Schraufnagel, R.A.: "A Review of the Physical and Mechanical Properties of Coal with Implications for Coalbed Methane Well Completion and Production," Geology and Coal-bed Methane Resources of the Northern San Juan Basin, Colorado and New Mexico, J.E. Fassett (ed.), Rocky Mountain Association of Geologists, Denver, Colorado (1988) 169-181.

[36]Kim, A.G.: "Estimating Methane Content of Bituminous Coalbeds from Adsorptive Data," U.S. Bureau of Mines, Report of Investigation, RI 8245.

[37]Franklin, R.E.: Fuel (1948) 27, 46.

[38]King J.G. and Wilkins, E.T.: Proc., Conference on Ultrafine Structure in Coal and Cores, London (1944).

[39]Analytical Methods for Coal and Coal Products, C. Karr, Jr. (ed.), New York: Academic Press (1978) 580.

[40]Bond, R.L. and Spencer, D.H.T.: Ind Carbon and Graphite (1958) 231.

[41]Zwietering, P. and van Krevelen, D.W.: Fuel (1954) 33, 331.

[42]Gray, I.: "Reservoir Engineering in Coalseams: Part 1-The Physical Process of Gas Storage and Movement in Coalseams," *SPERE* (February 1987) 2, No. 1, 28-34.

[43]Mavor, M.J. and McBane, R.A.: "Western Cretaceous Coalseam Project," Quarterly Review of Methane from Coalseams Technology (April 1992) 9-11.

[44]Mavor, M.J.: "Western Cretaceous Coalseam Project," monthly report, Gas Research Institute (January 1993) 1-5.

[45]Close, J.C. and Mavor, M.J.: "Influence of Coal Composition and Rank on Fracture Development in Fruitland Coal Gas Reservoirs of San Juan Basin," Coalbed Methane of Western North America, Guidebook for the Rocky Mountain Association of Geologists Fall Conference and Field Trip, Glenwood Springs, Colorado (September 1991) 109-121.

[46]Mavor, M.J. and McBane, R.A.: "Western Cretaceous Coalseam Project," Quarterly Review of Methane from Coalseams Technology (July 1991) 8, No. 4, 20-22.

[47]Close, J.C.: "Western Cretaceous Coalseam Project," Quarterly Review of Methane from Coalseams Technology (July 1992) 10, No. 1, 11-14.

[48]Law, B.E.: "The Relationship between Coal Rank and Cleat Spacing: Implications for the Prediction of Permeability in Coal," Proc., 1993 International Coalbed Methane Symposium, Birmingham, Alabama (May 1993) 435-441.

Chapter 3

Sorption

3.1 Principles of Adsorption

3.1.1 Theory Overview

In 1938, Brunauer[1] categorized the adsorption of a gas on a solid into five types of isotherms. "Isotherm" refers to the volume of gas adsorbed on a solid surface as a function of pressure for a specific temperature, gas, and solid material. According to Brunauer's classification, a Type I isotherm, as characterized by Fig. 3.1, applies to the adsorption of gases in microporous solids. At high pressures, the amount adsorbed becomes asymptotic with pressure. At higher temperatures, the amount adsorbed decreases. At low pressures, large volumes of gas adsorb or desorb with small changes of pressure. Consequently, a point to note from Fig. 3.1 is that at abandonment of a coalbed methane (CBM) well at a low reservoir pressure, the recovery factor will be highly dependent on how far the drawdown in the reservoir proceeds.

Type I isotherms closely describe the adsorption/desorption behavior of methane on coals, and the model has been applicable without exception.

The Langmuir equation fits the adsorption data of methane on coal and is used exclusively in the CBM process to describe the Type I curves. The model is such a close fit of the adsorption data of all coals that use of the Langmuir equation is universal in the industry. Further, its simplicity is appealing.

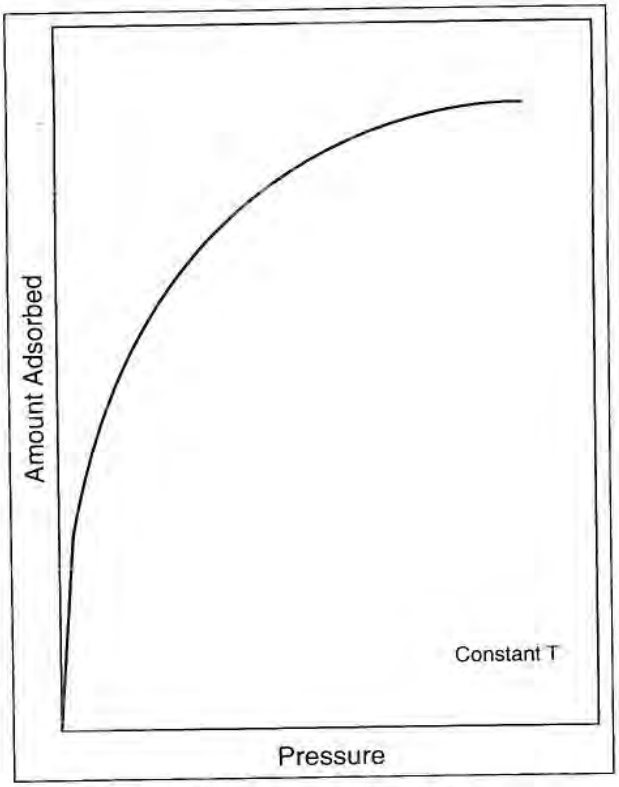

Fig. 3.1—Type I isotherm of Brunauer.

As pressures in coalseams increase with depth or with the hydrostatic head of water, the capacity of the coal for adsorbing more methane improves. It is also evident that present gas content of a coal may have been set by some previously lower or higher pressure in geologic time and that current depth may be misleading in estimating gas content.

3.1.2 Langmuir Isotherm

The most commonly used equation to describe the adsorption of gases on a solid is that of Langmuir, who developed the theory in 1918.[2] The major assumptions[3] in deriving the equation are as follows:

- One gas molecule is adsorbed at a single adsorption site.
- An adsorbed molecule does not affect the molecule on the neighboring site.
- Sites are indistinguishable by the gas molecules.
- Adsorption is on an open surface, and there is no resistance to gas access to adsorption sites.

The assumption of an open surface is a troublesome one in the Langmuir theory because micropore throats leading to cavities in the coal may be thousands of molecular diameters long[4] and only several molecular diameters wide. Therefore, the adsorbate does not have unrestricted access to the adsorption sites, which are far from comprising an open surface. The development of the Langmuir equation reveals how the faulty assumption still serves the true phenomenon.

At equilibrium for a given temperature, the rate of molecules of adsorbed gas leaving adsorption sites will equal the rate of those attaching to adsorption sites, somewhat similar to evaporation from the surface of liquid water. This state of equilibrium can be described if we let

r = rate of adsorption and desorption from complete monolayer coverage at constant temperature
θ = fraction of sites covered or fraction of monolayer coverage
P = pressure

For the case of desorption in the coals, or by analogy of evaporation from a free water surface,

$r\theta$ = rate of gas molecules leaving those occupied adsorption sites

Conversely, upon adsorption or upon condensation by analogy,

$k(1-\theta)P$ = rate of gas molecules attaching to adsorption sites

where

k = adsorption equilibrium constant

That is, the number of molecules striking the uncovered surface is proportional to pressure, and k represents an equilibrium constant. Note that k may be derived from the kinetic theory of gases and, thus, relates the fraction of molecules sticking to an adsorption site with the number that strike it at a given temperature.

Equating the adsorption and desorption rates at equilibrium conditions in Eq. 3.1,[3]

$$r\theta = k(1-\theta)P \qquad (3.1)$$

Rearranging Eq. 3.1 gives for the subject temperature the fraction of sites covered, θ, in Eq. 3.2.

$$\theta = \frac{(k/r)P}{1+(k/r)P} \qquad (3.2)$$

Or, considering θ as the fraction of monolayer coverage $\theta = \frac{V}{V_{max}}$

where

V = gas volume adsorbed per unit weight of solid at pressure, P

V_{max} = maximum monolayer volumetric capacity per unit weight of solid

Now, since k/r would be constant at a given temperature, let B denote the constant to represent k/r in Eq. 3.3. Then,

$$V = V_{\max} \frac{BP}{1 + BP} \qquad (3.3)$$

Eq. 3.3 is the Langmuir equation. The constant B is the Langmuir constant, or reciprocal of the Langmuir pressure, P_L; P_L is defined as the pressure that gives a gas content equal to one-half of the monolayer capacity. The equation can be derived thermodynamically or from the kinetic theory of gases.

At low pressures attainable in the laboratory but difficult to attain in a coalseam in the field, $(1 + BP) \approx 1$ and Eq. 3.3 reduces to that of a straight line passing through the origin on a graph of adsorbed volume vs. pressure. This low-pressure region is referred to as Henry's law region[5] and is given by Eq. 3.4.

$$V = V_{\max} BP \qquad (3.4)$$

One should also realize that gas desorption increases rapidly as pressures are lowered on the coals in the Henry's law region. For a given pressure drop, much more gas is evolved at these low pressures than at the higher pressures where CBM production usually starts. A practical limit exists for lowering total pressures on the coalseam to take advantage of this fact, but it is feasible to achieve the same result by reducing partial pressures of the methane into the Henry's law region, for example, by injecting nitrogen into the reservoir.

In Eq. 3.4, $V_{max}B$ is a constant, and the equation may be rewritten as $V = C_H P$

where

C_H = Henry's law constant

The steep slope of the Type I curve in Fig. 3.1 where it is linear at low pressures would reflect a monomolecular layer of adsorbate on the solid surface of the micropores according to Langmuir's model and assumptions.

It is seen from the Langmuir equation that at high pressures, when $BP/(1+BP)\approx 1$, then $V = V_{max}$; all adsorption sites become filled and maximum coverage results.

Eq. 3.3, the Langmuir equation, may be used to construct the isotherm of methane sorption on coal as pressure is varied while keeping temperature constant, a path similar to CBM production. The model has been found to fit the adsorption characteristics of coalseams at the pressures and temperatures pertinent to the CBM process. Therefore, with laboratory data from a crushed coal sample at reservoir temperature and pressures equal or less than initial reservoir pressure, the resulting Langmuir isotherm can be extrapolated to the maximum gas content at higher than tested pressures. More importantly, the model provides a guide to gas content of the coal at any time as pressure is decreased while production proceeds.

To determine the Langmuir constant, B, and the monolayer capacity, V_{max}, Eq. 3.3 can be rearranged. When these empirically derived constants are known, the entire isotherm can be reconstructed.

$$\frac{P}{V} = \frac{1}{V_{\max} B} + \frac{P}{V_{\max}} \qquad (3.5)$$

Thus, a plot of P/V vs. P gives a straight line with an intercept of $1/V_{max}B$ and a slope of $1/V_{max}$. Commonly, the CBM data will be plotted as pressure units of psia and volume units of standard cubic feet per ton of coal (scf/ton). By collecting data in the laboratory from experimental pressures up to the reservoir pressure, the two Langmuir constants may be determined and the curve accurately extrapolated to higher or lower pressures.

As an example, Eq. 3.5 was used to evaluate the adsorptive characteristics of the

Cameo seam in the Piceance basin of Colorado.[6] Table 3.1 presents the adsorption data of Rakop and Bell for a core extracted from the Cameo D seam at a depth of 5,612.5–5,614.5 ft. After extraction, the coal was powdered before being used to generate the isotherm in the laboratory.

Table 3.1—CH_4 Adsorption of Cameo Coals (After Rakop and Bell[6])

Pressure (psia)	Gas Content (scf/ton)
100	66
413	207
1,016	306
1,917	378

Their corresponding data in Table 3.2 represent methane desorption from the same coal. The adsorption and desorption data are plotted as P/V vs. P in Fig. 3.2 to evaluate the Langmuir constants and to establish the complete isotherm.

Table 3.2—CH_4 Desorption of Cameo Coal (After Rakop and Bell[6])

Pressure (psia)	Gas Content (scf/ton)
1,513	364
1,014	328
767	287
417	215
211	143
163	118
113	88
63	53
12	0

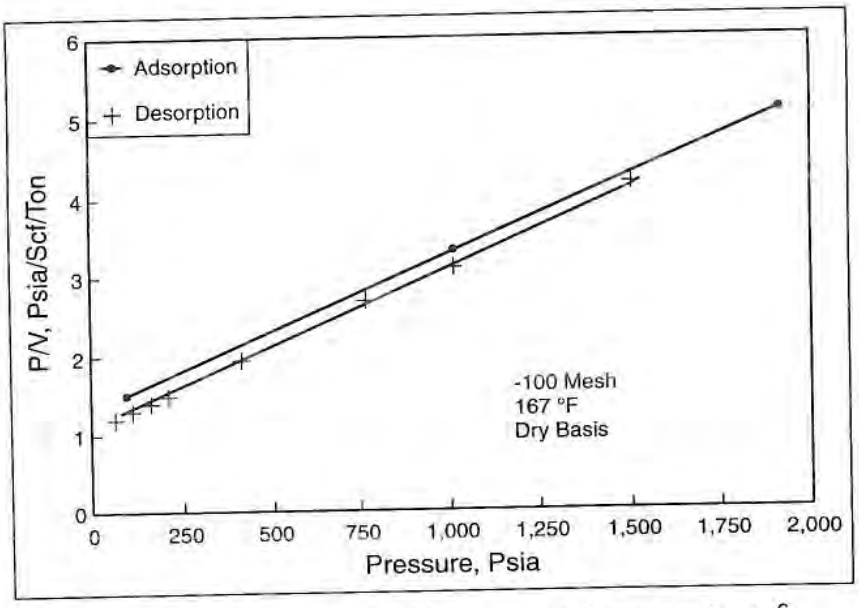

Fig. 3.2—Langmuir coefficients of Cameo coal, Piceance basin.[6]

A straight line fits the data in Fig. 3.2, indicating the applicability of the Langmuir model to the adsorption and desorption of methane on the Cameo coal. A slight hysteresis effect is also evident as plots of desorption and adsorption data are slightly offset. Theoretically, some hysteresis could occur in the adsorption and desorption from microporous solids, but a slight divergence of the adsorption and desorption curves may also indicate a small error in laboratory technique. Although simple in principle, the apparatus to collect the data is very sensitive to small leaks and to pressure monitoring. From Fig. 3.2, the constant B is found to be 0.00157 psia^{-1}. V_{max} is found to be 504 scf/ton for the adsorption, which would be the molecular monolayer capacity of the Cameo coal—the maximum gas content to be expected if the coal were to be saturated with methane at higher pressures.[6]

These coefficients are then used in the Langmuir equation to construct the complete isotherm of Fig. 3.3. With superposition on the laboratory data, a close fit is indicated.

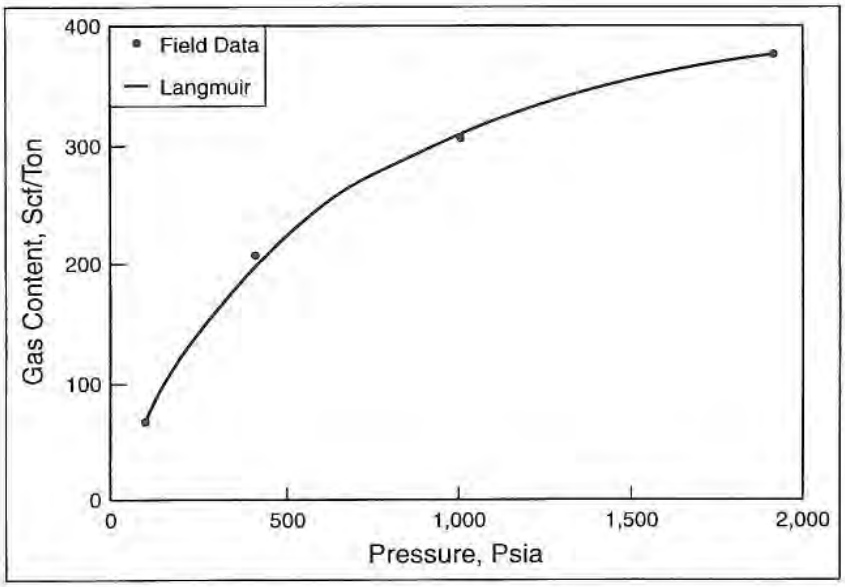

Fig. 3.3—Cameo adsorption isotherm (from a 100-mesh sample at 167°F, on a dry basis).[6]

3.1.3 Similarities of Adsorbed Methane and Liquid Behavior

Eq. 3.4 for the adsorption of methane at low concentrations of adsorbate is the counterpart of Henry's law for ideal liquid solutions, which applies at low concentrations of solute. The similarity is not incidental, and other similarities of adsorbed gas with liquids become apparent for adsorption on microporous solids.

Paradoxically, the Langmuir equation models CBM isotherms exceptionally well even though there are anomalies from the assumptions in the development of the

equation for the microporous solids. Despite the failure of some assumptions to meet the conditions in the micropores of coal, the resulting equation has been proven applicable.

Physical adsorption on microporous solids (as in the case of methane on coal) results from van der Waals's forces between adsorbate and solid surface as well as between the adsorbate molecules. The force between solid and gas is the stronger. Energy fields that attract the gas molecules toward the surface extend outwardly from the solid surface. In the case of micropore capillaries with diameters only a few adsorbate molecules in thickness, these energy fields overlap to create sufficient forces to adsorb multimolecular layers instead of monomolecular layers. Therefore, although Langmuir's equation is based on the assumption of monomolecular coverage, the overlapping energy fields in the micropores create strong forces on upper-layer molecules that approximate the forces on monolayers of an open solid surface.

Thus, Langmuir's assumptions give the proper result. A packing of methane molecules in the capillaries occurs, and the adsorbed molecules are held together by van der Waals's forces as in a liquid. In such a case, the methane in the capillaries is similar to a liquid. The higher-pressure portion of the Type I isotherm represents the filling of the pores.

Data for the adsorption of methane indicate that the adsorbed gas must be liquid-like at saturation. Otherwise, the volumes of methane adsorbed by coal are so large as to require each carbon atom of the coal to be exposed as an adsorption site for one molecule of methane for all of the methane to be accommodated. This is a highly improbable occurrence.[4] The plausible explanation is that methane is packed liquid-like in the micropores and capillaries.

Upon desorption, the rate of detachment of the methane molecules from the interior surface of the micropores is rapid, but the adsorbate traverse of the pore opening is many times slower. These micropore passageways may be 100–1,000 methane molecular diameters in length, compared to an average diameter of the passageways of 8 Å and relative to a molecular diameter of methane of 4.1 Å.

Movement of methane along these passageways is by Knudsen diffusion, surface diffusion, bulk diffusion, and combinations of the three diffusion mechanisms.

Knudsen diffusion refers to the molecular movement of the gas through the capillaries when the walls are closer than the mean free path of the methane molecules, so the molecules strike the walls instead of colliding. Surface diffusion refers to the movement along the capillary walls of the pseudoliquid adsorbed on the surface. Bulk diffusion is the diffusion by concentration gradient of the desorbed methane gas between walls further apart than the mean free path.

Since physical adsorption by van der Waals's forces is similar to attractive forces in liquids, inert gases not easily forming a liquid are also not much adsorbed. For example, helium has insignificant adsorption on coal, and it is also the most difficult of the gases to liquefy.

Like liquids, vapor pressure of the adsorbed methane on coal is related to temperature by the Clapeyron equation, Eq. 3.6.

$$lnP_v = -\frac{\Delta H_{ad}}{RT} + C \qquad (3.6)$$

where

P_v = partial pressure above liquid-like adsorbed phase
T = absolute temperature
R = universal gas constant
ΔH_{ad} = heat of adsorption
C = constant of integration

A heat of adsorption is associated with the adsorption of methane, other hydrocarbons, carbon dioxide, or nitrogen onto the surface of coal. The heat of adsorption is of greater magnitude than the heat of vaporization of the adsorbate as a liquid[7] because the van der Waals's forces between the gas and the solid

surface of adsorption are usually stronger than the molecular attraction in a liquid state.

Unlike other adsorbents, such as molecular sieves, the coal has no selective adsorption for water so that no large heat of vaporization associated with water enters into the adsorption applications of activated carbon or coals. Therefore, by plotting the natural logarithm of pressure vs. the reciprocal of absolute temperature at the same degree of surface coverage by methane, a straight line should result with which the heat of adsorption can be calculated from the slope. Also, an estimation of the heat of adsorption comes from application of the Clausius-Clapeyron equation, Eq. 3.7.[8]

$$\ln\frac{p_{v2}}{p_{v1}} = \frac{\Delta H_{ad}}{R}\left(\frac{T_2 - T_1}{T_1 T_2}\right) \qquad (3.7)$$

where

P_{v1}, P_{v2} = equilibrium pressures in gas phase
T_1, T_2 = absolute temperatures at equilibrium
ΔH_{ad} = heat of adsorption, maintaining a constant amount adsorbed
R = universal gas constant

Adsorption of the gases on coal is exothermic, but the heat of adsorption associated with methane on coal is small. The heat of adsorption of ethane on coal will be larger than that of methane, and the value of ΔH_{ad} will continue to increase up the homologous series.[9] The latent heat associated with adsorption or desorption would go to raising or lowering the temperature of the adsorbent bed, however imperceptible, in coalseams.

A slight hysteresis of adsorption and desorption paths is exhibited by adsorbates that fill the capillaries of microporous solids as a pseudoliquid.[4] Adsorption is

layer by layer in the capillaries, where the final layer makes the surface a continuum and the meniscus that forms near V_{max} lowers the vapor pressure. Thereafter, when the first increment of methane in the saturated state desorbs, it must be subjected to a lower pressure than the last increment of adsorption, which causes some hysteresis in the isotherm. The effect is similar to the lowering of vapor pressure above the meniscus of a liquid in a capillary (Fig.3.4).

When multiple layers of gas molecules pack into the capillaries by the forces of overlapping energy fields, a large pressure is exerted on the walls, resulting in matrix swelling.[7] Adsorbates, such as CO_2 strongly held by the coal surface, are more readily adsorbed and will create more swelling of the coal matrix than methane or nitrogen. The swelling effect is significant enough with the adsorption and desorption of methane to impact permeability of the coalseam.

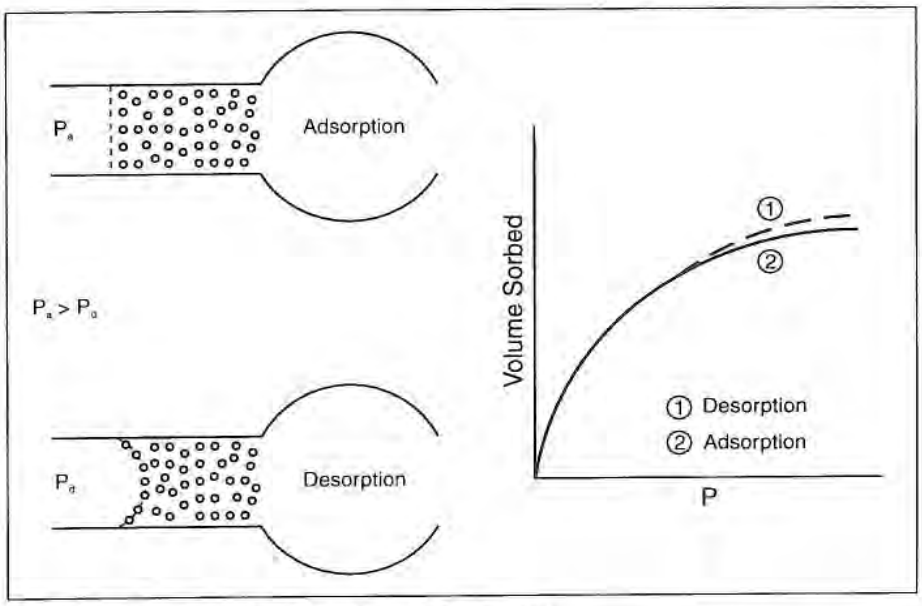

Fig. 3.4—Packing of adsorbate and hysteresis

3.1.4 Extended Langmuir Isotherm

Methane adsorption on coal as a single component is described satisfactorily for CBM work by the Langmuir isotherm. In practice, however, multicomponent gases desorb from the coal in addition to methane. In a study by Scott[10] of 1,400 CBM wells in the major basins of the United States, the average composition of produced gases was found to be the following: (1) CH_4 = 93%; (2) $C_2H_6^+$ = 3%; (3) CO_2 = 3%; and (4) N_2 = 1%.

Individual wells occasionally show extreme values of a carbon dioxide fraction, especially in the San Juan and Piceance basins, where about 40% CO_2 has been recorded in isolated cases. Maximum nitrogen contents range from 7.5–11.2% in the San Juan, Black Warrior, Powder River, and Cherokee basins.[10] The minimum values of both components are zero.

If coalbed production gases contain CO_2 initially, there is a subsequent increase in CO_2 content and decrease in CH_4 content with time.[11] Underestimation of treating costs and overestimation of methane reserves could be a consequence of not accounting for the CO_2 production trend.

Carbon dioxide and nitrogen lower both the heating value of the produced coalbed gas and the ultimate recovery of methane. Also, adsorbed hydrocarbon gases heavier than methane on the coal affect the accuracy of methane reserve calculations. Primarily, it is carbon dioxide and nitrogen that compete with methane for adsorption sites. Carbon dioxide has a stronger affinity to the coal surface than methane, and nitrogen is less readily adsorbed than methane.

The Langmuir model has been extended to account for adsorption of multiple gas components in a mixture.[9,12] The extended Langmuir isotherm is represented by Eq. 3.8.

$$V_i = \frac{(V_{\max,i}) B_i P_i}{1 + \sum_{j=1}^{n} B_j P_j} \qquad (3.8)$$

where

V_i = gas volume of component i adsorbed per unit weight of solid at partial pressure, P_i

$V_{max,i}$ = monolayer volumetric capacity of component i per unit weight of solid, scf/ton

n = total number of j gas components in mixture

B_j = reciprocal of Langmuir pressure of j component

In the derivation[9] of Eq. 3.8, it is implicitly assumed that the monolayer volumetric capacity, $V_{max,i}$, is the same for each molecular species, i. For the assumption to be correct, all gas components must have equal access to adsorption sites in the micropores of the coal. Therefore, using the extended Langmuir isotherm to describe multicomponent gas adsorption in coals would be expected to be more in error for gas components with widely divergent molecular diameters.

Table 3.3 gives the molecular diameters of the gases of concern in CBM operations.

Table 3.3—Molecular Diameters of Coalbed Gases

Gas Molecule	Diameter (Angstroms)
CH_4	4.36
CO_2	5.12
N_2	4.10
C_2H_6	5.50
C_3H_8	6.28

A comparison of methane, carbon dioxide, and nitrogen molecular diameters suggests access to similar micropores and surface areas for these three main components of coal gas. Not accounting for any shape factor, the carbon dioxide molecular diameter is only about 17% larger than the methane diameter, suggesting the validity of the extended Langmuir equation for coalbed gases.

Harpalani[12] found good agreement of Eq. 3.8 with experimental adsorption data of a carbon dioxide and methane binary gas mixture adsorbed on a pulverized Fruitland coal. Only 4% error was indicated by use of the equation.

Deo and coworkers[11] used the extended Langmuir relationship in a computer simulation model to predict the profile of methane composition at the wellbore in a producing well as a function of dimensionless time. Note the decrease in the methane fraction with time in Fig. 3.5 that resulted from their simulation.

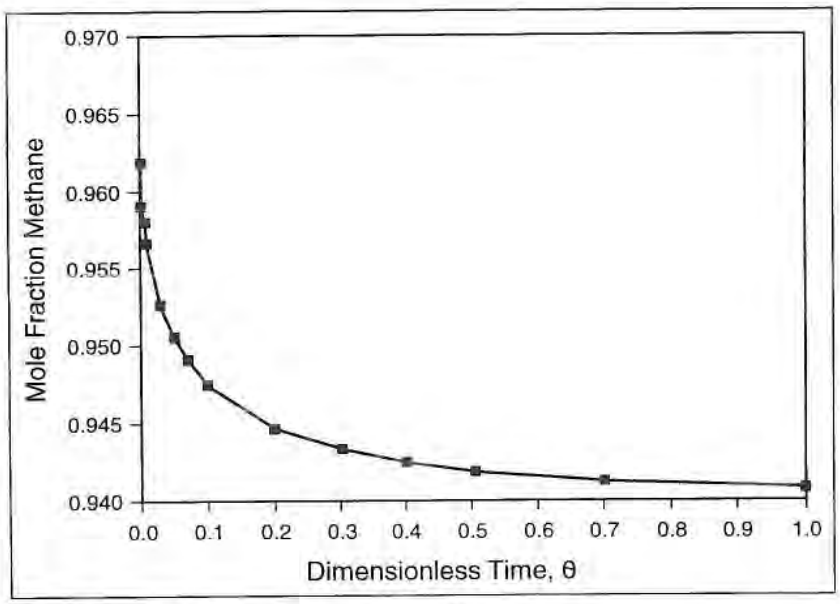

Fig. 3.5—Changing gas composition.[11]

The dimensionless time, θ, is given by Eq. 3.9.

$$\theta = \frac{t\, k_f\, P}{L^2\, \mu\, \phi} \qquad (3.9)$$

where

t = time, sec
k_f = permeability of coalseam, m^2
P = pressure in the coalseam, atm
L = total length of the reservoir, m
μ = viscosity of produced gas, atm-sec
φ = porosity of coalbed

As the CBM industry matures, production of nonhydrocarbon gases and alkanes heavier than methane will increase, making it more important to use an isotherm model for a multicomponent gas mixture. The extended Langmuir isotherm is satisfactorily accurate to fulfill the need, and it also resolves a complex laboratory procedural problem for establishing the isotherm of a gas mixture.

3.1.5 Industry Uses of Adsorbents

Activated carbon may have surface areas of 1 sq mi/5 lb of carbon, which is several hundred times greater than charcoal adsorbents.[13] Activated carbon or charcoal has long been used in gas masks and for recovery of solvents and fractionation of mixed gases.

Activated carbon is being studied as a means to store natural gas at relatively low pressures for use as an alternative fuel in vehicles. The Type I adsorption curve characteristic of large amounts of gas adsorbed on the activated carbon at low pressures would be beneficial for on-board gas storage in vehicles. It presents

advantages (such as safety and lower pressure storage) over the high pressures of compressed natural gas.

Molecular sieve adsorbents and other solid adsorbents are used to dry gas or liquid streams in industry. Parallel beds are used to dry the streams; the adsorbent is regenerated cyclically. The regeneration cycle is accomplished by the following techniques used singly or in combination: (1) lowering total pressure, (2) raising temperature, (3) displacing adsorbate with a species of greater affinity, (4) lowering partial pressure, or (5) sweeping desorbed material away with a flowing gas stream of material that does not adsorb.

By analogy with the regeneration of industrial adsorbents, the CBM process lowers total pressure at constant temperature to remove methane. Recovery of methane from coalbeds by any of the other preceding adsorbent regeneration techniques is limited only by practicality of the process.

3.2 The Isotherm Construction

An isotherm presents the relationship of a coal's adsorptive capacity for methane as a function of pressure at a constant temperature, and thus the isotherm is plotted as scf/ton of methane volume adsorbed vs. psia of pressure. Isotherms are necessary to estimate reserves of methane in a coal property and to estimate ultimate recovery and the recovery factor. At any point in the production process, the prevalent reservoir pressure can be related to current gas content by means of the isotherm.

At constant formation temperature, the gas content-pressure relationship will be influenced by coal rank, mineral matter content of the coal, and bed moisture. Because of the variability of these parameters in the field, multiple core samples are necessary to establish representative adsorption isotherms. Only with numerous cores and analyses can inhomogeneities in the reservoir be accounted for.

Isotherms are established in the laboratory using crushed samples (particles that will pass through a 60-mesh screen[14]) of the coal to shorten the mass transfer time during adsorption/desorption. The crushed coal reduces test time without significantly affecting adsorption data for the isotherm. The additional external surface areas of the smaller particles created by crushing increase total surface area of the sample by only 0.1% to 0.3%.[14] To collect data for the isotherm, methane is alternately added to and removed from the cell containing crushed coal, and pressure is correlated with a material balance for each incremental step. A proximate analysis of the original coal sample gives moisture and ash content with which to correct the adsorption data to a standard dry, ash-free (daf) basis.

Gravimetric, chromatographic, or volumetric methods could be used to measure gas adsorption and desorption on the coal, but the volumetric method is commonly used. The volumetric procedure measures pressure and volume of a reference and test cell that are held at a constant temperature (Boyle's law) and that contain the granulized coal. A schematic of the basic laboratory process for establishing the isotherm is given in Fig. 3.6.

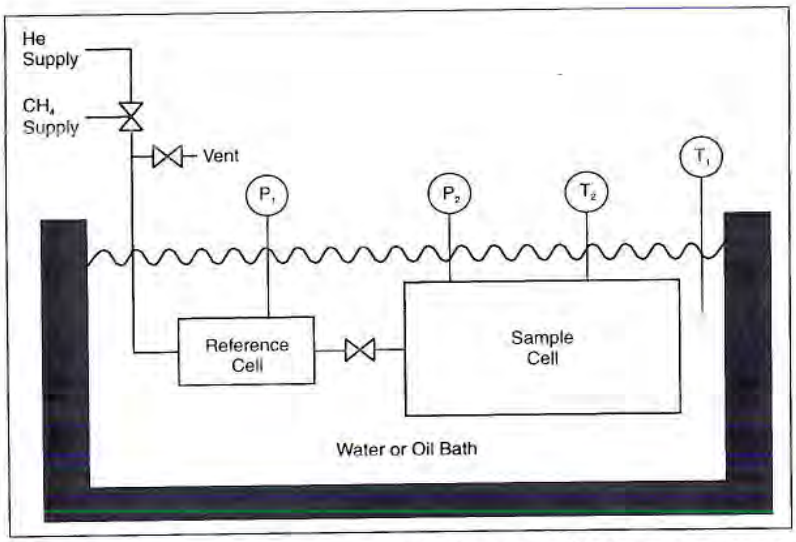

Fig. 3.6—Establishing the adsorption isotherm.[14] *Copyright 1990, Society of Petroleum Engineers.*

The apparatus can be modified to collect data in addition to that for establishing an isotherm for a pure component. For example, Greaves and coworkers[15] modified the apparatus to sample gas from the test cell in determining the isotherm of a multicomponent gas mixture. Kalluri[16] used a backpressure regulator and gas meter downstream of the test cell in displacement studies of adsorbed methane with nitrogen or carbon dioxide. A brief description of the procedure is as follows:

1. The test cell is filled with the crushed coal.
2. A proximate analysis of the coal is obtained.
3. A helium porosimeter is used to establish dead volumes of the lines, test cells, and free pore space in the sample; helium is appropriate because it is not adsorbed by the coal.

4. The reference cell is pressurized with a metered amount of methane from a positive displacement mercury pump or otherwise raised to a pressure higher than the test cell.
5. An incremental amount of methane is input to the coal sample in the test cell, and initial and final pressures of both cells are noted. Pressure stabilization in the test cell may require 4 to 8 hours, and accurate pressure measurements are critical. A constant temperature bath maintains the cells at the desired temperature. Methane fills void spaces and pore spaces of the coal sample in the test cell; it is also adsorbed to decrease pressure.

Additional increments of known volumes of methane are admitted to the vessel over the desired pressure range. By use of the compressibility equation of state, the standard cubic feet of methane as free gas occupying the known volume of the pore space and dead spaces of the cell are calculated. The difference between input volumes of methane and helium gases is the volume of methane adsorbed at that pressure.

Desorption data from the apparatus are obtained by a reversal of the adsorption process. In the modified apparatus, desorption data are obtained by lowering the backpressure regulator in a stepwise manner and measuring with a gas meter the amount of gas released.

The following discussion illustrates the establishment of an isotherm. Table 3.4 presents sorption data of methane on coal from the Jagger seam of the Mary Lee coal group in the Warrior basin. The data are plotted in Fig. 3.7 as P/V vs. P, and the Langmuir constants are calculated from the slope and intercept. With the Langmuir constants known, the entire isotherm can be constructed as in Fig. 3.8. The resulting isotherm is of the form of a Type I curve described by Brunauer for adsorption on microporous solids. With the Langmuir constants derived from Fig. 3.7 for laboratory data points below 1,000 psia, the curve of Fig. 3.8 can be accurately extrapolated to higher pressures.

Table 3.4—Sorption Data for Jagger Coal at 104°F

Pressure (psig)	Gas Adsorbed (scf/ton)	Gas Desorbed (scf/ton)
100	146	173
200	235	233
300	290	295
400	315	330
500	352	353
600	385	365
700	401	377
800	401	385
900	440	419
1,000	410	410

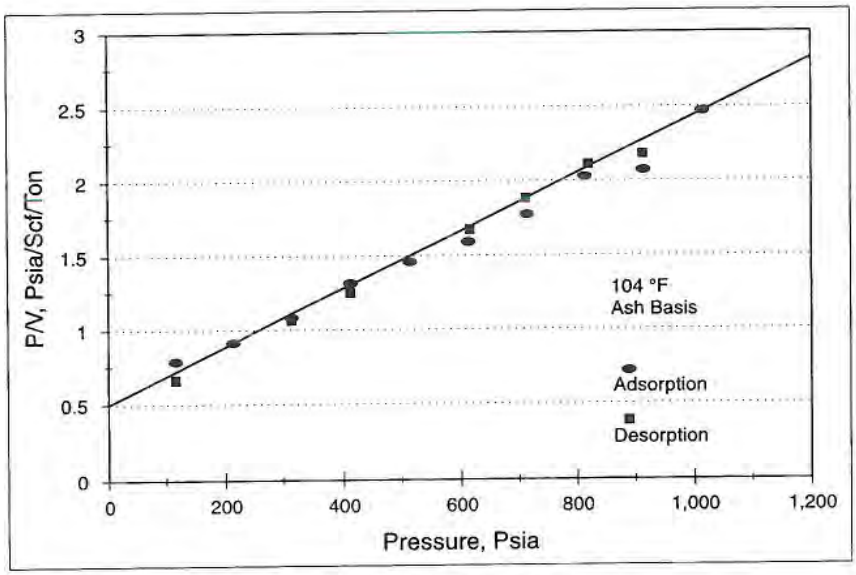

Fig. 3.7—Langmuir coefficients of Jagger seam.

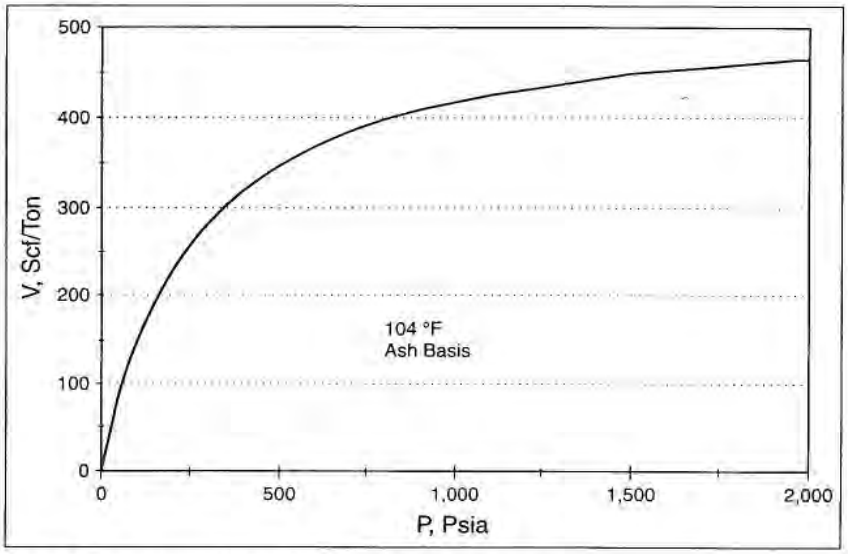

Fig. 3.8—Langmuir isotherm for Jagger coal.

3.3 CH_4 Retention by Coalseams

During the early stages of the coalification process, methane is slowly generated until a threshold is reached in the bituminous ranks where its quantity exceeds the adsorptive capacity of the micropores. Beyond this threshold, additional methane generation serves as the driving force to expel excess gas into the macropore network.[17] The volume of methane generated during coalification depends upon the coal's stage of thermal maturity, as well as the coal's maceral content. It was evident in Fig. 2.22 that lower-rank coals generate a small fraction of the thermogenic methane ultimately generated during the complete maturation process and that prolific methane generation begins at the coalification break near the attainment of hvAb.

The amount of methane generated by the in-place coal during maturation is by no means a sure indicator of current gas content of the coal in the field. Methane in excess of the adsorptive capacity of the coal would have been dissipated, and the coal may not be saturated at current reservoir pressure and temperature. Because of geologic events between the time of coal maturation and the present, current gas content may represent saturation at a pressure lower than current pressure. The amounts of methane generated and retained are put into perspective by Fig. 3.9.

The amount of methane a coal is capable of retaining is much less than is generated after the coalification break near hvAb. This is evident in Fig. 3.9. The anthracite and low-volatile bituminous coals are shown to retain only 5–20% of the thermogenic methane generated. (Of course, it is feasible that biogenic methane could be generated over geologic time periods, migrate to the coalbeds, and be adsorbed by the coal. It is also feasible that thermogenic methane from non-coal sources could migrate and be adsorbed similarly.)

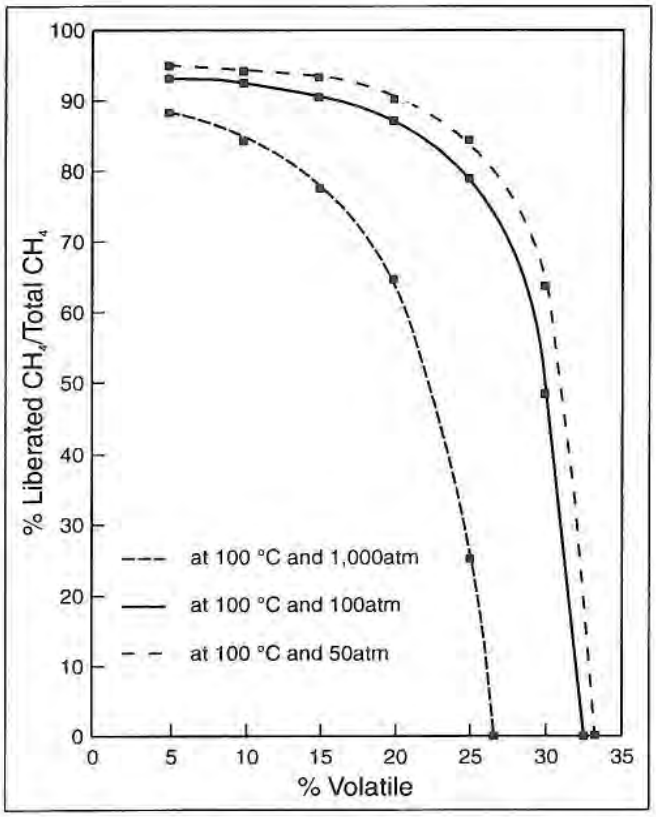

Fig. 3.9—Generation and retention of methane.[17,18]

Another illustration of the low percentage of methane retention by the bituminous coals is given in Fig. 3.10, where the data for gas content of Central Appalachian basin coals at 2,000-ft depths are graphically superposed on the data for methane output of coals of this rank in general. Retention is an order of magnitude less in the Appalachian coals than methane generation for that rank.[19,20] It is estimated that as much as 30,000 scf/ton of methane could be generated through the anthracite rank.

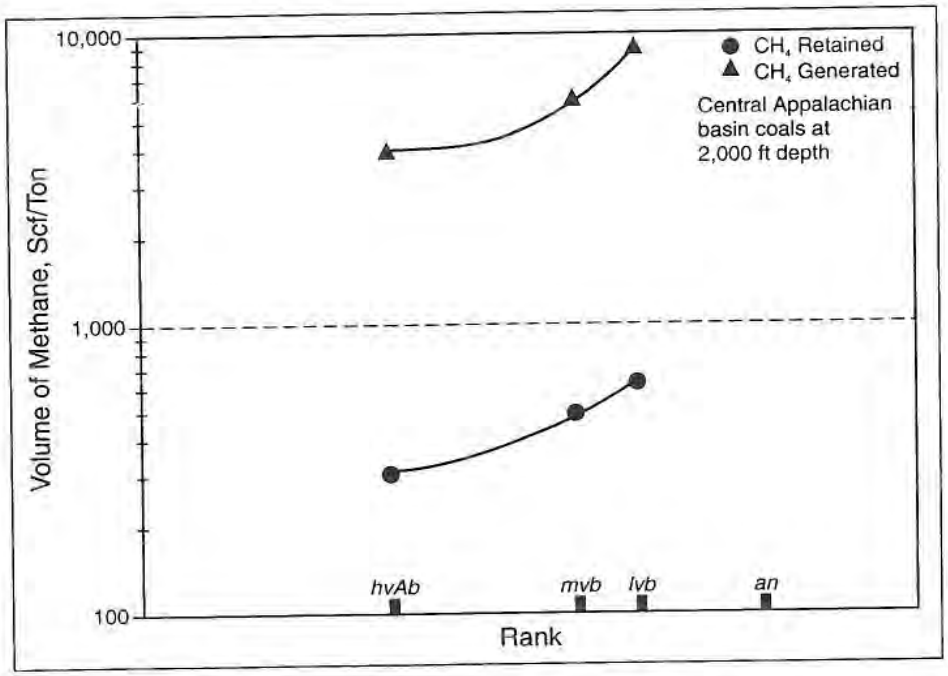

Fig. 3.10—Retention of CH_4 in Central Appalachian coals.[19,20]

The methane generated in excess of retained gas is lost to the surface by: (1) fissures, (2) uplifting and eroding that bring the coal closer to the surface at lower pressure, or (3) charging adjacent sandstone and carbonate formations through a permeable connection. As in the case of the Appalachian coals illustrated in Fig. 3.10, the excess gas dissipated may be large. Consequently, conventional gas reservoirs have been produced in the proximity of coalseams in the San Juan, Powder River, Appalachian, Warrior, and other basins.

About 98% of the methane retained in coalseams will be adsorbed in the micropores and the other 2% retained as free gas or dissolved in the bulk waters in the macropores.[21] Factors determining the amount of methane adsorbed in the

micropores are current pressure and temperature, historical pressure and temperature, coal rank, ash content, moisture content, and the presence of other adsorbates, such as carbon dioxide or heavier hydrocarbons.

Under favorable conditions, a unit volume of coal will contain more methane than the same volume of conventional reservoir sandstone. This attests to the potential of coal for large reserves of natural gas. A lack of understanding of the complex mechanism of methane generation and retention is one reason the adsorbed coal gas has been overlooked as a major energy source until recent times.

3.4 CH_4 Content Determination in Coalseams

Gas content data are vital to determination of the commercial potential of a field, and core analyses provide that information. The measurement of gas content in conventional sandstone or carbonate reservoirs by logs is a benefit not yet available in coalseams without extensive calibration of the logs from previous core analyses. Therefore, gas contents of coals are determined in the laboratory from cores taken from the field. Coring and analyzing in the laboratory for gas content of coalseams are costly and time consuming.

Additional problems arise. Nonuniformities in ash content and in the coal structure laterally through individual seams, as well as from seam to seam, necessitate the analysis of enough cores to be representative. Another problem is that the gas lost during the core retrieval process can only be approximated.

An even less desirable option than coring for determining gas content of the coalseam is the use of drill cuttings, which are used more in openhole completions or as a last resort in the absence of cores. With cuttings, even more uncertainty exists in estimating lost gas during sample retrieval because of questions about exact depth and time of retrieval of the coal fragments.

The procedure for analyzing the core for gas content of a coalseam involves these steps:

1. Remove cores from the coalseam with conventional coring equipment.
2. Transport cores in core barrels rapidly to the surface. Record transit time.
3. Place cores in canisters immediately upon reaching the surface.
4. Measure desorbed gas as a function of time in the sealed canister at the temperature of the reservoir.
5. Calculate lost gas.
6. Determine residual methane in the coal at atmospheric pressure after crushing the coal.
7. Analyze moisture, ash, and mass of coal in the canister.

Finally, gas content of the core is the sum of residual gas, desorbed gas in the canister, and lost gas. The relationship is given by Eq. 3.10.

$$G = G_R + G_C + G_L \qquad (3.10)$$

where

G = gas content of the coal in the formation, scf/ton
G_R = residual gas of core, scf/ton
G_C = gas released by the core in the canister, scf/ton
G_L = gas lost from the core in the coring process, scf/ton

It is assumed that all gas remaining adsorbed in the coal below atmospheric pressure should not be considered because it would not be recovered in practice.

Residual gas, G_R, is that which would be produced if atmospheric pressure were attained at the pore opening. By crushing the coal, pressure gradients in the flow of methane are effectively eliminated, and atmospheric pressure is established for

the micropores of the core. Northern Appalachian coals have long sorption times. (Diffusion of the methane through the sample is lengthy.) Therefore, those Appalachian coals have a high residual gas content that may be found to be as much as 50% upon crushing. In contrast, coals with short sorption times may have only 5% methane left in the core after a few hours;[22] its residual gas content is low. The U.S. Bureau of Mines (USBM) specifies 100 days as the maximum time to allow for gas desorption in the canister, after which the coal should be crushed and residual gas determined.

Desorbed gas, G_C, is gas collected from the whole core in the canister at seam temperature and atmospheric pressure during days or weeks of this controlled environment in the canister. Temperature during desorption of the core in the canister must be kept at that of the reservoir to give accurate assessment of gas to be desorbed from the coalseam. Elevating temperature above formation temperature or lowering pressure below atmospheric pressure are not permissible ways therefore to shorten the time of the canister desorption; inaccurate measurements of gas contents result.

The effect of temperature on quantity of adsorbed methane on coal can be seen in Fig. 3.11. The coal sample was of the Pittsburgh seam of the northern Appalachian basin from the data of the USBM. Note the decrease in adsorbed methane from increasing temperatures.[23,24]

Lost gas, G_L, refers to gas desorbed from the core from the time the core is extracted from the formation to the time the core is placed in the canister and sealed. The gas lost as the core is retrieved to the surface is an unknown amount. The need to minimize the transfer time is apparent, but the difficulty in standardizing the procedural time in the field can be readily surmised. Compensation for the lost gas is made by noting the core transfer time and using the initial canister desorption rate as the same rate of loss during the core transfer time. Consequently, coals with shorter sorption times will have more lost gas for which to account.

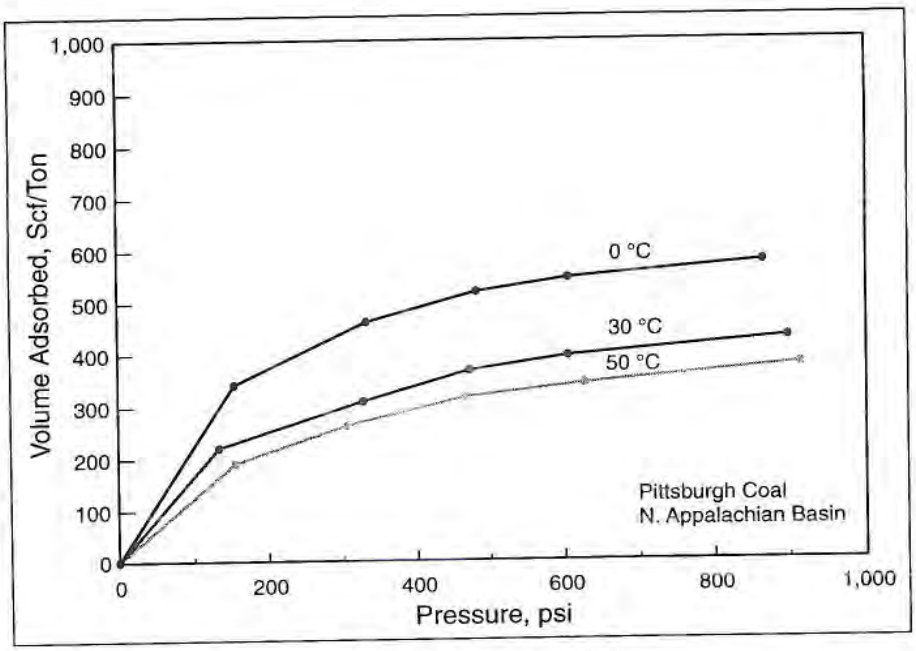

Fig. 3.11—Temperature effects on adsorption.[23,24]

According to Eq. 3.11, gas desorption quantity should be linear with the square root of time if the mechanism of gas flow is diffusion controlled. That was found to be the case when both V/Vt < 0.5 and surface concentration of gas at the pore entrance were constant.[25]

$$\frac{V}{V_t} = \frac{6}{\sqrt{\pi}}\sqrt{\frac{Dt}{r_p^2}} \qquad (3.11)$$

where

V_t = total volume of gas adsorbed
V = volume of gas adsorbed at any time, t
D = diffusion coefficient
t = time
r_p = particle radius

Therefore, lost gas is estimated by extrapolating a plot of V/V_t vs. $t^{1/2}$ from the time the core was put into the canister to the beginning time when the core was extracted.

Laboratory studies indicate that calculation of the lost gas by extrapolation may give a 20–50% under-estimation of gas that is actually lost.[26] Extrapolation has less error for cores from shallow, low-pressure reservoirs than for deeper seams because of greater accuracy in estimating the shorter retrieval times. Likewise, the error is less for coals of long sorption times.

One complicating factor in gas content determination from canister tests is the lack of standardized procedures. Olszewski and McLennan investigated the effect of lack of standardized procedures by having different laboratories analyze the same cores from an Appalachian basin well and then comparing results.[26] The analyses of gas contents were inconsistent. Large discrepancies in gas content were reported by the different laboratories in the canister tests for the following reasons:

- Lack of documentation on core retrieval conditions.
- Inadequate data immediately after placing core in canister (necessary for lost-gas extrapolation).
- Inadequate temperature controls on the canister.
- Inconsistent reporting on a dry, ash-free basis.

The error in lost-gas estimation can be eliminated with a pressure core barrel that immediately seals the cut core in a gas-tight compartment at the pressure of the reservoir. Meridian reports[27] promptly wrapping the barrel with heating tape and insulation followed by reheating to reservoir temperature when brought to the surface. Gas content is then measured conventionally. Advantages of the more accurate procedure must be weighed against additional costs.

3.5 The Isotherm for Recovery Prediction

The adsorption of methane on coals follows a Type I curve of Brunauer, and the data fit a Langmuir mathematical model as depicted by Fig. 3.12. After the isotherm has been established, it may be used to follow the progress of the CBM process and to estimate a percentage recovery. For example, assume the isotherm of Fig. 3.12 has been generated in the laboratory from crushed coal samples.

If P_i in Fig. 3.12 is the pressure on the coalseam initially, then an undersaturated state exists. Pressure must be reduced by dewatering until the saturation pressure, P_s, is reached on the isotherm. Subsequently, further dewatering proceeds to the abandonment pressure, P_a, where it is no longer economical to further reduce pressure and produce methane. Unfortunately, Pa falls on the steep part of the curve where a small incremental pressure decrease involves the greatest incremental volume of methane production. The percentage recovery is then given by Eq. 3.12.

$$R = (V_s - V_a)/V_s \, x \, 100 \qquad (3.12)$$

where

R = % recovery
V_a = methane content of coal at abandonment, scf/ton
V_s = saturated gas content after initial dewatering, scf/ton

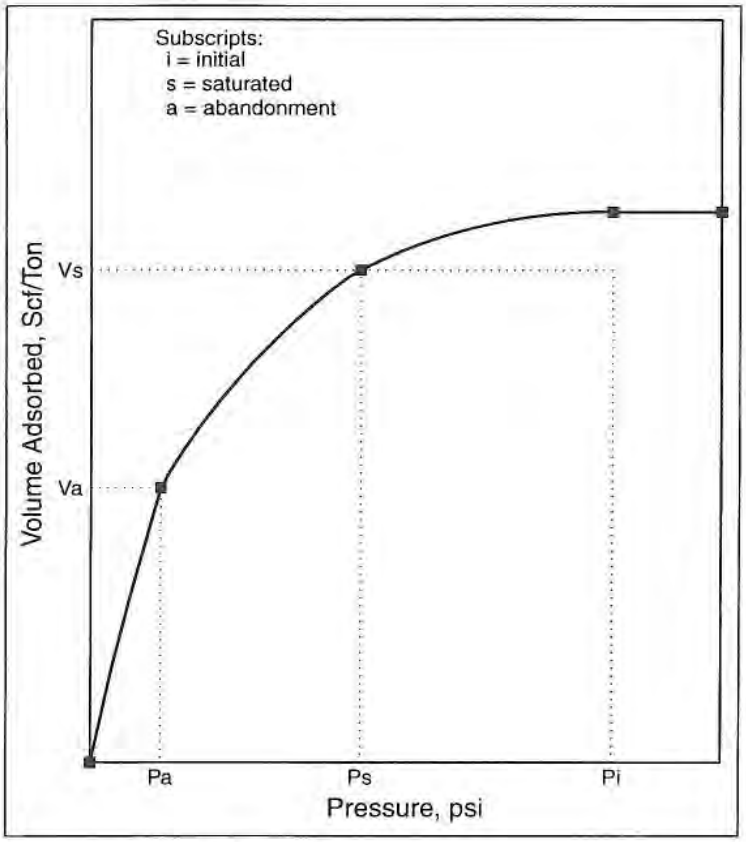

Fig. 3.12—General isotherm.

With respect to Fig. 3.12, one may speculate on the possible causes of the unsaturated condition: temperature, pressure, and burial depth may have changed over geologic time to cause the apparent unsaturated anomaly. For example, temperatures may have been higher at an earlier time. Another explanation of the undersaturated condition is an error in the determination of gas content of the coalseam.

3.6 Model of the Micropores

3.6.1 Pore Geometry

The micropore geometry and dimensions are important in determining rate of diffusion of methane from adsorption sites and in determining capacity of the micropores. A model of the micropore network is especially helpful in visualizing the mechanism of sorption and the mass transport of methane from the micropores' network to the cleats.

Insight into micropore geometry is given from a study of the specific surface areas of coals of lvb rank reported by Gregg and Pope.[28] The amount of nitrogen adsorbed on coals in their laboratory at the warmer 183°K was greater than at the colder 197°K for coals of about 90% fixed carbon content. The increasing adsorption with higher temperatures suggests a pore opening constricted by the lower temperature that requires an activation energy for the adsorbate to enter if its molecular diameter is only slightly less than the pore diameter.

Constricted pore openings in coal are substantiated by the adsorption preference for the smaller carbon dioxide molecule over the larger butane molecule.[4] Also, easier access of flat molecules than branched ones of similar molecular weight suggests a slit port of entry. The slit geometry is consistent with the plate-like structure of the aromatic clusters constituting the higher ranked coals of most importance to the CBM process.

Smith and Williams[25] report differing mechanisms for the diffusion of methane and helium in an anthracite coal. Bulk diffusion dominates with methane. Knudsen diffusion dominates with helium. This signifies smaller passageways than the methane can penetrate but in which the smaller helium moves through apertures of wall space smaller than its mean free path. A model that explains these behaviors is given in Fig. 2.23.[29]

Note in the sketch that adsorbate molecules must first pass through the constricted passageway to reach the larger chamber. If the molecular diameters are only slightly smaller than the pore throat diameters, the adsorbate molecules must possess an activation energy to enter. The inner pores of the micropore network may be interconnected through additional constrictions that are not uniformly the same size.

3.6.2 Carbon Molecular Sieves

Some insight into the structure of the pores of coal is given by the diffusion in carbon molecular sieves.[5] By imparting a throat opening of approximately 5 Å to the pores in the carbon, kinetic separations of gases can be made by making the diffusion into the pores of one gas molecule more rapid than another component from a gas mixture flowing by the face of the solid. In 1977, Kamishita reported a technique to control the pore throat size of a carbon molecular sieve by cracking methane at 855°C in the pores of a charred lignite.[30] Consequently, with the carbon molecular sieve product, nitrogen may be separated from the oxygen in air and CH_4 from CO_2 (Fig. 3.13).

The controlled adjustment of pore throat size in the sieves and the resulting effect on molecular species diffusion suggest the importance these constrictions have in CBM diffusion and pore selectivity.

By analogy of the carbon molecular sieves with coal, matrix swelling/contraction occurs in the coal micropores with adsorption/desorption of methane or other adsorbates, such as CO_2. The result may be some blockage of passageways to molecular species larger than methane. By further extension of the analogy, generation during coalification of hydrocarbons heavier than methane may partially block the entrance to large pores to give smaller apertures. By the same mechanism, some smaller micropores may restrict the passage of methane itself.

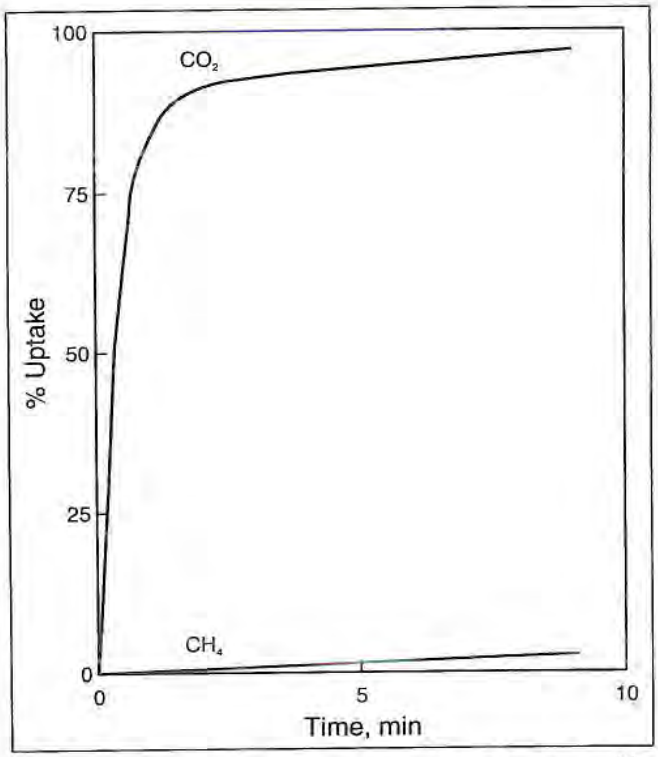

Fig. 3.13—Separation of carbon molecular sieves.[31]

The molecular sieve effect helps explain why paraffins block the pore entrance of coals in one section of the San Juan basin. It also adds to understanding of how polymer components of the fracturing fluid could block larger micropore openings.

3.7 Coal Sorption of Other Molecular Species

3.7.1 Swelling of Coal Matrix

Adsorption on coals swells the matrix. Adsorption of CO_2 is reported to create matrix swelling of coals[21] to the extent of an average linear strain of 1.255×10^{-5} psi^{-1} in coals from Metropolitan Colliery, New South Wales, Australia.[32] Coals from Hokkaido with an average linear strain of 8.621×10^{-7} psi^{-1} are reported[33] to swell much less upon adsorption of methane. Although CO_2 has a more pronounced swelling effect on the coal matrix, the desorption of large volumes of methane during production shrinks the matrix enough to increase permeability of the coalseam.

Matrix shrinking upon desorption improves permeability of coal as production of methane proceeds; shrinking of the matrix increases cleat width and reduces resistance to flow in the cleats, especially at the lower pressure end of the adsorption isotherm where larger volumes of methane are desorbed for a given increment of pressure decrease.

3.7.2 Heavier Hydrocarbons

The larger pore sizes of lignite trend to the small micropore sizes of anthracite as coalification progresses. Also consider that methane adsorption reaches a minimum near lvb coal ranks of 90% total carbon content (Fig. 3.14).[34]

The hydrocarbons produced in the coalification process and their subsequent blocking of pore throats may account for part of the decreased sorption of methane at low-volatile bituminous rank coals; subsequent geothermal conditions on the coal (especially very high temperatures) may clear the blockage as rank increases to anthracite.[35]

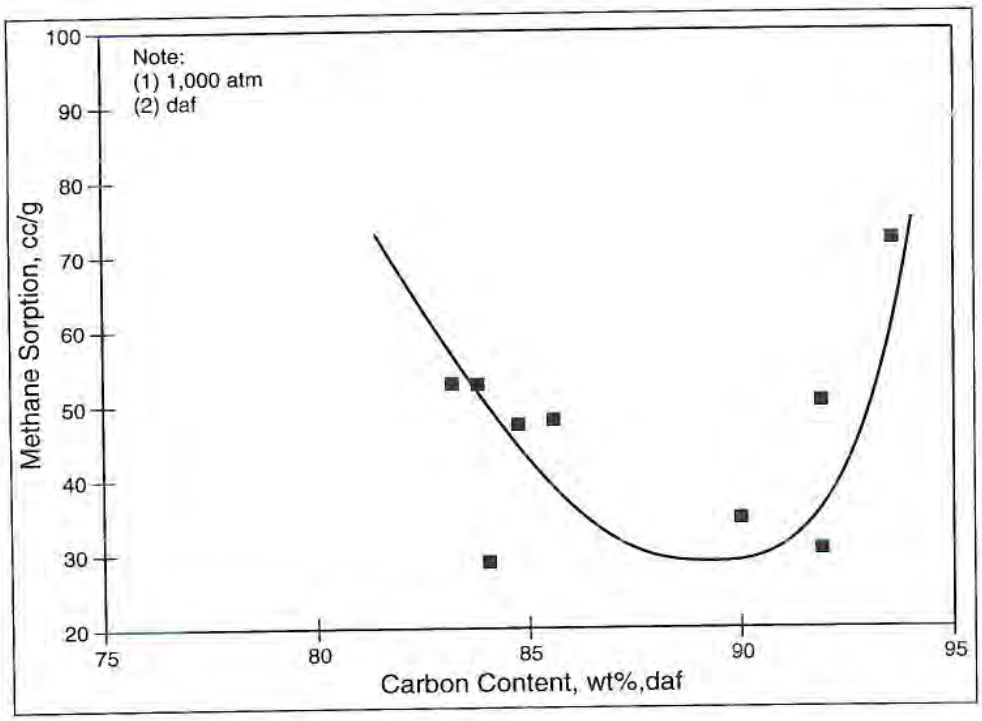

Fig. 3.14—Coal's minimum sorption.[34]

Levine reports that two coals of hvAb rank from the Fruitland formation of the northern San Juan basin differed in the waxy deposits of hydrocarbons (Table 3.5).[35] The core with waxy constituents gave a lower measured surface area by CO_2 adsorption and substantially lower gas desorption. The production of the heavier hydrocarbons during coalification evidently occurred at the hvAb stage in the waxy coal, probably obstructing the pore entrances of the waxy sample, thereby limiting passage in the pores to moisture, carbon dioxide, and methane.

Table 3.5—Waxy Constituent Effect on Sorption of Two hvAb Fruitland Coals[35]

	Sample 1	Sample 2
Sample Depth (ft)	2,989	3,068
R_{O2MAX} (%)	0.94	1.03
C_{15+} in Extract (ppm)	6,853	12,061
Saturated Hydrocarbons in Extract (%wt)	8.1	24.0
Equilibrium Moisture (%wt)	2.16	0.95
CO_2 Surface Area (m^2/gm)	122.7	61.75
Desorbed Gas (cm^3/gm)	21.5	12.7

Paraffins are reported to have reduced the flow of some CBM wells in the San Juan basin to uneconomical rates. Productivity was restored in one case, however, by injecting microbes into the well. The microbes fed on the paraffins in the micropore throats and cleaned them for passage of methane.

The Fruitland coals of the San Juan basin are rich in liptinite (exinite),[36] the maceral composed of higher percentages of hydrogen and aliphatics. The paraffins, oil, and alkanes heavier than methane that have been produced in modest quantities in the basin originated from these liptinite macerals in the coals of the southern part of the basin.

Any wet gases generated in coalification are subjected to further degradation to methane with increasing thermal maturity. An example of this is the 99+% CH_4 dry gases in the more thermally mature northern part of the basin. The dry methane may also be the result of bacterial action on the higher-weight aliphatics. The bacteria enter into the coalseams of the northern San Juan basin with meteoric waters at the coal's outcrop.

3.7.3 Carbon Dioxide and Nitrogen

Carbon dioxide is preferentially adsorbed over methane by coal. Because CO_2 affinity to the solid surface is greater than CH_4, an increasing desorption rate of CO_2 will result as the removal of free water lowers reservoir[28] pressures and as the less readily adsorbed methane depletes. A chromatographic effect results during the flow of gases in the coalseam because of the different affinities of methane, nitrogen, carbon dioxide, and ethane.

Data from the adsorption of methane-carbon dioxide mixtures on a Northern Appalachian coal are given in Fig. 3.15.[26] Note that substantially more pure carbon dioxide could be adsorbed by the coal than pure methane.

Gases from the Fruitland coals of the San Juan basin vary in composition across the basin with some produced gases being 99% methane. Some coals in the basin may contain as much as 13% carbon dioxide, while ethane or nitrogen may also be present. Ayers studied over 280 CBM wells in the Fruitland formation to determine variations in gas composition and to establish distribution patterns.[37] Consequently, this much-studied basin has the best characterization of gas composition and distribution. Gases are indistinguishable in the southern portion of the basin regarding origin in the Pictured Cliffs formation or Fruitland sandstones or coal. The high CO_2 contents occur in the hvAb coals in the basin.

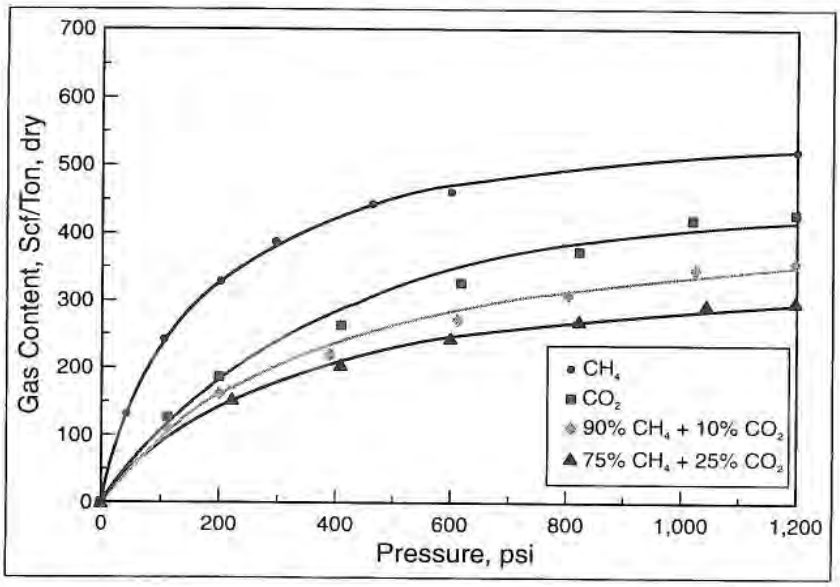

Fig. 3.15—Influence of CO_2 on adsorption isotherm.[26]

Significantly, the overpressured region of the San Juan basin has a greater presence of CO_2. Bacteria entering the meteoric waters at the high-elevation outcrops in the north produce CO_2 from organic matter encountered on its down-dip trek. The carbon dioxide is subsequently adsorbed by the coal to be released upon pressure reduction[36] of the CBM process.

3.8 Effects of Ash and Moisture on Ch_4 Adsorption

Gas content of a coalseam is affected by ash content and moisture in the coal matrix. The presence of either ash or moisture reduces the amount of methane that can be retained. A large volume of adsorbed moisture exists in lignite and the

rapid, steady decline of this moisture with the coal's maturation is a good indicator of rank in the lower-rank coals.[38]

The importance of bound water in the micropores is to reduce adsorption space for methane although bound water does not impede movement of methane through the micropores.[39,40] However, the moisture is more strongly adsorbed to the micropore surface than the components of air or methane, and some swelling of the matrix can be expected upon moisture adsorption in a dry coal.[41]

The reduction in gas content of an Appalachian coal because of moisture is evident in Fig. 3.16. An increasing bed moisture content reduces methane content at all pressures for these coals of the Pittsburgh seams of Greene County.[19]

The ash content of a coal, taken as representative of the mineral matter of coal as determined by a proximate analysis, correlates with the capability of that coal to adsorb methane. The methane content of the coal decreases linearly with ash content. Fig. 3.17 shows the importance of correcting the mass of the coal sample for ash content[42] from the standpoint of potential gas capacity of the coal. This is in addition to the deleterious effect that ash has on the coal's fracturing capability.

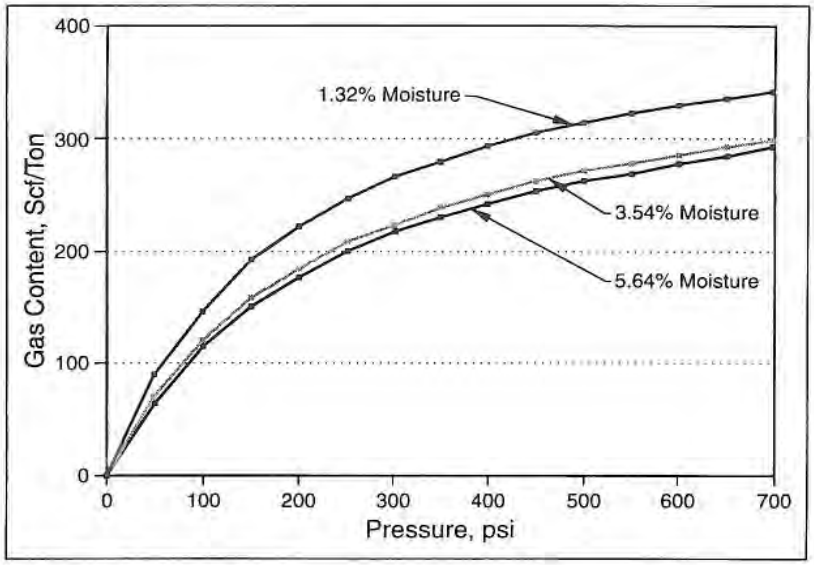

Fig. 3.16—Moisture reduces CH_4 capacity.[19]

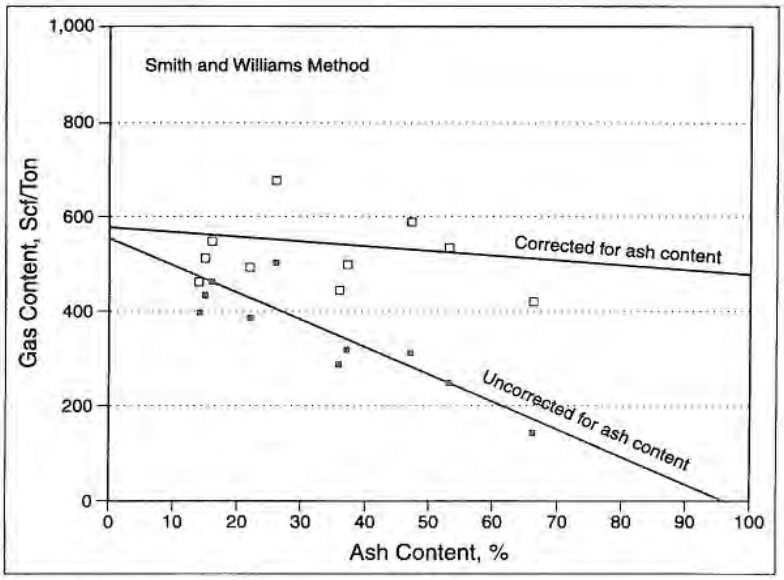

Fig. 3.17—Ash lowers CH_4 content.[42]

References

[1]Brunauer, S., Emmett, P.H., and Teller, E.: "Adsorption of Gases in Multimolecular Layers," *J. of Am. Chem. Soc.* (1938) 60, 309.

[2]Langmuir, J.: "The Adsorption of Gases on Plane Surfaces of Glass, Mica, and Platinum," *Am. Chem. Soc.* (1918) 40, 1361.

[3]Daniels, F. and Alberty, R.A.: *Physical Chemistry*, John Wiley & Sons, Inc., New York (1957) 524.

[4]Gregg, S.J. and Sing, K.S.W.: *Adsorption, Surface Area and Porosity*, Academic Press, London and New York (1967) 197.

[5]Yang, R.T.: *Gas Separation by Adsorption Process*, Butterworth Publishers, Boston (1987) 14.

[6]Rakop K.C. and Bell, G.J.: "Methane Adsorption/Desorption Isotherms for the Cameo Coalseam Deep Seam Well, Piceance Basin, Colorado," final report, Terra Tek, Inc., REI (July 1986) 30.

[7]De Boer, J.H.: *The Dynamical Character of Adsorption*, Clarendon Press, Oxford (1953) 55.

[8]*Chemical Engineers' Handbook*, third edition, J.H. Perry (ed.), McGraw-Hill Book Company, Inc., New York (1950) 301.

[9]Ruthven, D.M.: *Principles of Adsorption and Adsorption Processes*, John Wiley & Sons, New York (1984) 433.

[10]Scott, A.R.: "Composition and Origin of Coalbed Gases from Selected Basins in the United States," Proc., International Coalbed Methane Symposium, Vol. I, Birmingham, Alabama (May 1993) 207-222.

[11]Deo, M.D., Whitney, E.M., and Bodily, D.M.: "A Multicomponent Model for Coalbed Gas Drainage," Proc., International Coalbed Methane Symposium, Vol. I, Birmingham, Alabama (May 1993) 223-232.

[12]Harpalani, S. and Pariti, U.M.: "Study of Coal Sorption Isotherms Using a Multicomponent Gas Mixture," Proc., International Coalbed Methane Symposium, Vol. I, Birmingham, Alabama (May 1993) 151-160.

[13]Shreve, R.N.: *The Chemical Process Industries*, second edition, McGraw-Hill Book Company, Inc., New York (1956) 163.

[14]Mavor, M.J., Owen, L.B., and Pratt, T.J.: "Measurement and Evaluation of Coal Sorption Isotherm Data," paper SPE 20728 presented at the 1990 Annual Technical Conference and Exhibition of the Society of Petroleum Engineers, New Orleans, Louisiana, 23-26 September.

[15]Greaves, K.H., Owen, L.B., McLennan, J.D., and Olszewski, A.: "Multi-Component Gas Adsorption-Desorption Behavior of Coal," Proc., International Coalbed Methane Symposium, Vol. I, Birmingham, Alabama (May 1993) 197-205.

[16]Kalluri, V.: "Enhanced Recovery of Methane from Coalbeds," MS thesis, Mississippi State University, Starkville, Mississippi (May 1994).

[17]Tissot, B.P. and Welte, D.H.: Petroleum Formation and Occurrence, second edition, Springer-Verlag, New York (1984) 497.

[18]Jüntgen, H. and Karweil, J.: "Gas Formation and Gas Storage in Anthracite Coal Layers, Part I and Part II," Petroleum and Coal Gas Petrochemicals (1966) 19, 251-258 and 339-344.

[19]Hunt, A.M. and Steele, D.J.: Coalbed Methane Technology Development in the Appalachian Basin, GRI 90/0288 topical report, Contract No. 5089-214-1783 (January 1991).

[20]Das, B.M., Nikols, D.J., Das, A.U., and Hucka, V.J.: "Factors Affecting Rate and Total Volume of Methane Desorption from Coalbeds," Guidebook for the Rocky Mountain Association of Geologists Fall Conference and Field Trip, Glenwood Springs, Colorado (September 1991) 69-76.

[21]Gray, I.: "Reservoir Engineering in Coalseams: Part 1-The Physical Process of Gas Storage and Movement in Coalseams," SPE Reservoir Engineering (February 1987) 28-34.

[22]Hunt, A.M. and Steele, D.J.: "Coalbed Methane Development in the Appalachian Basin," *Quarterly Review of Methane from Coalseams Technology* (July 1991) 8, No. 4, 10-19.

[23]Olszewski, A.J. and Schraufnagel, R.A.: "Development of Formation Evaluation Technology for Coalbed Methane Development," *Quarterly Review of Methane from Coalseams Technology* (October 1992) 10, No. 2, 27-35.

[24]Kim, A.G.: "Estimating Methane Content of Bituminous Coalbeds from Adsorption Data," U.S. Bureau of Mines Rept. of Investigations 8245 (1977) 22.

[25]Smith, D.M. and Williams, F.L.: "Diffusional Effects in the Recovery of Methane from Coalbeds," *SPEJ* (October 1984) 529-535.

[26]Olszewski, A.J.: "Development of Formation Evaluation Technology for Coalbed Methane Development," *Quarterly Review of Methane from Coalseams Technology* (July 1992) 10, No. 1, 27.

[27]Bent, P.W., Radford, S.R., and Eaton, N.G.: "Reheat Cores to Measure Gas Better," *Pet. Eng. Int.* (October 1991) 46-55.

[28]Gregg, S.J. and Pope, M.I.: *Fuel* (1959) 38, 501.

[29]Zwietering, P. and van Krevelen, D.W.: *Fuel* (1954) 33, 331.

[30]Kamishita, M., Mahajan, O.P., and Walder, P.L. Jr.: *Fuel* (1977) 56, 444.

[31]Carrubba, R.V. *et al.*: *AIChE Symp. Ser.* (1984) 80, No. 233, 76.

[32]Hargraves, A.J.: "Instantaneous Outbursts of Coal and Gas," PhD dissertation, U. of Sydney, Sydney, Australia (1963).

[33]Gray, I.: "Overseas Study of Japanese Methane Gas Drainage Practice and Visits to Coal Research Centres, June-August 1980," Australian Coal Industry Research Laboratories Ltd., Sydney, report no. P.R. 80-15 (1980).

[34]Moffat, D.H. and Weale, K.E.: "Sorption by Coal of Methane at High Pressures," *Fuel* (1955) 34, 449-462.

[35]Levine, J.R.: "The Impact of Oil Formed During Coalification on Generation and Storage of Natural Gas in Coalbed Reservoir Systems," *Proc., Coalbed Methane Symposium*, Tuscaloosa, Alabama (May 1991) 307-315.

[36]Scott, A.R. and Kaiser, W.R.: "Relation between Basin Hydrology and Fruitland Gas Composition, San Juan Basin, Colorado and New Mexico," *Quarterly Review of Methane from Coalseams Technology* (November 1991) 9, No. 1, 10-17.

[37]Ayers, W.B. Jr.: "Geologic Evaluation of Critical Production Parameters for Coalbed Methane Resources," *Quarterly Review of Methane from Coalseams Technology* (February 1991) 8, No. 2, 27-33.

[38]Berkowitz, N.: An Introduction to Coal Technology, Academic Press, New York (1979) 31.

[39]Reznik, A.A., Dabbous, M.K., Fulton, P.F., and Taber, J.J.: "Air-Water Relative Permeability Studies of Pittsburgh and Pocahontas Coals," *SPEJ* (December 1974) 14, No. 6, 556-562.

[40]Olague, N.E. and Smith, D.M.: "Diffusion of Gases in American Coals," *Fuel* (November 1989) 68, 1381.

[41]Dabbous, M.K., Reznik, A.A., Taber, J.J., and Fulton, P.F.: "The Permeability of Coal to Gas and Water," *SPEJ* (December 1974) 14, No. 6, 563-572.

[42]Close, J.C. and Erwin, T.M.: "Significance and Determination of Gas Content Data as Related to Coalbed Methane Reservoir Evaluation and Production Implications," *Proc., Coalbed Methane Symposium*, Tuscaloosa, Alabama (April 1989) 37-55.

Chapter 4

Reservoir Analysis

4.1 Coal as a Reservoir

During the progression of coalification from peat to anthracite, an order of magnitude more methane may be generated than can be retained by the coal. Under proper conditions, the expelled gas may charge adjacent sands as evidenced by Pictured Cliffs sandstone conventional gas fields below Fruitland coals of the San Juan basin and by Trinidad sandstone below Vermejo coals of the Raton basin. Coal is an important source rock for natural gas, and commercial advantage has long been taken of this fact.

Coal is also a reservoir rock, but only in the development of the coalbed methane (CBM) process has this fact been commercially exploited. Even though the coal may retain only a fraction of the gas it generates as a source rock, that fraction may represent two to seven times more gas per unit volume as a reservoir rock than a conventional gas reservoir. This is because the coal may have 1 million ft^2/lbm of adsorption surface area,[1,2] and the adsorbed methane concentration may approach liquid density.

Similarities between the coalbed reservoir and the conventional sandstone or carbonate reservoir exist, and because of some similarities, oilfield technology may be used. However, differing phenomena in the relatively low-pressure coalbed reservoir have necessitated innovations, modifications, and limitations to conventional oilfield technology. Applied research has allowed adaptation of the oilfield processes. For example, different mechanical properties of the coal and formation susceptibility to chemical damage required study and modification of conventional fracturing and completion techniques. The concept of adsorption and attendant water problems was introduced into the analysis of a reservoir.

Comparisons of general properties of a conventional gas reservoir and a coal reservoir are presented in Table 4.1.

Table 4.1—Coalbeds and Conventional Reservoirs Compared[3]

Conventional Gas	Coalbed
Darcy flow of gas to wellbore.	Diffusion through micropores by Fick's Law.
	Darcy flow through fractures.
Gas storage in macropores; real gas law.	Gas storage by adsorption on micropore surfaces.
Production schedule according to set decline curves.	Initial negative decline.
Gas content from logs.	Gas content from cores. Cannot get gas content from logs.
Gas to water ratio decreases with time.	Gas to water ratio increases with time in latter stages.
Inorganic reservoir rock.	Organic reservoir rock.
Hydraulic fracturing may be needed to enhance flow.	Hydraulic fracturing required in most of the basins except the eastern part of the Powder River basin where the permeability is very high. Permeability dependent on fractures.
Macropore size:[3] 1μ to 1 mm	Micropore size:[3] <5A° to 50A°
Reservoir and source rock independent.	Reservoir and source rock same.
Permeability not stress dependent.	Permeability highly stress dependent.
Well interference detrimental to production.	Well interference helps production. Must drill multiple wells to develop.

To develop the coalbeds economically, gas content and permeability of the reservoir must meet minimum criteria that may be about 150 scf/ton gas content in thin seams and 1 md permeability. A minimum criterion of permeability is required before hydraulic fracturing can successfully interconnect the natural cleat system to the wellbore. Exceptions exist. For example, the extraordinarily thick coalseams of the Powder River basin are economical at lower gas contents.

Ordinarily, these reservoir characteristics must be determined to be above their minimum values before developing a field. Later, development centers around resolving questions of water production, water disposal, well interference effects, completion techniques, and well spacing.

The mechanism for gas flow in the coal involves three steps: (1) desorption of the gas from the coal surface inside the micropores, (2) diffusion of the gas through the micropores, and (3) Darcy flow through the fracture network to the wellbore.

Multiple wells in the field are necessary to remove water, where well-to-well interference is a positive factor. Faults and joints throughout the formation play an important role. Therefore, the interplay of many parameters in the reservoir is a complexity that requires simulation to fully understand overall performance. Consequently, simulation has been used extensively from the beginning of the CBM process, making the coalbed process possible and establishing itself as an essential analysis tool.

4.2 Permeability

Permeability is the most critical parameter for economic viability of a gas-containing coal; the network of natural fractures along with any hydraulic fractures must supply the permeability for commercial flow rates of methane. It is also the most difficult parameter to evaluate accurately. Therefore, the frequency of the natural fractures, their interconnections, degree of fissure aperture opening, direction of butt and face cleats, water saturations, burial depths, matrix shrinkage upon desorption, and in-situ stresses all affect permeability. The determination of gas effective permeability is further complicated by the changing nature of gas relative permeability with water content in the flow path.

Spafford and Schraufnagel[4] estimated with a simulator the effect of coalseam permeabilities on production for various hydraulic fracture half-lengths in the Warrior basin. Their results are presented in Fig. 4.1. It is evident from the work

that natural permeabilities of this Warrior basin coal:

- Less than 0.1 md hold little promise of improvement in gas production from fracturing.
- With initial permeabilities between 0.1 and 1.0 md are marginal for development after fracturing.
- With permeabilities between approximately 1.0 and 10.0 md can have production enhanced greatly by fracturing.

Although the results are derived for the Mary Lee coal group at Rock Creek, the effect of permeability on well performance and fracture design should be qualitatively representative of other basins.

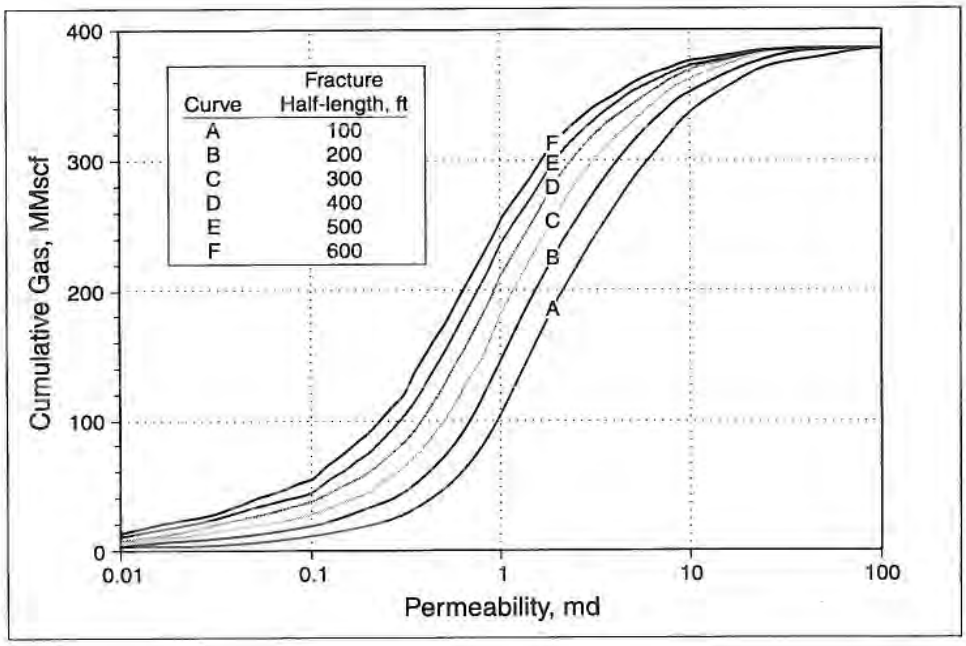

Fig. 4.1—Results of a simulator estimation of the effect of coalseam permeabilities on production for various hydraulic fracture half-lengths in the Warrior basin.[4]

Therefore, how the reservoir is treated depends on permeability, and the permeabilities of natural cleat systems vary from basin to basin and from coalseam to coalseam. Values can range from impermeable to >100 md.

How are the cleats formed? Insight into this question might assist the engineer in planning and managing the reservoir development. Natural fractures occur during coalification from shrinkage of the coal matrix after loss of volatiles. Folding or tectonic action over geologic time further extends the fracturing network.[5] Additionally, differential compaction of coalseams and adjacent sediments possibly contribute to the cleat network in coals, but the effect is probably minor. Maceral content influences the frequency of cleats in the coal, as does the coal rank at the time tectonic action occurred. Mineral matter in the coal has a deleterious effect on cleat formation.

Table 4.2 gives a few representative, absolute permeabilities of major coalseams where active CBM projects exist. The tabulation implies a diversity of permeabilities in commercial projects, and it also suggests a dependence of permeability on depth and the in-situ stresses that normally increase with depth. The CBM process for the first time has emphasized the importance of in-situ stresses in the formation.

Table 4.2—Representative Permeabilities

Location	Permeability (md)
Cedar Cove, Brookwood, Oak Grove Fields in Warrior Basin[6]	100 at 100 ft 10 at 1,000 ft
U.S. Steel Well 1036, Appalachian Basin[7]	20
Upper Fruitland, NE Blanco Unit, San Juan Basin[8,9] Upper Fruitland, Tiffany Project Area[10] Basal Fruitland, Tiffany project Area[10]	 1.5 to 8.8 1.5 4.5
Mary Lee (Upper Group) Black Creek (Lower Group)	10 to 25 0.5 to 3.5
Cedar Hill, San Juan Basin[11] • Butt Cleat Direction • Face Cleat Direction	 4 12

Determining the permeability of a prospective coal reservoir is of major importance. Insight into permeability from the extent and direction of fracturing in coals of undeveloped areas has been sought through the study[12] of surface lineaments revealed by satellite and aerial photographs. From these photographs, directional trends can be defined, but an acceptable general correlation with permeability has not been achieved.

Even with core tests, accurate measurement of permeability is difficult. Because permeability of coal is a function of stress, values measured in the laboratory cores may not be accurate. Also, since the permeability of coal is a function of sample size,[13] values measured in the laboratory tend to be less than those realized in the field because the small cores may not sample fractures or joints.[14] Laboratory results can be a factor of 10 lower than permeabilities experienced in the field.[15] It is possible that damage to the cores may result upon extraction, and it may be impossible to reproduce the formation stresses in the laboratory. Hence, it is necessary to determine permeability from history matching production data or from one of the following pressure transient tests:

- Drillstem test (DST).
- Slug test.
- Injection falloff tests (IFT).
  - Tank test.
  - Below fracture pressure injection falloff test (BFP-IFT).
  - Diagnostic fracture injection test (DFIT).
- Pressure buildup test (PBU).
- Multi-well interference test.

4.2.1 Drillstem Test (DST)

This test is similar to the drillstem tests performed in conventional wells. They are performed openhole and are usually conducted during the drilling of the well rather than after reaching the total depth of the well. Openhole drillstem tests are performed because the coals are least damaged at this time. Individual zones are isolated with packers (see Fig. 4.2) and tested to determine permeability, skin damage, fluid properties, and reservoir pressures. Like conventional well drillstem tests, there are four periods in this test, namely:[16]

a) Pre-flow period.

b) First/initial shut-in period.

c) Main flow period.

d) Final shut-in period.

The first flow period is usually performed to clean up the well, and the shut-in that follows lets the well equilibrate from the pre-flow-period pressure variations. The main flow period is usually longer than the pre-flow period and is performed to determine the formation flow characteristics. Fluid samples taken during this period can be analyzed following the conclusion of the test. The final shut-in that follows the flow period will help determine the formation permeability and skin damage (if any). The drillstem test is not the most commonly applied pressure transient test in coals because of safety issues, higher costs, and short radius of investigation.

Fig. 4.2—DST tool string.

4.2.2 Slug Test

The slug test involves the instantaneous addition (or withdrawal) of a specific volume of fluid into (or from) a wellbore and measuring the pressure response as the fluid level returns to equilibrium conditions. It is relatively simple to perform and the main requirements to perform this test are the following:

- Tool to isolate the test interval.
- A way to instantaneously inject (or withdraw) the specific volume of fluid.
- A way to measure the pressure as the well returns to equilibrium conditions.

The following are the main advantages of a slug test:

- Executed simply.
- Costs less.
- Requires no flow rate control mechanism.
- Requires relatively simple analysis.
- Can be performed if the well is underpressured.

The main disadvantages of a slug test are:

- Test duration could be excessively long for low-permeability coals.
- Radius of investigation is relatively small.
- Results may be incorrect if gas saturation is present.
- Results may not be as unique as other test types.

The slug test is undertaken before fracturing while only water is being produced. Besides permeability, initial formation pressure may be determined from the test. Likewise, if porosity-compressibility is known, a skin factor may be calculated to estimate well damage.

The test procedure establishes a hydrostatic head of water in the wellbore above the coalseam that is higher than the equilibrium level of water above the seam. The water influx rate into the seam at the known hydrostatic head of the imposed water column is then measured. Test pressures are kept below fracturing pressures. The test is simple to perform with a minimum of equipment and a foolproof operating procedure. One shortcoming of the slug test is that the penetration distance into the formation may be short. In the CBM process, a short radius of investigation may not incorporate important fractures contributing to formation permeability.[17] A schematic of the setup is presented in Fig. 4.3.

A pressure transducer placed by wireline below the equilibrium water level monitors pressure as a function of time, and from this data, the rate of water influx into the seam is calculated. The water influx rate is determined from the difference in volume of water in the tubing before and after the tests. A takeoff on the procedure is to draw down the initial equilibrium hydrostatic head above the seam and subsequently monitor water inflow to the well by means of the transducer as a function of time.

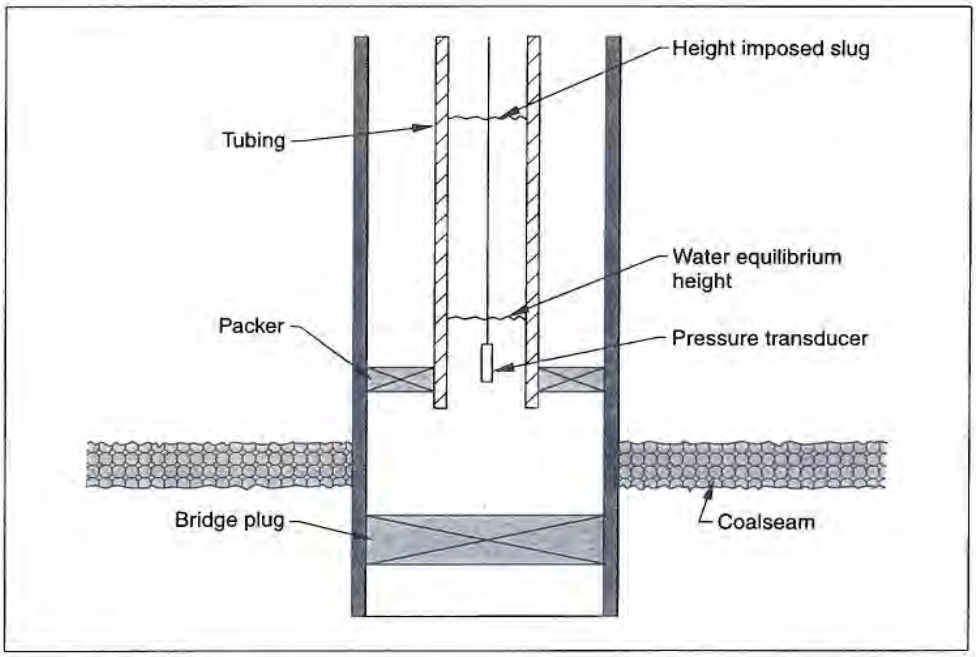

Fig. 4.3—Slug test.

Time to conduct the test depends on permeability of the formation and on the volume of the hydrostatic head in the wellbore according to Eq. 4.1.[18] It is important to note that test time increases with the square of the wellbore diameter.

$$t_s = \frac{75.9\mu D_i^2}{kh} \qquad (4.1)$$

where

t_s = time to perform slug test, hr
μ = viscosity of water test fluid, cp
D_i = inside diameter of casing, tubing, or open hole confining the test fluid, in.
k = formation permeability, md
h = height of coalseam tested, ft

The test time, t_s, may be estimated by assuming a permeability of the formation. Viscosity of the water test fluid, casing diameter, and height of the seam will be known. The test time as a function of casing, tubing, or wellbore diameter is given in Fig. 4.4 for various formation permeabilities.[7,19] A seam height of 10 ft and a 1-cp water viscosity were assumed to prepare the curves. In practice, the test time can be regulated by choice of tubing diameter.

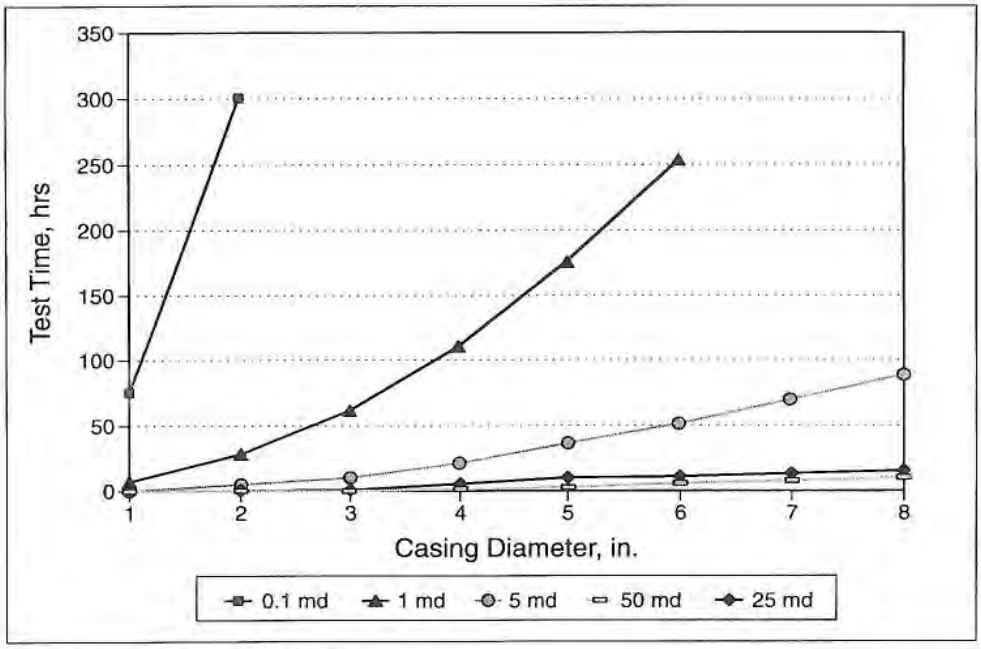

Fig. 4.4—Slug test time.[19,22]

The absolute permeability of the seam is calculated from Eq. 4.2. Type curves are used to make the determination of permeability.[20]

$$k = \frac{5.68x10^{4}\,\mu\,D_c^{2}}{\rho_{wf}\,ht^{*}} \qquad (4.2)$$

where

k = permeability, md
μ = test fluid viscosity, cp
D_c = casing diameter, ft
h = net pay thickness, ft
ρ_{wf} = test fluid density, lb/ft^3
t^* = time from type curve match, hr

The time, t^*, in Eq. 4.2 is obtained from the match point of the type curve first developed by Ramey[21] and presented by Earlougher,[16] which is superimposed on a plot of the slug test data (ratio of water heights on Y-axis vs. test time on logarithmic X-axis) on the same coordinates and scale as the type curves.[22]

The wellbore storage coefficient, C_D, is calculated[20] from Eq. 4.3. The parameters of doubtful value will be the porosity and the total compressibility of the formation. Porosity will be less than 5%, where 2.5% is a typical value.

$$C_D = \frac{72 D_c^2}{\rho_{wf} \phi c_t h D_w^2} \tag{4.3}$$

where

φ = porosity
D_w = diameter wellbore
c_t = total compressibility

The total compressibility of the formation is commonly given[23] by the following equation:

$$c_t = c_w S_w + c_f + c_g S_g$$

where

c_w = water compressibility, psia^{-1}
S_w = water saturation, fraction
c_f = formation compressibility, psia^{-1}
c_g = gas compressibility, psia^{-1}
S_g = gas saturation, fraction

Skin factor from any drilling and completion damage may be calculated from Eq. 4.4. With a value of the wellbore storage factor, C_D, obtained from Eq. 4.3, and

$C_D e^{2s}$ obtained from the match point of the type curve, a dimensionless skin factor, s, can be determined from Eq. 4.4.[20]

$$s = \frac{1}{2} \ln \frac{C_D e^{2s}}{C_D} \tag{4.4}$$

Primary limitations to the slug test are the following:

- Does not apply after fracturing.
- Valid for water-saturated seams.
- Applicable to homogeneous reservoir of one seam.
- Short depth of penetration.

The test is also limited to underpressured reservoirs, and its accuracy is influenced by the stress dependency of the permeability of the coal. Since coal properties may vary laterally within a single seam and the variation is even greater vertically among parallel seams, interpretation of the slug test is best for a single seam with deep penetration of the test fluid. Penetration as radius of investigation, r_d, may be estimated by Eq. 4.5.

$$r_d = 0.029 \sqrt{\frac{kt}{\phi \mu c_t}} \tag{4.5}$$

where

r_d = penetration of slug, ft
k = permeability, md
t = time, hr
φ = porosity
μ = viscosity, cp
c_t = total compressibility, psi^{-1}

It should be noted that penetration distance into the formation of the slug, as given by r_d, is increased at the expense of longer test times.

4.2.3 Injection Falloff Tests

4.2.3.1 Tank Test

The tank test falls into the category of injection falloff test because it uses gravity drainage to inject water instead of using pumps (Fig. 4.5). For gravity drainage to occur, the reservoir pressure should be lower than the hydrostatic gradient. The difference between the reservoir pressure and the hydrostatic head of the tank and wellbore creates the injection potential. Since the reservoir pressure is very low, it is always recommended to use a downhole shut-in valve and avoid any wellbore storage effects. Conventional leakoff analysis methods can be used to analyze the shut-in data because a fracture is not created during gravity injection.

The main benefits of this test are that it:

- is conducted under single-phase testing conditions and hence there is no need for relative permeability curves.
- can be applied to both pre- and post-stimulated coalseams.
- costs comparatively less.

The main disadvantages of this method include the following:

- A small breakdown treatment is required to establish good communication between the wellbore and the coal.
- The radius of investigation is limited to the created water bank.[24]
- Because of the limitation above (bullet 2), a long injection period is required to create a sufficiently large water bank before the falloff data is affected by two-phase flow.[24]

If radial/pseudo-radial flow was observed during shut-in, a "unique" solution for pore pressure and permeability can be obtained. If by any chance a fracture is created during injection, the falloff data cannot be analyzed using conventional leakoff analysis techniques.

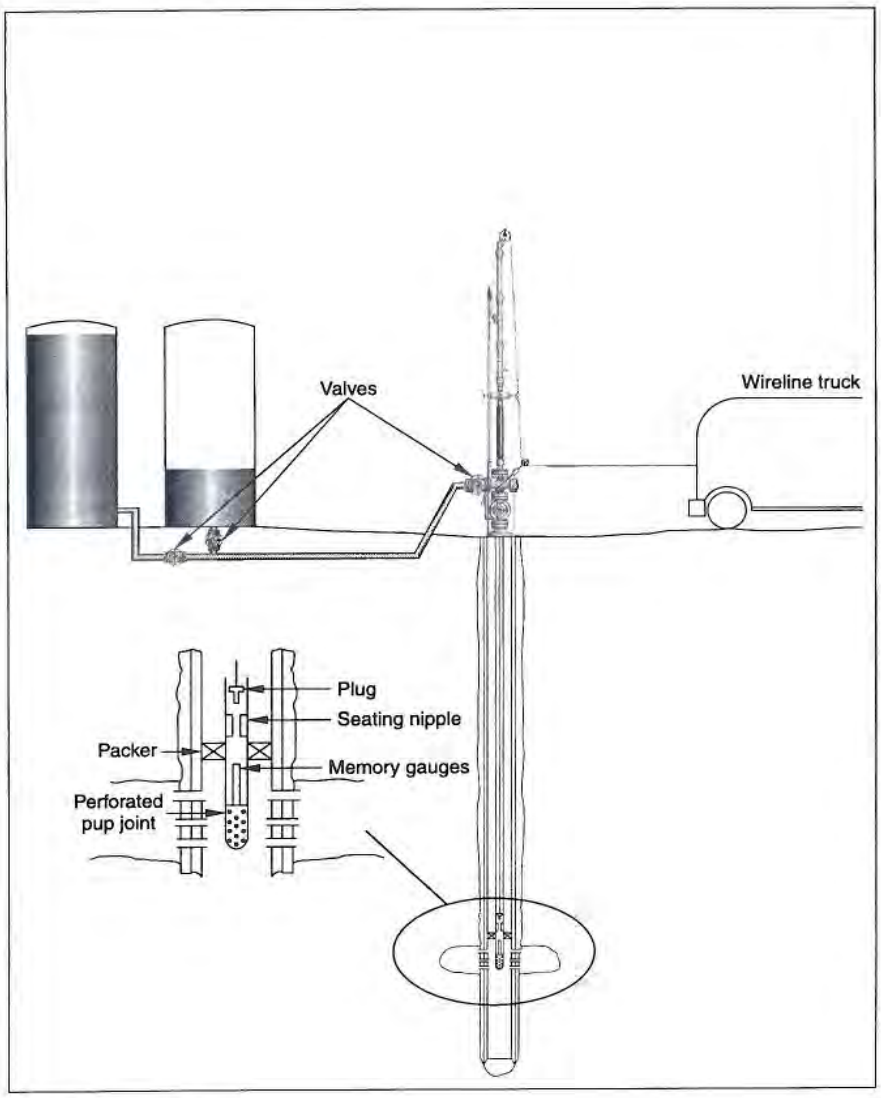

Fig. 4.5—Tank test

4.2.3.2 Below Fracture Pressure-Injection Falloff Test (BFP-IFT)

The BFP-IFT is also referred to as the "matrix injection test." It has been widely used in the industry to test the coals and obtain pore pressure, skin, and permeability. If the reservoir pressure is too high to conduct a gravity drainage injection, pumping equipment will be required to perform a conventional injection. This test can be applied in both over-and under-pressured reservoirs as long as the fracture pressure is not exceeded during injection.

In the BFP-IFT test, water is injected into the formation at sufficiently low rates (sometimes at less than 0.5 gal/min) such that a fracture is not created. If the permeability of the coal is very low, then accordingly, low injection rates are needed to prevent fracturing the zone. The shut-in period has to be at least four times the injection period. The shut-in falloff pressure data are then analyzed to obtain pore pressure, permeability, and skin damage. If fracture pressure is exceeded during injection, conventional falloff analysis is not applicable to analyze the data.

The advantages of the BFP-IFT test are the following:

- Does not need relative permeability curves because of single-phase testing conditions.
- Can be applied to both pre- and post-stimulated coals.
- Will provide a unique solution if conducted properly.

The main disadvantages of this test are the following:

- The injection fluid has to be pumped below fracture pressure (if the data are to be analyzed using conventional falloff analysis).
- A breakdown is needed before the test because a poor connection between the wellbore and the reservoir can lead to erroneous results.[25]
- A non-stable reservoir pressure before the test can result in non-unique solutions.[24]
- The test is not applicable to very low-permeability coals because pumping below fracture pressures may not be possible.

4.2.3.3 Diagnostic Fracture Injection Test (DFIT)

DFIT is a form of injection falloff test that first found use in conventional reservoirs and later in coals. DFIT is a small-volume, cost-effective, and short-duration test that has been used successfully in conventional and CBM reservoirs. The test consists of the following analyses:

1. G-function derivative analysis to identify the leakoff mechanism and closure.
2. Calibrated before-closure analysis using modified Mayerhofer method to determine permeability and fracture-face resistance.
3. After-closure analysis to determine pore pressure and permeability.

The uniqueness in applying this test to coals derives from the following:

- Injection rates are not limited by fracture pressure.
- Creation of a fracture during injection is taken into consideration.
- Is mainly dependent on after-closure analysis.
- Can be applied whether a fracture is created or not.

Since the injection volume is low, and the shut-in time is long enough to observe pseudoradial flow, the late-time, after-closure data can be analyzed for pore pressure and permeability. DFIT is similar to the impulse fracture test proposed by Abousleiman, *et al.*[26] The impulse fracture analysis method uses the late-time data and hence can be applied whether the formation is fractured or not. Thus, if the fracture pressure is exceeded during a conventional below fracture pressure-injection falloff test (BFP-IFT), the falloff data can still be analyzed using the DFIT after-closure analysis method.

In addition to its uniqueness, there are seven main advantages of this test.

1. It is a short-duration test and thus economical for the operator.
2. There is no need for a breakdown treatment before the test to establish good communication between the wellbore and the reservoir.
3. The test can be applied to both pre- and post-stimulated coals.
4. It can determine unique pore pressure and permeability values.
5. It is the only test of coals in which closure pressure and leakoff type can be determined in conjunction with pore pressure and permeability.

6. The results from this test can also be used to optimize stimulation treatments.
7. The test can analyze BFP-IFT data if it exceeded the fracture pressure.

The results obtained from DFIT in some coals were compared with the below-fracture, pressure-injection falloff test results performed in the same coals and were found to be similar.[27]

The two main disadvantages of the DFIT test are that (1) it cannot obtain quantitative skin damage values, and (2) if pseudoradial flow was not observed during shut-in, the results may not be unique.

Fig. 4.6 shows a typical coal DFIT treatment plot. In this case, approximately 1,195 gal of 2% KCl water was injected into a 24-ft thick coal at an average rate of 3.9 bbl/min. The bottomhole instantaneous shut-in pressure obtained was 2,464 psi, resulting in a fracture gradient of 0.84 psi/ft. The resulting G-function derivative analysis plot is shown in Fig. 4.7, which clearly shows pressure-dependent-type leakoff with hydraulic fracture closure estimated to be 2,149 psi. Fissure opening pressure was estimated to be 2,301 psi. The data following closure were then used in the after-closure analysis.

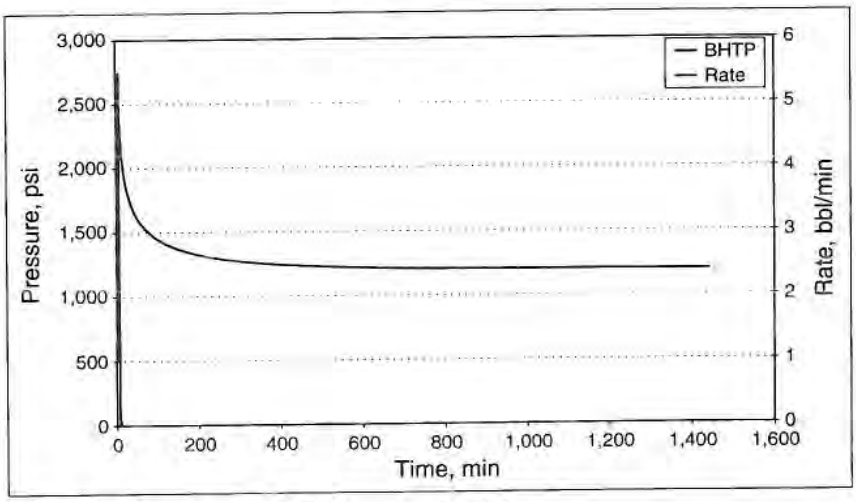

Fig. 4.6—Typical coal DFIT treatment plot.

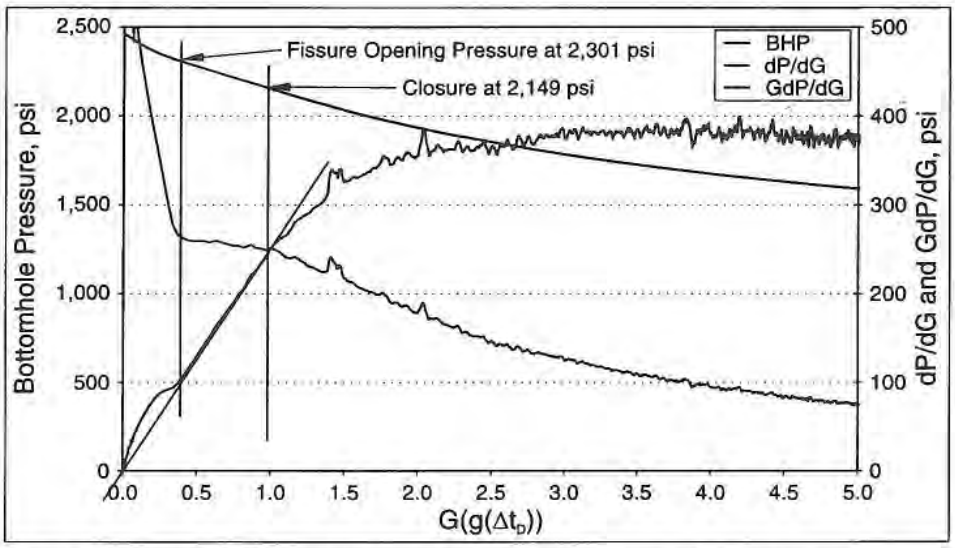

Fig. 4.7—Pressure-dependent-type leakoff with hydraulic fracture closure estimated to be 2,149 psi.

Fig. 4.8 shows the after-closure log-log diagnostic analysis plot. This plot is used to verify whether pseudolinear and pseudoradial flows were observed during shut-in. Pseudolinear flow occurs soon after fracture closure, and it precedes pseudoradial flow. According to Nolte,[28] pseudolinear flow behavior is described by Eq. 4.6.

$$P(t) - P_r = M_L F_L(t, t_c) \qquad (4.6)$$

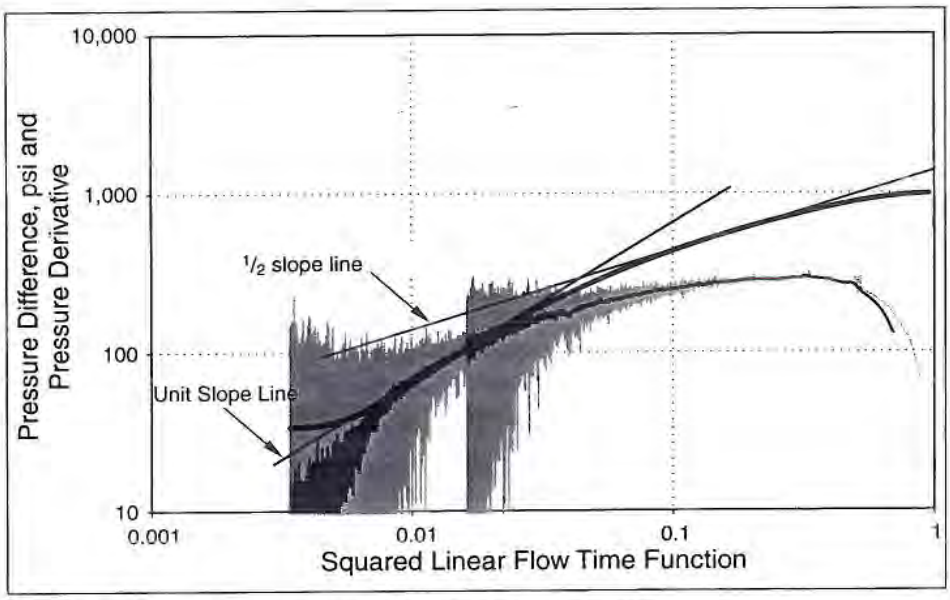

Fig. 4.8—After-closure log-log diagnostic analysis plot.

In Eq. 4.6, M_L is a constant during pseudolinear flow. The linear flow time function, $F_L(t,t_c)$, is defined in Eq. 4.7.

$$F_L(t,t_c) = \frac{2}{\pi}\sin^{-1}\sqrt{\frac{t_c}{t}}, t \geq t_c \qquad (4.7)$$

Talley, *et al.*[29] state that pseudolinear flow regime can be verified by plotting the pressure difference, P(t) - P_r, and pressure derivative vs. the squared linear flow time function, $F_L(t,t_c)^2$, on a log-log plot. This plot should result in a one-half slope for pseudolinear flow. Pseudolinear flow is indicated when the pressure difference and the derivative curves fall on a half-slope line and is offset by a factor of 2. Fracture half-length can be determined with the use of before-closure information and the transition time from pseudolinear to pseudoradial flow. This

can be used to verify the fracture length obtained from before-closure analysis. It is recommended that the reader refer to work done by Nolte[28] for further discussion on this topic.

The late-time pressure decline of a diagnostic fracture injection test develops into pseudoradial flow that allows the determination of transmissibility (and thus permeability) using a method similar to Horner analysis.[29] Pseudoradial flow is not dependent on the pumping schedule, but instead it depends on the injection volume, reservoir pressure, formation transmissibility, and closure time.[26,29-31] When pseudoradial flow regime is reached the pressure behavior is defined as in Eq. 4.8.

$$P(t) - P_r = M_R F_R(t, t_c), t > t_c \qquad (4.8)$$

In Eq. 4.8, P_r is the initial reservoir pressure. The radial flow time function, F_R, which is functionally equivalent to Horner time in conventional well testing, is defined[32] in Eq. 4.9.

$$F_R(t, t_c) = \frac{1}{4}\ln\left\{1 + \frac{\chi t_c}{t - t_c}\right\}, \chi = \frac{16}{\pi^2} \cong 1.6 \qquad (4.9)$$

Hence, a Cartesian plot of pressure vs. radial flow time function yields reservoir pressure from the y-intercept and reservoir transmissibility is then determined from the slope, M_R, using Eq. 4.10.

$$\frac{kh}{\mu} = 251{,}000\left[\frac{V_i}{M_R t_c}\right] \qquad (4.10)$$

In Eq. 4.10, V_i is the injected volume in units of barrels. Thus, permeability can be determined from the equation.[6]

Pseudoradial flow regime can be verified by plotting the pressure difference, $P(t) - P_R$, and the pressure derivative vs. the radial flow time function, F_R, or squared linear flow time function, $F_L(t,t_c)^2$, on a log-log plot. When the pressure curve and the derivative curves overlay on a unit slope line, pseudoradial flow is confirmed.

In this example, Fig. 4.8 clearly shows that both pseudolinear and pseudoradial flows were observed during shut-in. Sometimes, it is difficult to identify the offset factor of 2 when pseudolinear flow occurs early, as in this case. Since pseudoradial flow was observed during shut-in, the intercept of the extrapolated straight line through the pseudoradial flow data provides an estimate of the pore pressure (1,164 psi) and is shown in Fig. 4.9. Transmissibility (and thus permeability) is then obtained from the slope of the extrapolated straight line. In this example, the permeability estimated from after-closure pseudoradial flow analysis is 2.82 md.

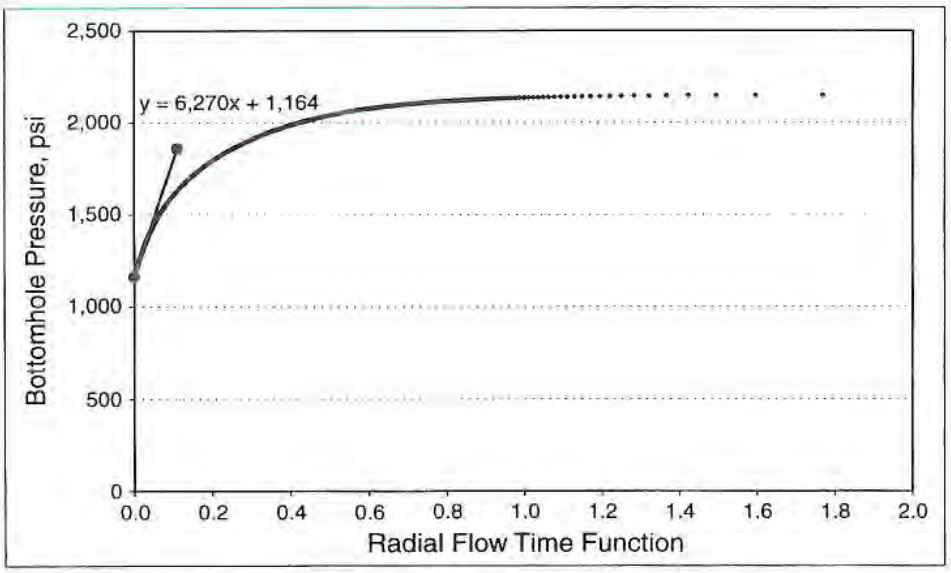

Fig. 4.9—The extrapolated straight line through the pseudoradial flow data provides an estimate of the pore pressure (1,164 psi).

4.2.3.4 Pressure Buildup (PBU) Test

Pressure buildup tests in coals are performed similar to the conventional reservoirs. When designing a PBU test in coal, it has to account for the coal properties. A PBU test can be performed in coal only when the reservoir pressure is sufficiently high (high deliverability). Permeability, skin, and average reservoir pressure can be obtained from this test. The two main advantages of this test are as follows:

- Drawdown/buildups are preferred for estimating reservoir properties in reservoirs with initial gas saturation.
- The test can be applied in both pre- and post-fracture stimulated coals.

The disadvantages of this test include the following:

- For wells with low deliverability, drawdown/buildup may not be feasible.
- Because drawdown occurs, the probabilities are high for two-phase flow.
- The test requires relative permeability curves to account for possible two-phase flow conditions.
- If not applied correctly, the test can lead to non-unique solutions.

4.2.3.5 Multi-Well Interference Test

Multi-well interference tests are performed to determine the interwell properties of absolute permeability and porosity-compressibility product. This test helps determine the heterogeneity of the CBM reservoir along with the degree of connectivity. Essentially, the test helps determine the permeability in the face and butt cleat directions. The test is conducted by producing or injecting into an active well and monitoring the responses in at least three observation wells.

Usually the face and butt cleats are perpendicular to each other. Hence interference testing may require only two observation wells present in the face and butt cleat directions to determine the magnitude of the low- and high-permeability trends. It is possible that the direction of the maximum permeability may be in a different direction than the face cleat direction as seen in the Black Creek coal at the GRI sponsored research project in the Black Warrior basin.[33] This was caused by some larger fractures being present that caused the direction of the maximum permeability to be in a different direction

than the face cleat direction. In such cases, three observation wells are required. There are four main advantages of performing a multi-well interference test:

- To understand the magnitude and orientation of the permeability in the butt and face cleat directions.
- To understand the heterogeneity of the CBM reservoir.
- To help determine well locations.
- To help optimize the CBM well spacing.

The two main disadvantages of the multi-well interference tests are:

- It is very expensive to perform.
- When two-phase reservoir conditions exist, only small saturation gradients should exist between wells.[24]

Simulation using a history match of production data is also a common practice in the CBM industry for determining coalseam permeability. However, to determine permeability, it is preferred to perform well tests under initial conditions when the coalseams are fully saturated with water and before any well production.[34] Then, the tests can be conducted under single-phase flow conditions and do not have to depend upon relative permeability relationships. After two-phase flow is established, the absolute permeability becomes dependent upon the chosen relative permeability curves. Hence, injection falloff tests are preferred since they test the coalseams under single-phase flow conditions.[35]

4.2.4 Depth Effects on Permeability

Because deep coal resources hold no interest for mining, data on seams below 4,000 ft are sparse. The deeper coals have been verified from logs of conventional wells near the center of the Warrior basin at 4,000- to 10,000-ft depths.[36-38] Coals at these depths are abundant in the Piceance basin and the Menefee formation of the San Juan basin. Coals below 5,000 ft are common in numerous other countries.[39]

Gas content may be higher at the pressures of the deeper coals. According to the Langmuir isotherms of coal, more gas can be adsorbed as pressure increases. Additionally, conditions of the deep coals promote the maturation process in its generation of methane and progression of rank. The higher formation pressures would be beneficial as a driving force for gas production. Therefore, in these important ways deep coals have the potential of being better producers.

The primary problem of the deep coals, however, is a decrease in coal permeability with depth. McKee, Bumb, and Bell[6] collected permeability data for coalseams in the San Juan, the Warrior, and the Piceance basins. Their correlation of permeability with depth predicts potential problems in producing deep CBM wells (see Fig. 4.10).

As shown in Fig. 4.10, permeabilities of the three basins decline rapidly below 4000-ft depths, decreasing at a rate of nearly 20% per 1,000 ft. At 0.1 md, where hydraulic fracturing becomes ineffective, a depth of approximately 7,000 ft would be expected.

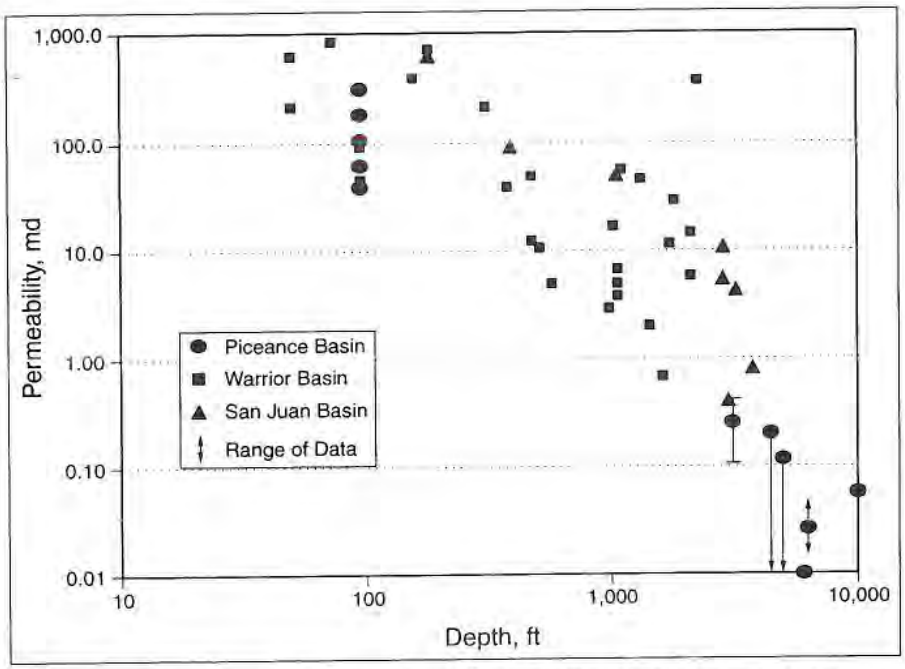

Fig. 4.10— Permeability of deeper coals.[6] Copyright 1984, Society of Petroleum Engineers.

However, Kuuskraa and Wyman[39] detailed three reasons why the relationship of Fig. 4.10 may be overly pessimistic. First, the correlation assumes a minimum horizontal stress gradient equal to the vertical stress gradient. Minimum horizontal stresses lower than the vertical stresses have been reported that indicated 10 to 100 times higher permeabilities than those from Fig. 4.10. Second, permeabilities in the correlation measured by slug tests may have been unduly low because of skin effects from formation damage near the wellbore.

Third, the Carman-Kozeny equation was used to relate permeability to porosity as given by Eq. 4.11.

$$k = f\left(\frac{\phi^3}{(1-\phi)^2}\right) \qquad (4.11)$$

where

k = permeability
φ = porosity

The Carman-Kozeny equation developed for sandstone formations is unproven for fractured coal formations.[39]

4.2.5 Klinkenberg, Shrinkage, and Stress Effects on Permeability

When pressure declines in coalseams as a consequence of production of water and gas, permeability changes because of three mechanisms: Klinkenberg effect, matrix shrinkage, and effective stress. Two of these mechanisms increase permeability, and the third reduces permeability.

The Klinkenberg effect increases effective permeability of methane at low pressures.[40] Flow of a gas through the cleats of coal is described by the Darcy equation, which includes the assumption that the layer of gas closest to the fracture walls is stagnant and does not move. In conventional sandstone reservoirs, as well as coal reservoirs, slippage of the adjacent layer does occur at low pressures to give a higher flow rate than would be calculated by Darcy's law, that is, the Klinkenberg effect. In the coalseams, pressures are likely to be lower than in conventional reservoirs, especially as production approaches abandonment, making the Klinkenberg effect more important in coal.

The correction of permeability for the Klinkenberg effect on gases flowing through porous media at low pressures is described by Eq. 4.12.

$$k = k_{\infty}(1 + b/p) \qquad (4.12)$$

where

k = corrected permeability
k_{∞} = permeability at high pressure
b = slippage factor
p = mean pressure

At very high pressures, the permeability is denoted by k_{∞}. At low pressures, Eq. 4.12 shows that slippage increases effective permeability of the gas linearly with reciprocal pressure.

The phenomenon is illustrated in Fig. 4.11 where the permeability of a porous rock to hydrogen, carbon dioxide, and nitrogen increases linearly with reciprocal pressure as pressure is decreased from a common value for all three gases at an initially high pressure.[41]

The effect on production rates of slippage of gas at the gas-coal interface at low pressures is greater than predicted from the Darcy equation. When pressures in the cleats are reduced with production, the Klinkenberg effect becomes increasingly important at low formation pressure because the largest amount of gas is desorbed and produced for a given increment of pressure decline. The Klinkenberg effect coupled with high gas storage at low pressures according to the Langmuir isotherm makes it especially important to extend the process to the lowest possible abandonment pressure.

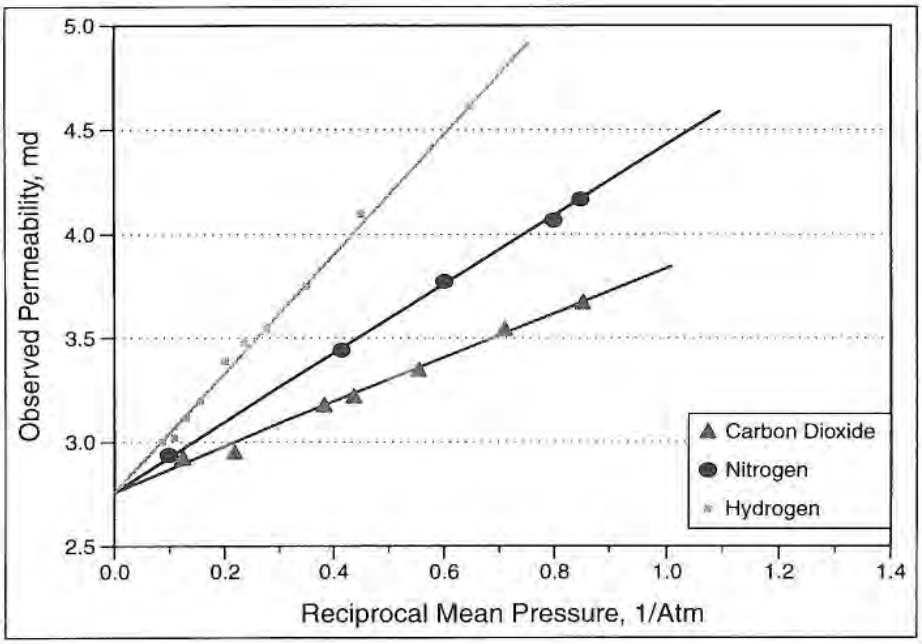

Fig. 4.11—Klinkenberg effect on permeability.[41] *Copyright 1990, Society of Petroleum Engineers.*

The coal matrix shrinks as gases desorb, which causes an enlargement of the adjacent cleat spacing.[42] The effect increases with adsorbate affinity for the coal. For example, the effect is greater for desorption of CO_2 than for methane because of the stronger affinity of the coal for CO_2. The cumulative shrinkage from the methane desorption is greater near the end of the well life for two reasons. First, most of the methane has been desorbed, and most of the matrix contraction has occurred. Second, at this point on the Langmuir isotherm, more methane is desorbed for a unit pressure decrease, so the greatest rate of matrix contraction occurs (see Fig. 4.12).

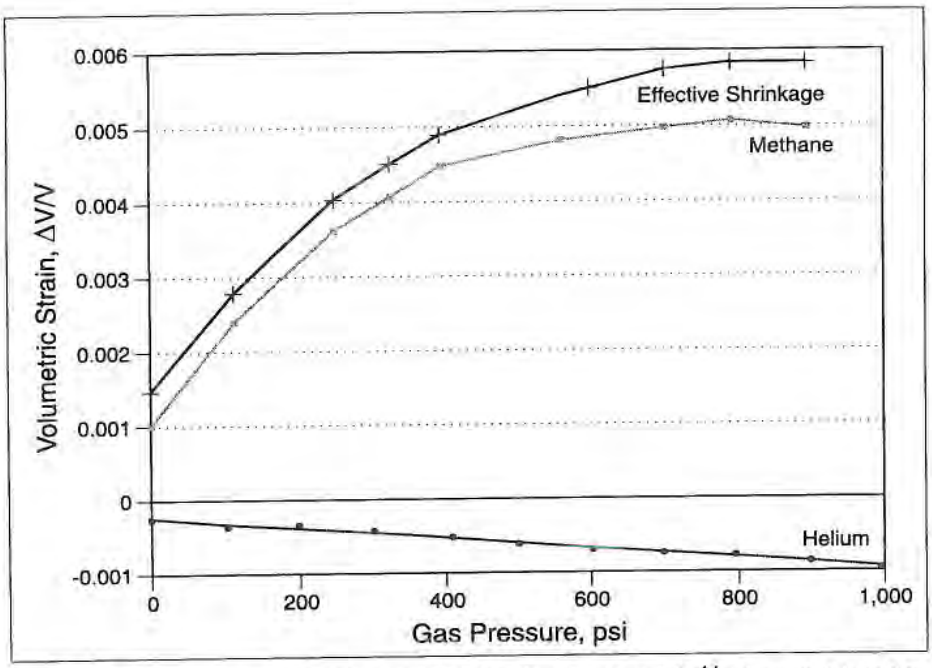

Fig. 4.12—Desorption of methane shrinks the coal matrix.[41] *Copyright 1990, Society of Petroleum Engineers.*

Fig. 4.12 shows the net effect of methane desorption on the volumetric change in a coal. In collecting data for Fig. 4.12, Harpalani used the nonadsorbing helium to isolate the effect of grain compressibility.[41] The effective shrinkage is a sum of the two phenomena.[42]

When methane adsorbs in capillaries of a diameter equal to a few molecular diameters of the gas, multilayers of adsorbate form because of the overlapping energy fields from the surrounding walls.[43] The stacking of these molecules in the confined space exerts a high pressure upon the pore walls of the coal and expands them outwardly. Upon desorption, the walls contract.[44] Thus, shrinkage with desorption increases the production rate of methane through enhancement of permeability by widening the cleat apertures.

The reverse effect, swelling of the matrix upon adsorption, is also greater for those compounds more strongly adsorbed. For carbon dioxide, adsorption should cause a larger expansion of the matrix than methane.[45] This would be a negative factor in using carbon dioxide for enhanced recovery of CBM (see Fig. 3.15). Helium creates negligible swelling. Nitrogen adsorption is intermediate to the methane and to the helium.

Theoretically, the matrix swelling from adsorption would apply to any intrusive molecular species on adsorption sites of the coal micropores. Any organic compound could be potentially damaging, although polymers of the fracturing fluid would be limited by their size to the external surface or blocking the entrance of the micropores. A consequence of adsorption-induced matrix swelling is the possible permeability impairment from the adsorption of chemicals injected during drilling, completion, or production. Some chemicals of crosslinked gels, in addition to the polymers, could create a problem.[46]

Corrosion inhibitors and broken polymers, although too large to diffuse through the micropores, could attach to the external surface by ionic bonding to the negatively charged surface of the coal. Their obstruction of the micropores would also reduce cleat permeability.[47]

Water production reduces pressure in the cleats. As pressure declines, the increasing effective stress acts to close the cleats and to reduce permeability.[48] A schematic of the cleat contraction after water removal is given in Fig. 4.13. It is seen that the phenomenon acts in opposition to the shrinking of the matrix in its effect on permeability.[42]

Therefore, in Fig. 4.13, it becomes evident that the permeability of the coalseam is a dynamic property. Of the three mechanisms affecting permeability during production, one decreases permeability and the other two increase permeability. It is hypothesized that matrix shrinkage and the Klinkenberg effect increase permeability as production proceeds; effective stress decreases permeability.

Harpalani studied the dynamic permeability in the laboratory. Fig. 4.14 gives his results of the combined effects of the Klinkenberg phenomenon, the matrix adsorption swelling, and the cleat contraction from increasing effective stress.

The Langmuir adsorption curve of methane is superposed on the data in Fig. 4.14.

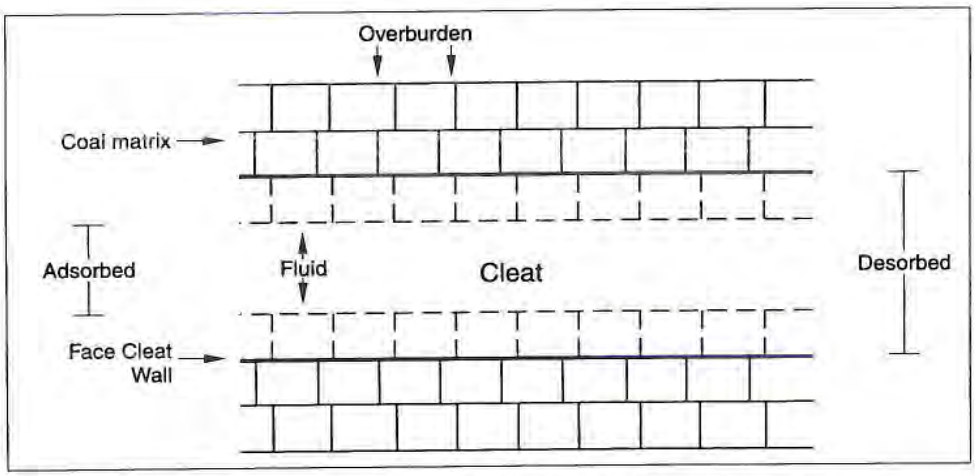

Fig. 4.13—Effective stress and desorption effects on cleat dimension.

One can see from Fig. 4.14 that as pressure is decreased from 1,000 psia, the three parameters are interactive. Two of them (matrix deswelling and the Klinkenberg effect) tend to increase permeability while the third (cleat contraction) has a negative impact and dominates at the higher pressures. The positive effect of matrix deswelling dominates cleat contraction at the point on the Langmuir isotherm at about 300 psi in which desorption accelerates; the greater volume of methane desorbed in that portion of the isotherm for a unit pressure drop emphasizes the positive effects of deswelling. Then, the Klinkenberg phenomenon becomes important at even lower pressures and contributes to large positive permeability increases near what would be abandonment pressures. Therefore, the Klinkenberg effect compounds the effect of deswelling.

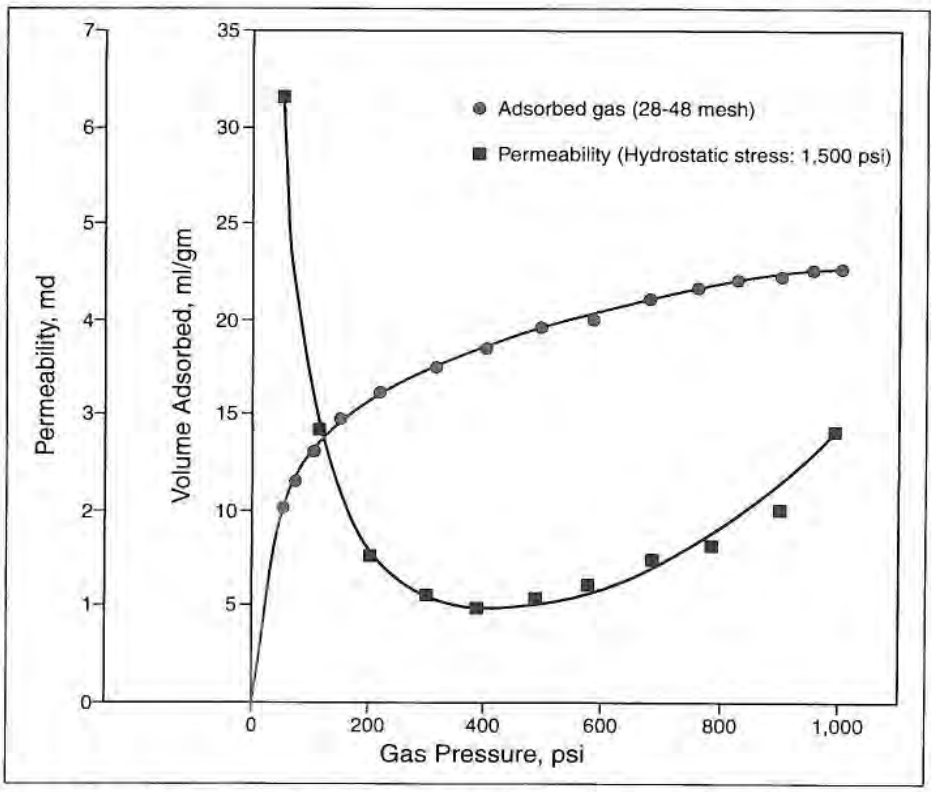

Fig. 4.14—Permeability changes with production.[4] *Copyright 1990, Society of Petroleum Engineers.*

The permeability curve of Fig. 4.14 is fitted with Eq. 4.13 by Harpalani.

$$k = A + \frac{B}{P} + CP^2 \qquad (4.13)$$

where

k = effective permeability
A,B,C = constants
P = operating pressure

At low pressures, where $B/P \gg CP^2$, the equation reduces to the form of the Klinkenberg relationship of Eq. 4.12. At high cleat pressures where the term CP^2 is dominant in the equation, the importance of a low effective stress is indicated.[41]

4.2.6 Water Composition as Permeability Indicator

An interesting insight into the permeability of a coalseam from the ion composition of its formation waters is reported in the San Juan basin. In the Fruitland formation, a high concentration of the HCO_3^- bicarbonate ion in coalbed waters is a positive indicator of favorable permeability while high concentrations of the Cl^- ion imply stagnant waters of insignificant meteoric recharge.[49]

If meteoric waters access the coalseams (as they do at high elevations of the northwestern part of the San Juan basin), waters of permeable coals may be high in the bicarbonate ion and low in the chloride ions that are swept away.

4.2.7 Relative Permeability

To evaluate accurately the productivity of a CBM well over its life, it is important to know the effective permeability of methane in the reservoir at all production stages. Initially, the cleats are expected to be fully occupied by formation waters. At this point of one-phase saturation, an injection falloff test can determine the absolute permeability. After the peak gas production rate is reached, water content in the coal slowly trends toward an irreducible amount, and the production rate of the water eventually should become small. As Seidle[50] points out, this eventual condition approaching single-phase gas flow may endure for a large fraction of the economic life of the well. In such cases, the effective permeability of the gas can be estimated.

In the period of two-phase flow, however, effective gas permeability is very sensitive to water content of the cleats. As water is extracted to start gas desorption, the water relative permeability decreases rapidly until the immobile

water concentration is reached. Conversely, the relative permeability of the gas increases rapidly with its increasing saturation in the cleats as water content wanes.

Relative permeability of gas is the ratio of effective permeability of the gas to absolute permeability as given in Eq. 4.14.

$$k_{rg} = \frac{k_g}{k} \tag{4.14}$$

where

k_{rg} = relative permeability to gas
k_g = effective gas permeability
k = absolute permeability as defined by Darcy's law

Accurate experimental data are not easily obtained for relative permeability.[51] Aside from difficulties in establishing experimental conditions, the difficulty of determining gas/water relative permeabilities of coal in the laboratory results from the misrepresentation of the seam fracture network by a small core. Also, any gravity separation of water/gas in the seam in the field improves the effective permeability of gas over that measured in a small core.[11]

A history match of computer simulations was performed on methane production from the Cedar Hill field of the San Juan basin.[11] As seen in Fig. 4.15, the relative permeability of gas must increase much more sharply with water reduction than analogous laboratory data would indicate to match actual gas production. This difference translates into a better production rate of gas in the field than would be predicted from laboratory data of relative permeability.

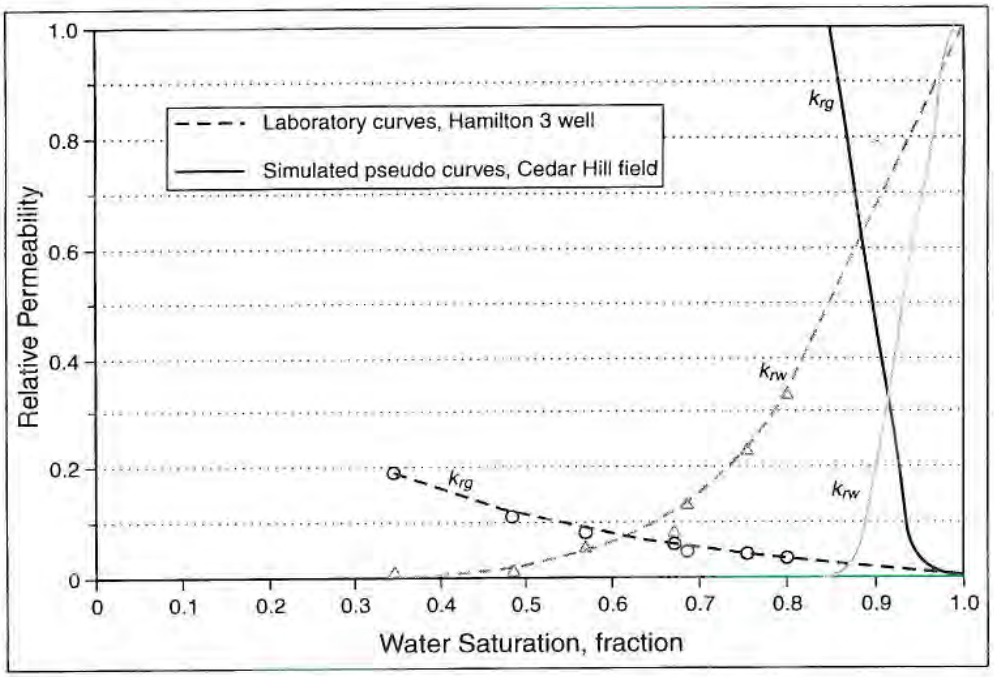

Fig. 4.15—Determining relative permeabilities, San Juan basin.[11]

Similar results of relative permeability simulations were obtained in the Warrior basin. The history match of production from the Black Creek seam indicates substantially higher gas relative permeability than laboratory values from a Blue Creek sample.[4] Fig. 4.16 suggests water/gas gravity separation that improves relative permeability in the field, which would be difficult to duplicate in the laboratory.

Likewise, from Fig. 4.16 a similar result is obtained for the relative permeability of water. Note that the immobile water content of the cleats is a high 45–50% saturation.[19,52,53] It is recommended that laboratory relative permeability curves not be used directly to simulate CBM production.[54]

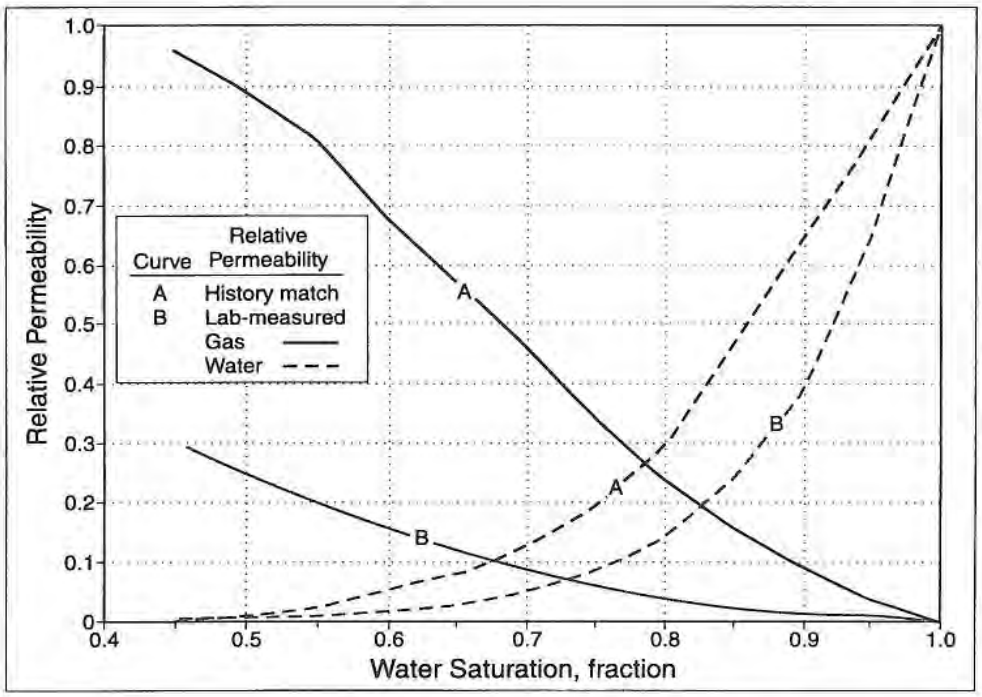

Fig. 4.16—Relative permeabilities from simulation and laboratory, Warrior basin.[4]

4.2.8 Butt and Cleat Permeabilities

Consider further some characteristics of cleats because the most decisive attribute of a gas-containing coal for the CBM process to be successful is permeability of the cleat system.

The primary continuous face cleat is orthogonal to the secondary discontinuous butt cleat. Fig. 4.17 presents a rosette diagram of cleat trends in the Cedar Hill field of New Mexico.[55] Note the face cleats perpendicular to butt cleats, and also note a third set of natural fractures oriented differently than the primary and secondary fractures. These tertiary cleats also promote permeability.

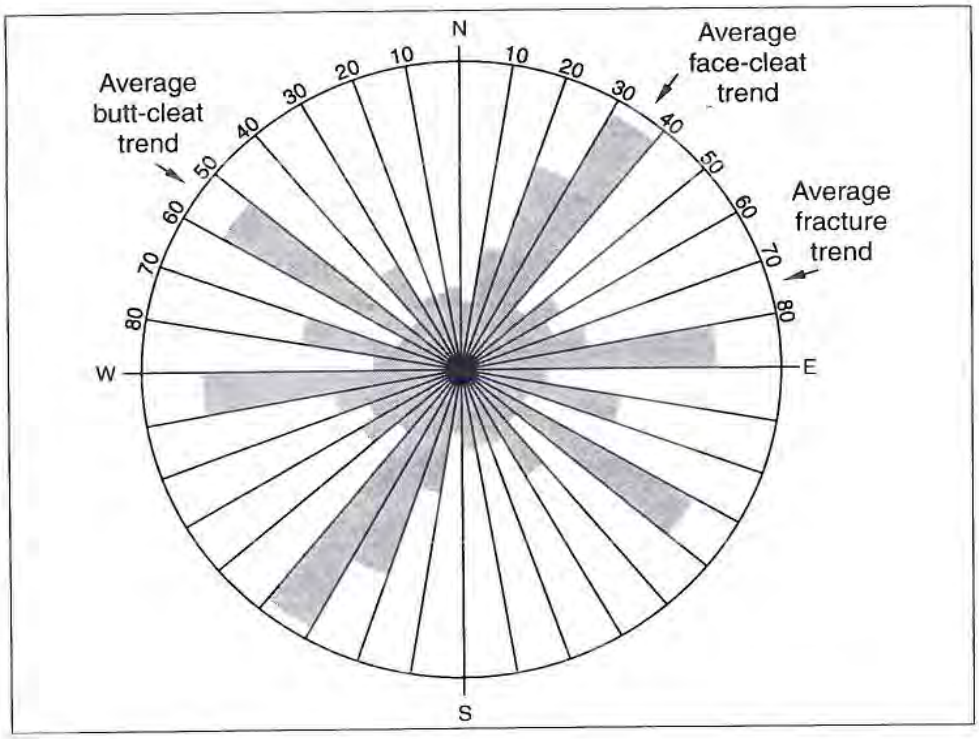

Fig. 4.17—Cleat and fracture orientations.[55]

Fluid moves in a tortuous path through both butt and face cleats with the continuity favoring the face cleat if rock stresses are favorable. An increase in the number of cleats per unit volume improves permeability, that is, the closeness of cleats assists in production. Cleat aperture opening as well as length or continuity of the cleat also impact permeability. Cleat aperture width in a Fruitland coal of the northwestern San Juan basin ranges from 0.0004 to 0.05 in. with an average width of 0.002 in.[56] A high cleat density creates a friable coal susceptible to damage from drilling, completions, and hydraulic fracturing, as well as presenting a problem in coring, but Weida[57] and Ramurthy[58] have shown that high cleat density is an important factor for successful dynamic cavity completions in the San Juan basin.

Some representative coals illustrate the cleat spacing dimensions. Reported values are in fairly close agreement. Cleats in the western U.S. coals are generally 0.50–1.00 in. apart;[59] they also range from less than 0.2 in. to several inches apart and are uniformly spaced.[60] In the Northern Appalachian basin of the Lower Freeport seam, the face cleats as well as the butt cleats are reported to be 0.79–1.18 in. apart.[61] Australian coals exhibit cleat spacings of 0.8–5.9 in.,[42] typical of the wide variability of cleat spacings encountered around the world and their unpredictability.

The cleating system of coal is a function of the historical tectonic action and its timing, the rank, the maceral content, and the mineral matter content. The network of cleats is most highly developed in low-volatile bituminous coals, whereas the lowest ranks and anthracite show the poorest cleat systems. In the low ranks, geochemical reactions have not proceeded to break sufficiently the large organic polymers with the release of volatiles to reduce the coal's plasticity; the shrinkage of the coal matrix upon loss of volatiles and water creates strain and develops fissures in the coal. Furthermore, burial depth of the subbituminous coals is usually insufficient to subject the coals to the high stresses of compaction and tectonic forces required for fracturing. As coalification progresses past low-volatile bituminous to anthracite, crosslinking under high pressures and very high temperatures of maximum burial may help seal those cleats.[3]

Permeability anisotropy is observed in all basins. Extremes of face/butt permeability ratios may range from 1:1 to 17:1.[1] Some permeabilities in the Fruitland formation are reported to be 9–13 md in the butt-cleat direction, substantially less than the 23.5–25.0 md permeability of the orthogonal face cleats.[62] The values check with those obtained by Young from history matching with the simulator in the Cedar Hill field (the oldest producing San Juan basin CBM field located in New Mexico) where face-cleat permeabilities are 2 to 4 times greater than butt-cleat permeabilities.[11]

Permeability anisotropy of the butt-and-face cleat system has significance in orientation and in spacing of wells. Ideally, wells and hydraulic fractures would be placed perpendicular to the plane of the face cleats to intersect the most joints and to increase drainage area. Wells drilled perpendicular to face cleats are

reported to produce 2.5 to 10 times as much methane[63] and is the main reason why vertical wells drain an elliptical area with the major axis parallel to the face cleat. A rule of thumb presented by McElhiney, Koenig, and Schraufnagel[1] states that at face/butt permeability ratios greater than 4:1, larger well spacings are warranted in the face-cleat direction, weighted according to Eq. 4.15.

$$E_{sp} = \sqrt{\frac{k_f}{k_b}} \qquad (4.15)$$

where

E_{sp} = well spacing factor to reduce number of wells in the face-cleat direction
k_f = permeability in the direction of the face cleats
k_b = permeability in the direction of the butt cleats

With this difference in directional permeability, a more realistic value for permeability of a seam may be a geometric average rather than either butt or cleat directional values. A geometric average permeability can be calculated with Eq. 4.16.

$$k_{ga} = (k_{butt} \times k_{face})^{0.5} \qquad (4.16)$$

where

k_{ga} = geometric average absolute permeability
k_{butt} = absolute permeability in butt cleat direction
k_{face} = absolute permeability in face cleat direction

Butt- and face-cleat permeabilities were determined for the Cedar Hill field by Young[11] by means of a three-dimensional simulation of the reservoirs. Some representative permeabilities from the study are presented in Table 4.3. Young arrived at a geometric average permeability of 7 md for the group of wells studied from the Cedar Hill field.

Table 4.3—Butt- and Face-Cleat Permeabilities[11]

Well No.	k_{ga} (md)	k_{butt} (md)	k_{face} (md)
1	6.9	4.0	12.0
2	10.0	5.0	20.0
3	6.9	4.0	12.0
4	6.9	4.0	12.0
5	0.5	0.5	0.5

4.3 Porosity

Coal has a dual porosity system. Macropores are the spaces within the cleat system and other natural fractures essential for the transport of water and methane through seams but relatively unimportant for methane storage. The storage space of the cleats and other natural fractures contains water, free methane, and methane dissolved in water, but primarily the porosity of the macropores determines the storage capacity for water. The macropore porosity has a direct impact on operating costs to handle and to dispose of formation waters that are produced.

Less than 10% of the in-place gas of a coalseam resides in the cleats. The porosity of the macropores of the cleat system is generally considered to range between 1–5%. The primary porosity of the Oak Grove, Alabama coals is reported at 2.8% for the Jagger group. The cleat porosity of the San Juan basin, Ignacio, is reported to be 2.4%. In the simulation work of Young,[11] porosities in the Cedar Hill field of the San Juan basin were estimated by history matching of production data to be an average of 0.25%. Such low porosities would give significantly less water storage and have a positive impact on process economics.

Micropores refer to the capillaries and cavities of molecular dimensions in the coal matrix that are essential for gas storage in the adsorbed state. Most of the gas

is contained in the micropores, adsorbed on the particle surface; Gray[42] estimates that 98% of the methane is typically adsorbed in the micropores.

Although coal porosity may be only 2% in the cleat system, it may have a storage capacity for methane in the micropores equivalent to that of a 20% porosity sandstone of 100% gas saturation at the same depth.[1] A large surface area necessarily exists for adsorption. It is reported that a 1-lb sample of Fruitland coal contains an internal surface area of 325,000 sq ft. McElhiney states an internal surface area of nearly 1 million sq ft per pound of coal.[1] Thus, a seeming paradox exists because very large volumes of methane can be stored in the coal's micropores despite a low porosity.

4.4 Gas Flow

4.4.1 Diffusion in Micropores

A unit of coal taken as a cube and bounded by butt (secondary) and face (primary) cleats is depicted in Fig. 4.18. Within the cube, a network of micropores and interconnecting capillaries leads to the thoroughfare of the bounding cleats. Methane molecules that desorb must pass through the maze of capillaries to reach cleats that are also interconnected to the wellbore by a network.

Diffusion through the coal's micropores is singly or by a combination of the three mechanisms of bulk, Knudsen, or surface diffusion.[43,64]

- **Bulk diffusion** occurs within the gas phase, driven by a concentration gradient, as adsorbate molecules encounter gas-to-gas collisions. Larger pore diameters, larger molecules, and higher pressures are conducive to bulk diffusion.
- **Knudsen-type diffusional flow** occurs in capillaries of diameters less than the mean free path of the gas molecules that move through the capillaries in the direction of lower concentration of their own species. As a consequence,

collision with the walls occurs before collision of gas molecules, and the adsorbate thus moves down the length of the capillary under the driving force of a concentration gradient. Therefore, smaller diameter capillaries and lower pressures of the gas are conducive to Knudsen flow.

- **Surface diffusion** is a second type of diffusional flow that occurs if the adsorbed gas, or pseudoliquid, moves along the micropore surface somewhat like a liquid.

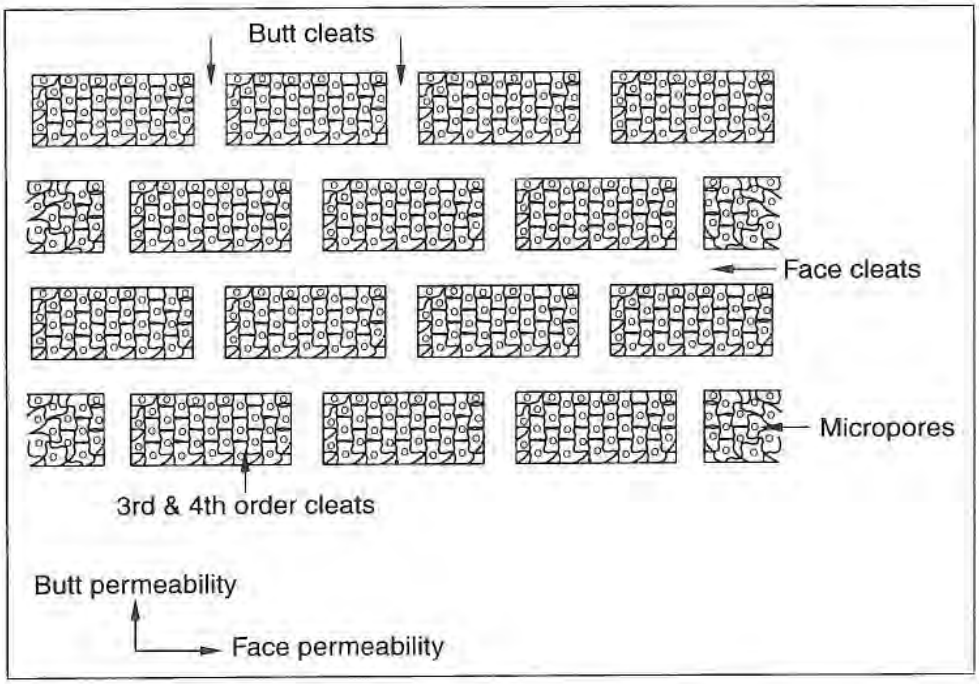

Fig. 4.18—Matrix blocks.

Diffusion of gas through the micropores of coal is described by Fick's law, which may be applied to transport through microporous spheres[56,65] by Eq. 4.17.

$$\frac{D}{r^2}\frac{\delta}{\delta r}\left(\frac{r^2 c}{r}\right)=\frac{\delta c}{\delta t} \qquad (4.17)$$

where

c = gas concentration
t = time
D = effective diffusion coefficient
r = radial distance from center of particle

The diffusion coefficient for methane in coal is a function of temperature, pressure, pore length, pore diameter, and water content.[66,67] Collins[43] hypothesizes that D is a composite diffusion coefficient that reflects the three mechanisms of surface, Knudsen, and bulk diffusion.

Fig. 4.19 is a simplified depiction of the micropore and cleat networks. It is apparent that the passage of the molecules of gas through the micropores will be influenced by the molecular size and passageway dimensions.

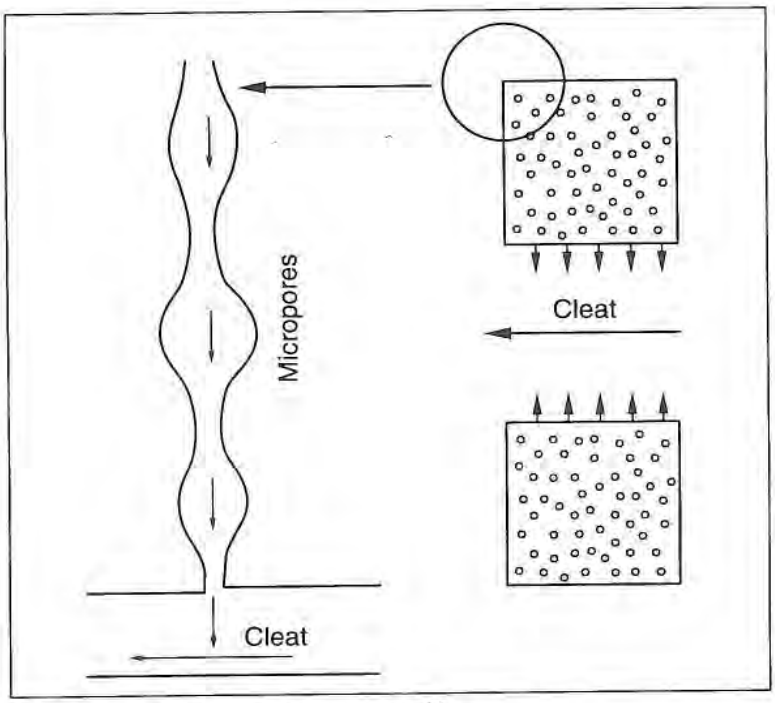

Fig. 4.19—Sketches of flow paths.[69]

To put the relative sizes of micropores and gas molecules into perspective, a tabulation of molecular diameters of species pertinent to the CBM process is presented in Table 4.4.[63] Note that the smaller helium molecule can traverse small passageways not accessible to methane.

Although a distribution of micropore sizes exists for a particular coal and although each rank of coal has a characteristic distribution, an average capillary diameter of 8 Å leading to a cavity of 40 Å is taken as representative.

Table 4.4—Sizes of Adsorbed Molecules[63]

Molecule	Effective molecular Diameter[45] (Angstroms)	Van Der Waals Molecular Diameter[44] (Angstroms)
Methane	4.1	3.24
Carbon dioxide	4.7	3.24
Helium	2.6	2.66
Nitrogen	3.0	3.15
Water	4.1	2.89
Ethane	5.5	—

The pore size distributions of coals, based on 12 different samples[68] of rank from lignite to anthracite, are presented in Table 4.5. According to the tabulation, the coals of most interest in the CBM process, hvAb to lvb in rank, exhibit multiple pore sizes that are predominantly less than 12 Å in diameter.

Table 4.5—Pore Size Distribution in Coal[68]
(By Permission of the Publishers, Butterworth–Heinemann Ltd.©)

Rank	Pore Size (Angstrom)		
	<12 (%)	12–300 (%)	>300 (%)
an	75.0	13.1	11.9
lvb	73.0	0.0	27.0
mvb	61.9	0.0	38.1
hvAb	48.5	0.0	52.0
hvBb	29.9	45.1	25.0
hvCb	41.8	38.6	19.6
lig	19.3	3.5	77.2

To describe mathematically the flow of gases through the micropores' cavities and capillaries, diffusion models have been developed for a single-pore size in coal (unipore model) and for a two-pore size network (bidisperse pore model).[64] Eq. 4.18 is a unipore model that allows, because of the equation simplicity, convenient estimating of the fraction of gas desorbed with time. Note that Eq. 4.18 indicates a linear change in sorption with the square root of time.

$$\frac{V}{V_t} = \frac{6}{\sqrt{\pi}}\sqrt{\frac{Dt}{r_p^2}} \qquad (4.18)$$

where

V/V_t = fraction of gas desorbed at time t
V_t = total volume of gas
D = diffusion coefficient
t = time
r_p = particle radius

The model assumes that pores are cylindrically shaped of only one diameter and that the desorption is controlled by the diffusion.[64] Smith and Williams superposed the curve of the unipore model calculated from Eq. 4.18 on experimental data. Their results are presented in Fig. 4.20, which is a plot of the fraction of methane desorbed from coal as a function of time. For a desorbed fraction up to 0.5 of the total methane, the unipore model of Eq. 4.18 fitted the data well. The divergence of the curve from the data at longer times and at $V/V_t >$ 0.5 indicates that more than one diameter of micropores are present in coal to affect diffusion. Olague and Smith[67] and Airey[70] also concluded that the unipore model was deficient in describing diffusion in coals.

Bidisperse models have been shown to be more accurate and representative of the true micropore size distribution for the diffusion of methane through coal.[64,70,71] Although more difficult to apply, these bidisperse models give results that check more closely with the size distributions of Gan in Table 4.5.[68]

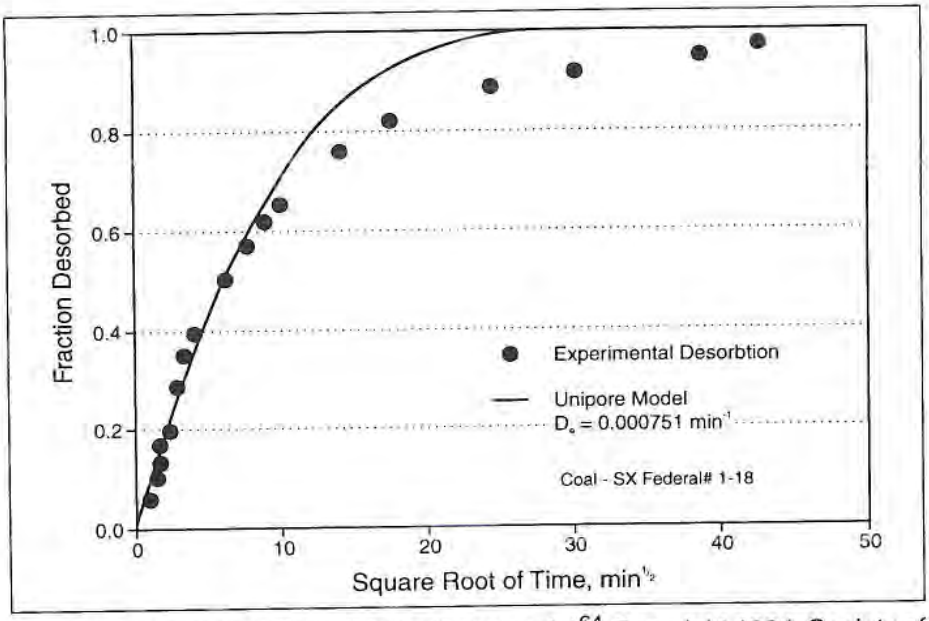

Fig. 4.20—Limited applicability of unipore model.[64] *Copyright 1984, Society of Petroleum Engineers.*

Airey[70] derived Eq. 4.19 empirically for the diffusion of desorbed methane through coal particles of a single coal. The model retains the simplicity of a unipore model but better represents the multimodal pore size distribution.

$$\frac{V_t}{V_\infty} = 1 - \exp\left[-\left(\frac{t}{t_o}\right)^n\right] \qquad (4.19)$$

where

V_t = volume of gas at time t
V_∞ = total volume of gas
t = time
t_o = empirical constant dependent on particle size, water content, and initial gas pressure[72]
n = empirical constant, approximately 0.33

4.4.2 Darcy Flow in Cleats

After local diffusion of gas through the micropores of the coal, transport of gas and water to the wellbore must proceed by flowing through the network of fractures and cleats. A joint or hydraulic fracture may improve the flow greatly (see Fig. 4.21).

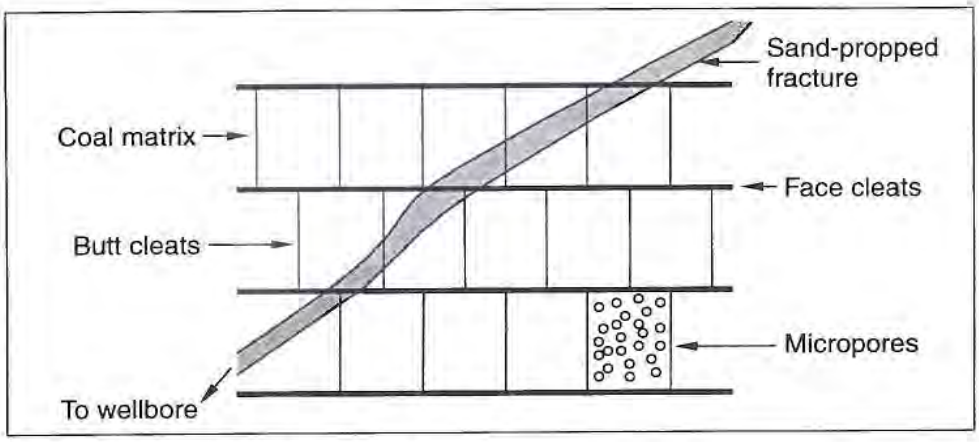

Fig. 4.21—Coal fracturing network.

Tertiary cleats are discontinuous fractures that formed after butt and face cleats, and they terminate at the face and butt cleats at about 45° angles. These tertiary cleats also represent an important pathway for gas flow into the network of primary and secondary cleats. The tertiary cleats are present, for example, in the fairway section of the San Juan basin where high permeabilities and low-strength mechanical properties of the coals contribute to the success of cavity completions.[57]

The flow of fluids through the cleats is by Darcy's law. When the well is first drilled, water may fully occupy the cleat space. In terms of the Langmuir isotherm, the seams may be undersaturated with respect to gas, and some water must be removed to lower the pressure and initiate desorption. As water is produced with time, a two-phase flow regime near the wellbore is established[1] (see Fig. 4.22).[69]

Sawyer, *et al.*[69] showed that the gas flow in this early two-phase flow regime is followed by pressure drops deeper within the seam as more water is produced. Then, gas movement originates from further into the cleats. It is an important occurrence that gas relative permeability improves greatly and rapidly as the water saturation decreases.

Finally, a flow regime is reached where the gas moves through the cleats accompanied by only small amounts of water. Actually, this simpler flow regime lasts through most of the life of the CBM well, as Seidle[50] points out. Seidle developed models for the flow in this regime based on the assumptions of low water flows and of constant effective gas permeability. When the one-phase gas flow regime develops, gas flow becomes analogous to a conventional dry-gas well.

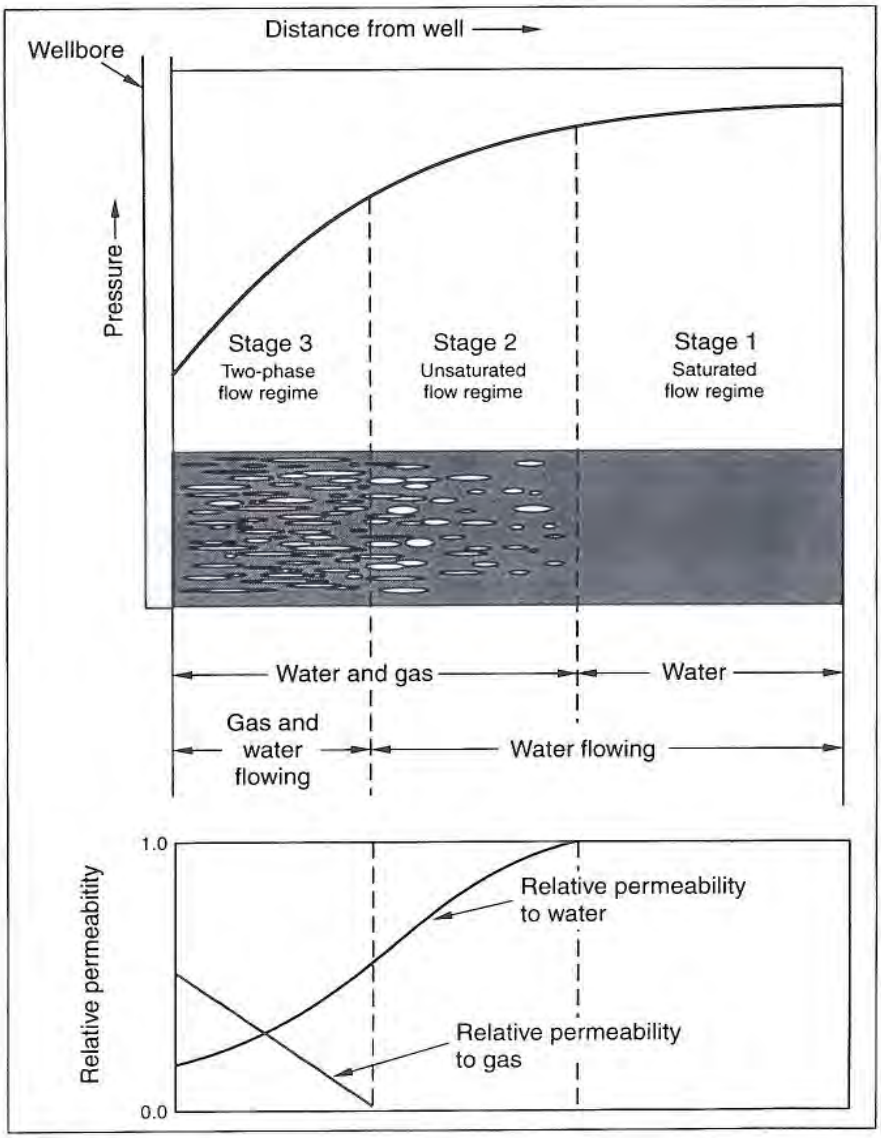

Fig. 4.22—Flow regimes early in gas production.[1]

4.4.3 Sorption Time

For a unit of the reservoir, such as a single block of coal bounded by butt and face cleats depicted in Fig. 4.18, King and Ertekin[72] give Eq. 4.20 for rate of diffusion in the unit under the driving force of a concentration gradient.

$$\frac{dV_i}{dt} = -D_i a(V_i - V_e) \qquad (4.20)$$

where

D_i = diffusion coefficient, ft^2/hr
V_i = adsorbate volumetric concentration, scf/ft^3
V_e = equilibrium sorption isotherm, scf/ft^3
dV_f/dt = volumetric gas flow per unit time
a = Warren and Root shape factor

The Warren and Root shape factor of Eq. 4.21 influences the flow through the matrix block between the micropores and macropores.[73]

$$a = \frac{8\pi}{S^2} \qquad (4.21)$$

where

S = spacing between cleats, that is, the size of the block

Substituting Eq. 4.21 into Eq. 4.20, Sawyer *et al.*[69] derive Eq. 4.22 for the flow rate of adsorbate through the pores as influenced by the size of the coal block.

$$\frac{dV_i}{dt} = \frac{8\pi D_i}{S^2}(V_i - V_e) \qquad (4.22)$$

Let

$$\tau = \frac{S^2}{8\pi D_i} = \frac{1}{D_i a} \qquad (4.23)$$

where

t = sorption time in the units of time used in the diffusion coefficient

$$\frac{dV_i}{dt} = -\frac{1}{\tau}(V_i - V_e) \qquad (4.24)$$

Integrate and impose the following boundary conditions on Eq. 4.24.

$V_i = V_o$ at $t = 0$
$V_i = V_t$ at external boundary for $t \geq 0$

Eq. 4.25 results.

$$V(t) = V_e + (V_o - V_e)e^{-t/\tau} \qquad (4.25)$$

In the special case of $t = \tau$,

$$V(\tau) = V_e + (V_o - V_e)e^{-1}$$

Rearrange to give the following:

$$\frac{V_o - V(\tau)}{V_o - V_e} = 1 - \frac{1}{e}$$

Here, V_e is the equilibrium CH_4 content of the coal at 1 atm pressure. The right side of the preceding equation represents the fraction of methane released by time, τ, as given by Eq. 4.26.

$$1 - \frac{1}{e} \approx 0.63 \qquad (4.26)$$

Since the concentration is proportional to mass, Eq. 4.26 means that 63% of the adsorbed methane will have diffused to the boundary of the particle by the time of $t = \tau$. Therefore, sorption time is defined as the time required to release 63% of the total adsorbed methane from a coal sample initially saturated at reservoir temperature and pressure[74] as it goes to atmospheric pressure.

The volumetric flow rate of methane from the matrix to the cleats is governed by Fick's first law. In terms of sorption time, this volumetric flow rate is given by Eq. 4.27.

$$Q = \frac{V_m}{\tau}(V_e - V_i) \qquad (4.27)$$

where

Q = volumetric flow rate of methane from block, ft^3/hr
V_m = matrix volume, ft^3
V_i = volumetric concentration of methane at matrix/cleat face, scf/ft^3
V_e = gas content given by Langmuir equation, scf/ft^3
τ = sorption time, hrs

Substituting the expression of sorption time of Eq. 4.23 into Eq. 4.27 gives the resulting Eq. 4.28.

$$Q = \frac{8\pi D_i V_m}{S^2}(V_e - V_i) \qquad (4.28)$$

In a CBM simulator, values of sorption time, τ, and distance between cleats, S, are input to determine the diffusion coefficient. Some sorption times measured for representative coals are presented in Table 4.6. A wide range of values occurs. Some Northern Appalachian cores were reported after 2 years to still desorb in the canister where they were placed to measure gas content.

Table 4.6—Sorption Times

Coal	Sorption Time
Fort Union, sub	<1 day[13]
Fruitland, mvb	<1 day[13]
Pennsylvanian Age	>80 days[13]
Fruitland (NW San Juan Basin)	4.1 hours[74]
Northern Appalachian	100 to 900 days[55]
Central Appalachian	1 to 3 days[55]
Warrior	3 to 5 days[55]

In the method commonly used for determining gas content of coal formations from extracted cores, sorption times of the coal have an important implication. At short sorption times, unaccounted lost gas from the core during extraction increases the error in gas content estimation.

Sorption times provide the information needed to calculate diffusion coefficients for simulations utilizing Fick's law. They were used by Sawyer[69] with a simulator to illustrate the effect of sorption times on production rates with time.

For a selected formation permeability of 10 md and a well spacing of 80 acres, early production rates can be expected to be much higher for the short sorption times (see Fig. 4.23).

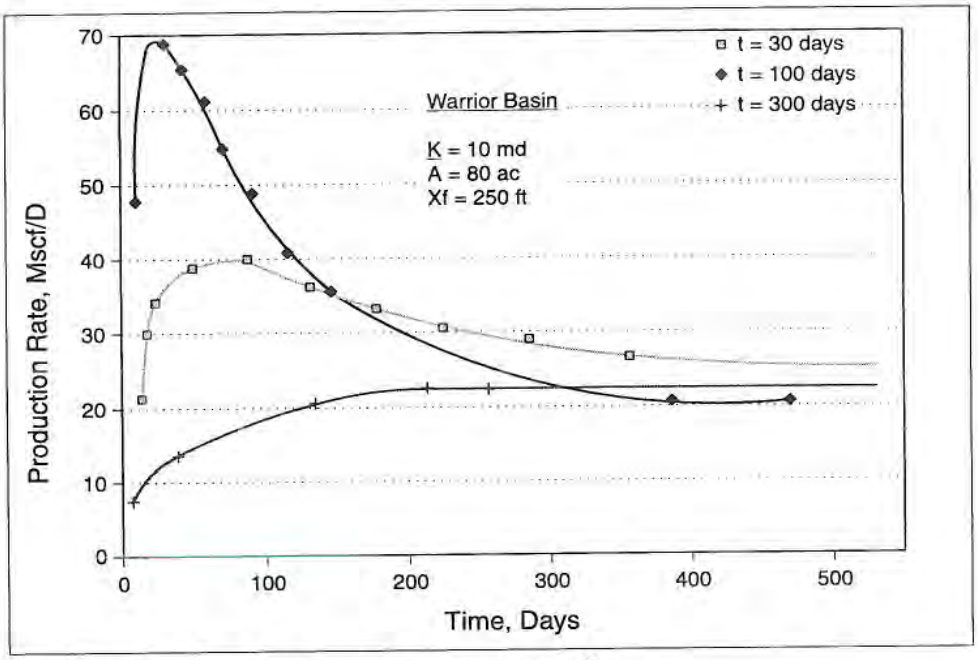

Fig. 4.23—Sorption times evident in production.[69]

4.5 Reserve Analysis

4.5.1 Gas In Place

To estimate the value of methane reserves in coalbeds, as in the development of a conventional gas property, an estimate is first made of the initial in-place gas.[76] However, estimation of in-place gas in coalseams is less accurate and more difficult than conventional reservoir engineering methods. One of the complicating factors is the inability to use well logs to obtain gas content of the coal. Because the geophysical logs cannot detect gas contained in the coals, as with sandstone or carbonate reservoirs, the methane content must be determined from a controlled desorption of retrieved cores—a costly, time-consuming task. In the method of core analysis, gas content is the sum of the quantity of gas desorbed from the coal in the canister and an estimated quantity of gas lost during core retrieval.

The procedure for determining gas content of a reservoir from cores is as follows.[10]

1. Cores are removed from the formation, retrieved to the surface, and transferred rapidly to a sealed container to minimize lost gas.
2. Reservoir temperature is established in the canister.
3. The rate and quantity of gas desorbed in the canister at reservoir temperature are recorded.
4. When gas flow stops at atmospheric pressure, the sample is crushed, and the gas released from the crushed coal is monitored. This gas is residual gas.
5. The gas lost during removal of the core from the well is estimated from a plot (according to Eq. 4.18) of the quantity of gas desorbed when the core is initially placed in the canister vs. $t^{1/2}$ by extrapolating to the time of extraction from the formation. The sum of gas desorbed in the canister, residual gas, and lost gas represents gas content of the coal.

There are six ways the gas content of a coal can be reported:[24,74]

a) Raw or As-Received.

b) Inert Gas-Air Dry.

c) Dry, Ash-Free.

d) Dry, Ash-Residual Moisture-Sulfur Free.

e) Theoretically Pure-Coal.

f) In-situ.

It is very important to understand the definition of each basis and use them accordingly.

4.5.1.1 Gas Content: Raw or As-Received

The gas content of a coal reported on a raw basis is determined using the weights of all material in the original sample. Therefore, the reported weight contains original moisture as well as any non-carbonaceous materials. This method provides a preliminary estimate of total gas content.[74] Eq. 4.29 describes the gas content determined on this basis.

$$GC_{RAW} = 32.0368\left\{\frac{V_{LG} + V_{RG} + V_{MG}}{W_{RAW}}\right\} \tag{4.29}$$

where,

GC_{RAW} (scf/ton) = gas content-Raw

V_{LG} (cm^3) = lost gas volume at STP

V_{RG} (cm^3) = residual gas volume at STP

V_{MG} (cm^3) = measured gas volume at STP

W_{RAW} (grams) = weight of the raw coal sample

4.5.1.2 Gas Content: Inert Gas-Air-Dry

The main difference between raw and inert-gas-air-dry basis is that the gas content determined on a raw basis is corrected by removing the weight of water from the raw sample. Basically, any extra material is removed from the sample by allowing the raw sample to air-dry in a laboratory environment until an equilibrium weight is obtained. This usually takes about 48 hours and is done in an inert environment to prevent oxidation. Eq. 4.30, shown below provides the gas content obtained in this basis.

$$GC_{Air-dry} = 32.0368\left\{\frac{V_{LG} + V_{RG} + V_{MG}}{W_{Air-Dry}}\right\} \qquad (4.30)$$

where,

$GC_{Air\text{-}Dry}$ (scf/ton) = gas content-inert gas-air-dry basis
$W_{Air\text{-}Dry}$ (grams) = weight of the air-dry coal sample

The sample weight determined here is the basis for estimating the next two gas contents.

4.5.1.3 Gas Content: Dry, Ash-Free

Once the sample is air-dried, there is still some moisture left in the coal referred to as residual moisture. There is also some ash left in this coal. The weight of the residual moisture and ash are determined as per ASTM standards[77,78] D3173-03 and D3174-04 and the air-dry sample weight is adjusted for these two weights using Eq. 4.31.

$$W_{DAF} = W_{AIR-DRY}\{1 - WF_{RMC} - WF_{DASH}\} \qquad (4.31)$$

where,

WF_{RMC} (weight-fraction) = residual moisture content
WF_{DASH} (weight-fraction) = dry ash content
W_{DAF} (grams) = weight of the dry, ash-free coal sample

After the weight of dry, ash-free coal, W_{DAF} is estimated, the gas content is then determined using Eq. 4.32.

$$GC_{DAF} = 32.0368\left\{\frac{V_{LG} + V_{RG} + V_{MG}}{W_{DAF}}\right\} \qquad (4.32)$$

where,

GC_{DAF} (scf/ton) = gas content-dry, ash-free basis

If dry, ash-free gas in place is to be determined, the density of coal on a dry, ash-free basis is required. This density can be estimated using Eq. 4.33.[79-81]

$$\rho_{DAF} = \left\{\frac{\rho_a * \rho * (100 - DASH)}{100 * \rho_a - \rho * DASH}\right\} \qquad (4.33)$$

where,

ρ_{DAF} (gm/cm^3) = density of coal, dry, ash-free basis
ρa (gm/cm^3) = density of dry ash
ρ (gm/cm^3) = density of dry coal containing ash
DASH (weight %) = dry ash content

The dry, ash-free gas content should be reported only for coals containing less than 40% by weight ash and moisture because it can otherwise be incorrect if a significant amount of mineral matter is present in coals of lower quality.[74] Please note that during the ash analysis, sulfur gets vaporized and therefore ash analysis cannot sufficiently account for the weight effect of sulfur present in coals.[78] How to account for the weight fraction of sulfur present in coals is discussed in the next section.

4.5.1.4 Gas Content: Dry, Ash-Residual Moisture-Sulfur-Free

The non-coal components in coal are residual moisture, ash, and sulfur. Adjusting for moisture and ash content weight would be sufficient to account for the non-carbonaccous components in many coals except when pyrite or carbonate minerals are present.[74] In such cases, the sulfur content in coals should also be accounted for since it is also a non-carbonaceous component. The weight fraction of sulfur should be determined as per the ASTM standards, D3177-02[82] and D1757-03,[83] and must be corrected from the weight of the air-dry sample. The dry, ash-residual moisture-sulfur-free sample weight can then be estimated using Eq. 4.34.[74,84]

$$W_{DAMSF} = W_{AIR-DRY}\left\{1-\left(WF_{RMC}+1.08WF_{AR-ASH}+0.55WF_{AR-TSC}\right)\right\} \tag{4.34}$$

where,

W_{DAMSF} (grams) = weight of the dry, ash-residual moisture-sulfur-free coal sample
$W_{Air\text{-}Dry}$ (grams) = weight of the air-dry coal sample
WF_{RMC} (weight-fraction) = residual moisture content
$WF_{AR\text{-}ASH}$ (weight fraction) = as-received ash content
$WF_{AR\text{-}TSC}$ (weight fraction) = as-received total sulfur content

Once the weight of residual moisture, ash, and sulfur are accounted for, the dry, ash-residual moisture-sulfur-free gas content can be determined using Eq. 4.35.

$$GC_{DAMSF} = 32.0368\left\{\frac{V_{LG}+V_{RG}+V_{MG}}{W_{DAMSF}}\right\} \tag{4.35}$$

where,

GC_{DAMSF} (scf/ton) = gas content-dry, ash-residual moisture-sulfur-free basis

4.5.1.5 Gas Content: Theoretically Pure Coal

The maximum gas content obtained by performing regression analysis on inert gas-air-dry, gas content data obtained from multiple samples plotted against the corresponding non-carbonaceous weight fraction data and extrapolated to zero non-carbonaceous weight percent is referred to as the pure-coal gas content. This term has been loosely used and incorrectly switched with dry, ash-residual moisture-sulfur-free gas content.

Like any statistical analysis, this method can be applied only when sufficient sample volumes containing a wide range of ash, sulfur, and residual moisture contents are available. It is essential to have sufficient sample numbers to obtain statistically accurate theoretically pure-coal gas content estimates. This gas content estimate is mainly used as a basis to compare gas contents from coal samples in various other locations.

The example in Fig. 4.24 is from a CBM well in the Tiffany area of the San Juan basin. As shown, there is an inverse relationship between the total air-dry basis gas content and the corresponding non-coal component weight fraction. The theoretically pure-coal gas content estimated in this example using linear regression is 495 scf/ton. The correlation coefficient obtained from this linear regression analysis is 0.77. Additional desorption sample test data would have improved the correlation coefficient. By comparing it with the isotherm storage capacity, the theoretically pure-coal gas content is used to determine the degree of saturation and also the effect of other gases like carbon dioxide and nitrogen.[1]

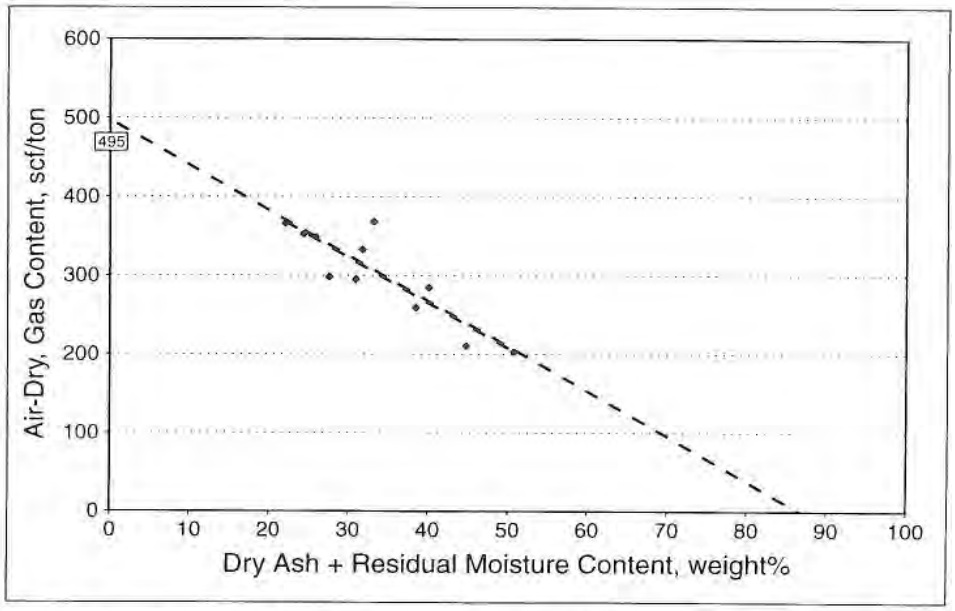

Fig. 4.24—"Pure Coal" gas content estimation, San Juan Basin.

4.5.1.6 Gas Content: In-Situ

Once the theoretically pure coal gas content is known, the in-situ gas content can be estimated using the residual moisture and dry ash content. In-situ gas content can be determined using Eq. 4.36.

$$GC_{In-situ} = GC_{PC}\{1 - WF_{DASH} - WF_{RMC}\} \qquad (4.36)$$

where,

$GC_{In\text{-}situ}$ (scf/ton) = gas content-in-situ basis
GC_{PC} (scf/ton) = gas content-pure-coal basis
WF_{RMC} (weight-fraction) = residual moisture content
WF_{DASH} (weight-fraction) = dry ash content

When pure coal gas content is not available, it can be replaced by dry, ash-free or dry, ash-residual moisture-sulfur-free gas content estimates.[74] It was found that a correlation exists between ash content and bulk density measured by wireline logs. The correlation is represented by Eq. 4.37.

$$WF_{DASH} = \left\{ \frac{\rho - \rho_c}{\rho_a - \rho_c} \right\} \tag{4.37}$$

where,

WF_{DASH} (weight fraction) = dry ash content
ρ (g/cm^3) = measured bulk density of coal
ρ_c (g/cm^3) = density of "pure" coal
ρ_a (g/cm^3) = density of ash

Based on this correlation, it is possible to determine gas content of coal from the logs. However, if the log data are not calibrated for accurate pure coal and ash densities, the resulting gas content estimates will be inaccurate.[74]

Therefore, adequate core sampling, representative of the reservoir, proper laboratory analyses, correct accounting of lost gas, and correct interpretation of data make the methane reserve estimation more difficult and more costly than for conventional reservoirs.

Once the in-situ gas content is known, the in-place gas is calculated by multiplying it by the weight of coal and then adding a term for the free gas in cleats as in Eq. 4.38.

$$G_I = V_C + 1359.7 A h \overline{\rho} \left(GC_{In\text{-}situ}\right) \qquad (4.38)$$

where,

G_I (scf) = initial gas in place
V_C (scf) = volume of free gas in cleats
A (acres) = surface area of the reservoir (drainage area)
h (ft) = net coal thickness
$\overline{\rho}$ (g/cm^3) = average bulk density of coal
$GC_{In\text{-}situ}$ (scf/ton) = gas content-in-situ basis

The height of the seam should come from high-resolution density logs. To determine accurate values of the thickness and to exclude the inorganic partings, high-resolution density logs are desirable for the thin seams. Use of conventionally run logs may result in overestimating the seam thickness. If gas content and density of coal in Eq. 4.38 is to be reported on a mineral-free basis, the height of the coalseam must be mineral-free.[85] When reporting gas in place, mixing the measurement bases can lead to errors, especially in coals with high ash content.

The volume of free gas in the cleats in Eq. 4.38 is expanded by Holditch and Zuber[19] into a more useful form as given in Eq. 4.39.

$$G_I = A(\Sigma h)\{43{,}560\phi_C(1-S_{WC})B_g + 1.36\overline{\rho}(GC_{In-situ})\} \qquad (4.39)$$

where,

G_I (Mscf) = initial gas in place
ϕ_C (fraction) = cleat porosity
S_{WC} (fraction) = water saturation in cleats
B_g (Mscf/ft^3) = formation volume factor of gas
Σh (ft) = net coal thickness

Only a relatively small portion, less than 10% of the total gas in place will be in the cleats in free-form. Hence Eq. 4.39 can be simplified into Eq. 4.40.

$$G_I = 1359.7Ah\overline{\rho}(GC_{In-situ}) \qquad (4.40)$$

Eq. 4.40 can be rearranged to represent dry, ash-free gas content in the manner of Eq. 4.41.

$$G_I = 1359.7Ah\overline{\rho}_{DAF}(GC_{DAF})(1-WF_{DASH}-WF_{RMC}) \qquad (4.41)$$

where,

G_I (scf) = initial gas in place
GC_{DAF} (scf/ton) = gas content, dry, ash-free basis
$\overline{\rho}_{DAF}$ (gm/cm^3) = average density of coal, dry, ash-free basis
WF_{RMC} (weight-fraction) = residual moisture content
WF_{DASH} (weight-fraction) = dry ash content

Recoverable reserves of methane may be calculated from initial gas in place. Estimated recoveries by volumetric calculations are the product of initial hydrocarbons in place times a recovery factor,[86,87] which may be represented by Eq. 4.42.

$$G_R = G_i R_f \qquad (4.42)$$

where

R_f = recovery factor
G_i = initial gas in place
G_R = methane recoverable reserves

The recovery factor is estimated from the isotherm for that coal[10,13] (refer to Fig. 4.25).

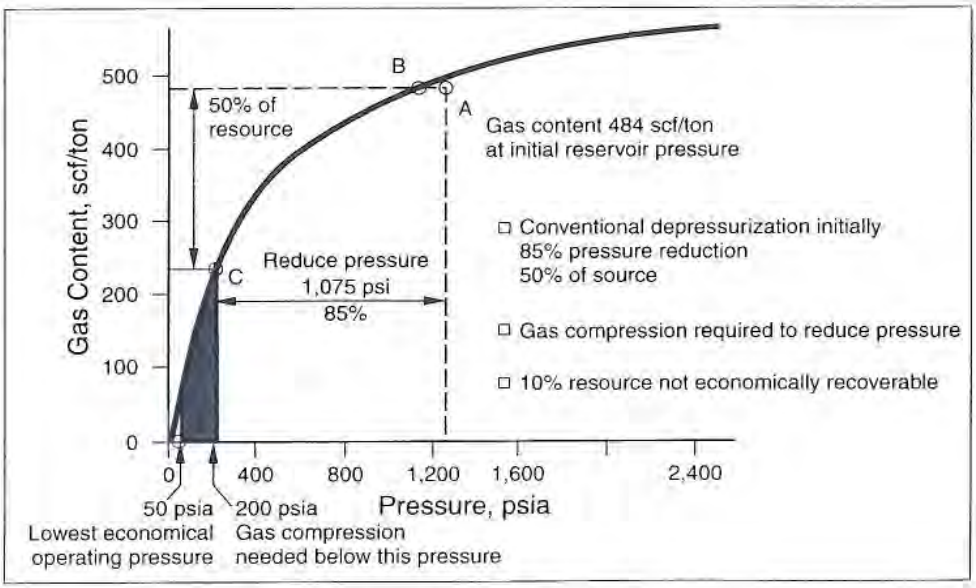

Fig. 4.25—Estimating reserves and recovery factor.[13]

The abandonment pressure establishes the residual gas in the coal at abandonment.

$$R_f = \frac{V_i - V_a}{V_i} \tag{4.43}$$

where

R_f = recovery factor
V_i = initial volumetric gas content, scf/ton
V_a = abandonment gas content, scf/ton

In Fig. 4.25, it is seen that 50% of the gas is recovered from reducing pressure by 1,075 psi to the pressure where gas compression is needed for the sales line. At the abandonment pressure of 50 psi, a recovery factor of about 90% is calculated from Eq. 4.43.

4.5.2 Decline Curves

A classical method to determine conventional oil and gas reserves is decline curve analysis. Decline curves have long been used in the oil and gas industry to fit the production time data of producing properties. After an initial decline pattern has been established, the subsequent decline usually follows an exponential, hyperbolic, or harmonic pattern that allows the prediction of each year's production until abandonment. Anticipation of cash flows and ultimate profitability of the producing unit are possible if future production rates can be determined. An adequate period of production is necessary in the beginning to establish the decline pattern of conventional wells.

The profile of CBM production vs. time differs dramatically from conventional gas production during early stages of production. For the CBM process, gas production increases (negative decline) initially while water is being removed, followed by a peak in gas production and then a long decline. Fig. 4.26 gives the

production profile of Well OG-134 of the Oak Grove field in the Warrior basin. Note that about 11 months was required for dewatering and gas desorption near the wellbore to establish peak gas production, plus another 7 months to begin a steady decline rate.[88]

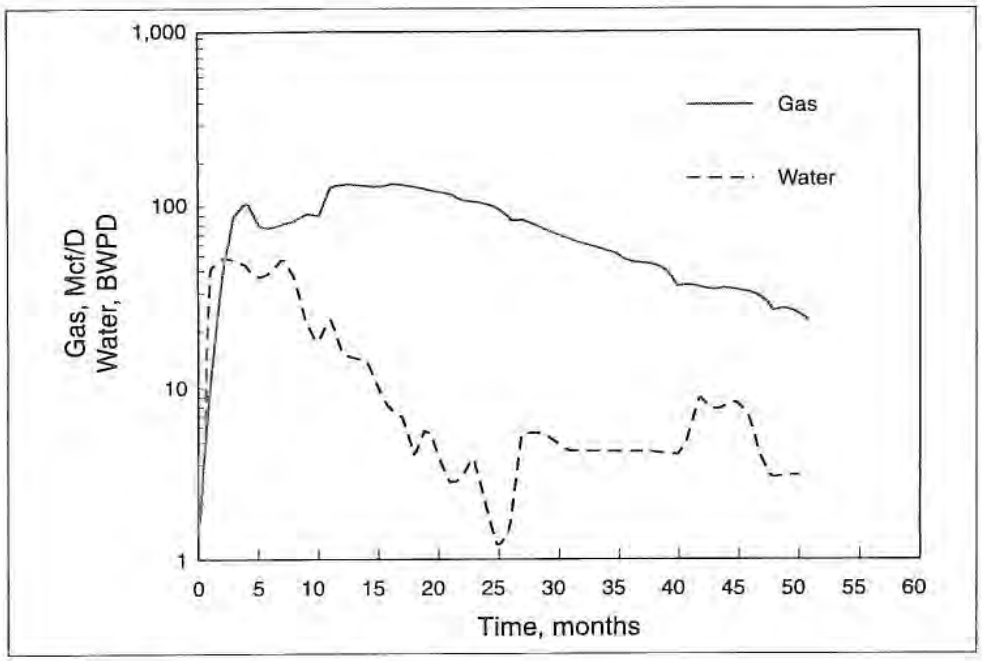

Fig. 4.26—Typical production curve.[88]

For the negative decline prior to the peak production, decline curve analysis would be inapplicable, but on the positive decline side, it may be beneficial if the production from the subject well has no interference from adjacent wells. Therefore, it is desirable to forego decline curve analysis until the decline side of the gas production curve represents at least 22 months of production, of which at least 6 months show a consistent decline slope.[88]

Hanby,[15] Richardson, *et al.*[88] and then Seidle,[89] followed by Mavor, *et al.*,[90] studied the use of decline curve analysis in coal wells. Hanby[15] studied the decline of 148 wells in the Deerlick Creek, Cedar Cove, and Oak Grove fields of

the Alabama Warrior basin. He selected only those wells with at least 2 years of production and uninfluenced by nearby mining. Production after the peak year declined exponentially in individual wells of the three fields.

Exponential decline is described by Eq. 4.44.

$$q = q_i e^{-Dt} \tag{4.44}$$

where

q = producing rate at time t, vol/unit time
q_i = producing rate at time 0, vol/unit time
D = nominal exponential decline rate, 1/time
t = time
e = base of natural logarithms, 2.718

Any consistent set of units is permissible.

A plot of production rate vs. time on semilog paper should give a straight line if the well exhibits exponential decline. Fig. 4.27 is an example of exponential decline in the Deerlick Creek field of the Warrior basin after peak production.[15]

Production from the well depicted in Fig. 4.27 declines at the rate of 15.1 year^{-1} to an assumed economic limit of 40 Mcfd in 137 months. From the information, a schedule of cash flows can be made, abandonment time predicted, and ultimate reserves estimated. Profitability of the well can then be estimated.

In Hanby's study,[15] peak gas production rates occurred 20, 33, and 15 months after flow initiation in the Cedar Cove, Deerlick Creek, and Oak Grove fields, respectively. Although decline curves could not be used until after the peaks were reached, the applicable post-peak production constitutes most of the production life since wells in general could produce 10–20 years.

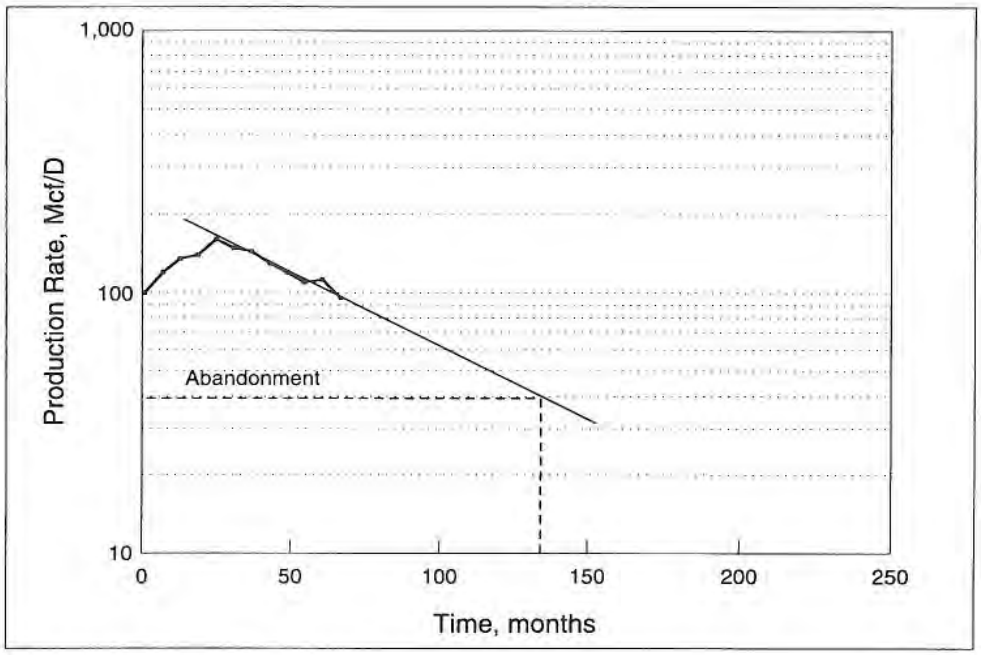

Fig. 4.27—Exponential decline, Deerlick Creek well.[15]

Example 4-1: Ultimate Reserves from Decline Curve

Determine the ultimate reserves of the Deerlick Creek Well of Fig. 4-27. When peak gas production is reached, 95,877 Mcf of gas will have been produced.

Solution:

Remaining reserves + cumulative production = ultimate reserves

Ultimate reserves should be the cumulative production at the time of abandonment.

Calculate from Eq. 4.45 by decline curve analysis the remaining reserves to be produced after peak until abandonment.

$$G_D = \frac{q_p - q_a}{D} \tag{4.45}$$

where

G_D = remaining reserves after peak
q_p = production rate at peak
q_a = production rate at abandonment
D = exponential decline rate

$$\text{GD} = \frac{160 \text{ Mcf/D} - 40 \text{ Mcf/D}}{0.151(1/\text{yr}) \times 1/12(\text{yr/mos.}) \times 1/30.2(\text{mos./days})} \tag{4.46}$$

From Eq. 4.46,

GD = 287,632 Mcf (from peak to abandonment)

The ultimate reserves are then obtained by adding the cumulative production before the peak was reached.

Ultimate reserves = 287,632 Mcf + 95,877 Mcf = 383,509 Mcf

In this case, about 75% of the production life of the well can be represented by an accurate decline curve analysis.

Richardson, *et al.*[88] used the decline curve analysis method in a comprehensive study of the reserves in the TEAM project, Oak Grove field of the Warrior basin. They also observed that the coal well gas production rates exhibited exponential decline once the peak production was obtained. Seidle,[89] in his work, derived and presented the decline coefficients for gas and water in coals, from which the

estimated ultimate recoveries and drainage area can be determined respectively. The gas decline coefficient as derived by Seidle[89] is given by Eq. 4.47.

$$D_g = \frac{2Jpp_i Z^*}{Z_i^* G_i} \frac{1}{\left[1 - \frac{p}{Z^*}\frac{dZ^*}{dp}\right]} \tag{4.47}$$

In Eq. 4.48, J is defined as:

$$J = \frac{kh}{1422\mu ZT\left\{\ln\left(\frac{r_e}{r_w}\right) - 0.75 + s\right\}} \tag{4.48}$$

where

k (md) = effective permeability to gas
h (ft) = coalseam thickness
μ (cp) = gas viscosity
Z (dimensionless) = real gas deviation factor
T (deg. R) = reservoir temperature
r_e (ft) = external radius
r_w (ft) = wellbore radius
s (dimensionless) = skin
p (psia) = average reservoir pressure
p_i (psia) = initial reservoir pressure
G_i (MMcf) = initial gas in place
Z* = pseudo-gas deviation factor defined by Eq. 4.49

$$Z^* = \frac{Z}{\left(1-c_f\left(p-p_i\right)\right)\left(1-S_w\right)+\dfrac{ZTp_{sc}V_{Ldaf}\left(1-WF_{DASH}-WF_{RMC}\right)\rho}{32.0368Z_{sc}T_{sc}\left(P_L+p\right)\phi_i}} \tag{4.49}$$

where,

c_f (1/psia) = cleat volume compressibility
S_w (fraction) = water saturation
V_{Ldaf} (scf/ton) = dry, ash-free Langmuir volume constant
ρ (g/cm^3) = measured bulk density of coal
P_L (psia) = Langmuir pressure constant
ϕ (fraction) = cleat porosity
D_g (%/yr) = nominal gas decline rate.
sc = at standard conditions

The water decline coefficient is given by Eq. 4.50.

$$D_w = \frac{q_p}{21.256Ah\phi\left(S_{w_i}-S_{w_{irr}}\right)\dfrac{1}{B_w}-q_p t_p} \tag{4.50}$$

where,

S_{wi} (fraction) = initial water saturation
S_{wirr} (fraction) = irreducible water saturation
B_w (res. bbl/stb) = water formation volume factor
q_p (bpd) = plateau (maximum) water rate
t_p (years) = duration of water production rate plateau
D_w (%/yr) = nominal water decline rate

As shown in Eq. 4.51, Mavor, *et al.*[90] simplified the gas decline coefficient derived by Seidle[89] using the real-gas potential.

$$D_g = \frac{\left(3.65\times10^{-4}\right)2J_g k_a k_{rg}}{\mu Z G_i}\frac{p}{P_L}\left[\frac{p_i}{p_i+P_L}\right](p+P_L)^2 \qquad (4.51)$$

where,

$$J_g = \frac{\left(1.987\times10^{-5}\right)hT_{sc}}{p_{sc}T\left\{0.5\ln\left(\frac{2.245A}{C_A r_w^2}\right)+s\right\}} \qquad (4.52)$$

k_a (md) = absolute permeability
k_{rg} (dimensionless) = relative permeability to gas
A (ft^2) = drainage area
G_i (Mscf) = initial gas-in-place volume
T (deg R) = reservoir temperature
C_A (dimensionless) = drainage area shape factor
$_{sc}$ = at standard conditions

4.6 Well Spacing and Drainage Area

Interference of one well with an adjacent well has a positive effect on methane production if dewatering of the seams is facilitated by the interference. Permeability, hydraulic fracturing length, and well spacing are especially important to know for field development because of the desired interference effect. The important consideration of these three parameters in field development is their effect on rate and quantity of water removed from a continuous coalseam.

It also means that CBM projects develop field-wide instead of as isolated wells. A five-spot pilot project is a minimum requirement to evaluate ultimate field performance where the center well will be most representative of field performance.

Studies of the combined effects of wells in the field are best done by simulation.

Young,[11] using data from the first 8.7 years of production, studied the effects of well spacing and interference by history matching in the Cedar Hill field of the San Juan basin. The center well of the field produced for 4.5 years without interference before two corner wells of a 320-acre, 5-spot pattern were drilled. As a result of the positive effect on production from the interference, cumulative production of gas improved over the total 8.7 years.[11] The up-dip well benefited most from the adjacent wells. It experienced the lowest initial water production and improved initial gas rates.

The Cedar Hill study also confirmed that gas and water production extended further in the face-cleat direction. The design of well patterns and spacing should take into account the permeability anisotropy.

Another parameter influencing well spacing and well-to-well interference is the fracture length. At Rock Creek in the Warrior basin, a history match was performed by Spafford[4] to arrive at a relationship of gas recovery, permeability, and well spacing (see Fig. 4.28).

Note that well densities could conceivably be reduced with greater fracture lengths at permeabilities between 1 and 100 md. At permeabilities below 1 md, any fracture length will probably be insufficient for commercial production. Also at high permeabilities, fracture length becomes inconsequential. The paradox exists, therefore, of possibly lower gas production from larger spacings because of the difficulty in removing the water. Dewatering depends on permeability of the coal (cleats and induced fractures) and well spacing.

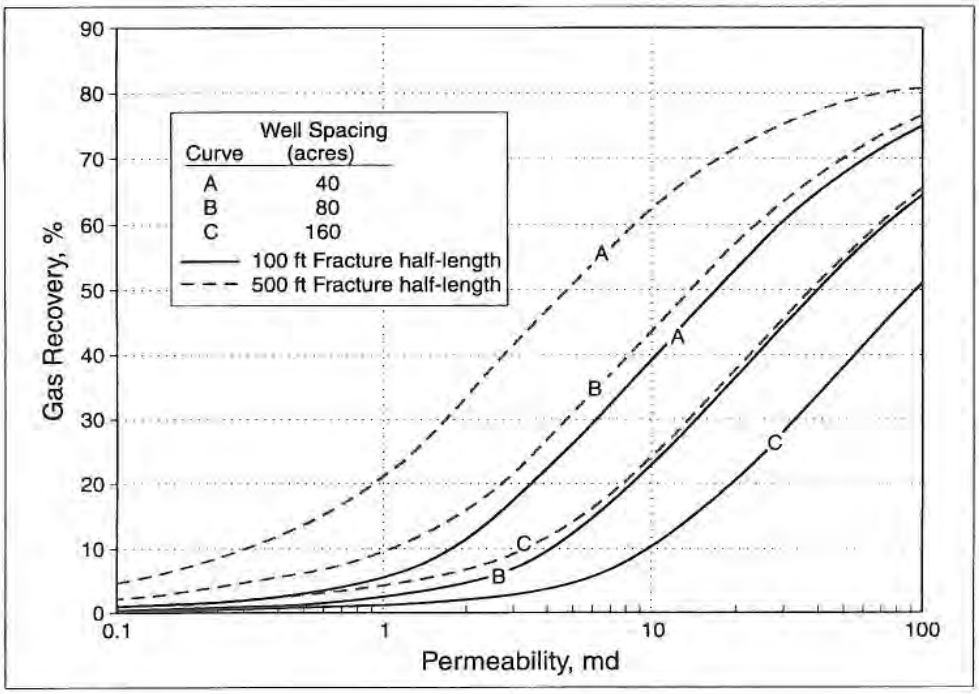

Fig. 4.28—Fracture length influences well spacing choice.[4]

Another simulation study by Sawyer[69] using properties of the San Juan basin shows the effect of well spacing on gas production rate (see Fig. 4.29). The 80-acre spacing provided a peak production rate much sooner than larger spacings because of the positive influence of dewatering.

An optimum well spacing for the most economical development of a CBM field can be obtained by simulation where effects on interference from permeability, fracture lengths, and permeability anisotropy are considered.

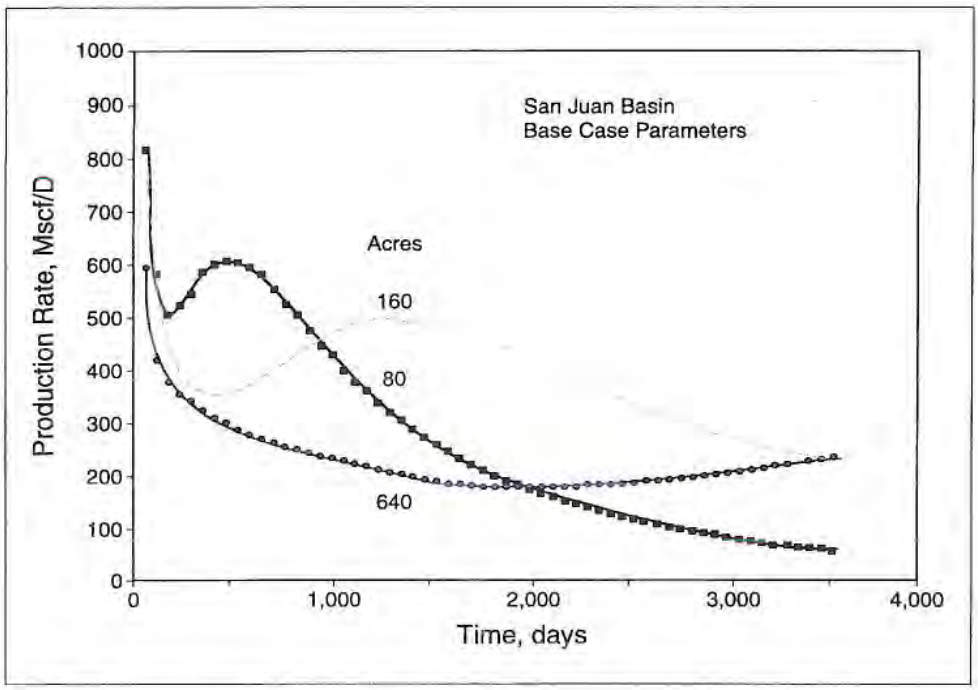

Fig. 4.29—Influence of well spacing.[69]

4.7 Enhanced Recovery

Technical advancements have made the CBM process a commercial reality, and it has been the additional technical innovations that have sustained the process. Enhanced recovery could possibly provide the breakthrough in the future that would make marginal coal properties economically attractive and possibly make deep coals viable targets. Three accomplishments would be desired:

1. Increase the ultimate reserves.
2. Accelerate the production.
3. Improve the process profitability.

The ultimate reserves are defined as the initial methane adsorbed on the coal plus free gas in the cleats minus the amount of the gas that must be left adsorbed and free in the coal at the economic limit of production. To increase ultimate reserves significantly, the enhanced recovery process would need to reduce the amount of gas left adsorbed in the micropores at the economic limit and accomplish the reduction economically.

If time to produce the reserves could be shortened (even without increasing ultimate reserves), improvements in rates of return on the investment might justify additional costs. A 20-year production schedule of a CBM well, for example, reduced in time to a few years, would take advantage of the time value of money.

Enhanced recovery of methane is possible using two methods. Using the first method, the partial pressure of methane is reduced by injecting an inert gas, such as helium or a gas that adsorbs more weakly than methane in coal, such as nitrogen (N_2), into the coalseams and thus maintaining the total pressure. Since the partial pressure of methane is reduced, it desorbs to achieve partial pressure equilibrium. Since helium is more expensive and scarce to obtain, nitrogen, which is cheap and abundant, is used in this process. This process is also referred to as methane stripping.[91] Amoco (now BP) reported initial laboratory research on this enhanced methane recovery process[92] and then field tested the method in a pilot project. They hold a patent on the process.[93]

The second method uses the injection of carbon dioxide (CO_2) to displace methane from coalseams. Carbon dioxide is more strongly adsorbed on coals than both nitrogen and methane in coals and so it displaces methane by better adsorption. As an added benefit, this process also helps sustain the total system pressure.

Conventionally, water removal from coalseams facilitates methane desorption according to the pressure-gas content relationship of its Langmuir isotherm, that is, total pressure is reduced to desorb methane. The desorption, however, is a function of partial pressure instead of total pressure for a binary or multicomponent gas environment. Based on the Amoco process, as methane is swept away from the adsorption site by nitrogen, it was found that the partial

pressure of methane could be reduced more rapidly and to a greater extent than the total pressure by water removal. The end result according to the Langmuir isotherm is the same, but the partial pressure reduction by injecting nitrogen will be faster and attain a lower partial pressure of methane while maintaining the positive effects of a high total pressure on permeability.

Laboratory experiments[94] show a 90%+ recovery of methane from the flowing of two pore volumes of nitrogen in a crushed Jagger coal at 104°F (see Fig. 4.30).

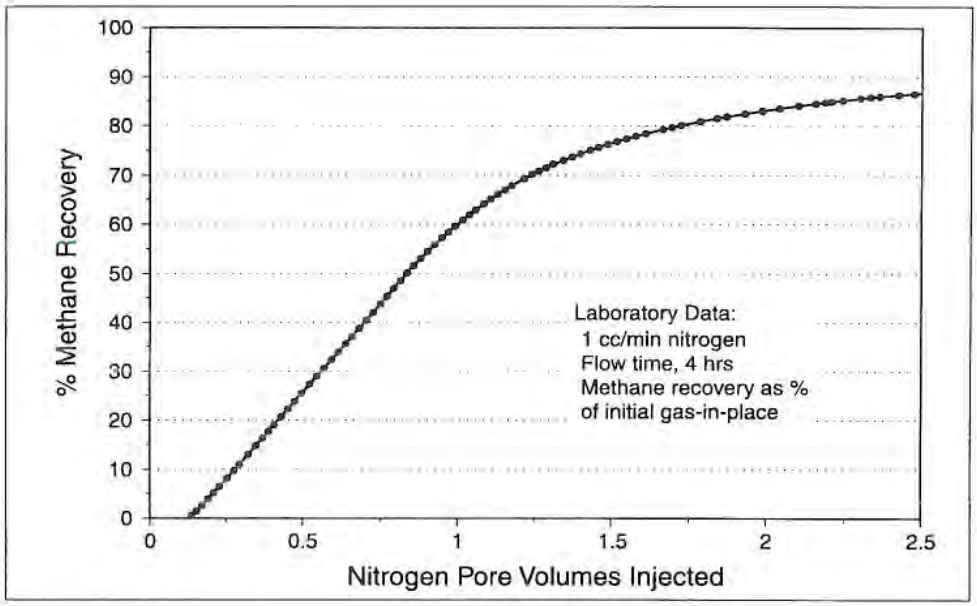

Fig. 4.30—Enhanced recovery of methane from coal.[94]

Another important potential of the process accrues from the maintenance of a high total pressure from injecting nitrogen or carbon dioxide throughout production. By maintaining the high pressure, lower effective stresses are maintained throughout production, and higher permeabilities are realized. Closure of the fissures in the coal by a progressively increasing effective stress is avoided.

It is important to understand the treatment response for these two processes when planning for enhanced CBM (ECBM) recovery. With nitrogen injection, the initial recovery rate is higher, but the breakthrough time of N_2 is also earlier, hence, nitrogen must be separated from the produced gas for a longer period of time.[95]

With CO_2 injection, the initial recovery is lower but the total recovery of original gas in place is earlier than with nitrogen. The breakthrough of CO_2 is delayed when compared to nitrogen because the affinity for CO_2 is very high in coals and so carbon dioxide moves through the coalbed very slowly. This increases the production of methane-rich gas for a longer time interval and reduces the amount of separation required.[95,96] A coalbed's affinity for carbon dioxide makes it a viable candidate for CO_2 sequestration and this also helps enhance the methane production. The dual function of CO_2 injection has caught the attention of the U.S. Department of Energy (DOE), which has sponsored several research projects in this area.

Two commercial ECBM recovery projects have been implemented in the San Juan basin, namely at the Allison and Tiffany units.[91] Allison unit is operated by Burlington Resources, and they injected CO_2 into the Fruitland coals. The objective here is to recycle the CO_2 produced from the Fruitland coals at the same time increasing the methane production from coals.[97] Approximately 4.7 Bcf of CO_2 has been injected continuously into the coals for more than 5 years. Of the 4.7 Bcf that has been injected, 4.2 Bcf of CO_2 has been sequestered.[97] In the project, the ratio of CO_2 injection to methane production was 3.1:1.0, which resulted in total incremental methane recovery of 1.5 Bcf.[97]

Tiffany unit is located in the southwestern part of LaPlata County, Colorado in the San Juan basin and is operated by BP America. A pilot project was commenced to understand the effects of nitrogen injection into the Fruitland coals in an area of approximately 10,000 acres.[91] It consisted of 36 production wells and 12 injection wells.[91] The injection was started in February 1998 and continued intermittently until it was suspended in January 2002. Nitrogen for

injection came from a cryogenic air separation plant in BP's Florida River gas processing facility northwest of the Tiffany unit.[91] It was reported that the increase in methane production was approximately five-fold because of the nitrogen injection. However, early nitrogen breakthrough was observed in almost all the production wells. Approximately 20% cut was reported in all but one well after the first year of injection, causing the need for separation.[91]

The net result of a nitrogen-injection enhanced CH_4 recovery process could be faster recovery of a larger ultimate CH_4 reserve. The process could be economical if the value of additional methane produced earlier exceeded the higher cost of process implementation, such as nitrogen injection and separation of the product gases. Carbon dioxide ECBM pilot projects are underway[97] in Canada, China, and Poland indicating an added interest in this method because of the need for sequestering CO_2. The main obstacle to the ECBM process is increased uncertainty regarding economics of CO_2 injection, transportation, and separation processes rather than the operational costs at the wellheads.[97] Once these issues are addressed via research, more and more operators will consider using this option.

References

[1]McElhiney, J.E., Koenig, R.A., and Schraufnagel, R.A.: "Evaluation of CBM Reserves Involves Different Techniques," *Oil & Gas J.* (October 1989) 87, No. 44, 63-72.

[2]Kuuskraa, V.A. and Brandenburg, C.F.: "CBM Sparks a New Energy Industry," *Oil & Gas J.* (October 1989) 87, No. 41, 49-56.

[3]Levine, J.R.: "Coal Petrology with Applications to CBM R & D," short course presented at Tuscaloosa, Alabama, 13 September 1990.

[4]Spafford, S.D. and Schraufnagel, R.A.: "Multiple Coalseams Project," *Quarterly Review of Methane from Coalseams Technology* (July 1992) 10, No. 1, 15-18.

[5]Ayers, W.B. Jr. and Kelso, B.S.: "Coalbed Resources Grows, But Needs More Study," *Oil & Gas J.* (October 1989) 87, No. 43, 64-67.

[6]McKee, C.R., Bumb, A.C., and Bell, G.J.: "Effects of Stress-Dependent Permeability on Methane Production from Deep Coalseams," paper SPE 12858 presented at the Unconventional Gas Recovery Symposium, Pittsburgh, Pennsylvania, May 1984.

[7]Hunt, A.M. and Steele, D.J.: *CBM Technology Development in the Appalachian Basin*, topical report, Gas Research Institute (January 1991) 27.

[8]Logan, T.L., Clark, W.F., and McBane, R.A.: "Comparing Different CBM Completion Techniques, Hydraulic Fracture and Openhole Cavity, at the Northeast Blanco Unit, San Juan Basin," *Proc., CBM Symposium*, Tuscaloosa, Alabama (April 1989) 265-272.

[9]Ramurthy M. *et al.*, "Case History: Reservoir Analysis of the Fruitland Coals Results in Optimizing CBM Completions in the Tiffany Area of the San Juan Basin," paper SPE 84426 presented at the 2003 SPE Annual Technical Conference and Exhibition, Denver, Colorado, 5-8 October.

[10]Close, J.C. and Erwin, T.M.: "Significance and Determination of Gas Content Data as Related to CBM Reservoir Evaluation and Production Implications," *Proc., International CBM Symposium*, Tuscaloosa, Alabama (April 1989) 37-55.

[11]Young, G.B.C.: "Coal Reservoir Characteristics from Simulation of the Cedar Hill Field San Juan Basin," *Quarterly Review of Methane from Coalseams Technology* (July 1992) 10, No. 1, 6-10.

[12]Decker, A.D., Close, J., and McBane, R.A.: "The Use of Remote Sensing, Curvature Analysis, and Coal Petrology as Indicators of Higher Coal Reservoir Permeability," *Proc., International CBM Symposium*, Tuscaloosa, Alabama (April 1989) 325-340.

[13]Hughes, B.D. and Logan, T.L.: "How to Design a CBM Well," *Pet. Eng. International* (May 1990) 16.

[14]Schraufnagel, R.A., McBane, R.A., and Kuuskraa, V.A.: "CBM Development Faces Technology Gaps," *Oil & Gas J.* (February 1990) 88, No. 6, 48-54.

[15]Hanby, K.P.: "The Use of Production Profiles for CBM Valuations," *Proc., CBM Symposium*, Tuscaloosa, Alabama (May 1991) 443-452.

[16]Earlougher, R.C. Jr.: Advances in Well Test Analysis, SPE of AIME, New York (1977) 131-132.

[17]Saulsberry, J.L.: "A New Low Cost Method of Performing Well Tests in Under Pressured Coalseams," *Proc., International CBM Symposium*, Vol. I, Birmingham, Alabama (May 1993) 273-283.

[18]Schraufnagel, R.A.: "CBM Shortcourse Overview of GRI Research at the Rock Creek Site, Black Warrior Basin," GRI Short Course, Birmingham, Alabama (October 21, 1992).

[19]Holditch, S. and Zuber, M.: "CBM Engineering Methods," SPE Short Course, presented at the 1992 SPE Annual Technical Conference and Exhibition, Washington, DC, 4-7 October.

[20]Koenig, R.A. and Schraufnagel, R.A.: "Application of the Slug Test in CBM Testing," *Proc., CBM Symposium*, Tuscaloosa, Alabama (November 1987) 195-205.

[21]Ramey, H.J. Jr., Agarwal, R.G. and Martin, I.: "Analysis of 'Slug Test' or DST Flow Period Data," *J. Can. Pet. Tech.* (July-September 1975) 37-47.

[22]McKee, C.R.: "Well Testing," The CBM Workshop, Gas Research Institute, Pittsburgh, Pennsylvania (February 6-7, 1989).

[23]Wattenbarger, R.A.: "Well Performance Equations," *Petroleum Engineering Handbook Society of Petroleum Engineers*, H.B. Bradley (ed.), Richardson, Texas (1989) 35-2.

[24]*A Guide to CBM Reservoir Engineering*, GRI 94/0397, Published by the Gas Research Institute, Chicago, Illinois.

[25]Hopkins, C.W. *et al.*,: "Pitfalls of Injection/Falloff Testing in CBM Reservoirs," paper SPE 39772 presented at the 1998 SPE Permian Basin Oil and Gas Recovery Conference, Midland, Texas, 25-27 March.

[26]Abousleiman, Y, Cheng, A. H-D and Gu, H.: "Formation Permeability Determination by Micro or Mini-Hydraulic Fracturing," *J. of Energy Resources Technology*, Vol. 116, pp.104-114 (June 1994).

[27]Ramurthy, M., Marjerisson, D.M. and Daves, S.B.: "Diagnostic Fracture Injection Test in Coals to Determine Pore Pressure and Permeability," paper SPE 75701 presented at the 2002 SPE Gas Technology Symposium, Calgary, Alberta, Canada, 30 April-2 May.

[28]Nolte, K.G.: "Background for After Closure Analysis of Calibration Tests," unsolicited paper, SPE 39407, July 1997.

[29]Talley, G.R., Swindell, T.M., Waters, G.A. and Nolte, K.G.: "Field Application of After-Closure Analysis of Fracture Calibration Tests," paper SPE 52220 presented at the 1999 SPE Mid-Continent Operations Symposium, Oklahoma City, OK, March 28-31.

[30]Nolte, K.G., Maniere, J.L. and Owens, K.A.: "After-Closure Analysis of Fracture Calibration Tests," paper SPE 38676 presented at the 1997 Annual Technical Conference and Exhibition, San Antonio, TX, October 5-8.

[31]Gu, H., Elbel, J.L., Nolte, K.G., Cheng, A. H-D., and Abousleiman, Y.: "Formation Permeability Determination Using Impulse-Fracture Injection," paper SPE 25425 presented at the 1993 Production Operations Symposium, Oklahoma City, OK, March 21-23.

[32]Chipperfield, S.T. and Britt, L.K.: "Application of After-Closure Analysis for Improved Fracture Treatment Optimization: A Cooper Basin Case Study," paper SPE 60316 presented at the 2000 SPE Rocky Mountain Regional/Low Permeability Reservoirs Symposium, Denver, CO, March 12-15.

[33]*Quarterly Review of Methane from Coalseams,* Technology Gas Research Institute, Chicago, Illinois (July 1986) Vol 4, No.1, pp 33-36.

[34]Koenig, R.A., *et al.*: "Hydrologic Characterization of Coalseams for Methane Recovery," Final Report (Jan 1987-April 1989), Report No. GRI 89/0220, Gas research Institute, Chicago, IL (Sept. 1989).

[35]Zuber, M.D., *et al.*: "Design and Interpretation of Injection/Falloff tests for CBM Wells," paper SPE 20569 presented at the 1990 Annual Technical Conference and Exhibition of the Society of Petroleum Engineers, New Orleans, LA, September 23-26.

[36]Grazzier, C.A. and Henderson, K.S.: "Interest Aroused Over Coal, Coalbed Gas Resource Potential of Mississippi Region," *Oil & Gas J.* (August 1989) 87, No. 35, 61-63.

[37]Rogers, R.E.: "Development of CBM in Mississippi Warrior Basin," final report, M.M.R.I. Grant #91-7F (August 1991).

[38]Rogers, R.E. and Carlson, K.W.: "Corehole to Evaluate Coalbeds in Mississippi," *Oil & Gas J.* (December 1991) 89, No. 49, 70-71.

[39]Kuuskraa, V.A. and Wyman, R.E.: "Deep Coalseams: An Overlooked Source for Long-Term Natural Gas Supplies," paper SPE 26196 presented at the 1993 SPE Gas Technology Symposium, Calgary, Canada, June 28-30.

[40]Patching, T.H.: "Variations in Permeability of Coal," *Proc., Rock Mechanics Symposium*, U. of Toronto (January 15-16, 1965).

[41]Harpalani, S. and Schraufnagel, R.A.: "Influence of Matrix Shrinkage and Compressibility on Gas Production from CBM Reservoirs," paper SPE 20729 presented at the 1990 SPE Annual Technical Conference and Exhibition, New Orleans, Louisiana, 23-26 September.

[42]Gray, I.: "Reservoir Engineering in Coalseams Part 1: The Physical Process of Gas Storage and Movement in Coalseams," *SPERE* (February 1987) 28-34.

[43]Collins, R.E.: "New Theory for Gas Adsorption and Transport in Coal," *Proc., International CBM Symposium,* Tuscaloosa, Alabama (April 17-20, 1989) 425-431.

[44]De Boer, J.H., *The Dynamical Character of Adsorption*, Oxford University Press, London (1953) 235.

[45]Olszewski, A.J.: "Development of Formation Evaluation Technology for CBM Development," *Quarterly Review of Methane from Coalseams Technology* (July 1992) 10, No. 1, 27.

[46]Puri, R., King, G.E., and Palmer, I.D.: "Damage to Coal Permeability During Hydraulic Fracturing," *Proc., CBM Symposium*, Tuscaloosa, Alabama (May 1991) 247-255.

[47]Conway, M.W.: "Coal-Fluid Interactions," CBM Shortcourse, Gas Research Institute, Birmingham, Alabama (October 21, 1992).

[48]Puri, R. and Seidle, J.: "Measurement of Stress Dependent Permeability in Coals and Its Influence on CBM Production," *Proc., CBM Symposium*, Tuscaloosa, Alabama (May 13-16, 1991) 415-424.

[49]Kaiser, W.R. and Swartz, T.E.: "Fruitland Formation Hydrology and Producibility of CBM in the San Juan Basin, New Mexico and Colorado," *Proc., CBM Symposium*, Tuscaloosa, Alabama (April 17-20, 1989) 87.

[50]Seidle, J.P.: "Long-Term Gas Deliverability of a Dewatered Coalbed," paper SPE 21488 presented at the 1991 SPE Gas Technology Symposium, Houston, Texas, January.

[51]Hyman, L.A., Brugler, M.L., Daneshjou, D.H., and Ohen, H.A.: "Advances in Laboratory Measurement Techniques of Relative Permeability and Capillary Pressure for Coalseams," *Quarterly Review of Methane from Coalseams Technology* (January 1992) 9, No. 2, 9-16.

[52]Dabbous, M.K., Reznik, A.A., Mody, B.G., Fulton, P.F., and Taber, J.J.: "Gas-Water Capillary Pressure in Coal at Various Overburden Pressures," *SPEJ* (October 1976) 16, No. 5, 261-268.

[53]Bond, R.L., Griffith, M., and Maggs, F.A.P.: "Water in Coal," *Fuel* (1950) 29, No. 4, 83.

[54]Zuber, M.D., and Olszewski, A.J.: "The Impact of Errors in Measurements of CBM Reservoir Properties on Well Production Forecasts," paper SPE 24908 presented at the 1992 Annual Technical Conference and Exhibition of the Society of Petroleum Engineers, Washington, DC, October 4-7.

[55]Mavor, M.J. and McBane, R.A.: "Western Cretaceous Coalseam Project," *Quarterly Review of Methane from Coalseams Technology* (June 1989) 6, Nos. 3 and 4, 24.

[56]Hunt, A.M. and Steele, D.J.: "CBM Development in the Appalachian Basin," *Quarterly Review of Methane from Coalseams Technology* (July 1991) 8, No. 4, 10.

[57]Weida, S.D.: "The Mechanics of Dynamic Cavity Completions for Coalseam Degasification Wells," M.S. thesis, Mississippi State University (December 1993) 147.

[58]Ramurthy, M., "Analysis of the Success of Openhole Cavity Completions in the Fairway Zone of the San Juan basin," M.S. thesis, Mississippi State University, December 1994 (SPE 55603).

[59]Puri, R., Evanoff, J.C., and Brugler, M.L.: "Measurement of Coal Cleat Porosity and Relative Permeability Characteristics," paper SPE 21491 presented at the 1991 SPE Gas Technology Symposium, Houston, Texas, January.

[60]King, G.R. and Ertekin, T.: "Comparative Evaluation of Vertical and Horizontal Drainage Wells for the Degasification of Coalseams," *SPERE* (May 1988) 720.

[61]Bell, G.J., Jones, A.H., Morales, R.H., and Schraufnagel, R.A.: "Coalseam Hydraulic Fracture Propagation on a Laboratory Scale," *Proc., CBM Symposium*, Tuscaloosa, Alabama (April 1989) 417-425.

[62]Mavor, M.: "Cavity Completion Well Performance," presented at the 1992 Eastern CBM Forum, Tuscaloosa, Alabama, 1 September.

[63]Rightmire, C.T.: "CBM Resource," CBM Resources of the United States, American Association of Petroleum Geologists Studies in Geology (1984) No. 17, 8-9.

[64]Smith, D.M. and Williams, F.L.: "Diffusional Effects in the Recovery of Methane from Coalbeds," *SPEJ* (October 1984) 24, No. 5, 529-535.

[65]Crank, J., *The Mathematics of Diffusion*, 2nd edition, Oxford Press (1975).

[66]Bird, R.B., Stewart, W.E., and Lightfoot, E.N., *Transport Phenomena*, John Wiley & Sons, Inc., New York (1960) 542.

[67]Olague, N.E. and Smith, D.M.: "Diffusion of Gases in American Coals," *Fuel* (November 1989) 68, 1381.

[68]Gan, H., Nandi, S.P., and Walker, P.L.: "Nature of the Porosity in American Coals," *Fuel* (1972) 51, 272-77.

[69]Sawyer, W.K., Zuber, M.D., Kuuskraa, V.A., and Horner, D.M.: "Using Reservoir Simulation and Field Data to Define Mechanisms Controlling CBM Production," *Proc., CBM Symposium*, Tuscaloosa, Alabama (November 1987) 295-307.

[70]Airey, E.M.: "Gas Emission from Broken Coal: An Experimental and Theoretical Investigation," *Int. J. of Rock Mech. and Mining Sci.* (1968) 5, 475.

[71]Ruckenstein, E., Vaidyanathan, A.S., and Younquist, G.R.: "Sorption by Solids with Bidisperse Pore Structures," *Chem. Eng. Sci.* (1971) 26, 1305-18.

[72]King, G.R. and Ertekin, T.M.: "A Survey of Mathematical Models Related to Methane Production from Coalseams, Part I: Empirical & Equilibrium Sorption Models," *Proc., CBM Symposium*, Tuscaloosa, Alabama (April 1989) 37-55.

[73]Warren, J.E. and Root, P.J.: "The Behavior of Naturally Fractured Reservoirs," *SPEJ* (September 1963) 245-255.

[74]Mavor, M.J. and McBane, R.A.: Quarterly Review of Methane from Coalseams Technology (November 1991) 9, No. 1, 19-23.

[75]*A Guide to Determining Coalbed Gas Content*, GRI-94/0396, Published by the Gas Research Institute, Chicago, Illinois (1995).

[76]Kuuskraa, V.A. and Brandenburg, C.F.: "CBM Sparks a New Energy Industry," *Oil & Gas J.* (October 1989) 49-53.

[77]D3173-03-Standard Test Method for Moisture in the Analysis Sample of Coal and Coke, *Annual Book of ASTM Standards*, Vol. 05.06-Developed by Subcommittee D05.21, ASTM, Philadelphia, PA (2003).

[78]D3174-04-Standard Test Method for Ash in the Analysis Sample of Coal and Coke, *Annual Book of ASTM Standards*, Vol. 05.06-Developed by Subcommittee D05.21, ASTM, Philadelphia, PA (2003).

[79]Berkowitz, N., *An Introduction to Coal Technology*, Academic Press, New York (1979) 27.

[80]van Krevelen, D.W., *Coal*, Elsevier Publishing Company, Amsterdam (1961) 315.

[81]Mahajan, O.P. and Walker, P.L. Jr.: "Porosity of Coals and Coal Products," C. Karr (ed.), *Analytical Methods for Coal and Coal Products*, Vol. 1, Academic Press, Inc., New York (1978) 131.

[82]D3177-02-Standard Test Method for Total Sulfur in the Analysis Sample of Coal and Coke, Annual Book of ASTM Standards, Vol. 05.06-Developed by Subcommittee D05.21, ASTM, Philadelphia, PA (2003).

[83]D1757-03-Standard Test Method for Sulfate Sulfur in Ash from Coal and Coke, Annual Book of ASTM Standards, Vol. 05.06-Developed by Subcommittee D05.29, ASTM, Philadelphia, PA (2003).

[84]Parr, S.W.: "The Classification of Coal," Bulletin No. 180, Engineering Experiment Station, University of Illinois (1928).

[85]Levine, J.R.: "New Methods for Assessing Gas Resources in Thin-bedded, High-ash Coals," *Proc., CBM Symposium,* Tuscaloosa, Alabama (May 1991) 115-125.

[86]Thompson, R.S. and Wright, J.D., *Oil Property Evaluation*, Thompson-Wright Associates, Golden, Colorado (1985) 4.1.

[87]Craft, B.C. and Hawkins, M.F., *Applied Petroleum Reservoir Engineering*, R.E. Terry (ed.), Prentice Hall, Englewood Cliffs, New Jersey (1991) 77.

[88]Richardson, J.S., Sparks, D.P., and Burkett, W.C.: "A Comprehensive Evaluation to Predict Ultimate Recovery of CBM," *Proc., CBM Symposium*, Tuscaloosa, Alabama (May 1991) 293-306.

[89]Seidle, J. P.: "Coal Well Decline Behavior and Drainage Areas: Theory and Practice" paper SPE 75519 presented at the 2002 SPE Gas Technology Symposium, Calgary, Alberta, Canada 30 April-2 May.

[90]Mavor, M.J., Russell, B. and Pratt, T.J., "Powder River Basin Ft. Union Coal Reservoir Properties and Production Decline Analysis," paper SPE 84427 presented at the 2003 SPE Annual Technical Conference and Exhibition, Denver, Colorado, 5-8 October.

[91]Wo, S. and Liang, J.T.: "Simulation Assessment of N_2/CO_2 Contact Volume in Coal and Its Impact on Outcrop Seepage in N_2/CO_2 Injection for Enhanced CBM Recovery," paper SPE 89344 presented at the 2004 SPE/DOE Symposium on Improved Oil Recovery, Tulsa, Oklahoma, 17-21 April.

[92]Puri, R. and Yee, D.: "Enhanced CBM Recovery," paper SPE 20732 presented at the 1990 SPE Annual Technical Conference and Exhibition, New Orleans, Louisiana, 23-26 September.

[93]Puri, R. and Stein, M.H.: "Method of CBM Production," U.S. Patent 4,883,122.

[94]Kalluri, V.: "Enhanced Recovery of Methane from Coalbeds," M.S. thesis, Mississippi State University, Starkville, Mississippi (1994).

[95] Zhu, J., Jessen, K., Kovscek, A.R. and Orr, F.M. Jr.,: "Analytical Theory of CBM Recovery by Gas Injection," *SPE Journal*, pp 371- 379 December 2003.

[96]Seidle, J.P.: "Fundamentals of CBM", Short Course, presented by Sproule Associates Inc. April 2002.

[97]Pashin, J.C.: "Enhanced CBM Recovery and CO_2 Sequestration," *Scribe's Report*, SPE Applied Technology Workshop, Denver, CO, Oct 27-29, 2004.

Chapter 5

Well Construction

5.1 Drilling

The drilling of coalbed methane (CBM) wells requires attention to the reservoir data collected from the assessment corehole. Minimizing damage by drilling underbalanced is preferred. The term underbalanced describes the well condition when there is more pressure in the formation "pushing up" than there is in the wellbore "pushing down." In normally pressured basins, this would mean air drilling vertical holes to total depth (TD). In over-pressured basins, the use of liquids with some solids and air may be required to maintain backpressure and control fluid influx.

Permeability testing will have determined the spacing of wells and whether or not an operator needs to consider horizontal drilling. Low-permeability coals with 3 ft or greater thicknesses are candidates for horizontal completions. Several techniques for drilling horizontal wells in unconventional reservoirs have been proven. Drilling multi-laterals in-seam using two wellbores has proven successful for one operator.[1]

Air drilling may be required to drill through an area of strip mining that has been reclaimed. The rubble pile, or spoils, that are buried at the surface have high permeability and will not allow circulation of conventional fluids. Air drilling allows circulation of the hole while drilling to surface-casing depth.

Conventional drilling with fluids may be needed to maintain hole stability because of soft formations or influx of fluids. In this case, fresh water or formation brine is preferred to limit damage to the coals, but achieving a slight underbalance is still desirable.

5.1.1 Drill Bits

The choice of bits used in drilling coal is determined by the drilling technique. Air drilling is done with air-hammer bits. Fluid drilling is commonly done with tri-cone rotary bits. Coal is generally softer than limestone or sandstone. Horizontal penetration rates can approach 100 ft/hr using water to circulate through a rotary bit.

5.1.2 Drilling Fluids

The selection of a drilling fluid for CBM wells should be made only after review of the geologic setting of the coals. Minimal use of surfactants, lost-circulation solids, and polymers will reduce the risk of permeability damage. If air or mist is chosen for a drilling fluid, no other additives are required. Foams will require the addition of a surfactant to provide foaming properties when mixed with the air. Drilling mud may be required for pressure maintenance.

Air drilling and use of freshwater systems are both economical and environmentally appealing. Air drilling increases rate of penetration and reduces cost because no mud is used; many wells are drilled to TD in 1 or 2 days. Lost-circulation problems are greatly reduced with air drilling and fewer cuttings are generated for disposal. Most coal basins now have access to air-drilling units.

Horizontal sections may be drilled with water and tri-cone bits, but the vertical portion of the hole is lightened with injected air. This maintains an underbalance pressure on the formation. The operator must be ready to process and control an increasing volume of methane gas liberated by the drilling of multiple horizontal laterals in the coalseam. Some patterns can approach 25,000 linear feet of openhole horizontal coal.

5.2 Cementing

Cementing CBM wells is comparable to cementing conventional wells except for the need to control fluid invasion into the delicate cleat system. While the hole may be drilled underbalanced with air or lightweight fluid systems, the cementing operation must be slightly overbalanced to prevent free-gas migration into the cement column after placement is accomplished. Following best practices for optimum flow rates, conditioning of the hole and centralization of the casing will help ensure complete isolation of the coal intervals and aid in directing the stimulation treatment.

Optimum flow rates should remove mud, drilling fluids, coal fines, and lost-circulation material (LCM); in general, higher pump rates clean the hole more effectively. Because most CBM wells are drilled with clear fluids, mud removal is not a major factor; placing a cement blend without damaging the coal is the fundamental objective.

Conditioning a CBM well vertically drilled with drilling mud would include reducing the viscosity (Pv) and yield point (Yp) as low as possible to obtain a flat gel-strength profile. Fluid-loss control should be lowered to reduce the filter cake across permeable zones. In horizontal sections, the viscosity may need to be increased to improve hole stability.

For air-drilled holes, circulating the hole with water or gel sweeps, to remove fines and to pre-wet the hole, allows placement of cement and helps prevent dehydration of the cement slurry before placement. Reactive spacers may be needed to help prevent lost circulation.

For compatibility, spacers and flushes should be matched to the drilling system. Separating reactive spacers from the cement slurry is a must. Follow the service company's guidelines for spacers and flushes with specific cement blends and for volumes recommended for various holes sizes. Cementing best practice is to provide 7–10 minutes of exposure to the spacer fluids for adequate hole cleaning in the annular space. Pump rates that provide turbulent flow while maintaining low circulating pressures (equivalent circulating densities [ECD]) are recommended.

Pipe centralization across the coalseams is required to obtain maximum zonal isolation. If cementing back into a surface pipe, additional centralization should be used to ensure a complete cement sheath. Standoff calculations can be made by a service company to determine the recommended number of centralizers. In horizontal sections, the use of rigid centralizers is recommended to reduce sticking of the pipe while running.

Pipe movement is preferred to improve cement coverage, and rotation of the pipe is preferred over reciprocation. The chance of sticking the pipe at the wrong depth is minimized with rotation; surge pressures on the coalseams are also eliminated. Pipe movement is not recommended if cementing through a packer shoe or multiple stage cementer.

Gas-flow potential can be difficult to measure for wells drilled underbalanced. Gas migration will leave channels in the cement and can result in a poor cement bond that compromises the containment of the stimulation treatment. The use of "short transition-time cements," such as thixotropic blends, is preferred. Cement additives that generate gas in situ after the cement is placed can also alleviate gas migration.

5.2.1 Foam Cement

Foam cement provides ductile, secure, and long-lasting zonal isolation for CBM wells. The light weight of foam cement places less pressure on the unique cleat structures of coalbeds, reducing the tendency of the cement to exceed the fracture gradient of the coal. If the gradient is exceeded, the coal formation may break down and cause the cement to be lost to the formation rather than cementing the casing into place as designed.

In extensive laboratory testing, foam cement surrounding casing was exposed to hundreds of casing expansions and contractions caused by internal casing pressure changes without apparent damage to the cement sheath. Conventional cements tested simultaneously did not demonstrate such ductility and lost bond with the casing. The tests demonstrated that a foam-cemented annulus could absorb elastically the pressure-induced stresses.[2]

During primary cementing, foam cement can help prevent formation breakdown, lost circulation, and post-job cement fallback. The extremely light weight of foam cement makes it especially useful as lost-circulation plugs where conventional methods of cementing may not be applicable. Slurries that contain less water are usually stronger than those that carry a high percentage of water. With inert gas as a filler material, slurries of even very low density can still have high solids content, which contributes to the ultimate strength of the cement sheath.

5.2.2 Lightweight Additives

Although many types of cement have been used, the simplest type is Class A (Type 1) common Portland cement. This cement is mixed at a density of 15.6 lb/gal for neat blends; the density can be lowered with additional additives. Bentonite, pozzolans, glass microspheres, particles of coal or asphalt, and fibrous materials can all be used to lighten the density and help prevent lost circulation. Because coal contains many natural fractures, or cleats, it is preferable to use a granular material for curing lost circulation. Acid-soluble additives can make removal easier during the completion but usually add to the density. A number of blends have been developed that incorporate combinations of the above additives to reduce weights to a 11.5–12.0 lb/gal cement density while still helping prevent lost circulation and providing excellent zonal isolation. Best practice is to contact the local service company representative to learn about blends being used in the area. Blend modifications can be made to fit the requirements of a particular project.

References

[1]Schoenfeldt, H.V., Zupanik, J., Wight, D.R., and Stevens, S.H.: "Unconventional Reservoirs in the US and Overseas," *Proceedings, International Coalbed Methane Symposium*, Tuscaloosa, AL (May 3-7, 2004) 441.

[2]Technical Data Sheet HO2656: "Foam Cement Delivers Long-Term Zonal Isolation and Decreases Remedial Costs," Halliburton Energy Services, Inc. ©2001.

Chapter 6

Formation Evaluations, Logging

6.1 Introduction

Historically, the wireline logging services employed by the coal industry provided means to assist in mapping the coal, measuring its thickness, and locating water tables in formations above the coal. The wells drilled for coal exploration were typically cored continuously from the surface by small, truck-mounted drilling rigs drilling boreholes of less than 4 in. diameter.

This procedure enabled the mine owners to analyze the coal from the coring operations to answer their questions concerning rank, mineral matter, and BTU content. Wireline logging in these wells was essentially done for qualitative purposes. The mineral logging industry uses small-diameter tools with short sensor spacing to provide sharp contrasts between the coal and the surrounding roof and floor rock.

The advent of extracting methane before mining for coal required use of a larger-diameter borehole for optimum production. This methane production also brought oil and gas exploration companies into the coal industry; these companies were more comfortable evaluating the wireline logs that were used in the oil and gas industry. It was only natural that the major wireline companies entered the coalbed methane (CBM) exploration and production arena. Coring began to take a back seat as the primary evaluation tool.

Now that we have quantitative coalwireline log measurements available, what do they mean and how do we quantify the key parameters for evaluating coal for its gas production properties? This chapter is dedicated to helping the reader understand wireline log measurements and how to determine some of the key parameters that need to be understood to successfully analyze a CBM gas-production play. The critical reservoir parameters addressed in this chapter

on wireline logs are:

- Coal thickness.
- Gas content.
- Coal tonnage and volumetric gas in place.
- Cleat permeability.
- Evaluation of sands near the prospective CBM target.
- Natural fracture orientation.
- Modern-day stress orientation.

In this chapter, we will evaluate four major categories of wireline logging tools (nuclear, electrical, acoustic, and magnetic resonance) and determine how they react in coal.

6.2 Borehole Environment

Before we evaluate wireline logs, we should examine the environment in which wireline logs are run.

6.2.1 Downhole Environment

The downhole environment is not friendly to wireline measurements. The greatest concern is the borehole shape because irregularly shaped boreholes can often create misleading wireline log measurements. As an example, coalbeds that are well cleated can often be eroded by the drilling process, creating a washed-out section of borehole that shows as an enlarged caliper measurement. When this occurs, the wireline measurements that rely on good contact with the borehole wall may be reading a mixture of formation and mud properties, which could be interpreted as showing coal where there really is no coal. An integral part of any interpretation of wireline logs is a consideration of the rugosity of the borehole environment and its relationship to the individual measurement devices.

6.2.2 Wireline Logging

Wireline logging measurements are recorded at various distances from the bottom of the logging tool, as shown in Fig 6.1. This means that if there is any sticking of the logging tool as the log is being recorded, the irregular tool movement will affect each sensor in a different place on the log. For example, if a logging tool is 75 ft long, the measurement sensors will be distributed as follows: at 8 ft for resistivity, 35 ft for bulk density and caliper, 50 ft for neutron porosity, and 70 ft for gamma ray. If the tool physically stops while the wireline cable is being extracted from the well, the pull on the cable will increase until the tool starts moving again or the maximum tension that can be applied to the cable is reached. If the tool starts moving, each sensor will have been stationary at a different depth in the wellbore. As the log is recorded, the surface equipment in the wireline logging unit delays each measurement so all the measurements are printed on depth. Tool pulls can cause a mismatch of the position of a particular measurement.

Each logging service company manufactures its own logging tools. It is important to examine the log heading for information related to the position of each sensor in areas of wireline tension pulls or washed-out boreholes. Fig. 6.2 shows an example of a quad combination log through several coalseams. The quad combination log consists of the three porosity tools and a resistivity measurement device discussed in this chapter.

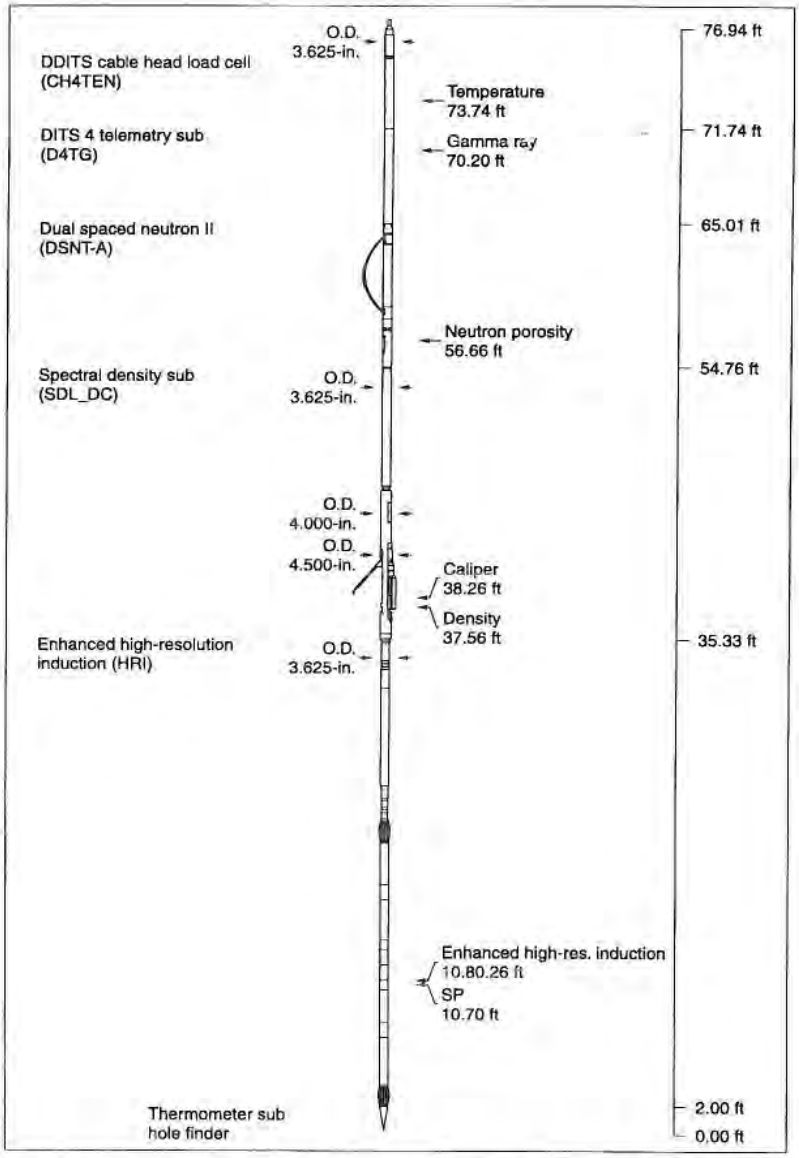

Fig. 6.1—Combination toolstring with the location of the different sensor measurement points.

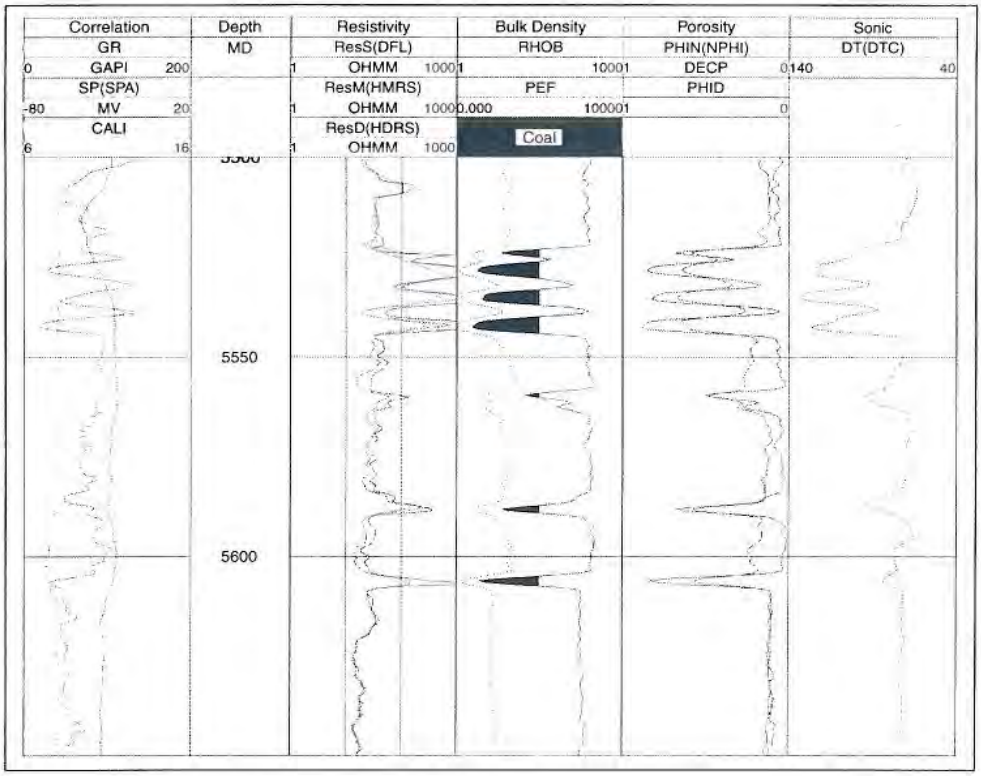

Fig. 6.2—Quad combination log in a coal.

6.3 Tool Measurement Response in Coal

6.3.1 Natural Gamma Ray

The natural gamma ray tool measures bulk gamma rays emitted from the radioactive minerals in the immediate vicinity of the wellbore. Most of the naturally occurring radioactivity in sedimentary formations comes from three general types of minerals: thorium, potassium, or uranium. Clay minerals generally contain large amounts of naturally occurring radioactive minerals (NORM). Uranium, being a more soluble mineral, can be transported by groundwater moving through the formation. Typically, a gamma ray measurement is interpreted as follows: the high readings are shales and the low readings are potential reservoirs. Coals usually have a very low natural gamma ray response because the concentration of clay minerals is low (Fig. 6.3). Occasionally, a coal will have some radioactive material (typically uranium) that was deposited by groundwater movement (Fig. 6.4), making the gamma ray measurement much higher.

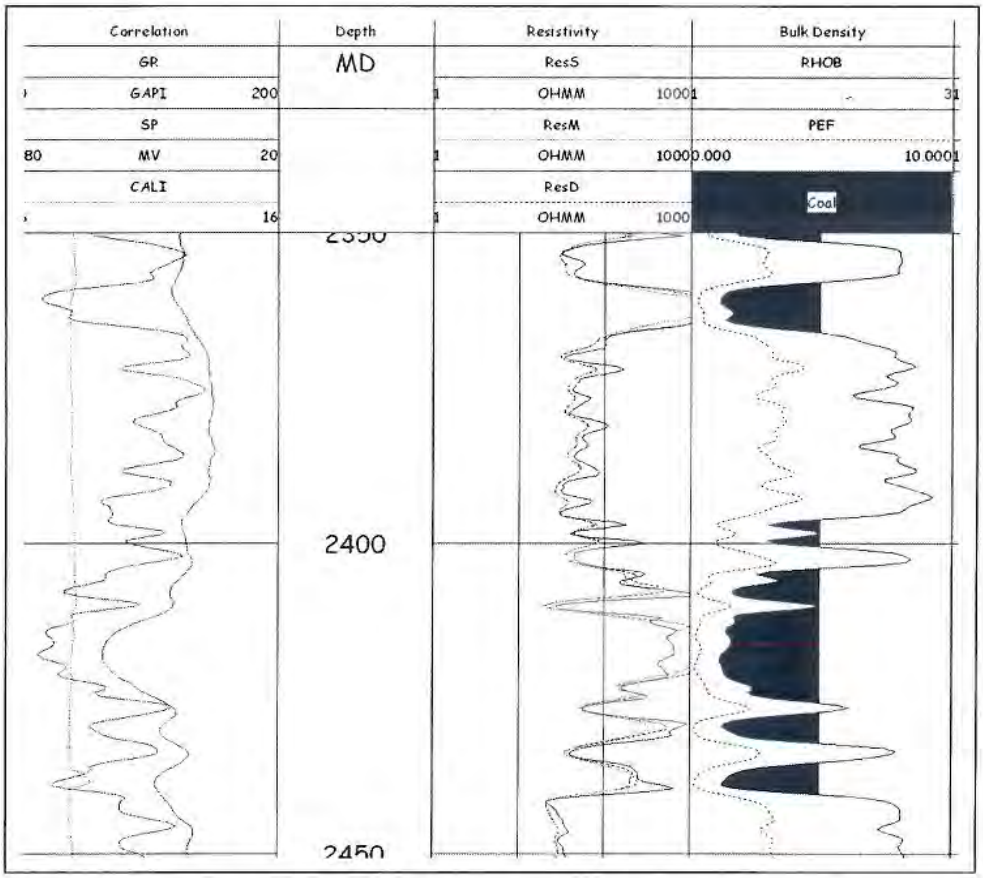

Fig. 6.3—The natural gamma ray tool response in a typical coal.

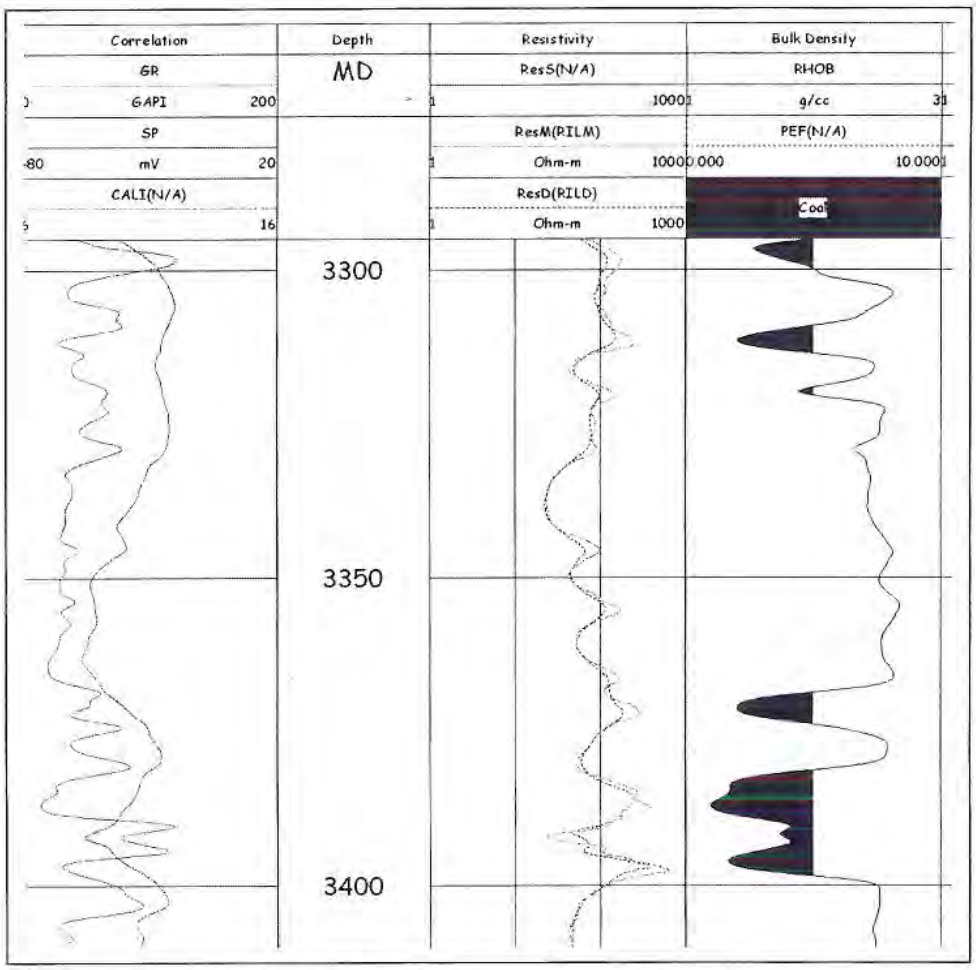

Fig. 6.4—The natural gamma ray tool response in a hot coal.

Enhanced vertical resolution processing of the natural gamma ray measurement is a recommended practice in CBM applications. This processing mathematically reduces the vertical resolution of the measurement, sharpening the bed boundary to help highlight the detail within the coal and result in a more accurate coal-thickness measurement.

6.3.2 Spontaneous Potential

The spontaneous potential (SP) measurement is a voltage potential difference created by three phenomena: salinity difference between the borehole fluid and reservoir fluid, streaming potential, and electrochemical invasion. The most common source of this SP is the salinity difference between connate water and borehole fluids. SP is generated by fluids moving from the borehole to the reservoir. Electrochemical SP effects are most common in carbonates where ions are traded between the reservoir rock and the borehole fluids. The SP is measured as a voltage in reference to the zero baseline value in shale (Fig. 6.3, first log track). When the SP measurement deflects to the left of the baseline, it indicates that the salinity of the borehole fluid is lower than the salinity of the formation water. When the SP measurement deflects to the right of the shale baseline, the borehole fluid salinity is greater than the salinity of the formation water. The shale content of the formation tends to decrease the magnitude of the SP response, as do thin beds, hydrocarbons, and low permeability. The magnitude of the SP deflection (no matter which way it goes) times the thickness of the coal is a good qualitative indication of permeability.[1]

In coals, SP deflection tends to reflect the bulk permeability in the coal. It is most likely due to a combination of salinity difference and streaming potential effects. A greater SP deflection observed across from a coal indicates greater permeability in a coal. When measuring production potential of coalbeds less than 10 ft thick, one should consider applying some thin-bed corrections to the SP measurement either by software bed-resolution enhancement or chart-book corrections to arrive at the most realistic SP response.

6.3.3 Resistivity Measurements

Resistivity tools come in two general categories, induction or laterolog. While each service company's resistivity devices may differ in name, they are all in one of these two categories.

The choice of resistivity tools is usually based upon the salinity of the borehole fluids. Induction tools are typically run in wells with less than 30,000 ppm chlorides in the drilling mud. In saltier mud systems, the dual laterolog tool is the tool of choice.

The most common resistivity devices run for CBM applications are induction-based tools. While the principles of measurement behind the tools differ, interpreting the resistivity log response in coal is similar.

Generally, coal tends to exhibit rather high resistivity measurements (Fig. 6.3, second log track). Coal, in its purest form, is a good insulator and has very high resistivity. Impurities in coal such as clays, pyrites, volcanic minerals, and fluid-filled cleating tend to reduce the resistivity in coals.

With dual induction-type resistivity measurements, the resistivity of the roof and floor rock encasing the coal can have a significant impact on the resistivity measured in the coal; these shoulder beds should be considered in coals less than 30 ft thick.

Modern induction logs and dual laterolog tools can be processed to reduce the effects of the shoulder beds so that vertical-bed resolution can be reliably in the 1–2 ft range. Older electrical logs can be very confusing when used to evaluate coal because these logs have a much coarser vertical resolution and are not the best indicator of coal thickness.

In salty mud systems, the dual laterolog has been used to indicate permeable coal (Fig. 6.5) from non-permeable coal (Fig. 6.6). Permeable coal is observed as having a typical invasion profile while the tight coal shows very high resistivity with no invasion.

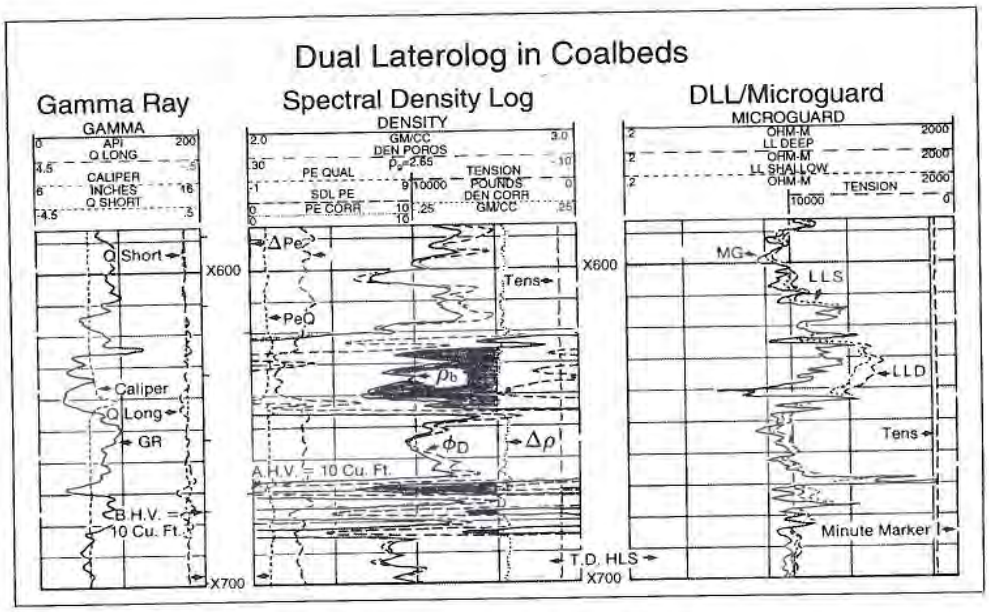

Fig. 6.5—Dual laterolog tool response in a well-cleated coal.

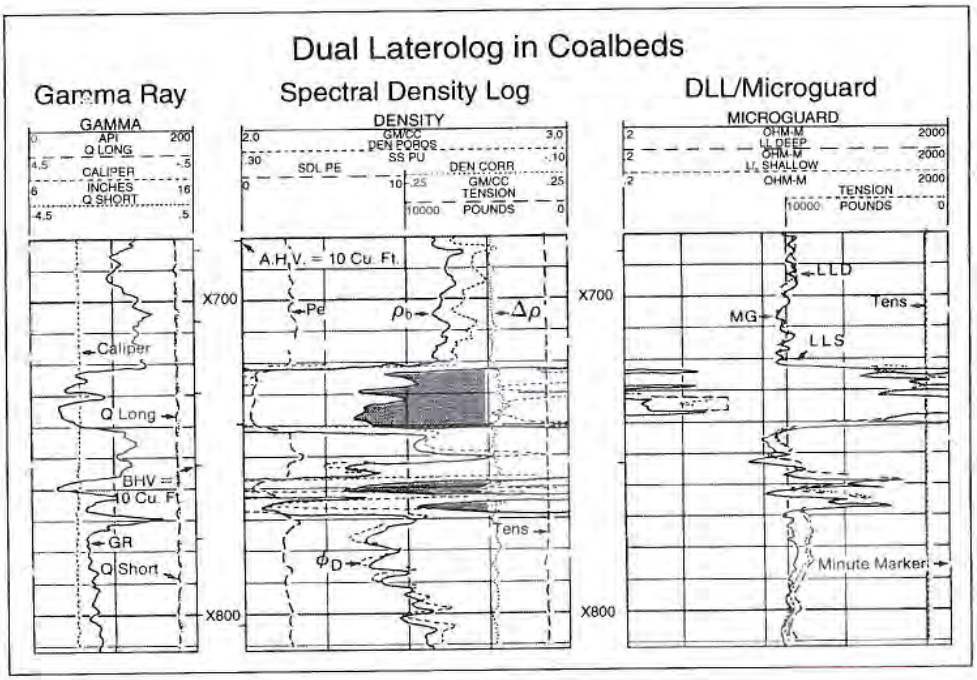

Fig. 6.6—Dual laterolog tool response in a non-cleated coal.

6.3.4 Micro-Resistivity Measurements

Microlog resistivity measurement is a very shallow, non-focused resistivity measurement, taken from a rubber pad about the size of a human hand (Fig. 6.7). The two measurements on the microlog tool are the normal and inverse. The normal resistivity reads slightly deeper than the inverse measurement. The microlog has historically been used as an indicator of mud cake across from permeable zones. In relation to coal, the microlog can be an excellent indicator of the degree of cleating in coalbeds (Fig. 6.8).[2] Although cleat permeability is not directly determined using the microlog, many studies have demonstrated a good

correlation between the cleated footage and production. Fig. 6.9 shows an example of the variation of permeability indications among coalbeds in the same wellbore.

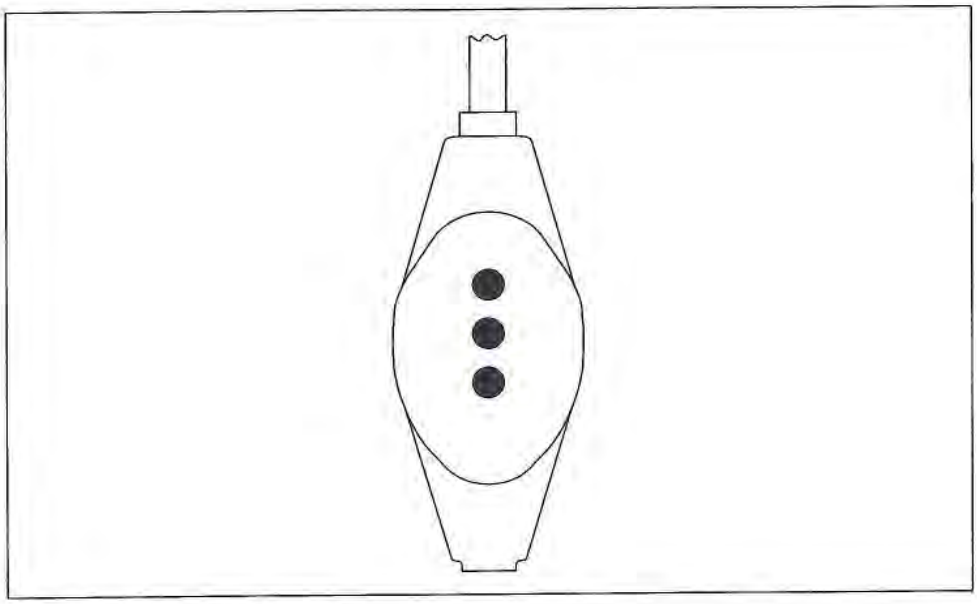

Fig. 6.7—The microlog pad.

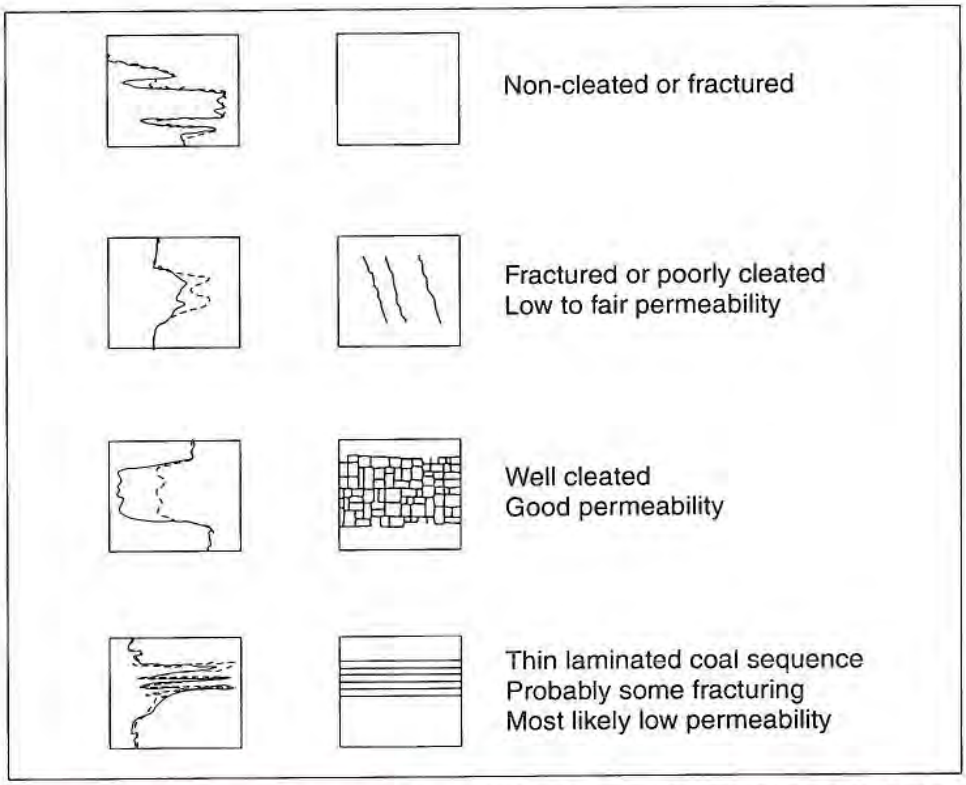

Fig. 6.8—Microlog tool response characterization chart for identifying cleating in coal.

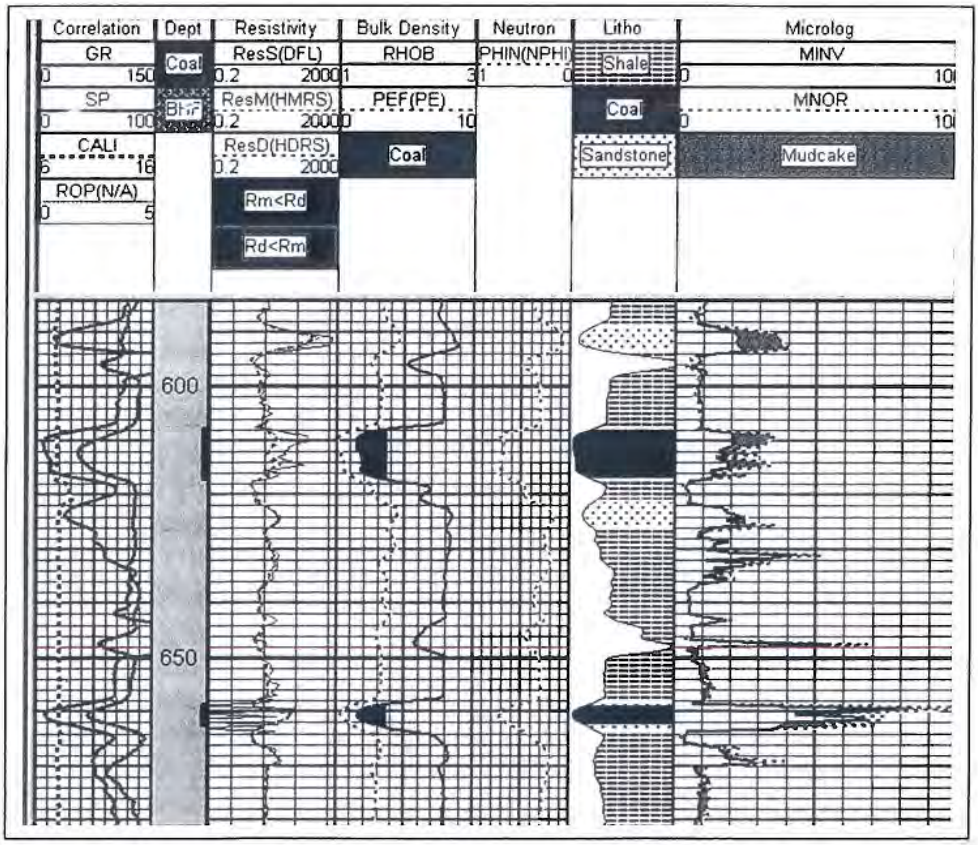

Fig. 6.9—Microlog response showing differences in permeability between coals in the same wellbore.

6.3.5 Nuclear Measurements

Nuclear measurements are divided into two categories: tools using high-energy gamma rays and tools using high-energy neutrons. The high-energy gamma ray tools measure the electron bulk density of the formation, while the high-energy neutron tools respond to the hydrogen index of the formation.

High-energy gamma ray tools are commonly called density tools; high-energy neutron tools are referred to as neutron tools. Typically, when they are run in combination, the log is called a density-neutron log.

Most CBM evaluation is performed with the density log. Many studies have shown good correlation between the bulk-density[3,4] measurement and the proximate analysis and gas content in coal. Most pre-1988 density logs did not display the curve measurement below 2 g/cc, so quantitative evaluation work in wells with older density logs is limited. The range of bulk-density measurements in coal is typically between 1.2 g/cc and 2 g/cc. Gas content has been measured in coaly shales with a bulk density up to 2.6 g/cc. The bulk-density log (Fig. 6.3, third log track) is a high-energy gamma ray tool that requires good contact with the borehole wall for the most accurate measurement. The porosity measurement is then calculated from the bulk density, assuming a matrix density. Washouts along the borehole wall can create pockets of mud between the tool and the borehole wall. The density tool will measure the bulk density of everything in front of the pad. If there is formation and water in front of the measurement pad, the bulk density of the formation will be reduced by the volumetric portion of fluid the tool encounters. The end result is that washouts cause the bulk-density measurement to spike to low bulk-density values. Thus, if one uses only a bulk-density measurement for coal identification without regard for the borehole environment, coal thicknesses could be greatly overestimated.

An integral measurement with modern density logs is the photoelectric (PE) measurement. PE measurement is an excellent measure of lithology as well as a good coal identifier. The PE measurement typically reads below 1.0 in coals.

The neutron porosity tool, often referred to as a compensated neutron tool, responds to the hydrogen index of the matrix rock adjacent to the tool (Fig. 6.10).

Coal, by its chemical composition, has one of the highest hydrogen index values of common minerals encountered in sedimentary deposits. Thus, in coal, the compensated neutron (CN) tool records a very high apparent porosity. The CN is a good tool to identify coal in either open holes or cased wellbores.

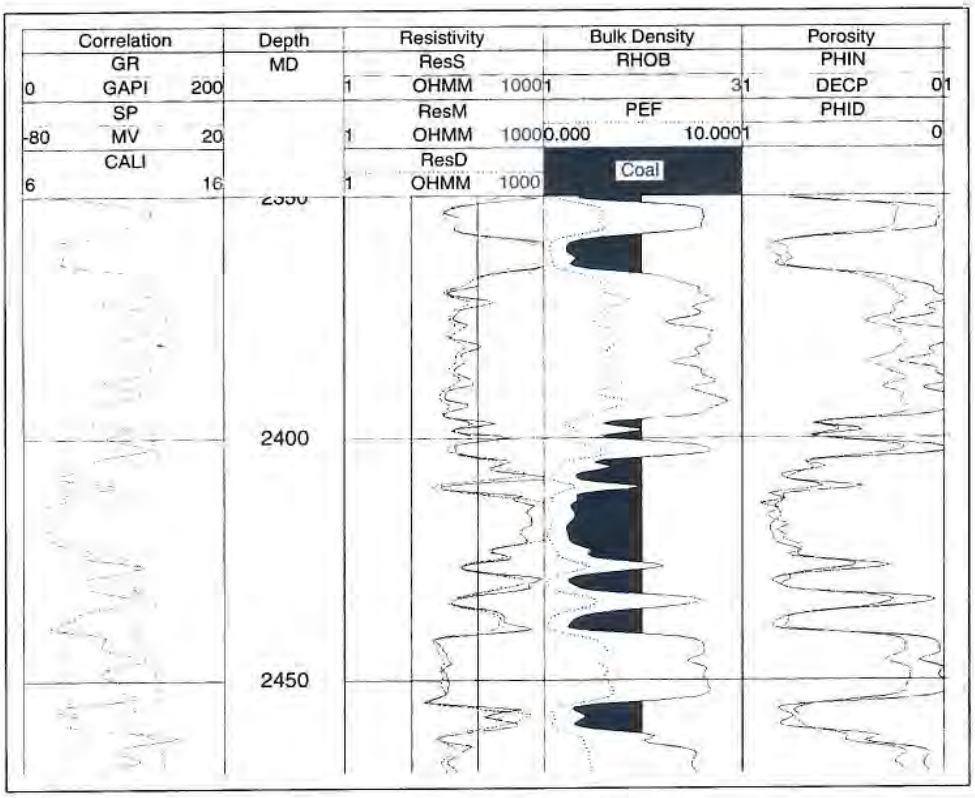

Fig. 6.10—Compensated neutron log response in coal.

The CN porosity tool is not typically used as an indicator of other coal properties because it is usually run in combination with the density log. The bulk-density measurement is more accurate in the low-density end of the measurement and the neutron porosity is most accurate in the low-porosity measurements. In

cased-hole applications, the CN tool can be used quite efficiently to drive coal property calculations by correlating the neutron porosity with the bulk-density measurement in a well where both tools are run (Fig. 6.11).

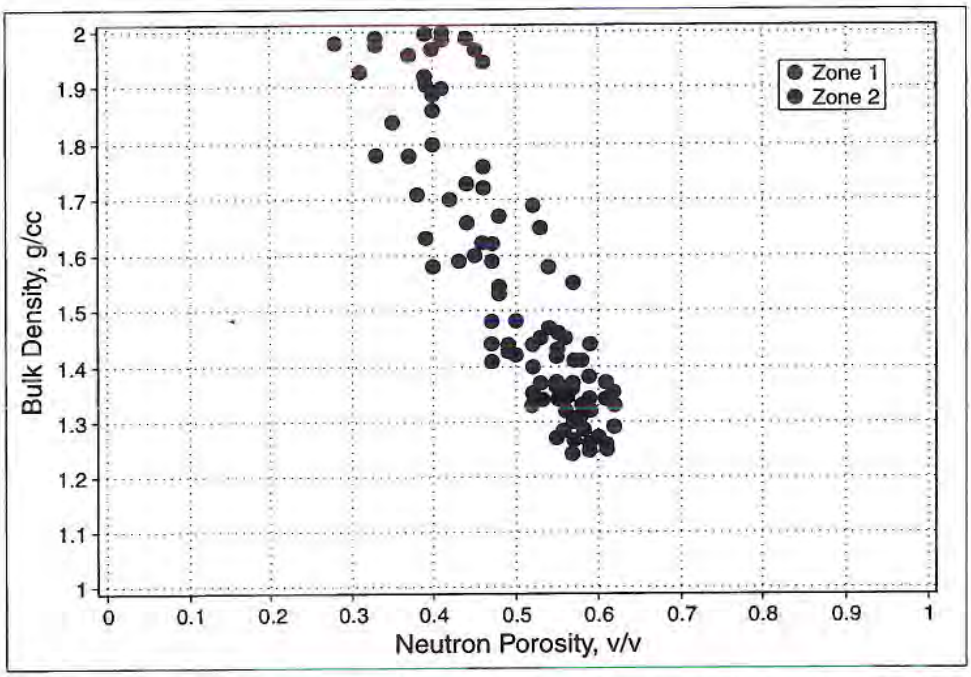

Fig. 6.11—A Crossplot showing the relationship of compensated neutron porosity and bulk density.

For conventional wireline log displays, the neutron porosity is overlain with the density porosity. A rule of thumb when interpreting these two porosity measurements is that when the curves overlay each other, the formation is fluid filled. When there is a crossover effect observed, wherein the neutron porosity reading shows lower porosity than the density porosity, the pore space is gas filled. In coals, this is not necessarily the case. However in some areas, a dry coal, i.e., coal that produces mostly gas and very little water initially, has the

neutron porosity recording a lower porosity than the density porosity, Fig 6.12.

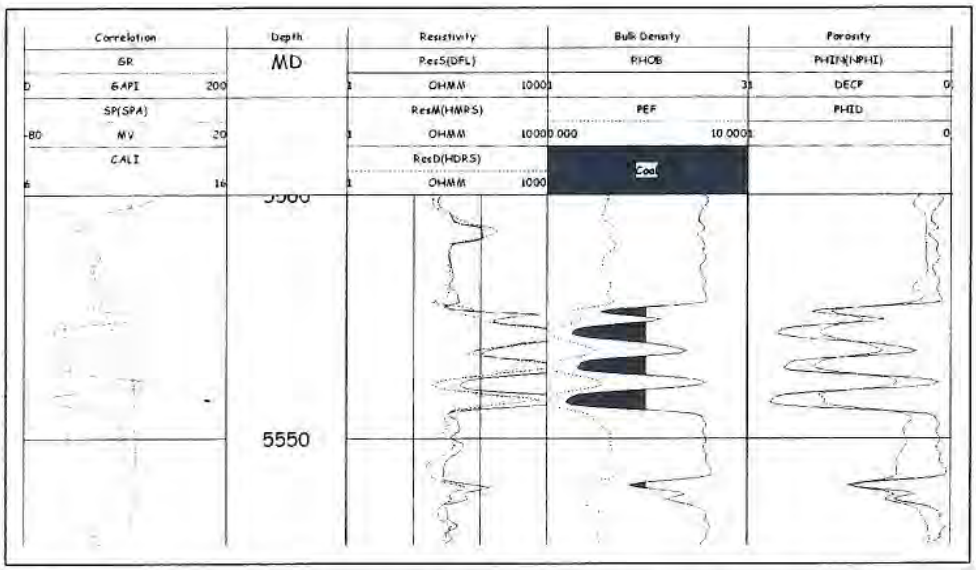

Fig. 6.12—An example of a dry coal tool response from the density-neutron porosity measurements.

A wet coal (a typical coal that produces water as the mechanism to reduce pressure in the cleat system for gas desorption) is often observed as a stacking of the neutron and density porosity. This observation may vary based upon the minerals present, geographic area, and service-company logging tool response.

Another category of neutron tools, the pulsed neutron tools, are small-diameter devices typically run through casing for formation evaluation. Instead of measuring high-energy neutrons elastically reflected to the logging tool, these tools measure the gamma rays given off when a high-energy neutron is slowed down by inelastic atomic scattering then captured by atoms in the formation. The rate of gamma ray decay from a short, high-energy neutron burst is inversely proportional to the formation capture cross-section called the formation sigma. The formation sigma is inversely proportional to the formation resistivity. Higher values of sigma correspond to lower resistivity. The pulsed neutron tools usually

have dual detectors in which the total count rate ratio is calibrated to neutron porosity. The inelastic count rates available from these tools are good indicators of mineralogy by determining the hydrogen yield and carbon-oxygen ratio from the spectral decay (Fig. 6.13).

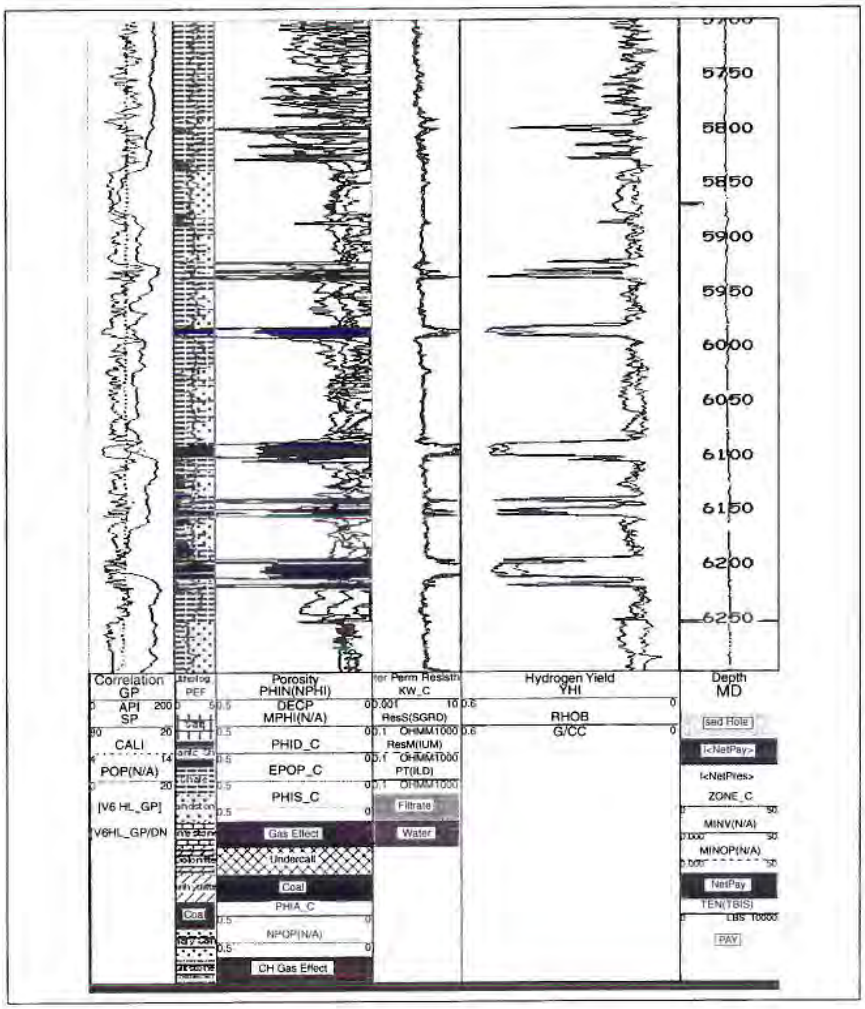

Fig. 6.13—Pulsed neutron log response in coal.

6.3.6 Acoustic Measurements

Acoustic tools come in two varieties, a monopole sonic and a dipole sonic. The monopole sonic tools are typically used when measuring compressional slowness. Dipole sonic tools offer both a monopole transmitter and a dipole transmitter (Fig. 6.14). Most modern dipole sonic tools have two shear transmitters at an orthogonal orientation, which allows an X and Y shear slowness measurement. When coupled with a navigational package, it is often possible to detect the orientation of the modern stress field and open fractures orientation. Occasionally, the magnitude of the stress field differences can be determined. Sonic logs identify coals by their long transit times, which will typically be longer than most any other formation in the well. Sonic tools can be run in either open holes or cased wellbores.

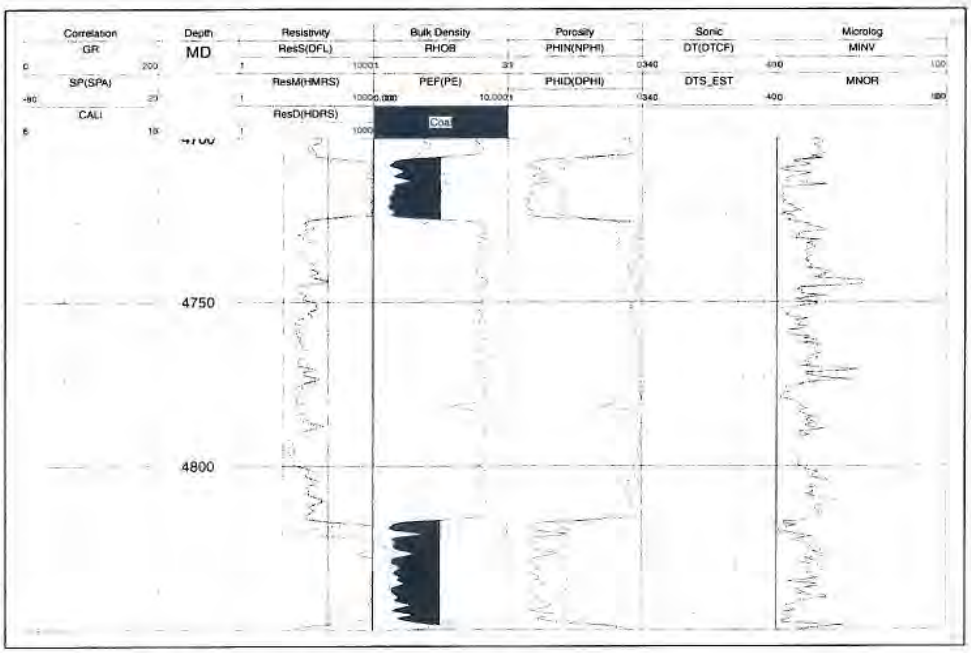

Fig. 6.14—Dipole Sonic tool response in coal.

6.3.7 Magnetic Resonance Measurements

The magnetic resonance imaging tool (MRIL) is a porosity device that measures only the pore space filled with fluid; its porosity measurement is independent of the lithology of the formation. Hence, it is the only porosity device that can accurately measure the porosity in a coal (Fig. 6.15). The porosity measured in coal is primarily the cleat porosity. Some coals do have "matrix" porosity, for example, the coals in the Powder River basin. But in general, the bulk-density measurement is used for a gross coal thickness and the coal with MRIL porosity is reflective of the net coal thickness.[6]

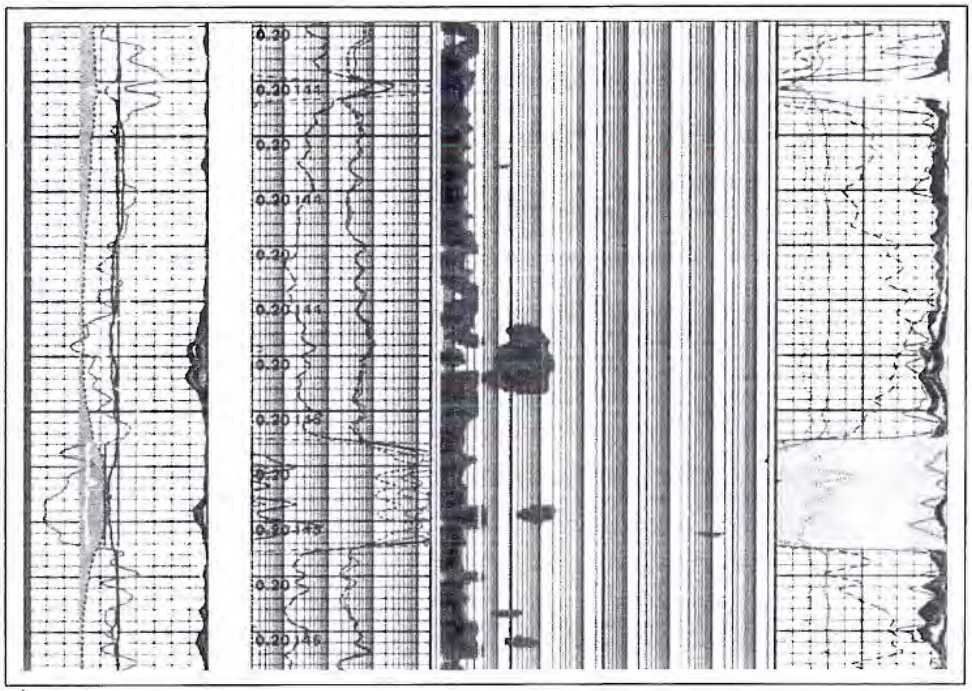

Fig. 6.15—MRIL tool response in coal.

Based upon the assumption that there exists a good correlation between cleat porosity and permeability in coal, the magnetic resonance measurement is a very valuable tool for providing permeability information in multi-seam coal plays.

6.3.8 Electrical Imaging

Over the past decade, micro-electrical imaging (MEI) technology has come a long way in its capability to image high-resistivity formations, such as coalbeds. MEI tools have an array of micro-resistivity buttons mounted on multiple pads to give a representative view of the inside of the borehole. These tools have either four or six arms carrying the micro-electric pad array.

The resolution of these devices is on the order of 0.1 in.; therefore, it is possible in some cases to see the difference between cleated coal (Fig 6.16) and fractured coal (Fig 6.17). In poorly cleated coal, cleat orientation may be observed. The information derived from electrical imaging is critical in understanding any CBM play. Present-day stress orientation, borehole breakout, fracture identification, fracture connection from the coals to adjacent sands along with partings, and cleating information in the coal are essential elements of information to obtain early when developing a CBM play. Much of this information is made available through the analysis of micro-electrical imaging logs.

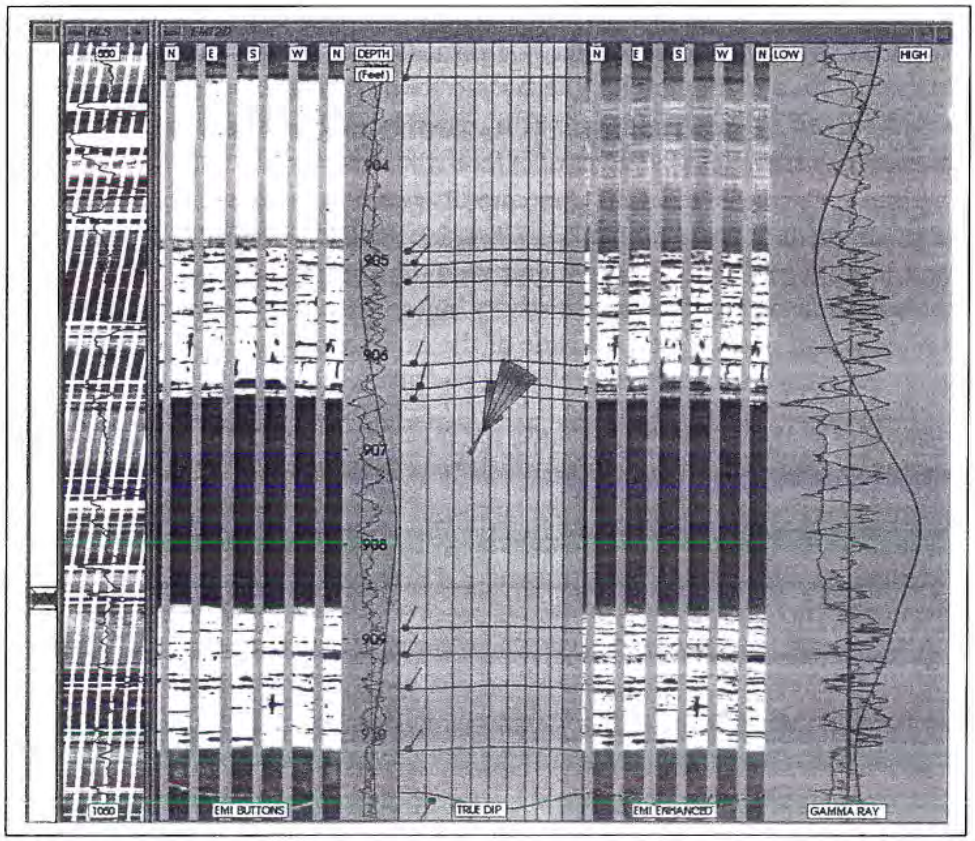

Fig. 6.16—An electrical-image log in thin coals showing individual cleats and thin partings.

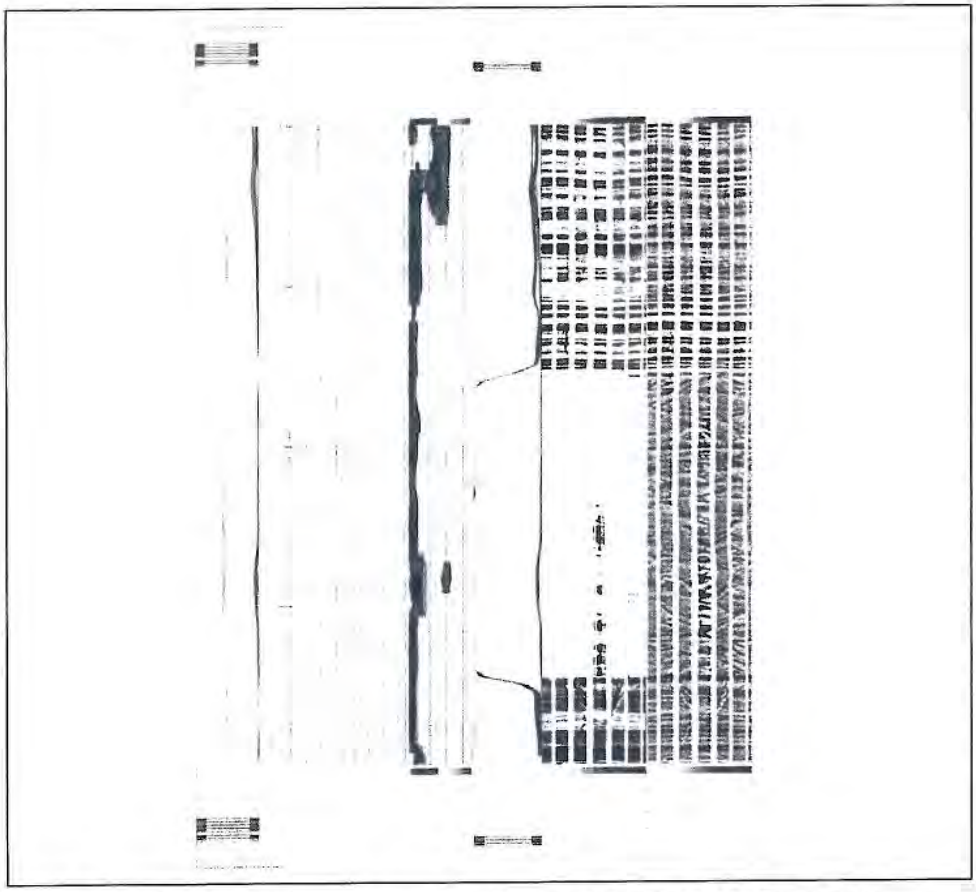

Fig. 6.17—An electrical-Image log in a thick coal that is highly fractured.

6.4 Wireline Log Evaluation of CBM Wells

To make a meaningful assessment of the CBM potential of a particular prospect, the analyst must consistently apply a methodical, structured evaluation. Understanding the key parameters in CBM reservoir evaluation early in the lifecycle of a project can help the analyst make pertinent decisions on project development.[7] Many of these key parameters can be determined with wireline measurements. A methodical process for utilizing wireline logs in conjunction with analytic data to evaluate the CBM potential is the next topic of discussion.

6.4.1 Coal Identification

The gross thickness of a particular coalseam is determined by following these general wireline log measurement cutoffs:

1. Bulk-density measurements less than 2 g/cc.
2. Gamma ray measurements less than 60 API.
3. Neutron porosity measurements greater than 50%.
4. Sonic transit time greater than 80 μs/ft.
5. Shear transit time greater than 180 μs/ft.
6. Resistivity greater than 50 $\Omega m^2/m$.

All of the preceding cutoffs must to be determined locally. The condition of the borehole in which the wireline log was recorded must be considered when using wireline logs for the identification of coal. As mentioned previously, rugose boreholes can give a false indication of coal. Using multiple coal indicators helps minimize the negative effects of borehole rugosity on coal thickness.

6.4.2 Coal Tonnage

A convenient measure to assess analog CBM projects compares coal tonnage per acre. Since no two CBM fields are identical, there is no reason for two CBM fields with similar coal tonnage per acre to be identical. However, coal tonnage per acre gives a starting place with stimulation treatment design. Determining coal tonnage in the project area is the first step to quantify the available resource. Coal tonnage is calculated using Eq. 6.1.

$$CTpA = 1359.7 * h * RHOB \qquad (6.1)$$

where

CTpA = coal tonnage per acre
h = coal thickness, feet
RHOB = minimum bulk density in the coal, g/cc

6.4.3 Proximate Analysis

The proximate analysis is a routine coal analysis to derive the mineral matter content, moisture content, volatile matter, and fixed carbon content of the coal. Of primary interest to the CBM project development are the mineral matter and moisture content. Mineral matter, often called ash content, is residue after the coal sample has been burned. When compared, one notices a good correlation between mineral matter content and bulk-density measurement from wireline logs.[3] It is possible to derive the proximate analysis using the correlations between the wireline log measurement of bulk density and the constituents of the proximate analysis. Because each coal is unique, the modeling between core measurements and wireline log measurements provides essential information that should be obtained early in the lifecycle of the project.[7]

6.4.4 Gas Content in Coal

Determining gas content in coal is the primary goal of CBM reservoir analysis. It is essential to have representative measurements of the initial gas content in a distribution of coals as well as in the organic-rich shale around the wellbore. This information is used to construct a linear correlation between initial gas content and the wireline log measurement of bulk density. From the basic correlation, initial gas content can be derived for a larger area than just the pilot project.

When expanding the gas content algorithm for a more descriptive case, the effects of pore pressure from dewatering the coal need to be taken into consideration. Eq. 6.2 is the characterization of the Langmuir isotherm most commonly used to model the gas content through the lifecycle of the well8.

$$GC\_L = Lc * [1- Mc+ Ac] / [PR/(PR+Pc)] \qquad (6.2)$$

where

GC_L = Langmuir desorbed gas content, scf/ton
Lc = Langmuir constant, scf
Mc = Moisture content in the coal, %
Ac = Ash content in the coal, %
Pc = Langmuir pressure, psi
Pr = Reservoir pressure, psi

Comparing the measured gas content at initial reservoir conditions with the calculation Langmuir gas content is another step in CBM reservoir understanding. The use of the Langmuir isotherm is discussed in Chapter 3. Coupling the calculated desorbed gas content using wireline log data with the Langmuir isotherm is a powerful tool to help users understand CBM production response.[8] This is especially important through the later stages in the lifecycle of the CBM reservoir when it is time to select infill drilling locations.

6.5 Gas-In-Place Calculations

Total gas-in-place (GIP) calculations are derived by multiplying the project area, coal tonnage, and the gas content together.

$$GIP = GC\_L * CTpA * A \quad (6.3)$$

where

GIP = Gas in place, scf
GC_L = Langmuir gas content, scf/ton
CTpA = Coal tonnage per acre
A = Total area in acres

6.6 Recovery Factor

The recovery factor, discussed in Chapter 3, is estimated using the Langmuir isotherm to obtain gas content at initial and abandonment reservoir pressure. The recovery factor is estimated as the ratio of the initial gas content and the gas content at abandonment. The gas content at abandonment pressure is not a strict engineering calculation because it falls on the steep portion of the isotherm curve. The actual recovery factor will be a combination of drainage patterns, well interference, production operations, and economic variables. When gas prices are high, projects can be economic longer than with low gas prices. The actual recovery factor determination may be decades in the future, but this method is a good first approximation of the recovery factor. The recovery factor (Eq. 3.12) can be calculated using the units described in this chapter as Eq. 6.4.

$$R = GC\_A / GC\_L \quad (6.4)$$

where

R = Recovery factor
GC_A = Gas content at abandonment pressure from the Langmuir isotherm, scf/ton
GC_L = Initial desorbed gas content, scf/ton

6.7 Drainage Area Calculations[8]

As a CBM project matures, infill drilling may be deemed necessary for optimum gas recovery. In Lifecycle 4, mature asset development, many wells have numerous years of production history. The cumulative gas production can be used to calculate the volumetric drainage area by rearranging the volumetric gas-in-place calculations. Note that the units of cumulative gas production and GIP must be the same.

$$CDA = \text{Cumulative gas production} / GIP \qquad (6.5)$$

where

CDA = Current drainage Area, Acres
GIP = Original recoverable Gas-in-place calculation per acre

When a circular drainage pattern is assumed, the drainage radius, DR, can be calculated from Eq. 6.6.

$$DR = (CDA * 43560 / 3.14159)^{0.5} \qquad (6.6)$$

The assumption of a circular drainage pattern is not always a direct reflection of the reservoir condition; however, it is a reasonable way to compare the production of wells when looking for permeability trends, offset, or infill locations.

6.8 Coal Permeability/Cleating

Successful CBM production depends on good coal permeability. Permeability is the single-most important parameter that must be determined early in the lifecycle of the CBM play. Chapter 4 discusses several methods for determining permeability in single seams. When pressure transient test permeability is used to calibrate certain wireline log measurement indications of permeability, the wireline logs can be a very powerful analysis tool used to rank individual coalseams that were not tested for permeability by pressure transient tests.

Wireline log measurements used to indicate permeability are SP deflections from a shale baseline, microlog response, porosity measured by the magnetic resonance imaging logs, and visual observations using MEI devices.

To quantify the microlog response in coal, the log response is first normalized for the mud resistivity and then categorized as well cleated, moderately cleated, and poorly cleated.[2]

In quantifying MEI logs, most service providers treat cleating as they would a vuggy carbonate to export some volume fraction of cleats.

To calibrate the wireline log measurements to give a reasonable permeability determination, the following procedure is recommended. Crossplot the permeability-ft, Kh, from the well testing against the following:

- Maximum absolute value of the SP deflection times coal thickness.
- Microlog well-cleated footage + 0.75 * moderately cleated footage + 0.5 * poorly cleated footage.
- Maximum magnetic resonance porosity times the permeable thickness.
- Image volume fraction of cleating times the thickness observed.

6.9 Natural Fracturing and Stress Orientation

The presence of natural fracturing must be considered when evaluating the total formation analysis around the CBM prospect area. Natural fractures can serve as conduits between the coals and aquifers. If the coalbeds are somehow connected to aquifers, the production analysis can be very confusing to interpret. The best way to examine the wellbore for natural fracturing is to use MEI tools, as described previously in this chapter. Fig. 6.17 shows an example of a fractured coal with a fracture orientation 10–20°N. The production from this coal is over 2,000 BWPD.

An additional benefit of running MEI logs is the identification of borehole breakout, modern-day fracture orientation, and modern-day stress orientation. Drilling-induced fractures tend to reflect the modern-day stress orientation. Borehole breakout is indicated by borehole elongation and usually occurs in the

minimum stress orientation. The best situation occurs when the natural fracture orientation is in some oblique angle to the modern-day stress orientation.

6.10 Mechanical Rock Properties in CBM Evaluation

Mechanical rock properties include Poisson's ratio and Young's modulus, which are commonly used in hydraulic-fracture stimulation design. Coal does not behave according to the uni-axial strain model; therefore, it is difficult to model a hydraulic-fracture treatment in coal. In general, a hydraulic fracture initiated in the coal tends to stay in the coal. Mechanical rock properties are a necessary input when analyzing post hydraulic-fracture treatment history matching. Mechanical rock properties can either be calculated from measured compressional and shear slowness using dipole sonic logs or derived through use of a lithologic model.

6.11 Summary

The goal of this chapter was to show the value and utility of incorporating wireline logs as an integral component of modern CBM project assessment. Wireline logs are a very useful evaluation tool when calibrated with core measurements, not only for gas content or estimating proximate analysis, but for identifying stress orientation, natural fracturing, and permeability in coalbeds. These are essential parameters to understand early in the lifecycle of the field and throughout the years as the project matures.

References

[1]Mullen, M.J.: "Log Evaluation in Wells Drilled for Coalbed Methane" RMAG Coalbed Methane San Juan Basin Symposium, 1988.

[2]Mullen, M.J.: "Cleat Detection in Coalbeds Using the Microlog," RMAG Coalbed Methane Symposium, Glennwood Springs, CO, May, 1991.

[3]Mullen, M.J.: "Coalbed Methane Resource Evaluation from Wireline Logs in the Northeastern San Juan Basin: A Case Study," paper SPE 18946 presented at the Rocky Mountain Regional/Low Permeability Reservoirs Symposium, Denver, CO, March 6-8 , 1989.

[4]Mullen, M.J.: "Cased Hole Coal Analysis in Producing Gas Wells in the San Juan Basin" paper presented at the Coalbed Methane Symposium, University of Alabama/Tuscaloosa May 13-16, 1991.

[5]*Halliburton Energy Services Chartbook*, 1991.

[6]Lipinski, P., Mullen, M.J., and Gegg, J.: Piceance MRIL paper.

[7]Blauch, M.E., Weida, D., Mullen, M., and McDaniel, B.W.: "Matching Technical Solutions to the Lifecycle Phase is the Key to Developing a CBM Prospect," paper SPE 75684, presented at the SPE Gas Technology Symposium, Calgary, Alberta, Canada, 30 April-2 May, 2002.

[8]"Coalbed Methane Play and Prospect Evaluations Using GeoGraphix Software," Customer White Paper published on \\http:www.geographix.com, 2003.

Completions

7.1 Introduction

Well completions in coalseams are similar to conventional gas well completions, but modifications have been incorporated into the procedures because of unique properties of the coal. Some coal properties and attendant problems associated with developing the coals for methane include the following:

- Coal is friable. The coal of optimum rank for coalbed methane (CBM) production is also the most fragile.
- Coal has an extensive natural fracture system that must be connected to the wellbore to provide adequate permeability. The fracture network is sensitive to blockage from cement or drilling muds.
- Adsorptive properties that lead to swelling of the coal matrix, especially from organic compounds, make the coal susceptible to drilling mud and fracturing fluids.
- Bothersome coal fines are generated during completion and production.
- Higher treating pressures are often encountered in fracturing coals.

As a consequence of these coal properties, completing CBM wells has become a study in choosing and modifying a method to give the best procedure for each set of conditions.[1] Costs of completing the well must be minimized in all CBM operations but particularly the many projects that are marginally economical.

7.2 Openhole Completions

Openhole completions of single seams were the first type of completion used in the Warrior basin where, before 1982, the completion goal was recovery of gas from a single seam with minimum formation damage.[2] The technique was simple

in principle, and it involved minimum risk. The single-seam, openhole completions were directed toward the most prolific group, the Mary Lee/Blue Creek.

Basically, the procedure was the following:

1. A 4 1/2-in. diameter casing was set above the coal.
2. Drilling was completed through the coal.
3. The seam was hydraulically fractured.
4. The well was cleaned with compressed air.
5. A tubing string and pumping equipment were inserted.[3]

Similarly, the CBM wells drilled in the Appalachian basin in the 1950s through the 1970s were openhole completions of a single seam. These wells ordinarily had no hydraulic fracturing, or at most a small-scale fracture. The gas production was less than 150 Mscf/D in all cases[4] and usually in the range of 30–50 Mscf/D. The procedure was favored by the mining industry because the open hole left no casing obstacle for eventual mining through the coal. However, downtimes to clean loose coal from the open hole were frequent.

During 1982–84, Taurus began initial developmental work on multizone completions in openhole[2] because of the potentially lower cost to develop marginal properties. As a result, the single-seam completion was replaced briefly with an openhole, multizone completion. A sketch of the openhole, multizone completion used early in the Warrior basin developmental period is shown in Fig. 7.1 for the case of the Deerlick Creek field.[2]

In this instance, the Black Creek, Mary Lee, and Pratt groups were completed. The Mary Lee was the prolific producer, but significant production came from the other two groups.

The openhole completion has these advantages:

- No casing is left to obstruct mining.
- The cementing process does no damage to the coal face.
- The open hole gives unobstructed access to the coal face from the wellbore.

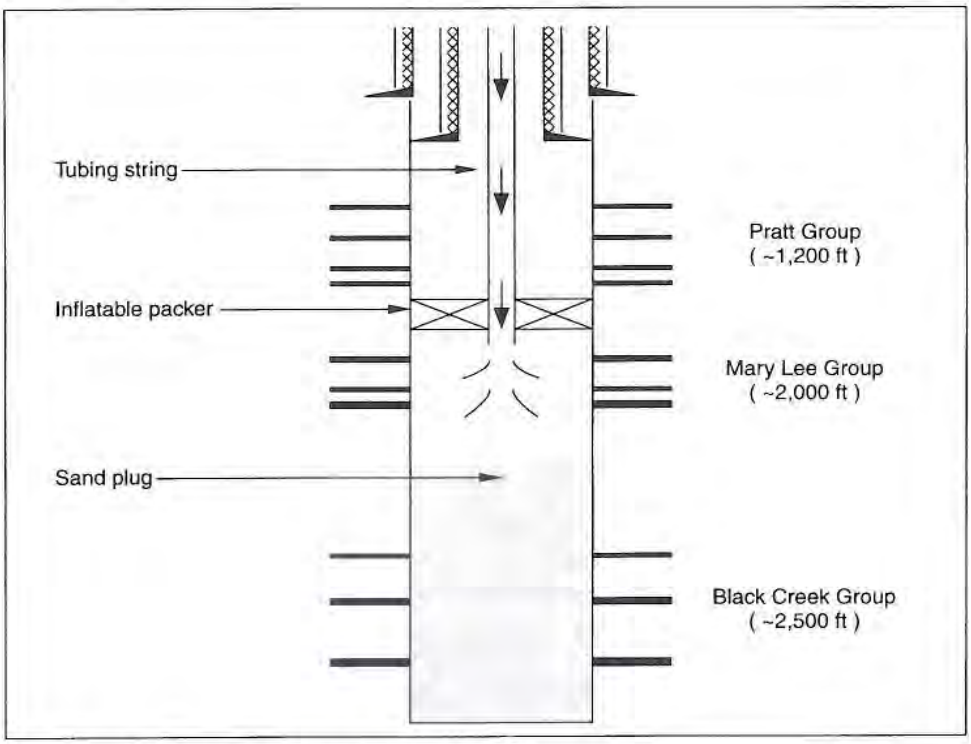

Fig. 7.1—Openhole multizone completion.[2]

Despite these secondary benefits, the time and expense of the multizone completion by open hole proved prohibitive in the Warrior basin for the multiple, thin coalseams. Openhole completions were also common in the San Juan basin where much thicker seams made the technique more practical.

7.3. Openhole Cavitation Process

7.3.1 Introduction

Reaming the coal face underneath the casing, as well as a natural cavitation phenomenon, led to the realization that great improvements in production could sometimes result in the San Juan basin if a cavity was created in the open hole and the hole was swept free of rubble. The dynamic cavity completion developed in open hole as a specialized completion method for thick, overpressured seams of high permeability in a northwest to southeast trending area, referred to as the fairway, along the Colorado/New Mexico border of the basin.

Therefore, completions in the thick seams of the San Juan basin have evolved into two schools: openhole cavity completions and cased-hole perforated completions with fracturing.

The cavity completion method grew rapidly after prolific production was reported by Meridian in 1986, and within a few years almost 1,000 such completions had been made. In these wells of the fairway of the northwest San Juan basin, cavity completions may produce at six times (or more) of the rate of fractured wells in the area.[5] Outside the fairway, however, the technique is not necessarily more successful than a fracturing technique.

The cavity completions of the San Juan basin act as a standard for project selection internationally, and other sites in the United States are sought for application of the process. Factors identified as contributing to success of the cavity completion include:

- Thick seams.
- Good permeability.
- Extensive cleating.
- Ranks of coal beyond the coalification break.
- Low ash content.
- Overpressuring.
- High in-situ stress.

The procedure has been successfully applied in 30- to 80-ft thick seams of coal of at least high-volatile A bituminous rank. Good permeabilities are present (22 md); third and fourth order cleats are present and the cleats are closely spaced. A 30% overpressuring has been reported in areas of successful applications.[6] Only a small part of the success of a cavity completion comes from the reduction in skin factor at the wellbore[7] or the effective enlargement of the wellbore.[8]

To explain the mechanism of the dynamic cavity effect on production, Weida[7] modeled the interactions of in-situ stresses, coal's bulk mechanical properties, and cavity dimensions. The results were stress-relaxed and stress-altered regions of exceptional permeability emanating from the cavity elliptically to intersect naturally occurring fractures and to effectively connect the formation cleat network to the wellbore. In the model of Weida, high natural permeabilities of the formation are symptomatic of a high-order cleat system that reduces mechanical properties of the coal for the process to be successful; thick seams result in longer stress-relaxed regions of enhanced permeability. A threshold value of minimum in-situ stress was suggested for the cavity mechanism to be effective.

There are some negative aspects of the fracturing process in the San Juan fairway that make the cavity completion excel in comparison, including the following.

- Fracturing may cause near-wellbore damage where fines collect around the wellbore to hinder gas flow. The hvAb to mvb coals are most susceptible to fines generation. (Fines may accumulate in the cavity without immediate effect. Near the wellbore, the cavity creates a repository where fines can accumulate without deleterious effects on production.)
- The closely spaced primary, secondary, and tertiary cleats are susceptible to fracturing fluid infiltration and damage.
- A fracture is apt to follow the trend of the face cleat, to increase the stress of adjacent coal, and to close the parallel face cleats in the low-modulus coal. This forces the flow of gas through the butt cleats of lower permeability. For maximum gas production, flow should be directed through the face cleats.

Although costly, holes already cased may be recompleted with a cavity-type completion or converted from a cased and hydraulically-fractured well to an openhole cavity completion. By jet-milling through the casing above the

coalseam, the hole can be sidetracked and redrilled through the coal. It is then cavity completed.

As a result of cavity completing, production was increased by a factor of 7.8 in 7-ft seams at 3,396 ft and 14-ft seams at 3,417-ft depths in the South Shale Ridge #11-15 well of Conquest Oil Company.[9] In a computer simulation of the operation, Weida[7] predicted a stress relaxation region of enhanced permeability extending 10.8 ft from the cavity in the 7-ft seam and 23.1 ft from the cavity in the 14-ft seam; these extended regions are postulated to have intersected natural fractures to increase production.

Different field procedures for the cavitation process have been investigated and will be discussed in the following sections.

7.3.2 Case Study: Cavitation Research Project

Using two producing wells and three observation wells, Amoco, the Gas Research Institute, and Resource Enterprises Inc. (REI) evaluated the cavitational technique in the fairway region of the San Juan basin near the Colorado and New Mexico border.[10] The original reservoir permeability was 22.5 md. Table 7.1 gives average characteristics of the wellsite.

Table 7.1—Average Reservoir Properties[10]

Depth, Top of Coal (ft)	3,150
Coal Thickness (ft)	47
Gas Content (scf/ton)	553
Ash Content (%)	30%
Langmuir Volume, Ash-free (scf/ton)	1,118
Langmuir Pressure (psia)	606
Sorption Time (hr)	4.1
Coal Density (g/cc)	1.50
Temperature (°F)	120
Initial Pressure (psia)	1,525
Permeability, Horizontal (md)	22.5

A flow diagram of the surface facilities used in the test well is presented in Fig. 7.2.[11]

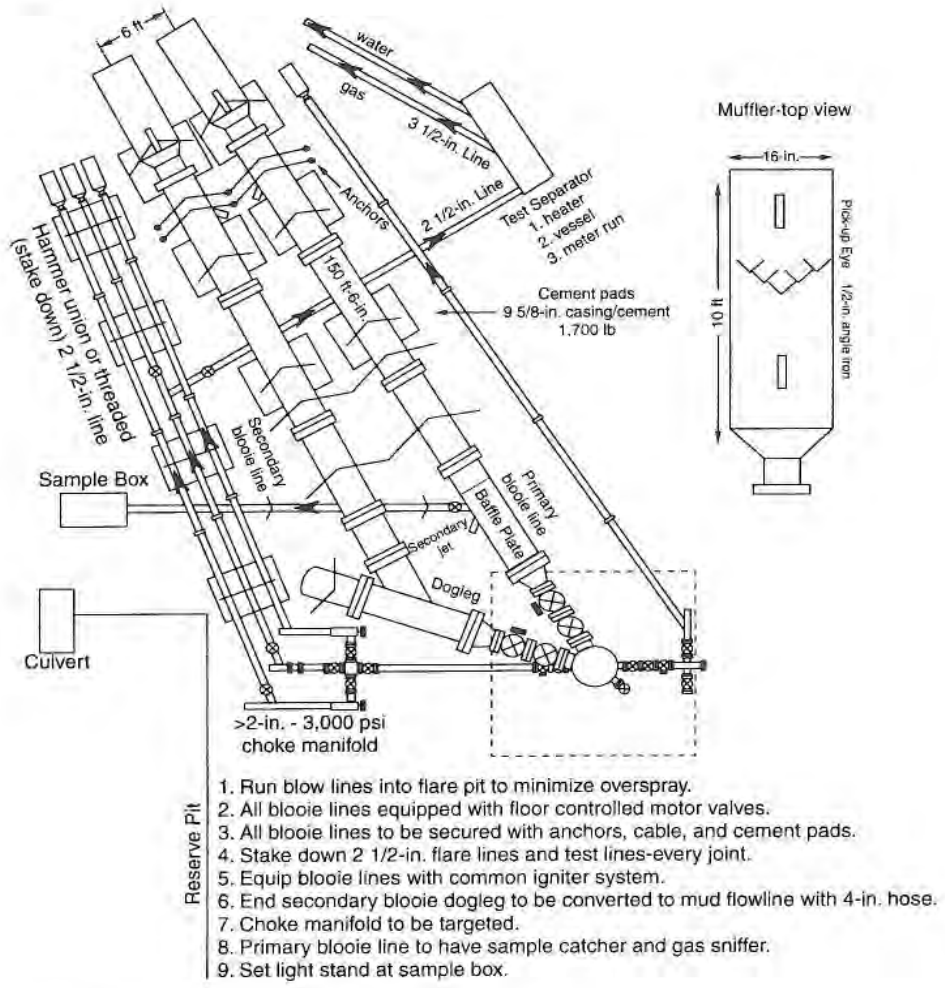

Fig. 7.2—Flow diagram of surface facilities.[11]

After drilling through the Fruitland coal, cavities were established by REI in the test well by injection cavitation, a process inducing sloughing of coal into the wellbore by pressure cycles, in which the following steps were taken in each cycle:

1. Pull drillpipe and bit into the casing above the open hole.
2. Close pipe rams around the drillpipe, sealing the annulus.
3. Close hydraulically operated valves in the blooie lines to give complete pressure sealing.
4. Inject 25 bbl water and follow with 2,625 scfm of air (approximately 10% of the rate to fracture[12]) through the drillpipe until 1,350 psig is reached.
5. Open the blooie lines. Allow the hole to blowout into the flare pit.

The cavitation cycles were continued by the consortium as reported by Mavor and McBane[10] through 9 days. Cost was estimated at $10,000 per day.

Elsewhere, a jetting tool to facilitate a cavity formation has been used in the Piceance basin. Consequently, the production rate of methane increased from 22 to 108 Mcf/D.[5] Permeability in the butt-cleat direction was 9–13 md and in the face-cleat direction 23.5–25.0 md.

Natural cavitation is the process of coal sloughing into the wellbore by release of natural in-situ stresses. The controlled blowout in the process comes from formation pressure buildup rather than injected air. A natural cavitation process was evaluated by Mavor and McBane in a test hole where the following steps were taken:[10]

1. Pull drillbit into casing.
2. Seal annulus with pipe rams.
3. Close hydraulic valves of blooie lines.
4. Allow surface pressure to increase to 500 psig (approximately 30 minutes).
5. Open valves; let well blow out into flare pit.

The steps are similar to the injection cavitation except there is no injection of water or air.

The sequence of steps was repeated 29 times. After production flow tests, the 60-mesh to 1/4-in. particles that had entered the cavity during flow periods were removed. Water and air were circulated through the drillpipe at total depth to remove the debris.

During the eighth day of cavitation cycling after about 15 injection cavitations and natural cavitations, a breakthrough was achieved.[10] Not only did the test gas flow reach a maximum at that time, but the pressure of an observation well 176 ft away was substantially affected. A production profile as a function of number of cycles is given in Fig. 7.3 that illustrates when additional cycles gave no more improvement in production.

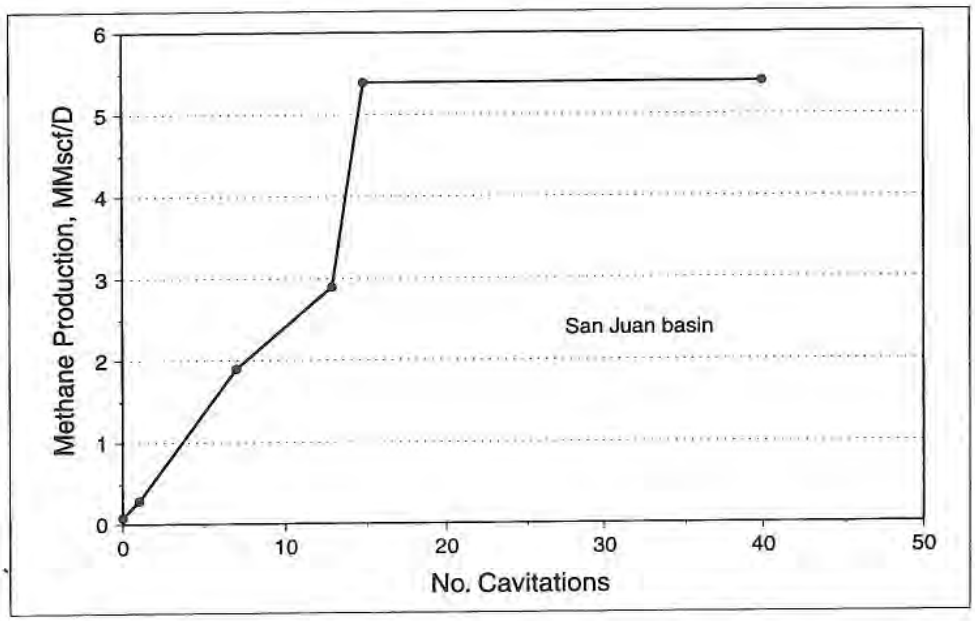

Fig. 7.3—Cavity cycles at Amoco test site.[11]

7.3.3 Case Study: Devon Cavity Process

In the fairway of the San Juan basin, 50 miles east of Farmington, New Mexico, and 50 miles south of the Fruitland coal outcrops at Durango, Colorado, 102 wells were drilled by Devon on 320-acre spacing and completed by the openhole cavity method.[13] The cost of creating the cavities was $180,000 per well and required 8–14 days to accomplish.

Although the maximum burial at one time was 8,800 ft, coal in the unit is now at 3,000 ft. Overpressured by 30%, the high-volatile bituminous coals average a seam thickness in the region of 50 ft; maximum thickness reaches 80 ft.

A sketch of the cavity completion technique as practiced by Devon at this location is presented in Fig. 7.4. An uncemented, perforated liner was run to total depth where the perforations were kept clear of fines buildup by circulating fresh water or, as a last resort, by pulling the liner.

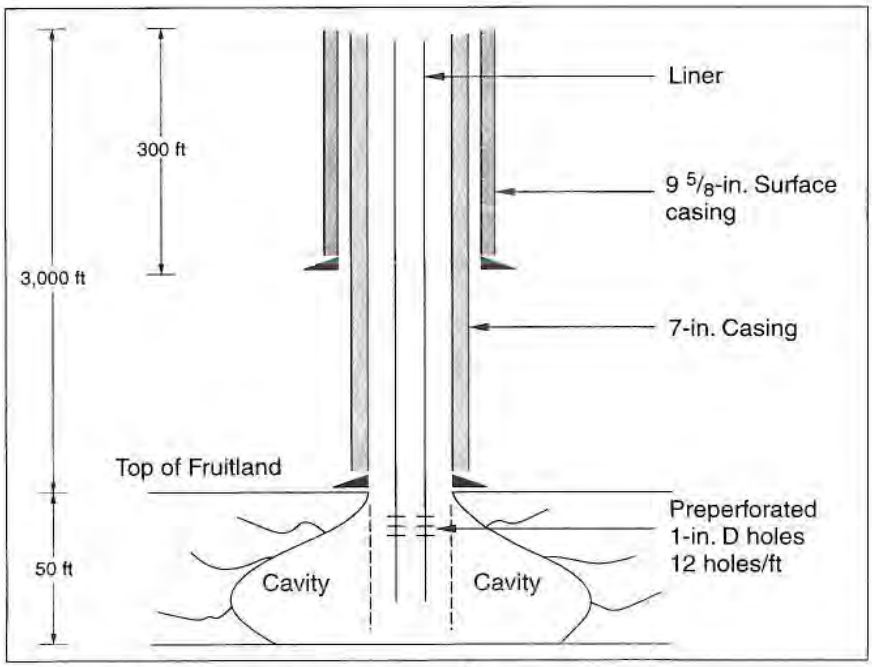

Fig. 7.4—Openhole cavity completion.[13]

From a horizontal distance of 0.2–0.4 miles away, wells were drilled directionally in an S-shaped hole to a destination under Navajo Lake to minimize the environmental impact.[12]

The openhole section completed in the coal was kept vertical since shale stringers that do not cavitate would otherwise have restricted pipe placement.[13] Four such wells were drilled to a depth of 2,000 ft underneath the lake and subsequently tested at a total rate of 35.3 MMcf/D.

A direct comparison between fracturing and cavity methods is possible here, as Devon replaced 10 fractured wells with nearby cavity completions, which gave 6.7 times as much stabilized gas flow as the initial rate of the fractured wells.[14] An even greater contrast of initial flow ratio existed in a 21:1 ratio of initial cavity rates to the initial fracture rates.

The cavity dimension from a sonar probe agrees with the cavity size calculated by Mavor from a material balance on solids collected at the surface[14] (see Fig. 7.5). The sonar probe gives a profile of the cavity in which fingerlike shale remains in the 8-ft diameter cavern. The gamma ray and density logs verify the sonar evaluation.

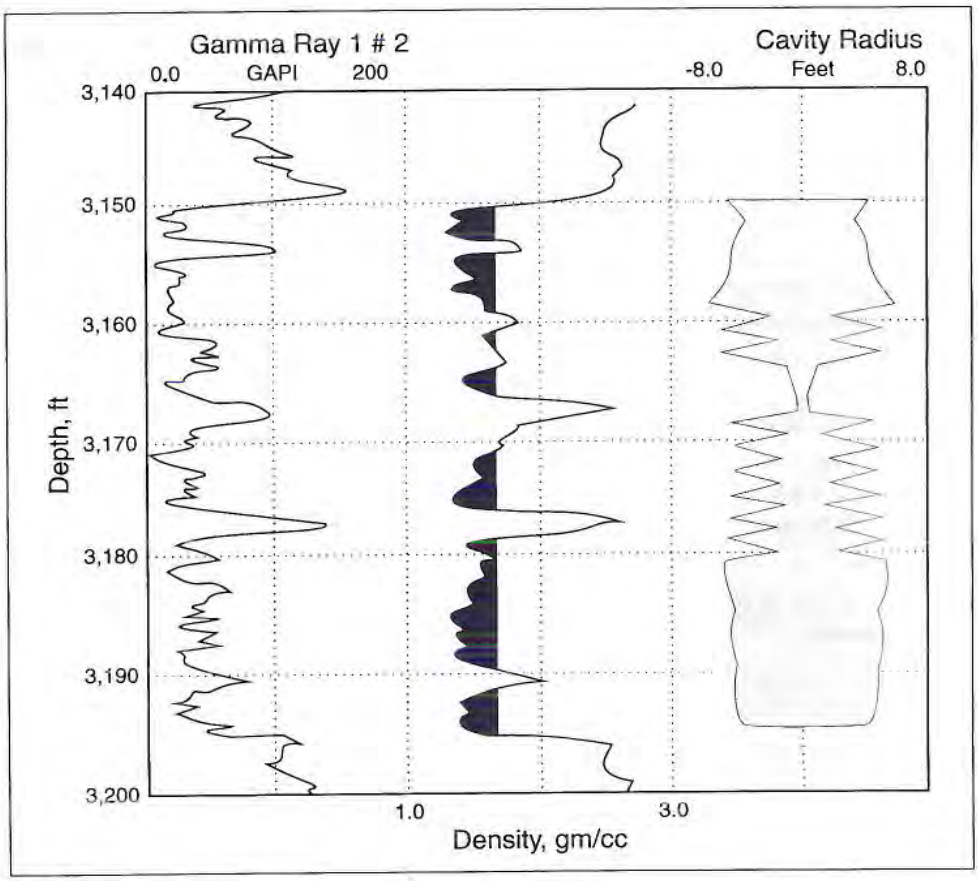

Fig. 7.5—Sonar probe of cavity.[15]

The diameter of the cavity should be 6–8 ft; a larger cavity provides only limited improvement of production rate.[5]

7.4 Cased-Hole Completions

7.4.1 Conditions for Cased Hole

Characteristics of multiple groups of coals with thin seams in the Warrior basin are typical of the other coals in the eastern United States. Completions in the Warrior serve as models for these other thin seams in Appalachia, and they may serve as models for completions of multiple, thin seams in basins around the world. Completion of these multiple seams must be done as cheaply as possible. The seams in a typical Warrior well may consist of the Pratt, Mary Lee/Blue Creek, and Black Creek coals. The shallow Pratt group has relatively high permeability and low gas content, the intermediate Mary Lee is the primary target from which most of the production comes, and the deep Black Creek seams have high gas content but low permeability.

The generalized configuration of the borehole and casing through the three coal groups before entry is made to the formation by slots or perforations is given in Fig. 7.6. The diagram refers to the experimental P2 well at the Rock Creek research site.[16] Note the 5 1/2-in. diameter casing in the 7 7/8-in. diameter hole established from surface into a sump below the lowermost seam.

Many completion techniques have been used throughout the Warrior basin. Influencing their choice are the following:

- Multiple seams per well.
- Thin seams of inches to a few feet thick.
- Marginal economics for producing.
- Large volumes of water produced early in the life.
- Normally pressured (some underpressured).
- Depth (1,000–4,500 ft).
- Coal fines.
- Optimum coal rank, hvAb-lvb.
- Good permeability.

Conditions usually combine to require a cased hole with access to the seams that allows maximum control of fracturing. Economics requires simplicity.

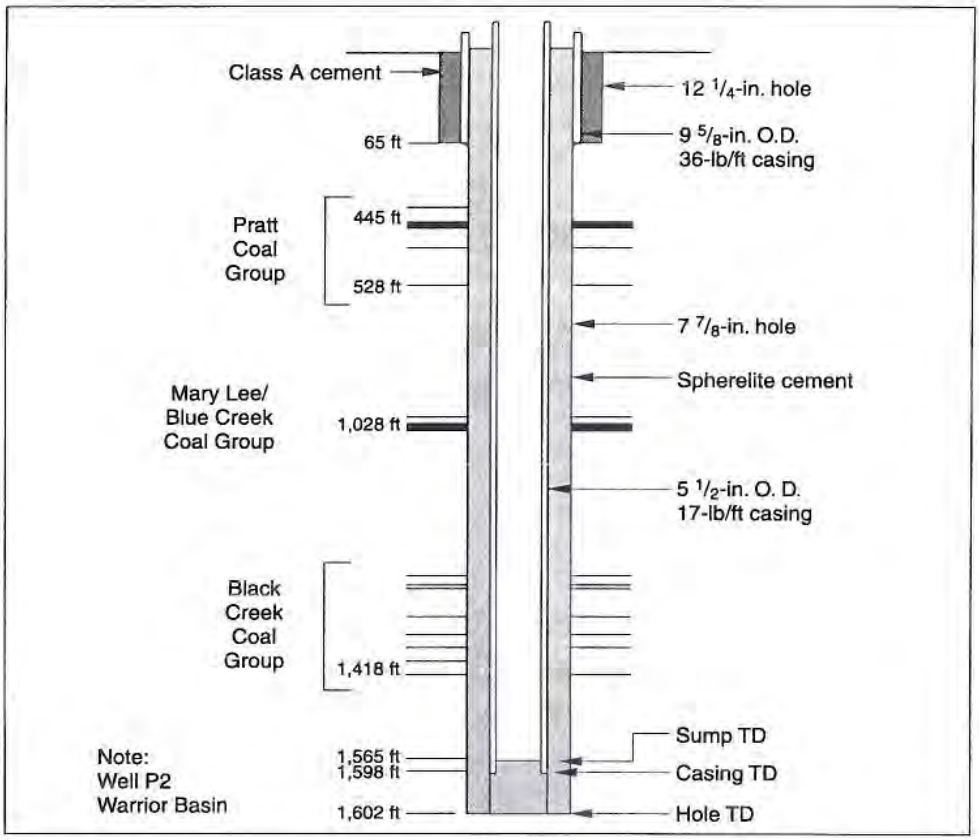

Fig. 7.6—Generalized diagram of cased hole at Rock Creek prior to seam entry.[16]

7.4.2 Access by Slotting

The slotted-casing technique was introduced to correct problems with fracturing control and fines control in openhole completions while retaining the best

attributes of the openhole completions used early in the development of the Warrior basin. The concept aims to retain a large area open to the face of the coal while providing a means to isolate each zone and control fracturing fluid entry more easily.

The procedure involves drilling and cementing casing through the coal intervals. A jetting tool is attached to the end of the tubing string, and slots are cut through the casing and cement with high velocity streams of an abrasive water-sand solution.

A sketch of the slotting tool is presented in Fig. 7.7. A high-velocity high-pressure water and sand fluid (4 bbl/min) is pumped through a 3/16-in. diameter tool to impinge on the casing; two nozzles are set 180° apart. The tool is cyclically lowered and raised to create slots approximately 48-in. long by a maximum of 1.4-in. wide.[17]

During the slotting operations, sand control in the carrier fluid, orientation of the tool, and overcutting prolong slotting times and increase costs. Overcutting is especially troublesome because early breakthrough at some point on the casing traverse will expose the coal to the high-pressure jet. The result can be small-scale fracturing that affects any subsequent permeability tests of the formation.

Slotted casing prevents fines and spallings from plugging access as in perforations.

Unfortunately, the problems associated with the slotting technique overshadow the advantages.[2]

1. Placing and orienting the cutting jet are difficult.
2. Slots weaken the casing and make it susceptible to failure during fracturing.
3. Additional time to perform the slotting operation adds to the cost.

The additional cost of slotting limits its use to those wells used for injection and falloff tests, where it is useful because of the slot's large entry area and lack of plugging.

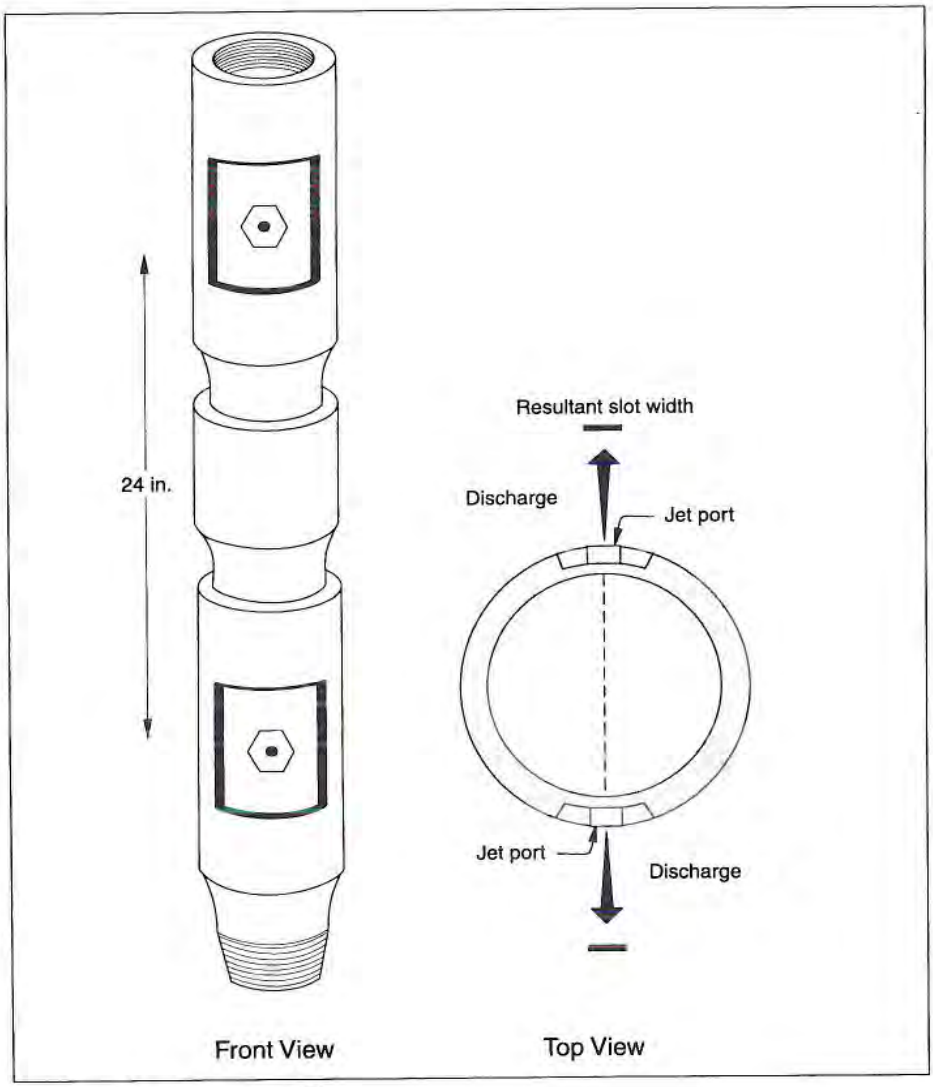

Fig. 7.7—Jet slotting tool.[17]

7.4.3 Access by Perforating

After the slotting attempts, a more conventional approach was taken. Casing was set to total depth, and a sand plug was placed successively below each zone before perforating at four shots per foot and fracturing above the sand. Although additional time was required to clean sand from the hole, completion times were reduced from 2 weeks to about 2 days, and the completion was for all of the coalseams present.[11]

Perforating is inexpensive compared to slotting. Schraufnagel and Lambert estimate an 80% greater cost for slots to give access to an equivalent section.[18] Perforating as the conventional method of accessing the formation has the following advantages:

- Inexpensive.
- Versatile.
- Selective stimulations.
- Formation stability around borehole; reduction of fines.
- Routine operation understood and performable by workers in the field.
- A repeatable process, applicable to large-scale field development.

A difficulty with perforating is the plugging of the perforations with coal fines and chips. It is especially troublesome if casing strength is inadequate to accommodate high fracturing initiation pressures in coals. Disadvantages may be summarized as follows:

- Greater costs for casing to total depth.
- Plugging of perforations.
- Danger of formation damage.

Despite the drawbacks, perforating cased holes has developed into the preferred method of accessing the coalseams in the eastern U.S. basins (Fig. 7.8). The preferred procedure is to cement casing to total depth followed by successively perforating and fracturing each zone up the hole. After a lower zone has been treated, a wireline bridge plug is set to isolate the zone above. The procedure allows completing two or three zones per day—a much faster procedure than openhole or slotting methods.[19]

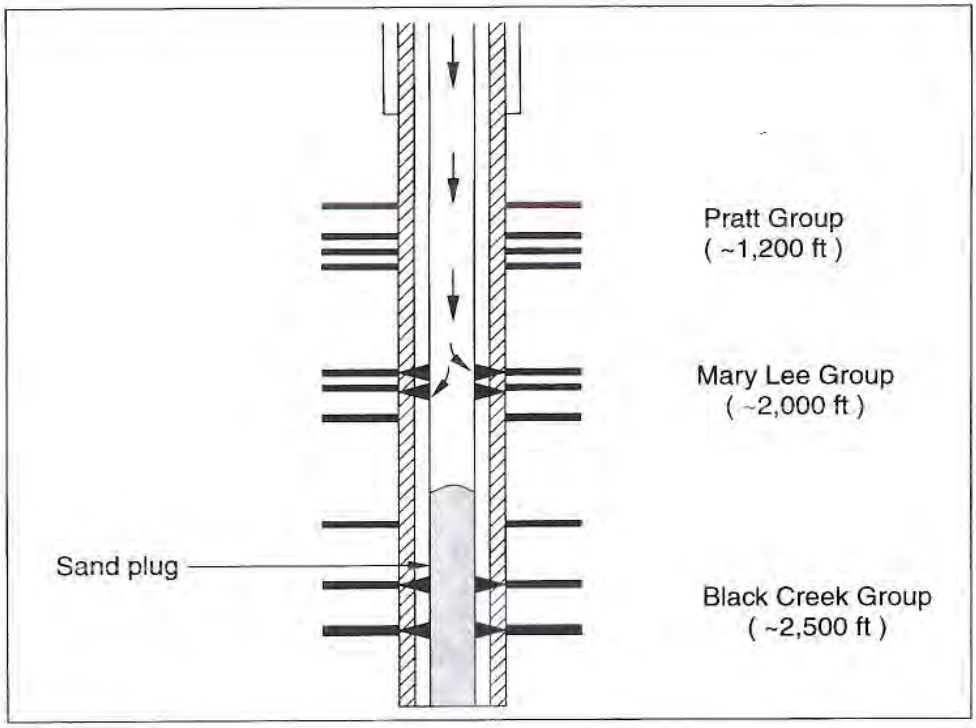

Fig. 7.8—Perforated multizone completions.[2]

7.5 Multizone Entry in Cased Hole

7.5.1 Baffled Entry

In the baffled fracturing technique, baffle plates are placed on the casing before installing and cementing the casing for locations between coal groups that are to be individually fractured. The upper baffle is a template that will pass a larger ball than the lower baffle. A sketch of the process is given in Fig. 7.9 where the placement of baffles and the relative size of the balls are indicated.[16,20]

From Fig. 7.9 it is seen that after perforating and fracturing the Black Creek, a sealing ball was dropped into place to isolate the Black Creek, whereupon the Mary Lee group was perforated and fractured. Finally, the Pratt group was isolated with a sealing ball, perforated, and fractured. In such manner, multiple zones can be treated in 1 day.

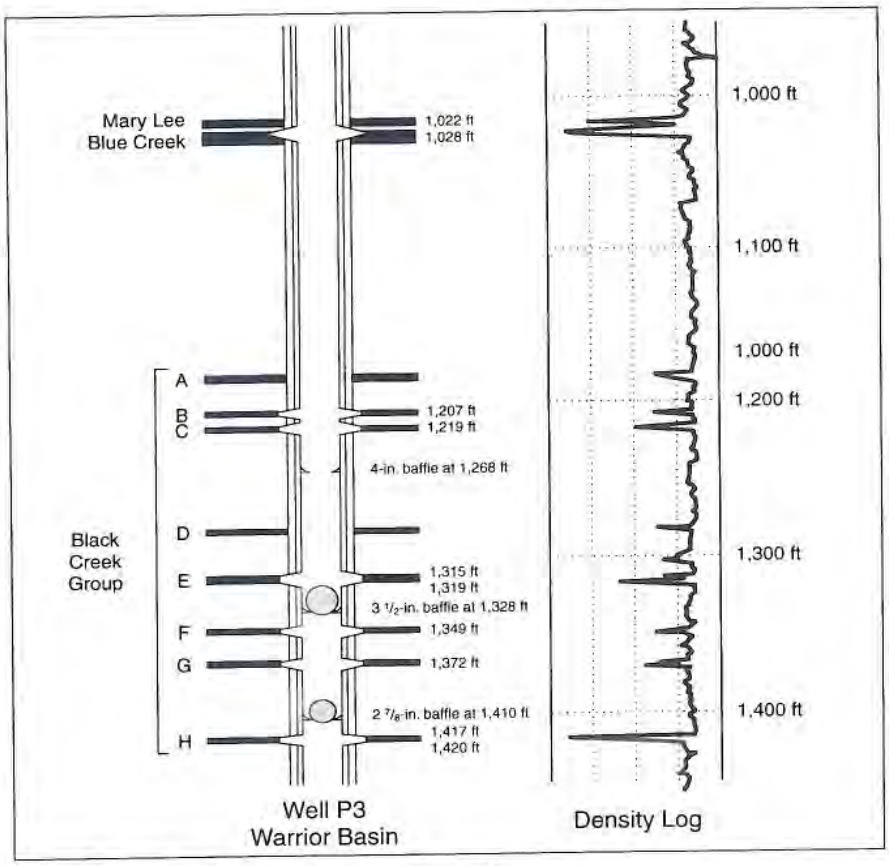

Fig. 7.9—Baffled fracturing technique.[20]

At the experimental P3 well at the Rock Creek research site in the Warrior basin, the Gas Research Institute fractured eight seams of the Black Creek group, which

contain 12 net feet of coals in four stages using three sets of baffles preset on the 5 1/2-in. casing. Fig. 7.10 shows their casing configuration with the three sets of baffles of 4 in., 3 1/2 in., and 2 7/8 in. and with decreasing diameters proceeding down the hole.[20]

Taurus and GRI developed a sequence of operations for baffled entry that goes as follows:

1. Perforate and fracture bottom seam at eight shots per ft. Drop ball to 2 7/8-in. baffle to seal off bottom seam.
2. Perforate the target seam directly above. Stimulate. Drop ball to 3 1/2-in. baffle.
3. Continue the procedure uphole until all seams are treated.

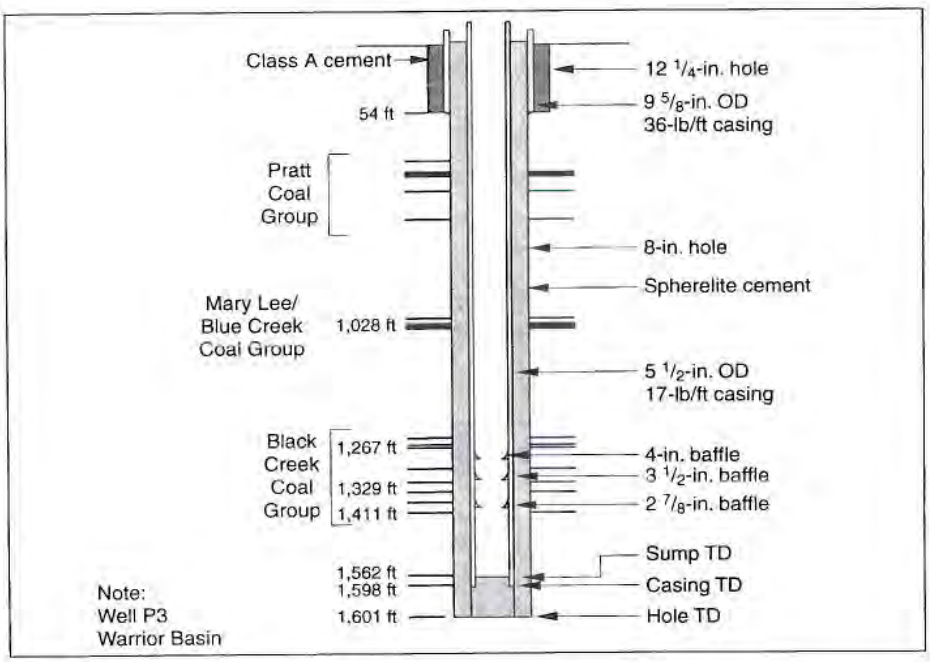

Fig. 7.10—Use of baffles to fracture multiple seams.[16]

7.5.2 Frac Plug Entry

Frac plugs originated from the desire of the operator to individually treat different zones after the casing had already been cemented in place. With the benefits seen in the baffled fracturing technique, frac plugs allowed the operator to set a plug-type tool on electric wireline in the casing after perforating a zone above (Fig. 7.11 shows a composite bridge plug).

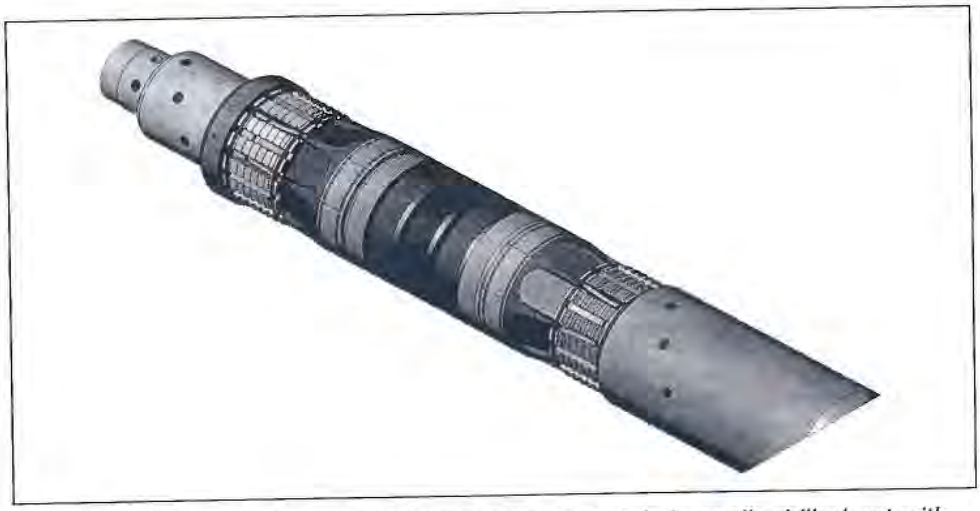

Fig. 7.11—A bridge plug made of composite materials is easily drilled out with conventional bits.

A frac plug is hollow through the center. A ball, much like that used in the baffle technique, could be dropped or placed in the top of the tool to allow shutoff of the casing (below) when initiation of the next frac stage (above) has commenced. Any number of plugs could be set coming out of the hole to allow for individual staging of treatments. While the frac plugs cost more than the baffle and ball combination, no restrictions for the perforators meant normal casing guns could be used in a pressurized well under lubricator. This allowed for better perforations and reduced breakdown pressures. One drawback of the steel frac plugs was the removal time. Use of two or three steel frac plugs led to lengthy

drillouts as the top tool would partially drill up, then fall down on the next plug and spin, preventing timely removal. It was not uncommon for an operator to take 7–10 days to remove the steel frac plugs. Steel frac plugs also meant that a large amount of iron debris would settle to the bottom of the well.

In 1997, Halliburton introduced a composite frac plug that would enable multiple plugs to be set in the hole for stage completions and easy removal via drillout in a single day. Composite plugs consist of composite material and rubber elements that contain minimal metal content. During the drilling operation of a composite frac plug, the composite material drills up and will float out with the return fluids because it is lighter than water. Drilling time for a plug using the recommended weight and drill bit averages 30 minutes. This saves rig time and reduces casing damage caused by a long drillout. The design of the lower shoe on the tool prevents spinning of the upper tool remnants after they drop onto the next tool. Improved efficiency of completions in CBM was noted by Guoynes, *et al.*[21]

7.5.3 Partings Entry

Thin seams of the Warrior basin and Appalachian coals are often marginally economical to develop because of the expense of completing and gaining access to multiple seams. For example, the Mary Lee group may be the most prolific producer, but the low-permeability Black Creek group below may have the potential of adding substantial gas flow from the same well. Similarly, the shallow Pratt group above the Mary Lee may have potential for the same well. The problem becomes one of tapping the reserves of the secondary seams to supplement the flow from the Mary Lee but doing so at acceptable incremental rates of return for the investment. The problem was addressed at the GRI field research site at Rock Creek in the Oak Grove Field of the Warrior basin.[22]

A single entry into the bottom of the Black Creek group was made with the goal of propagating a vertical fracture through the seven seams dispersed over a 250-ft interval as depicted by Spafford[22] in Fig. 7.12.

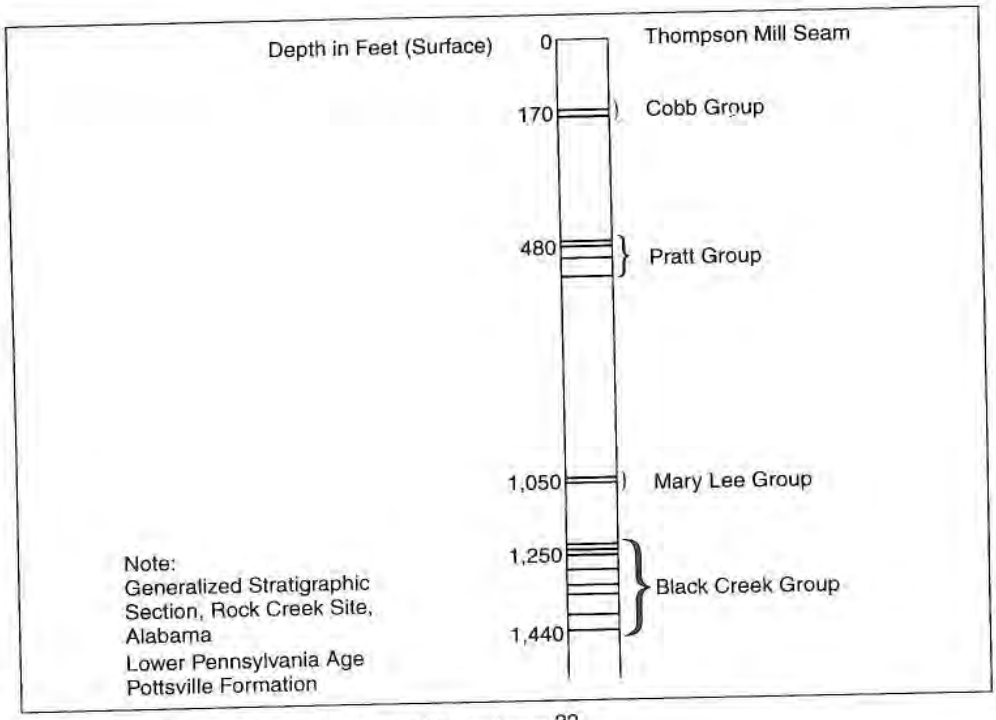

Fig. 7.12—Rock Creek stratigraphic column.[22]

Such a procedure is dependent upon having stress data on the coal and surrounding rock; it depends on a favorable minimum horizontal stress profile that would give assurances of fracture containment. Stresses in the formation at Rock Creek are presented in Fig. 7.13. Vertical growth downward of a fracture would appear to be limited to the bottom of the Black Creek coal group by high stresses located at 1,440 ft.[23] There would be the hope of encompassing all eight seams of the Black Creek group in one fracture initiated at an entry near the bottom of the coal group but above the stress barrier.

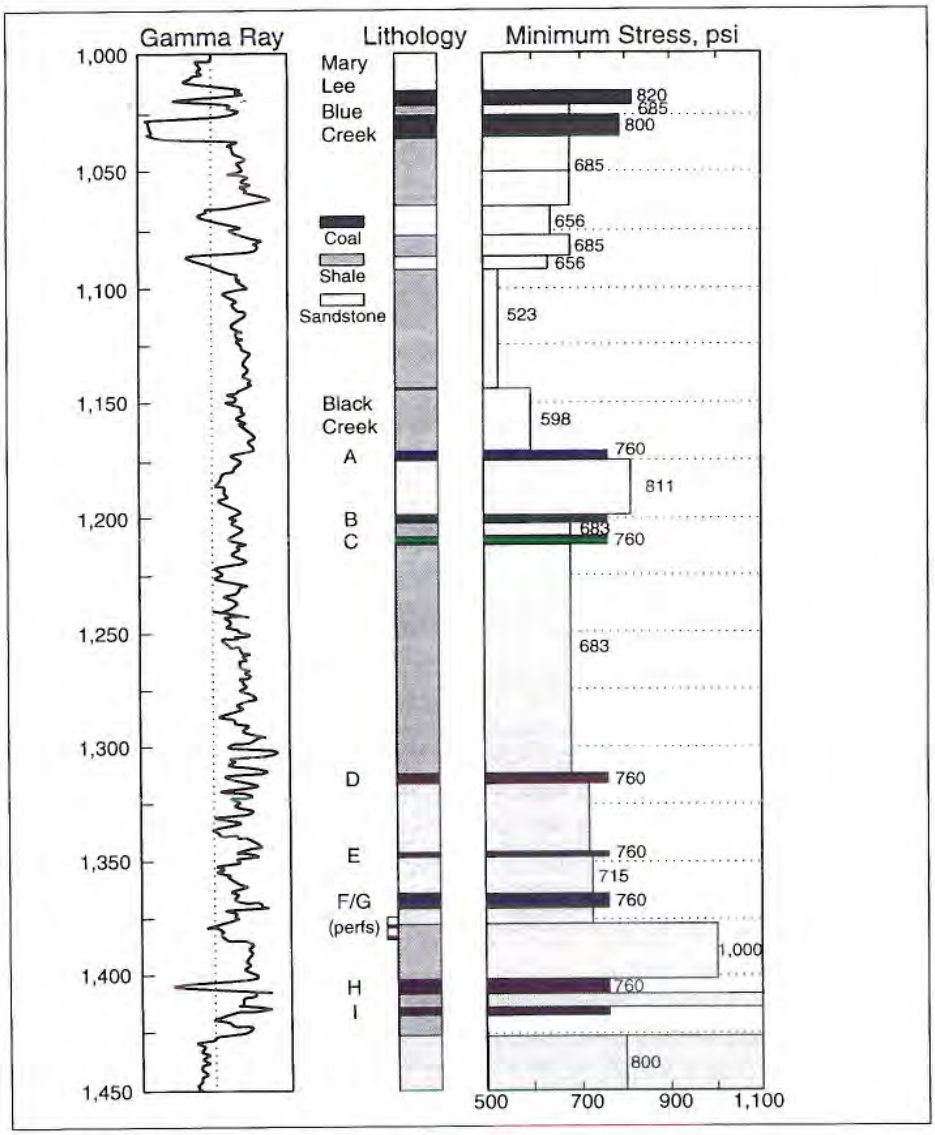

Fig. 7.13—Stress profile at Rock Creek.[23]

The hypothesis was evaluated by Schraufnagel, Spafford, and Saulsberry.[24] Consequently, perforations were made in the lower seam in a control well and in the rock parting between G and H seams on another well with the expectation of a fracture in each well encompassing the area of Fig. 7.14. Fracturing with a crosslinked gel resulted in a single, vertical fracture through the eight Black Creek seams. As expected, the fracture was limited in downward growth by a high stress. A water tracer dye later showed the fracture to have penetrated the Mary Lee group also.

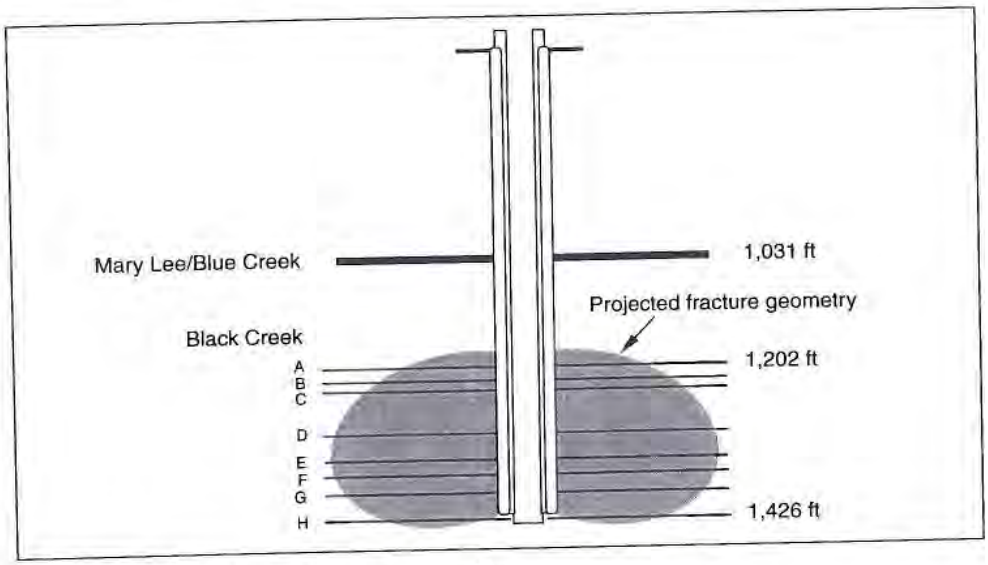

Fig. 7.14—Desired fracture geometry.[24]

Perforating and gaining access to the formation through the adjacent inorganic rock reduces generation of fines at the point of fracture initiation that would occur from bursting of the coal. When producing water and gas, fines generated from the eroding of coal at high fluid velocity near the wellbore are reduced, and additional fines are collected in the partings segment of the fracture before reaching the wellbore. Multiple, parallel fractures occurring at higher pressures that might occur in coal are avoided.

However, when accessing the formation through noncoal partings, there is the possibility of communicating with adjacent sands that could create questionable production to qualify for the Section 29 tax credit. Unless the stress profile of the formation is certain, the operator will not have the confidence of containing the fracture or of connecting all of the seams to the wellbore. Finally, shales adjacent to the coals may not offer a medium in which to generate and to maintain a conductive fracture.

Spafford[22] reported positive results at Rock Creek. Fines gave fewer problems than usual; a sucker rod pump for water removal was maintenance-free for 1 year as compared to ordinarily being down three to four times per year for maintenance. There was evidence that the fracture connected all eight Black Creek seams to the wellbore, and the fracture was contained by high stress below the coal group.[22]

7.5.4 Coiled Tubing and Packer Completions

Advances in the use of large-bore coiled tubing (CT) strings, 2 3/8- to 2 7/8-in. diameter, in conjunction with development of a unique bottomhole packer assembly (BHPA, Fig. 7.15) finally enable the stimulation engineer to isolate and treat as many coalseams as required on an individual basis with one trip to the well. Pinpoint placement of treatments can be tailored for each coalseam based on conductivity requirements. An integrated CT rig (Fig. 7.16) allows the operation to proceed in a safe, timely, and economical manner that was impossible to repeat with prior completion methods.

Rodvelt, *et al.*[25] used a 2 3/8-in. CT string and proprietary BHPA to fracture-treat as many as 19 stages (21 coalseams) in a CBM pilot in Buchanan County, Virginia. This project used 70-quality nitrogen foam to place proppant in each stage at an average rate of 8 bbl/min and 4,000 psi.

Fig. 7.15—Bottomhole packer assembly.

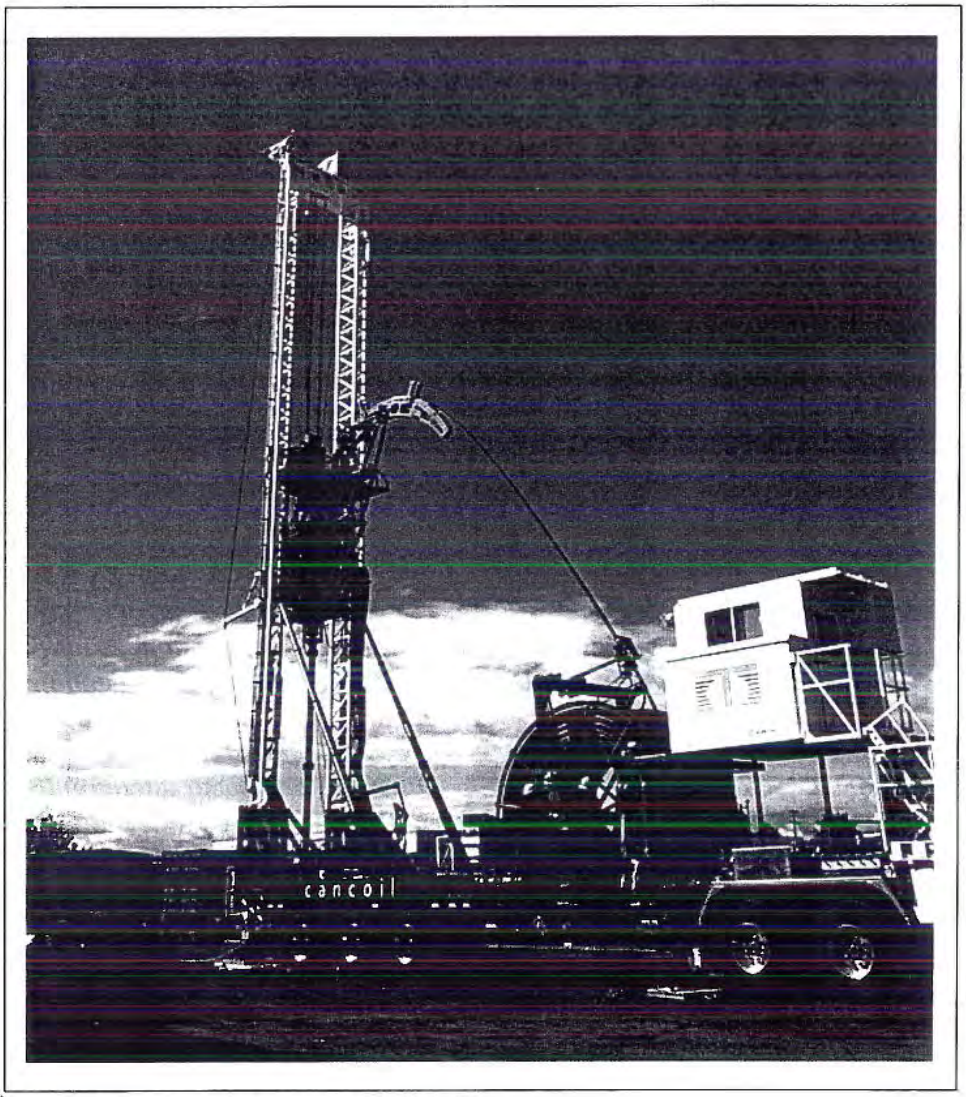

Fig. 7.16—Integrated coiled-tubing rig.[25]

The operation consists of perforating all prospective intervals in the well in 1 or 2 days before the fracturing equipment arrives on the well site. An integrated CT rig picks up the BHPA and trips into the well to a known depth on bottom. The BHPA is then positioned across the lowest, prospective coalseam with the bottom packer approximately 24 in. below the bottom perforation. CT movement sets the lower packer, and circulation is begun through the annulus past the upper cups and back up the coil string. Once the hole is circulated clean, a new stage is begun down the CT. At the completion of the treatment stage, the pressure is equalized across the BHPA, which is then moved to the next upward zone. After the BHPA is positioned and set, the hole is circulated clean and the next stage started. In the event of a screenout, the BHPA is moved, reset, and the hole circulated clean. If communication between treatment perforations and the next upward perforations is observed, the treatment is moved to the next upward zone and restarted; additional treatment volume can be added to this stage to account for the communicated zone.

CT fracturing has been used with foamed fluids, crosslinked fluids, and commingled gas-fluid systems. Other benefits of CT and the BHPA include reduction of screenouts, less environmental impact, and fewer pieces of fracturing equipment to achieve the same outcome. At the end of fracturing the upper-most interval, the BHPA can be withdrawn from the well and a CT cleanout performed. No baffles, plugs, or sand-fill remain to hinder placing the well on production. Negatives include higher treatment pressures (friction through coil) and limited rates and proppant concentrations through the coil string.

Jetting through the casing to allow entry to the coalseam has been discussed previously (7.4.2). Advances in jet technology coupled with CT provide a method of completing multiple intervals at the speed and versatility of coil. Benefits over the CT and packer (CTP) technique allow for maximum injection rate, maximum proppant volume, and maximum proppant concentration according to formation need. This completion technique allows the operator to perforate and fracture-treat a well during the same trip into the hole with the speed and versatility of coiled tubing.

The process entails pumping through a CT string using a proprietary jet (Fig. 7.17) to create perforations and to initiate fractures (Fig. 7.18).[26] Fracture extension and placement is done via the CT/casing annulus. At the completion of the treatment, a sand plug is placed to pack the perforations and provide isolation for the next stage. At the completion of pumping, the jet tool is raised through the sand plug to clear the pipe. The casing is then reverse-cleaned as the CT is lowered to spot the jet for the next interval treatment (Fig. 7.19). Once all prospective coals have been stimulated, the jet tool can be removed and coil run back to bottom to clean the casing to bottom. As with the CTP method, no baffles, plugs, or sand-fill remain to hinder placing the well on production.

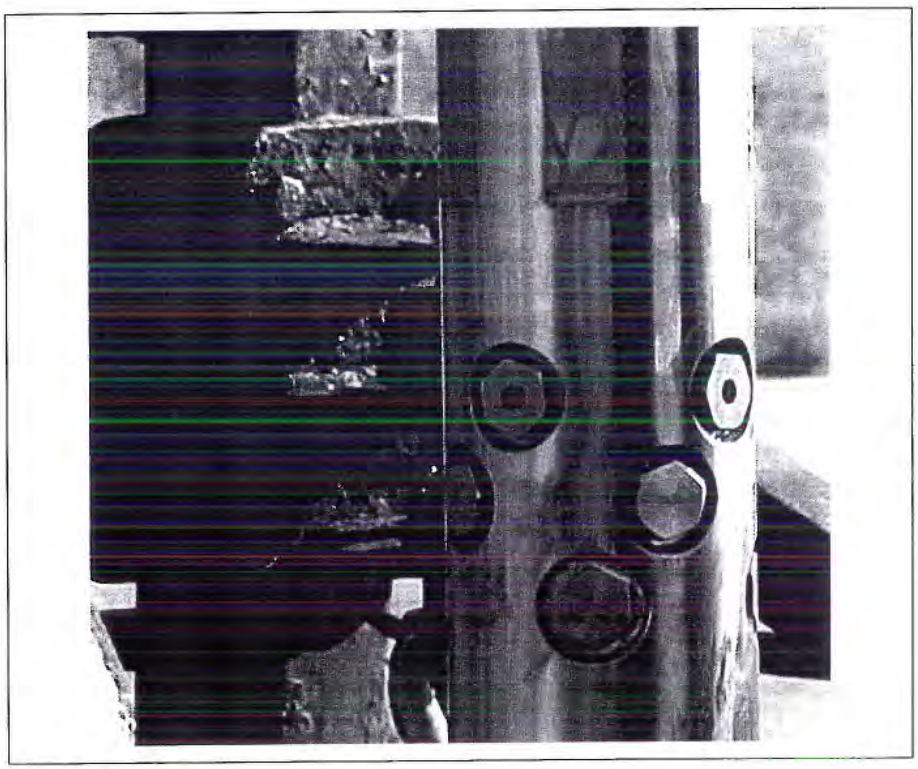

Fig. 7.17—Jet-perforation nozzles.

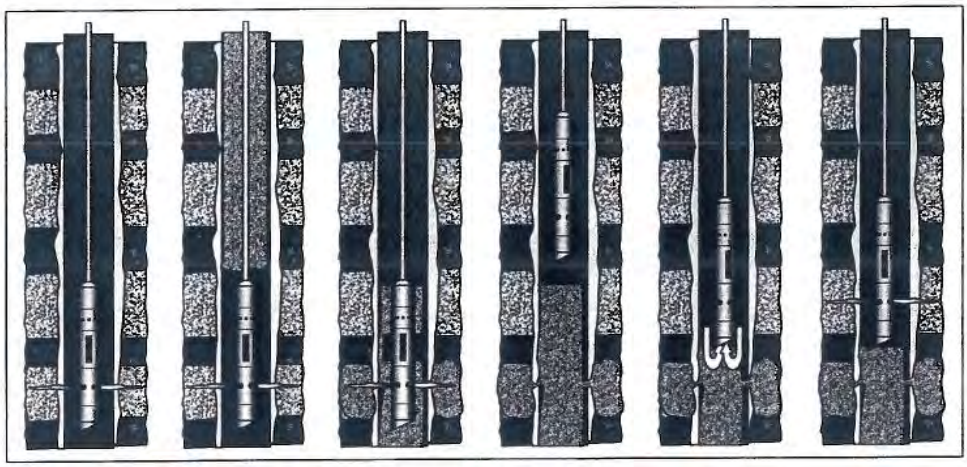

Fig. 7.18—CT string performing jet perforation and initiating fractures.

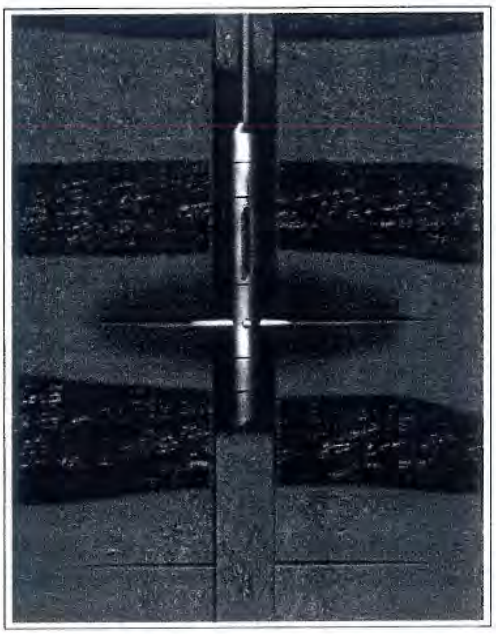

Fig. 7.19—Jet-perforating tool being lowered into the next interval to be treated.

References

[1]Holditch, S.A.: "Completion Methods in Coalseam Reservoirs," paper SPE 20670 presented at the 1990 SPE Annual Technical Conference and Exhibition, New Orleans, Louisiana, 23-26 September.

[2]Lambert, S.W., Niederhofer, J.D., and Reeves, S.R.: "Multiple-Coal-Seam Well Completions in the Deerlick Creek Field," *JPT* (November 1990) 42, No. 11, 1360-1363.

[3]Lambert, S.W. and Graves, S.L.: "Production Strategy Developed," *Oil & Gas J.* (November 1989) 87, No. 47, 55-56.

[4]Hunt, A.M. and Steele, D.J.: "Coalbed Methane Development in the Appalachian Basin," *Quarterly Review of Methane from Coalseams Technology* (July 1991) 8, No. 4, 10-19.

[5]Mavor, M.: "Cavity Completion Well Performance," paper presented at the 1992 Eastern Coalbed Methane Forum, Tuscaloosa, Alabama, 1 September.

[6]Logan, T.L.: "Western Basins Dictate Varied Operations," *Oil & Gas J.* (December 1989) 87, No. 49, 35-39.

[7]Weida, S.D.: "The Mechanics of Dynamic Cavity Completions for Coalseam Degasification Wells," MS thesis, Mississippi State U. (December 1993) 147.

[8]Mavor, M.J.: "Summary of the Completion Optimization and Assessment Laboratory Site," GRI Contract No. 5088-214-1657, Resource Enterprises, Inc. (December 1991).

[9]Close, J.C., Pratt, T.J., Logan, T.L., and Mavor, M.J.: "Summary of the Conquest Oil Company South Shale Ridge #11-15 Well, Piceance Basin, Western Colorado," GRI Contract No. 5088-214-1657, Resource Enterprises, Inc. (April 1993).

[10]Mavor, M.J. and McBane, R.A.: "Western Cretaceous Coalseam Project," *Quarterly Review of Methane from Coalseams Technology* (January 1992) 9, No. 2, 17.

[11]Mavor, M.J. and McBane, R.A.: "Western Cretaceous Coalseam Project," *Quarterly Review of Methane from Coalseams Technology* (November 1991) 9, No. 1, 19.

[12]Duckworth, J.M. and Rector, C.A.: "Devon Blends Drilling Methods in Fruitland Coal," *Western Oil World* (July 1991) 47, No. 49, 26-27.

[13]Mavor, M.J.: "Coal Gas Reservoir Cavity Completion Well Performance," paper presented at the 1992 International Gas Research Conference, Orlando, Florida, 16-19 November.

[14]Petzet, A.G.: "Devon Pressing Fruitland Coalseam Program," *Oil & Gas J.* (November 1990) 88, No. 45, 28-30.

[15]Palmer, I.D., Mavor, M.J., Seidle, J.P., Spitler, J.L., and Volz, R.F.: "Openhole Cavity Completions in Coalbed Methane Wells in the San Juan Basin," paper SPE 24906 presented at the 1992 SPE Annual Technical Conference and Exhibition, Washington, DC, 4-7 October.

[16]Schraufnagel, R.A. and Lambert, S.W.: "Multiple Coalseam Project," *Quarterly Review of Methane from Coalseams Technology* (March 1988) 5, Nos. 3 and 4, 33-44.

[17]Schraufnagel, R.A. and Lambert, S.W.: "Multiple Coalseam Project," *Quarterly Review of Methane from Coalseams Technology* (December 1987) 5, No. 2, 25-36.

[18]Schraufnagel, R.A. and Lambert, S.W.: "Multiple Coalseam Project," *Quarterly Review of Methane from Coalseams Technology* (November 1988) 6, No. 2, 27-34.

[19]Zebrowitz, M. and Thomas, B.A.: "Coalbed Stimulations Are Optimized," *Oil & Gas J.* (October 1989) 87, No. 41, 67-70.

[20]Spafford, S.D. and Schraufnagel, R.A.: "Multiple Coalseams Project," *Quarterly Review of Methane from Coalseams Technology* (October 1992) 10, No. 2, 17-21.

[21]Guoynes, J.C., et al.: "New Composite Fracturing Plug Improves Efficiency in Coalbed Methane Completions," paper SPE 40052 presented at the 1998 SPE Rocky Mountain Regional Meeting/Low Permeability Reservoirs Symposium and Exhibition, Denver, Colorado, April 5-8.

[22]Spafford, S.D.: "Stimulating Multiple Coalseams at Rock Creek with Access Restricted to a Single Seam," *Proc., Coalbed Methane Symposium, Tuscaloosa, Alabama* (May 1991) 243-246.

[23]Schraufnagel, R.A. and Lambert, S.W.: "Multiple Coalseam Project," *Quarterly Review of Methane from Coalseams Technology* (June 1989) 6, No. 3 and 4, 28-37.

[24]Schraufnagel, R.A., Spafford, S.D., and Saulsberry, J.L.: "Multiple Seam Completion and Production Experience at Rock Creek," *Proc., Coalbed Methane Symposium*, Tuscaloosa, Alabama (May 1991) 211-221.

[25]Rodvelt, G., Toothman, R., Willis, S., and Mullins, D.: "Multiseam Coal Stimulation Using Coiled-Tubing Fracturing and a Unique Bottomhole Packer Assembly," paper 72380 presented at the 2001 SPE Eastern Regional Meeting, Canton, Ohio, October 17-19.

[26]Halliburton Energy Services, Inc., Internal Data-CobraMax^{SM} data sheet, 2004.

Chapter 8

Hydraulic Fracturing of Coalseams

8.1 Need for Fracturing Coals

The coalbed methane (CBM) industry began after the realization that large methane contents of coals could often be produced profitably if the seams were dewatered and if a permeable path to the wellbore could be established for the gas. Hydraulic-fracturing technology, developed in the oil and gas industry after 1948, proved to be the answer in many cases for facilitating dewatering and elevating gas production rates to economic levels.

Although hydraulic fracturing had been highly developed for conventional gas reservoirs of low-permeability sands, adjustments to the process were necessary for the coal because of the following phenomena:

- The surface of the coal adsorbs chemicals of the fracturing fluid.
- The coal has an extensive natural network of primary, secondary, and tertiary fractures that open to accept fluid during hydraulic fracturing but close upon the fluid afterwards, introducing damage, fluid loss, fines, and treating pressures higher than expected.
- Fracturing fluid can leak deep into natural fractures of coal without forming a filter cake.
- Multiple, complex fractures develop during treatment.
- High pressures are often required to fracture coal.
- Young's modulus for coal is much lower than that for conventional rock.
- Induced fractures in some vertical CBM wells may be observed in subsequent mine-throughs.
- Horizontal fractures occur in very shallow coals, such as the Pratt group in the Warrior basin.
- Fines and rubble result from fracturing brittle coal.
- Coalseams to be fractured may be multiple and thin, perhaps only 1 or 2 ft thick, requiring a strict economical approach to the operations.

Successful application of fracturing to coalseams has been helped by research during the 1980s in the Black Warrior basin at the Gas Research Institute's Rock Creek site. The research helped reduce the costs and improve the performance of hydraulically fractured coalseams, serving somewhat as a field laboratory for the development of the process. Improvements continue, especially in preventing damage to the coal.

8.1.1 Appalachian Wells Inadequately Stimulated

The central and northern Appalachian basins have an estimated 66 Tcf of CBM in place. Several decades before the CBM process became commercially viable, coal gas from vertical wells in the Appalachian basins was being produced, but low production rates from these early wells contrast sharply with current rates.

Vertical, unstimulated, or inadequately stimulated CBM wells in the northern Appalachian basin completed before 1980 produced methane at modest rates of less than 140 Mcf/D with most of the wells at 10–30 Mcf/D.[1] (Those that produced more than 100 Mcf/D had permeabilities greater than 10 md.) Of the wells that were hydraulically fractured, the sizes of the hydraulic projects were smallscale. Although production could be sustained for long times at these rates, it was not economical to produce for pipeline sales.

It became apparent in these early wells that the low-permeability formations could benefit from fracturing and that the benefit depended upon fracture length. The effect of fracture length is indicated from the field data and the simulation results of a test well drilled in 1975 into the Pittsburgh seam in Greene County, Pennsylvania.[1] (The Pittsburgh seam is mined in the area.) Permeability of the coal was about 1.3 md and gas content 190 scf/ton. The coalseam was about 1,000 ft deep and about 6.5 ft thick. The well was not fractured, and it gave a maximum production of 21 Mcf/D. Simulation results of Hunt and Steele for 150-ft and 250-ft half-length fractures are compared to the unstimulated well data in Fig. 8.1. The results demonstrate the need for hydraulic fracturing under these conditions, which could have yielded 80 Mcf/D with a 250-ft fracture

half-length. Peak gas production would have occurred several years sooner in fractured wells.

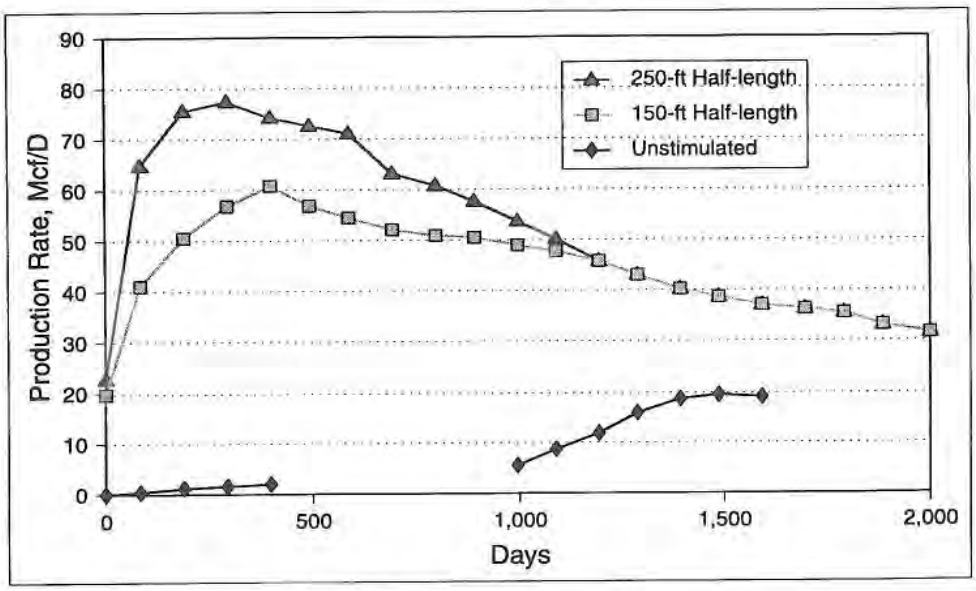

Fig. 8.1—Extent of fracturing effects.[1]

Further computer simulation by Hunt[1] with data from wells in Greene County gives added insight into the positive effect of longer fracture half-lengths on gas production rate over a period of 10 years. Production rates increase dramatically over the first few years from coals of low permeability when fracture half-length increases. Production rates from three half-length fractures of 150 ft, 250 ft, and 350 ft converge at 10 years, but at the peak rate after 2 years the 350-ft half-length would produce at a rate 66% higher (see Fig. 8.2).

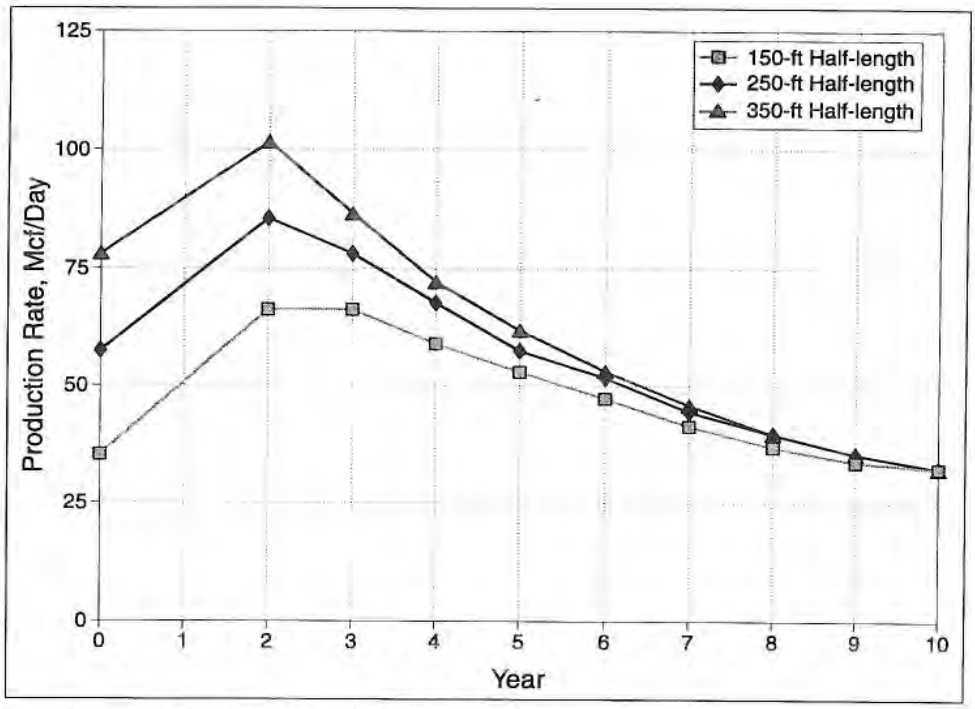

Fig. 8.2—Sensitivity to fracture half-length.[1]

The benefit of the fracture length at infinite fracture conductivity is qualified by the absolute permeability of the seam. Simulations by Spafford and Schraufnagel[2] (Fig. 8.3) are based on reservoir parameters indigenous to the Black Warrior basin and show 5-year cumulative gas production as a function of fracture half-length and as a function of absolute permeability. A range of permeabilities exists in which longer fractures show marked production improvements, but beyond the high end and the low end of the permeability range, fracture length becomes unimportant.

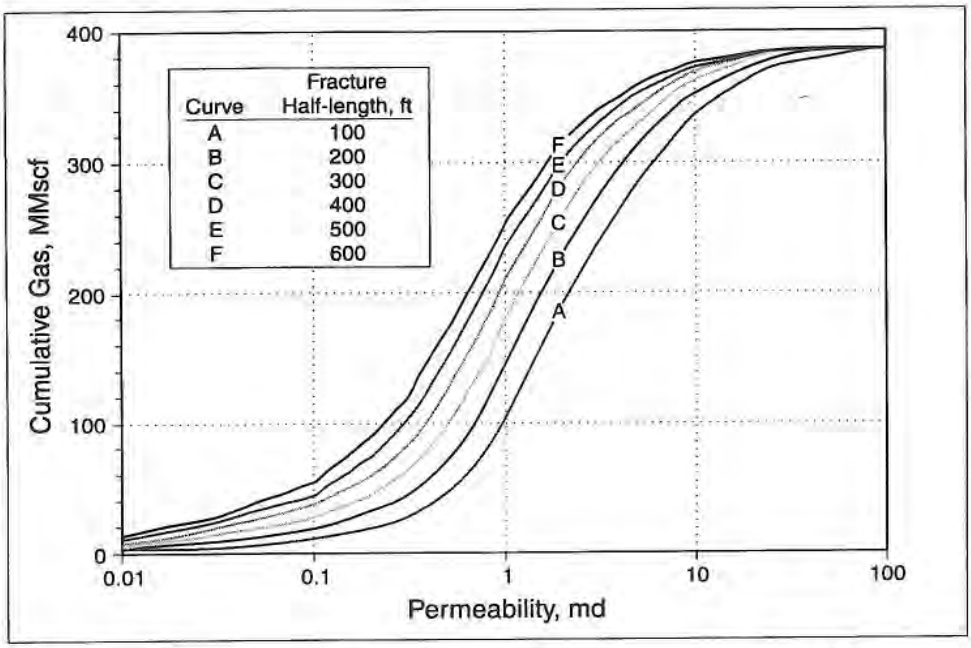

Fig. 8.3—Efficacy of fracture length dependent on permeability level.[2]

Fracture length assists productivity especially between 0.5 and 6.0 md. Therefore, if the absolute permeability of a prospect is too low, the property cannot be made economical by fracturing.

The length becomes inconsequential as permeabilities exceed 10 md. Therefore, above the propitious permeability range, the goal of stimulation may be to connect the wellbore with the natural fracture system, circumventing any near-wellbore damage.

8.1.2 Unstimulated Wells in Big Run Field

An interesting case history is the Big Run field in Wetzel County, West Virginia. Conventional gas was produced from the Big Injun and Gordon sands below the seam of coal from 1905 until 1932, at which time the well was to be abandoned and plugged. Upon pulling the casing, flow of gas was initiated from the coals above the abandoned sands; nearby mining in the Pittsburgh seam had reduced water saturations to a low level. Recompletion of the well in the Pittsburgh seam (about 1,070-ft depth) proceeded to produce 200 MMcf of methane over the next 30 years, albeit at a slow rate, without stimulation.[1] Other wells were drilled and 52 unstimulated wells have produced from the field. After 43 years, 2 Bcf of methane cumulative production has resulted (see Fig. 8.4). Typical production rates from the low-permeability Pittsburgh seam amounted to only 38 Mcf/D without fracturing.

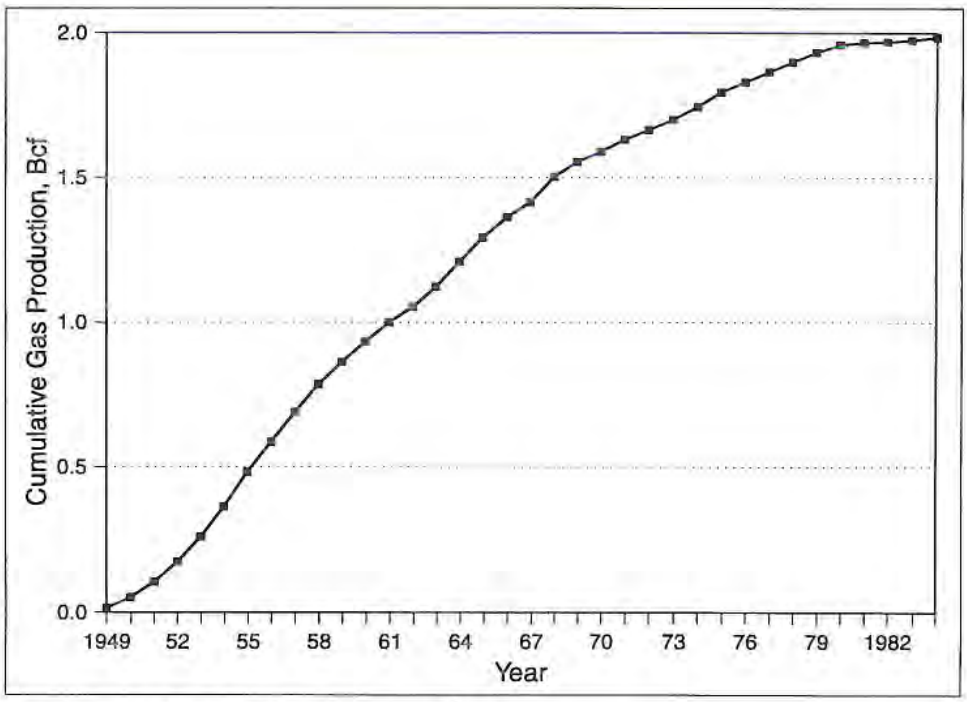

Fig. 8.4—Big Run field, unstimulated.[1]

8.2 Unique Problems in Fracturing Coals

Most anomalies in fracturing coals result from uncommon values of properties of the coal reservoir, such as rock mechanical properties and extensive natural fractures in the coals. As a consequence of these coal reservoir properties, induced fractures are very sensitive to complex in-situ stress profiles and the altering of those stresses when drilling and fracturing. Treating pressures may be higher than conventional reservoir fracturing. The cleat system influences the path of the fracture and may introduce multiple fractures to increase treating pressures. Rubble generated near the wellbore or fines introduced during fracturing may contribute to higher treating pressures.

Excessive fines are generated during fracturing because of the friable nature of the coal. Unfortunately, the fines continue to be generated during subsequent gas production to reduce conductivity. Unlike the conventional reservoir, the particles can be the size of powder or blocks large enough to plug perforations.

The organic composition of the reservoir rock makes it susceptible to damage. Fluid damage to the coals occurs by two mechanisms. First, the organic surface of the coal is especially susceptible to fluid damage by adsorption of chemicals from the fracturing fluid or drilling fluid. Second, the fluids may become trapped in the intricate fissure network that constitutes the flow path.

Perhaps the more pervasive problem is the trapped fluids. Cement and drilling fluids have been found to permeate surprisingly long distances from the wellbore through the natural cleat system to physically block these conduits of gas flow. During fracturing, the imposed pressures open the cleats to allow fluid penetration, subsequently trapping the gel upon closure to obstruct gas flow.

A consequence of the experience gained by the industry in fracturing a reservoir rock of such different and complex properties is an advancement in the knowledge and understanding of fracturing in general.

8.2.1 Fines

Fines contribute to elevated pressures during fracturing.[3] Fines are known to deteriorate fracture conductivity with time, possibly packing into secondary and tertiary natural fractures to damage permeability.

Some research has helped explain qualitatively the contribution of fines to high fracturing pressures. Several mechanisms are offered.[4,5] Fines could load the fracturing fluid to increase its viscosity and consequently increase pressure drop as the more viscous fluid moves through the fracture. Parting of the coal could create rubble and fines near the wellbore for a more tortuous flow path. The fines could pack in the tips of developing fissures or bridge elsewhere in the fracture to cause higher treating pressures. A more important question revolves around the quantitative impact of fines on fracture treating pressures.

Laboratory burst-tests verify the generation of fines but in volumes that will not load the fracturing fluid appreciably. Therefore, there should not be excessive frictional pressure drops introduced by fines in the flow of the fluid through the fracture. In coal burst-tests in the laboratory by Jeffrey and coworkers,[6] an average of 0.0144 lb of fines per sq ft of fracture surface area was created.

Jeffrey determined the increase in apparent viscosity from loading a 40 lb/1,000-gal noncrosslinked fluid with 120- to 170-mesh coal fines. The volume of fines generated in his tests would not significantly increase the pressure drop in the flow of the fracturing fluids in coals.

More important effects on treating pressures come from fines concentrating near the wellbore to create high pressure drops in the fluids flowing through them. Injection falloff tests in CBM wells that reveal high skin factors are indicative of this.

Fines are also created from the attrition of the fracturing fluid, loaded with sand, flowing past the coal surface. In a laboratory experiment,[6] a 40 lb/1,000-gal hydroxypropyl guar (HPG) gel with 8 lb/gal sand flowing at typical fracturing rates in a coal-simulated fracture generated fines linearly with time (see Fig. 8.5).

A tortuous fluid path causing high-velocity fluid flow, such as near the wellbore or through opened butt or tertiary cleats, would contribute to the attrition of fines. Shear stresses on the coal that move one face of the fracture or cleat relative to the other face would also be expected to generate fines.

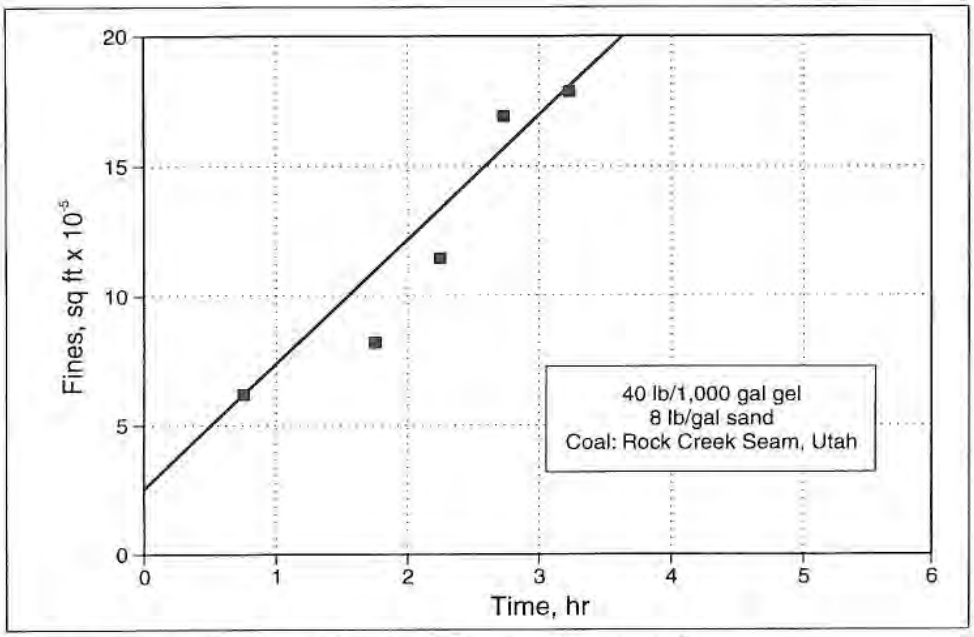

Fig. 8.5—Fines from fluid abrasion laboratory flow tests.[6]

Perforating only in the rock partings between seams proved effective at Rock Creek in preventing pump repairs and workovers, primarily because fewer fines were generated.[3] Since the fracturing fluid loaded with sand increases in abrasiveness with velocity, most damage occurs in the vicinity of the wellbore where the cross-sectional area of the flow channel is smallest and the velocity of the fracturing fluid is greatest. In the case of thin, multiple seams, perforating in the inorganic rock avoids the high attrition of coal fines near the wellbore. Perforating in an acceptable rock parting may later help remove coal fines entrained with production fluids by screening those fines in the sand-propped fracture of the inorganic rock before they concentrate at the wellbore.

In many cases, it is desirable to perforate only the coalseams to avoid directing the hydraulic fracture treatment into a lower-stress sandstone or carbonate. The operator must then have a remedial process for alleviating damage caused by fines plugging the sandpack and wellbore area.

A post-fracture service that helps remove wellbore damage and coal fines blockage through a powerful backflush has been developed. The mobility of the fines is then restricted with a proprietary chemical formulation that makes the surface of the coal particle "tacky," enabling them to stick together and cling to formation features away from the critical flow paths in the proppant pack. Fig. 8.6 shows how fines "clots" can accumulate near the wellbore in the pack. The thin carrier fluid is pumped under high pressure into the damaged fractures, helping break down the clots of coal fines and displacing them to the outer limits of the fracture system. The clots are immobilized at the far reaches of the pack, restoring conductivity to the wellbore.

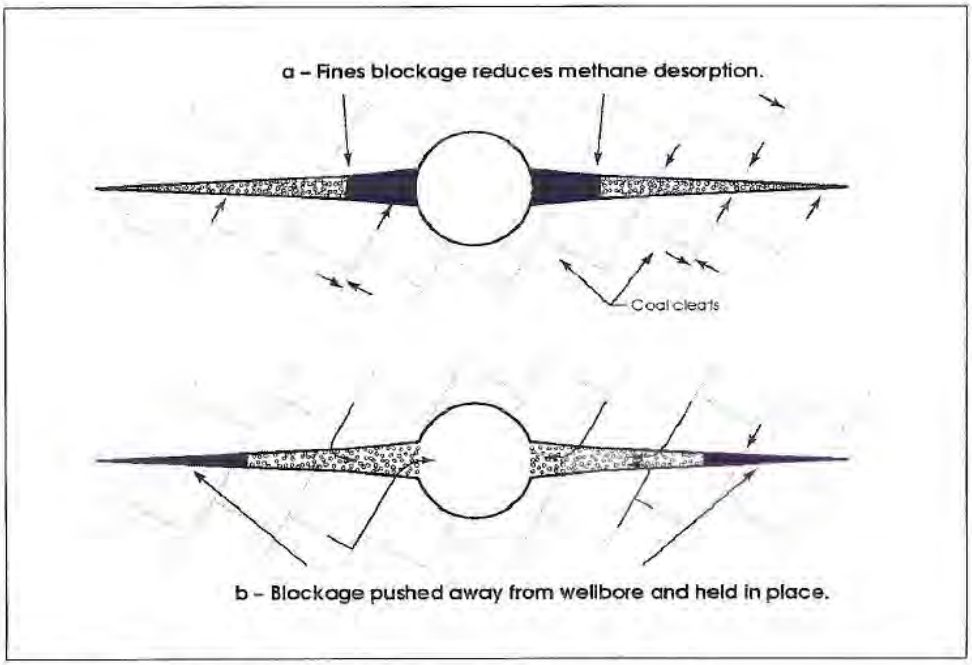

Fig. 8.6—Removing and holding fines away from the wellbore.

This proprietary system (marketed by Halliburton as CoalStim® Service) can also be formulated to remove polymer damage from fracturing treatments. While the well is shut in after treatment to allow the chemical process to alter the coal fines' surface, polymer breakers will have time to dissolve residue to improve pack conductivity. Both guar and polyacrylamide polymers have been removed with this treating fluid.

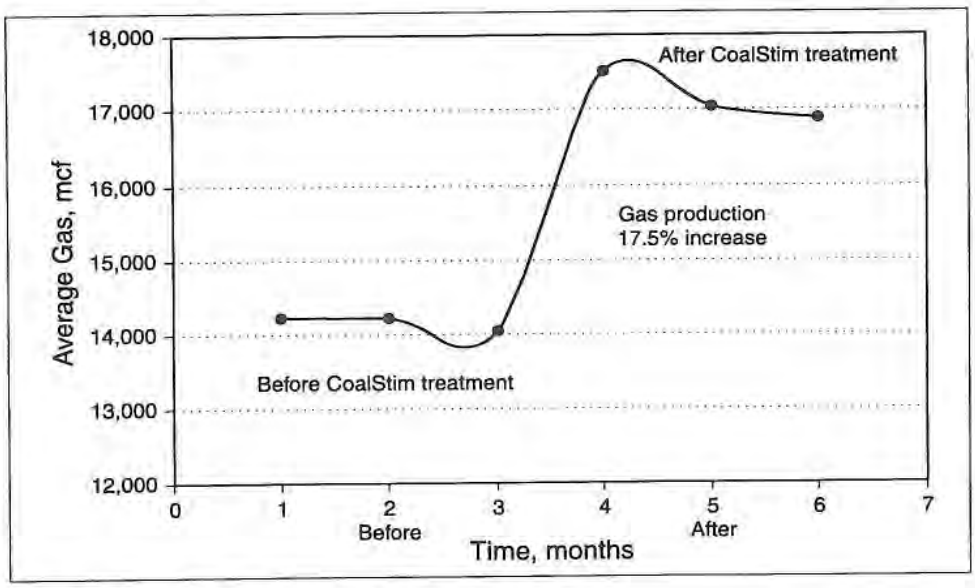

Fig. 8.7—Production increase from controlling fines.

This process has been used in the Rocky Mountain and Appalachian basins to increase gas production from 17.5% to 25% with payouts of less than 9 days. Fig. 8.7 depicts one operator's success in using the process. Another operator used the service on a 30-well program, increasing production an average of 66 Mcf/D with a payout of 32 days.[7]

Another improvement in fines control is the use of a surface modification agent (SMA) on the surface of the proppant grains during hydraulic fracturing that provides several benefits:

- Helps maintain a high well production rate for a longer period of time.
- Enhances the frac fluid cleanup (see Fig 8.6).
- Reduces proppant settling to help improve permeability of the proppant pack.
- Helps reduce proppant flowback.
- Adds surface modification agent (SMA) on-the-fly to help eliminate leftover coated proppant.
- Stabilizes the proppant pack/formation interface to reduce the intrusion of formation material into the proppant pack.

With the amount of fines generated during a stimulation treatment, a stabilized pack/formation interface is critical to maintaining conductivity through the proppant pack (Fig. 8.8). Intrusion of fines into the pack is the major cause of production decline in a CBM producer. Besides plugging the pack, fines can be the beginning point for scale precipitate formation. Using SMA, the operator can place the rod pump below the lowest perforations, allowing a more efficient de-watering of all coals. All CBM projects can benefit from lowering the pumps to provide lower backpressure on the coals.

SMA was used in the Fruitland Coal in the San Juan basin[8] for an operator to increase production from no production up to 200 Mcf/day in a re-frac case history. Low-gel borate (LGB) fluid was used to place 300,000 lb of SMA-treated proppant in two of three re-fracs confirming the process performance. LGB was used on all three wells. However, in the two wells using SMA, production showed a four-fold increase that was being maintained several months after treatment. Economic value to the operator was $720,000 per year.

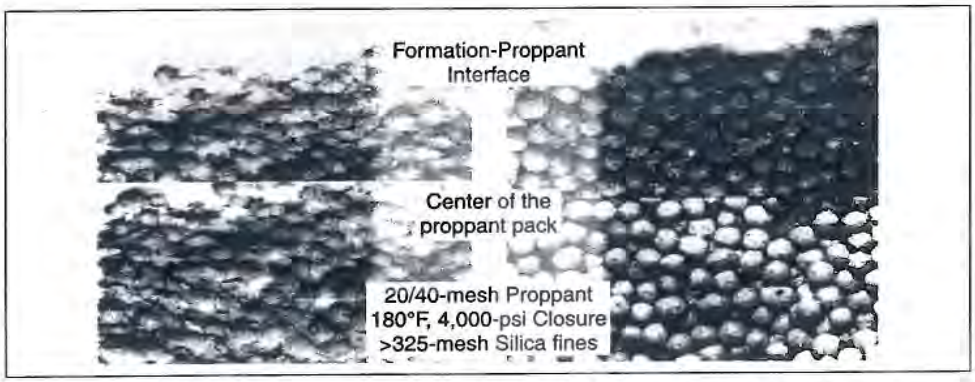

Fig. 8.8—A stabilized proppant pack/formation interface helps maintain conductivity through the proppant pack.

8.2.2 Fluid Damage

The organic surface of coal has the potential of being damaged from adsorption of ingredients of the fracturing fluid (or drilling fluid) in a manner unlike that of the inorganic surfaces of conventional reservoirs. Adsorption and physical entrapment of polymer molecules in the coal obstructs butt and face cleats, tertiary fissures, and micropore openings to restrict methane desorption, diffusion, and Darcy flow.

Molecules small enough to enter the micropores, such as CO_2, that are strongly adsorbed in the micropores cause swelling of the coal matrix with attendant permeability reduction. The degree of swelling is dependent upon the affinity of the adsorbate for the solid surface.

A possible problem of chemicals in crosslinked gels altering permeability by matrix swelling from adsorption has been investigated by Puri, *et al.*[9] Cores of 3.5-in. diameter (from the San Juan basin) and 2.0-in. diameter (from the Warrior basin) were evaluated in the laboratory by Amoco for polymer damage to permeability. The flow tests were structured to isolate permeability damage from

sorption effects and to minimize extraneous effects of cleats physically bridging and packing with gel. The gel in the tests had been broken and the fracturing fluid filtered. It was found that HPG decreased permeability by a factor of 10 in each of the two coals. In Fig. 8.9, the Fruitland coal exhibits a precipitous decline in permeability simultaneously with the commencing flow of the fracturing fluid. After deterioration of permeability from sorption, permeability could not be reinstated. The damage was mostly irreversible.

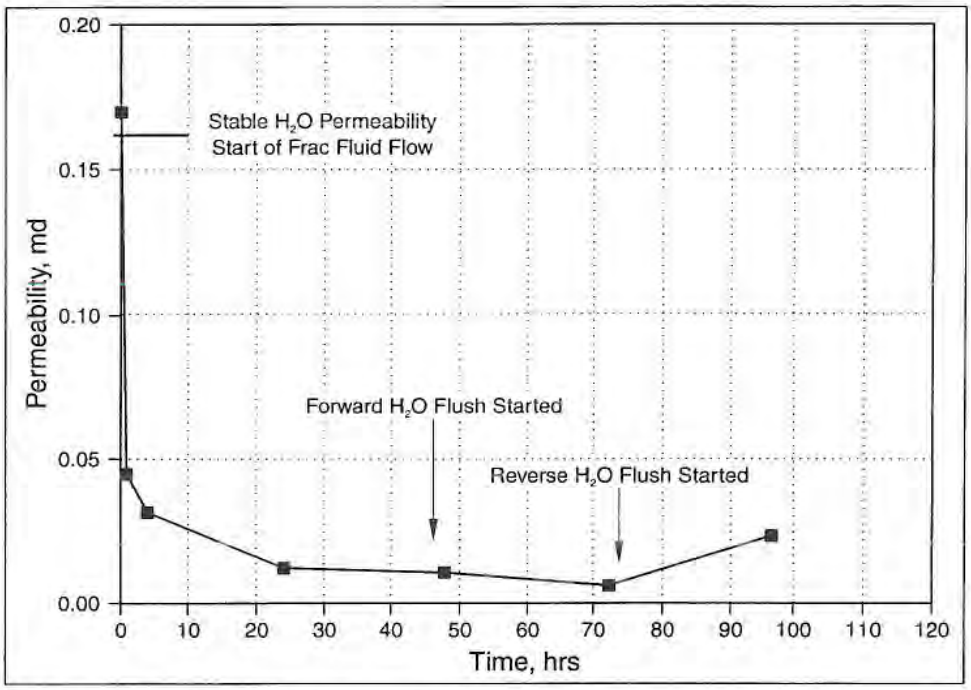

Fig. 8.9—Gel damage, San Juan core.[9]

In Fig. 8.10, the higher permeability Warrior basin coal demonstrated a similar damage from the broken polymer in the Amoco test.

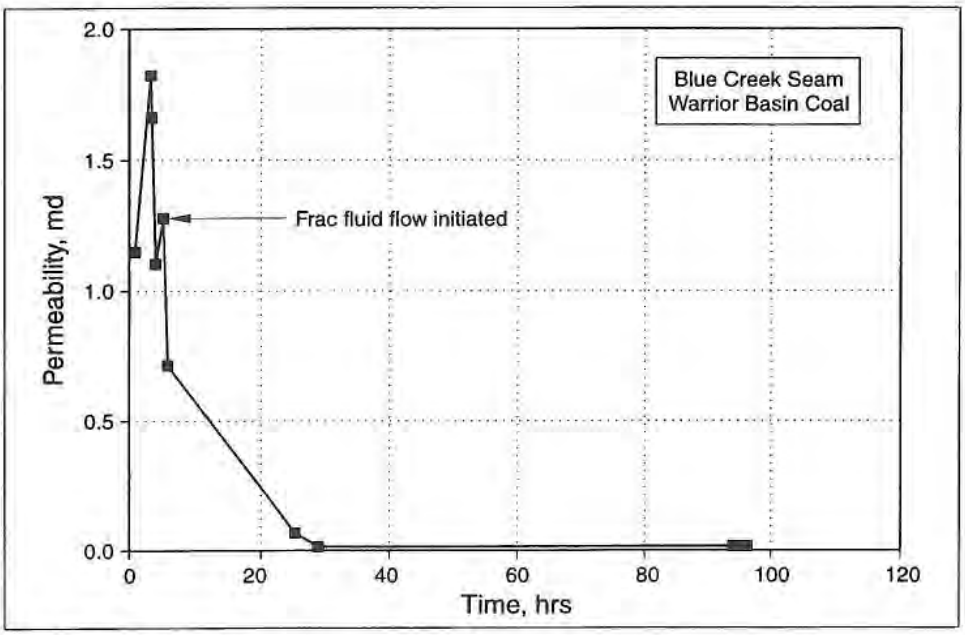

Fig. 8.10—Gel damage, Warrior coals.[9]

It is recognized that the primary and secondary cleat system as well as the tertiary fissures of coals represent the flow system for future gas production and must be protected during the drilling or completion process.[10] Besides chemical damage of gels to the organic surface, blockage of the natural fractures can occur as high treating pressures open fissures for fluid invasion and as the gels become trapped by closure; filter cakes may not limit fluid invasion as in sandstone formations. Mineback has revealed unbroken gels in fractures far from the wellbore at extended times after treatment. An estimated 25% of the gel remained in the formation in an Oak Grove, Alabama test conducted by Amoco.[11]

It should be emphasized that fracturing with gel fluids has produced many successful wells that are economical and operate with no apparent deleterious effects from the fluid. However, gel damage does often occur, and it can be substantial.

At the Rock Creek test site, remedial treatments of poorly performing wells[12] were conducted. The criteria for selecting the wells for corrective action were as follows. The criteria reflect the probability of the original fracturing fluid damaging the coal:

- Original stimulations used guar-based fracturing fluids with an enzyme breaker.
- Fluid returned at high viscosity after fracturing.
- Some wells underachieved in the midst of good performers.

The restimulation of Well P3 at Rock Creek is a classic example.[13] HPG gel had been used originally to fracture the well. Production rates from the well were retarded at 65 Mcf/D. The well was refractured with nitrogen foam containing hydroxyethyl cellulose (HEC). After the remedial treatment, production reached 380 Mcf/D (see Fig. 8.11).

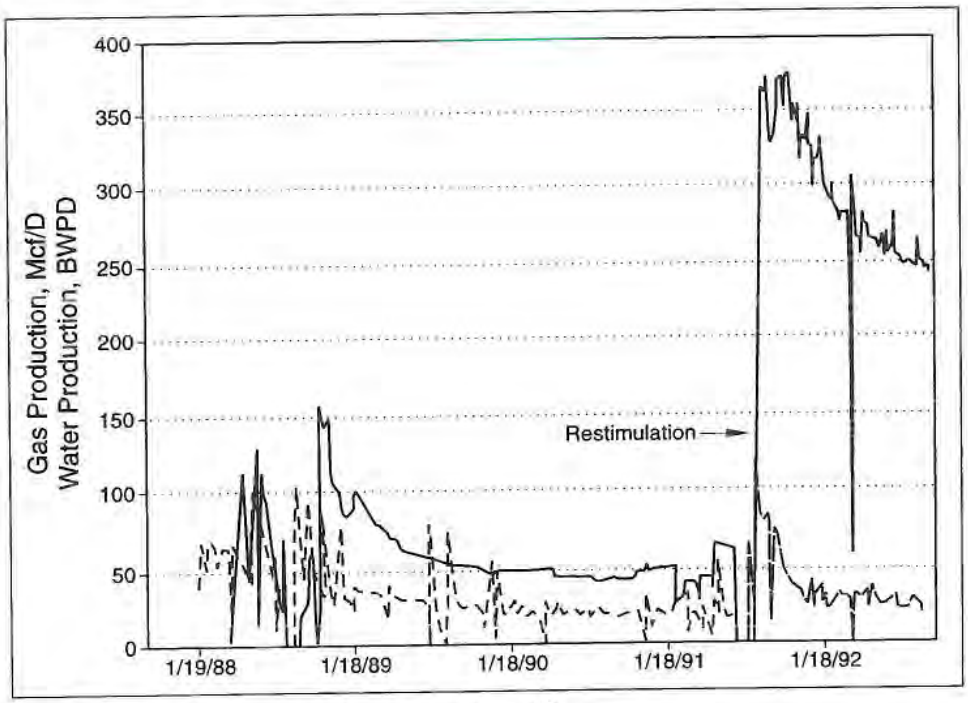

Fig. 8.11—Restimulation with nitrogen foam.[13]

8.2.3 Excessive Treating Pressures

A higher pressure than ordinary may be necessary to initiate a fracture in coal.[14] With normal expectations of overburden pressure gradient of 1.0–1.2 psi/ft and of minimum horizontal stress of 0.6–0.8 psi/ft, the pressure to initiate the fracture should be approximately 100 psi greater than the minimum horizontal stress to create a vertical fracture,[5] or no more than a 1 psi/ft gradient. Instead, a fracture gradient greater than 1.0 psi/ft is often encountered in coals.[9] A survey[5] of the fracturing gradients encountered in the Black Warrior basin of Alabama indicated the distribution as presented in Fig. 8.12.

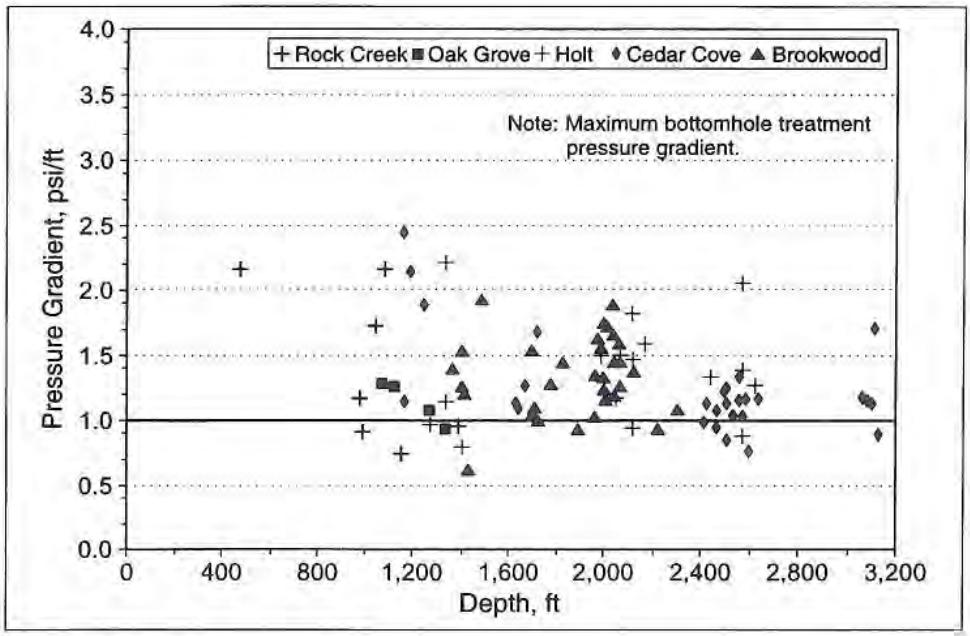

Fig. 8.12—High fracture gradients in Warrior basin.[5]

It is evident that most of the fracture gradients in the Warrior basin exceed the normal 1.0-psi/ft gradient. Note that some pressures exceeded 2.0 psi/ft. The

preponderance of wells were within the 1.0–2.0-psi/ft range. Only about 20% of the wells exhibited gradients less than 1.0 psi/ft.

The following mechanisms have been postulated to account for the higher than expected fracturing pressures in coal:

1. Borehole instability or perforating causes rubble at the point of fracture initiation. Any stress relief of the coals results in breakup of the coal block. Drilling the wellbore, perforating, and even fracturing realign stresses surrounding the borehole. The unconsolidated coal chips retard initiation of the hydraulic fracture.
2. Bursting of the rock at fracture initiation generates fines that bridge the crack near the wellbore. Further from the wellbore, the accumulation of fines and chips blocks the fracturing fluid front, redirecting the path of the fracture.
3. Tortuous fracture path develops as the path follows cleats, slippage at joints occurs, and horizontal components at the rock interface develop. A tortuous path may develop at the wellbore if the perforations are not aligned with the maximum horizontal stress.[15] Otherwise, the fracture may propagate radially until extending in the direction of maximum horizontal stress. The tortuous path causes greater pressure drops in the fluid, requiring higher pressures to open the apertures sufficiently for sand traverse.[16]
4. A network of fractures, multiple fractures, and parallel fractures develops. These have been documented in minethroughs. They tend to divert fracturing fluid, necessitating higher pressures to propagate the primary fracture.
5. Fracture tip anomalies occur from fines at the tip or fluid lag.[17] This is similar to (3), but it occurs at the fracture tip.
6. Raising pore pressures near the wellbore makes the coal subject to failure.

The proposed mechanisms causing high fracturing pressures are depicted in Fig. 8.13. The most likely causes of the high fracturing pressures are rubble near the wellbore from poroelastic effects, tortuous path near the wellbore and beyond, and multiple fractures.

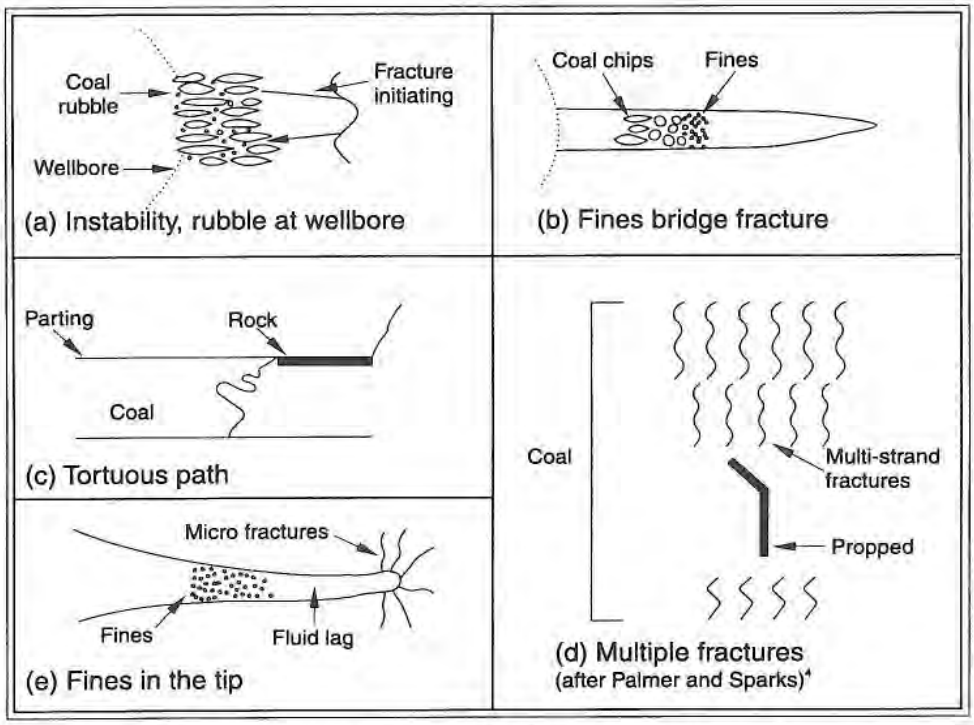

Fig. 8.13—Mechanisms causing excessive fracturing pressures.[4]

Laboratory and simulator uses of field data by Khodaverdian, McLennan, and Jones indicate that coal fragments in the fracture near the wellbore help cause the high pressures.[5] The pressures in the fracture as a function of distance from the wellbore show the effect of near-wellbore damage, as pressures drop off rapidly a short distance from the well[18] (see Fig. 8.14).

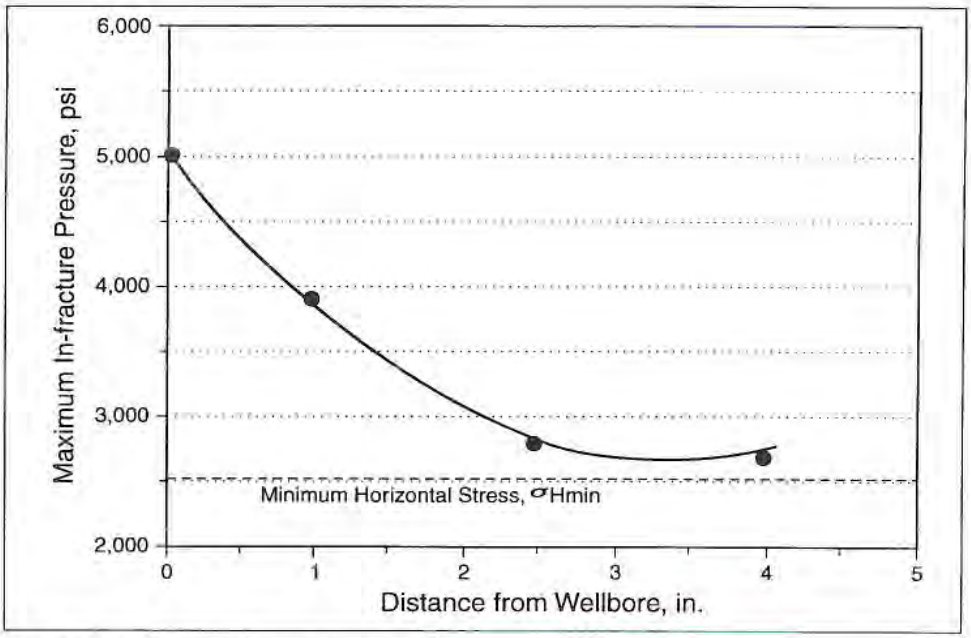

Fig. 8.14—Near-wellbore damage.[18]

Fluid leakoff from the fracturing process increases pore pressure to the extent that mechanical properties of coal deteriorate near the wellbore. Young's modulus decreases and Poisson's ratio increases in such instances, thereby increasing the fines generation and causing the failure of the coal matrix.

In the case of multiple, thin seams, perforating below the coalseam or in the parting between seams, if the bounding rock is suitable, reduces coal rubbling from perforations, fines generation from the bursting of the coal at fracture initiation, and attrition of fines from the high velocity of the fluid near the wellbore. It also may avoid degrading poroelastic effects.

The five proposed mechanisms presented in Fig. 8.13 may work in consort or individually. Most have been verified. The amount of the pressure drop due to each mechanism is unknown in the coal fracturing process.

8.2.4 Leakoff

Historically, when coalseams were encountered in the hydraulic fracturing of conventional formations, the coal acted as a barrier to fracture growth because of fluid leakoff, elastic properties of the coal, and the likelihood of slippage at the coal-rock interface. With the advent of the CBM process and the objective to penetrate or stay within the bounds of the coal, the problem of leakoff became magnified.

The following deleterious effects result from leakoff in coals:

- Loss of fluid limits penetration of the fracture.
- Fracturing efficiency decreases.
- Formation damage likely occurs.
- Screenout probability increases.

The severity of the leakoff problem in coals is substantiated from mineback observations. For example, cement was observed in a natural fracture in the roof of a coal mine 133 ft from the wellbore at Oak Grove in the Black Warrior basin. In another instance, unbroken gel was spotted in a fracture 7 months after the stimulation was completed.[19] In a third case of eight field treatments in a government-sponsored test where fluorescent paint was part of the fluid system during fracturing, paint was observed as far as 630 ft from the wellbore in unpropped face and butt cleats. The paint in some intercepted fractures revealed stair-stepped butt and cleat joints propagating through the coal.[20]

In extensive natural fracture networks of coals, the pressures imposed during hydraulic fracturing open the fissures to compound the leakoff problem. This factor may be accentuated in the fairway section of the San Juan basin where the hvAb-rank coal has an elaborate network of cleats, closely spaced, including superposed tertiary cleats from a reoriented stress field. The high-permeability coal in the fairway is more susceptible to leakoff of fracturing fluids upon pressurizing, and greater damage to the coals may result from fracturing with gels.

Penny and Conway[21] addressed the leakoff problem in laboratory experiments with 3.5-in. × 2.9-in. mined coal samples taken from the Fruitland formation of

the San Juan basin. Because of the randomness of the cleat system, the permeabilities of the samples ranged from 1 to 100 md with an average value in his tests of 40 md. Although 1-md samples were impermeable to all fracturing fluids, both crosslinked and noncrosslinked HPG fluids moved into the natural fractures of the 40-md samples unhindered by any filter-cake buildup at modest driving pressure differentials (see Fig. 8.15). Note that no filter cake develops to obstruct leakoff at any pressure. At the higher pressures, loss of fluid increased.

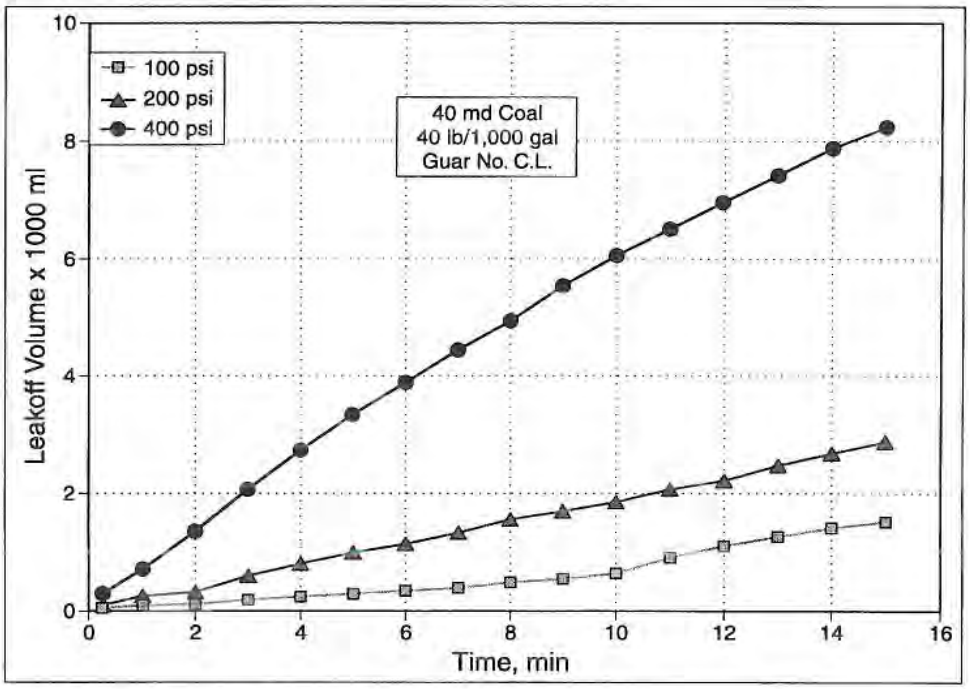

Fig. 8.15—Leakoff in Fruitland cores.[21]

Although the polymers do not bridge the cleat openings to initiate a filter cake, it is possible to do so with the correct proppant size. The proppant may bridge the gap and polymer build upon it to prevent leakoff. The bulk of the fracturing fluid and larger size proppant is then diverted to a primary induced fracture. It is intimated that multiple fractures might be reduced to a single dominant fracture

and tortuosity of the single fracture reduced by use of proppant slugs.[16] Slugs of 100-mesh or 40/70-mesh sand early in the pad could direct the fluid and proppant to a single fracture.

Sand of 100-mesh in concentrations as low as 2 lb/gal proved effective in reducing leakoff to an insignificant level by facilitating the formation of a filter cake in the laboratory experiments of Penny and Conway[21] (see Fig. 8.16).

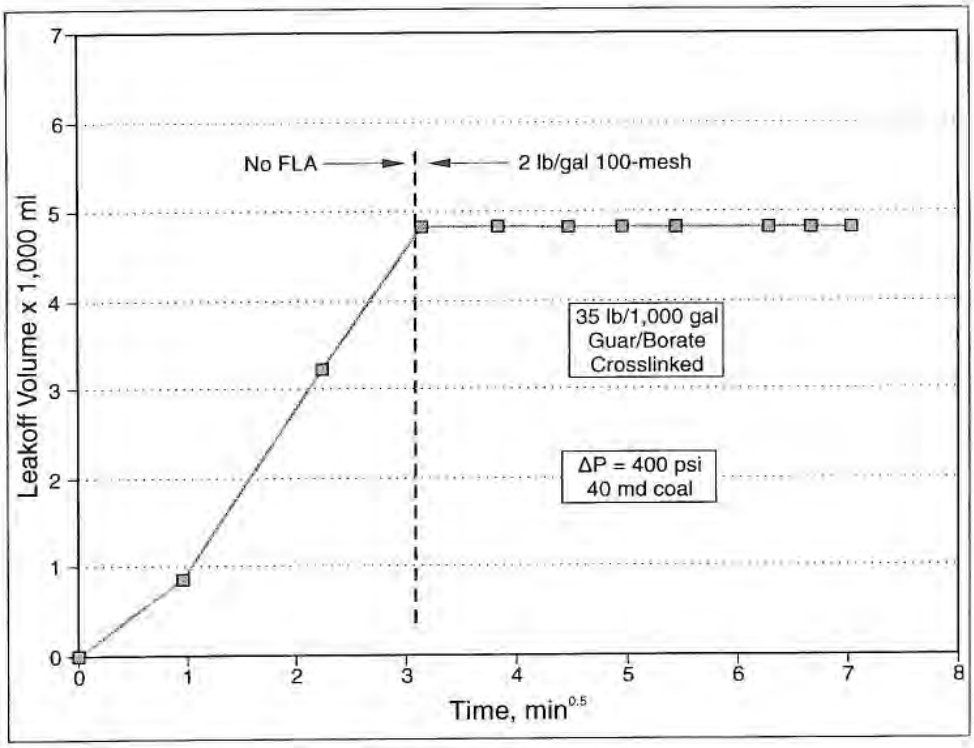

Fig. 8.16—Leakoff prevention in Fruitland cores.[21]

Note in Fig. 8.16 that leakoff progressed unabated until the 100-mesh sand was added. Immediately, a filter cake formed to eliminate the loss of fluid at the

higher 400-psi test condition. The results have implications for reducing fluid damage to the coals and for creating a single dominant hydraulic fracture.

A leakoff coefficient, C_w, may be calculated using Eq. 8.1[22] to provide an approximation of how much fluid will leak into the formation, affecting height and penetration of the fracture.

$$C_w = 0.0328 \frac{m}{2A} \tag{8.1}$$

where

C_w = leakoff coefficient, ft/min$^{1/2}$

m = slope of fluid-loss curve (filtrate volume/$\sqrt{(flow\ time)}$), ml/min$^{0.5}$

A = cross-sectional area of sample, cm^2

For the case of the 40-md Fruitland samples of Fig. 8.16, C_w is determined to be 0.001 ft/min$^{0.5}$ with the 100-mesh sand in the fluid.

The fine-mesh sand should be scheduled so that it is present as the cleats and fissures initially spread apart.[10] Injecting the fine mesh later after the apertures are dilated may compound the problem.

Cramer[23] reports the effective use in the field of 40/70-mesh sand in the San Juan basin to seal cleats and to prevent leakoff. Palmer and Kutas[24] also relate an effective use of 40/70-mesh sand preceding a coarser 12/20-mesh sand to seal the cleats and secondary pathways that open when fracturing San Juan coals. The mechanism was verified when radioactive tracers in the two sands indicated a segregation of the two sand sizes in the coal and placement of the two sizes in different fractures. The fine sand went to close secondary and tertiary fissures; the coarser sand propped the main fracture.

A 100-mesh sand was used to control leakoff in the U.S. Department of Energy's multiwell experiment, resulting in completing the fracturing as designed.[10]

Since fluids may enter the cleats and secondary fissures when they are dilated from treating pressures, later cleanup at reduced pressures may leave gel trapped to reduce permeability.[10] It becomes important, therefore, to restrict as much as possible the growth of complex fractures and fluid loss to them by properly selecting proppant size and schedule.

Partly because of better control of leakoff, nitrogen foams are increasingly used in fracturing coals.

8.3 Types of Fracturing Fluids for Coal

For methane production rates to be economical, permeability of the formation must be adequate. Permeability of the coalseam depends on the natural fracture system and the connection of the fracture system to the wellbore. Connecting the fissures to the wellbore must be by hydraulic fracturing or by regionally limited cavity completions.

There has been uncertainty in the industry on the choice of the proper fracturing fluid—whether to use linear polymer, crosslinked gel, water with proppant, water without proppant, or nitrogen foam. The history of changing popularity of each of the preceding fluids reflects the uncertainty.

Cost, formation damage, proppant placement, and propped fracture length dictate the choice. Table 8.1 summarizes the general attributes of the fluid selections, and it is surmised from the tabulation that either crosslinked gels or nitrogen foams would be preferred. Formation damage evolved as an important consideration in selecting a fluid, moving the preferred fluid selection from crosslinked gels toward nitrogen foams.

Table 8.1—Fracturing Fluid Ratings

	Cost	Formation Damage	Proppant Placement	Propped Length
Water w/o proppant	Good	Good	Poor	Poor
Water w/ proppant	Good	Good	Poor	Poor
Linear gel	Fair	Poor	Fair	Fair
Crosslinked gel	Fair	Poor	High	High
Nitrogen foam	High	Good	Good	Good

8.3.1 Crosslinked Gels

In the many CBM wells that have been fractured in the San Juan basin and the Black Warrior basin, the fracturing fluid most frequently used has been a 30–35 lb per 1,000 gal HPG in 2% KCl water solution crosslinked with the borate ion.[25] Polymer content of the gel is minimized to reduce residual unbroken gel, cost, and additional produced-water treatment requirements to meet BOD specifications.

The water-soluble HPG polymer is derived from guar by combining it with propylene oxide to achieve a polymer with less residue and higher temperature stability. The structure of HPG is presented in Fig. 8.17.[26] It contains one galactose unit to two mannose units as the basic repetitive group of the polymer chain.

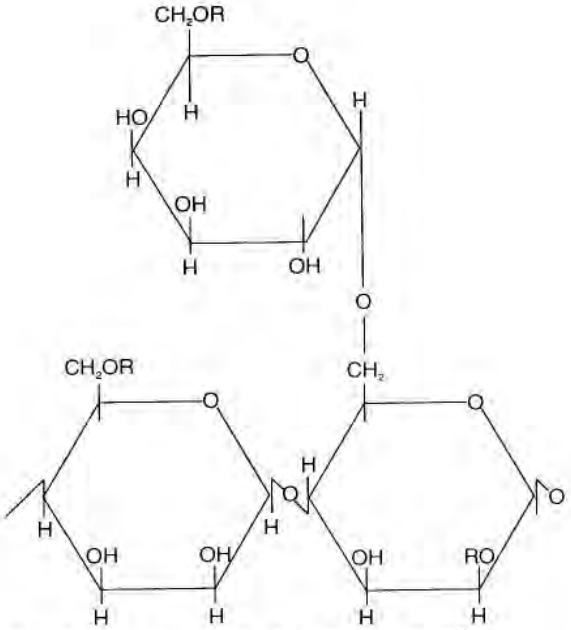

Fig. 8.17—Structure of HPG polymer.[26]

Crosslinking increases viscosity of the fluid with a minimum amount of polymer. The borate ion is most commonly used as the crosslinker in CBM fracturing fluids. It links the polymer as shown in Fig. 8.18.[26]

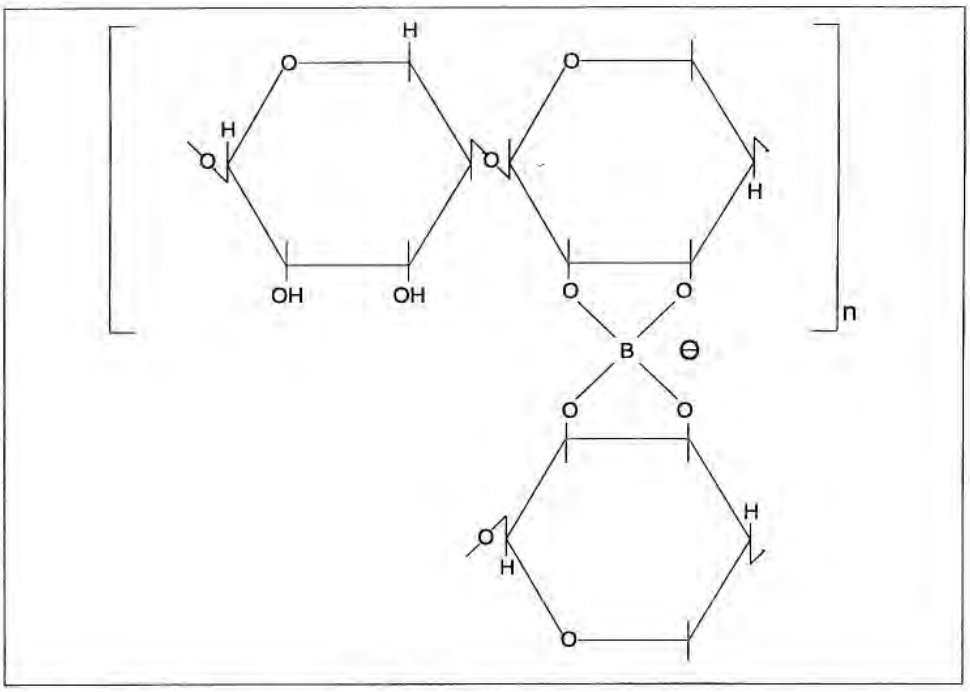

Fig. 8.18—HPG crosslinked with borate.[26]

The gel is shear thinning but reforms its structure with the borate ion crosslinker, making it easy to work with in the field. Apparent viscosity of the borate-crosslinked gel is high, and it provides excellent proppant transport. At the temperatures encountered in CBM wells, structures of the gel are stable and thus provide the viscosity needed for sand transport.[27] Black Warrior basin and San Juan basin temperatures of 105 to 120°F are in ranges that provide good proppant transport by fracturing fluids.[28]

The relationship of apparent viscosity to temperature for one HPG gel with borate crosslinker is given in Fig. 8.19.[27] Note that the apparent viscosity of HPG without crosslinker follows the relationship with temperature of Eq. 8.2, where the natural logarithm of the apparent viscosity is linear with the reciprocal of absolute temperature at temperatures where the polymer molecular structure does not dissociate. The gel's apparent viscosity is much higher, but its viscosity

decreases at the same rate as the polymer solution at temperatures encountered in CBM wells; the gel viscosity declines with temperature according to Eq. 8.2.

$$\mu_a = \beta\, e^{\alpha/T} \qquad (8.2)$$

where

μ_a = apparent viscosity
β, α = constants
T = absolute temperature

Higher temperatures above those encountered in CBM wells break the gel abruptly, and its viscosity declines to that of the base polymer solution.

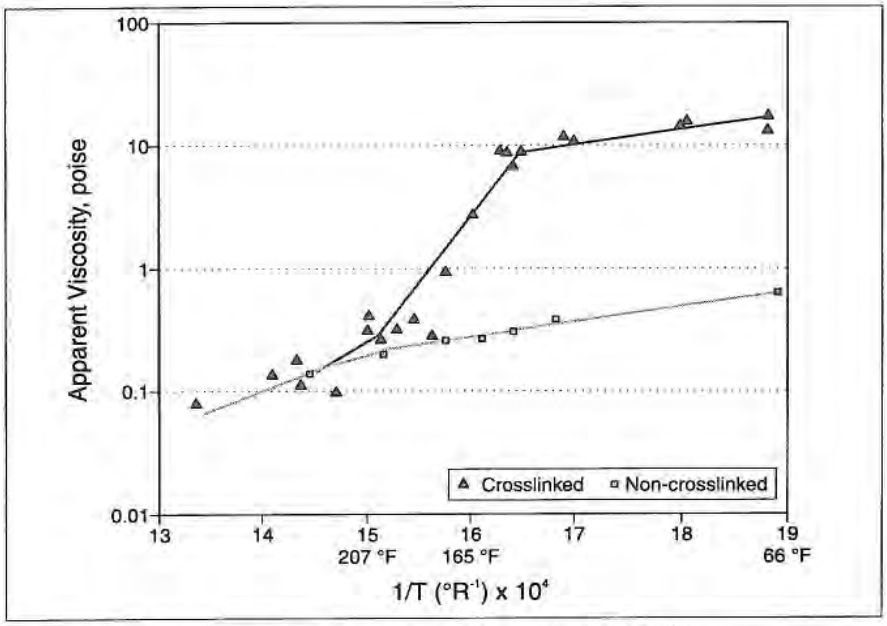

Fig. 8.19—Apparent viscosity of gelled fracturing fluids.[27]

Fracturing with gels maximizes the fracture length and increases proppant loading over longer distances. Good results have been reported in the Warrior basin as well as the San Juan basin. HPG polymers crosslinked with the borate ion as 30–35 lb of polymer per thousand gallons of solution are commonly used; less than 10 lb/gal of 20/40-mesh sand is common.[11]

Two examples of fracturing treatments of coalbeds are as follows. A typical fracture conducted by Taurus in the Mary Lee group was designed to use 12/20-mesh sand, filtered water, hydroxypropyl guar, and borate ion crosslinker. The process involved 63,000 gallons of fluid with 145,000 lb of proppant injected at 40 bbl/min; proppant load was ramped.[29]

In a second example, a 4,000-ft well in the San Juan basin was fractured with a 35 lb/1,000-gal HPG crosslinked with the borate ion. Fluid was injected at 55 bbl per minute, and proppant was injected in two stages: 22,000 lb of 40/70-mesh sand and 210,000 lb of 20/40-mesh.[28]

When compared to water as the fracturing fluid, crosslinked polymers have four possible disadvantages.

1. The cost is higher. For similar jobs, fracturing with a gelled fluid costs $50,000 while water fracturing costs $28,000 in the Oak Grove field of the Warrior basin.[7]
2. Chemicals in the gelled fluid may alter the surface properties of the coal.
3. The polymer or gel may plug flow channels. Gel may penetrate into the coal 50 ft from the vertical fracture and be trapped upon closure.[11]
4. Breakers added to the gel may be inadequate and leave unbroken gel in seams.

After research of fracturing fluids identified the possible damage mechanisms to coal, service companies have improved the performance of the crosslink gels. LGB systems have been optimized to provide high viscosity with 50% less polymer. Typical gel loadings have been reduced to 15–20 lb/Mgal of fluid. It is desirable to use a high-viscosity fluid that will transport sand efficiently while reducing fluid lost to the coal cleat system. Whole fluid invasion is the primary damage mechanism when deciding which fluids to use. Shallow coal plays

generally have low bottomhole pressure. The driving force to produce back fluids lost into the cleat system may not be present. The addition of nitrogen to the fluid system can help alleviate fluid loss and provide energy to return treatment fluids. Regardless of which fluid system is chosen, minimizing contact time with the coal is the best method of reducing damage. It is recommended that wellbores be cleaned and the well placed on pump within 72 hours of performing the stimulation treatment. This may mean delaying the stimulation treatment until production equipment is in place.

Guar systems are preferred over HPG systems to lower the cost of gelled fluids. High-performance enzyme breakers have been developed that eliminate instances of unbroken gel even at bottomhole temperatures as low as 55°F. Cleaner breaks mean higher regained conductivity (Fig. 8.20). In a survey done by Palmer, *et al.*,[30] LGB fluid was the predominant fluid used in the Raton basin with good results. In Appalachia, the use of nitrogen foams predominates. Crosslinked foams have been used to provide improved sand transport on higher permeability coals.

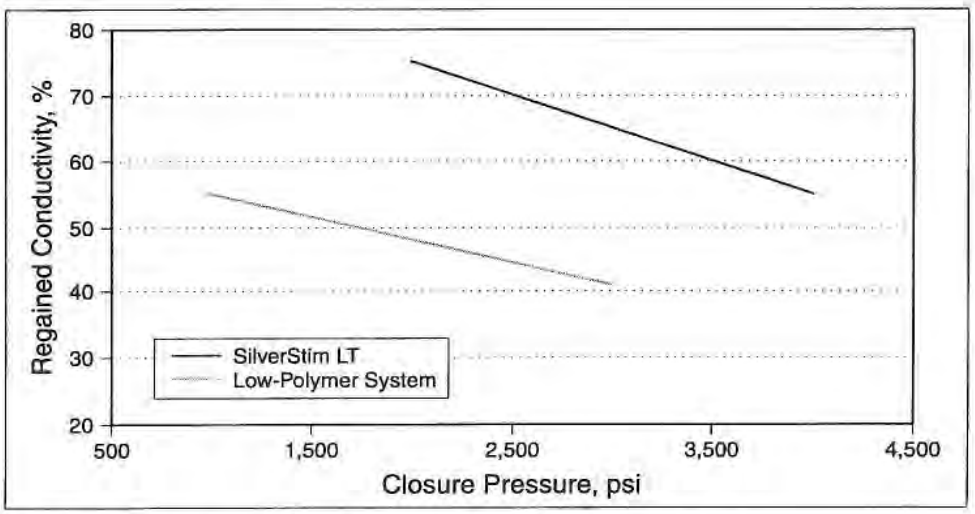

Fig. 8.20—Cleaner gel breaks yield higher regained conductivity.

8.3.1.1 Hydrogen Peroxide

As discussed in the previous section, polymers can penetrate the cleat system and cause damage. Even the lower gel-loading systems used today can leave residual damage. One emerging solution is the use of hydrogen peroxide (H_2O_2) as a cleanup aid. H_2O_2 is a strong oxidizer capable of dissolving guar and polyacrylamide, commonly used products in fracturing. Placement of H_2O_2 has been an issue of concern in the past.

Lack of process knowledge and understanding of risk have limited the use of H_2O_2. The rapid reaction of H_2O_2 with steel manifolding and tubulars prevented service companies from pumping it; operators did not want the safety liability. Halliburton has designed a process using composite coiled tubing, stainless pumping equipment, and a chemical stabilization system that allows safe placement of the product in the coal with minimal surface risk. Operators now have a safe, remedial, treatment process for removing gel damage from past treatments.

In addition, the reaction of H_2O_2 on minerals in the coal serves to enhance the cleat aperture, effectively increasing permeability. Reaction products are carbon dioxide and water, both commonly found in coal. This is highly desired by coal operators when the target zone is later to be mined.

One drawback of the process could be cost. Proximity of location to an inexpensive supply of H_2O_2 delivery could make the process economical. Cost of the delivery system would best be minimized with a sequence of wells when equipment is mobilized.

8.3.2 Water

Water has been used as the ultimate cheap, nondamaging fracturing fluid but with the major deficiency of reduced sand transport. Less than 5 lb/gal of a 12/20-sand has been used. Fracturing with water in coalbeds may pump only 1–1.5 lb/gal of sand without screenout; if the water flow rate is increased to carry more sand, the height of the fracture may grow. Excessive height growth of the

fracture in sand/water fracturing increases the problem of sand settling from the water. Propping a limited portion of the fracture is indicated in Fig. 8.21 from a simulation run by Amoco[6] to match the results of fracturing the Black Creek group in Alabama with water-carrying sand. Possibly, only one-third of the seams in the group were propped by the sand.

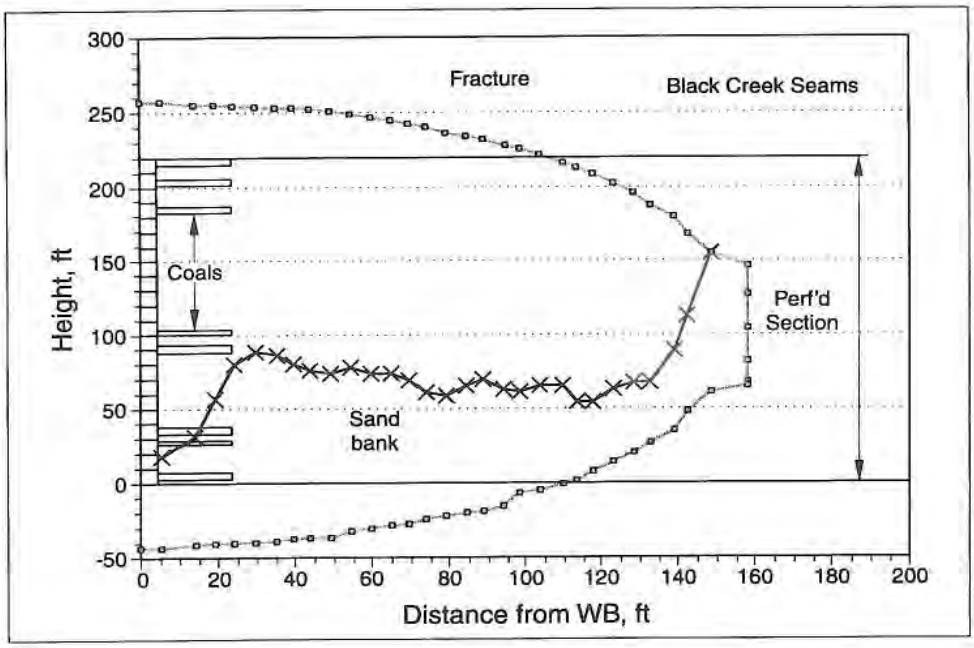

Fig. 8.21—Schematic of proppant distribution in water fracture.[11]

In the Oak Grove field, Amoco[30] evaluated the use of water without sand to fracture the Pratt, Mary Lee/Blue Creek, and Black Creek seams using ball sealers to direct fluid flow. The concept is to create fractures that are self-propping; slippage of the ragged fracture faces from shear stresses of the formation is supposed to support the fracture upon closure. Amoco concluded that the water fracture treatments with sand gave better gas production in the field than treatments with water alone.

Without proppant present, coal fragments may help support the fissure. If in-situ shear stresses cause slippage at the interface during fracturing, the rugosity of the faces may provide a propped fracture. Some successes with water fracturing in thin, multiple seams have been seen.

It is possible that water fracturing without sand creates fractures of less width and less stress redistribution. These restricted widths may close face cleats parallel to them less than wider fractures propped with sand, where closing of the parallel face cleats would divert gas flow to the less permeable butt cleats.[31]

8.3.3 Comparison of Gel and Water

A field study in the Oak Grove field of the Warrior basin compared water fracturing with gelled-fluid fracturing under controlled conditions.[11] Twenty-three wells were fractured, 13 with water-soluble crosslinked polymer and 10 with water. The selected wells were interspersed to avoid bias of location. Characteristics of the water and water-gel treatments are compared in Table 8.2. The tabulation shows approximately a 50% cost saving from the water-fracturing treatment, but the gel fluid transported more than twice as much proppant. The coals were of good permeability and boreholes were cased and perforated as indicated in Table 8.3. After 12 months of production, the water-fractured wells had 20% more methane production with less formation water production. Apparently, although the gel created longer and better propped fractures through more seams, the shorter and poorly propped water fractures had negligible formation damage. The tradeoff in this case of a high-permeability coal favored the water treatment.

Table 8.2—Comparison of Water and Gel Fractures[11]

Characteristic	Water	Gel
Chemicals	No polymer	Borate crosslink, HPG, 30 lb/1,000 gal
Proppant	<5 lb/gal 12/20 70,000 lb/zone	10 ppg 12/20, 100,000 lb/zone
Flow rate, bbl/min	50 to 60	40
Number of wells	10 Oak Grove	13 Oak Grove
Production	12 months	12 months
Cost, USD	$28,000	$50,000
Efficiency, %	<20	50 to 80

Table 8.3—Field Properties of Oak Grove Pilot[11]

Parameter	Comments
Permeability	5 to 20 md
Completions	• Cased and perforated. • Individual seams of Black Creek and Mary Lee/Blue Creek. • Perforated, stimulated Black Creek. • Repeated Mary Lee/Blue Creek.
Depth	2,000 ft—Black Creek 1,500 ft—Mary Lee/Blue Creek

The comparison was broadened to include the results from additional fracturing fluids in the San Juan basin as well as the Warrior basin. Sandless water fractures, water with sand fractures, crosslinked gel fractures, sandless water refractures, and cavity completions were compared[30] (see Table 8.4).

Table 8.4—Comparisons of Stimulation Treatments[30]

Basin	X	Y	Gas Production X/Y	Stimulation Cost X/Y
San Juan	Cavity	Gel	5 to 10	11.0
San Juan	WFS	Gel	2.5	0.5
Black Warrior (Oak Grove)	WFS	Gel	1.2 to 1.4	0.5
Black Warrior (Oak Grove)	WFS	SWF	1.9	2.0
Black Warrior	SWF refracture	Gel original fracture	2.0	0.25

The results indicate a cost savings with the water, formation damage with gels, and a need for proppant support of the fracture. A special case is indicated in the San Juan basin where a good permeability and cleat system are sensitive to formation damage.

A somewhat similar study by Taurus in the Cedar Cove field of the Warrior basin indicated a better performance of the crosslinked polymer than the water fracturing fluid in the first nine months of production,[29] where a long, propped fracture apparently overshadowed formation damage to increase production.

8.3.4 Foam

Nitrogen foam is a gas-in-water emulsion made stable by the addition of a surfactant and a viscosifying agent, such as HEC or HPG. The quality of the foam, or volume percentage of nitrogen in the foam, may range from 60–90%.

Nitrogen foam reduces formation damaging effects of the fracturing fluid for the following reasons:

- The nitrogen provides energy to clean the fracturing fluid from the formation.
- The foam requires about 70% less water than a gel.[32]
- HEC is used at reduced levels and is a less damaging viscosifier.
- Foam has better leakoff characteristics.

In addition to assisting fluid cleanup, the nitrogen released from the foam acts to enhance methane desorption and production. The mechanism is to reduce partial pressure of methane in the coal, thereby creating a concentration gradient for diffusion of methane from the micropores.

Nitrogen does not cause appreciable swelling of the coal because it is less readily adsorbed than the methane. Carbon dioxide, if used in the foam, could induce detrimental matrix swelling because it is preferentially adsorbed by the coal.

Advantages of nitrogen foam as a fracturing fluid may be summarized as follows:

- Cleans up quickly from the induced fracture.
- Leaves virtually no unbroken fluid.
- Leaves a minimum residue to plug the reservoir.
- Inflicts minimum damage to coal.
- Enhances CH_4 desorption by lowering CH_4 partial pressure.
- Provides good proppant transport.
- Reduces leakoff.

The disadvantages of a foam fracturing fluid for coals are as follows:

- More expensive.
- More difficult quality control.
- Difficult to characterize rheologically.

A laboratory analysis of permeability damage to Warrior basin coal (Blue Creek seam) from flow contact with a 70% nitrogen foam showed a high recovery of permeability after the test. The continuous phase of the foam was 2% KCl in water, viscosified with HEC polymer as 30 lb of polymer per 1,000 gal of liquid. The results in Fig. 8.18 illustrate the nondamaging aspects of N_2 foam fracturing fluids,[33] as 78% of the permeability had been recovered shortly after foam

treatment, and improvement was continuing at that time. Although more expensive than HPG, the HEC polymer is less damaging to the formation.[34]

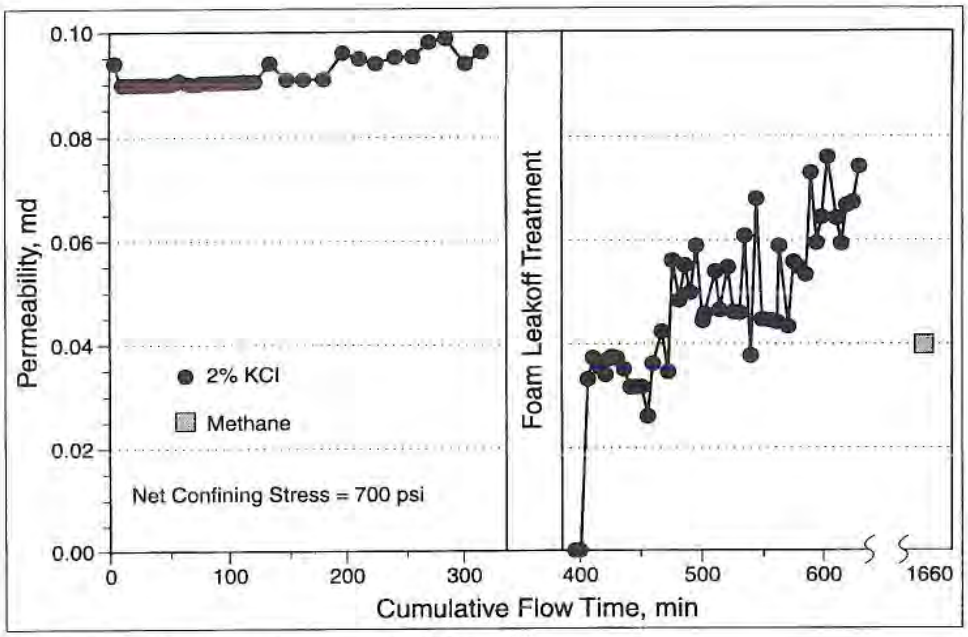

Fig. 8.22—Nondamaging aspects of foam.[33]

8.3.5 Proppant Considerations

Sand proppant has sufficient strength for CBM applications, so it is the economical and practical choice.

Some common problems encountered in conventional fracturing involving proppant are magnified in coalbed fracturing: (1) embedment of proppant into the matrix of the soft formation, (2) trapping of large volumes of fines by the proppant, (3) leakoff of the sand-bearing fluid into secondary fissures and cleats, and (4) transport of the proppant through a tortuous path.

Because of the soft, elastic properties of coal, proppant embeds in the coal matrix to reduce conductivity. In doing so, it causes spalling of the fracture face. Consequently, the coal chips that collect in the sandpack further contribute to the deterioration of fracture conductivity.[25] As described by Eq. 8.3, the initial width of the packed sand in the fracture is decreased to eventually give an effective sandpack width, W_{eff}.

$$W_{eff} = W_i - \Delta W_c - \Delta W_{emb} - \Delta W_s \qquad (8.3)$$

where

W_{eff} = effective sandpack width
W_i = initial sandpack width
ΔW_c = sandpack compression
ΔW_{emb} = sand embedment
ΔW_s = sand width loss due to spalling

Hardness of coal, the property affecting embedment, is difficult to measure in the laboratory because of the randomness of fissures and the introduction of fractures from handling of the sample.[35] A general indication of the susceptibility to proppant embedment as a function of coal rank is given in Fig. 8.23. It is evident from Fig. 8.23 that the hardness of coal increases rapidly at the anthracite rank. Low-volatile bituminous and medium-volatile bituminous coals are most subject to proppant embedment.[35,36]

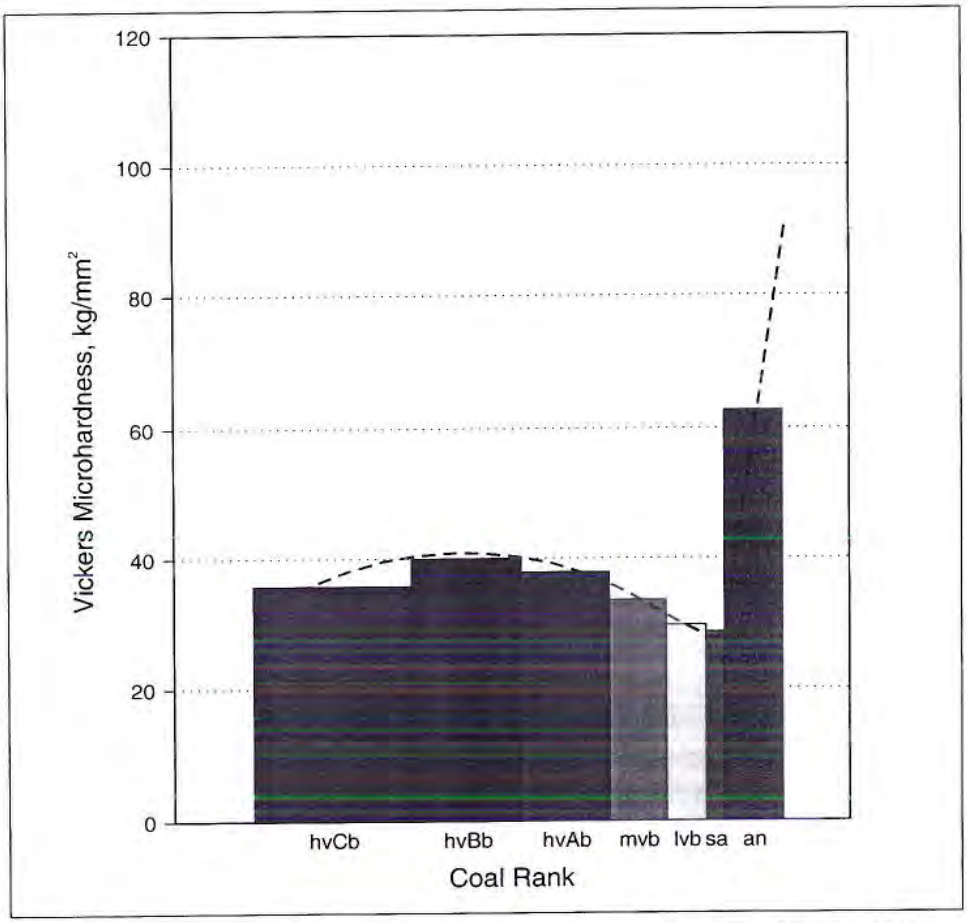

Fig. 8.23—Relative embedment potential of coal ranks as determined by Vickers microhardness.[35,36]

Higher loadings of the proppant in the fracture will alleviate the problem. Holditch[37] concludes that the fracture design should be for proppant loadings of 1.0 lb/ft^2.

Three other problems—fines, leakoff, and tortuous path—might be alleviated by proper selection of size distribution for proppant and their schedule of introduction. Radioactive tracers amid 100-mesh, 40/70-mesh, and 12/20-mesh proppant used in the San Juan basin confirmed[24] that the 100-mesh and 40/70-mesh sands become segregated from the 12/20-mesh sand, each size situated in a particular part of the induced and natural fracture system.[24] The mechanism is one of the small particles located at the openings of secondary and tertiary cleats and obstructing flow into the cleats, thereby forcing more fracturing fluid to be diverted into the main induced fracture. The diverted flow creates larger widths in the main fracture to accommodate the 12/20-mesh sand. Therefore, not only does the finer fraction of proppant reduce leakoff, but in the process indirectly helps place the larger proppant in the primary fracture, prevents bridging in the primary fracture, and reduces tortuosity of the primary fracture.

A proper size distribution of proppant helps prevent the movement of sand and coal fines through the proppant bed to the wellbore. Holditch, *et al.*[37] propose a schedule of the following: 100-mesh sand for secondary fissure blocking and deep penetration, followed by 40/70-mesh sand to screen coal fines and proppant flowback, followed by 20/40-mesh sand to reduce flow resistance near the wellbore.[37]

8.4 In-Situ Conditions

8.4.1 Rock Properties

The mechanical properties of the coal determine the reaction of the rock to imposed stresses of fracturing. Elastic properties determine the effect of imposed or in-situ stresses on existing natural fractures or previously created hydraulic fractures, directly affecting the permeability of the rock system. In coalbed reservoirs, rock mechanical properties and related stresses are of great concern.

Young's modulus is an elastic property of rock defined by Eq. 8.4 that gives a measure of fractional elongation as a consequence of stress imposed on the rock.

$$E_x = \frac{\sigma_x}{\varepsilon_x} \qquad (8.4)$$

where

E_x = Young's modulus (psi)

σ_x = stress, x direction (psi)

ε_x = strain (x direction)

Young's modulus is important in establishing the width of the fracture in the coal, and it plays a minor role in limiting fracture height. Maximum width, w, of a fracture near the wellbore is inversely proportional to the fourth power of Young's modulus[38] as in the fracturing model of Geertsma and de Klerk.[38]

$$w \sim \left(\frac{1}{E}\right)^{1/4}$$

Soft, elastic coal of low Young's modulus will be conducive to a wide fracture. Conversely, hard formations may be adjacent to the coalseam and have a constricted flow path in the fracture.[32] Minethrough observations in the Oak Grove field show sand-propped fractures 1.5 to 2.5 in. wide within 10 ft of the wellbore.

Some representative rock properties of coal and its bounding rock from microfracture tests are presented in Table 8.5.[39-41] The table illustrates a factor of ten contrast in Young's modulus, E, of coal and adjacent rock, as well as its substantially higher Poisson's ratio, ν.

The surrounding rock will represent a high percentage of the overall formation thickness in the multiple, thin seams of basins similar to the Black Warrior.

The high modulus of adjacent rock contrasted with the low modulus of coal will contribute to confining a fracture in the coal, but the confinement from modulus is secondary to restraints to fracture growth from in-situ stresses.

Table 8.5—Contrasting Elastic Properties of Coal and Bounding Rock[39-41]

E_{coal} (psi)	$E_{bounding}$ (psi)	ν_{coal}	$\nu_{bounding}$
290,000 German Creek	3,481,000	0.35	0.22
300,000 Bowen Basin	2,320,000	0.39	0.23
400,000 Mary Lee	7,000,000	0.35	0.20 Shale

Data from van Krevelen[42] illustrate the effect of coal maturation on Young's modulus in Fig. 8.24. For hvAb-rank coal through lvb-rank, Young's modulus is unchanging, but beginning with anthracite, the modulus increases rapidly. Again, the modulus is affected by fissures in the rock, and it is difficult to make laboratory measurements that are representative of field conditions.

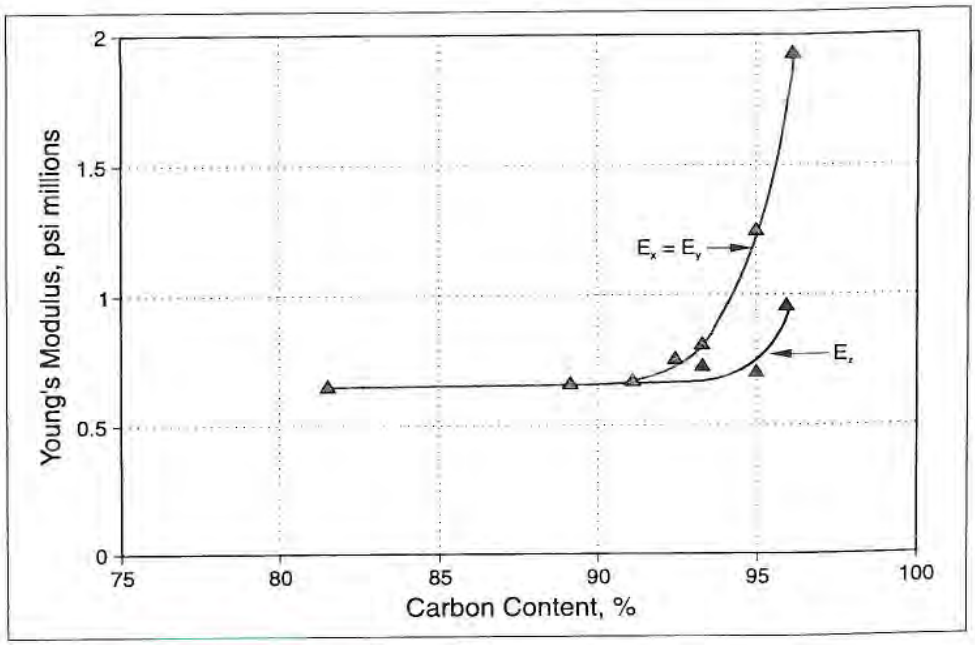

Fig. 8.24—Young's modulus of coal.[42,43]

Young's moduli measured[44] from core analyses across the Mary Lee zone and the Black Creek zone (formations from Black Creek to Mary Lee/Blue Creek seams) in Alabama are illustrated as a function of the depth in Fig. 8.25. An average non-coal value of $E = 2.5 \times 106$ psi was determined by Palmer and Sparks[4] to exist across the zones. (Typically, Young's modulus for coal would be 100,000–500,000 psi.[37]) History matching with the simulator by Lambert, *et al.*[45] showed that a value of Young's modulus of about 1.3×106 psi would best account for pressures encountered during the fracturing.[45] Fractures in the formation would effectively reduce Young's modulus so that core evaluations in the laboratory supply an upper-limit value.[37]

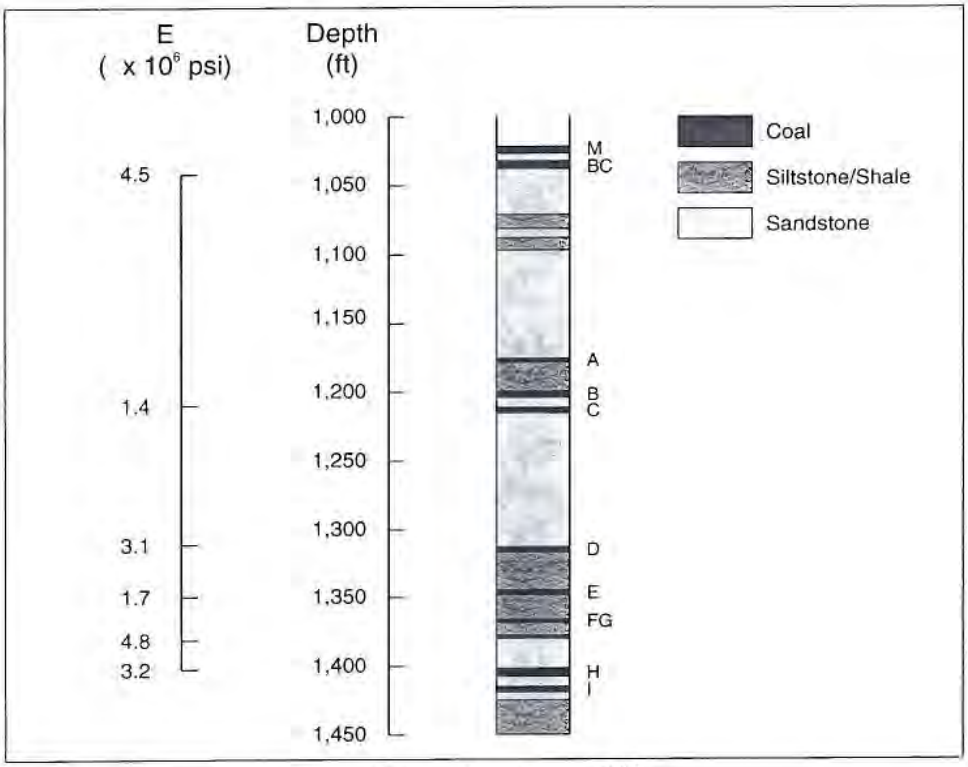

Fig. 8.25—Young's modulus of Black Creek zone.[4,45]

Poisson's ratio is an elastic property of rock defined by Eq. 8.5 that is a measure of the lateral expansion as compared to the longitudinal contraction for a longitudinally imposed load, the ratio of transverse strain to longitudinal strain.[46]

$$\nu = -\frac{\varepsilon_2}{\varepsilon_1} \qquad (8.5)$$

where

ν = Poisson's ratio

ε_2 = strain or fractional lateral expansion

ε_1 = strain or fractional deformation in longitudinal direction

The sign convention establishes expansion as the negative direction. Poisson's ratio for the reservoir rock and surrounding rock influences the stress profile, the reservoir parameter that defines fracture boundary and orientation. It is a factor in determining fracture width. Poisson's ratio and Young's modulus are essential for fracture model evaluations.

8.4.2 Stress

In-situ minimum stress differences of strata limit fracture height growth, and large differences in the strata of Young's modulus limit fracture height growth. Coal usually has a much smaller Young's modulus than the surrounding rock, and in the case of the Fruitland coal adjacent to the Pictured Cliffs sandstone, an order of magnitude less.[24] It has been determined that modulus contrasts are subservient to in-situ stresses in limiting fracture height growth. The effect is for the fracture induced in such strata of different modulus to conform to the stress pattern, so that strata of high stress rather than elastic properties of the rock will restrict fracture height growth.

For an idealized depiction of high-stress areas confining a fracture to the coalseam, consider Fig. 8.26. A vertical fracture propagates perpendicular to the minimum horizontal stress and is limited in height by bounding strata of high stress.

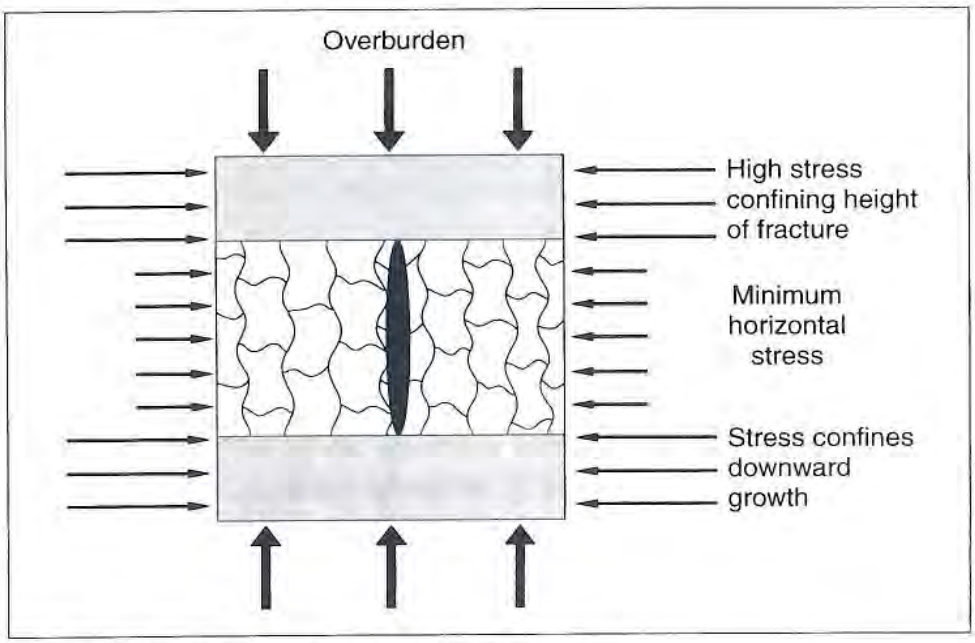

Fig. 8.26—Fracture height confined by stresses.

Fracture height is controlled by in-situ stresses of the formations. As an example, minifrac tests determined stress variations at the Department of Energy's multiwell experiment site in the lower Mesaverde group of the Piceance basin.[47] The results showed a large in-situ stress variation of about 2,000 psi over a short distance of 100 ft of formation between the Cozzette sandstone and the highly stressed Mancos shale, seen in Fig. 8.27. The stressed shale would limit fracture height growth if the sandstone were to be fractured; the fracture would be confined to the Cozzette. A lateral, high-stress area would pinch out the vertical growth of the fracture.[48]

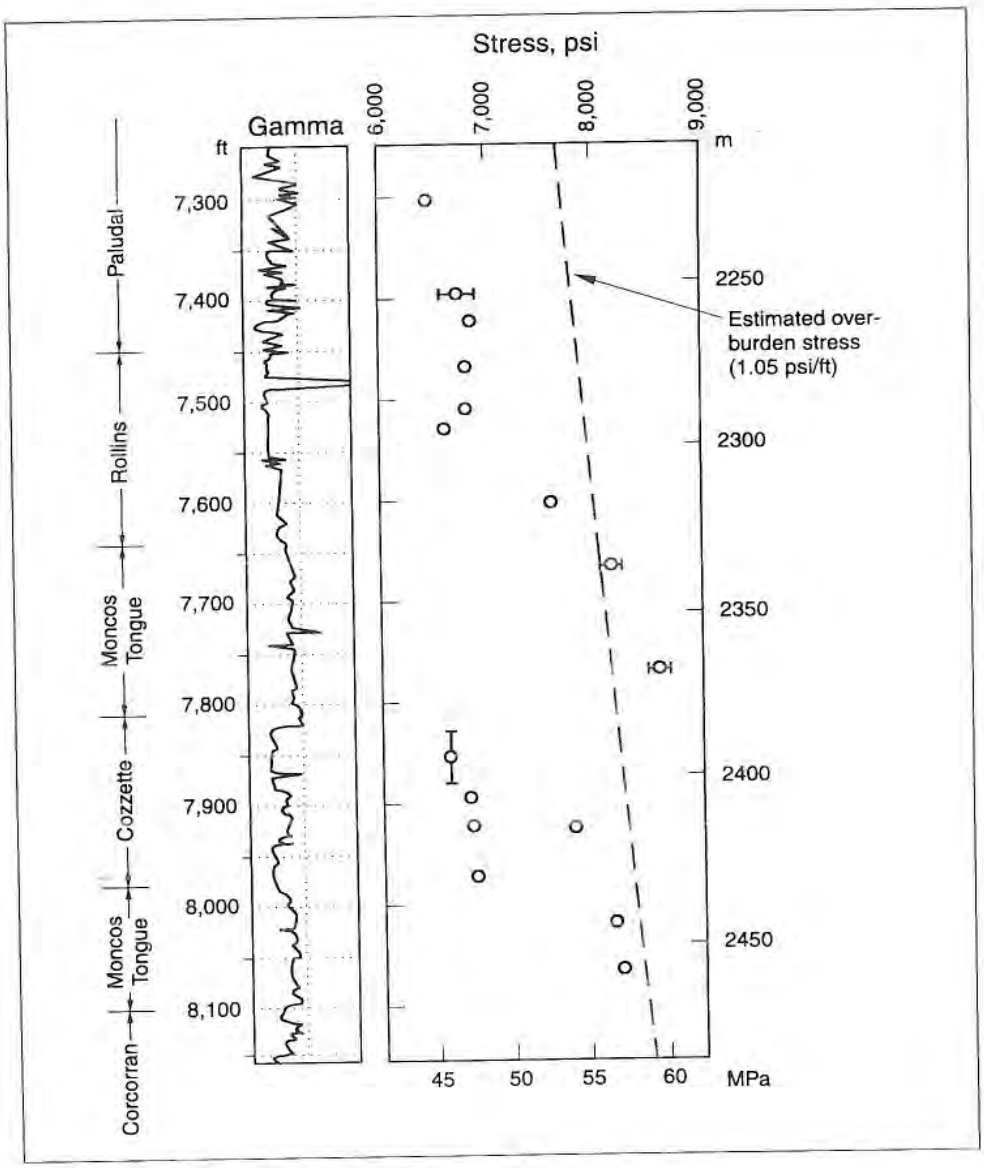

Fig. 8.27—In-situ stress measurements.[47]

Minimum in-situ stress profiles were established from microfracture tests made at the Rock Creek site of the Warrior basin.[45] The profile for depths of 1,000–1,450 ft spanned the Mary Lee/Blue Creek seams at about 1,200 ft to the deepest Black Creek seam at approximately 1,415 ft. The stress profile is presented in Fig. 8.28. Forty miles from Rock Creek at Moundville in the Warrior basin, stress profiles have been found to be similar.

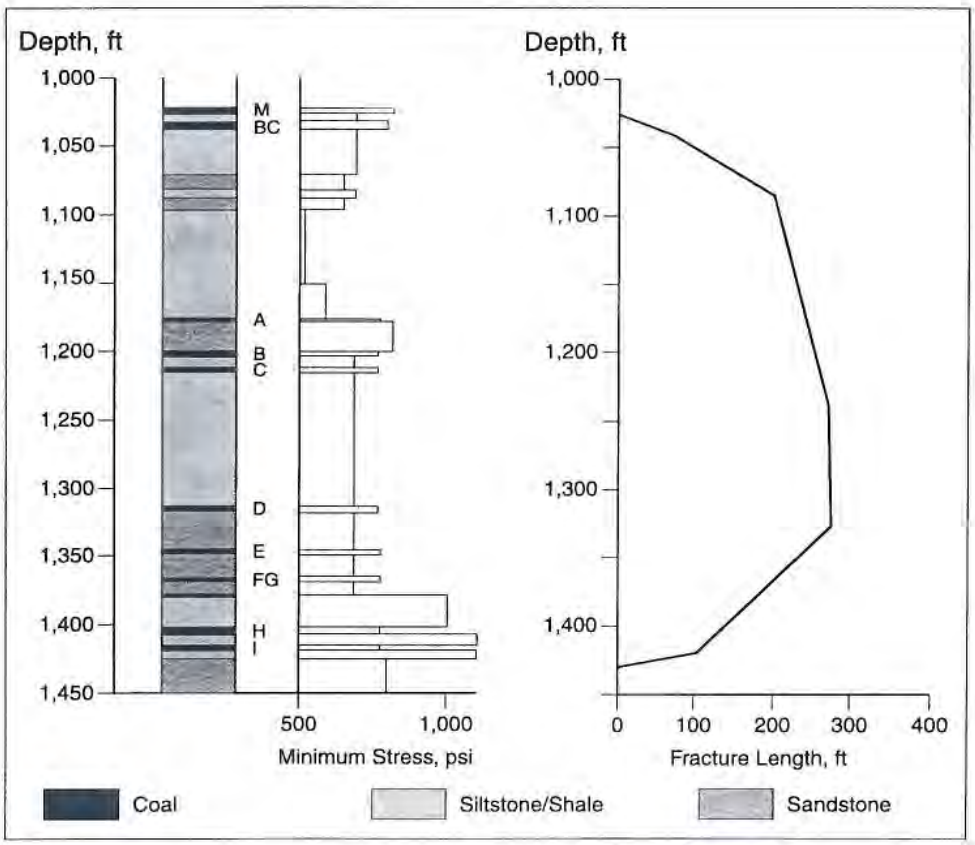

Fig. 8.28—Stress profile Black Creek zone.[45]

Note the high stress in the siltstone/shale interbedded with the lower seams of the Black Creek group. A fracture initiated through perforations in the lower Black Creek should not grow downward but possibly extend upward into the Mary Lee/Blue Creek seams. Fig. 8.28 depicts the fracture that spanned the multiple seam interval.

After the stress profile was obtained, fracturing with crosslinked gel resulted in a fracture propagating from the perforations at 1,375–1,383 ft upward into the Mary Lee/Blue Creek seams, and the fracture propagated downward far enough to intercept the lowermost Black Creek seams. Communication between the coal groups was evident.

The stress profile over an interval of multiple seams shown in Fig. 8.28 raises the possibility of lowering costs of completing and making marginally economical properties profitable by fracturing all the seams of one zone in one operation. The stresses must limit the fracture to the desired interval.

Another example of the effects of stress contrasts of the coal and bounding strata occurs in the northwestern part of the San Juan basin, where Pictured Cliffs sandstone below the coalseam at about 2,900 ft has a stress value 746 psi less than the coal; the fracture grows across the interface into the sand, even though Young's modulus of the sandstone is an order of magnitude larger.[24]

A general indication of the orientation that a fracture will take is given in Fig. 8.29 where a vertical fracture develops perpendicular to the least principal stress, which in this case is the minimum horizontal stress. Similarly, Fig. 8.29 depicts the case where a horizontal fracture is possible if the overburden weight is less than the lateral stress, as might be the case in a very shallow coalseam. The minimum in-situ stress orientation determines the orientation of the fracture.[49] This is true of the general trend of the fracture. Localized trends follow butt and face cleats in a highly irregular path.

The advent of CBM operations with minethrough afforded visual observations of the hydraulic fracture. Consequently, minethroughs gave insight into when a horizontal or a vertical fracture would occur.

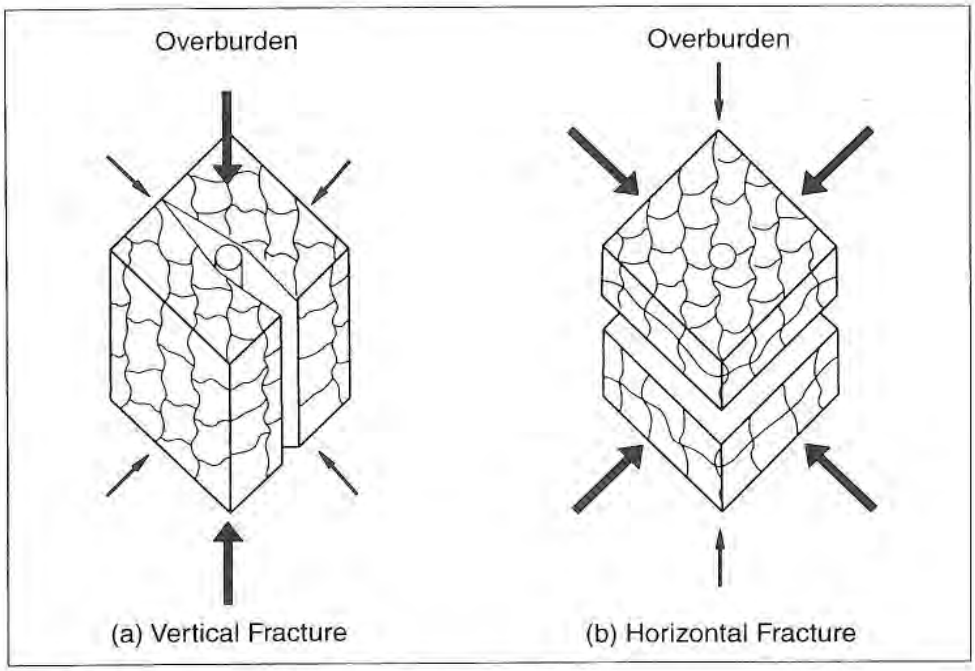

Fig. 8.29—Stresses orient fracture in coals.[48]

Horizontal fractures have been observed shallower than about 750 ft; vertical fractures occur in the coalseams deeper than 2,000 ft.[38] In between either of the two, orientations or inclined fractures occur.

A horizontal component of the fracture may be created at the coal and roof rock interface if the shear strength, τ, of the interface described by Eq. 8.6[32] is less than the tensional stress of the propagating fracture. Therefore, if a low coefficient of friction of the interface or a low normal stress acting on the interface or the product of these two parameters are present, slippage at the interface will occur to terminate the vertical growth of the fracture. The amount and type of fill material at the interface and the rugosity of the two faces determine τ_o and μ_f. The normal stress decreases at shallower depths.

$$\tau = \tau_o + \mu_f \sigma_n \qquad (8.6)$$

where

τ = shear stress at interface to overcome cohesive and friction forces

τ_o = cohesive shear strength of interface

σ_n = normal stress

μ_f = coefficient of friction

The combination of normal stress and friction coefficient that gives a low value of shear stress will be conducive to the horizontal propagation of the fracture at unbonded interfaces. If the overburden stress is low, as it is at the depth of many CBM seams, the T-shaped fracture is more likely to occur. The T fracture has been amply documented in minethroughs.

With the relationship of increasing normal stress with depth, the horizontal component of the T is more often found in the roof than in the floor of the seam.[24] Fractures of T shape with a horizontal component have been observed at the roof of coalseams in the San Juan and Warrior basins of the United States and the German Creek mine of Australia.[19,39]

If the coal and bounding strata at the interface are bonded and the minimum stresses of the two strata at the interface are similar, the relative elastic properties of the two rocks and strength of the interface, τ_o, determine whether the fracture propagates across the boundary.[47]

Slippage also may occur as the fracturing fluid increases macropore pressure within the coal in the natural fracture system. Thus, by decreasing coefficient of friction and allowing coal faces to slip relative to each other, permeability of the coals may be permanently altered.[10]

Stress profile is the most important parameter for designing fracture heights. The stress is also important in determining proppant embedment, horizontal or vertical fractures, proppant crushing, surface treating pressures, fracture azimuth, and widths of the fracture.[32]

8.4.3 Determining Stress Values

Stress profiles of the coal and other rock strata between coal groups may be obtained by pump-in microfracture tests. Microfractures involve pumping a small volume of fluid into the formation and measuring the instantaneous shut-in pressure (ISIP), which is close to the value of the minimum horizontal stress. The method is reliable when used in low-permeability rock having less than 1 md of restricted leakoff.[47] Microfracturing provides stress measurements for the few discrete points tested. The procedure is relatively expensive and often neglected. However, an increasing emphasis is being placed on importance of in-situ stresses to CBM production.

Two important series of in-situ, state-of-stress (ISSOS) tests were conducted for the GRI in the Piceance and Warrior basins.[50,51] The steps used in their microfracture techniques were similar in each basin. The procedure is summarized as follows:

1. Isolate the test interval of the formation with straddle packers.
2. Inject 10–20 gal of fresh water at 4–6 gal/min.
3. Break the formation.
4. Extend the fracture at constant pressure for 1 minute.
5. After shut-in, monitor the pressure decline.
6. Take the ISIP as the minimum horizontal stress.

If the comprehensive pump-in tests require unacceptable time and expense, an estimate of minimum horizontal stress can be made with Hubbert's equation (Eq. 8.7).

$$\sigma_{\min} = \left(\frac{\nu}{1-\nu}\right)(\sigma_z - p_R) + p_R + \sigma_E \qquad (8.7)$$

where

σ_{min} = minimum horizontal stress (psi)
ν = Poisson's ratio
σ_E = externally generated stress (psi [must be measured])
p_R = reservoir pressure (psi)
σ_z = overburden stress

To profile the stresses in the coal zone, Poisson's ratio is needed. With Poisson's ratio, reservoir pressure, and overburden stress the horizontal stress may be calculated according to linear elastic theory. The calculation would be complete if external horizontal stresses were not present and if the rock were in a relaxed state. When tectonic action or nearby mountain ranges have created significant horizontal stresses, the calculations without external stresses are not accurate. For example, Warpinski showed that calculated values of stress from the equation on the lower Mesaverde group in the Piceance basin, which is subjected to large external stresses, did not match well with measured values.[47]

In the most comprehensive evaluation of Eq. 8.7, Sparks detailed the importance of σ_E in the Cedar Cove field of Alabama.[52] Fig. 8.30 presents the minimum principal stress as calculated from Eq. 8.7 without any contributing compressional tectonic forces, where this calculation is presented as the lower straight line. Closure pressures from microfracture tests in the 400 wells throughout the field, as an approximation of the minimum principal stress, were then superimposed on the calculated line of Fig. 8.30. Most of the closure pressures fall above the calculated base line, and their distance above the base line represents the magnitude of tectonic stress, σ_E. It is evident that tectonic forces cannot be neglected in most of the Cedar Cove field.

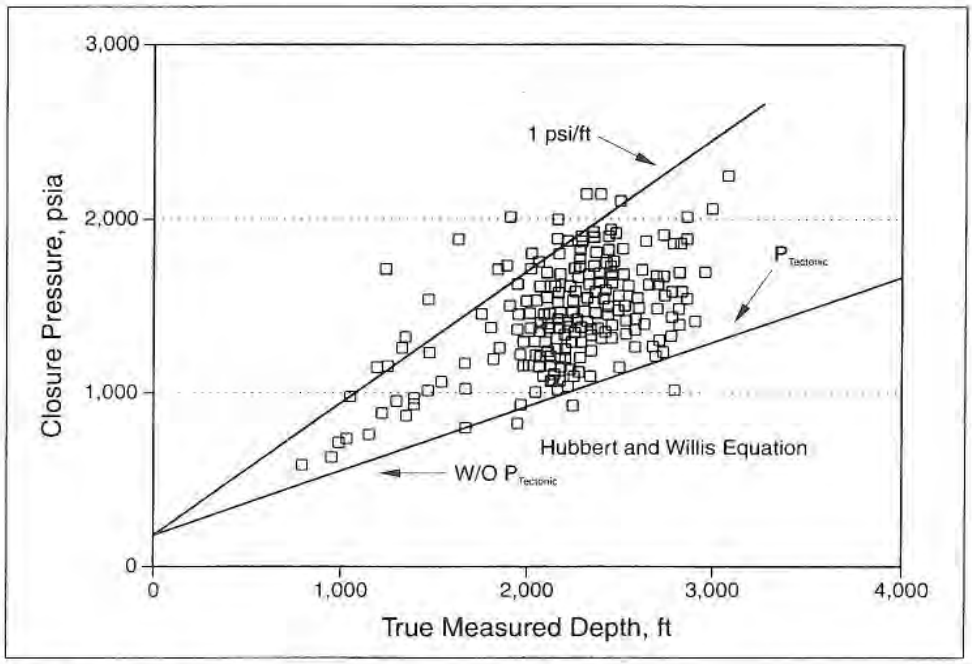

Fig. 8.30—Minimum principal stresses at Cedar Cove.[52]

Poisson's ratio may be determined from cores stressed in the laboratory in a static test, or it may be determined on undisturbed coal in place in the formation from analysis of sonic logs as a dynamic test. Unfortunately, static tests result in a lower elastic constant, as the cleats and fissures of the coal are not affected in the dynamic tests but are in the static tests.

8.5 Visual Observation of Fractures

The intersection of hydraulically induced fractures by mines has afforded the first opportunity to view fracture characteristics. A study by the U.S. Bureau of Mines investigated the fracture characteristics of 22 stimulation treatments that had

been mined through. From those investigations, Diamond and Oyler[19] reported the sand-propped fracturing of a 5.6-ft coalseam with a vertical fracture 0.5 in. wide. A T-shaped fracture formed at the coal/shale interface of the roof, and the horizontal fracture component was filled with sand (see Fig. 8.31). No horizontal component occurred at the floor interface.

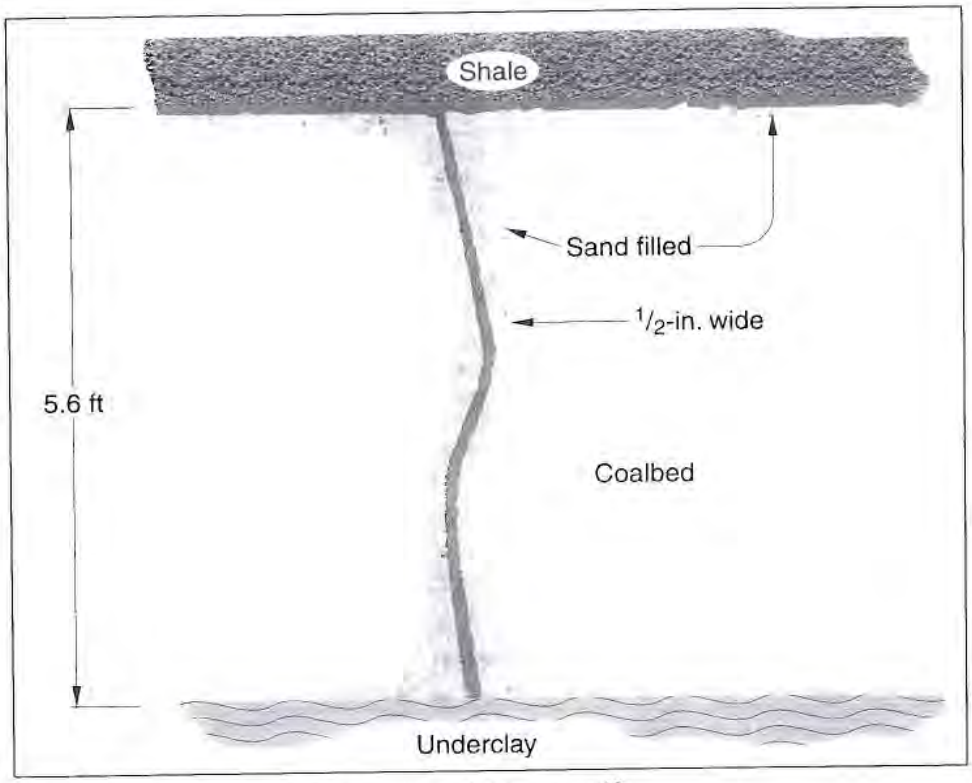

Fig. 8.31—Minethrough observation of T fracture.[19]

Fractures of T shape were observed in minethroughs at the German Creek mine in Australia.[39] The horizontal segment of the fracture occurred at the roof interface, where most of the proppant was deposited. The horizontal fracture was elliptical with the major axis in the direction of maximum stress.

Further documentation of the horizontal component of the fracture at the roof parting of the coal comes from radioactive proppant tracer used in fracturing Fruitland coals of the San Juan basin.[24] The tracers profile horizontal components of the fracture at the roof of the coal. Furthermore, the horizontal fracture is found more often at the top of the coal than at the floor.

The vertical fracture is terminated by a high in-situ stress rather than a difference in rock elastic properties. The phenomenon is indicated in the minethrough observations of Warpinski.[49] In his noncoal application, a hydraulic fracture was induced from a horizontal wellbore in a low modulus formation. The induced fracture propagated across the interface without a horizontal component, as the induced crack moved in a continuous fashion without offset upon entering a high modulus formation. However, the fracture terminated in the downward direction at a high-stress peak in the low modulus formation below.

The offset of a fracture at the coal interface was also observed in the downhole telemetry of Palmer and Sparks.[4] Their observations in the Black Creek coals of the Warrior basin are presented in Fig. 8.32.

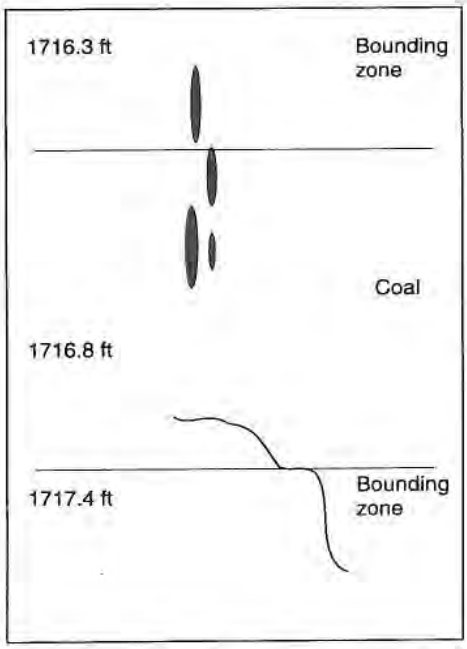

Fig. 8.32—Downhole camera results.[4]

Extensive fractures that were induced by hydraulic fracturing in vertical CBM wells have been observed in minethroughs. A long fracture, generated by a large water treatment with 100-mesh and 20/40-mesh sand and documented by minethrough, is reported by Steidl[20] and illustrated in Fig. 8.33. The fracture was observed to extend 525 ft from the wellbore and to be propped with sand at point I, 352 ft from the well.[20] The maximum observed width of the fracture was 0.3 in.

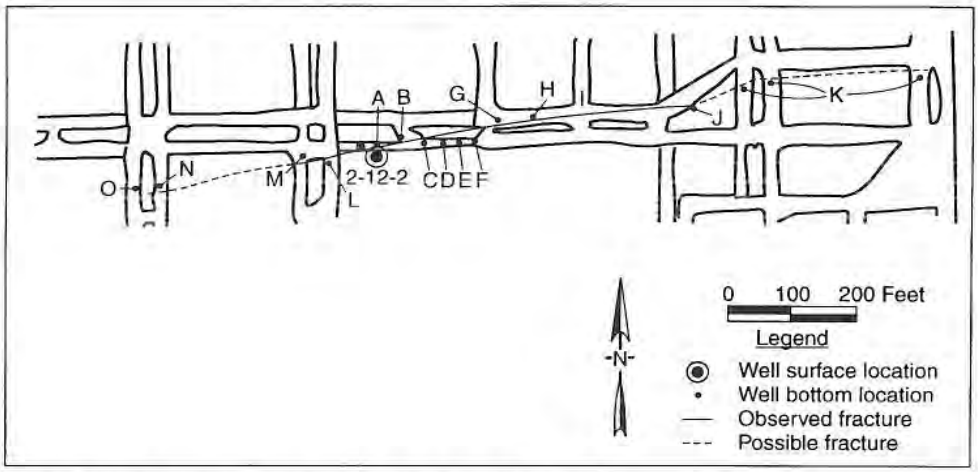

Fig. 8.33—Minethrough documents long fracture.[20]

References

[1]Hunt, A.M. and Steele, D.J.: "Coalbed Methane Development in the Northern and Central Appalachian Basins—Past, Present and Future," *Proc., Coalbed Methane Symposium*, Tuscaloosa, Alabama (May 1991) 127-141.

[2]Spafford, S.D. and Schraufnagel, R.A.: "Multiple Coal Seams Project," *Quarterly Review of Methane from Coal Seams Technology* (July 1992) 10, No. 1, 15-18.

[3]Spafford, S.D.: "Stimulating Multiple Coal Seams at Rock Creek with Access Restricted to a Single Seam," *Proc., Coalbed Methane Symposium*, Tuscaloosa, Alabama (May 1991) 243-246.

[4]Palmer, I.D. and Sparks, D.P.: "Measurement of Induced Fractures by Downhole TV Camera in Black Warrior Basin Coalbeds," *JPT* (March 1991) 43, No. 3, 270.

[5]Khodaverdian, M., McLennan, J.D., and Jones, A.H.: "Spalling and the Development of a Hydraulic Fracturing Strategy for Coal," final report, GRI-91-0234 (April 1991) 43.

[6]Jeffrey, R.G., Hinkel, J.J., Nimerick, K.H., and McLennan, J.: "Hydraulic Fracturing to Enhance Production of Methane from Coal Seams," *Proc., Coalbed Methane Symposium*, Tuscaloosa, Alabama (April 1989) 385-394.

[7]HO3679, Halliburton Internal Sales Data Sheet.

[8]HO2289, Halliburton Internal Sales Data Sheet.

[9]Puri, R., King, G.E., and Palmer, I.D.: "Damage to Coal Permeability During Hydraulic Fracturing," *Proc., Coalbed Methane Symposium*, Tuscaloosa, Alabama (May 1991) 247-255.

[10]Warpinski, N.R.: "Hydraulic Fracturing in Tight, Fissured Media," *JPT* (February 1991) 43, No. 2, 146.

[11]Palmer, I.D., Fryar, R.T., Tumino, K.A., and Puri, R.: "Comparison Between Gel-Fracture and Water-Fracture Stimulation in the Black Warrior Basin," *Proc., Coalbed Methane Symposium*, Tuscaloosa, Alabama (May 1991) 233-242.

[12]Spafford, S.: "Re-Stimulation Treatments for Poorly Performing Wells," paper presented at the 1992 Eastern Coalbed Methane Forum, Tuscaloosa, Alabama, 1 September.

[13]Spafford, S.D. and Schraufnagel, R.A.: "Multiple Coal Seams Project," *Quarterly Review of Methane from Coal Seams Technology* (October 1992) 10, No. 2, 17-21.

[14]Bell, G.J., Jones, A.H., Morales, R.H., and Schraufnagel, R.A.: "Coal Seam Hydraulic Fracture Propagation on a Laboratory Scale," *Proc., Coalbed Methane Symposium*, Tuscaloosa, Alabama (April 1989) 417-425.

[15]Davidson, B.M., Saunders, B.F., Robinson, B.M., and Holditch, S.A.: "Analysis of Abnormally High Fracture Treating Pressures Caused by Complex Fracture Growth," paper SPE 26154 presented at the 1993 SPE Gas Technology Symposium, Calgary, Canada, 28-30 June.

[16]Cleary, M.P. *et al.*: "Field Implementation of Proppant Slugs to Avoid Premature Screen-out of Hydraulic Fractures with Adequate Proppant Concentration," paper SPE 25899 presented at the 1993 SPE Rocky Mountain Regional Meeting/Low Permeability Reservoirs Symposium and Exhibition, Denver, Colorado, 26-28 April.

[17]Jones, A.H.: "Spalling and the Development of a Hydraulic Fracturing Strategy for Coal," *Quarterly Review of Methane from Coal Seams Technology* (March 1990) 7, No. 3, 33-35.

[18]McLennan, J.D.: "Spalling and the Development of a Hydraulic Fracturing Strategy for Coal," *Quarterly Review of Methane from Coal Seams Technology* (February 1991) 8, No. 2, 25-27.

[19]Diamond, W.P. and Oyler, D.C.: "Effects of Stimulation Treatments on Coalbeds and Surrounding Strata--Evidence from Underground Observations," U.S. Bureau of Mines RI 9083 (1987).

[20]Steidl, P.F.: "Inspection of Induced Fractures Intercepted by Mining in the Warrior Basin, Alabama," *Proc., Coalbed Methane Symposium*, Tuscaloosa, Alabama (May 1991) 181-191.

[21]Penny, G.S. and Conway, M.W.: "Coordinated Laboratory Studies in Support of Hydraulic Fracturing of Coalbed Methane," *Quarterly Review of Methane from Coal Seams Technology* (April 1992) 9, No. 3 and 4, 26-29.

[22]*Petroleum Engineering Handbook*, second printing, H.B. Bradley (ed.), SPE, Richardson, Texas (1987) 55-4.

[23]Cramer, D.D.: "The Unique Aspects of Fracturing Western U.S. Coalbeds," *JPT* (October 1992) 44, No. 10, 1126-1133.

[24]Palmer, I.D. and Kutas, G.M.: "Hydraulic Fracture Height Growth in San Juan Basin Coalbeds," paper SPE 21811 presented at the 1991 Rocky Mountain Regional Meeting and Low-Permeability Reservoirs Symposium, Denver, Colorado, 15-17 April.

[25]McBane, R.A., Penny, G.S., and Conway, M.W.: "Coordinated Laboratory Studies in Support of Hydraulic Fracturing of Coalbed Methane," *Quarterly Review of Methane from Coal Seams Technology* (July 1991) 8, No. 4, 33-39.

[26]Economides, M.J. and Nolte, K.G.: *Reservoir Stimulation*, Schlumberger Educational Services, Houston, Texas (1987).

[27]Rogers, R.E., Veatch, R.W. Jr., and Nolte, K.G.: "Pipe Viscometer Study of Fracturing Fluid Rheology," *SPEJ* (October 1984) 24, No. 5, 575-581.

[28]Hinkel, J.J., Nimerick, K.H., England, K., Norton, J.C., and Roy, M.: "Design and Evaluation of Stimulation and Workover Treatments in Coal Seam Reservoirs," *Proc., Coalbed Methane Symposium*, Tuscaloosa, Alabama (May 1991) 453-458.

[29]Sparks, D.P. and Richardson, J.S.: "A Comparison of Completion Techniques in the Cedar Cove Field, Black Warrior Basin, Alabama," *Proc., Coalbed Methane Symposium*, Tuscaloosa, Alabama (May 1991) 223-231.

[30]Palmer, I. and Kinard, C.: "Sandless Water Fracture Treatments with Ball Sealers," paper presented at the 1992 Eastern Coalbed Methane Forum, Tuscaloosa, Alabama, 1 September.

[31]Mavor, M.: "Cavity Completion Well Performance," paper presented at the 1992 Eastern Coalbed Methane Forum, Tuscaloosa, Alabama, 1 September.

[32]Gidley, J.L., Holditch, S.A., Nierode, D.E., and Veatch, R.W. Jr.: "Recent Advances in Hydraulic Fracturing," Monograph Series 12, SPE, Richardson, Texas (1989) 67.

[33]Penny, G.S. and Conway, M.W.: "Coordinated Studies in Support of Hydraulic Fracturing of Coalbed Methane," annual report, GRI Contract No. 5090-214-1983 (April 1992) 73-74.

[34]Penny, G.S. and Conway, M.W.: "Coordinated Laboratory Studies in Support of Hydraulic Fracturing of Coalbed Methane," *Quarterly Review of Methane from Coal Seams Technology* (February 1993) 10, No. 3, 30-32.

[35]Berkowitz, N., *An Introduction to Coal Technology*, Academic Press, New York (1979) 90.

[36]Honda, H. and Sanada, Y.: *Fuel* 35 (156) 451.

[37]Holditch, S.A., Ely, J.W., Carter, R.H., and Semmelbeck, M.E.: "Coal Seam Stimulation Manual," topical report, GRI-90/0141 (April 1990) 33.

[38]Geertsma, J. and de Klerk, F.: "A Rapid Method of Predicting Width and Extent of Hydraulically Induced Fractures," *JPT* (December 1969) 21, No. 12, 1571-81.

[39]Jeffrey, R.G., Enever, J.R., Ferguson, T., and Bride, J.: "Small-Scale Hydraulic Fracturing and Mineback Experiments in Coal Seams," *Proc., International Coalbed Methane Symposium*, Vol. I, Birmingham, Alabama (May 1993) 79-88.

[40]Morales, H. and Davidson, S.: "Analysis of Coalbed Hydraulic Fracturing Behavior in the Bowen Basin (Australia)," *Proc., International Coalbed Methane Symposium*, Vol. I, Birmingham, Alabama (May 1993) 99-109.

[41]Layne, A.W. and Byrer, C.W.: "Analysis of Coalbed Methane Stimulations in the Warrior Basin, Alabama," *SPEFE* (September 1988) 3, No. 3, 663-669.

[42]van Krevelen, D.W.: "Coal," *Coal Science and Technology 3*, Elsevier Scientific Publishing Co., New York (1981) 407.

[43]Schuyer, J., Dijkstra, H., and van Krevelen, D.W.: *Fuel* 33 (1954) 409.

[44]McBane, R.A. (ed.) *Quarterly Review of Methane from Coal Seams Technology* (June 1987) 3, No. 1, 38.

[45]Lambert, S.W., Graves, S.L., and Jones, A.H.: "Warrior Basin Drilling, Stimulation," *Oil & Gas J.* (November 13, 1989) 87, No. 46, 87-91.

[46]Johnston, D.J.: "Geochemical Logs Thoroughly Evaluate Coalbeds," *Oil & Gas J.* (December 24, 1990) 88, No. 52, 45-51.

[47]Warpinski, N.R., Branagan, P., and Wilmer, R.: "In-Situ Stress Measurements at U.S. DOE's Multiwell Experiment Site, Mesaverde Group, Rifle, Colorado," *JPT* (March 1985) 37, No. 3, 527-536.

[48]Veatch, R.W. Jr.: "Overview of Current Hydraulic Fracturing Design and Treatment Technology-Part I," *JPT* (April 1983) 35, No. 4, 677-687.

[49]Warpinski, N.R., Schmidt, R.A., and Northrop, D.A.: "In-Situ Stresses: The Predominant Influence on Hydraulic Fracture Containment," *JPT* (March 1982) 34, No. 3, 653.

[50]"Deep Coal Seam Project," *Quarterly Review of Methane from Coal Seams Technology* (May 1985) 3, No. 1, 30.

[51]"Multiple Coal Seam Project," *Quarterly Review of Methane from Coal Seams Technology* (September 1985) 3, No. 2, 43-47.

[52]Sparks, D.P., Lambert, S.W., and McLendon, T.H.: "Coalbed Gas Well Flow Performance Controls, Cedar Cove Area, Warrior Basin, U.S.A.," *Proc., International Coalbed Methane Symposium*, Vol. II, Birmingham, Alabama (May 1993) 529-548.

Chapter 9

Water Production and Disposal

9.1 Introduction

Water production and disposal assume a greater degree of importance in coalbed methane (CBM) projects than in conventional oil or gas operations. In marginally economic coalbed projects, the water disposal costs and the attendant environmental accounting are critical factors in the investment decision; water disposal costs economically make or break a marginal project.

Normally, water must be removed from the coal to lower the pressure and to initiate methane desorption; however, near mining operations there may be only small amounts of water to produce. The operator can also anticipate large amounts of water being produced early in the process but decreasing thereafter to an eventual low level. Therefore, water disposal problems decrease with time, and the greatest economic burden is placed on the operator in the first few years.

Water purity ranges from nearly fresh in the Powder River basin to marginally saline in the Warrior basin to a brine in the deepest coals. Water purity and the quantity produced determine the means of disposal and the costs of disposal. Suspended solids, total dissolved solids, and oxygen demand of produced waters have the most impact on water treatment.

High initial water flow rates normally decline as the hydrocarbon production rate increases, which is counter to the conventional oil and gas process. Lack of understanding of the unusual pattern of water flow and its relation to methane desorption probably delayed recognition that methane could be produced profitably from the country's vast coal reserve. As a result, operators lacked the persistence to produce and dispose of enough waters to flow commercial amounts of methane until the early 1980s.

Another dissimilarity with conventional wells is that well-to-well interference in CBM fields is beneficial because of the mutual assistance in water removal. The interference results in more rapid gas production, especially in interior wells of a field pattern. The interference characteristic imposes another economic demand on the process: a commitment to develop the entire field and a large capital investment. Development of a lone well is impractical.

Before investing in a CBM process, a multiplicity of questions are to be answered concerning the water to be produced—questions concerning quantity, flow rates, chemical content, disposal means, monitoring, and environmental regulations. Perhaps no other factor affects the economics and feasibility of CBM projects as much as water removal and disposal. It has been suggested[1] that a truer indicator of the value of a well would be a plot of gas/water ratio rather than gas production alone. As a whole, CBM operations result in 0.31 barrels of water produced per 1,000 cu ft of methane.[2]

Water associated with a CBM project involves three forms: adherent moisture, inherent moisture, and chemically bound water.

Adherent moisture or bulk moisture refers to the free water contained in the cleat system having a normal vapor pressure.[3] Production of the adherent water from a single well may begin at a rate as high as 1,500 BWPD from saturated cleats and decline thereafter to a value as low as 10 BWPD for most of the producing life. The adherent moisture or bulk moisture represents the water to be disposed of in CBM work.

Inherent moisture or adsorbed moisture is the water in the micropore system that decreases the adsorptive capacity of the coal for methane. Inherent moisture is inconsequential in water disposal problems, but it is detrimental from the standpoint of limiting gas content.

Other forms of water may be present in coal but do not directly affect methane production. First, chemically bound water may have been incorporated in the molecular structure of coals at the start of peatification but then mostly dissipated as volatiles during maturation; the loss contributed to the cleating process. Second, water of hydration may be contained in minerals dispersed in the coal. In

both cases, temperatures higher than any encountered in the coalbed-methane process are required to release these two water sources.

9.2 Water Production Rates from Methane Wells

9.2.1 Initial Water Production Rates

There are wide variations of water production rates from coals in any basin. Ease of dewatering any well depends on the coal's permeability, interference with other wells or mines, and link to an aquifer or meteoric waters. Past mining in the area, even though presently inactive, may have depleted water in the seams.

It is informative to study the average water production rate of wells in the highly developed Warrior basin. Pashin[4] reports from Oil and Gas Board records that 420 wells in the Warrior basin had initial water production rates of 17 to 1,175 BWPD, averaging 103 BWPD. An initial value less than 250 BWPD (70% of all wells) can be expected in the Warrior basin. For wells developed by Taurus, initial flow rates in the Warrior basin ranged from 10 to 1,500 BWPD, and the average initial rate for that company's wells throughout the basin was estimated to be 150 BWPD.[5] However, the production rate is dependent on the location in the basin,[6] and these initial rates decline to a much lower, steady value for most of the producing life of any well.

By June 1992, average water production per well throughout the Warrior basin had declined to the values given in Table 9.1. Note that only Cedar Cove water production rates in 1992 approached the average initial values stated previously. (Because of the proliferation of wells, total coalbed water production in the Warrior basin increased from 100,000 bbl/month to 9,000,000 bbl/month over the decade of the 1980s.[7])

Table 9.1—Chloride Content of Waters from Warrior Fields[8]

Field	Chloride (mg/l)	
	Average	Range
Oak Grove	1,500	40 to 18,000
Cedar Cove	5,500	100 to 14,900
Brookwood	3,000	80 to 18,800
Deerlick Creek	5,000	2,500 to 13,500
Moundville	28,000	4,000 to 36,000

Other factors influence the amount and the rate of water production. In the Warrior basin, for example, wells on the periphery of the pattern of the Oak Grove field produce more water than those in the interior because of interference between wells in the midst of the pattern. The peripheral wells may be the only ones demonstrating water influx on a continuing and significant basis.[9] Initially then, the negative decline of CBM production develops rapidly in the interior of the pattern. If a well is up-dip of other wells in the formation, its relative production rate of water may be less than that of the other wells.

Generally, water production rates in coalbed wells of the Warrior basin decrease significantly by the end of the first month of production.[10] Fig. 9.1 gives the water production schedule from Well Permit #3440-C in the Oak Grove field.[4,11] Note that water production decreased by 75% after 2 years from an initial rate of approximately 380 BWPD to less than 20 BWPD. A consequence of the production profile of Fig. 9.1 is a drop in operating costs with time and a decrease in water disposal costs with time.

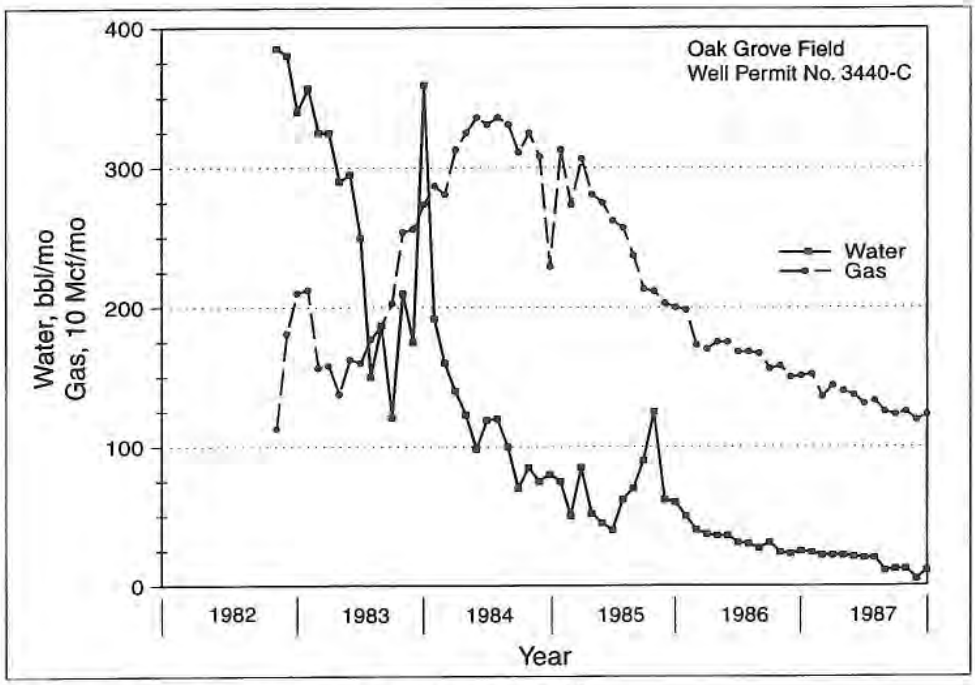

Fig. 9.1—Water production in Oak Grove field.[11]

As a point of comparison with the Black Warrior basin, initial water production rates on the southern Ute Reservation of the San Juan basin ranged from 14 to 1,000 BWPD per well with an average rate of 70 BWPD.

9.2.2 Water Decline Rates

The anticipated schedule of water production throughout the life of the project is needed for an accurate economic evaluation. Water disposal and operating costs depend upon knowing the water production rate from an entire field. The water production with time data of a production unit in the field may be described with decline curve analysis if the subject production unit does not experience interference. Then, either a field or an isolated well as a unit would be appropriate.

If the data are treated as an exponential decline, then the resulting straight line can be extrapolated to any later time as in Fig. 9.2, which represents the water production schedule of a single well in the Oak Grove field without interference from other wells. If the decline rate can be established for all production units or for the field as a whole, the total load schedule can be determined for the water treatment facilities, discharge into surface streams, or injection into disposal wells.

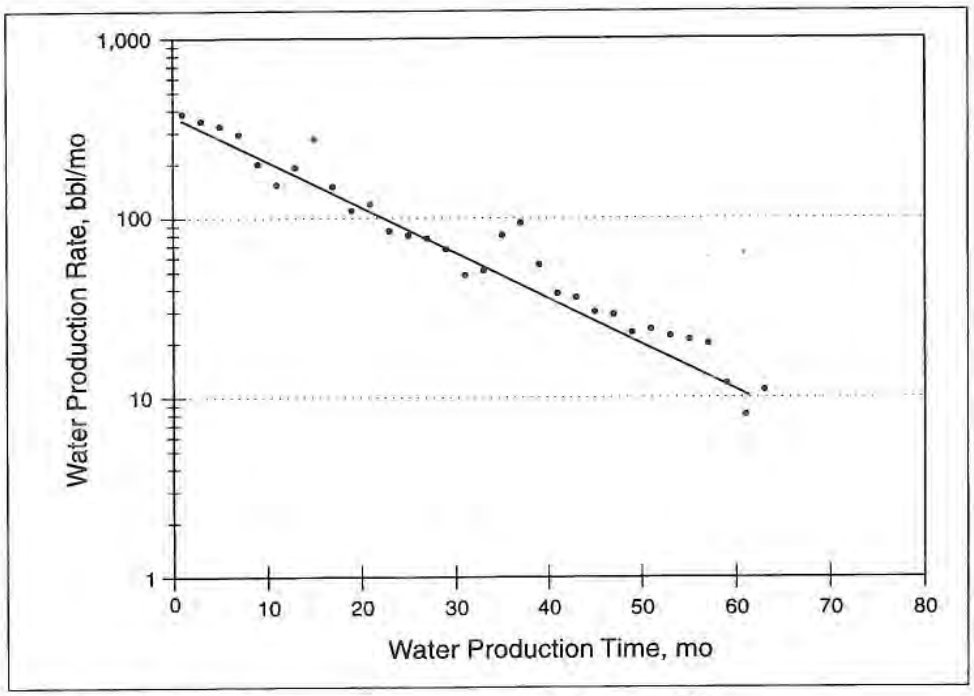

Fig. 9.2—Exponential decline of water in Well #3440-C.[4,11]

9.2.3 Anomalous Water Production Rates

Early and improved CBM production with less accompanying water has been noted in the vicinity of coal mines. In the northern Appalachian basin, effects of

coal mine drainage were observed at a vertical methane well 2 1/2 miles away.[12] The effects are not unique to the Appalachian nor to the Warrior basins.

Fig. 9.3 shows the effect of a Jim Walter well on the potentiometric level of water in the surrounding Warrior basin coalfield.[4]

Anomalously low rates of water production occur in wells other than those in the vicinity of mining. Wells in the southern San Juan basin have little or only small amounts of water production.[6] Also, shallow coals on the eastern edge of the Powder River basin exhibit minimal water production.[9] Gas production from sandstones intermingled with the coalbeds may result in smaller than expected water production rates.

9.3 Chemical Content

Quantity and chemical content are the two important considerations of waters produced from coalseams. Some treatment at the surface is necessary regardless of the disposal method.

Representative analyses of coalbed waters are given in Table 9.2, which is a compilation by Lee-Ryan[13] for waters in the San Juan and the Warrior basins. Note the great variability of the chemical content of the waters. The pH of the waters of both basins is basic. More iron and chloride ions by a factor of 10 must be removed from eastern coalbed waters; about twice as high average total dissolved solids (TDS) exist in the eastern waters.

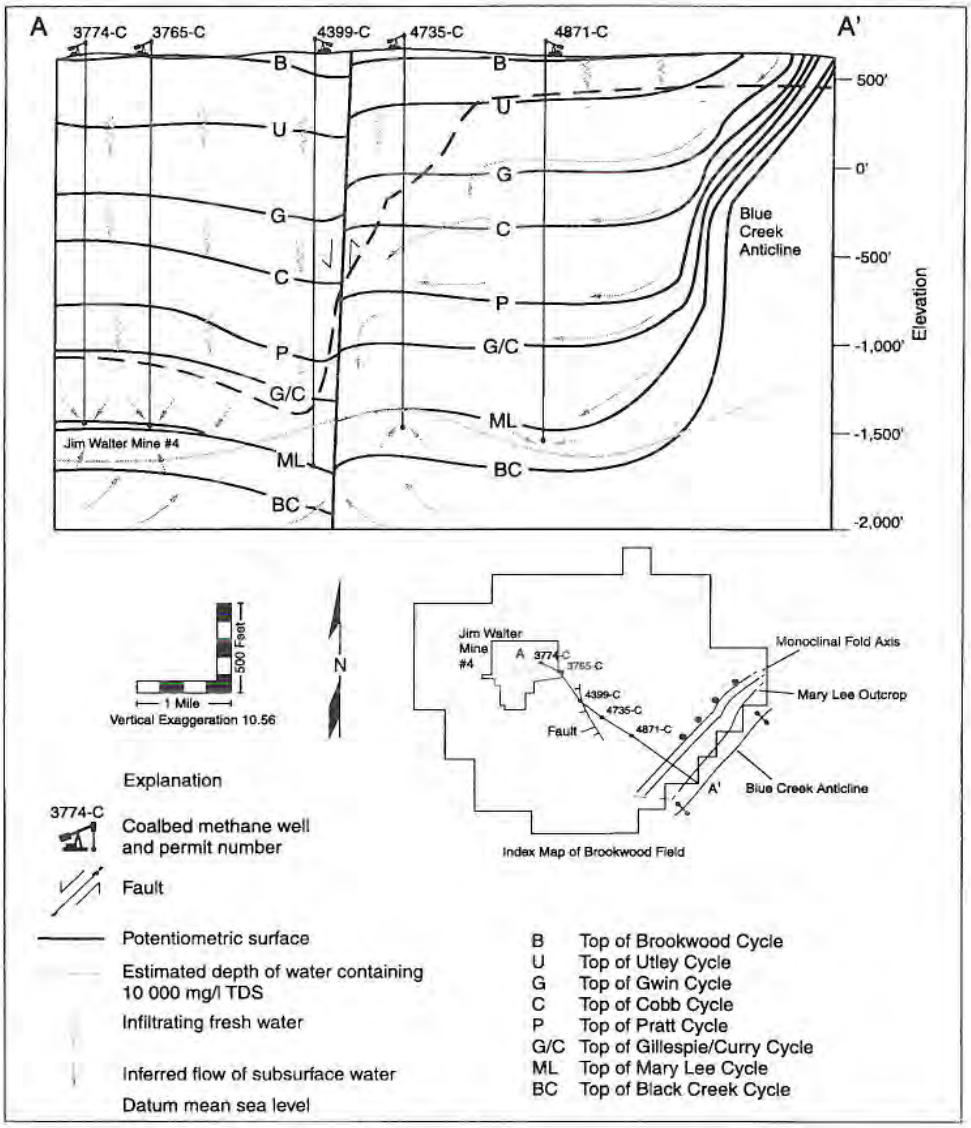

Fig. 9.3—Potentiometric level of water.[4]

Table 9.2—Chemical Compositions of Coalbed Water[13]

	Eastern Waters		Western Waters	
Parameters	**Range**	**Average**	**Range**	**Average**
pH	6.5 to 9.2	7.8	7.4 to 8.8	8.0
Anions (mg/l)				
Bicarbonate	76 to 12,000	596.5	7.8 to 1,450	501.1
Chloride	19 to 15,000	2,000	1 to 720	43.3
Fluoride	ND to 20	2.6	0.1 to 3.6	0.82
Sulfate	ND to 650	12.9	ND to 2,700	323.2
Metals (mg/l)				
Barium	0.2 to 37	2.78		
Cadmium	ND to 0.026	0.005		
Calcium	ND to 620	89	3 to 460	52
Iron	0.005 to 246	9.8	ND to 5	0.43
Lithium	0.18 to 3.3	0.49		
Magnesium	0.3 to 420	33.1	0 to 150	17
Manganese	0.005 to 3.8	0.25		
Potassium	0.3 to 24	7.5	1.1 to 8.5	3.5
Silicon	0.2 to 14	7.3	6.8 to 15	9.3
Sodium	0 to 6,800	1,905	26 to 1290	282.4
Strontium	0 to 56	5.8		
Zinc	0 to 0.36	0.1		
TDS	550 to 26,700	4,000	263 to 4,050	996.5
BOD	100 to 300	200		
Hydrocarbons	<1 to 62	5		

In 1987, effluent CBM waters from the Cedar Cove field of the Warrior basin had a chloride content at the point of discharge throughout the year graphed in Fig. 9.4.[13] The chloride content varied between 1000 mg/L and 2000 mg/L during the year in a fairly consistent pattern. O'Neil found that below 593 mg/L chloride content of a stream, plant and fish life are unaffected.[13]

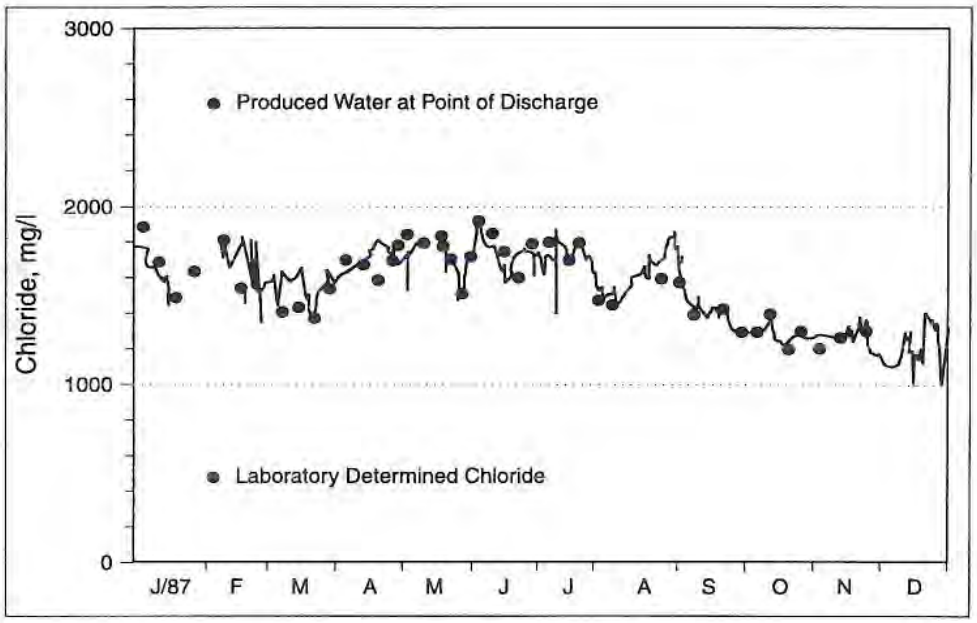

Fig. 9.4—Chloride content of produced CBM waters.[13]

A more comprehensive study of 122 wells of the Cedar Cove field 5 years later by Davis, *et al.*[8] showed a higher average chloride content of 5500 mg/L and a range of 100 to 14,900 mg/L. This demonstrates the wide swing in chloride content from wells within a single field (see Table 9.3).

Table 9.3—Average Water Production in Warrior Basin[8]

Field	Number of Wells	June 1992 Average Flow (bbl/well/d)	Range of Water (bbl/well/d)
Oak Grove	650	100	1 to 1,000
Cedar Cove	441	213	0 to 960
Brookwood	319	50*	<1 to 2,100
Deerlick Creek	223	38	<1 to 500
Moundville	87	57	20 to 1,200

*Average flow based on 122 vertical wells.
Low-flow gob and horizontal wells not included.

TDS, oxygen content, and suspended solids must be controlled for discharge into surface streams, and conformance to the federal regulations is closely watched by the U.S. Environmental Protection Agency working with state agencies. Chloride content, TDS, particulate matter, and formation compatibility must be established for water disposal by well injection.

Besides establishing disposal requirements, water composition gives some insight into the permeability of the formation. The bicarbonate ion exists in larger concentrations in those formations having meteoric waters continually replenishing the coalseams. The chloride ion occurs in greater concentration in those more stationary coalbed waters. Therefore, the anion HCO^{3-} is indicative of a good permeability in the coals and of a continuity in the seams that allows water circulation along an uninterrupted path. The Cl^- anion, on the other hand, suggests a discontinuity in the seams or a lack of permeability that leaves the waters uncirculated.

The relationship of overpressured seams, high permeabilities, and artesian flows with low chloride content has been observed in the Piceance basin as well as in the San Juan basin.[15]

The data of Pashin[4] for the Black Warrior basin show a chloride concentration as a function of depth as given in Fig. 9.5. Note the scatter of the data for formations shallower than about 2,000 ft, which is consistent with extreme variations in reported chloride concentrations of Table 9.3.

Hanor presented the relationship of chloride content with depth for oilfield waters of northern Louisiana and southern Arkansas in a regional diffusion model of the chloride ion,[16] and his trend of chloride content with depth is superimposed in Fig. 9.5. Comparison of the two sets of data helps explain the variation of the chloride data, particularly at shallow depths.

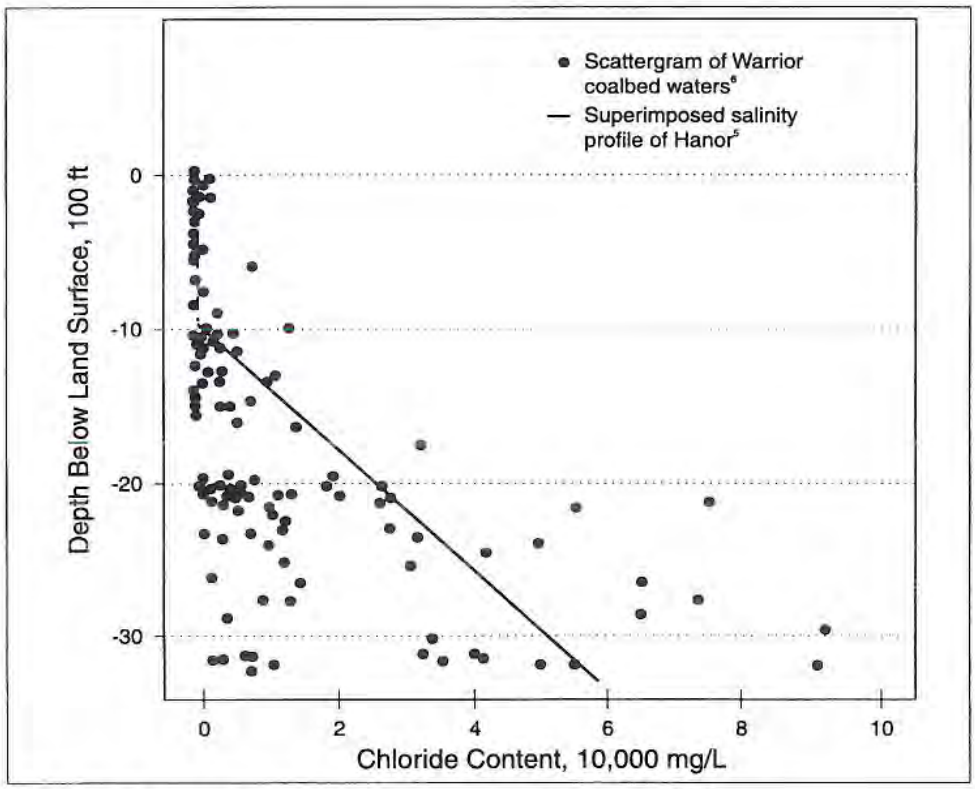

Fig. 9.5—Chloride ion in coalbed waters, Warrior basin.[4,16]

The chloride content in Fig. 9.5 is shown to decrease from about 9,000-ft depths in a linear fashion until about 1,100 ft from the surface where the Cl^- ion concentration drops precipitously. Diffusion of the Cl^- ion occurs from a highly concentrated brine at depths to 1,100 ft to give the linear decline of Hanor. However, near the surface, meteoric waters sweep the brine away but only where large variations in permeabilities or in faulting cause irregular concentrations of the chloride.

By analogy it is hypothesized that where surface waters mix in the coalseam, the Cl^- concentration will be low, and the bicarbonate ion will be high. A Cl^- concentration envelope would exist that covers the range of concentrations resulting from variations in depths of surface mixing.

If disposal wells are used for produced coalbed waters, it is not permissible to reinject the produced coalbed waters into any formation having less than 10,000 ppm TDS.[17] In this case, chloride concentration with depth takes on additional importance.

The Fruitland formation of the San Juan basin provides a case study in hydrology, as presented by Kaiser.[6] A cross-section of the basin with potentiometric surfaces is presented in Fig. 9.6. The chloride ion and the bicarbonate ion concentrations differ widely by region in the basin but are explained in Kaiser's model in the following manner.

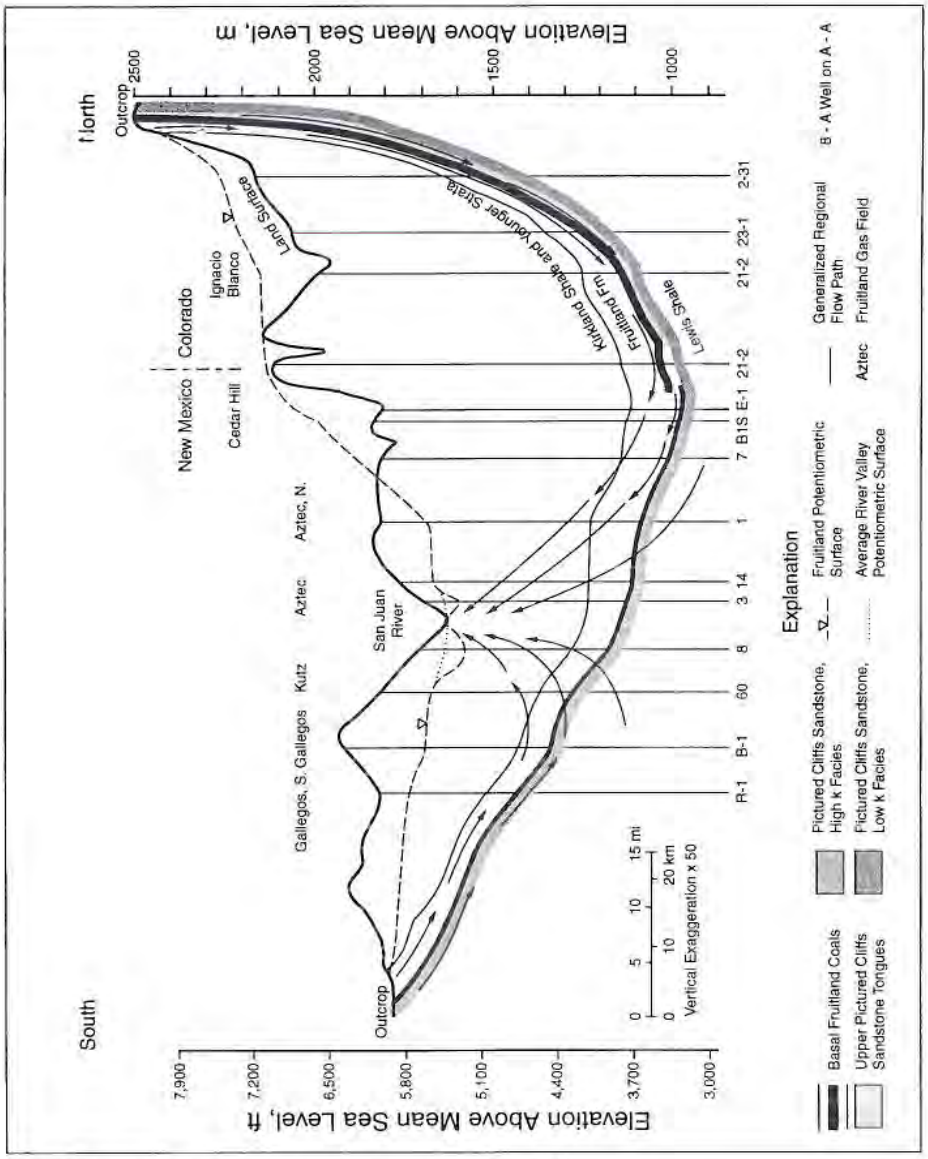

Fig. 9.6—Water circulation in San Juan basin.[6]

Waters from the north and north-central regions of the San Juan basin exhibit a high concentration of HCO_3^-, but in the south and east, Cl^- is prevalent.[6] Where the coals outcrop in the north, waters recharge the seams and proceed to the southwest to discharge into the San Juan River. At a GRI facility 16 miles south of the northwestern outcrop of Fruitland coal and 27 miles from the northern outcrop, bicarbonate in formation waters is estimated to be 38,000 years old from carbon-14 dating.[18] Scott and Kaiser further predict a residence time of 15,000 to 28,000 years for the travel of the waters from the outcrops to the site. The coals are overpressured in parts of the north and north-central region, as can be seen by comparing potentiometric and surface elevations in Fig. 9.6. Although some of the bicarbonate in waters of the overpressured region may come from calcite in cleats, Kaiser postulates some of it is of biogenic origin from bacteria entering with meteoric waters at the outcrop.[18]

Coals also outcrop in the southwestern region of the San Juan basin, and waters recharge those coals. They, too, eventually discharge into the San Juan River, but the chloride ion is high in the region and the bicarbonate ion is low, indicating at best a sluggish flow. To the east, low permeabilities exist, and there are no coal outcrops. The waters are not replenished by surface waters, and the chloride ion concentration is high.

The Kirtland and Lewis shale bounds the Fruitland formation above and below and helps make the Fruitland one hydrological unit. Wherever the Pictured Cliffs sandstone is interfingered through the Fruitland coals, water chemistry and pressures are similar to those of the coals. Around the overpressured coals of the north and north-central region of the San Juan basin is an underpressured region.[6] Methane is produced from both regions, although the most prolific wells occur in the north.

9.4 Environmental Regulations

9.4.1 Toxicity Limitations of Coalbed Water

Coalbed waters are regulated to specify the following chemical contents and conditions:

- Dissolved oxygen (DO).
- Biochemical oxygen demand (BOD).
- Iron.
- Manganese.
- Total dissolved solids (TDS).

The first four of the preceding five regulated conditions are dependent on adequate oxygen being added to the waters from the coalbeds before the waters can be disposed of in surface streams. Dissolved oxygen must be input to the produced waters because the waters from the coalseams are devoid of oxygen. Upon aerating the waters at the surface, iron and manganese are oxidized and precipitate as solids. Additionally, aerating supplies the oxygen for BOD; about 1.2 lb oxygen is required for 1.0 lb BOD.[2] Therefore, supplying oxygen is a primary requirement for surface treatment of produced waters, and 5 mg/L of O_2 is required for waters discharged from the treating process.

Table 9.4 summarizes important characteristics of oxygen in water.[8] Note from Table 9.4 that oxygen solubility in water is naturally limited to 7.6–11.3 mg/L under ordinary conditions. As temperature or chloride content increases, oxygen solubility is more diminished.[19] In the hot months, therefore, O2 solubility in Alabama's surface waters decreases, and supplying or maintaining the oxygen in produced waters becomes more difficult.

Table 9.4—Oxygen in Coalbed Waters[8]

Oxygen in water from coalseam	0.0
Oxygen required in discharged waters	≥5 mg/L
Oxygen for ferrous ion oxidation	1 mg/L O_2 per 7 mg/L Fe^{2+}
Oxygen for manganous ion oxidation	1 mg/L O_2 per 3 mg/L Mn^{2+}
Per 1.0 lb of BOD	1.2 lb O_2
7.6 to 11.3 mg/L O_2 dissolves in H_2O	at 50 to 86°F w/o Cl^-

In the Warrior basin, produced coalbed waters are discharged into surface streams. The formations suitable for deep-well injection are not present. Because of its lower cost, a surface disposal becomes economically vital in marginal properties of the Warrior basin. Despite the freedom of surface disposal, strict regulations are imposed on the treatment, disposal and monitoring of waters in surface streams. A series of treating ponds in any producing field of the basin serves as staging points for the treatment process.

The first treatment must be to provide oxygen to the waters collected in the ponds using one of three methods:

- **Spraying**. The surface area of the water is increased to absorb oxygen from the air.
- **Agitating mechanically**. The surface area of water in contact with air is renewed constantly. The new surface absorbs more oxygen; the concentration gradient is increased for more rapid absorption of the oxygen.
- **Pumping air beneath the water surface**.

A primary objective in the initial treatment is to transfer oxygen to the water for feeding the growth of microorganisms that degrade organic matter in the water. The three preceding methods increase surface areas of water exposed to air to enhance absorption of oxygen. Then agitation is supplied to bring bacteria, oxygen, and organic matter into contact.[19]

Bates, *et al.*[19] give the rate of oxygen transfer across the gas and liquid films of the liquid/air interface in Eq. 9.1.

$$dC/dt = k_L a(C_s - C) \qquad (9.1)$$

where

C = concentration of oxygen
C_s = saturation concentration of oxygen in water
a = area of interface per unit volume of liquid
t = time
k_L = proportionality constant

Biochemical oxygen demands (BOD) result from the bacteria that degrade organic compounds in the water. It is this oxygen that must be supplied to the bacteria to degrade the mass of organic matter in the water within a certain length of time. The microorganisms increase their activity exponentially with temperature so that a standard temperature must be set. The standard is 20°C. BOD_5—the biochemical oxygen demand over a 5-day test period at 20°C—must not exceed 30 mg/L in the disposal waters, which is applicable across the United States as established by the Environmental Protection Agency (EPA) and the Clean Water Act.[2,10,19]

The organic constituents of the produced coalseam waters that the microorganisms feed upon may come from organic compounds of the coal or from decaying organic matter in the treatment ponds. However, the greatest amounts of organic matter that must be biodegraded come from fracturing fluids expelled from the formation. Consequently, the fracturing fluids place a heavy periodic demand on the waters for oxygen. After fracturing, these stimulation fluids continue to be returned for several months during production of the methane. The hydroxypropyl guar and other water-soluble polymers used in fracturing are the main culprits.

To correct the heavy surge of BOD_5 upon startup of a field, Taurus added hydrogen peroxide to supply oxygen demand as a temporary fix to a problem that could have required large capital expenditures for more facilities. The startup BOD_5 demand resulted from return of stimulation fluids used to fracture wells in the field.[19]

Removal of the manganese and iron is more straightforward than TDS removal. The oxidized manganese and iron forms precipitate in the holding ponds. Their oxidation is much faster at higher pH, which should be maintained above 7.2. Manganese content in the effluent waters must be less than 2 mg/L as a monthly maximum.[2,8] Total iron must be less than a 3.0 mg/L monthly maximum; coalbed waters of the Warrior basin average less than 15 mg/L.[8] After oxidation of the ferrous ion, ferric hydroxide precipitate flocculates to settle slowly because of a specific gravity only slightly above unity (1.002). Furthermore, high levels of BOD_5 interfere with the flocculation of the iron precipitated.[10] To assist gravity settling, the following conditions are imposed in the treating ponds:

- Quiescent settling waters.
- >24-hr Detention time.
- Ponds of 10-ft depth that accumulate several years of precipitates before cleanout.
- Baffled exit of water from the ponds.

The TDS are the most troublesome chemical content of produced waters and the most damaging to plant life. Sodium chloride is the main constituent of the dissolved solids. It is evident from Table 9.3 that chloride content varies in Warrior basin waters from an average of 1500 mg/L at Oak Grove to 28,000 mg/L at Moundville. Aeration or detention in holding ponds has no effect on TDS content. Membrane processes can remove the sodium chloride, but those processes are too costly at present or have not been sufficiently developed for large-scale use in the industry.

Reduction of chloride content and disposal of coalbed waters in the Black Warrior basin rely on diluting the produced water in the receiving stream to less than the 230 mg/L deemed nondamaging to aquatic life. Although permits allow

only 230 mg/L in the streams, discharge to the stream must be interrupted if 190 mg/L is registered by in-stream monitors for a stream with less than a 100/1 diluting capability. The interruption point increases to 210 mg/L for a ratio greater than 100/1.[10,17]

The standards for chloride content were set and are checked by its toxicity to living organisms. The Alabama Department of Environmental Management requires two representative living organisms, a fathead minnow and a water flea, be able to live in effluent coalbed waters to verify lack of toxicity.[8]

To dilute the effluent coalbed waters in the river or tributary, a diffuser is placed below the surface of the indigenous stream. Beyond a mixing zone, the blended waters must not exceed 230 mg/L of TDS. The mixing zone radius is set in Alabama as five times the low-flow stream depth, but it cannot exceed one-half the stream width.[8]

9.4.2 Regulatory Agencies of the Warrior Basin

Important regulations in Alabama that relate to the CBM industry deal with the following:

- Wetlands restrictions on site selection.[20]
- Drilling, site maintenance, wellbore configuration, production procedures.
- Water disposal to surface streams.
- Injection wells for water disposal.

The wetland restrictions on site selection are comprehensive, and authority is given to the Army Corps of Engineers (ACOE) and to the EPA under Section 404 of the Clean Water Act.[20] Permits are required in any wetlands involving 10 acres or more before dredging, drilling, or filling can be done.

Drilling and operation of CBM wells are regulated by the Alabama Oil and Gas Board. Permits are granted by this agency.[10]

Water disposal to surface streams is regulated by the EPA through powers granted in a series of federal Congressional acts: the Federal Water Pollution

Control Act of 1972, the Clean Water Act of 1977, and the Water Quality Act of 1987.[8] The Alabama Department of Environmental Management (ADEM) administers the program for the EPA, and ADEM is authorized to grant national pollutant discharge elimination system (NPDES) permits to discharge into surface streams as a mining operation in Alabama.[2] The permits must be renewed every 5 years.

Water disposal to injection wells is regulated by the Alabama Oil and Gas Board.[17] The authority comes from the Safe Drinking Water Act. Disposal wells for coalbed waters are categorized as Class II disposal wells under the Underground Injection Control Program.[2,10] A primary limitation under the act is that injection cannot be made into an aquifer of less than 10,000 mg/L of TDS unless the aquifer is already contaminated. Proof must be made of contamination and of TDS before the license is given.[13]

9.4.3 Regulatory Agencies of the San Juan Basin

In the San Juan basin, the transport and disposal of waters from CBM wells are controlled by state, federal, and tribal regulations (see Table 9.5).

Table 9.5—Regulations for Coalbed Water Disposal/Transportation, San Juan Basin[21]

Brine Conveyance	Lease or Land Status	Regulatory Agency	Comments
Trucking and pipelines	Fee minerals	Colorado Oil and Gas Commission	Section 325 of Colorado Oil and Gas Commission regulations
Trucking and pipelines	Indian lands (allotted and tribal)	Bureau of Land Management	Removal of brines from lease must be approved
Brine disposal			
Direct use	Indian lands (all lands within reservation boundary)	EPA	• NPDES permits of reservation issued by EPA • Subject to agricultural and wildlife water use subcategory (40 CFR 435.50) • Tribes eligible for program primacy
Evaporation pits	Fee minerals	Colorado Oil and Gas Commission	Section 325 of Colorado Oil and Gas Commission regulations
Evaporation pits	Indian lands (allotted and tribal)	Bureau of Land Management	NTL–2B (1/1/76)
Evaporation pits	Commercial pits	Colorado Department of Health/county commissioners	• Colorado solid waste regulations • County issues permit (certificate of designation) with technical assistance from the state • Enforcement by state
Underground injection	Fee minerals	Colorado Oil and Gas Commission	State Class II UIC program approved April 1984
Underground injection	Indian lands (all lands within reservation boundary)	EPA	Tribes eligible for program primacy

9.5 Water Disposal Techniques

Four techniques are possible to dispose of produced coalbed waters: (1) well injection, (2) discharge into surface streams, (3) land application, and (4) membrane processes.

Disposal in deep wells is practiced in the San Juan basin. Here, an intricate network of pipelines and trucks serve the wells.

Surface stream disposal is used in the Warrior basin. Here, the option of deep-well disposal is unavailable because of the lack of permeable formations below the coal-containing Pottsville formation. Land applications were used early in the process in the Warrior basin but have mostly been phased out and permits are no longer given. Any future applications to land depend on making one of the membrane processes economical, which would give an effluent pure enough to apply to the land surface.

Potentially, water purification could produce usable water, which would be preferable if economics were satisfactory. For example, separation by semipermeable membranes might eventually produce water of sufficient quality for agricultural use.[22] In its environmental impact study in the Uinta basin, the U.S. Bureau of Land Management recommended a reverse osmosis project with subsequent land application as one option for water disposal.[23] If the capacities of acceptable sandstone formations in the San Juan basin become insufficient to disseminate peak coalbed production waters, the use of membranes to purify the water eventually may be needed.[2] At any site, economics, geology, and environmental restrictions dictate the choice.

9.5.1 Surface-Stream Disposal

A flow diagram[8] of the surface treating facilities for coalbed waters in the Black Warrior basin is given in Fig. 9.7. The waters pass through an aeration pond, a sedimentation pond, and possibly a storage pond before being disposed of through a diffuser into the surface stream.

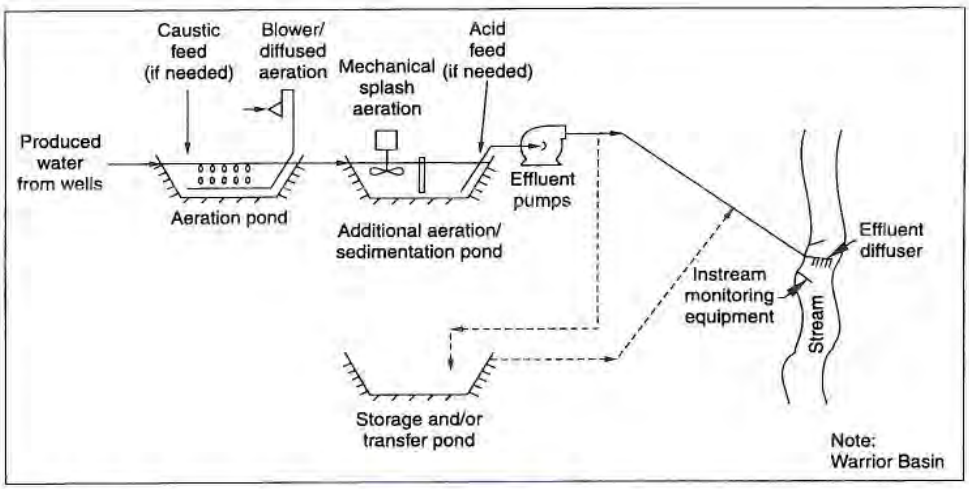

Fig. 9.7—Surface treatment of coalbed waters.[8]

Aeration of the "dead" coalbed waters having no dissolved oxygen is an important step in processing because the introduction of oxygen into the water has multiple beneficial effects. Foremost of benefits is the oxidation and resulting precipitation of the suspended solid iron and manganese. Oxidation of the two metals in the aeration and sedimentation ponds removes these metals from the waters and from further consideration. (After several years, the solid sediments must be removed from the bottom of the pond.) Volatile organic matter is lost during the aeration in the holding pond. Also, the aeration adds dissolved O_2 and decreases biological oxygen demand by as much as 50–90%.[9] The aeration process, however, decreases neither the chloride content nor the TDS of the coalbed waters.

In the case of emergencies, the storage and transfer pond of Fig. 9.7 is designed to hold waters temporarily, primarily during the low flow of surface streams in the dry summer months.

Chloride removal would require a more expensive and higher technology treatment, specifically, ion exchange, reverse osmosis, or electrodialysis; evaporation is also feasible. Consequently, the most difficult problem for any

type of surface disposal lies with meeting the TDS specifications, primarily for chlorides. The options are to remove chlorides at considerable expense or to dilute the water to acceptable chloride concentration levels.

In the Warrior basin, disposal plans for production waters are coordinated with the onstream schedule of new wells in the field to determine the impact upon surface streams from addition of new production. State and federal environmental regulations limit TDS and chloride content of the natural streams.

The regulations specify that under no circumstances may the instream chloride content exceed 230 mg/L. If the instream content reaches 190 mg/L for streams having a dilution capability of less than 100/1, the discharge must be shut in. More leniency exists for streams such as the Warrior River with a dilution capability greater than 100/1, and shut-in is not mandated until the instream chloride content reaches 210 mg/L.[10]

Upon addition of production waters, the content of the natural stream becomes the sum of innate TDS and Cl^- plus TDS and Cl^- added from CBM waters. Timing of CBM water disposal in streams must allow for the prescribed dilution, a feat dependent upon the highly variable, seasonal surface stream flow.

Four parameters are necessary to develop the surface disposal plan:[9] (1) water quality of the produced and natural streams, (2) well start-up schedule, (3) projected flow history of the well, and (4) natural stream capacities.

The relationship of these four parameters is given in Eq. 9.2. The surface stream flow rate, Q_s, is the minimum river flow rate that will accommodate the coalbed well effluent. It will depend upon the volumetric flow rate, Q_e, of effluent waters from production facilities to be dispersed in a surface stream; the effluent concentration, C_e, of TDS; the inherent concentration, C_s, of the stream; and the concentration, C_m, that the stream reaches after mixing with the effluent.[5,10]

$$Q_s = Q_e \frac{C_e - C_m}{C_m - C_s} \qquad (9.2)$$

where

C_m = instream quality limitation
C_s = background stream concentration
Q_s = minimum surface stream natural flow to accommodate
Q_e = effluent from coalbed methane wells
C_e = effluent water concentration of TDS

Environmental regulations would set C_m. Assimilative capacities of streams can therefore be calculated.

If consistent units of C are used, if Q_e is given in units of BWPD, and if Q_s is desired in units of cubic feet per second, the relationship becomes that of Eq. 9.3.

$$Q_s = 6.5\ 10^{-5} Q_e \frac{C_e - C_m}{C_m - C_s} \qquad (9.3)$$

Example 9.1—The "A" Creek in the month of July has an average minimum monthly flow rate of 12 cu ft/sec (184,814 bbl/D). Inherent background TDS in its waters amounts to 10 mg/L. Government regulations limit raising the TDS to a maximum of 190 mg/L. Coalbed methane wells in the adjacent field produce waters having an average TDS content of 1790 mg/L. What maximum volumetric rate of the produced waters in BWPD could be disposed of in "A" Creek in July?

Example 9.1 Solution:

$$Q_e = Q_s \frac{C_m - C_s}{C_e - C_m}$$

where

Q_e = coalbed well effluent, b/d

Q_s = 12 cfs

C_e = 1790 mg/l

C_m = 190 mg/l

C_s = 10 mg/l

$$Q_e = \frac{12 \qquad (190 - 10)}{0.00006493\,(1790 - 190)}$$

$$Q_e = 20{,}792 bpd$$

Therefore, during the low-flow period of July (assuming an average river flow rate for the month) 20,792 BWPD of the coalbed produced waters could be disposed in "A" Creek without exceeding the total dissolved solids' limit of the stream. August, September, and October would be the low-flow months, so the low allowable in July would be expected to decrease further in the subsequent 3 months.

To determine whether a surface stream will accommodate the waters from numerous coalbed wells in its drainage sphere of influence, to determine how many wells can be drilled and drained in the area, or to determine the amount of supplementary storage capacity one must provide, the following steps are taken:

1. Determine the water production decline profile of the wells in the control group.
2. Determine water production of each well at a selected point in time.
3. Add water production of all wells at the selected point in time.
4. Estimate the flow rate of the natural surface stream.
5. Calculate the assimilative capacity of the natural surface stream.
6. Superimpose the total methane-well and waste-water flow rate on the graph of assimilative capacity of the natural surface stream vs. time.

Example 9.2—Determine if "B" Creek in the area of a planned CBM project will have the capacity to receive expected production waters throughout the first year from the wells without exceeding TDS limits of governmental regulations. Initially, 25 wells will be simultaneously brought onstream on January 1. One hundred days later, a second group of 50 will be brought onstream. Thereafter, in 100 days a third group of 25 wells will be brought onstream. Assume each well follows the production pattern given in Fig. 9.8.[10]

Example 9.2 Solution: The production of the water follows an exponential decline as presented in Fig. 9.8. Determine the total flow from the wells of the 25-well group from initial startup, January 1, for the first year of operation. Do likewise for the second group of 50 wells that come onstream 100 days later as well as the third group of 25 wells.

1. Use the decline curve of Fig. 9.8 for each group of wells and summarize in Table 9.6.
2. Convert the units of bbl/D to cu ft/sec for the total input from the CBM wells to the creek.
3. Determine the flow rate of the creek.

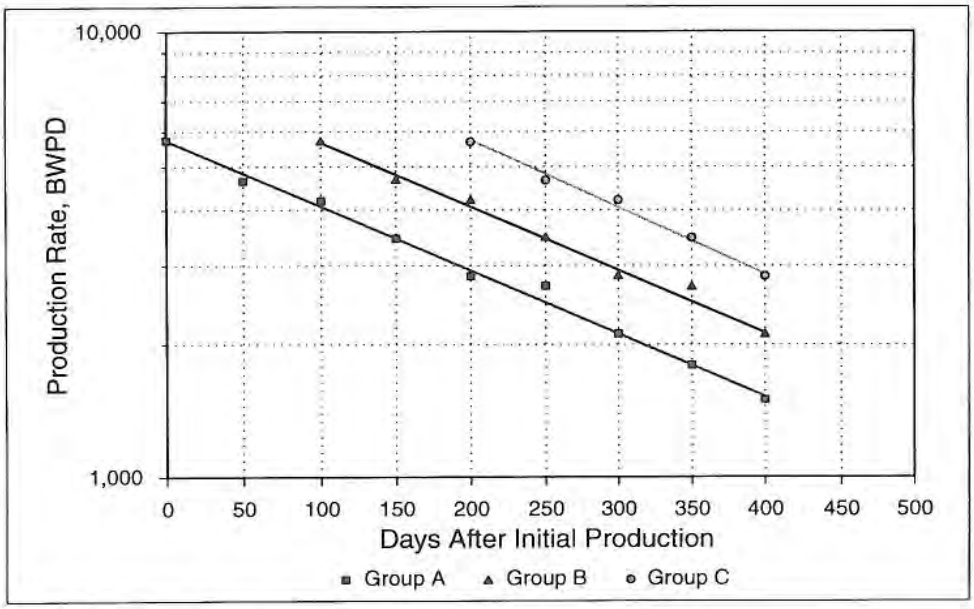

Fig. 9.8—Project water production decline curve.

Table 9.6—Coalbed Waters to Dispose of in Stream

Time (Days)	Water Produced Group 1 Wells (BWPD)	Water Produced Group 2 Wells (BWPD)	Water Produced Group 3 Wells (BWPD)	Total Stream Flow (BWPD)
0	5,700	—	—	5,700
50	4,650	—	—	4,650
100	4,200	5,700	—	9,900
150	3,450	4,650	—	8,100
200	2,850	4,200	5,700	12,750
250	2,700	3,450	4,650	10,800
300	2,100	2,850	4,200	9,150
350	1,800	2,700	3,450	7,950
400	1,500	2,100	2,850	6,450

Fig. 9.9 presents the year's trace of the creek's flow rate. Four of the largest peak flows have been truncated.

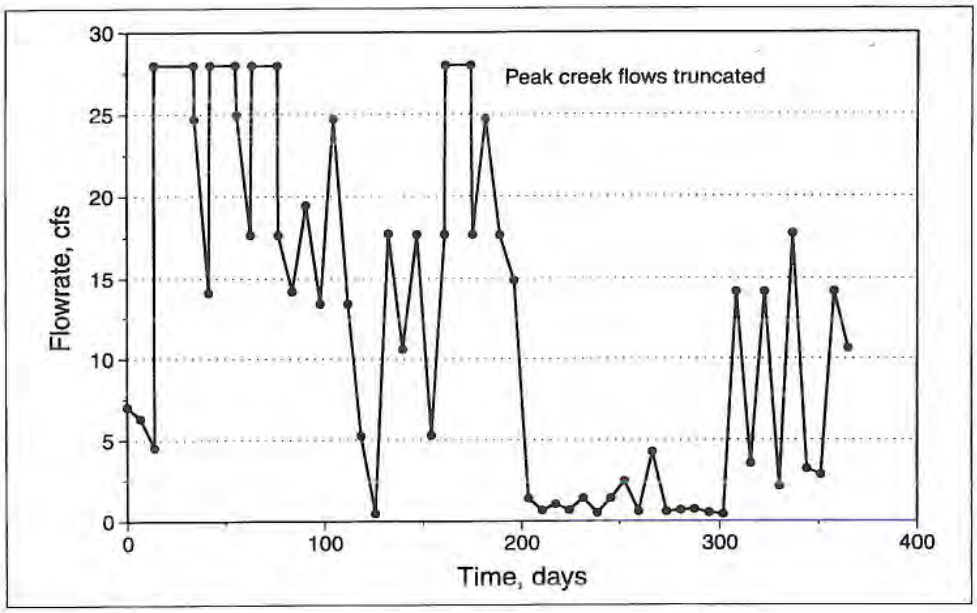

Fig. 9.9—B Creek seasonal flow rates.[11]

With the creek flow rate established, the assimilative creek capacity is determined from the values of Fig. 9.9 by rearranging Eq. 9.2 to obtain Eq. 9.4.

$$Q_e = Q_s \frac{(C_m - C_s)}{(C_e - C_m)} \qquad (9.4)$$

where

Q_s = values from Fig 9.9, cu ft/sec

C_e = 1790 mg/L

C_m = 190 mg/L

C_s = 10 mg/L

Q_e = assimilative capacity of stream, cu ft/sec

Eq. 9.4 and the stated values result in the following:

$$Q_e = 0.1125\, Q_s$$

Finally, the total effluent flow rate from the CBM wells are superposed on the assimilative capacity of the stream (see Fig. 9.10). The results show that supplementary storage or alternative disposal must be provided during the three dry months and briefly for one other time in late spring. The example is similar to conditions in the Black Warrior basin.

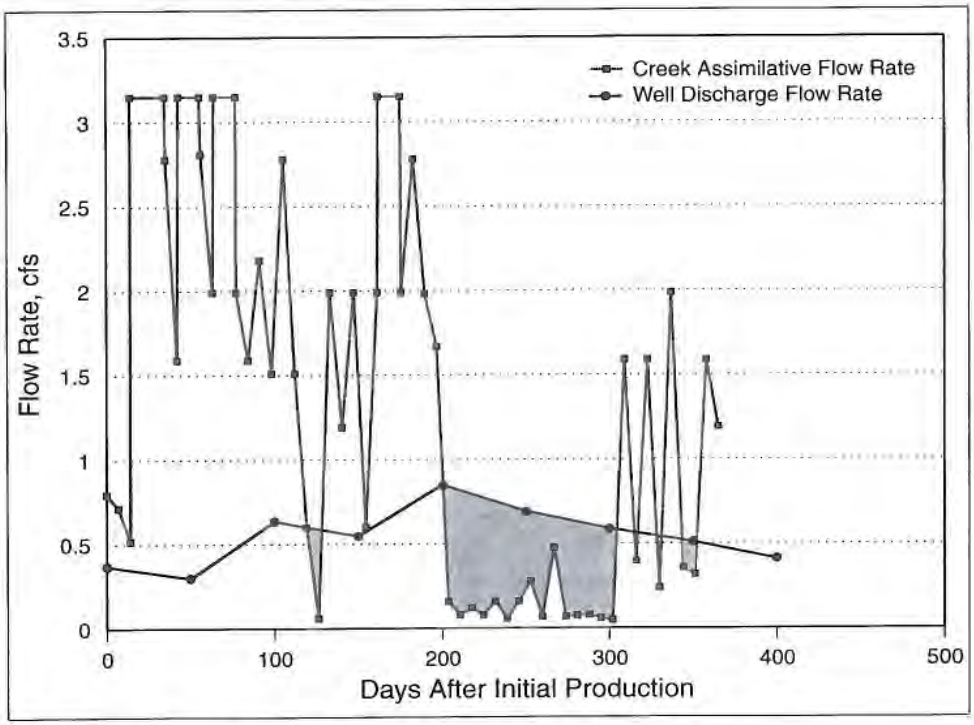

Fig. 9.10—Creek's assimilative capacity limits brine discharge.

The San Juan basin, in contrast, is severely limited in surface water disposal. Initial water production rates in the southern Ute Reservation of the San Juan basin range from 14 to 1,000 BWPD per well with an average rate of 70 BWPD.

Furthermore, the chemical content varies from a relatively pure TDS <1,000 mg/L in the northwestern and western part of the reservation to 10,000–15,000 mg/L TDS in the south.[21]

Therefore, only about 25% of the water production in the southern Ute Reservation contains a solids content low enough to be considered for use on the surface for livestock without treatment (no harmful chemicals are present).[21] The terrain limits available crops for irrigation uses of the water.

Table 9.7 gives reference values for water use based solely on TDS. The table is presented to put into perspective the magnitudes of TDS in water. Ionic composition also enters into the acceptable use.[24]

Table 9.7—Acceptable Uses of Coalbed Methane Waters[21]

TDS Content (mg/L)	Toleration
<3000	Crop irrigation, hay meadows, stock watering
<2500	Cattle
<5000	Sheep
<500	Drinking water, humans

Passive evaporation ponds could be used in the San Juan basin to dispose of the water if production rates declined to less than 5 BWPD, perhaps in the latter stages of a well's productive life. Average evaporative rates of about 5 in./month in the warmer New Mexico part of the basin are more conducive to evaporative ponds than the wetter, colder areas in Colorado. One large evaporation pit covers 45,000 sq ft and evaporates 88 BWPD in the New Mexico section.[21]

Active evaporation ponds that use a spray system increase evaporation rates by a factor of five to ten times and require smaller areas. Costs, however, are increased by additional maintenance, and entrainment of spray in the wind is a problem near the pit.

Other problems with evaporation ponds exist. They must be designed both to handle large volumes of brine and to present a large surface area. Any oil on the

surface reduces evaporation rates, and risk to the environment from seepage, spills, or windblown sprays exists.

9.5.2 Injection Wells

In the Black Warrior basin, injection wells for produced CBM waters are not used, mostly because of lack of suitable formations for disposal. Only five saltwater disposal wells have been used; these were drilled into the Pottsville sandstone formations and the deeper Knox carbonate formations. Reinjection is allowed by the Alabama Oil and Gas Board only into formations having greater than 10,000 ppm TDS.[13] Any disposal well must be evaluated after drilling and before injection to establish TDS. The target formations between 4,000 ft and 10,000 ft in the Warrior basin have in some instances had water fresher than the 10,000 ppm TDS level.[17]

By contrast, in the southern Ute land of the San Juan basin, injection wells are the preferred choice, and depleted gas sands include Point Lookout sandstones, Entrada sandstones, and Pictured Cliffs sandstone.[21] On the Southern Ute Reservation, the target for disposal-the Mesaverde group-would be 5,000 to 8,000 ft deep. In the San Juan basin 65% of the disposal wells for coalbed waters have been drilled into the Jurassic sandstones. For the entire basin, 66 million barrels of produced water per year as a maximum is anticipated.[25]

A combined CBM production and brine disposal well is given in Fig. 9.11. In such a well, the water can be reinjected into the Point Lookout sandstone below the Fruitland coals from whence the methane comes.[21] In the Uinta basin of Utah, similar dual injector/producer wells were chosen as a means of water disposal.[23]

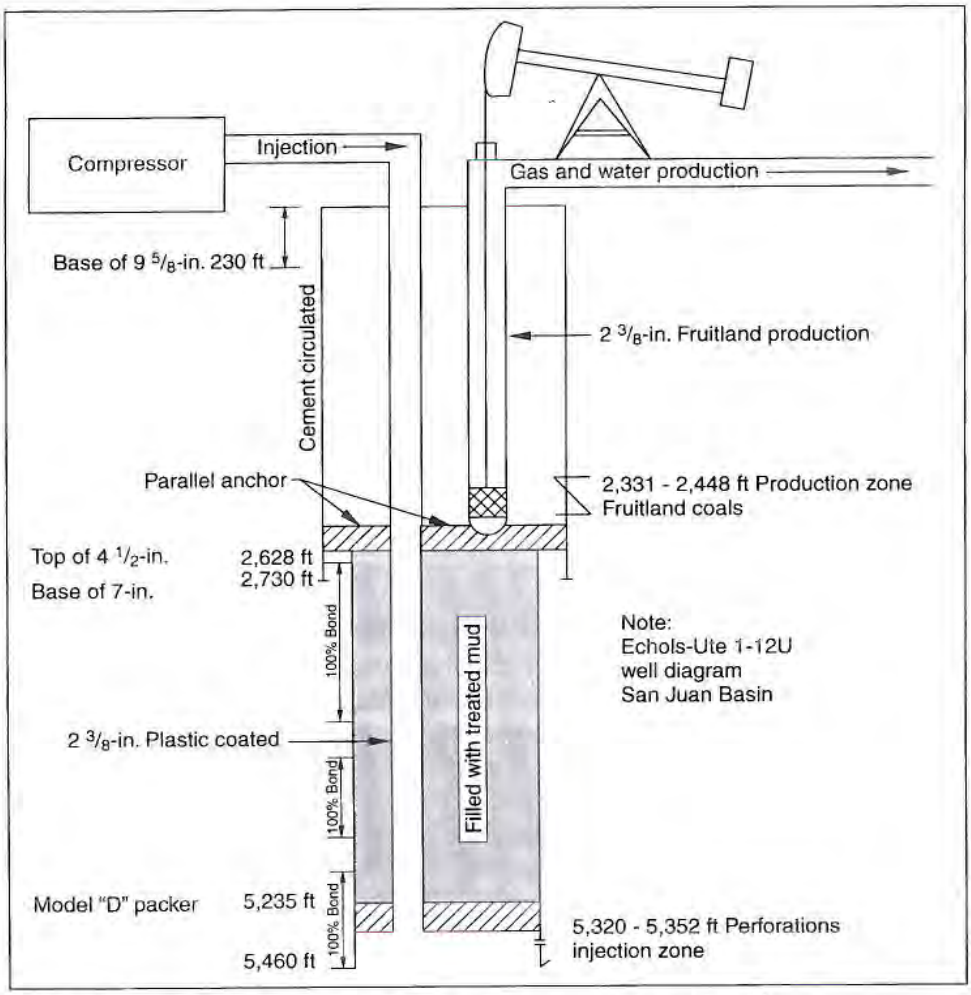

Fig. 9.11—Dual production and brine disposal well schematic.[21]

More commonly, multiple CBM wells serve a single disposal well. Holding tanks at the injection site receive incoming brine by pipeline and by truck. Low-cost

polyethylene pipe is used in the pipelines.[21] The brine must be filtered before pumping into the receiving sandstone.

On the southern Ute Reservation, the ratio of producing wells to injection wells is optimum at 70 to 1.[21] Devon reports using injection wells in the San Juan basin to accommodate 8,000 to 9,000 BWPD/well. Before injecting, the water is filtered with 25-micron and 1-micron filters.[26]

9.6 Summary

Water production profiles of CBM wells give rates that peak within 1 year and then decline throughout the remaining life unless the well is on the periphery of the pattern or unless the coal has high permeability accessing an aquifier or meteoric waters. Early in the life of an individual well, therefore, the most demands are placed upon disposal. Eventually, the relative permeability of water in the coal decreases rapidly as the gas fraction increases. Then, attendant costs of disposal decline; a corresponding decline in operating costs occurs. The water-treating facilities must be designed for the peak loads that account for the expectancy of peak production per individual well and the number of producing wells.

The inorganic chemical content of the produced waters is primarily a function of depth and permeability of the formation. The chloride ion creates the main problem to surface-stream disposal of the water. The chloride content of coalbed waters increases as the permeability of the coals decreases. At low permeabilities, the waters cannot be replaced by meteoric waters. On the other hand, the bicarbonate ion may be indicative of high permeability.[27] The inorganic chemical content of ferrous and manganous ions is readily oxidized and precipitated in holding ponds to remove them from discharged waters.

Methods available for water disposal are discharge into surface streams, injection wells, surface use without treatment, surface use with direct treatment, and evaporation pits. Environmental regulations, economics, suitable formations for disposal wells, climate, and chemical content dictate the choice.

The preferred disposal method varies with the basin. Surface disposal is the most economical means. Fortunately, the water quality, the number of surface streams, and the volumetric flow rates of the streams allow surface disposal in the Warrior basin, which is environmentally acceptable under strict controls. In the San Juan basin, the preferred disposal method is injection wells. Here, disposal into surface streams is not allowed, but numerous sandstone formations are available for injection wells. Land application is rarely allowed, and any eventual land application is tied to technical and economical development of membrane processes.

Coalbed water production is an integral part of the CBM process. Unlike conventional oil and gas operations, the volumes of produced waters and the attendant operating costs decrease with time. Initial water purification and disposal create a primary problem that must be overcome to establish profitable methane production. Water disposal is a deciding factor in developing marginally economical properties.

References

[1]Allison, M.: "Production Trends in the Brookwood Field as Influenced by Stimulation Design and Geology," presented at the 1992 Eastern Coalbed Methane Forum, Tuscaloosa, Alabama, 1 September.

[2]Lawrence, A.W.: "Coalbed Methane Produced-Water Treatment and Disposal Options," *Quarterly Review of Methane from Coal Seams Technology* (December 1993) 11, No. 2, 6-17.

[3]Berkowitz, N., *An Introduction to Coal Technology*, Academic Press, New York (1979) 30-32.

[4]Pashin, J.C., Ward, W.E., Winston, R.B., Chandler, R.V., Bolin, D.E., Hamilton, R.P., Mink, R.M.: "Geologic Evaluation of Critical Production Parameters for Coalbed Methane Resources," annual report, Part II-Black Warrior Basin, Gas Research Institute (February 1990) 130.

[5]Luckianow, B.J. and Hall, W.L.: "Water Storage Key Factor in Coalbed Methane Production," *Oil & Gas J.* (March 1991) 89, No. 10, 79-84.

[6]Kaiser, W.R. and Swartz, T.E.: "Fruitland Formation Hydrology and Producibility of Coalbed Methane in the San Juan Basin, New Mexico and Colorado," *Proc., Coalbed Methane Symposium*, Tuscaloosa, Alabama (April 1989) 87.

[7]Mount, D.R., O'Neil, P.E., and Evans, J.M.: "Discharge of Coalbed Produced Water to Surface Waters-Assessing, Predicting, and Preventing Ecological Effects," *Quarterly Review of Methane from Coal Seams Technology* (December 1993) 11, No. 2, 18-25.

[8]Davis, H.A., Simpson, T.E., Lawrence, A.W., Miller, J.A., and Linz, D.G.: "Coalbed Methane Produced Water Management Strategies in the Black Warrior Basin of Alabama," *Proc., International Coalbed Methane Symposium*, Vol. I, Birmingham, Alabama (May 1993) 317-338.

[9]Seidle, J.P.: "Long-Term Gas Deliverability of a Dewatered Coalbed," paper SPE 21488 presented at the 1991 SPE Gas Technology Symposium, Houston, Texas, January.

[10]Burkett, W.C., McDaniel, R., and Hall, W.L.: "The Evaluation and Implementation of a Comprehensive Production Water Management Plan," *Proc., Coalbed Methane Symposium*, Tuscaloosa, Alabama (May 1991) 43.

[11]O'Neil, P E.: "Biomonitoring of a Produced Water Discharge from the Cedar Cove Degasification Field, Alabama," Alabama Geological Survey, Circular 135 (1989) 195.

[12]Hunt, A.M. and Steele, D.J.: "Coalbed Methane Development in the Northern and Central Appalachian Basins-Past, Present and Future," *Proc. Coalbed Methane Symposium*, Tuscaloosa, Alabama (May 1991) 127-141.

[13]Lee-Ryan, P.B., Fillo, J.P., Tallon, J.T., and Evans, J.M.: "Evaluation of Management Options for Coalbed Methane Produced Water," *Proc., Coalbed Methane Symposium*, Tuscaloosa, Alabama (May 1991) 31-41.

[14]O'Neil, P.E., Harris, S.C., and Mettee, M.F.: "Stream Monitoring of Coalbed Methane Produced Water from the Cedar Cove Degasification Field, Alabama," *Proc., Coalbed Methane Symposium*, Tuscaloosa, Alabama (April 1989) 355-361.

[15]Kaiser, W.R.: "Geologic Evaluation of Critical Production Parameters for Coalbed Methane Resources," *Quarterly Review of Methane from Coal Seams Technology* (January 1992) 9, No. 2, 25-31.

[16]Hanor, J.S.: "Variation in the Chemical Composition of Oilfield Brines with Depth in Northern Louisiana and Southern Arkansas: Implications for Mechanisms and Rates of Mass Transport and Diagenetic Reaction," *Trans., Gulf Coast Association of Geological Societies* (1984) 34, 55.

[17]Ortiz, I., Weller, T.F., Anthony, R.V., Franck, J., Linz, D., and Nakles, D.: "Disposal of Produced Waters: Underground Injection Option in the Black Warrior Basin," *Proc., International Coalbed Methane Symposium*, Vol. I, Birmingham, Alabama (May 1993) 339-364.

[18]Scott, A.R. and Kaiser, W.R.: "Relation between Basin Hydrology and Fruitland Gas Composition, San Juan Basin, Colorado and New Mexico," *Quarterly Review of Methane from Coal Seams Technology* (November 1991) 9, No. 1, 10-18.

[19]Bates, R.L., McDaniel, R., and Luckianow, B.: "Chemical Oxidation by H_2O_2 Addition to Satisfy Wastewater Oxygen Demands During Production Field Startup Operations," *Proc., International Coalbed Methane Symposium*, Vol. I, Birmingham, Alabama (May 1993) 365-374.

[20]Luckianow, B.J., Burkett, W.C., and Bertram, C.: "Overview of Environmental Concerns for Siting of Coalbed Methane Facilities," *Proc., Coalbed Methane Symposium*, Birmingham, Alabama (May 1991) 1-11.

[21]Zimpfer, G.L., Harmon, E.J., and Boyce, B.C.: "Disposal of Production Waters from Oil and Gas Wells in the Northern San Juan Basin, Colorado," *Rocky Mountain Association of Geologists Guidebook*, Denver, Colorado (1988) 183-198.

[22]Simmons, B.F.: "Treatment and Disposal of Waste Waters Produced with Coalbed Methane," *Proc., Coalbed Methane Symposium*, Tuscaloosa, Alabama (May 1991) 459.

[23]Schwochow, S.D. (ed.): "Uinta Basin, Utah," *Quarterly Review of Methane from Coal Seams Technology* (April 1993) 10, No. 4, 2-3.

[24]Oldaker, P., Stevens, S.H., Lombardi, T.E., Kelso, B.S., and McBane, R.A.: "Geologic and Hydrologic Controls on Coalbed Methane Resources in the Raton Basin," *Proc., International Coalbed Methane Symposium*, Vol. I, Birmingham, Alabama (May 1993) 69-78.

[25]Cox, D.O.: "Coal-Seam Water Production and Disposal, San Juan Basin," *Quarterly Review of Methane from Coal Seams Technology* (December 1993) 11, No. 2, 26-30.

[26]Petzet, G.A. (ed.): "Devon Pressing Fruitland Coal Seam Program," *Oil & Gas J.* (November 1990) 88, No. 45, 28-30.

[27]Decker, A.D., Klusman, R., and Horner, D.M.: "Geochemical Techniques Applied to the Identification and Disposal of Connate Coal Water," *Proc., Coalbed Methane Symposium*, Tuscaloosa, Alabama (November 1987) 229.

Chapter 10

Economics of Coalbed Methane Recovery

10.0 Introduction

The profitability of a coalbed methane (CBM) project is highly dependent on factors of seam thickness, gas content, and permeability. Its economics are influenced by other variables, such as depth, water disposal volumes, access to market, and gas price. Well tests, logging, and core analyses add to the costs in regions without prior coal mining or core analyses of the coal.

The San Juan basin has proved to be the most profitable of any coal basin because two favorable factors, gas content and permeability, combine there with thick seams. In the San Juan basin, the completions in its single 50-ft thick seams have been more cost-effective than completions in multiple, thin seams of the Appalachian and the Warrior basins. As another example of profitable combinations, low gas contents of subbituminous coals in the Powder River basin are compensated for by shallow seams 100 ft thick.

In the Warrior basin, favorable combinations of rank, permeability, and gas content exist. Property access, market access, moderate depths, and abundant data from previous years of mining and conventional drilling compensate for thin seams to give success. Although more properties are marginally profitable because of thin seams in the Warrior basin, research (mostly from support of the Gas Research Institute of the Rock Creek research site) has helped sustain economical production by developing fracturing, multizone completion techniques, computer simulations, well spacing, and water handling techniques to reduce costs and improve gas production.

Whatever combinations of reservoir parameters exist, high initial costs will be encountered in developing CBM properties. Unlike developing a conventional

gas field, a CBM venture requires drilling a group of wells where interference between them will improve overall gas production by facilitating the more rapid removal of large volumes of water. A large capital investment is needed to develop a field.

It is understandable that the Section 29 tax credit established by the federal government assisted in the early development of the process, especially in the Warrior and Appalachian basins where some marginal properties became attractive with the credit. Moreover, Section 29 provided the impetus for the CBM process to be established. Since then, technical advances have improved the economics of the process, and technology holds the best hope for process viability in the future.

10.1 Tax Credit

10.1.1 History of the Credit

Tax credits for fuels from specified unconventional sources were incorporated into the Windfall Profit Act (WPT) of 1980 at a time of high oil prices.[1] The tax credit for CBM became known simply as the Section 29 credit when it was retained after the WPT act provisions expired. Over a 10-year period from its start, about $270 million of credits in the Warrior basin and $860 million of credits on production of CBM in the San Juan basin were realized by producing companies.[1] Another $900 million of credits seemed probable for the subsequent 5 years.

The credit was enacted at a fortuitous time for CBM development and played a key role in the development of the new process, as Congress intended. Although the tax credit was written to end on the last day of 1990, the 1988 Technical and Miscellaneous Revenue Act (TMRA) stipulated a 1-year extension of the credit from January 1, 1990, until January 1, 1991. The Omnibus Budget Reconciliation Act of 1990 again extended the deadline for drilling qualifying wells 2 years until January 1, 1993.[1]

For CBM production to qualify, the well must have been spudded between December 31, 1979, and January 1, 1993. The site must have been prepared, the drilling rig set up, and the initial borehole begun. Further, capital to drill to total depth must have been committed.[2]

The two extensions of the tax credit shortly before expiration caused a rash of drilling before the three deadlines. Wells drilled in the three flurries of activity were then later brought onstream at a leisurely pace. At the end of December 1992, Congress allowed Section 29 to expire.

10.2 Measures of Profitability

10.2.1 Criteria for Economical Methane Project

Many factors are necessary to make a CBM property profitable and attractive for investment. Access to pipelines, proximity to markets, ownership certainty, infrastructure of oilfield services, and local regulations on water disposal impact a CBM property's profitability and are specific to a region to be evaluated on an individual basis.

For multiple, thin seams similar to the ones of the Pennsylvanian Age in the eastern United States, critical parameters for development are gas content, permeability, and pressure. A discussion reiterating the importance of each follows.

Gas content of the coal must be sufficient to justify the expenses of developing. For profitable development in the Appalachian and Warrior basins, a minimum gas content of the coals is 125–150 scf/ton.[3] Because of nonuniformities in coal rank and of ash content within a field, representative sampling is needed to give a reliable estimate of gas content in a property. For example, the River Gas Corporation obtained 31,844 ft of core before developing its 32,480 acres in Tuscaloosa County, Alabama.[4]

A permeability of at least 0.1 to 0.5 md is needed for the eastern coals to be economically attractive.[3] Above the threshold values, hydraulic fracturing may be used to enhance production rates.

Adequate reservoir pressure must supply the driving force for movement of gas and water through the system and accommodate higher gas contents according to Langmuir's isotherm. A minimum initial pressure that would encourage development of coals of multiple, thin seams would be 125–175 psi.[3] Because the Langmuir isotherm predicts more gas evolved per unit pressure drop at low pressures, abandonment pressure becomes more important than in conventional gas production.

Gas prices during the life of the project directly impact expected profitability. Here, the investor is subject to the vagaries of gas prices determined by supply and demand. In a study by Hobbs, Holland, and Winkler,[5] the profitabilities of a hypothetical development project designed to be representative of typical wells in the Warrior basin were compared when actual prices over a 2-year period were 32–42% less than the initial forecast price. The lower gas prices reduced internal rate of return (ROR) to unacceptable values.

Three common measures of profitability for analysis of CBM projects are payout, net present value profit, and discounted cash flow ROR.

Payout is the time required to have the original investment returned as cash flow. Undiscounted payout establishes the equality of investment value with cumulative cash flows with no regard for the time value of money. Discounted payout is the time to return the value of the investment in discounted cash flows.

Payout's utilities are its simplicity and its indication of when the investment will be returned. This information is especially important for independents with smaller cash flows and capital limitations. Additionally, payout may assume greater importance in investments in a country of political instability by answering the question of how soon the investment can be retrieved.

As a stand-alone measure, payout does not fully include a time value of money, it says nothing of the profitability beyond the time of investment retrieval, risk is not included, and it depends on the early pattern of cash flows.

In the CBM process, the pattern of cash flows makes payout deceiving as a profitability indicator. Water disposal during the first year after startup incurs its maximum expense in the life of the project, and income from methane production is low during that initial dewatering stage. Furthermore, a heavy front-end investment is required for CBM projects because multiple wells must be committed for any size of development. The combined effect is a longer payout that may not reflect an ultimate attractive project profitability.

Undiscounted payout, P_{ud}, is described by Eq.10.1.

$$\sum_{j=1}^{P_{ud}} NCF_j = I \qquad \text{(Eq. 10.1)}$$

where

P_{ud} = year of undiscounted payout or value of j when $I\text{-}\Sigma NCF_j = 0$
NCF_j = net cash flow of year j
I = investment
j = year

Net present value (NPV) profit is a measure of profitability that is the present value of cash flows discounted at an average opportunity rate, i_o, in excess of the present value of the investment. It is defined by Eq.10.2.[6]

$$NPV = \sum_{j=0}^{L} \frac{NCF_j}{(1+i)^j} \qquad \text{(Eq. 10.2)}$$

where

L = producing life of the unit
NCF = net cash flow
j = year (the investment is represented as $j = 0$)

NPV profit introduces the time value of money into the analysis, and it uses an interest rate representative of the company's reinvestment opportunity. If the NPV profit is positive, a viable investment is indicated. If the NPV is negative, the investment should be rejected. In the economic analysis of CBM projects, NPV profit is most often used in conjunction with payout and a ROR. These are combinations most frequently used in the oil industry.[7]

The ROR presents profitability in terms of a compound discount rate, which can be compared directly to interest rates of borrowing or to internal rates generated by ongoing projects. DCFROR is the interest rate necessary to make the sum of the present value of the investment equal to the sum of the present values of each year's net cash flow (see Eq. 10.3).

$$\sum_{j=0}^{L} \frac{NCF_j}{(1+i)^j} = 0 \qquad \text{(Eq. 10.3)}$$

When the equality of Eq. 10.3 holds, DCFROR is equal to i.

Mavor[8] presents discounted cash flow rates of return for five wells in the San Juan basin as a function of a composite reservoir parameter. (Assume a constant cleat system and attendant permeability.) The composite factor is the product of initial reservoir pressure, gas content, and coal height in the completed interval. Permeability is held constant at 5 md in the correlation (see Fig. 10.1). A linear relationship of DCFROR with the composite factor results. In this example, DCFROR is calculated on an after-federal-tax basis, and it includes the Section 29 tax credit. Calculation of the ROR implicitly says the reinvested cash flows receive the same interest rate as the DCFROR of the project when reinvested for the duration of the project.

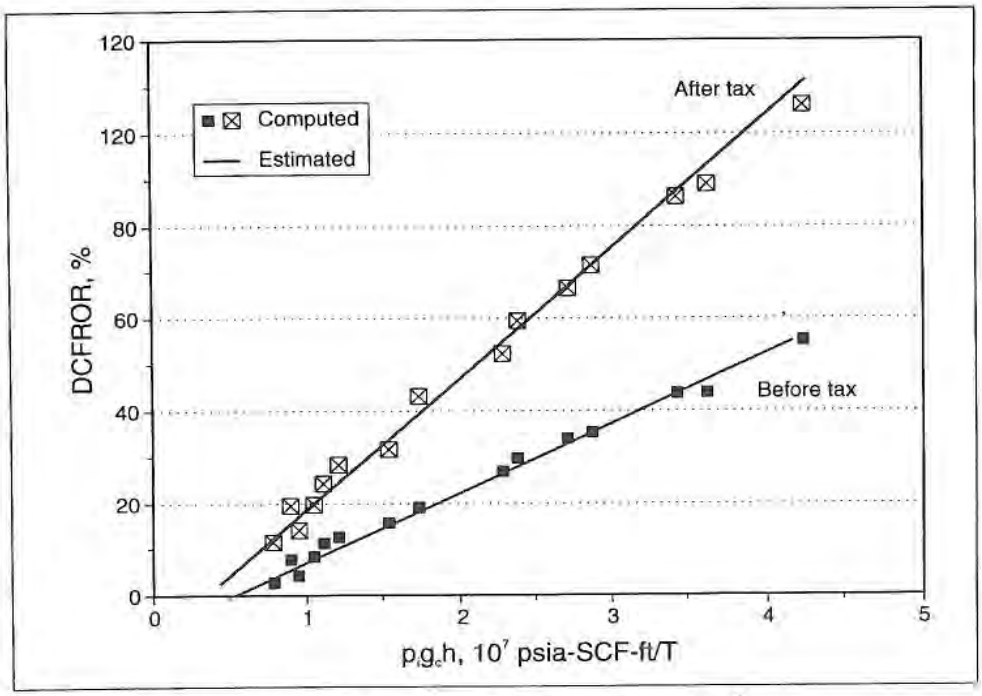

Fig. 10.1—DCFROR depends on critical coalbed properties.[8]

10.2.2 Comparison of Measures of Profitability

No single measure of profitability has all the characteristics needed to evaluate a CBM property. Combinations of several yardsticks of profitability are desirable. The initial capital demand for drilling multiple wells, the negative decline of gas production initially, and the weighting of early water-disposal costs especially impact payout and ROR.

Rates of return of properties in general would be expected to exceed typical minimum value criterion of 20%; payout would ordinarily indicate a desirable

criterion of less than 1.5 years for a conventional project under consideration. In Example 10.1 the profitability to be anticipated from a typical producing CBM well in the Warrior basin is calculated. Profitability will be represented by those measures previously discussed.

Example 10.1—A well drilled in the Warrior basin began production in 1992 amid expectations of continuing for 20 years. What will be the profitability, measured as discounted cash flow ROR and net present value profit?

1. Make the calculations on the basis of after-federal-income tax.
2. Determine the impact of the tax credit on profitability.
3. Evaluate profitability for three levels of reserves.

Example 10.1 Solution—Three levels of reserves were considered:

- "A" Level = best well
- "B" Level = average well
- "C" Level = poor well

The following costs establish this Warrior basin investment:[9-11]

	Percentage of Total Cost
Land acquisition, preparation	7
Tangibles	30
Intangibles	55
Facilities	8

The cost of a typical, completed well in the basin is assumed to be $300,000. A refracturing procedure, at a cost of $27,000 (cost of fracturing with water), is performed in the eighth year, and its present value adds to the investment.[12] The operating costs are assumed to average $1,200 per month.

It is necessary to make assumptions that will vary among operators and properties. Values most representative are chosen. A conservative approach to forecasting gas price is taken, where gas prices are considered constant for a 5-year period but show a compounded growth rate of 10% at the end of each 5-year period. The conservative pricing approach does not inflate the resulting profitability values.

Other assumptions include the following:

- 3/16 Royalty; 81.25% revenue interest; 100% working interest.
- Maximum production Warrior: 221 Mcf/D; 927.1 MMcf reserves per well.
- Average production Warrior: 147 Mcf/D; 616.5 MMcf reserves per well.
- Poor production Warrior: 111 Mcf/D; 463.8 MMcf reserves per well.
- 10% Average opportunity rate assumed for discounting.
- Compounding of gas price at 10% every 5 years.
- Depreciation by double declining balance; SLM fifth year.
- 20-Year life of the CBM well.
- Full utilization of the tax credit on this or other projects.

Net income and federal income tax were calculated with a spreadsheet for each of the three levels of reserves over the 20-year life of the well. The resulting profitability measures are summarized in Table 10.1. All three levels of reserves provide a lucrative ROR with a fully utilized tax credit. However, the wells of average or poor levels of reserves without the tax credit in the Warrior basin would not be good investments under the assumptions established for the example. The results show the essential role the tax credit had as an incentive for early development of the CBM process, especially for marginal properties.

Table 10.1—Results of Profitability Analysis, Warrior Basin

	AFIT w/ Tax Credit			AFIT w/o Tax Credit		
	Good Well	Average Well	Poor Well	Good Well	Average Well	Poor Well
DCFROR (%)	46.6	29.0	19.5	16.2	6.8	0.9
NPV ($)	486,025	231,713	106,730	81,582	–31,219	–95,593
Well Reserve (MMcf)	927.1	616.5	463.8	927.1	616.5	463.8
Annual Peak Production (MMcf)	80.7	53.7	40.4	80.7	53.7	40.4
Peak Rate (Mcf/D)	221	147	111	221	147	111

10.3 Costs

10.3.1 Drilling and Completion

In general, the well costs—including drilling to a typical depth of about 3,000 ft in the Warrior basin, perforating, and fracturing three zones—amount to $190,000 to $200,000.[13] The cost to drill, perforate, fracture, dispose of water, and bring the methane onstream of a Black Warrior development well 3,500 ft deep is estimated to be $319,300.[5] The cost of a typical well of the River Gas Corporation in Tuscaloosa County, Alabama, is broken down in Table 10.2.[4] The cost of drilling, completing, and gel fracturing a single zone of the Mary Lee/Blue Creek in the Oak Grove field was $125,000.[14] In the San Juan basin, the openhole cavitation process costs $8,000–$10,000 per day to create the cavity. An average well cost in the San Juan basin is approximately $500,000, which includes installations at the surface; the figure also includes the monthly operating costs and the water disposal.[8]

Table 10.2—Typical Costs of Tuscaloosa County Well[4]

Typical Well Expenditure Item	Average Well Cost ($)
Intangible costs	101,000
Equipment	67,000
Geological/transportation/pipeline	6,000
Overhead	13,000
Total	**190,000**

Perforating evolved into the accepted completion procedure to access the formation for multiple-seam wells in the Black Warrior basin and to give maximum control over the initiation of hydraulic fractures. The choice is based on a procedure long used in the oil and gas industry that workers in the field can accomplish in a reproducible manner and in a short time. A major consideration in the eventual selection of perforating, however, was a lower cost than slotting or openhole completions. Lambert[13] estimated the relative costs of the three completion procedures given in Table 10.3. The higher costs of the openhole and slotting procedures go along with less reliability and more lost time than perforating. Thus, perforating may cost 45% of openhole completion or 68% of the slotting procedure costs.

Six different completion techniques in the Deerlick Creek field of the Warrior basin over a span of 3 years were evaluated by Lambert, Niederhofer, and Reeves.[15] The ratio of cost to methane flow rates attained with each completion was determined. The study was undertaken as part of the effort to make the marginally economic wells in the region cost-effective (see Fig. 10.2).

From Fig. 10.2, several conclusions are evident. The openhole completion with a linear gel exhibited the lowest methane flow rate, while the slotted case that involved only a water fracturing fluid gave the highest flow rate. The limited entry and the baffled fracturing techniques gave the lowest costs, and the second most cost-effective procedure used baffles for fracturing. Although the slotted casing provided high flow rates, it was not as cost effective. Baffled fracturing and limited entry methods were most attractive.

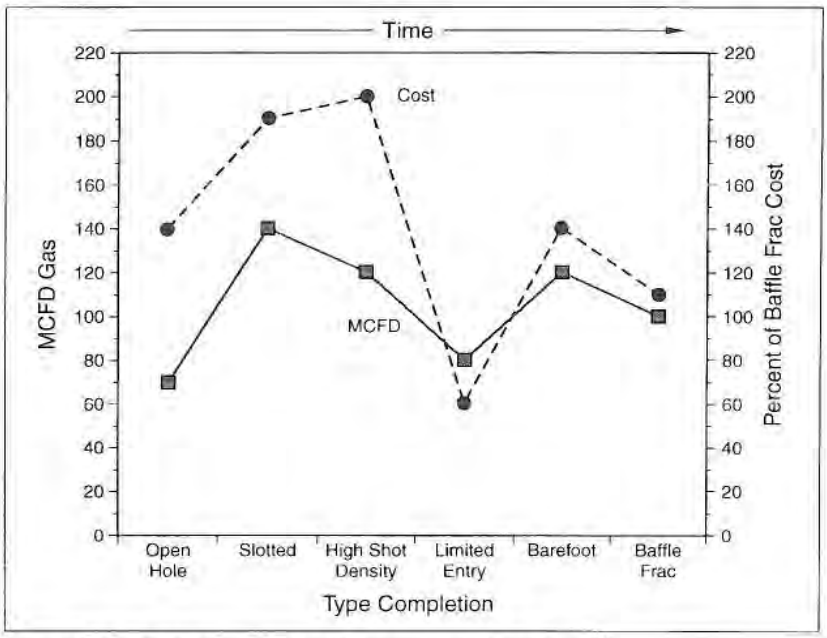

Fig. 10.2—Relative completion costs at Deerlick.[15]

Table 10.3—Relative Costs of Completion Methods[13]

Openhole Item[a]	Openhole Cost ($)
Top packer for 8-in. diameter hole, minimum rental	2,688.00
Bottom packer for 8-in. diameter hole, minimum rental	2688.00[b]
Supervision, 2 hr at $60/hr	120.00
Total	**5,496.00**
Perforating Item[c]	**Perforating Cost ($)**
Service charge	500.00
Rig time, 2 hr at $120/hr	240.00
Perfs, 16 at $36.75/3 each	588.00
Supervision, 2 hr at $60/hr	120.00
Retrievable bridge plug	980.00
Total	**2,428.00**
Slotting Item[d]	**Slotting Cost ($)**
Sand, 20/40-mesh, 100 sks at $6.00 each	600.00
Water hauling, 5 hr at $40/hr	200.00
Rig time, 2 hr at $120/hr	240.00
Sand transport (100 sks)	340.00
Jet tool (double stack) rental	750.00
Jets, 4 at $43 each	172.00
Supervision, 4 hr at $60/hr	240.00
Abrasive fluid charge, $.25 × 100 sks	25.00
Retrievable bridge plug	980.00
Total	3,547.00[e]

[a] Isolated 4-ft interval.

[b] Backfilling the hole with sand is an alternative method to provide lower isolation. The costs associated with removal of such sand is considered equivalent to the bottom packer rental cost quoted.

[c] 4 SPF, 61-in. EHD, 4-ft interval

[d] 4-ft slot, 1 coalseam frac

[e] No service equipment or related standby or mileage considered. No rig trip time or related standby considered. Actual costs on individual slotting jobs are estimated at $5,000, if not performed in conjunction with the hydraulic stimulation process.

10.3.2 Water Disposal

Zimpfer, Harmon, and Boyce[16] determined relative costs of transportation by truck or pipeline and of disposal of CBM production waters by evaporation pit, underground injection, or direct surface use on the southern Ute Reservation of the San Juan basin. Their estimate for truck conveyance was based on a 160-bbl tanker moving brines 10 miles for disposal. Their cost of transporting by truck is presented in Eq. 10.4.

$$T = 11.1\,Q^{-0.195} \qquad \text{(Eq. 10.4)}$$

where

T = cost of truck transport of brine, $/bbl
Q = volume transported

Truck conveyance costs range from $0.50 per bbl at high rates to $2.90 per bbl at low rates of brine production (see Fig. 10.3).

A more practical carrier for large volumes of brine in mountainous areas, such as the San Juan basin, is pipeline. The range of costs were determined by Zimpfer, *et al.*[16] to be $0.44/bbl at 5,000 BWPD to $0.97/bbl for higher rates. Fig. 10.3 presents the relative costs of the two transportation modes.

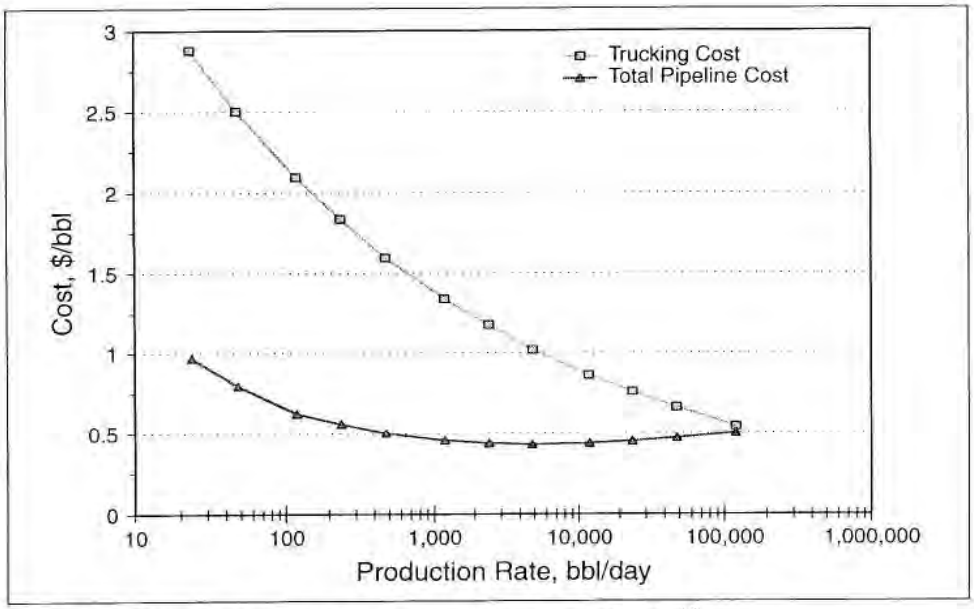

Fig. 10.3—Brine transportation costs of San Juan basin.[16]

Relative costs of injection well and evaporation pit water disposal are shown in Fig. 10.4 for the southern Ute Reservation of the San Juan basin.[16] Transportation costs to each site must be added to costs of each disposal method of Fig. 10.4.

It can be seen from Table 10.4 that other possible means of disposal are either economically prohibitive with state-of-the-art technology or would violate environmental codes.[16]

Reid and coworkers[17] studied production from five wells in the Wyodak-Anderson coals of the Fort Union formation in the Powder River basin. They history-matched data from the five wells by means of a three-dimensional, two-phase simulator. These shallow, thick (139-ft) subbituminous coals were shown to be profitable for CBM production over a reasonable range of natural gas prices if water disposal costs could be controlled. The low solids content of

the produced water, 1,500–2,500 ppm, makes disposal more favorable. Their results showed that water disposal costs below about $2.00/bbl are needed in the Powder River basin for satisfactory ROR (see Fig. 10.5).

Table 10.4—Costs of Other Water Disposal Means[16]

Application	Cost ($/bbl)
Direct surface use, no treatment	0.01 to 0.10
Direct use, distillation	5.00
Direct use, reverse osmosis	>5.00
Direct use, ion exchange	5.00

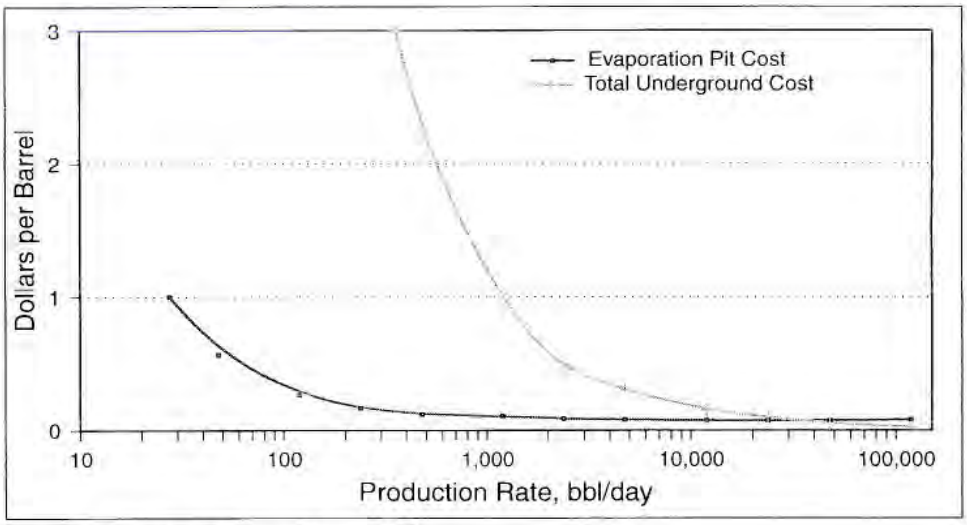

Fig. 10.4—Water disposal costs.[16]

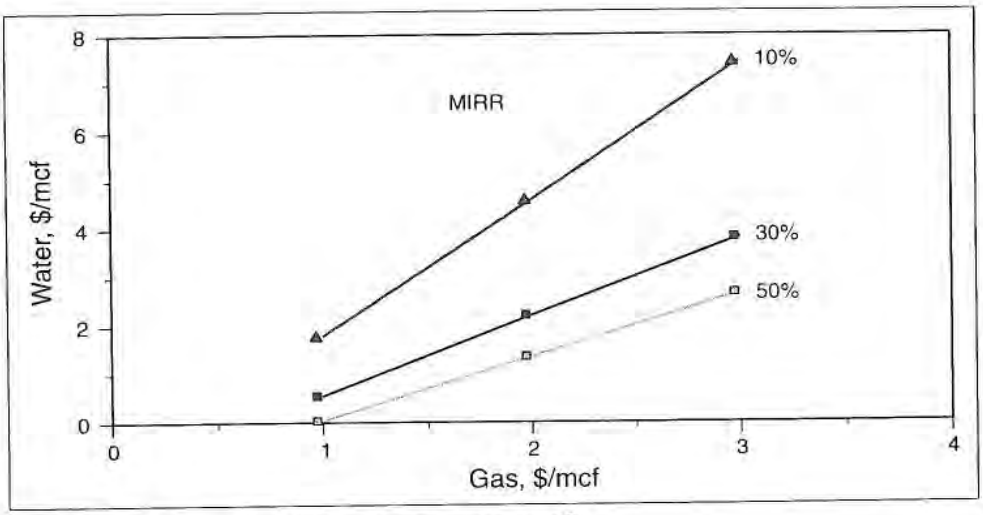

Fig. 10.5—Profitability in Powder River basin.[17]

10.3.3 Finding Costs

Reserves and production rates for wells in the San Juan basin are higher than in the Warrior or other eastern basins. The differences are emphasized by comparing finding costs in the two basins. Hobbs presented the comparison as recorded in Table 10.5.[18]

Table 10.5—Finding Costs of Basins[18]

Basin	Reserves Per Well (Bcf)	Find Costs ($/Mcf)
San Juan	0.4 to 9.0	0.08 to 0.24
Black Warrior	0.3 to 1.2	0.28 to 0.67

The 400–900 Tcf of CBM estimated to be in coals less than 4,000 ft deep is in addition to unknown quantities of gas in deeper coals in the United States. Technical capabilities and economics will determine how much of this in-place gas will be produced. The trend toward clean energy indicates that the resource will be increasingly needed in the future. In the brief history of the process to recover methane from coals, rapid progress has been made both technically and economically in the process. Continued progress would make development of the CBM process one of the most important innovations in clean energy supply.

10.4 Structured Resource Evaluation

Maximizing CBM profitability requires an early assessment of critical reservoir parameters. Gas content, seam thickness, and permeability have already been discussed. In addition, determination of the permeability anisotropy ratio must be evaluated as a decision point between vertical development and the use of horizontal wellbores to access CBM gas. Even if vertical development is the optimum, spacing of the vertical wells must be determined to maximize return on investment.

Historically, CBM exploration has followed two evaluation paths. The first, and most commonly employed path, is to drill a single well or a five-spot and place the wells on production. While this may give an indication of productivity of water or "free" gas, it does not allow the operator to make an informed decision about what spacing would optimally develop the project, nor does it give a true indication of what the coals are capable of producing because water influx will inhibit gas desorption. Without reservoir data (gas content, isotherms, permeability data), it is impossible to simulate what the center well of a five-spot should produce. A representative model cannot be built to allow economic analysis for optimization. History-matching can require gathering of several years of data to enable the operator to draw conclusions about the resource value.

The second technique involves understanding the reservoir and productivity early in the exploration process. An aggressive data acquisition program must be conducted in a step-wise manner that proceeds from collecting the least costly parameters to more costly data and from a basin-wide to site-specific assessment.

Programs for unexplored basins will have evaluation programs that differ from those used for expanding production in a proven basin.

Basin evaluation programs acquire information that points to preferred sites for initial production development. Both geologic and hydrologic models are constructed from available public and private data. These evaluations include estimating gas in place (GIP) and gas and water production. Economics are evaluated based on expected gas price sales, water disposal costs, and pipeline access costs. From this assessment, a site-specific drilling program is developed where core holes will be located.

Once the core hole locations are drilled and cores taken, gas content data will be measured and desorption isotherms determined; adsorption isotherms can be developed. Economic modeling can then begin to assess viability of the project. Table 10.6 lists some measured values applicable to an Appalachian project review.

10.4.1 Gas Content Sensitivity

Fig. 10.6 depicts the relationship of gas content to production rate based on simulation runs using the parameters in Table 10.6. Mother Nature rules in the CBM world—higher gas content leads to higher gas production rates when all other variables are held constant. NPV calculations indicate that an operator must have 400 scf/ton or higher gas contents to make a positive NPV profit from this scenario (Table 10.6).

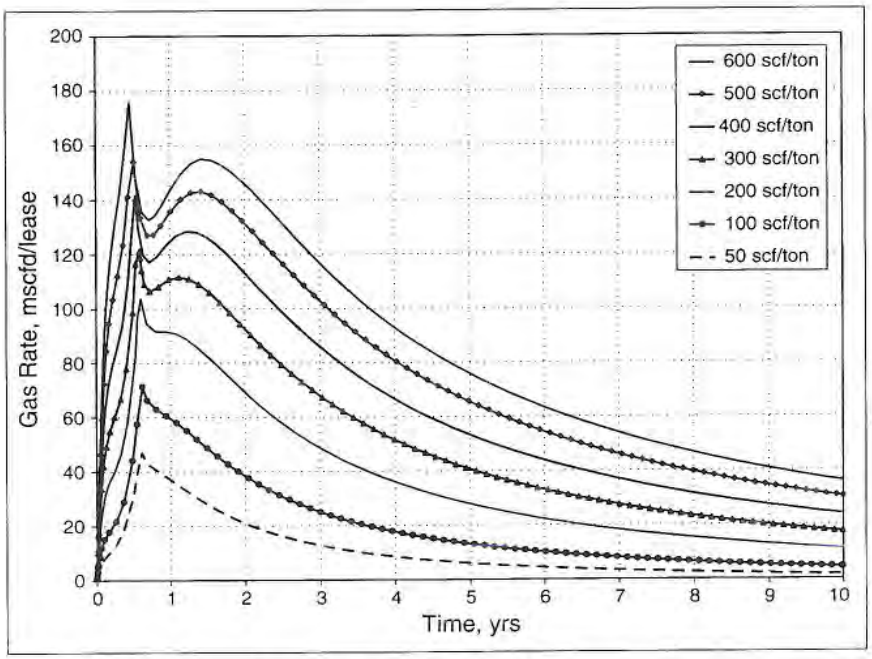

Fig. 10.6—Gas rate for various gas contents.

Table 10.6—Reservoir and Economic Parameters

Base Case Reservoir Parameters		
Lx/Ly =1	kx = ky = 6 md	Xf = 200 ft
GRI rel perm	Sw = 95%	Porosity = 1%
600 scf/ton	WHFP 50 psia	Hn = 15 ft
PRI 500 psia	40-acre spacing	
Economic Parameters		
Interest rate		10%/yr
Net back price		$3/Mcf
Water disposal		$2/bbl
Ops cost		$800/month
D & C cost		($300,000)
Life		10 years

10.4.2 Permeability Sensitivity

Sensitivity to different permeability values can likewise be simulated and displayed (Fig. 10.7). Economic calculations indicate permeability of 3 md or higher is needed for positive NPV profit (Table 10.7).

Table 10.7—NPV Calculations for Different Gas Contents

	Prod NPV	Well NPV
600 scf/ton	$665,276	$214,361
500 scf/ton	$589,784	$139,095
400 scf/ton	$499,303	$49,135
300 scf/ton	$401,847	($47,741)
200 scf/ton	$296,675	($152,170)
100 scf/ton	$163,543	($283,202)
50 scf/ton	$90,272	($353,752)

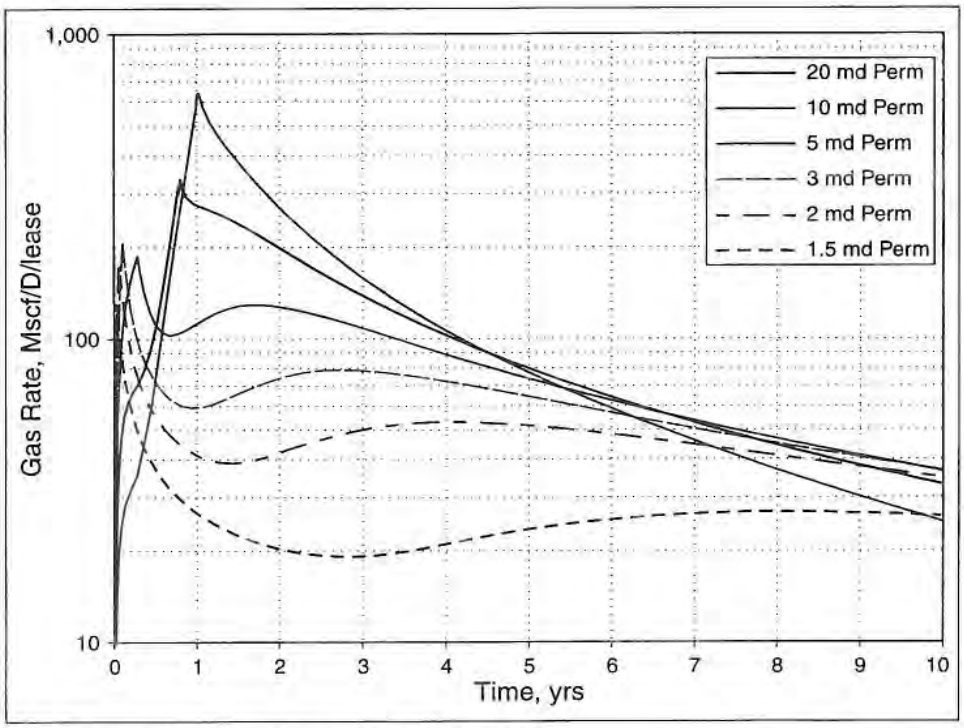

Fig. 10.7—Gas rates as permeability is varied.

10.4.3 Spacing Sensitivity

Interference between CBM wells is imperative to promote gas desorption. This may be the biggest difference between conventional production and CBM production. Peak gas desorption rates are functions of gas content and permeability, parameters an operator cannot control. Spacing of wells can be controlled to obtain maximum gas desorption once the other variables are determined.

Sensitivity to various spacing designs is depicted in Fig. 10.8. Note the increasing peak rates and reduction in time to achieve them as spacing is decreased. This is why spacing is so important to the development of a CBM field and the reason it is the main controlling factor of the economics in a project. A review of the economics of the simulations (Table 10.8) would indicate that 80-acre spacing is correct, based on well NPV. However, in a lease situation where the infrastructure (lease roads, compression, gathering lines) is established by the first few wells, additional wells do not cost as much to drill and connect. As a result, the 40-acre spacing finally yields the better return.

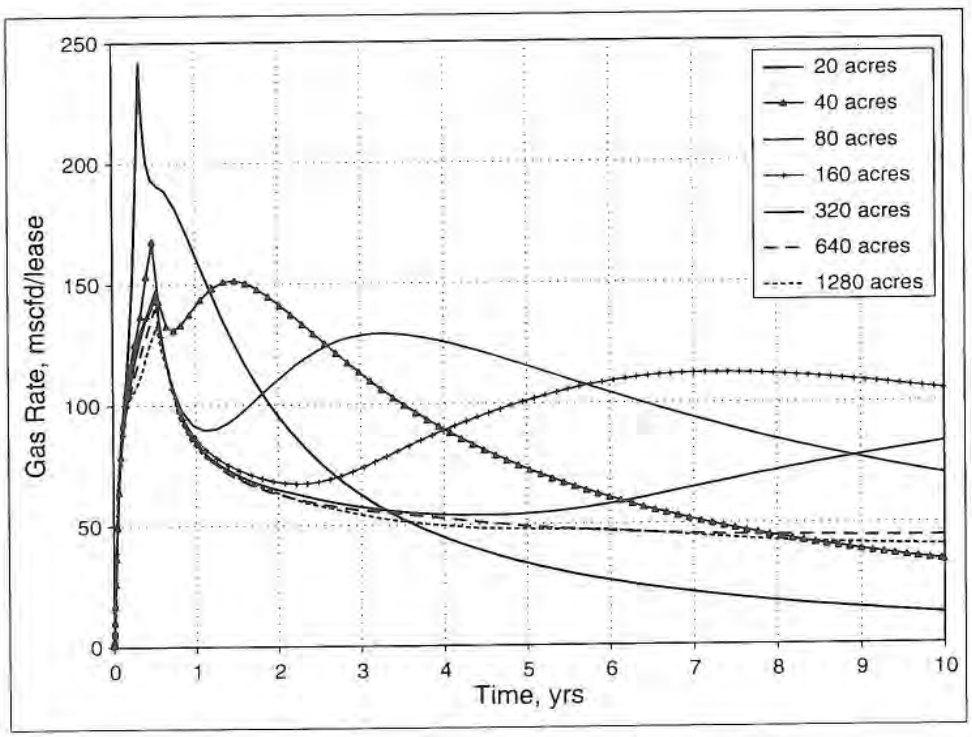

Fig. 10.8—Gas production sensitivity to various well spacings.

Table 10.8—NPV Calculations for Different Permeabilities

	Prod NPV	Well NPV
20 md	$991,689	$537,407
10 md	$809,562	$357,417
5 md	$606,743	$157,815
3 md	$448,712	$3,393
2 md	$336,067	($105,764)
1.5 md	$182,045	($251,822)

10.4.4 Permeability Anisotropy Sensitivity

Determination of permeability anisotropy is an early objective of a five-spot production test. High-permeability anisotropy substantially reduces production rates in spite of what appears to be an adequate in-situ permeability measured from a pre-stimulation injection-falloff test. Sensitivity of production rate to anisotropy can be seen in Fig. 10.9 for a ratio k_x:k_y=2.0. Fig. 10.10 shows some separation of production rate profiles based on a rectangular pattern given anisotropy for k_x:k_y=5.0 with the pattern being twice the distance in the x-direction over y-direction. NPV analysis (Table 10.9) reveals that for a ratio of 2, all patterns make positive cash flow. In the case of anisotropy =5.0, the rectangular pattern is the only choice with positive cash flow.

Table 10.9—Net Present Value (NPV) Calculations for the Different Spacings

Spacing	Prod NPV	Disposal NPV	Well NPV	Lease NPV
20 acres	474,414	-31085	49610	393884
40 acres	642090	-57140	191231	764925
80 acres	727737	-100716	233301	466603
160 acres	650236	-164974	91543	91543
320 acres	482693	-233177	-144203	
640 acres	420668	-260535	-233586	
1280 acres	409330	-261584	-245973	

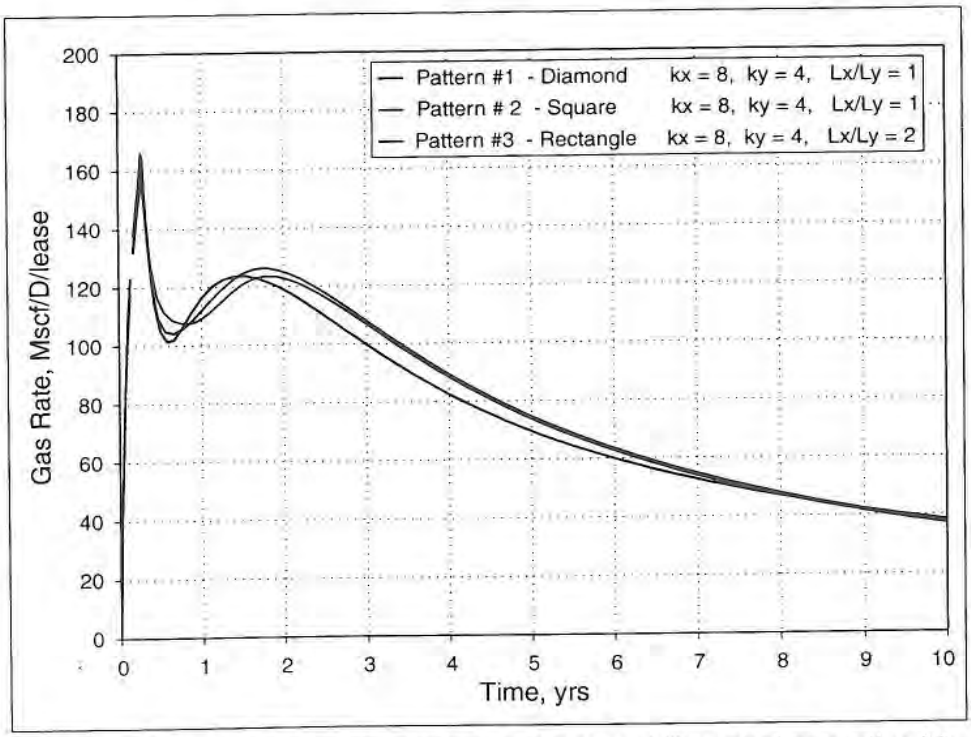

Fig. 10.9—Gas rates for various patterns and permeability anisotropy ratio of 2.

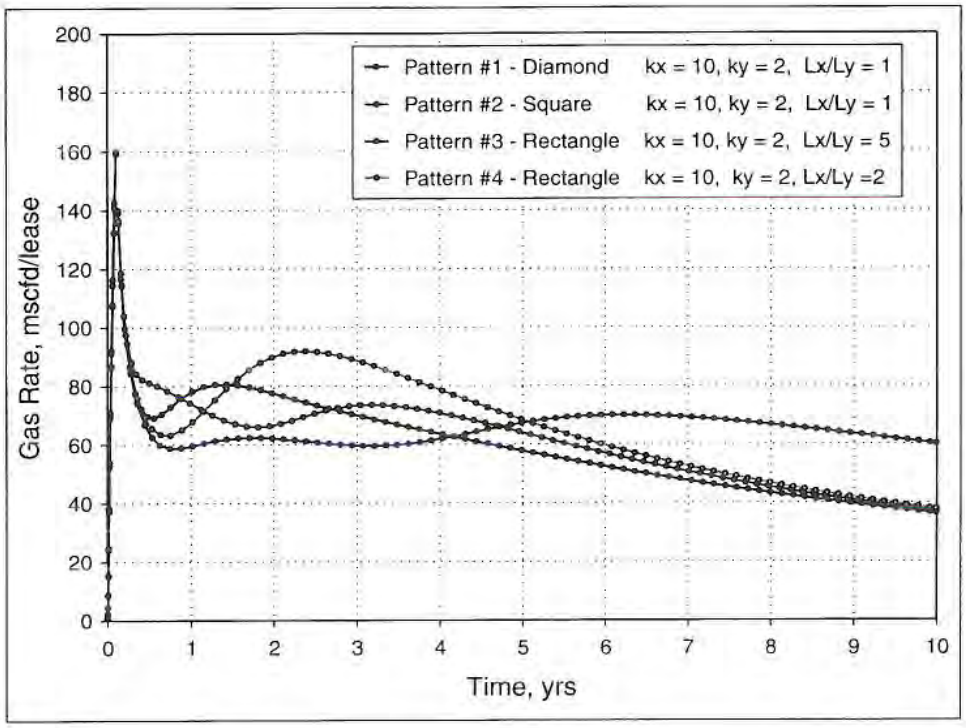

Fig. 10.10—Gas rates for various patterns and perm anisotropy ratio of 5.

A high anisotropy of k_x:k_y >10 might indicate the need for horizontal drilling or for selecting an alternative production test site. High anisotropy will yield low production vertical wells regardless of spacing and pattern. A low anisotropy, such as k_x:k_y <3, could indicate that anisotropy does not warrant further investigation. A standard square pattern should be adequate for optimum production.

10.4.5 Fracture Length Sensitivity

Net present value analysis has been done for a number of years in conventional fracture design work for CBM designs with a change in x-axis to reflect the optimum spacing. Fig. 10.11 indicates the optimum spacing to be 40–50 acres with a 300–400 ft fracture. While simulations of fracture length sensitivity are easily done, measurement of actual fracture geometry is much more difficult. Currently, the most economic method is a post-fracture injection fall-off test to calibrate fracture volumes used.

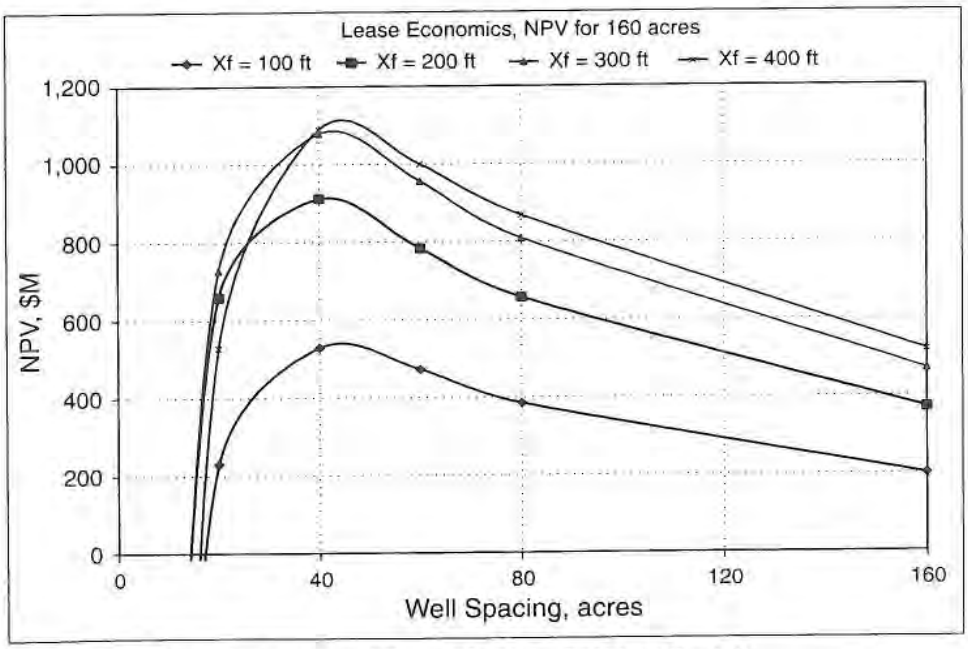

Fig. 10.11—NPV analysis for different fracture half-lengths (xf).

Continual reservoir characterization is required as site development progresses to the scale of field development. Local geology and hydrology will dictate an appropriate expansion program from the original site-specific assessment. If permeability and gas content remain consistent from well to well, development should proceed as concentric rings of wells around the original five-spot pilot on

the optimum spacing determined from simulation assessment. Step-outs approximately 3 miles from the original test location should be validated for permeability and gas content to confirm the field model. History-matching of production can begin right away with the first field model, provided the operator records daily gas rate, water rate, and backpressure data. This history-matching will allow changes to the field model sooner in the field development lifecycle.

References

[1]Soot, P.M.: "Tax Incentives Spur Development of Coalbed Methane," *Oil & Gas J.* (June 1991) 89, No. 23, 40.

[2]Lemons, B.N. and Nemirow, L.: "Maximizing the Section 29 Credit in Coal Seam Methane Transactions," *The Journal of Taxation* (April 1989) 238-245.

[3]Hunt, A.M. and Steele, D.J.: "Coalbed Methane Development in the Appalachian Basin," *Quarterly Review of Methane from Coal Seams Technology* (July 1991) 1, No. 4, 10-19.

[4]Willis, C.P.: "A Case History of River Gas Corporation's Black Warrior Project," *Quarterly Review of Methane from Coal Seams Technology* (July 1992) 10, No. 1, 33.

[5]Hobbs, G.W., Holland, J.R., and Winkler, R.O.: "Economic Model Predicts Coal-Bed Methane Development," *Pet. Eng. Int.* (July 1992) 64, No. 7, 34-38.

[6]Thompson, R.S. and Wright, J.D., *Oil Property Evaluation*, second edition, Thompson-Wright Associates, Golden, Colorado (1985).

[7]Boyle, H.F. Jr.: "Investment Analysis: U.S. Oil and Gas Producers Score High in University Survey," *J. Pet. Tech.* (April 1985) 37, No. 4, 680-690.

[8]Mavor, M.J.: "Western Cretaceous Coal Seam Project," *Quarterly Review of Methane from Coal Seams Technology* (April 1991) 8, No. 3, 19-21.

[9]Hobbs, W.G. and Winkler, R.O.: "Coalbed Methane Shows Its Potential," *Pet. Eng. Int.* (May 1990) 62, No. 5, 26-33.

[10]Kuuskra, V.A., Boyer, C.M., and McBane, R.A.: "Steps to Assess Resource Economics Covered," *Oil & Gas J.* (December 1989) 87, No. 52, 121-125.

[11]Willis, C.: "Core Tests Speed Coalbed Methane Gas Development," *Oil & Gas J.* (June 1991) 89, No. 22, 93-96.

[12]Palmer, I.D., Tumino, K.A., Fryar, R.T., and Puri, R.: "Water Fracs Outperform Gel Fracs in Coalbed Pilot," *Oil & Gas J.* (August 1991) 89, No. 32, 71.

[13]Lambert, S.W.: "Comparison of Open Hole, Slotting and Perforating Completion Methods for Multiseam Coalbed Gas Wells," *Proc., Coalbed Methane Symposium*, Tuscaloosa, Alabama (April 1989) 262.

[14]Zuber, M.D. and Wicks, D.E.: "Methane from Coal Deposits Technical Evaluation and Data Base," *Quarterly Review of Methane from Coal Seams Technology* (November 1988) 6, No. 2, 39-41.

[15]Lambert, S.W., Niederhofer, J.D., and Reeves, S R.: "Multiple-Coalseam Well Completions in the Deerlick Creek Field," *J. Pet. Tech.* (November 1990) 42, No. 11, 1360-1363.

[16]Zimpfer, G.L., Harmon, E.J., and Boyce, B.C.: "Disposal of Production Waters from Oil and Gas Wells in the Northern San Juan Basin, Colorado," *Rocky Mountain Association of Geologists Guidebook*, Denver, Colorado (1988) 183-198.

[17]Reid, G.W., Towler, B.F., and Harris, H.G.: "Simulation and Economics of Coalbed Methane Production in the Powder River Basin," paper SPE 24360 presented at the 1992 SPE Rocky Mountain Regional Meeting, Casper, Wyoming (May 1992) 425-432.

[18]Hobbs, G.W.: "Economics and Financing of Coalbed Methane Ventures," paper presented at 1990 Eastern Coalbed Methane Forum, Tuscaloosa, Alabama, 16 January.

Acronyms

AFIT	after federal income tax
API	American Petroleum Institute
ACOE	Army Corps of Engineers
ADEM	Alabama Department of Environmental Management
bbl	barrel(s)
bbl/min	barrels per minute
Bcf/D	billion cubic feet per day
BFP-IFT	below fracture pressure injection falloff test
BHPA	bottomhole packer assembly
BOD	biochemical oxygen demands
BTU	British thermal unit
BWPD	barrels of water per day

CBM	coalbed methane
CMOP	Coalbed Methane Outreach Program (EPA)
CN	compensated neutron
CNG	compressed natural gas
CTP	coiled tubing and packer
daf	dry, ash-free
DCFROR	The interest rate necessary to make the sum of the present value of the investment equal to the sum of the present values of each year's net cash flow.
DFIT	diagnostic fracture injection test
DOE	U.S. Department of Energy
DST	drillstem test
EIA	Energy Information Administration
EPA	U.S. Environmental Protection Agency
gal	gallons
g/cc	grams per cubic centimeter
GIP	gas in place
GRI	Gas Research Institute (now known as GTI)
HEC	hydroxyethyl cellulose
H.G.I.	Hardgrove grindability index
hp	horsepower
hr	hours
HPG	hydroxypropyl guar

IFT	injection falloff test
in.	inches
ISIP	instantaneous shut-in pressure
ISSOS	in-situ state-of-stress
LGB	low-gel borate
Mcf	thousand cubic feet
md	millidarcy
MEI	micro-electrical imaging
mg/L	milligrams per liter
MMcf/D	million cubic feet per day
MMcf/min	million cubic feet per minute
MRIL	magnetic resonance imaging tool
m.y.a.	million years ago
NGV	natural gas vehicles
NORM	naturally occurring radioactive minerals
NPDES	national pollutant discharge elimination system
NPV	net present value
PBU	pressure buildup (test)
PE	photoelectric
ppg	pounds per gallon
REI	Resource Enterprises Inc.
ROR	rate of return

scf	standard cubic feet
scfm	standard cubic feet per minute
SLM	straight line method of depreciation
SP	spontaneous potential
Tcf	trillion cubic feet
TD	total depth
TDS	total dissolved solids
TMRA	Technical and Miscellaneous Revenue Act (1988)
USBM	U.S. Bureau of Mines
WPT	windfall profit tax; Windfall Profit Act (1980)

Index

A

B

C

D

E

F

G

H

I

J

K

L

M

N

O

P

Q

R

S

T

U

V

W

Y

COALBED METHANE

PRINCIPLES & PRACTICES

Second Edition

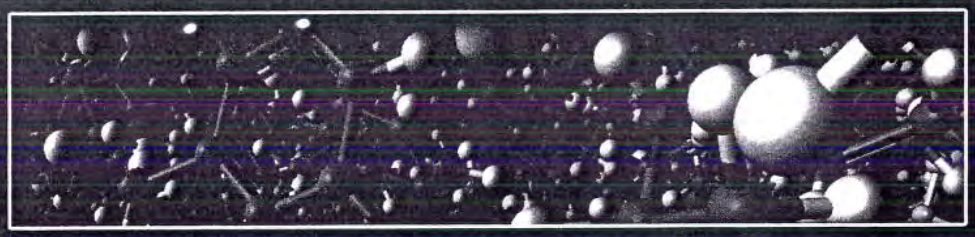

With today's heightened environmental awareness, decreased domestic oil production, and increased consumer demand for energy, the timing is right for the coalbed methane process. In this 2nd edition of *Coalbed Methane: Principles and Practices,* Halliburton engineers Ramurthy, Rodvelt and Mullen update and add valuable information on reservoir analysis, well construction, formation evaluations, logging, completions and hydraulic fracturing technology for successful coalbed methane production.

Chapters Include:

A. Overview of CBM reservoirs, major U.S. coal basins
B. Geological influences on coal, coal chemistry
C. Sorption
D. Reservoir analysis
E. Well construction
F. Formation evaluations, logging
G. Completions
H. Hydraulic fracturing of coalseams
I. Water production and disposal
J. Economics of CBM recovery

About the Authors

- **Rudy Rogers** is a professor in the Swalm School of Chemical Engineering at Mississippi State University, where he has taught petroleum engineering and chemical engineering for thirty years. His research covers coalbed methane and other energy topics. Prentice Hall published in 1994 the original ***Coalbed Methane: Principles and Practice*** by Dr. Rogers.

- **Muthukumarappan "Kumar" Ramurthy** is a Technical Professional, Team Lead with Halliburton's Tech Team in Denver. He received his Bachelor of Engineering in Mechanical Engineering in India and a M.S. in Petroleum Engineering from Mississippi State University. He has published numerous papers on coalbed methane and is a board member of the SPE Denver section. He serves on the Unconventional Gas Resources team with Halliburton.

- **Gary D. Rodvelt** is a Sr. Technical Services Advisor – Reservoir with 29 years of service to Halliburton in Mid-Continent, Illinois, and Appalachian Basins. Author of ten SPE papers on stimulation and evaluation processes in CBM and conventional reservoirs, he is a Project Advisor on Appalachian/Illinois CBM projects. He lives in West Virginia.

- **Mike Mullen** is Technical Professional Manager-Solution Team specializing in the integration of stimulation petrophysics, reservoir simulation and economic stimulation design in conventional and unconventional reservoirs with Halliburton in Denver, CO. He has authored numerous papers concerning Economic Stimulation and Production Log analysis.

H06263 06/08